Using Objective Methods to Measure the Underlying Mechanisms of Discomfort during Prolonged Standing

by

Stephanie A. Wiltman

BS Materials Science and Engineering, Virginia Tech, 2015

BS Psychology, Virginia Tech, 2015

Submitted to the Graduate Faculty of

Swanson School of Engineering in partial fulfillment

of the requirements for the degree of

Doctor of Philosophy

University of Pittsburgh

2020

UNIVERSITY OF PITTSBURGH

SWANSON SCHOOL OF ENGINEERING

This dissertation was presented

by

Stephanie A. Wiltman

It was defended on

March 5, 2020

and approved by

William J. Anderst, Ph.D., Assistant Professor, Department of Orthopedic Surgery

Theodore J. Huppert, Ph.D., Associate Professor, Department of Electrical and Computer Engineering

Subashan Perera, Ph.D., Professor, Department of Medicine

Mark Redfern, Ph.D., Professor, Department of Bioengineering

Scott Tashman, Ph.D., Director, Biomedical Engineering Program, Steadman Philippon Research Institute

Dissertation Director: April J. Chambers, Ph.D., Research Assistant Professor, Department of Bioengineering

Using Objective Methods to Measure the Underlying Mechanisms of Discomfort during Prolonged Standing

Stephanie Anne Wiltman, PhD

University of Pittsburgh, 2020

Prolonged standing is an occupational hazard that leads to higher likelihoods of joint and circulatory disorders. Existing measures of prolonged standing do not directly assess circulatory or joint responses. The goal of this research is to (Aim 1) identify novel weight transfer strategies, (Aim 2) investigate in vivo knee joint cartilage deformation, and (Aim 3) examine characteristics of lower extremity muscles during prolonged standing. Twenty-nine healthy adults were recruited in two body-mass index (BMI) subgroups, healthy weight (HW, 16 subjects, BMI<29.9 kg/m^2) and obese (OB, 13 subjects, BMI>29.9 kg/m^2). Subjects stood for two hours on two different flooring surfaces. Radiographs of the knee and near infrared spectroscopy (NIRS) of the soleus muscle were used to measure joint and circulatory effects of prolonged standing, respectively. Subjective surveys, electromyography (EMG), and underfoot vertical reaction forces were also collected.

A novel method was developed to determine two weight transfer strategies, termed shifts and fidgets, based on vertical force and temporal boundaries. Shifts and fidgets increased significantly over time. OB subjects displayed more shifts and fidgets over time than HW subjects. Tibiofemoral gap distance, determined using a fitted piecewise model, decreased over time. OB subjects reached terminal tibiofemoral gap sooner on a hard floor than mat, suggesting that the mat condition may have a beneficial effect on cartilage compression for OB subjects. The NIRS measured increases in blood volume and flow over time. The mat condition decreased blood volume and flow, especially for OB subjects.

Overall, OB subjects demonstrated different physiological responses to an anti-fatigue mat versus a hard floor, suggesting that ergonomic interventions may influence the response of heavier workers differently. Future research should include human factors—such as BMI, age, gender, pregnancy, or disease—when investigating occupational injuries associated with prolonged standing. These human factors should be considered when evaluating the effectiveness of ergonomic interventions and designing new interventions.

Table of Contents

Acknowledgements ..... **xlv**

1.0 Specific Aims **1**

2.0 Background and Significance **4**

2.1 Epidemiology and Clinical Significance **4**

2.2 Background **9**

2.2.1 Psychophysical Measures of Prolonged Standing **10**

2.2.2 Measures of Weight Transfer Changes during Prolonged Standing **13**

2.2.3 Measures of Joints during Prolonged Standing **18**

2.2.4 Measures of Muscles during Prolonged Standing **23**

2.3 Effects of Standing Surfaces on Prolonged Standing Outcome Measures **37**

2.4 Effects of Obesity on Prolonged Standing Outcome Measures **43**

2.5 Study Innovation **47**

3.0 Experimental Methods **49**

3.1 Subject Population **49**

3.2 Experimental Environment **50**

3.3 Experimental Protocol **55**

3.3.1 Standing Visits **55**

3.3.1.1 Subject Preparation **55**

3.3.1.2 Device Preparation **60**

3.3.2 CT Scan Visit **62**

3.4 Data Processing and Analysis **62**

3.4.1 Subjective Discomfort Measures 62

3.4.2 Weight Transfer Measures 63

3.4.2.1 Previously Published Method: Cham and Redfern, 2001 64

3.4.2.2 Previously Published Method: Wiggermann and Keyserling, 2013 . 64

3.4.2.3 New Proposed Method 64

3.4.3 Knee Joint Measures 65

3.4.4 Lower Extremity Muscle Measures 70

3.4.4.1 Electromyography 70

3.4.4.2 Near Infrared Spectroscopy 71

4.0 Results 73

4.1 Tiredness and Discomfort 73

4.2 Weight Transfer Measures 85

4.2.1 Development of a New Method 85

4.2.2 Comparison of Methods 92

4.2.3 Standing Strategies during Prolonged Standing 93

4.2.4 Standing Strategies and Subjective Tiredness and Discomfort 99

4.3 Knee Joint Measures 100

4.3.1 Introduction to MTFG Data Analysis 100

4.3.2 Exploration of the Relationship between MTFG and Kinematics during Prolonged Standing 102

4.3.3 Development of a Piecewise Model for MTFG Data 107

4.3.4 Knee Joint Measures and Subjective Tiredness and Discomfort 115

4.3.5 Knee Joint Measures and Standing Strategies 116

4.4 Lower Extremity Muscle Measures 118

4.4.1 Electromyography 118

4.4.1.1 Tibialis Anterior 118

4.4.1.2 Gastrocnemius 122

4.4.1.3 Soleus 126

4.4.1.4 Rectus Femoris 130

4.4.1.5 Hamstring 133

4.4.1.6 Electromyography Measures and Subjective Tiredness and Discomfort 138

4.4.1.7 Electromyography Measures and Standing Strategies 138

4.4.2 Near Infrared Spectroscopy 141

4.4.2.1 Near Infrared Spectroscopy Measures and Subjective Tiredness and Discomfort 148

4.4.2.2 Standing Strategies and Near Infrared Spectroscopy Measures 149

4.4.3 Correlations of Electromyography and Near Infrared Spectroscopy Data 150

5.0 Discussion 152

5.1 Tiredness and Discomfort 152

5.2 Weight Transfer Measures 154

5.3 Knee Joint Measures 163

5.4 Lower Extremity Muscle Measures 165

5.4.1 Electromyography 165

5.4.2 Near Infrared Spectroscopy 168

5.4.3 Correlations of Electromyography and Near Infrared Spectroscopy.....173

5.5 Correlations with Discomfort and Tiredness..... 175

5.6 Correlations with Standing Strategies..... 177

6.0 Limitations..... 179

7.0 Conclusion 183

Appendix A Tiredness and Discomfort..... 186

Appendix A.1 Overall Tiredness..... 187

Appendix A.2 Legs Tiredness..... 190

Appendix A.3 Hips..... 193

Appendix A.4 Upper Legs..... 196

Appendix A.5 Knees 199

Appendix A.6 Lower Legs 202

Appendix A.7 Ankles..... 205

Appendix A.8 Feet 208

Appendix B Weight Transfer Measures 211

Appendix B.1 Comparison of COP and P_R Data..... 211

Appendix B.2 Shift and Fidget Data 213

Appendix B.2.1 Shifts.....213

Appendix B.2.2 Fidgets.....216

Appendix B.2.3 Total Events.....219

Appendix B.3 Investigation of Strategy Usage..... 221

Appendix C Knee Joint Measures..... 256

Appendix C.1 MTFG and Kinematics Data..... 257

Appendix C.2 Comparison of Models using Two and Four Hours of Data 283

Appendix D Lower Extremity Muscle Measures 285

Appendix D.1 Electromyography Data 285

Appendix D.1.1 Tibialis Anterior MPF 286

Appendix D.1.2 Tibialis Anterior RMS 289

Appendix D.1.3 Gastrocnemius MPF 292

Appendix D.1.4 Gastrocnemius RMS 295

Appendix D.1.5 Soleus MPF 298

Appendix D.1.6 Soleus RMS 301

Appendix D.1.7 Rectus Femoris MPF 304

Appendix D.1.8 Rectus Femoris RMS 307

Appendix D.1.9 Hamstring MPF 310

Appendix D.1.10 Hamstring RMS 313

Appendix D.2 Near Infrared Spectroscopy Data 316

Appendix D.2.1 Oxy-Hemoglobin 317

Appendix D.2.2 Deoxy-Hemoglobin 321

Appendix D.2.3 Total Hemoglobin 325

Appendix D.2.4 Pulsatile Flow 329

Appendix D.2.5 Tissue Oxygen Saturation 333

Appendix D.2.6 Pulsatile Oxygen Saturation 337

Bibliography 341

List of Tables

Table 1: A collection of studies investigating the effects of various independent variables on subjective discomfort, fatigue, or unpleasantness. ***Significance (T, time; C, cycles; R, rest; SS, standing surface; S, shoe type; I, insoles) is denoted in superscript next to measurement locations.*** **..... 11**

Table 2: A collection of studies investigating the effects of various independent variables on weight transfer measures. ***Significance (T, time; SS, standing surface; SE, session) is denoted in superscript next to measurement locations.*** **..... 15**

Table 3: A collection of studies investigating the effects of various independent variables on muscle and circulatory outcomes of prolonged standing. ***Significance (T, time; SS, standing surface; S, shoe type) is denoted in superscript next to measurement locations.*** **.. 35**

Table 4: A collection of studies investigating the effects of standing surfaces interventions (anti-fatigue mats and shoe insoles) on subjective, behavioral, and physiological outcomes of prolonged standing. ***Significance (T, time; SS, standing surface; S, shoe type) is denoted in superscript next to measurement locations.*** **..... 38**

Table 5: Mean ± STD and range of subject demographics. An unpaired t-test was performed on age, height, weight, and BMI to confirm differences between groups. ***p < 0.0001, *; p > 0.05, NS*** **..... 50**

Table 6: Muscles measured using EMG's and accompanying anatomical landmarks. Distances were measured in centimeters to the center of the EMG to the center of the anatomical landmark. Anatomical landmarks were chosen based on the ability to access them for measurement while the subject was seated. 60

Table 7: A list of devices and whether data was collected at discrete time points or continuously throughout the standing visit. If data was collected continuously, the collection frequency is noted. 61

Table 8: Model-based tracking accuracy and precision for individual bones and rotational measurements. Adapted from [63]. 68

Table 9: Full factorial within subjects repeated measures mixed effects analysis of tiredness and discomfort. Factors included are flooring (F), BMI (B), and time (T). *p < 0.0001 **, *p < 0.001 ***, *p < 0.01 **, *p < 0.05 *, *p > 0.05 NS* 74**

Table 10: Pearson's correlation between methods of measuring behaviors during prolonged standing. *p < 0.0001 **, *p < 0.001 ***, *p < 0.01 ** 92**

Table 11: Results from repeated measures mixed effects model investigating the effects of flooring (F), BMI (B), and time (T) on shifts, fidgets, and total events performed during standing. *p < 0.0001 **, *p < 0.001 ***, *p < 0.01 **, *p < 0.05 *, *p > 0.05 NS* 94**

Table 12: Pearson correlations were performed to determine if tiredness and discomfort measures were related to standing strategies. *p < 0.0001 **, *p < 0.001 ***, *p < 0.01 **, *p < 0.05 *, *p > 0.05 NS* 99**

Table 13: Pearson correlation results comparing MTFG with flexion, abduction, and external rotation using all subject data. *p < 0.0001 **, *p < 0.05 *, *p > 0.05 NS* 102**

Table 14: Correlation coefficients between MTFG and flexion, abduction, and external rotation by subject. Significant and non-significant probabilities are indicated. *p < 0.0001 **, *p < 0.001 ***, *p < 0.01 **, *p < 0.05 *, *p > 0.05 NS* 104**

Table 15: All HW subject data, including subjects that did not converge or converged with errors. Values a, b, and c are coefficients for the quadratic piecewise equation, $at^2 + bt +$

$c = g(t)$, where t is time in minutes, and g is predicted gap distance. G_0 is the intercept value at 0 minutes of standing. T_T and G_T are the values for terminal gap, where quadratic and linear functions converged. Data that was not included in analyses is shaded in light grey. Data was omitted if a convergence error occurred or if the quadratic fit modeled an increase in gap distance over time. 109

Table 16: All OB subject data, including subjects that did not converge or converged with errors. Data that was not included in analyses is shaded in light grey. Values a, b, and c are coefficients for the quadratic piecewise equation, $at^2 + bt + c = g(t)$, where t is time in minutes, and g is predicted gap distance. G_0 is the intercept value at 0 minutes of standing. T_T and G_T are the values for terminal gap, where quadratic and linear functions converged. 110

Table 17: Pearson correlation results comparing MTFG outcome variables and subjective tiredness and discomfort. Only T_T was significantly correlated with feet discomfort. * *Denotes significance ($p < 0.05$), NS denotes non-significance.* 115

Table 18: Pearson correlations comparing standing behaviors and MTFG outcome variables. No significant correlations were found. $p > 0.05$ *NS* 116

Table 19: Tibialis anterior MPF and $RMS^{\%}$ results from repeated measures mixed effects model investigating the effects of flooring (F), BMI (B), and time (T). $p < 0.0001$ ****, $p < 0.001$ ***, $p < 0.01$ **, $p < 0.05$ *, $p > 0.05$ *NS*..... 119

Table 20: Gastrocnemius MPF and $RMS^{\%}$ results from repeated measures mixed effects model investigating the effects of flooring (F), BMI (B), and time (T). $p < 0.0001$ ****, $p < 0.001$ ***, $p < 0.01$ **, $p < 0.05$ *, $p > 0.05$ *NS*..... 122

Table 21: Soleus MPF and RMS$^{\%}$ results from repeated measures mixed effects model investigating the effects of flooring (F), BMI (B), and time (T). ***p < 0.0001 ****, p < 0.001 ***, p < 0.01 **, p < 0.05 *, p > 0.05 NS*** **..... 127**

Table 22: Rectus femoris MPF and RMS$^{\%}$ results from repeated measures mixed effects model investigating the effects of flooring (F), BMI (B), and time (T). ***p < 0.0001 ****, p < 0.001 ***, p < 0.01 **, p < 0.05 *, p > 0.05 NS*** **..... 131**

Table 23: Hamstring MPF and RMS$^{\%}$ results from repeated measures mixed effects model investigating the effects of flooring (F), BMI (B), and time (T). ***p < 0.0001 ****, p < 0.001 ***, p < 0.01 **, p < 0.05 *, p > 0.05 NS*** **..... 134**

Table 24: Pearson correlation results comparing EMG outcome variables and subjective tiredness and discomfort. ***p < 0.0001 ****, p < 0.001 ***, p < 0.01 **, p < 0.05 *, p > 0.05 NS*** **..... 139**

Table 25: Pearson correlation results comparing EMG outcome variables and subjective tiredness and discomfort. ***p < 0.0001 ****, p < 0.001 ***, p < 0.01 **, p < 0.05 *, p > 0.05 NS*** **..... 140**

Table 26: NIRS results from repeated measures mixed effects model investigating the effects of flooring (F), BMI (B), and time (T). ***p < 0.0001 ****, p < 0.001 ***, p < 0.01 **, p < 0.05 *, p > 0.05 NS*** **..... 142**

Table 27: Pearson correlation results comparing NIRS outcome measures and subjective tiredness and discomfort. All six NIRS outcome measures were significantly correlated with tiredness and discomfort measures. ***p < 0.0001 ****, p < 0.001 ***, p < 0.01 **, p < 0.05 *, p > 0.05 NS*** **..... 148**

Table 28: Pearson correlation results comparing NIRS outcome measures and standing strategies. ***p < 0.0001 ****, p < 0.001 ***, p < 0.01 **, p < 0.05 *, p > 0.05 NS*** **..... 149**

Table 29: Pearson correlations between EMG and NIRS outcome variables. ***p < 0.0001 ****, p < 0.001 ***, p < 0.01 **, p < 0.05 *, p > 0.05 NS*** **..... 151**

Table 30: Subjects included in Group 1. These subjects were ranked higher based on total fidgets displayed during standing, and lower based on total shifts displayed during standing. RankRatio was calculated using Equation B-3. 251

Table 31: Subjects included in Group 2. These subjects were ranked similarly based on total fidgets displayed during standing and total shifts displayed during standing. RankRatio was calculated using Equation B-3. 252

Table 32: Subjects included in Group 2. These subjects were ranked lower based on total fidgets displayed during standing, and higher based on total shifts displayed during standing. RankRatio was calculated using Equation B-3. 253

Table 33: MTFG model coefficients, T_T, and G_T for seven subjects (five HW and two OB) standing on the HF condition. 283

Table 34: MTFG model coefficients, T_T and G_T for seven subjects (five HW and two OB) standing on the MT condition. 284

List of Figures

Figure 1: Percent of the workday standing or walking by selected occupations. Number of people employed in each occupation is denoted in parentheses (in millions) [10, 13, 14]. . 5

Figure 2: Recreation of data from Rekant et. al. [44]. I. Displays a primary shifter in which the subject transferred weight between legs at a lower frequency than II. the primary fidgeter. It is unknown if these two different "strategies" are a defense mechanism used by the body to mitigate discomfort, or if it is a response to discomfort. 17

Figure 3: Schematic of the knee joint capsule. Adapted from Mow and Huiskes [53]..... 18

Figure 4: Overall and compartmental compressive strain in tibial cartilage measured as a function of walking time [68]. 22

Figure 5: I. Testing apparatus used to measure cartilage compression under a half-bodyweight load. This setup was designed to replicate loading due to standing. II. Recreation of figure from Marsh. Data follows a steep compression followed by an asymptotic tail [64]..... 23

Figure 6: Systematic blood flow leaves through the aorta and returns to the heart through the vena cava. Vessel diameters are solid bars and wall thicknesses are hashed bars. Red bars represent oxygenated blood, blue bars represent deoxygenated blood, and purple bars represent a mixture of both. Adapted from Klabunde [75]. 27

Figure 7: Flow (*Q*) into and out of the capillaries must be equal. Capillaries distribute flow by distributing it in series. As more capillaries are recruited, flow decreases within each capillary. 28

Figure 8: Extinction coefficients for oxygenated hemoglobin (red line) and deoxygenated hemoglobin (blue line). Black dot indicates the isobestic point, in which both lines intersect. The dotted lines indicate the two wavelengths of light used in this study (690 and 830 nm). At 690 nm, deoxygenated hemoglobin absorbs more light. At 830 nm, oxygenated hemoglobin absorbs more light. 32

Figure 9: Typical testing setup at the Orthopaedic Biodynamics Laboratory. X-rays, force plates, NIRS, and EMG are labeled. Anti-fatigue mats with tape rectangles where a subject stood are sitting on top of the force plates. NIRS and EMG data acquisition devices sat on a cart near the subject. X-ray emitters and intensifiers were positioned such that there would not be interference by the harness system or the standing desk. 52

Figure 10: I. Full document provided to subjects to complete their survey. II. Enlarged example of each scale used for separate body parts. 54

Figure 11: Shoes and socks used for testing. Subjects self-selected shoe size but all shoes were the same brand and model. 57

Figure 12: DSX placement to collect a radioscopic image of the right knee. 57

Figure 13: EMG placement on a typical subject. Following EMG placement, measurements were taken to maintain consistent placement between visits. 59

Figure 14: NIRS and EMG placement on a typical subject. The NIRS fiber-optic lead was lifted off the floor once standing and positioned away from the body as to avoid impeding natural movement. 60

Figure 15: X-rays taken simultaneously of the right knee during a single trial. I. Image collected from the posterior-medial side of the knee. II. Image collected from the posterior and slightly lateral side of the knee. 66

Figure 16: DRRs and x-ray renderings. Top row images are of the femur, and bottom row images are of the tibia. Images on the left (I) and right (II) sides were collected simultaneously using two x-rays. 67

Figure 17: Final right knee rendering for a single subject. I. View is posterior to anterior. II. Color mapping indicates gap distance between the femoral condyles and tibial plateaus. Gap distance is less on the medial side than the lateral side. 69

Figure 18: Change in I. Overall tiredness and II. Legs tiredness; and change in discomfort in III. Hips, IV. Upper Legs, V. Knees, VI. Lower Legs, VII. Ankles, and VIII. Feet from 0 minutes over time. Each point represents the average normalized value across subjects. Error bars represent standard error of the mean. Each measurement increased significantly with time. Time points labeled with different letters are significantly different. 76

Figure 19: Total change in discomfort after 120 minutes of prolonged for all surveyed body segments. Changes in discomfort standing increased as distally across body segments. 77

Figure 20: Average measurement of (I) knee discomfort and (II) foot discomfort across all time points and subjects standing on a hard floor (HF) or anti-fatigue mat (MT). Error bars indicate standard error of the mean. Standing on the MT resulted in significantly decreased knees and feet discomfort than on the HF overall. Bars not connected by the same letters are significantly different. 77

Figure 21: Change in I. Overall Tiredness and II. Legs Tiredness; and discomfort in III. Hips, IV. Upper Legs, V. Knees, VI. Lower Legs, VII. Ankles, and VIII. Feet from 0 minutes across time, split into flooring groups. Each point represents the average normalized value across subjects. Error bars represent standard error of the mean. No

multiple comparisons between time points were performed, as the interaction effects did not indicate significant differences. 79

Figure 22: Change in I. Overall tiredness and II. Legs tiredness; and discomfort in III. Hips, IV. Upper Legs, V. Knees, VI. Lower Legs, VII. Ankles, and VIII. Feet from 0 minutes across time, split into BMI groups. Each point represents the average normalized value across subjects. Error bars represent standard error of the mean. No multiple comparisons between time points were performed, as the interaction effects did not indicate significant differences..... 80

Figure 23: Average overall tiredness ratings across all time points and subjects, split into flooring and BMI groups are displayed. Error bars indicate standard error of the mean. The introduction of the MT condition displays an opposite effect for the HW group versus the OB group. While the main interaction effect was significant, no significant post hoc multiple comparisons were made. 82

Figure 24: Overall tiredness ratings across subjects, split into flooring and BMI groups over time. Error bars indicate standard error of the mean. The interaction effect of time, flooring, and BMI group was not statistically significant. However, it seems that the MT condition begins to have an effect on overall tiredness after 30 minutes of standing. The MT condition tends to have an opposite effect on HW subjects versus OB subjects—decreasing overall tiredness for HW subjects and increasing overall tiredness for OB subjects. 82

Figure 25: Average feet discomfort ratings across all time points and subjects, split into flooring and BMI groups are displayed. Error bars indicate standard error of the mean. The presence of the MT condition had a significant effect on foot discomfort within the

OB group. This effect was not present within the HW group. Bars not connected by the same roman numerals are significantly different. 84

Figure 26: Feet discomfort ratings across subjects, split into flooring and BMI groups over time. Error bars indicate standard error of the mean. The interaction effect of time, flooring, and BMI group was not statistically significant. However, it seems that the MT condition begins to have an effect on feet discomfort for the OB group even by 30 minutes of standing. The MT condition does not seem to have the same effect on the HW group. 84

Figure 27: HW subject standing on a HF condition (S10). I. P_R data for two hours of standing. Movement amplitudes and frequencies seem to increase over time. II. CWS counted every five minutes over two hours of standing. The number of CWS over time tends to increase, with a maximum number of CWS occurring between 95 and 100 minutes (283 shifts). III. P_R between 95 and 97 minutes of standing. This subject continuously transferred weight between the right and left side. 86

Figure 28: OB subject standing on a HF condition (S21). I. P_R data for two hours of standing. Movement amplitudes and frequencies do not seem to increase over time. II. CWS counted every 5 minutes over two hours of standing. The number of CWS does not seem to increase over time. III. WWS counted every 5 minutes over two hours of standing. The number of WWS increases over time for this subject. 88

Figure 29: Selection of data from Figure 28. I. P_R over a 2 minute time period between 98 and 100 minutes of standing. Movements were recorded as CWS, but not as WWS. II. P_R over a 2 minute time period between 104 and 106 minutes of standing. This stepwise movement was registered as both a CWS and WWS. 89

Figure 30: I. Each line represents the average number of events counted within a single five minute block of time across all subjects. This was performed iteratively for boundary conditions ranging from 0.01 BW to 0.49 BW. II. Slope of each line was calculated and plotted. III. The plot in II is zoomed in. at about 0.13 BW is where the slopes start to approach 0. This is where the amplitude boundary condition was set. 91

Figure 31: Average number of movement events registered every five minutes throughout two hours of standing. Each bar represents a single method. Error bars are standard error of the mean. Bars labeled with different letters are significantly different. 93

Figure 32: Time was a significant factor for I. Change in shifts, II. Change in Fidgets, and III. Change in total events. Error bars are standard error of the mean. Asterisks (*) represent time points that are significantly different from 0. 95

Figure 33: Average number of I. fidgets and II. Total events performed every 5 minutes across all flooring conditions and time points, split into BMI group. Error bars are standard error of the mean. Bars labeled with different letters are significantly different. 96

Figure 34: The interaction effect of flooring condition and BMI group is a significant factor for changes in shifts. Bars are the average change in shifts across all subjects and time points, split between BMI group and flooring conditions. 97

Figure 35: The interaction effect of flooring condition and BMI group is a significant factor for the change in I. Shifts, II. Fidgets, and III. Total events. Points represent average values across all subjects and flooring conditions split into BMI groups. Error bars are standard error of the mean. Letters represent time points that were significantly different from 0. 98

Figure 36: MTFG of two typical subjects. I. S10 (HF condition) MTFG seems to decrease over two hours of standing. However, MTFG unexpectedly increases again after 30 minutes of standing. II. S05 (HF condition) MTFG does not display any discernable changes in MTFG over time. These unexpected trends warranted an investigation of sources of variance in data, as well as development of a piecewise model to fit and analyze the data..... 101

Figure 37: Flow charts describing how correlations for I. Flexion, II. Abduction, and III. External Rotation relate to changes in MTFG and cartilage compression. 105

Figure 38: MTFG versus flexion, abduction, and external rotation for two subjects. I. S05 knee flexion is positively correlated with MTFG. II. S10 knee flexion is not correlated with MTFG. III. S05 knee abduction is negatively correlated with MTFG. IV. S10 knee abduction is not correlated with MTFG. V. S05 knee external rotation is positively correlated with MTFG. VI. S10 knee external rotation is not correlated with MTFG. 106

Figure 39: A typical subject that did not converge. Subject (S20) is from the obese subgroup and this data was collected while standing on the hard floor condition. 108

Figure 40: MTFG collected during 120 minutes of standing and model MTFG for a typical HW subject on the I. HF and II. MT conditions. Points represent the raw data used to develop the model values, displayed with a line. A red square denotes the location of terminal gap (T_T,G_T)..... 111

Figure 41: MTFG collected during 120 minutes of standing and model MTFG for a typical OB subject on the I. HF and II. MT conditions. Points represent the raw data used to develop the model values, displayed with a line. A red square denotes the location of terminal gap (T_T,G_T)..... 112

Figure 42: I. MTFG at start G_0 is similar within HW and OB groups when standing on different mats. G_0 may be slightly increased for the OB group versus the HW group. II. G_T calculated by the piecewise model. There is no discernable difference between flooring or BMI groups. III. Terminal gap normalized to start (G_T/G_0) may be slightly increased on the MT versus the HF. In other words, MTFG compressed less on the MT versus the HF. IV. Time to terminal gap (T_T) did not change within the HW group between flooring conditions. However, T_T did increase on the MT versus the HF for the OB group. 114

Figure 43: Raw MTFG and proportion of bodyweight over the right leg overlaid for a single subject visit (S20, HF). As the number of events increase over time, MTFG variance increases and MTFG becomes more spread out. 117

Figure 44: TA MPF changed significantly with time. Data points represent the average MPF value measured across all subjects at that time point. Error bars represent the standard error of the mean. No TA MPF values were significantly different from TA MPF at 0 minutes. However, TA MPF at 30 minutes and 55 minutes were significantly different from one another (labeled A and B, respectively)..... 120

Figure 45: TA $RMS^{\%}$ changed significantly with flooring condition. I. Average TA $RMS^{\%}$ split into HF and MT groups. Bars with different letter labels are significantly different. Error bars represent standard error of the mean. II. The interaction effect of flooring with time was not a significant factor for TA $RMS^{\%}$. Differences between overall flooring conditions may be due to spikes in MT data occurring at 30, 70, and 80 minutes of standing. 121

Figure 46: Average GAS MPF over all time points and flooring conditions, split into BMI groups. OB GAS MPF was significantly lower than the HW group. Error bars represent standard error of the mean. 123

Figure 47: GAS MPF split into BMI groups over time. The interaction effect of time and BMI group was not statistically significant for GAS MPF. However, BMI group as an effect on its own was significant—and this graph displays the OB group's decreased GAS MPF throughout the duration of standing. 123

Figure 48: The interaction effect of flooring and BMI group was statistically significant for GAS MPF. GAS MPF was significantly less for the OB group than the HW group. The HW group on the MT condition was significantly less than on the HF condition. Alternatively, the OB group on the MT condition was significantly more than on the HF condition..... 124

Figure 49: I. Flooring was a significant factor for GAS RMS$^{\%}$. Bars represent average GAS RMS$^{\%}$ across all subjects and time points, split into HF and MT conditions. Bars labeled with different letters are significantly different. Error bars are standard error of the mean. II. Flooring with time is not a significant factors for GAS RMS$^{\%}$. The overall difference between HF and MT is observed throughout the time course, as HF GAS RMS$^{\%}$ is larger than MT GAS RMS$^{\%}$. 125

Figure 50: The interaction effect of flooring condition and BMI group was a significant factor for GAS RMS$^{\%}$. Bars represent GAS RMS$^{\%}$ averaged across all time points for each flooring condition and BMI group. Bars labeled with different letters are significantly different. Error bars are standard error of the mean. 126

Figure 51: SOL MPF changed significantly with flooring condition. I. SOL MPF, across all time points and BMI groups, split into flooring conditions. Bars not labeled with the same letter are significantly different. Error bars represent standard error the mean. II. SOL MPF averaged within each time point, split into flooring conditions. Throughout the course of standing, the MT condition displayed a higher level of SOL MPF. 128

Figure 52: Flooring was a significant factor for SOL RMS$^{\%}$. All SOL RMS$^{\%}$ values, averaged across subjects and time, split into flooring conditions. Bars labeled with different letters are significantly different. Error bars are standard error of the mean. Both the HF and MT condition increased from baseline. 129

Figure 53: SOL RMS$^{\%}$ changed significantly due to the interaction effect of flooring condition and BMI group. Bars represent average SOL RMS$^{\%}$ values across all time points, split into BMI group and flooring conditions. Bars not connected by the same letter are significantly different. Error bars are standard error of the mean. 130

Figure 54: Time was a significant factor for RF MPF. Points represent average RF MPF data across all subjects and flooring conditions. Error bars are standard error of the mean. Significant differences from 0 minutes of standing are denoted with asterisks (*) at 75 and 85 minutes of standing. 131

Figure 55: RF MPF changed significantly due to the interaction effect of flooring and BMI group. Bars represent average RF MPF values across all subjects, split into BMI group and flooring conditions. Bars labeled with different letters are significantly different. Error bars are standard error of the mean. 132

Figure 56: RF RMS$^{\%}$ changed significantly due to the interaction effect of flooring and BMI group. Bars represent the average percent change across all subjects and time points, split

into flooring and BMI groups. Error bars are standard error of the mean. RMS% changed significantly between flooring conditions within BMI group. 133

Figure 57: I. HAM MPF on the HF condition was significantly different than on the MT condition. Bars represent the average HAM MPF value averaged across all time points and subjects, split into flooring conditions. Error bars are standard error of the mean. Bars not connected by the same letter are significantly different. II. The time and flooring condition interaction effect was not a significant factor for HAM MPF. However, the difference seen in I. may have occurred as a result of slight increases in HAM MPF on the HF after 80 minutes of standing. 135

Figure 58: HAM MPF changed significantly with the interaction effect of flooring and BMI group. Bars labeled with the same letter are not significantly different. Error bars represent standard error of the mean. 136

Figure 59: I. Flooring was a significant factor for HAM RMS%. Bars are the average HAM RMS% value across all subjects and time points, split into flooring conditions. Bars connected by different letters are significantly different. Error bars are standard error of the mean. II. 137

Figure 60: Change in I. HbO, II. HHb, and III. HbT over time. All data points represent average Hb values across all subjects and both flooring conditions at that time point. Error bars represent standard error of the mean. Values that are significantly different from the first time point (0) are labeled with asterisks (*). 143

Figure 61: Change in flow over time. Points represent averages of all subjects standing on both flooring conditions every five minutes. Error bars represent standard error of the mean. Flow became significantly different from flow at time 0 by 35 minutes of standing,

and continued to remain significantly different from 0 for the remainder of the standing trial. Values that are significantly different from 0 are labeled with asterisks (*). 144

Figure 62: I. HbO, II. HbT, III. Flow, and IV. StO_2 changed significantly with flooring condition. SpO_2 did not change significantly, but was trending towards significance, so is included. Bars are average values across all subjects and all time points, split into flooring conditions. Bars are standard error of the mean. Bars labeled with different letters are significantly different. 146

Figure 63: The interaction effect of flooring condition and BMI group was significant for I. HbO, II. Flow, and III. StO_2. Each bar represents average values, across all time points, split into BMI group and flooring conditions. Bars labeled with different letters are significantly different. 147

Figure 64: Overall Tiredness over time (I) and between flooring conditions (II) and BMI groups (III). Error bars are standard error of the mean. 187

Figure 65: Overall Tiredness between BMI groups, split into flooring conditions (I), and over time, split between flooring conditions (II) and BMI groups (III). Error bars are standard error of the mean. 188

Figure 66: Overall Tiredness over time, split between BMI groups and flooring conditions. Error bars are standard error of the mean. 189

Figure 67: Legs Tiredness over time (I) and between flooring conditions (II) and BMI groups (III). Error bars are standard error of the mean. 190

Figure 68: Legs Tiredness between BMI groups, split into flooring conditions (I), and over time, split between flooring conditions (II) and BMI groups (III). Error bars are standard error of the mean. 191

Figure 69: Legs Tiredness over time, split between BMI groups and flooring conditions. Error bars are standard error of the mean. 192

Figure 70: Hips discomfort over time (I) and between flooring conditions (II) and BMI groups (III). Error bars are standard error of the mean. 193

Figure 71: Hips discomfort between BMI groups, split into flooring conditions (I), and over time, split between flooring conditions (II) and BMI groups (III). Error bars are standard error of the mean. 194

Figure 72: Hips discomfort over time, split between BMI groups and flooring conditions. Error bars are standard error of the mean. 195

Figure 73: Upper Legs over time (I) and between flooring conditions (II) and BMI groups (III). Error bars are standard error of the mean. 196

Figure 74: Upper Legs discomfort between BMI groups, split into flooring conditions (I), and over time, split between flooring conditions (II) and BMI groups (III). Error bars are standard error of the mean. 197

Figure 75: Upper Legs discomfort over time, split between BMI groups and flooring conditions. Error bars are standard error of the mean. 198

Figure 76: Knees over time (I) and between flooring conditions (II) and BMI groups (III). Error bars are standard error of the mean. 199

Figure 77: Knees discomfort between BMI groups, split into flooring conditions (I), and over time, split between flooring conditions (II) and BMI groups (III). Error bars are standard error of the mean. 200

Figure 78: Knees discomfort over time, split between BMI groups and flooring conditions. Error bars are standard error of the mean. 201

Figure 79: Lower Legs over time (I) and between flooring conditions (II) and BMI groups (III). Error bars are standard error of the mean. 202

Figure 80: Lower Legs discomfort between BMI groups, split into flooring conditions (I), and over time, split between flooring conditions (II) and BMI groups (III). Error bars are standard error of the mean. 203

Figure 81: Lower Legs discomfort over time, split between BMI groups and flooring conditions. Error bars are standard error of the mean. 204

Figure 82: Ankles discomfort over time (I) and between flooring conditions (II) and BMI groups (III). Error bars are standard error of the mean. 205

Figure 83: Ankles discomfort between BMI groups, split into flooring conditions (I), and over time, split between flooring conditions (II) and BMI groups (III). Error bars are standard error of the mean. 206

Figure 84: Ankles discomfort over time, split between BMI groups and flooring conditions. Error bars are standard error of the mean. 207

Figure 85: Feet discomfort over time (I) and between flooring conditions (II) and BMI groups (III). Error bars are standard error of the mean. 208

Figure 86: Feet discomfort between BMI groups, split into flooring conditions (I), and over time, split between flooring conditions (II) and BMI groups (III). Error bars are standard error of the mean. 209

Figure 87: Feet discomfort over time, split between BMI groups and flooring conditions. Error bars are standard error of the mean. 210

Figure 88: Comparison of COP (gold) and P_R (navy). Fz and COP are related and show similar curves. Differences between COP and P_R are due to, Fx, My, and the location of the feet. 212

Figure 89: Change in Shifts over time (I) and between flooring conditions (II) and BMI groups (III). Error bars are standard error of the mean. 213

Figure 90: Change in Shifts between BMI groups, split into flooring conditions (I), and over time, split between flooring conditions (II) and BMI groups (III). Error bars are standard error of the mean. 214

Figure 91: Change in Shifts over time, split between BMI groups and flooring conditions. Error bars are standard error of the mean. 215

Figure 92: Change in Fidgets over time (I) and between flooring conditions (II) and BMI groups (III). Error bars are standard error of the mean. 216

Figure 93: Change in Fidgets between BMI groups, split into flooring conditions (I), and over time, split between flooring conditions (II) and BMI groups (III). Error bars are standard error of the mean. 217

Figure 94: Change in Fidgets over time, split between BMI groups and flooring conditions. Error bars are standard error of the mean. 218

Figure 95: Change in Total Events over time (I) and between flooring conditions (II) and BMI groups (III). Error bars are standard error of the mean. 219

Figure 96: Change in Total Events between BMI groups, split into flooring conditions (I), and over time, split between flooring conditions (II) and BMI groups (III). Error bars are standard error of the mean. 220

Figure 97: Change in Total Events over time, split between BMI groups and flooring conditions. Error bars are standard error of the mean. 221

Figure 98: Subject S01 weight transfer events counted every five minutes during standing. I. Change in Shifts and II. Change in Fidgets on the HF condition. S01 force plate data on the MT condition was not included for analyses. 223

Figure 99: Subject S02 weight transfer events counted every five minutes during standing. I. Change in Shifts and II. Change in Fidgets on the MT condition. S02 did not complete the standing protocol, and therefore only MT data is available. 223

Figure 100: Subject S03 weight transfer events counted every five minutes during standing. I. Change in Shifts and II. Change in Fidgets on the HF condition. III. Change in Shifts and IV. Change in Fidgets on the MT condition. 224

Figure 101: Subject S04 weight transfer events counted every five minutes during standing. I. Change in Shifts and II. Change in Fidgets on the HF condition. III. Change in Shifts and IV. Change in Fidgets on the MT condition. 225

Figure 102: Subject S05 weight transfer events counted every five minutes during standing. I. Change in Shifts and II. Change in Fidgets on the HF condition. III. Change in Shifts and IV. Change in Fidgets on the MT condition. 226

Figure 103: Subject S06 weight transfer events counted every five minutes during standing. I. Change in Shifts and II. Change in Fidgets on the HF condition. III. Change in Shifts and IV. Change in Fidgets on the MT condition. 227

Figure 104: Subject S07 weight transfer events counted every five minutes during standing. I. Change in Shifts and II. Change in Fidgets on the HF condition. III. Change in Shifts and IV. Change in Fidgets on the MT condition. 228

Figure 105: Subject S10 weight transfer events counted every five minutes during standing. I. Change in Shifts and II. Change in Fidgets on the HF condition. III. Change in Shifts and IV. Change in Fidgets on the MT condition. 229

Figure 106: Subject S11 weight transfer events counted every five minutes during standing. I. Change in Shifts and II. Change in Fidgets on the HF condition. III. Change in Shifts and IV. Change in Fidgets on the MT condition. 230

Figure 107: Subject S12 weight transfer events counted every five minutes during standing. I. Change in Shifts and II. Change in Fidgets on the HF condition. III. Change in Shifts and IV. Change in Fidgets on the MT condition. 231

Figure 108: Subject S13 weight transfer events counted every five minutes during standing. I. Change in Shifts and II. Change in Fidgets on the HF condition. III. Change in Shifts and IV. Change in Fidgets on the MT condition. 232

Figure 109: Subject S14 weight transfer events counted every five minutes during standing. I. Change in Shifts and II. Change in Fidgets on the HF condition. III. Change in Shifts and IV. Change in Fidgets on the MT condition. 233

Figure 110: Subject S15 weight transfer events counted every five minutes during standing. I. Change in Shifts and II. Change in Fidgets on the HF condition. III. Change in Shifts and IV. Change in Fidgets on the MT condition. 234

Figure 111: Subject S16 weight transfer events counted every five minutes during standing. I. Change in Shifts and II. Change in Fidgets on the HF condition. III. Change in Shifts and IV. Change in Fidgets on the MT condition. 235

Figure 112: Subject S17 weight transfer events counted every five minutes during standing. I. Change in Shifts and II. Change in Fidgets on the HF condition. III. Change in Shifts and IV. Change in Fidgets on the MT condition. 236

Figure 113: Subject S19 weight transfer events counted every five minutes during standing. I. Change in Shifts and II. Change in Fidgets on the HF condition. III. Change in Shifts and IV. Change in Fidgets on the MT condition. 237

Figure 114: Subject S20 weight transfer events counted every five minutes during standing. I. Change in Shifts and II. Change in Fidgets on the HF condition. III. Change in Shifts and IV. Change in Fidgets on the MT condition. 238

Figure 115: Subject S21 weight transfer events counted every five minutes during standing. I. Change in Shifts and II. Change in Fidgets on the HF condition. III. Change in Shifts and IV. Change in Fidgets on the MT condition. 239

Figure 116: Subject S22 weight transfer events counted every five minutes during standing. I. Change in Shifts and II. Change in Fidgets on the HF condition. Data for the MT condition was not included in analyses. 240

Figure 117: Subject S23 weight transfer events counted every five minutes during standing. I. Change in Shifts and II. Change in Fidgets on the HF condition. III. Data for the MT condition was not included in analyses. 240

Figure 118: Subject S24 weight transfer events counted every five minutes during standing. I. Change in Shifts and II. Change in Fidgets on the HF condition. III. Change in Shifts and IV. Change in Fidgets on the MT condition. 241

Figure 119: Subject S25 weight transfer events counted every five minutes during standing. I. Change in Shifts and II. Change in Fidgets on the HF condition. III. Change in Shifts and IV. Change in Fidgets on the MT condition. 242

Figure 120: Subject S26 weight transfer events counted every five minutes during standing. I. Change in Shifts and II. Change in Fidgets on the HF condition. III. Change in Shifts and IV. Change in Fidgets on the MT condition. 243

Figure 121: Subject S27 weight transfer events counted every five minutes during standing. I. Change in Shifts and II. Change in Fidgets on the HF condition. III. Change in Shifts and IV. Change in Fidgets on the MT condition. 244

Figure 122: Subject S28 weight transfer events counted every five minutes during standing. I. Change in Shifts and II. Change in Fidgets on the HF condition. III. Change in Shifts and IV. Change in Fidgets on the MT condition. 245

Figure 123: Subject S29 weight transfer events counted every five minutes during standing. I. Change in Shifts and II. Change in Fidgets on the HF condition. III. Change in Shifts and IV. Change in Fidgets on the MT condition. 246

Figure 124: Subject S31 weight transfer events counted every five minutes during standing. I. Change in Shifts and II. Change in Fidgets on the HF condition. III. Change in Shifts and IV. Change in Fidgets on the MT condition. 247

Figure 125: Subject S32 weight transfer events counted every five minutes during standing. I. Change in Shifts and II. Change in Fidgets on the HF condition. Data for the MT condition was not included in analyses. 248

Figure 126: Average change in shifts (I) and change in fidgets (II) split into strategy groups. Error bars are standard error of the mean. 254

Figure 127: Scatter plot of fidgets versus shifts every five minutes for all subjects and visits. 255

Figure 128: Subject S01 MTFG and kinematics data for all collected trials. On the HF condition: Flexion (I), Abduction (III), and External Rotation (V). On the MT condition: Flexion (II), Abduction (IV), and External Rotation (VI)..... 257

Figure 129: Subject S03 MTFG and kinematics data for all collected trials. On the HF condition: Flexion (I), Abduction (III), and External Rotation (V). On the MT condition: Flexion (II), Abduction (IV), and External Rotation (VI)..... 258

Figure 130: Subject S04 MTFG and kinematics data for all collected trials. On the HF condition: Flexion (I), Abduction (III), and External Rotation (V). On the MT condition: Flexion (II), Abduction (IV), and External Rotation (VI)..... 259

Figure 131: Subject S05 MTFG and kinematics data for all collected trials. On the HF condition: Flexion (I), Abduction (III), and External Rotation (V). On the MT condition: Flexion (II), Abduction (IV), and External Rotation (VI)..... 260

Figure 132: Subject S06 MTFG and kinematics data for all collected trials. On the HF condition: Flexion (I), Abduction (III), and External Rotation (V). On the MT condition: Flexion (II), Abduction (IV), and External Rotation (VI)..... 261

Figure 133: Subject S07 MTFG and kinematics data for all collected trials. On the HF condition: Flexion (I), Abduction (III), and External Rotation (V). On the MT condition: Flexion (II), Abduction (IV), and External Rotation (VI)..... 262

Figure 134: Subject S10 MTFG and kinematics data for all collected trials. On the HF condition: Flexion (I), Abduction (III), and External Rotation (V). On the MT condition: Flexion (II), Abduction (IV), and External Rotation (VI)..... 263

Figure 135: Subject S12 MTFG and kinematics data for all collected trials. On the HF condition: Flexion (I), Abduction (III), and External Rotation (V). On the MT condition: Flexion (II), Abduction (IV), and External Rotation (VI)..... 264

Figure 136: Subject S13 MTFG and kinematics data for all collected trials. On the HF condition: Flexion (I), Abduction (III), and External Rotation (V). On the MT condition: Flexion (II), Abduction (IV), and External Rotation (VI)..... 265

Figure 137: Subject S14 MTFG and kinematics data for all collected trials. On the HF condition: Flexion (I), Abduction (III), and External Rotation (V). On the MT condition: Flexion (II), Abduction (IV), and External Rotation (VI)..... 266

Figure 138: Subject S15 MTFG and kinematics data for all collected trials. On the HF condition: Flexion (I), Abduction (III), and External Rotation (V). On the MT condition: Flexion (II), Abduction (IV), and External Rotation (VI)..... 267

Figure 139: Subject S16 MTFG and kinematics data for all collected trials. On the HF condition: Flexion (I), Abduction (III), and External Rotation (V). On the MT condition: Flexion (II), Abduction (IV), and External Rotation (VI)..... 268

Figure 140: Subject S17 MTFG and kinematics data for all collected trials. On the HF condition: Flexion (I), Abduction (III), and External Rotation (V). On the MT condition: Flexion (II), Abduction (IV), and External Rotation (VI)..... 269

Figure 141: Subject S19 MTFG and kinematics data for all collected trials. On the MT condition: Flexion (I), Abduction (II), and External Rotation (III). No HF data is displayed, as the subject did not complete the HF visit..... 270

Figure 142: Subject S20 MTFG and kinematics data for all collected trials. On the HF condition: Flexion (I), Abduction (III), and External Rotation (V). On the MT condition: Flexion (II), Abduction (IV), and External Rotation (VI)..... 271

Figure 143: Subject S21 MTFG and kinematics data for all collected trials. On the HF condition: Flexion (I), Abduction (III), and External Rotation (V). On the MT condition: Flexion (II), Abduction (IV), and External Rotation (VI)..... 272

Figure 144: Subject S22 MTFG and kinematics data for all collected trials. On the HF condition: Flexion (I), Abduction (III), and External Rotation (V). On the MT condition: Flexion (II), Abduction (IV), and External Rotation (VI)..... 273

Figure 145: Subject S23 MTFG and kinematics data for all collected trials. On the HF condition: Flexion (I), Abduction (III), and External Rotation (V). On the MT condition: Flexion (II), Abduction (IV), and External Rotation (VI)..... 274

Figure 146: Subject S24 MTFG and kinematics data for all collected trials. On the HF condition: Flexion (I), Abduction (III), and External Rotation (V). On the MT condition: Flexion (II), Abduction (IV), and External Rotation (VI)..... 275

Figure 147: Subject S25 MTFG and kinematics data for all collected trials. On the HF condition: Flexion (I), Abduction (III), and External Rotation (V). On the MT condition: Flexion (II), Abduction (IV), and External Rotation (VI)..... 276

Figure 148: Subject S26 MTFG and kinematics data for all collected trials. On the HF condition: Flexion (I), Abduction (III), and External Rotation (V). On the MT condition: Flexion (II), Abduction (IV), and External Rotation (VI)..... 277

Figure 149: Subject S27 MTFG and kinematics data for all collected trials. On the HF condition: Flexion (I), Abduction (III), and External Rotation (V). On the MT condition: Flexion (II), Abduction (IV), and External Rotation (VI)..... 278

Figure 150: Subject S28 MTFG and kinematics data for all collected trials. On the HF condition: Flexion (I), Abduction (III), and External Rotation (V). On the MT condition: Flexion (II), Abduction (IV), and External Rotation (VI)..... 279

Figure 151: Subject S29 MTFG and kinematics data for all collected trials. On the HF condition: Flexion (I), Abduction (III), and External Rotation (V). On the MT condition: Flexion (II), Abduction (IV), and External Rotation (VI)..... 280

Figure 152: Subject S31 MTFG and kinematics data for all collected trials. On the HF condition: Flexion (I), Abduction (III), and External Rotation (V). On the MT condition: Flexion (II), Abduction (IV), and External Rotation (VI)..... 281

Figure 153: Subject S32 MTFG and kinematics data for all collected trials. On the HF condition: Flexion (I), Abduction (III), and External Rotation (V). On the MT condition: Flexion (II), Abduction (IV), and External Rotation (VI)..... 282

Figure 154: Tibialis Anterior MPF over time (I) and between flooring conditions (II) and BMI groups (III). Error bars are standard error of the mean. 286

Figure 155: Tibialis Anterior MPF between BMI groups, split into flooring conditions (I), and over time, split between flooring conditions (II) and BMI groups (III). Error bars are standard error of the mean. 287

Figure 156: Tibialis Anterior MPF over time, split between BMI groups and flooring conditions. Error bars are standard error of the mean. 288

Figure 157: Tibialis Anterior RMS over time (I) and between flooring conditions (II) and BMI groups (III). Error bars are standard error of the mean. 289

Figure 158: Tibialis Anterior RMS between BMI groups, split into flooring conditions (I), and over time, split between flooring conditions (II) and BMI groups (III). Error bars are standard error of the mean. 290

Figure 159: Tibialis Anterior RMS over time, split between BMI groups and flooring conditions. Error bars are standard error of the mean. 291

Figure 160: Gastrocnemius MPF over time (I) and between flooring conditions (II) and BMI groups (III). Error bars are standard error of the mean. 292

Figure 161: Gastrocnemius MPF between BMI groups, split into flooring conditions (I), and over time, split between flooring conditions (II) and BMI groups (III). Error bars are standard error of the mean. 293

Figure 162: Gastrocnemius MPF over time, split between BMI groups and flooring conditions. Error bars are standard error of the mean. 294

Figure 163: Gastrocnemius RMS over time (I) and between flooring conditions (II) and BMI groups (III). Error bars are standard error of the mean. 295

Figure 164: Gastrocnemius RMS between BMI groups, split into flooring conditions (I), and over time, split between flooring conditions (II) and BMI groups (III). Error bars are standard error of the mean. 296

Figure 165: Gastrocnemius RMS over time, split between BMI groups and flooring conditions. Error bars are standard error of the mean. 297

Figure 166: Soleus MPF over time (I) and between flooring conditions (II) and BMI groups (III). Error bars are standard error of the mean. 298

Figure 167: Soleus MPF between BMI groups, split into flooring conditions (I), and over time, split between flooring conditions (II) and BMI groups (III). Error bars are standard error of the mean. 299

Figure 168: Soleus MPF over time, split between BMI groups and flooring conditions. Error bars are standard error of the mean. 300

Figure 169: Soleus RMS over time (I) and between flooring conditions (II) and BMI groups (III). Error bars are standard error of the mean. 301

Figure 170: Soleus RMS between BMI groups, split into flooring conditions (I), and over time, split between flooring conditions (II) and BMI groups (III). Error bars are standard error of the mean. 302

Figure 171: Soleus RMS over time, split between BMI groups and flooring conditions. Error bars are standard error of the mean. 303

Figure 172: Rectus Femoris MPF over time (I) and between flooring conditions (II) and BMI groups (III). Error bars are standard error of the mean. 304

Figure 173: Rectus Femoris MPF between BMI groups, split into flooring conditions (I), and over time, split between flooring conditions (II) and BMI groups (III). Error bars are standard error of the mean. 305

Figure 174: Rectus Femoris MPF over time, split between BMI groups and flooring conditions. Error bars are standard error of the mean. 306

Figure 175: Rectus Femoris RMS over time (I) and between flooring conditions (II) and BMI groups (III). Error bars are standard error of the mean. 307

Figure 176: Rectus Femoris RMS between BMI groups, split into flooring conditions (I), and over time, split between flooring conditions (II) and BMI groups (III). Error bars are standard error of the mean. 308

Figure 177: Rectus Femoris RMS over time, split between BMI groups and flooring conditions. Error bars are standard error of the mean. 309

Figure 178: Hamstring MPF over time (I) and between flooring conditions (II) and BMI groups (III). Error bars are standard error of the mean. 310

Figure 179: Hamstring MPF between BMI groups, split into flooring conditions (I), and over time, split between flooring conditions (II) and BMI groups (III). Error bars are standard error of the mean. 311

Figure 180: Hamstring MPF over time, split between BMI groups and flooring conditions. Error bars are standard error of the mean. 312

Figure 181: Hamstring RMS over time (I) and between flooring conditions (II) and BMI groups (III). Error bars are standard error of the mean. 313

Figure 182: Hamstring RMS between BMI groups, split into flooring conditions (I), and over time, split between flooring conditions (II) and BMI groups (III). Error bars are standard error of the mean. 314

Figure 183: Hamstring RMS over time, split between BMI groups and flooring conditions. Error bars are standard error of the mean. 315

Figure 184: Change in HbO over time (I) and between flooring conditions (II) and BMI groups (III). Error bars are standard error of the mean. 317

Figure 185: I. Change in HbO split into BMI group and flooring condition and II. Change in HbO split into BMI group and flooring condition displayed over time. Error bars are standard error of the mean. 318

Figure 186: I. Change in HbO split into HF and MT flooring conditions and plotted over time. Error bars are standard error of the mean. II. Tukey HSD t statistic comparing mean change in HbO between flooring conditions at each five minute time interval. ... 319

Figure 187: I. Change in HbO split into BMI groups and plotted over time. Error bars are standard error of the mean. II. Tukey HSD t statistic comparing mean change in HbO between BMI groups at each five minute time interval..... 320

Figure 188: Change in HHb over time (I) and between flooring conditions (II) and BMI groups (III). Error bars are standard error of the mean. 321

Figure 189: I. Change in HHb split into BMI group and flooring condition and II. Change in HHb split into BMI group and flooring condition displayed over time. Error bars are standard error of the mean. 322

Figure 190: I. Change in HHb split into HF and MT flooring conditions and plotted over time. Error bars are standard error of the mean. II. Tukey HSD t statistic comparing mean change in HHb between flooring conditions at each five minute time interval. ... 323

Figure 191: Change in HHb split into BMI groups and plotted over time. Error bars are standard error of the mean. II. Tukey HSD t statistic comparing mean change in HHb between BMI groups at each five minute time interval..... 324

Figure 192: Change in HbT over time (I) and between flooring conditions (II) and BMI groups (III). Error bars are standard error of the mean. 325

Figure 193: I. Change in HbT split into BMI group and flooring condition and II. Change in HbT split into BMI group and flooring condition displayed over time. Error bars are standard error of the mean. 326

Figure 194: I. Change in HbT split into HF and MT flooring conditions and plotted over time. Error bars are standard error of the mean. II. Tukey HSD t statistic comparing mean change in HbT between flooring conditions at each five minute time interval..... 327

Figure 195: I. Change in HbT split into BMI groups and plotted over time. Error bars are standard error of the mean. II. Tukey HSD t statistic comparing mean change in HbT between BMI groups at each five minute time interval..... 328

Figure 196: Change in Flow (%) over time (I) and between flooring conditions (II) and BMI groups (III). Error bars are standard error of the mean. 329

Figure 197: I. Change in Flow split into BMI group and flooring condition and II. Change in Flow split into BMI group and flooring condition displayed over time. Error bars are standard error of the mean. 330

Figure 198: I. Change in Flow split into HF and MT flooring conditions and plotted over time. Error bars are standard error of the mean. II. Tukey HSD t statistic comparing mean change in Flow between flooring conditions at each five minute time interval. ... 331

Figure 199: I. Change in Flow split into BMI groups and plotted over time. Error bars are standard error of the mean. II. Tukey HSD t statistic comparing mean change in Flow between BMI groups at each five minute time interval..... 332

Figure 200: Change in StO_2 (%) over time (I) and between flooring conditions (II) and BMI groups (III). Error bars are standard error of the mean. 333

Figure 201: I. Change in StO_2 split into BMI group and flooring condition and II. Change in StO_2 split into BMI group and flooring condition displayed over time. Error bars are standard error of the mean. 334

Figure 202: I. Change in StO_2 split into HF and MT flooring conditions and plotted over time. Error bars are standard error of the mean. II. Tukey HSD t statistic comparing mean change in StO_2 between flooring conditions at each five minute time interval..... 335

Figure 203: I. Change in StO_2 split into BMI groups and plotted over time. Error bars are standard error of the mean. II. Tukey HSD t statistic comparing mean change in StO_2 between BMI groups at each five minute time interval..... 336

Figure 204: Change in StO_2 (%) over time (I) and between flooring conditions (II) and BMI groups (III). Error bars are standard error of the mean. 337

Figure 205: I. Change in SpO_2 split into BMI group and flooring condition and II. Change in SpO_2 split into BMI group and flooring condition displayed over time. Error bars are standard error of the mean. 338

Figure 206: I. Change in SpO_2 split into HF and MT flooring conditions and plotted over time. Error bars are standard error of the mean. II. Tukey HSD t statistic comparing mean change in SpO_2 between flooring conditions at each five minute time interval.... 339

Figure 207: I. Change in SpO_2 split into BMI groups and plotted over time. Error bars are standard error of the mean. II. Tukey HSD t statistic comparing mean change in SpO_2 between BMI groups at each five minute time interval..... 340

Acknowledgements

First and foremost, I would like to express my deepest appreciation to my advisor—April Chambers—and my committee members (Bill Anderst, Ted Huppert, Subashan Perera, Mark Redfern, and Scott Tashman) for their expertise, guidance, and support. I must also thank the Bioengineering Department for providing financial assistance to complete my degree. I am extremely grateful to those at the Human Movement and Balance Laboratory and the Orthopaedic Biodynamics Laboratory—especially Jenna Trout, Tom Gale, and Alex Maxim—whose help cannot be overestimated. Thank you to my friends in BMES and EGSO, who added some color to the fabric of my graduate school experience. In a special way, I wish to acknowledge the support and love of my friends and family—especially my Dad, Jim Wiltman, and my fiancé, Adam Joslin. Completion of this project would not have been possible without you.

1.0 Specific Aims

Previous research has established that prolonged standing is an occupational hazard leading to leg swelling, muscle fatigue, and joint compression in the lower extremities [1-11]. Repeated exposure to prolonged standing in the workplace is linked to a multitude of serious chronic diseases, including osteoarthritis, chronic venous insufficiency, carotid arteriosclerosis, varicose veins, increased blood pressure, and complications with pregnancy [10]. Despite the clear health risks associated with prolonged standing, the Bureau of Labor Statistics reports that workers in the United States spend on average 61% of the workday standing or walking—with retail salespersons, welders, waiters/waitresses, electricians, and pharmacists topping the list [12]. These select five occupations consist of nearly 9 million people spending over 75% of their workday standing [12].

Prior studies consistently find that musculoskeletal discomfort in the lower extremities is frequently associated with prolonged standing and identified as a risk factor in the development of pathologies (listed above) [2, 10]. Unfortunately, existing objective measures of body movements and the musculoskeletal system show varied results [1-11]. Studies consistently measure increases in discomfort and tiredness, blood pooling, weight transfers, and muscle fatigue over time [2-8]. However, comparing across ergonomic interventions and demographics lead to inconsistent results [1-11]. Many studies find no significant differences between standing interventions and controls [1-7, 11]. It is speculated that the lack of significant differences may be due to current measurement methods. Current methods are subjective or indirectly measure physiological outcomes of prolonged standing. As such, the underlying mechanisms of musculoskeletal discomfort and diseases remain unclear. The specific objective of this study is to introduce methodology and analysis novel to prolonged standing research to obtain new objective measures

of joint and muscle responses during standing. These measures include (1) weight transfer strategies used during prolonged standing, (2) cartilage deformation at the knee joint using a dynamic stereo x-ray system (DSX), and (3) blood volume and muscle oxygenation in the lower extremity muscles using near infrared spectroscopy (NIRS). This is motivated by a lack of consistent objective measures in the literature, with the intention of introducing methods that discern the underlying mechanisms of discomfort and injury. The long-term goal of this study is to better understand the physiological effects of prolonged standing to prevent musculoskeletal discomfort and injury in the workplace.

Specific Aim 1: To identify relationships among weight transfer strategies, psychophysical measure of discomfort and tiredness, and physiological changes during prolonged standing.

H1.1: Weight transfer strategies will vary based on temporal characteristics and amount of body weight that each leg is exposed to as a result of shifts and fidgets.

H1.2: Psychophysical measures of joint and muscle pain and discomfort will be correlated with differences in weight transfer strategies.

H1.3: Weight transfer strategies will be related to physiological changes in lower extremity joints and muscles reported in SA 2 and SA 3.

Specific Aim 2: To identify relationships between in vivo knee joint cartilage deformation, discomfort and tiredness, BMI group, and standing surface during prolonged standing.

H2.1: Articular cartilage deformation within the knee joint will increase over time during prolonged standing.

H2.2: Psychophysical measures of joint pain and discomfort will be correlated with changes in articular cartilage deformation.

H2.3: Effects of prolonged standing on articular cartilage deformation at the knee joint (H2.1) will be greater in obese individuals.

H2.4 Effects of prolonged standing on articular cartilage deformation at the knee joint (H2.1) will be less when using an anti-fatigue mat.

Specific Aim 3: To identify relationships between lower extremity muscles characteristics, discomfort and tiredness, BMI group, and standing surface during prolonged standing.

H3.1: Muscle oxygenation and oxy-hemoglobin levels of lower extremity muscles will decrease with time during prolonged standing, while blood volume will increase as measured with near-infrared spectroscopy. This finding will be correlated with muscle fatigue, as measured by electromyography.

H3.2: Psychophysical measures of muscle pain and discomfort will be correlated with changes in the physiological variables of the lower extremity muscles stated in H3.1.

H3.3 Physiological variables of the lower extremity muscles stated in H3.1 will be negatively affected by obesity.

H3.4 Physiological variables of the lower extremity muscles stated in H3.1 will be positively impacted by the use of an anti-fatigue mat.

2.0 Background and Significance

2.1 Epidemiology and Clinical Significance

Workers in the United States spend on average 61%—approximately 5 hours—of their workday standing [12]. Figure 1 displays the percent of workday standing over a collection of occupations. Many common occupations, such as waiters and waitresses, hairdressers, retail salespersons, and nurses are on their feet throughout the workday [10, 13, 14]. In some cases, workers are only afforded a 15 minute break after 4.5 hours of work—as mandated by the United States Department of Labor [15]. Despite its prevalence, prolonged standing has been identified as an occupational risk factor leading to increased chronic pathologies and accompanying medical costs, along with decreased productivity [10, 14]. Some of these chronic pathologies include osteoarthritis, chronic venous insufficiency, carotid atherosclerosis, varicose veins, increased blood pressure, and complications with pregnancy [10].

Epidemiological studies investigating the relationship between prolonged standing or walking and general musculoskeletal symptoms among various occupational settings have been performed [16-21]. Many of these studies only investigated "musculoskeletal discomfort" or general pathologies, not specific prognoses [16-21]. Over 500 supermarket checkout workers were evaluated for the presence of musculoskeletal symptoms [16]. A positive significant relationship was found between standing time and lower limb and foot symptoms [16]. Checkout workers, who spent 90% of their workday standing, showed the highest prevalence of lower limb musculoskeletal symptoms [16]. A cross-sectional study of assembly plant workers in Michigan reported that a 10% increase in time walking or sidestepping led to a 20% increased risk of

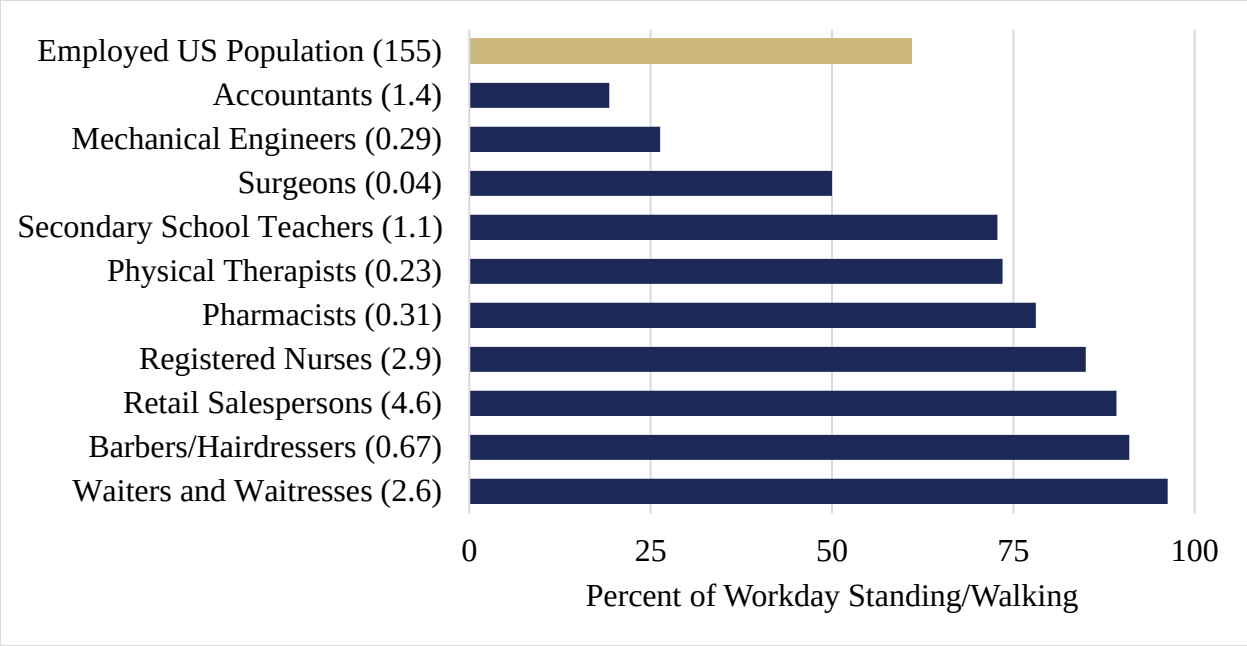

Figure 1: Percent of the workday standing or walking by selected occupations. Number of people employed in each occupation is denoted in parentheses (in millions) [10, 13, 14].

presenting with a foot or ankle disorder [17]. A review of over 10,000 studies across the world published between 1994 and 2014 indicated that the likelihood of nurses developing lower extremity musculoskeletal disorders is heavily associated with static posture and prolonged standing, among other factors [18]. A study of Egyptian female hairdressers indicated that back and knee pain were the most frequently reported chronic pain, in comparison with office workers [19]. A proportionality test revealed that hairdressers reported significantly more leg and foot pain throughout the workday than office workers [19]. Furthermore, there was a significant association between prolonged standing and leg and foot pain and knee pain [19]. A self-report study of nearly 300 Nigerian hairdressers indicated a significant association between hours working in a standing position and the prevalence of musculoskeletal disorders [20]. Gradual onset of a musculoskeletal disorder was reported by 91.3% of Nigerian hairdressers [20]. Bodily pain was reported in the

hips/thighs (16.6%), knees (32.8%), and ankles/feet (23.7%), among other locations [20]. Over 25% of those who reported musculoskeletal pain indicated that symptoms had a negative effect on their efficiency and job performance [20].

Primary knee joint disorders associated with prolonged standing are osteoarthritis (OA) and meniscal injury [22]. Healthy synovial joints are protected by layers of cartilage that provides a smooth, gliding surface for movement [23]. OA is characterized by a breakdown of cartilage over time resulting in joint pain due to increased friction between joints [23]. Development of OA is broadly associated with fixed and modifiable risk factors [24]. One such modifiable risk factor is occupation—especially those occupations that require continued compressive load on the lower extremities [23, 24]. A 12 year follow up study investigating prognostic factors of cartilage loss in OA of the knee determined that cartilage loss was associated with occupations requiring prolonged standing [25]. It was speculated that a lack of cyclic loading and cartilage rehydration during prolonged standing may lead to cartilage loss over time [25]. Over 200 employees from a large Finnish forestry company were evaluated on the basis of knee pain, development of OA, and occupational activities [26]. According to this study, the likelihood of the development of knee pain increased for those who worked in a kneeling or standing position with a forward flexed trunk [26]. A study of nearly 3,000 English men indicated that those who stand or walk for over 2 hours per day are at increased risk of meniscal injury [27].

Cardiovascular pathologies related to prolonged standing have been established. Studies investigated whether or not prolonged standing at work leads to excess risk of phlebopathy such as varicose veins and chronic venous insufficiency [28, 29]. Healthy veins transport blood from the body's tissues to the heart with the help of one-way valves that aid in blood flow [30]. The development of phlebopathies occurs when veins are damaged and cannot adequately pump blood

back towards the heart [30]. A three year prospective study of 1.6 million Danish adults determined that working in a standing position was associated with increased risk of hospitalization due to varicose vein development [28]. The risk ratio for the development of varicose veins was 1.85 and 2.63 for men and women, respectively [28]. A comparison of 336 male industrial workers (prolonged standing working condition), office workers (seated working condition), and stoneworkers (intermediary group) indicated that the prevalence of pathologies that significantly hinder venous functionalities are more likely to develop for industrial workers than office workers or stoneworkers [30]. More specifically, those in the study who stood for over half of the workday were more likely to develop major venous pathologies [30]. A Dutch study investigating diurnal changes in leg volume within a standing profession found a significant change in lower leg volume for those without chronic venous insufficiency (CVI), indicating that those with CVI may have been predisposed to the disease in some way [31]. Pathologies affecting arterial structures, including carotid atherosclerosis, have likewise been related to prolonged standing at work [32]. Arterial structures degrade or are damaged as a result of disturbed, turbulent flow of blood through the arterial system [32]. Within the scope of prolonged standing, turbulent flow occurs as a result of increased heart rate, changes in pulse pressure, and humoral responses [32]. Turbulent arterial blood flow has been linked to endothelial cell injury and atherosclerosis [32]. The development of atherosclerosis is measured through carotid intima media thickness measurements, in which increases in thickness indicate increased risk for development of carotid atherosclerosis [32]. The progression of carotid intima media thickness increased as standing time at work increased, indicating increased risk for carotid atherosclerosis [32].

Costs related to prolonged standing manifest in various forms, including costs due to sick leave, lost productivity, decreased job satisfaction, and direct medical costs. Out of all workplace

related injuries reported in the United States in 2017, approximately 24% (262,660) were due to lower extremity injuries [33]. Each workplace related lower extremity injury leads to a median 12 days of leave [34]. Decreased job satisfaction has been reported by assembly workers who developed foot or ankle disorders [17]. A study comparing productivity and cognitive effects of prolonged standing during office work measured attention, problem solving, and mental state over time standing. Reaction times became significantly slower over time standing [21]. Decreased reaction times may be especially concerning within professions that require the use of heavy machinery or dangerous tools [21]. While no "lifetime medical cost" of prolonged standing has been calculated, medical costs of the aforementioned injuries and diseases have been reported. The following individual costs reported are calculated using data collected from various sources and injury, disorder, or disease origins. The lifetime individual cost of osteoarthritis is approximately $140,300 per person [23, 35]. Venous disorders (chronic venous insufficiency and varicose veins) are commonly treated using laser ablation, a treatment that accrues a lifetime cost of approximately $30,000 [36]. The Journal of the American Heart Association cited that those with high blood pressure (hypertension) face increased medical costs of $2,000 per year compared with their normal blood pressure counterparts [37].

2.2 Background

The definition for "prolonged standing" varies between studies depending on the scope, application, and field of study [14, 30]. Standing for four hours has been loosely defined as "prolonged" based on circulatory changes and implications [14, 30]. A study investigating onset of fatigue using EMG measurements indicate that muscular fatiguing due to prolonged standing may occur in as little as 20 minutes [2]. In orthopedic knee joint imaging, ten minutes of maintained stance has been considered "prolonged standing" [38]. The scope of this dissertation considers any studies to be "prolonged standing" if subjects maintain bipedal stance for enough time to illicit a psychophysical or physiological response.

It has been hypothesized that the aforementioned chronic diseases are related to repeated exposure to lower extremity blood pooling, muscle fatigue, and joint compression that occurs during prolonged standing in the workplace [10, 14]. Prior literature has measured psychophysical and physiological outcomes of prolonged standing using various subjective and objective measurement methods [1-11, 39-46]. Subjective measures are generally self-reported and include measures of discomfort, fatigue, unpleasantness, or mental state [1, 3-6, 9, 11, 21, 39, 41-43, 46]. Objective measures primarily focus on muscular and circulatory characteristics over time—including electromyography (EMG) [1, 6, 43], leg volume or circumference [1, 3, 5, 6, 42, 43], leg temperature [1, 3, 6], and near-infrared spectroscopy (NIRS) [42, 43]. Standing movements—including weight fidgets, shifts, transfers, and center of pressure excursions—are also quantified, and are speculated to indicate physiological responses to discomfort [1, 6, 11, 42-44].

2.2.1 Psychophysical Measures of Prolonged Standing

Psychophysiology investigates the cognitive processing of physiological activity [47]. A commonly utilized psychophysical measure during prolonged standing is a subjective survey of discomfort, fatigue, or unpleasantness [1, 3-6, 9, 11, 21, 39, 41-43, 46]. Surveys are useful tools for studying detrimental effects of prolonged standing because they are a low-cost option that can be utilized in both laboratory and field study settings [14]. The effects of time, environmental factors, and human factors on psychophysical outcomes of standing have been measured by surveys [14]. While there is consensus among researchers that negative psychophysical outcomes do increase over time, psychophysical measurement definitions, total standing duration, and collection frequency vary between studies [1, 3-6, 9-11, 21, 39, 41-43, 46]. The rate at which psychophysical outcomes increase with time, and the manner in which standing interventions or anthropometry affect this increase, is difficult to compare across studies [10]. Effects of time are considered in this section while interventions and anthropometry factors are discussed in sections 2.3 and 2.4, respectively. A collection of studies published between 1995 and 2018 that utilized subjective psychophysical measurements as dependent variables are listed in Table 1. Primary measurement methods include visual analog scales [3, 6, 11, 21, 39, 42], CR-10 Borg discomfort scale [1, 9, 43], body part discomfort scales [11, 41], various Likert scales [4, 5], and study-specific scales [46]. The scales themselves may be matched with various body diagrams or questionnaires [1, 3-6, 9, 11, 21, 39, 41-43, 46]. Cross validation studies indicated that these various scales and questionnaires display similar results [48]. Due to the similarity in subjective survey results across studies, the term “discomfort” will be used to describe results obtained from subjective, psychophysical surveys.

Table 1: A collection of studies investigating the effects of various independent variables on subjective discomfort, fatigue, or unpleasantness.

Significance (T, time; C, cycles; R, rest; SS, standing surface; S, shoe type; I, insoles) is denoted in superscript next to measurement locations.

First Author *Year*	Study Type	Testing Duration	Frequency	Independent Variables	Measurement Locations
Baker, R [21] *2018*	Lab	2 hours	Every 30 min	Time	Hips/thighs/buttocks ^{T}, Knees ^{T}, Ankles/feet ^{T}
Garcia, M-G [42] *2015*	Lab	5 hours	0, 180, 300 min and 60 min post-work	Time, Cycle type, Rest type	Upper legs/hips $^{T, CxT}$, Knees ^{T}, Lower legs ^{T}, Ankles $^{T, RxT}$, Feet ^{T}
Brownie, J [39] *2015*	Lab	5 hours	Every 150 min	Time, Standing surface, Age	Buttocks ^{T}, Upper legs ^{T}, Knees ^{T}, Lower legs ^{T}, Feet $^{T, SS}$
Haney, J [43] *2015*	Lab	6 hours	Every 30 min	Time, Standing surface	Hips ^{T}, Upper legs ^{T}, Knees ^{T}, Lower legs ^{T}, Ankles ^{T}, Feet ^{T,SS}
Jefferson, JR [46] *2013*	Field	12 hours	End of shift	Insoles	Low back/buttocks ^{I}, Knees, Feet ^{I}
Wiggermann, N [11] *2013*	Lab	4 hours	0, 55, 110, 120, 175, 230 min	Standing surface	Overall body, Overall legs ^{SS}, Buttocks, Thighs, Knees, Lower legs ^{SS}, Feet ^{SS}
Lin, Y-H [5] *2012*	Lab	4 hours	55, 115, 175, 235 min	Time, Shoe type, Standing surface	Feet $^{T, S, SS, FxS}$
Drury, CG [41] *2008*	Field	40 min	40 min	Stool intervention	Combined lower extremity ^{SI}
King, PM [4] *2002*	Field	8 hours	End of shift	Insoles, Standing surface	General fatigue $^{SS, SSxI}$, Leg fatigue $^{SS, SSxI}$, Hips $^{SS, SSxI}$, Upper legs, Knees $^{SS, SSxI}$, Lower legs, Ankles, Feet $^{SS, SSxI}$
Cham, R [1] *2001*	Lab	4 hours	Every 60 min	Standing surface	Overall body ^{SS}, Overall legs ^{SS}, Hips ^{SS}, Upper legs ^{SS}, Lower legs ^{SS}, Knees ^{SS}, Ankles ^{SS}, Feet ^{SS}
Hansen, L [3] *1998*	Lab	2 hours	0, 30, 60, 115	Time, Shoe type, Standing surface	Legs ^{T}, Feet ^{T}
Madeleine, P [6] *1997*	Lab	2 hours	Every 15 min	Time, Standing surface	Overall unpleasantness $^{T, SS}$
Redfern, MS [9] *1995*	Field	8-10 hours	End of shift	Insole, Standing surface	General tiredness ^{SS}, Leg tiredness ^{SS} Hips ^{SS}, Upper legs ^{SS}, Knees ^{SS}, Lower legs ^{SS}, Ankles ^{SS}, Feet ^{SS}
Zhang, L [45] *1991*	Lab	2 hours	Every 15 min	Time, Standing surface, Shoe type	Frequency ^{T}, Severity ^{T}, Sum $^{T, TxS}$

The primary source of error inherent to discomfort surveys is likely due to response bias and demand characteristics [49]. Subjects may expect negative outcomes of standing to increase over time, so this may bias outcomes of the survey [49]. For this reason, the frequency of survey administration must be far enough apart to minimize response bias, but close enough to provide as many data points as possible [49]. While each study in Table 1 measuring the effects of time has indicated that discomfort and fatigue increase over time, the optimization of maximizing survey administration frequency and minimizing response bias has resulted in a range of survey administration frequencies [3, 5, 6, 21, 39, 42, 43, 45]. The frequency of survey administration during testing for studies measuring the impact of time on psychophysical outcomes range from 15 minutes [6, 45] to 3 hours [42], partitioning the total duration of standing into 3 [39, 42] to 13 [43] data points.

Standing duration in a laboratory setting has varied from 40 minutes [41] to 6 hours [43]. Alternatively, in a field study setting, standing duration was the length of a work shift [4, 9, 46]. Testing duration is generally dictated by the dependent variables of interest, such as standing time or interventions. Studies that have investigated the effect of time on psychophysical outcomes tended to test for at least two hours [3, 5, 6, 21, 39, 42, 43, 45]. It has been found that discomfort increases as early as 30 minutes after standing [10, 21, 43, 45].

Lower extremity measurement locations are displayed in Table 1. While some studies may have investigated the effects of standing on the back and upper body, only lower extremity locations are included for the purpose of this review. The part of the lower body most often surveyed are the feet [1, 3-5, 9, 11, 21, 39, 41-43, 45, 46]. Other frequent survey locations include buttocks, hips, upper legs/thighs, knees, lower legs, and ankles [1, 3-6, 9, 11, 21, 39, 41-43, 45, 46]. Some studies have also measured “overall” areas or created composite measurement locations

[1, 4, 6, 9, 11, 21, 41, 45, 46]. For example, Zhang et. al. measured the number of body parts that had discomfort (body part discomfort frequency), the mean of all non-zero discomfort ratings (body part discomfort severity), and an overall sum for ratings (sum of discomfort ratings) [45]. It has been shown that ratings of discomfort tend to decrease proximally in the lower extremities [9, 45]. In other words, the feet display the highest levels of discomfort, while the hips display the least over time [9, 45]. Discomfort located in muscle sites attributed to blood pooling and muscle fatigue have been measured, and authors posit that there may be a relationship between discomfort and these factors [3, 5, 6, 21, 39, 42, 43]. A single study compared discomfort areas representing joint structures (ankles, knees, and hips) and muscular sites (thigh, lower leg), and suggested that joint structures displayed increased discomfort in comparison to muscular sites during prolonged standing [4]. The relationship between joint discomfort and physiological outcomes during prolonged standing has only been speculated but never tested [11].

2.2.2 Measures of Weight Transfer Changes during Prolonged Standing

Behavioral responses to prolonged standing are primarily measured using weight transfer changes over time [1, 6, 11, 42-44]. During standing, a continuous effort is made by the neuromuscular system to maintain posture and balance [50]. It has also been speculated that weight transfers during standing are responses to joint or muscular discomfort [11]. Methods by which these movements are observed and measured are numerous. A description of theories related to upright stance, measurement methods, and consideration of findings related to weight transfer measures of prolonged standing are reviewed in this section.

Weight transfer changes over time are measured by observing changes in center of pressure (COP) or distribution of bodyweight over both feet [50]. In both instances, force plates—devices

that measure ground reaction forces and moments in vertical and shear directions—are used [50]. During standing, each foot applies forces to the force plate over a maintained contact surface area [50]. The force alone may be analyzed as a distribution of bodyweight [50]. The total force spread over the contact surface area is the COP [50, 51].

During prolonged standing, body movements are not only a corrective mechanism for stance but are also a behavioral response to discomfort during standing [1, 3, 6, 8, 11, 42-45]. This is especially true in the medial-lateral direction, in which weight is transferred from one foot to another [1, 3, 6, 8, 11, 42-45]. Weight transfer changes are used to describe behavioral changes as a result of time standing, interventions (standing surface, shoe types, work/rest cycles, etc.), or human factors (age, obesity, etc.). These changes are quantified by measuring changes in magnitude and temporal characteristics [1, 3, 6, 8, 11, 42-45]. A collection of studies investigating weight transfer changes over time standing are displayed in Table 2.

Studies included in Table 2 tested the effects of time standing, shoe type/footwear, standing surface, or age on weight transfer responses [1, 3, 6, 8, 11, 42-45]. The manner in which this was completed was through measuring COP [1, 3, 11, 42, 45] or the distribution of vertical force between both feet [8, 11, 43, 44]. Events were measured on the basis of reaching a magnitude threshold, temporal threshold, or both. Wiggermann and Keyserling measured a weight shift event if the distribution of vertical force between each foot transitioned between the following conditions: "(1) At least 20% of total body weight being supported by both the right and left foot, (2) >80% total body weight being supported by the right foot, or (3) >80% body weight being supported by the left foot" and the time spent in the condition was at least 7.5 seconds [11]. Unlike Wiggermann and Keyserling [11], Cham and Redfern measured a shift as a "change in lateral COP

Table 2: A collection of studies investigating the effects of various independent variables on weight transfer measures. ***Significance (T, time; SS, standing surface; SE, session) is denoted in superscript next to measurement locations.***

First Author *Year*	Testing Duration	Independent Variables	Weight transfer Measure	Dependent Variables
Rekant, J [44] *2019*	6 hours	Time	Fz	Shifting ^{T}, Fidgeting ^{T}
Garcia, M-G [42] *2018*	5 hours	Time Cycle type Rest type	COP	Speed ^{T}, Ellipse Area ^{T}
Haney, J [43] *2015*	6 hours	Time Flooring	Fz	Shifting ^{T}
Wiggermann, N [11] *2013*	4 hours	Time Standing surface Session	Fz COP	Shifting $^{T, SS, SE}$, Single Foot Stance ^{T}, Excursions $^{T, SS}$
Prado, J [8] *2011*	0.5 hours	Age	Fz	Weight Transfers ^{A}
Cham, R [1] *2001*	4 hours	Standing surface	COP	Shifting ^{SS}
Madeleine, P [6] *1997*	2 hours	Standing surface	COP	Displacement ^{SS}

beyond 10% of the total distance range seen for the trial" and there was no temporal requirement [1]. Prado et. al. used a moving magnitude threshold, which was dependent on the cumulative sum of the difference in proportion of bodyweight between both feet [8]. A weight transfer was measured when the cumulative sum reached user-defined thresholds, which included amplitude, event windows, and durations [8]. While time was not directly measured in this method, a drift parameter was included that allowed a subject to drift weight from one leg to another slowly without indicating a sharp weight transfer event [8]. A newer method for measuring weight transfer changes due to prolonged standing was published by Rekant et. al. [44]. This method was informed by methods published by Wiggermann and Keyserling [11], Cham and Redfern [1], and Prado et. al. [8] to measure how much weight was placed on the dominant leg over time, while

counting events (shifts and fidgets) in which transfers between each leg occurred [44]. Despite differences in methodologies, general trends have been observed between studies [1, 3, 6, 8, 11, 42-45]. Time standing is shown to be a predictor for weight transfer events [3, 11, 42-45]. Some studies correlated weight transfer events with changes in discomfort over time and between shoe type/footwear and standing surface [1, 43]. Cham and Redfern found significant correlations between COP weight shifts and overall fatigue, leg fatigue, hip discomfort, upper leg discomfort, and ankle discomfort [1]. Wiggermann and Keyserling found a weak positive correlation between weight shifting, percent time on single foot stance, and COP excursions and discomfort [11].

The manner in which people stand and the shape of their weight transfer curves over time have not been thoroughly investigated [44]. However, recent preliminary work by Rekant et. al. suggests that people may display different standing "strategies [44]." Figure 2 displays a representation of the data published by Rekant et. al. [44]. Figure 2, I displays a "primary shifter" while Figure 2, II displays a "primary fidgeter [44]." It has been speculated that fidgeting may be related to muscular discomfort, while shifting may be related to joint discomfort [11]. However, this direct relationship has not yet been tested. Whether standing strategies are inherent to the subject, a learned strategy, or change in association with varying levels of discomfort has not yet been determined [44].

I.

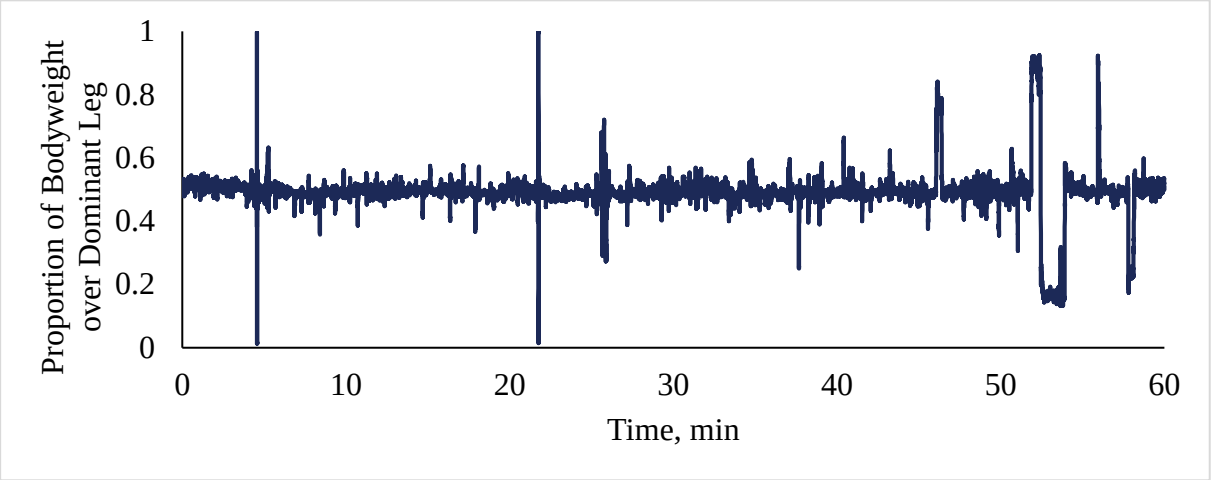

II.

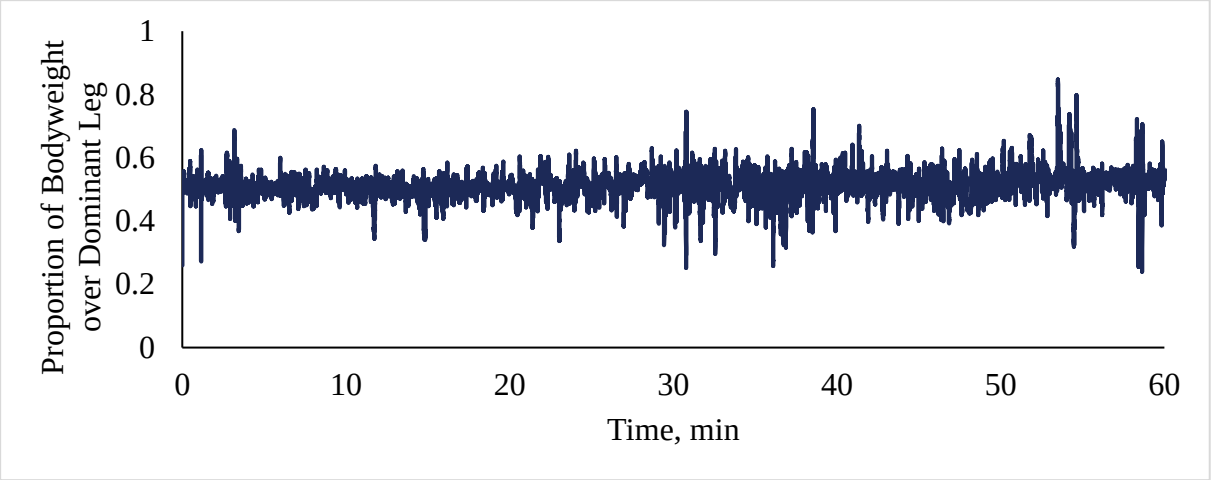

Figure 2: Recreation of data from Rekant et. al. [44]. I. Displays a primary shifter in which the subject transferred weight between legs at a lower frequency than II. the primary fidgeter. It is unknown if these two different "strategies" are a defense mechanism used by the body to mitigate discomfort, or if it is a response to discomfort.

2.2.3 Measures of Joints during Prolonged Standing

Articular cartilage is a thin (1-3 mm) viscoelastic connective tissue that provides a nearly frictionless surface in which compressive loads may be transmitted between bone articulations [52-54]. When a compressive load is applied to the knee (Figure 3), the load is transmitted through the bones towards the joint cavity [53]. The subchondral cortex provides a connection point between articular cartilage and cancellous bone [53]. The load is withstood by articular cartilage and dispersed with the help of the meniscus [53].

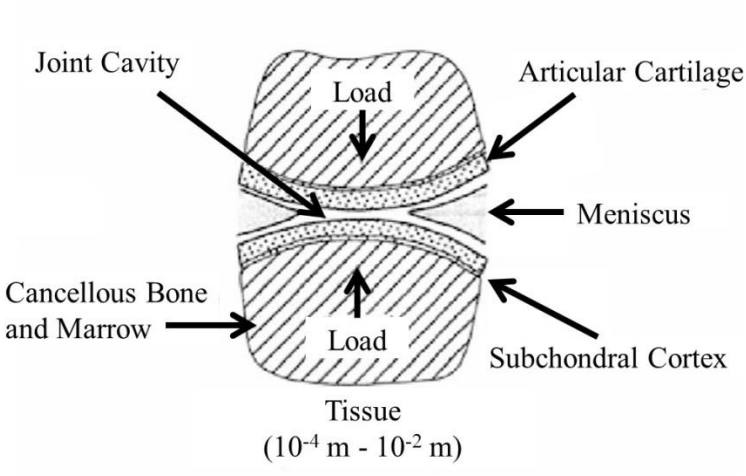

Figure 3: Schematic of the knee joint capsule. Adapted from Mow and Huiskes [53].

The manner in which compressive load is withstood by articular cartilage has been investigated using various forms of indentation creep tests [55, 56]. During a creep indentation test, a cartilage specimen is indented by an indenter with known compressive load and surface area [53]. The manner in which the material indents is then recorded, and compressive properties of

the material are measured [53]. Mechanical properties of articular cartilage have been largely defined by the results of these studies [53].

Based on these indentation studies, articular cartilage is defined as a biphasic viscoelastic material composed of two incompressible phases: a fluid phase (water and electrolytes) and a solid phase (collagen, proteoglycans, proteins, and chondrocytes) [52, 54-57]. The instant a compressive load is applied, interstitial fluid has not had a chance to escape [55]. Therefore, the cartilage behaves as a single-phase elastic solid the instant it is compressed [55]. During this stage, the load is withstood by the fluid state [55]. Subsequently, cartilage begins to compress as the fluid phase is expelled from the system, at which point the solid phase withstands more of the compressive load [52, 54-57]. The rate at which fluid is expelled from the system depends on permeability of the cartilage, length of the drainage path (distance the fluid has to flow to be expelled), and the stiffness of the cartilage [54]. These properties are a function of cartilage compression [54]. If a compressive load is held constant, the velocity of fluid flow will decrease until it reaches zero [54]. The time at which flow velocity reaches zero is considered the *characteristic time for drainage*, and has been cited at approximately 250 seconds or in some cases over 1000 seconds [54, 56, 58]. Defining this value is difficult, as it is dependent on the harvesting site, fluid flow constraints, types of indenters, and compressive forces [53, 54, 59].

When the compressive load is released, fluid is absorbed back into the cartilage interstitial space [53-55]. This occurs more slowly than fluid exudation [53-55]. Hysteretic energy losses due to fluid expulsion and reabsorption have been measured [54]. Energy lost has been shown to decrease as load frequency increases [54].

More recently, indentation studies have considered the tribological nature of cartilage [60-62]. Tribology, or the science of interacting surfaces and lubrication, may be used to investigate

how the movement of two bones is related to cartilage rehydration. Rather than performing an indentation or confined compression experiment, a tribometer translates a glass slide or indenter across a cartilage sample [60-62]. Results of these studies indicate that material and tribological properties of cartilage change with the rate of translation across the sample [60-62]. The faster the translation across the sample, the more load is withstood by the fluid phase, rather than the solid phase [61]. Likewise, a slower movement across the sample leads to less load being supported by the fluid phase [61]. In a single specific tribological study, the rate of compression increased during static contact in comparison to sliding contact (60 mm/sec) [60]. Therefore, cartilage not only responds to compressive force, but the manner and speed in which the force is translated across the joint [60-62].

Cadaver, *in situ*, and *in vivo* studies have also been used to investigate how cartilage behaves under different loading and kinematic conditions. Measuring cartilage responses in these environments allow for an increase in physiological relevance of the studies. These studies have largely supported claims also made through indentation, compression, and tribological studies. Imaging devices are utilized to measure joint gaps, cartilage thickness, compression, and biochemical responses to mechanical loading. One such imaging technique is biplane radiography in which bone location is tracked *in vivo* using a computer algorithm [63]. Subject specific bone morphology is collected using three-dimensional digitally reconstructed radiograph (DRR) models developed from computed tomography (CT) scans [63]. A computer algorithm maximizes the correlations between DRR and biplane radiographs [63]. This method may be used on its own to compare bones in space and measure the distances and angles between them [63]. Specifically, this method may output "tibiofemoral gap distance," in which the distance between the tibial plateaus and femoral condyles are measured [63]. The manner in which this distance is measured

(average, minimum, and compartment specific) is dependent on the study and applications in question [63, 64]. In many studies, this method is taken a step further by using an MRI to collect cartilage information and measure actual cartilage compression characteristics [38, 65-68].

A study measuring patellofemoral cartilage of six knee joint specimens through MRI indicated that thickness decreased following a viscoelastic trend over 500 seconds of testing [69]. Flow rate decreased in the same way [69]. Expectedly, the overall volume of the cartilage decreased as thickness decreased—indicating an expulsion of the fluid phase as cartilage compressed [69]. In another study, six healthy right knees of living subjects were imaged under load-bearing conditions at various flexion angles [67]. Cartilage thickness was shown to change as a result of flexion angle [67]. Generally, as flexion angle increases, medial compartment femoral cartilage decreases [67]. However, the nature of this relationship depends on the specific region (medial/lateral, anterior/posterior) of the condyle in question [67]. The contact point—the location within the knee where the distance between the tibial plateau and the femoral condyle is minimized—has been investigated during flexion exercises [65, 67]. It has been shown that the total excursion of the contact point is less over the medial compartment than the lateral compartment of the knee [65, 67]. The medial compartment acts as a pivot point for the lateral compartment to rotate about as a mechanism of the screw-home function of the knee [65, 67]. Furthermore, the manner in which cartilage compresses is not uniform through the depth of cartilage [56, 70]. Cartilage structure becomes more solid as depth increases [56, 70]. Because of this, the superficial layers compress more readily than the deeper layers of the tissue [70].

Time effects of exercise and standing on cartilage thickness *in vivo* have been measured [68]. Compressive strain percent as a function of walking duration has been investigated for healthy subjects [68]. Even during this highly dynamic activity, compressive strain follows a

biphasic compressive curve [68]. Figure 4 displays compressive strain measured over sixty minutes of walking [68].

Effects of standing on cartilage compression have been limited to highly controlled laboratory settings and have only been measured for up to ten minutes. Marsh measured tibiofemoral gap distance (a measurement of the gap between the femoral condyle and tibial plateau that is related to cartilage thickness) during a knee extension exercise [64]. The apparatus used during this experiment is displayed in Figure 5, I [64]. This study applied a load of 50% bodyweight to the foot while the knee was in full extension for 20 seconds [64]. The results of this study are displayed in Figure 5, II [64]. Over 20 seconds of constant loading, changes in gap distance displayed a biphasic viscoelastic curve [64].

Uzuner et. al. imaged right knee joints of two participants during ten minutes of standing [38]. Partial bodyweight was slowly applied over 5 to 7 seconds while images were collected [38]. A knee brace was used to constrain changes in kinematics during the trial [38]. During this time, displacement of the femur along the longitudinal axis in respect to the tibia was 0.24 mm for the female participant, and 0.36 mm for the male participant [38]. This change occurred following a biphasic curve [38]. Hosseini et. al. measured cartilage contact deformation during 300 seconds

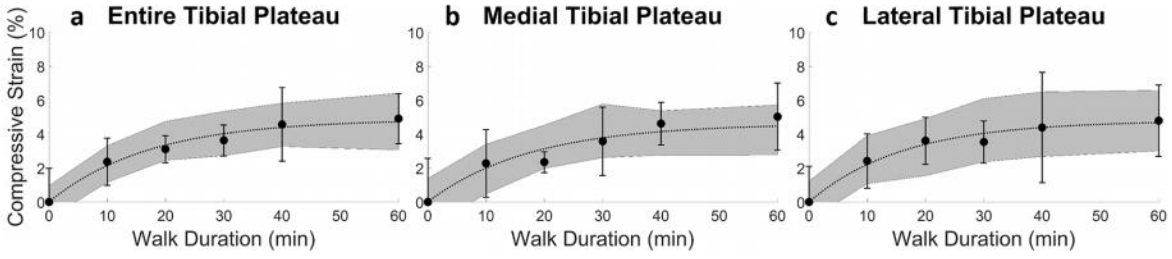

Figure 4: Overall and compartmental compressive strain in tibial cartilage measured as a function of walking time [68].

of static single-leg standing with full bodyweight [66]. Images of both knees were taken separately [66]. As expected, deformation increased quickly followed by a slow rate of increase [66]. The total percent deformation was approximately 12.1% in the medial compartment and 14.6% in the lateral compartment [66]. No studies to date have specifically investigated cartilage compression or gap distance changes as a result of *in vivo* prolonged standing. While this has not been investigated, related research indicates that changes over time may follow a biphasic curve, in which changes in cartilage compression occur quickly and plateaus.

I. **II.**

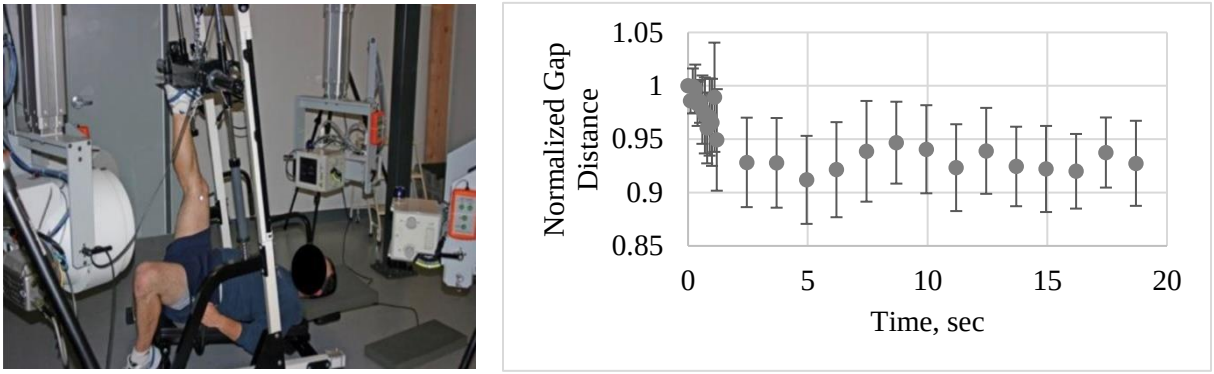

Figure 5: I. Testing apparatus used to measure cartilage compression under a half-bodyweight load. This setup was designed to replicate loading due to standing. II. Recreation of figure from Marsh. Data follows a steep compression followed by an asymptotic tail [64].

2.2.4 Measures of Muscles during Prolonged Standing

The primary biomechanical outcomes of prolonged standing on muscles are fatiguing and blood pooling [1, 3, 5, 6, 42, 43]. The two measurements are inextricably linked, as changes in the circulatory system affect muscular fatigue.

Muscle fatigue occurs when the muscle tissue can no longer supply sufficient energy either due to ischemia or a lack of metabolic substrates [50]. During prolonged standing, lower extremity muscles must maintain consistent submaximal contractions to sustain upright stance [50]. In most cases, fatigue is characterized by decreased observed tension [50]. However, sustaining upright stance requires maintained tension. Therefore, fatigue is characterized by increased motor unit recruitment [50].

The smallest unit of a muscle is a motor unit, comprised of a motor neuron and the muscle fibers innervated by that neuron [50]. Motor units are activated through a multi-step electrochemical pathway [71]. The primary motive proteins of motor unit contraction are actin and myosin fibers [72]. Movement is produced through a series of actin and myosin cross-bridges, which move with the use of adenosine tri-phosphate (ATP), an energy providing molecule [72]. ATP is created when myoglobin (a muscle oxygen carrier) uses oxygen to break down a glucose molecule in the muscle [72]. The energy released by ATP when a phosphate group is removed produces the movement of actin and myosin cross-bridges [72]. The movement of these cross-bridges results in motor unit contraction and relaxation [72]. The innervation and activation of many motor units result in the overall contraction and relaxation of a muscle [50].

In ergonomics and human factors research, fatiguing is measured using subjective measures (reviewed in section 2.2.1) or through objective measurements of electrical signals produced by neural stimulation of muscles over time [50]. Muscle tension varies based on two factors: a change in stimulation rate for a single motor unit, or by the recruitment of multiple motor units [50]. The quantitative indicators of muscle fatigue during prolonged standing are changes in median (or mean) power frequency (MPF) and root-mean squared (RMS) of the electrical signal measured during testing [71].

Surface electrodes are placed on the skin over the belly of a muscle and the electrical activity of muscle tissue may be measured in Volts [71]. An electromyography (EMG) signal has two components utilized for analysis: signal duration and amplitude [50]. As a muscle fatigues, less metabolic substrates are available to propagate an electrical signal [50]. Because of this, the duration increases [50]. A fatiguing muscle recruits the use of multiple motor units over time to fire synchronously to maintain tension [50]. Synchronous firing of motor units increases signal amplitude [50]. The increased signal duration and increased signal amplitude decreases the overall power spectrum of the signal, measured using MPF [50]. A change in activation of a motor unit during prolonged standing may be due to two sources: fatiguing and motor unit recruitment, or an acute contraction resulting in weight transfer movement [50]. RMS measures amplitude changes over time and may indicate fatigue if RMS increases over time (either due to new motor unit recruitment or increased weight transfer movement) [50].

To interpret the significance of lower extremity blood pooling as a result of prolonged standing, an explanation of circulatory mechanisms, metabolism, and hemodynamics is required. The circulatory system transports and distributes essential salts, proteins, carbohydrates, lipids, and gases to tissues and removes metabolic by-products from tissues [73]. Arteries carry blood away from the heart, while veins carry blood back to the heart [73]. Starting at the right ventricle, blood is pumped through the lungs and carbon dioxide (CO_2) is exchanged with oxygen (O_2) [73]. Oxygenated blood returns to the left ventricle of the heart and is distributed to all other tissues of the body [73]. Circulation to tissues within the body is referred to as systemic circulation, while circulation between the heart and lungs is referred to as pulmonary circulation [73].

Blood flows through the systemic circulatory system through a network of vessels that decrease in diameter as flow moves peripherally [73]. However, total cross-sectional area of

combined vessels increase towards the periphery [73]. Specifically, the diameter of each capillary is less than an arteriole, but the total cross-sectional area of the capillary bed is large [73]. High pressure regions of the circulatory system—namely the aorta, arteries, and arterioles have thick vessel walls [73]. Capillaries have very thin wall thicknesses to allow the flow of substances into and out of the vascular bed [73]. Thin walls also make veins more compliant than arteries under increased internal pressure [74]. Figure 6 illustrates the differences in diameter, wall thickness, and total cross-sectional area between vessels.

The changes in cross-sectional area though the systemic circulatory system is significant in the management of blood flow, velocity, fluid pressure, and oxygen transportation to tissues [73]. In a closed system, blood flow into and out of the heart is constant and depends on the pressure gradient, properties of the fluid, and the entire circulatory system [73]. Blood volume flow (Q) is a function of linear velocity (v) and cross-sectional area (A), as in Equation 2-1. Velocity changes inversely and proportionally with cross-sectional area [73]. According to Equation 2-1, as blood flows into capillaries (with low cross-sectional areas), linear velocity increases [73].

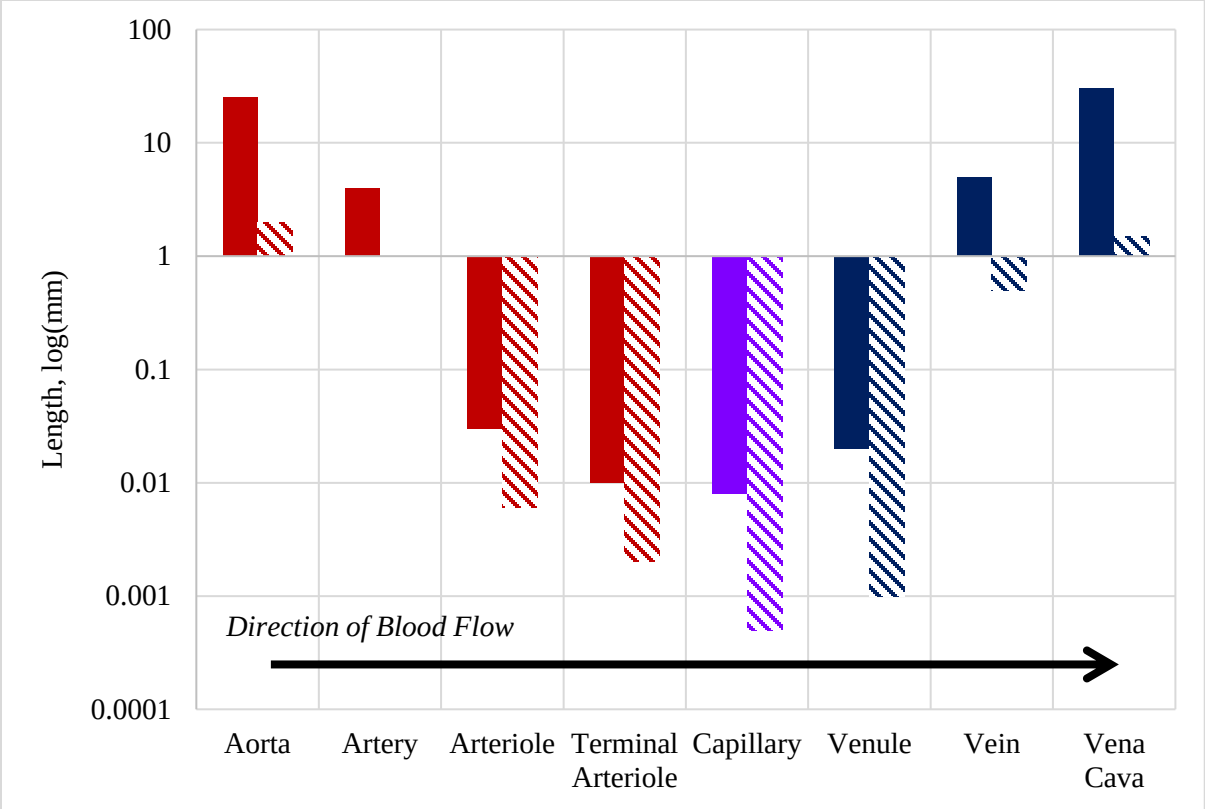

Figure 6: Systematic blood flow leaves through the aorta and returns to the heart through the vena cava. Vessel diameters are solid bars and wall thicknesses are hashed bars. Red bars represent oxygenated blood, blue bars represent deoxygenated blood, and purple bars represent a mixture of both. Adapted from Klabunde [75].

$$v = \frac{Q}{A} \tag{2-1}$$

The large number of capillaries—especially in muscle tissue—allow blood flow in parallel [73]. Total flow into and out of the capillary bed equals the sum of all flows through the parallel capillary elements, as is described in Figure 7 and Equation 2-2 [73]. This allows for each individual capillary to decrease in velocity despite low cross-sectional areas [73]. To maintain constant blood flow through the system, capillaries may collapse or be recruited as circulatory needs change [73]. Slow moving blood through capillaries allows for the diffusion of oxygen through capillary walls into muscles for metabolic processes [73].

$$Q_i = Q_1 + Q_2 + Q_3 + \cdots + Q_n = Q_o \tag{2-2}$$

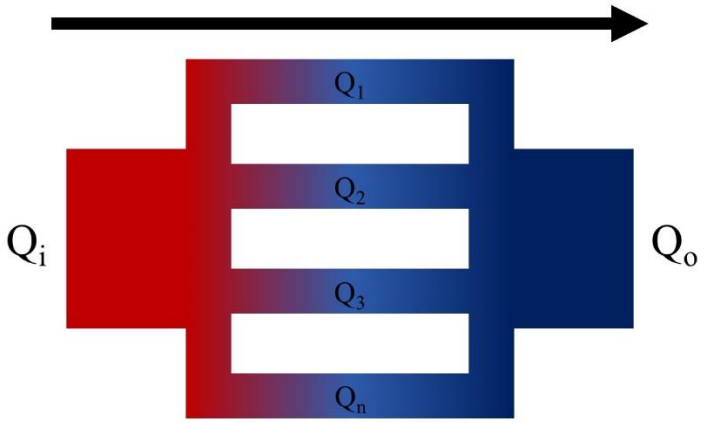

Figure 7: Flow (*Q*) into and out of the capillaries must be equal. Capillaries distribute flow by distributing it in series. As more capillaries are recruited, flow decreases within each capillary.

Erythrocytes are flexible cells that transport O_2 to the body tissues and transport CO_2 to the lungs. The carrier protein in erythrocytes is hemoglobin, a protein containing an iron moiety that binds with O_2 and CO_2 [73]. As blood flow velocity slows in the capillaries, hemoglobin releases O_2 for muscles to metabolize, and absorbs carbon dioxide as a metabolic by-product [73]. On its way back towards the heart, blood passes through venules and veins with the help of muscular pump mechanisms in the calf muscles [73].

The effect of prolonged standing on the circulatory system requires significant regulation mechanisms [73-75]. Mechanisms are mechanical, humoral, and nervous in origin [73-75]. When a person stands upright, the immediate result is increased blood volume accumulation in the lower extremities [74]. Approximately 70% of the total blood volume accumulates in the lower extremities [74]. Of that, 75% is located in venules and veins, as they are more compliant than arteries [74]. Mean capillary pressure also increases from 80 mmHg to 125 mmHg, and fluid filters from the capillaries into the interstitial space as a result of increased pressure [74].

As a response, the circulatory system begins to regulate operations [74]. The sympathetic nervous system signals vasoconstriction nerves to stiffen vein walls which in turn increases blood pressure in the veins [74]. Increased blood pressure helps force blood back towards the heart [74]. After approximately 30 minutes of standing, these mechanisms begin to lose out to the effects of gravity [74]. A person may increase movement to begin to contract lower extremity muscles to utilize the venous pump system to increase venous return [74]. Increased capillary pressures recruit more capillaries to alleviate increased hydrostatic pressures [75]. Fluid in the interstitial space results in increased diffusion distance for oxygen to be metabolized [74]. Oxygen release by hemoglobin is dependent on the partial pressure of oxygen in the capillary space [73]. Because the partial pressure increases, oxygen is not released by hemoglobin as readily—resulting in an

overabundance of oxygenated hemoglobin [73]. Eventually, the venous internal hydrostatic pressure matches that of the external pressures on the venous wall and dilation of the veins slows [73]. Blood settling in the lower extremities means that the volume of blood reaching the heart is less than that leaving the heart. In response, the central venous system signals a loss of blood—which results in the release of norepinephrine (vasoconstrictor) and vasopressin (antidiuretic hormone); increased heart rate, and nervous vasoconstriction [74].

The result of prolonged standing greater than 30 minutes on lower extremity hemodynamics should then be increased blood volume over time, increased oxygen over time, and a sharp increase and plateau of blood accumulation in veins [74]. It is also expected that, despite the increased oxygen accumulation in the lower extremities, muscles are not acquiring the oxygen—which may be linked to fatigue over time [74].

Changes in hemodynamics may be measured using indirect or direct quantitative methods. The "gold standards" for measuring overall lower extremity volume changes are leg/lower extremity volumetry and leg circumference measurements [1, 3, 5, 6, 42]. Both methods require little technology and cost to perform. Leg volumetry is performed by measuring the volume displacement of water when the leg is submerged in a large vessel [1]. Leg circumference measurements may be performed on a predetermined cross section of the leg [5, 6]. Both methods only measure overall swelling of the leg and cannot measure changes in oxygenation. Leg volumetry may only be performed at the beginning and end of standing if any electrical sensors (such as EMG's) are also being used. Measurements of muscle surface temperature have also been used and may indicate increased blood settling in the muscle or increased muscle metabolism [1, 3, 6].

More recently, near infrared spectroscopy (NIRS) has been used to measure changes in muscular hemodynamics due to prolonged standing [42, 43]. NIRS is an optical imaging method that measures changes in hemoglobin with high temporal resolution [76]. NIRS has been proven to be effective in measuring changes in hemodynamics in a variety of testing environments and physiological locations [76].

NIRS capitalizes on changes in optical properties between oxygenated (HbO) and deoxygenated (HHb) hemoglobin to measure the concentration of each in a localized area of interest [77]. A NIRS system emits light at two different wavelengths through fiber optic cables [77]. Optical properties of HbO and HHb are displayed in Figure 8 [78]. The extinction coefficient represents a molecule's ability to absorb light [78]. The isobestic point for HbO and HHb is at a wavelength of 798 nm [78]. Moving away from 798 nm, extinction coefficients diverge [78]. At wavelengths less than 798 nm, the extinction coefficient of HHb is greater than that of HbO [78]. Alternatively, at wavelengths greater than 798 nm, the extinction coefficient of HbO is greater than that of HHb [78]. Therefore, HHb absorbs more light at wavelengths less than 798 nm than HbO; and HbO absorbs more light at wavelengths greater than 798 nm than HHb [78]. To measure changes in HbO and HHb simultaneously, two discrete wavelengths of light greater than and less than the isobestic point and between approximately 700 and 1000 nm are emitted by the NIRS device [77]. Wavelengths that are too low result in high levels of scattering, while wavelengths that are too high result in increased absorption by water [77].

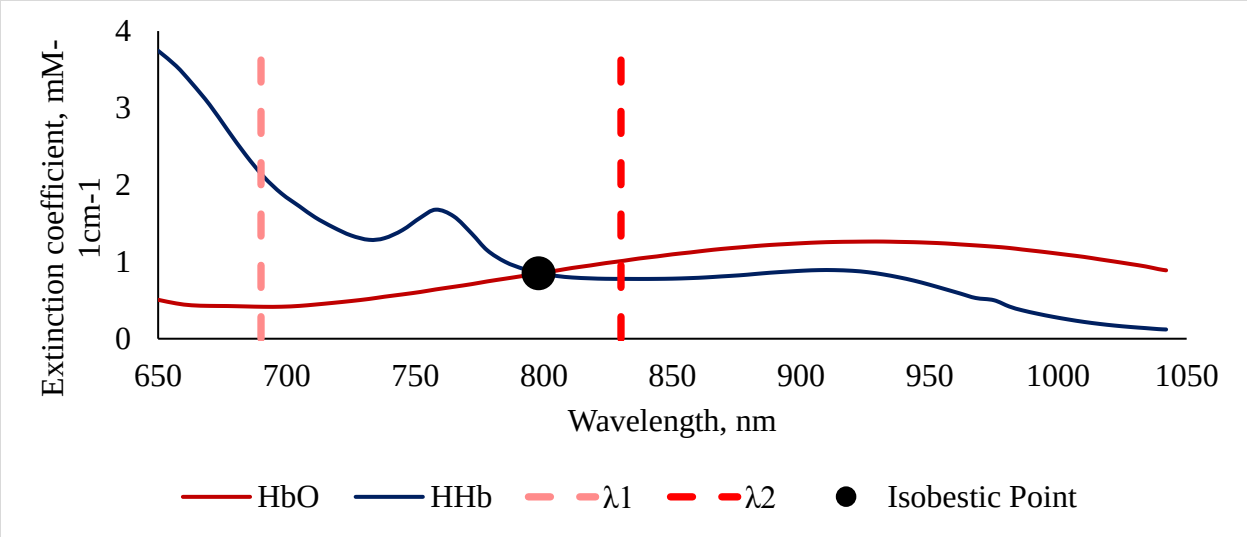

Figure 8: Extinction coefficients for oxygenated hemoglobin (red line) and deoxygenated hemoglobin (blue line). Black dot indicates the isobestic point, in which both lines intersect. The dotted lines indicate the two wavelengths of light used in this study (690 and 830 nm). At 690 nm, deoxygenated hemoglobin absorbs more light. At 830 nm, oxygenated hemoglobin absorbs more light.

Light emitted through fiber optic cables and into the muscle is attenuated by absorption and scatter [77]. The proportion of light absorbed versus scattered is dependent on the optical properties of the tissue in the light path (skin, fat, muscle, etc.) [77]. Fiber optic detectors measure attenuation of light, which may be related to the concentration of hemoglobin in the localized area of question [77]. The relationship between light attenuation and concentration has been defined by the Beer Lambert Law and is dependent on the type of hemoglobin (and therefore the extinction coefficient), light wavelength, and the distance traveled by the light photons [77]. Attenuation (A) is a ratio of the intensity of light emitted (I_e) versus detected (I_d), displayed in Equation 2-3 [77]. The basic Beer Lambert Law is outlined in Equation 2-4, where A is a product of a material's extinction coefficient (ε), concentration (C), and distance traveled by photons (d) [77].

The Beer Lambert Law has been modified for the purposes of measuring hemoglobin concentration in tissue [77]. The value of *d* is unknown given the multitude of tissues and unknown scattering effects of light through each of these tissues in series [77]. The Modified Beer Lambert Law, displayed in Equation 2-5, includes a differential path length factor (DPF), which is a scaling value to account for scattering of light as a function of the distance between emitter and detector optodes [77]. A multiplier (*G*) is added to the equation to account for the relationship between the geometry of the optodes and light scatter [77].

In the case of measuring HbO and HHb, a minimum of two wavelengths and two detectors must be used to solve for separate hemoglobin concentrations [77]. A system of equations may then be developed (Equation 2-3 – Equation 2-9) [77]. *G* is the same value for both HbO and HHb so it may be eliminated from the system of equations [77].

The primary limitation of using NIRS technology to measure hemodynamics in muscle tissue is that DPF is unknown [77]. Therefore, measurements made by this kind of NIRS device can only be used as a trend monitor [77].

Prior research investigating the effects of prolonged standing on muscular and circulatory mechanisms have been measured using EMG, maximal voluntary contractions, volume measurements, and surface temperature measurements [1, 3, 5, 6, 42, 43]. More recently, some studies have used NIRS as a means of measuring muscle oxygenation and blood volume over time [42, 43]. Summaries of these studies are outlined in Table 3.

Studies did not find significant changes in EMG measurements [1, 6, 43]. This indicates that MPF or RMS may not be sensitive enough to measure slow developments of fatigue over time. Subjects may also display different EMG responses to standing, where combining subjects for analysis may wash out subject specific behaviors of note.

$$A = \log\left(\frac{I_d}{I_e}\right) \tag{2-3}$$

$$A = \varepsilon * C * d \tag{2-4}$$

$$A = e * C * d * DPF * G \tag{2-5}$$

$$A = [\varepsilon_1 C_1 + \varepsilon_2 C_2 + \cdots + \varepsilon_n C_n] \tag{2-6}$$

$$\Delta A_{\lambda 1} = \begin{bmatrix} \varepsilon_{\lambda 1}^{HbO} & \varepsilon_{830}^{HHb} \end{bmatrix} * \begin{bmatrix} \Delta C^{HbO} \\ \Delta C^{HHb} \end{bmatrix} * (d * DPF)_{\lambda 1} * G \tag{2-7}$$

$$\Delta A_{\lambda 2} = \begin{bmatrix} \varepsilon_{\lambda 2}^{HbO} & \varepsilon_{\lambda 2}^{HHb} \end{bmatrix} * \begin{bmatrix} \Delta C^{HbO} \\ \Delta C^{HHb} \end{bmatrix} * (d * DPF)_{\lambda 2} * G \tag{2-8}$$

$$\begin{bmatrix} \Delta A_{\lambda 1} \\ \Delta A_{\lambda 2} \end{bmatrix} = \begin{bmatrix} \varepsilon_{\lambda 1}^{HbO} & \varepsilon_{\lambda 1}^{HHb} \\ \varepsilon_{\lambda 2}^{HbO} & \varepsilon_{\lambda 2}^{HHb} \end{bmatrix} * \begin{bmatrix} \Delta C^{HbO} \\ \Delta C^{HHb} \end{bmatrix} * \begin{bmatrix} (d * DPF)_{\lambda 1} & (d * DPF)_{\lambda 2} \end{bmatrix} \tag{2-9}$$

Table 3: A collection of studies investigating the effects of various independent variables on muscle and circulatory outcomes of prolonged standing.

Significance (T, time; SS, standing surface; S, shoe type) is denoted in superscript next to measurement locations.

First Author *Year*	Testing Duration	Independent Variables	Method(s)	Measurement Locations	Measurement Frequency
Garcia, M-G [42] *2018*	5 hours	Time, Cycle type, Rest type	Leg Volume	Lower-Leg ^{T}	0, 3, 6 hours
			NIRS, HbT	Soleus ^{T}	0, 45, 90, 135, 180, 225, 270, 315, 360 mins
			NIRS, StO_2	Soleus ^{T}	0, 45, 90, 135, 180, 225, 270, 315, 360 mins
Haney, J [43] *2015*	6 hours	Time, Standing surface	EMG RMS & MPF	Rect. Femoris, Tib. Anterior, Soleus, Med. Hamst.	Continuous
			NIRS, HbT & SpO_2	Soleus	Continuous
Lin, Y-H [5] *2012*	4 hours	Time, Shoe type, Standing surface	Leg circumf.	Thigh, Shank $^{T, SS, SSxS}$	Every hour
Cham, R [1] *2001*	4 hours	Standing surface	EMG, RMS & MPF	Soleus, Tib. Anterior	Every 15 mins
					Every 15 mins
			Leg Volume	Up to Tibial Plateau	0, 4 hours
			Leg Surf. Temp.	Soleus ^{SS}, Tib. Anterior ^{SS}, Quadriceps ^{SS}, Hamst. ^{SS}	Every 15 mins
Hansen, L [3] *1998*	2 hours	Time, Shoe type, Standing surface	Foot Volume	Entire foot ^{T}	0, 2 hours
			Foot Surf. Temp	Dorsal venous arc ^{T}	0, 30, 60, 115 min
Madeleine, P [6] *1997*	2 hours	Time, Standing surface	Leg circumf.	Shank (right calf)	Every 5 mins
			EMG, RMS & MPF	Soleus ^{SS}, Tib. Anterior ^{SS}	0, 30, 60, 90, 106, 110, 120 min
			Leg Surf. Temp	Shank (right calf)	0, 30, 60, 90, 106, 110, 120 min

Results from these studies agree that prolonged standing leads to increased leg volume or leg circumference [1, 3, 5, 6, 42]. Hansen et. al. found increases in foot volume over two hours of standing [3]. Garcia et. al. and Lin et. al. found significant changes in leg volume and circumference over time standing [5, 42]. Cham and Redfern and Madeleine et. al. did not test the effects of time directly [1, 6]. Rather, they discovered that the difference in leg volume or circumference between different shoe types and standings surfaces changed over time [1, 6]. These differences became more pronounced over time, suggesting time as a factor for increased leg volume or circumference [1, 6]. Those measuring leg surface temperature over time found that temperature increases over time [1, 6]. Madeleine et. al. found that shank muscle temperature increased by approximately 0.32 – 0.37 degrees Celsius while standing on a hard surface, though this relationship was not statistically tested [6]. Cham and Redfern did not directly measure effects of time on surface temperature [1]. However, they found that significant differences in shank surface temperature between standing surfaces occurred after the fourth hour of standing, suggesting that changes over time standing occur [1].

Studies that investigated circulatory effects of standing more directly—through the use of NIRS—see similar results [42, 43]. Haney investigated total hemoglobin and muscle oxygen saturation over six hours of standing, with short seated breaks between one-hour trials [43]. Garcia et. al. investigated the same variables over five hours of standing with various passive or active breaks [42]. Haney saw slight decreases in total hemoglobin over the first two hours, and then increases between three and six hours [43]. However, these trends were not significant [43]. Garcia et. al. did see significant increases in total hemoglobin over time [42]. These results suggest that the overall leg volume changes seen during prolonged standing may be at least in part due to increases in blood volume over time in the lower extremities [42, 43]. Haney did not find

significant changes over six hours of standing in muscle oxygen saturation [43]. However, within each hour, a sharp decrease, followed by a recovery and an overall increase within each hour of standing [43]. Garcia et. al. confirmed these results by finding a significant increase in muscle oxygen saturation over time [42]. This was not expected by the authors, given that muscle fatigue is many times related to a lack of oxygen available for metabolism [42]. Therefore, it is likely that fatigue may be due to an imbalance of other metabolic substrates or an inefficiency in oxygen diffusion over time [42].

2.3 Effects of Standing Surfaces on Prolonged Standing Outcome Measures

Standing surface interventions and suggested ergonomic practices have been developed for those who stand in the workplace [10]. Ergonomic interventions include, but are not limited to, anti-fatigue mats and shoe inserts [10]. The effects of anti-fatigue mats and shoe inserts on discomfort, muscular fatigue, and leg volume changes have been explored in laboratory and field settings under varying standing and walking conditions [10]. In response to these studies, workplaces have "best suggested practices" for employees to minimize the health effects of prolonged standing at work [79-81].

Anti-fatigue mats and shoe insoles are frequently implemented interventions in the workplace [79-81]. Table 4 displays a list of studies investigating the effects of various interventions on psychophysiological and physiological outcomes. Only standing surface and shoe types are considered in this list, as other methods are beyond the scope of this project.

Table 4: A collection of studies investigating the effects of standing surfaces interventions (anti-fatigue mats and shoe insoles) on subjective, behavioral, and physiological outcomes of prolonged standing. ***Significance (T, time; SS, standing surface; S, shoe type) is denoted in superscript next to measurement locations.***

First Author *Year*	Testing Duration	Study Type	Independent Variables	Method(s)	Measurement Frequency
Zhang, L [45] *1991*	2 hours	Lab	Time Standing Surface Shoe Types	Discomfort $^{S, SxT}$ Stabilography EMG	Every 15 mins Every 30 mins Every 30 mins
Wiggermann, N [11] *2013*	4 hours	Lab	Time Standing Surface	Discomfort ^{SS} Stabilography ^{SS}	Every 55 minutes Every hour
Hansen, L [3] *1998*	2 hours	Lab	Time Standing Surface Shoe Type	Discomfort ^{T} Stabilography ^{T} Foot Volume $^{T, SS, S}$ Foot Temperature ^{T}	Every hour 5, 55, and 115 min 0 and 2 hours 0, 30, 60, 115 mins
Lin, Y-H [5] *2012*	4 hours	Lab	Time Standing Surface Shoes	Discomfort $^{T, SS, S, SSxS}$ Leg Circumference $^{T, SS, SSxS}$	0, 50, 60, 110, 120, 170, 180, 230 min 0, 50, 60, 110, 120, 170, 180, 230 min
Lin, Y-H [5] *2012*	4 hours	Field	Standing Surface	Leg Circumference $^{T, SS}$	0, 2, 4 hour
Cham, R [1] *2001*	4 hours	Lab	Standing Surface	Discomfort ^{SS} Stabilography ^{SS} EMG Leg Volume Leg Temperature ^{SS}	0, 4 hours Every 15 min Every 15 min 0, 4 hours Every 15 min
Jefferson, JR [46] *2012*	12 hours	Field	Shoe Insoles	Discomfort ^{S}	End of workday
King, PM [4] *2001*	8 hours	Field	Standing Surface Shoe Insoles	P. Firmness Fatigue $^{SS, S}$ Discomfort $^{SS, S}$	End of workday
Redfern, M [9] *1995*	8-10 hours	Field	Standing Surface Shoe Insert	Tiredness ^{SS} P. Hardness ^{SS} Discomfort ^{SS}	End of workday
Haney, J [43] *2015*	6 hours	Lab	Time Standing Surface	Discomfort $^{T, SS}$ Stabilography EMG NIRS	Every 30 min Continuous Continuous Continuous
Madeleine, P [6] *1998*	2 hours	Lab	Time Standing Surface	Unpleasantness $^{T, SS}$ Stabilography ^{SS} EMG ^{SS} Leg Circumference ^{SS} Leg Temperature ^{SS}	Every 15 min Every 5 min Every 5 min Every 15 min Every 15 min

Those studying the effectiveness of standing interventions in the field most frequently used surveys in which subjects marked their overall tiredness or discomfort at the end of the workday [4, 9, 46]. Differences in discomfort, tiredness, and perceived flooring hardness were observed [4, 9, 46]. Subjects tended to report decreased discomfort and tiredness when standing on an anti-fatigue mat versus a hard floor [4, 9, 46].

Jefferson measured foot discomfort at the end of a workday in over 300 workers [46]. Those who experienced high levels of foot discomfort were given shoe insoles, which showed a statistically significant decrease in foot discomfort [46]. King investigated the effects of using an anti-fatigue mat, shoe insoles, and the combination of both interventions, finding that subjects noted a significant decrease in discomfort and fatigue when using either or both interventions [4]. However, ratings did not differ significantly between intervention types [4]. Redfern and Chaffin studied the effects of multiple anti-fatigue mats and a single shoe insert on standing discomfort, tiredness, and perceived floor hardness [9]. Mechanical properties of the mats, including bottom out depth and stiffness modulus were measured and compared to subjective ratings provided by subjects [9]. Mechanical properties were measured by performing stress deformation tests of the mats [9]. The stiffness modulus is an indicator of firmness, while bottom out depth is when the stiffness modulus significantly changed slope during the stress deformation test [9]. At this point, continued applied stress results in very little deformation [9]. This bottom out depth is related to both the thickness and the material properties of the mat [9]. This study determined that a combination of increased bottom out depth and decreased stiffness modulus were related to lower overall ratings of perceived hardness and tiredness [9]. An analysis of all mats used indicated that the feet and lower legs were most affected by the standing surface in question [9]. This effect dissipated as ratings moved proximally [9]. It was also found that, of shoe inserts and mats with

similar mechanical properties, shoe inserts resulted in significantly lower tiredness, perceived hardness, and discomfort ratings than the mat [9]. This may indicate that the direct application of shoe inserts to the foot may be more beneficial than an anti-fatigue mat—in which the effects are a result of the shoe and mat combination [9]. While helpful, studies using subjective surveys in the field shed little light on the physiological effects of standing and how they are mitigated by the use of standing surface and shoe insert interventions. Lin et. al. measured the effects of standing surface in the field on thigh and shank circumference over time [5]. Measurements were conducted at the beginning of the workday, two, and four hours into the workday [5]. It was determined that both thigh and shank circumference were significantly affected by flooring type and time standing [5]. However, only one anti-fatigue mat was used, and no mechanical properties of the mat were reported [5].

Standing sessions in laboratory settings ranged from two hours to six hours—some with seated or walking breaks [1, 3, 5, 6, 11, 43, 45]. Subjective measurements in laboratory studies are in agreement with field studies—in that discomfort, tiredness, and fatigue decrease when standing on an anti-fatigue mat or using shoe insoles as opposed to standing on a hard floor [1, 3, 5, 6, 11, 43, 45]. Discomfort in the feet is most often and most effectively in comparison to other body parts when anti-fatigue mats are used [11, 43, 45]. However, this effect only emerged after three hours of standing in some cases [1, 11].

Effects of anti-fatigue mats and shoe inserts on stabilography were measured [1, 3, 6, 11, 43, 45]. Anti-fatigue mats were shown to be significant factors influencing weight transfer events [1, 6, 11]. These events were measured in numerous ways, that are detailed in Table 4. Cham and Redfern tested many floors of varying mechanical properties, and discovered that standing on a floor mat characterized by increased elasticity, increased stiffness, and lower energy absorption

led to decreased weight shifts [1]. However, a significant decrease in weight shifts were only observed in the fourth hour of standing [1]. Likewise, Wiggermann and Keyserling discovered that weight shifting increased with standing time and hardness of the flooring condition [11]. Madeleine et. al. measured greater COP displacements in the frontal and sagittal planes on the hard floor condition than the soft floor condition, though specific mechanical properties of the flooring conditions were not reported [6]. Discomfort and weight transfer events over time have been positively correlated. However, it is not understood if behavioral responses are a result of discomfort or a method by which the body mitigates discomfort [1, 11]. Therefore, it is unknown if a lack of movement is related to a positive or negative physiological outcome.

Muscular and circulatory related effects of anti-fatigue mats and shoe inserts show significant results [1, 3, 5, 6]. Overall, volume or circumference increases in the lower extremities are significantly less as a result of standing on an anti-fatigue mat versus a hard floor [3, 5, 6]. Likewise, leg surface temperature shows a smaller increase over time standing on an anti-fatigue mat versus a hard floor condition [1, 6]. Changes in leg, foot volume or circumference or leg surface temperature are hypothesized to be related to circulatory effects of prolonged standing, including blood pooling [43]. Haney measured changes in total hemoglobin and muscle oxygen saturation over six hours of standing [43]. However, no significant differences between flooring conditions were observed [43]. The effect of flooring on EMG outcomes (MPF and RMS) were varied [1, 6, 43]. Madeleine et. al. found statistically significant increases in muscle activity (RMS) on the anti-fatigue mat compared to the hard surface [6]. However, soleus muscle activity decreased [6]. MPF was lower for both tibialis anterior and soleus on the anti-fatigue mat in comparison to the hard floor condition [6]. In other cases, MPF and RMS tended to be subject

specific or did not show significant differences between anti-fatigue mat and hard floor conditions [1, 43, 45].

A lack of significant differences comparing standing surfaces and shoe inserts to hard floor conditions may be related to the amount of time standing or the mechanical properties of the anti-fatigue mats in question. Hansen et. al. only measured effects of a single flooring and shoe insert type on discomfort over two hours of standing work, suggesting that two hours may not be enough time to see significant effects [3]. Likewise, Zhang et. al. measured discomfort over two hours of standing and did not find any significant differences in weight transfer events or EMG measurements between standing surfaces [45]. However, Haney measured differences in standing surfaces over six hours of standing and did not find significant differences in EMG, NIRS, or weight transfers between flooring conditions [43]. This may have been because the flooring conditions were too similar in mechanical properties to find distinguishable results [43].

Based on the results of laboratory and field prolonged standing studies, various governmental and professional associations have made suggestions for safe practice in professions that require prolonged standing. The Association of periOperative Registered Nurses (AORN) published a set of solutions for prolonged standing in perioperative settings to minimize musculoskeletal disorders due to static work [82]. These solutions include limiting continuous static stance, using anti-fatigue mats, using sit/stand stools, and choosing supportive footwear [82]. Occupational Safety and Health Administration (OSHA) published safety considerations for young workers in restaurants [81]. To minimize the effects of prolonged standing, OSHA suggests continually moving and avoiding static positions, well-cushioned shoes, and anti-fatigue mats [81]. The Canadian Centre for Occupational Health and Safety suggests providing a dynamic workplace

in which workers are able to choose among a variety of working positions [80]. Comfortable footwear and anti-fatigue mats are also suggested [80].

While intervention measures are overall helpful, it is unknown to what extent various interventions help minimize physiological effects of prolonged standing. It is also unknown if interventions have different effects on those with obesity.

2.4 Effects of Obesity on Prolonged Standing Outcome Measures

The Center for Disease Control reported in 2017 that 39.8% of adults and in the United States were obese [83]. Obesity is defined based on body mass index (BMI), which is an aggregate value derived from the mass and height of an individual [84]. A BMI of over 30 kg/m^2 is considered *obese*, while a BMI between 18 and 30 kg/m^2 is considered *healthy weight* or *overweight* [84]. Those with obesity are more at risk than those without obesity of development of musculoskeletal and circulatory disorders, such as osteoarthritis, chronic venous insufficiency, varicose veins, and more [10, 85, 86]. Furthermore, those with obesity may be more likely to experience negative outcomes of prolonged standing, but few studies have been done in this area [4, 17, 19]. While not directly measuring the effects of prolonged standing, a retrospective study including 11,728 health care and university employees in the North Carolina area compared rates of workers compensation claims, associated costs, and lost work days to BMI [87]. According to this study, the number rate of claims and dollars spent per claim increased with increasing BMI [87]. The claims most strongly affected by BMI included lower extremity injuries (pain or inflammation, sprain or strain, and contusion or bruise)—among other injuries [87].

Many studies have investigated the relationship between postural sway and obesity during short, quiet stance [88]. In a study in which 59 male subjects ($17.4 < BMI < 63.8$ kg/m^2) stood on a force platform for 35 seconds, COP speed was found to increase with BMI, suggesting that those with higher BMI are less stable [88]. In another study, 44 obese (BMI = 40.6 ± 4.6 kg/m^2) and 20 healthy controls (BMI = 21.6 ± 2.2 kg/m^2) stood for 60 seconds on a force plate [89]. Those in the obese group displayed higher COP displacements throughout the duration of stance [89]. Likewise, a study in which subjects stood on a force plate for 18 minutes discovered that the obese group displayed higher postural sway overall than the normal weight group [90]. Furthermore, postural sway increased over time for the obese group significantly faster than the normal weight group [90]. While it is known that obese adults stand differently during short periods of time, the impact of prolonged standing on obese adults is limited.

Epidemiological workplace research has cited obesity as a factor relating to the development of musculoskeletal and circulatory disorders [19]. A study investigating musculoskeletal pain amongst Egyptian hairdressers discovered that those who had leg, foot, and knee pain were more likely to have higher BMI compared to those who did not [19]. This study was able to discern statistically significant differences in leg, foot, and knee pain due to the wide range of subject BMI (19.5 – 30.7kg/m^2) [19]. Some studies, such as that performed by Werner et. al. did not find significant differences due to BMI [17]. Werner et. al. investigated risk factors for foot and ankle disorders among 407 assembly plant workers [17]. Out of these workers, 97 (24%) had a foot or ankle disorder [17]. While the overall range of BMI was wide (18 – 68 kg/m^2), the distribution was skewed and had a high mean BMI of 30.0 kg/m^2 [17]. Therefore, the authors suggest this may have had an effect on their ability to discern differences due to BMI [17]. King measured the effects of anti-fatigue mats and shoe insoles on discomfort and fatigue during the

workday [4]. No strong correlations between weight and discomfort associated with various standing conditions were found [4]. However, a strong correlation between height and discomfort was found [4]. As BMI is an aggregate index of the relationship between height and weight, BMI may have been a significant factor that was not investigated [4].

As obesity is a known risk factor for OA, studies have investigated mechanical and biochemical differences in cartilage of those with obesity and those of a normal weight [24, 85, 86]. Obesity is a significant risk factor associated with the prevalence of knee OA [24, 86]. Development of OA has been linked to mechanical factors, including increased forces and torques on the knee, suggesting that those who are obese are more likely to develop OA [86]. A study investigating the effects of BMI on gait discovered that, when correcting for gait speed, those with greater BMI have more abducted knees during the stance phase [91]. Higher abduction has been shown to lead to increased compression of the medial compartment of the knee and therefore medial compartment OA [91]. Those with obesity are approximately four times more likely to develop OA [24]. For women the likelihood jumps to nearly seven times [24]. Studies also indicate that biochemical properties of cartilage are affected by obesity [92]. Those with high BMI have significantly decreased resting tibial cartilage thickness, higher tibiofemoral cartilage strains, and higher T1ρ relaxation times [92]. Decreased tibial cartilage thickness and higher tibiofemoral cartilage strains are related to higher forces exerted on the joints due to increased bodyweight [92]. T1 ρ relaxation times are inversely related to proteoglycan content [92]. Proteoglycans are proteins that aid cartilage in withstanding compressive forces, and prior studies have indicated that high adipose tissue is related to cartilage proteoglycan loss and may induce OA even in non-weight bearing joints, such as the wrist and hand [92].

Those with obesity are more at risk for circulatory pathologies, such as cardiovascular disease, chronic venous insufficiency, varicose veins, and increased blood pressure [85, 93]. However, few studies have investigated the effects of obesity on circulatory outcomes as they relate to standing time at work. An investigation of risk factors of developing varicose veins—including BMI and standing at work—in the Japanese population discovered that prolonged upright standing at work and increased BMI demonstrated an additive effect to increase likelihood of varicose veins [94]. This relationship was not statistically tested, as the cohort was too small for significant statistical power [94]. A single study was found that investigated the effects of prolonged standing on shank circumference between normal weight ($18.5 < BMI < 24.9$ kg/m^2) and overweight ($25 < BMI < 29.9$ kg/m^2) groups [40]. Surprisingly, it was determined that those who were overweight showed significantly decreased changes in shank circumference over time standing in comparison with their normal weight counterparts [40]. This may be because the shank circumference of the normal weight group is more dynamic, while the overweight group may not see distinct changes [40]. Also, changes were reported as mean shank circumference increases and were not normalized to original shank circumference, which may affect interpretation of the results [40].

It is clear, based on quiet standing studies, that studies with intentional BMI groupings discover differences between groups during standing [88-90]. However, most prolonged standing studies treat BMI as a covariate and not as a main variable of the study. The lack of prolonged standing studies deliberately investigating the effects of BMI or obesity on physiological outcomes makes interpretation and design of standing interventions difficult.

2.5 Study Innovation

Millions of people in the United States spend their workday standing and are at risk for a multitude of joint and circulatory pathologies. Despite its prevalence, there are a paucity of studies that quantify underlying musculoskeletal and circulatory mechanisms of discomfort and injury due to prolonged standing. Past prolonged standing research has largely depended on subjective and behavioral data for interpretation. The main downfall of using these measurements of prolonged standing is their lack of objectivity. Furthermore, subjective or behavioral measurements lack the resolution to discern specific physiological effects of ergonomic interventions or varying human factors. The present study provides a critical step in understanding established connections between prolonged standing and resultant pathologies through introducing methods novel to prolonged standing research to quantify the underlying musculoskeletal and circulatory outcomes of prolonged standing using objective measures.

The instrumentation used in this study, DSX and NIRS, provide quantifiable and repeatable measures of possible underlying joint and circulatory injury-related mechanisms of prolonged standing. DSX imaging is novel to the field of prolonged standing and provides in-vivo measures of the knee joint. Until now, no studies have investigated the effects of standing on knee joint compression *in vivo* for more than ten minutes. This study utilizes a DSX device to measure the effects of prolonged standing over two hours. Circulatory effects of prolonged standing are directly quantified using a noninvasive, portable NIRS device, which has only been recently introduced to the field of prolonged standing.

This study offers insight into joint and circulatory injury-mechanisms during prolonged standing that may be influenced by flooring and BMI. Obesity is a growing problem in the United States workforce and increased BMI has been related to higher levels of work injury claims and

associated costs [87, 95]. Differences revealed in this study can be used to make improved worker-centric occupational recommendations that incorporating BMI. Anti-fatigue mats are a common intervention utilized in prolonged standing. The novel objective measures presented here can be used to better evaluate flooring interventions and redesign more effective surfaces. This study provides essential knowledge necessary to develop the most effective interventions, materials, and health directives, leading to less chronic occupational injuries and diseases in prolonged standing.

3.0 Experimental Methods

3.1 Subject Population

Twenty-eight healthy adults ages 21-35 in the greater Pittsburgh area were recruited for this study. Subjects were split into two body-mass index (BMI) subgroups, healthy weight (HW, 16 subjects, BMI < 29.9 kg/m^2) and obese (OB, 13 subjects, BMI > 29.9 kg/m^2). Subject demographics are listed in Table 5. Preliminary statistical analyses were performed on demographics data. Each subject performed two standing visits in which demographics data (age, height, weight, and BMI) were collected. A paired t-test determined that demographics data were not significantly different between visits. Age, height, weight, and BMI were compared between BMI groups using unpaired t-tests. Age and height were not significantly different between BMI groups. However, weight and BMI were significantly different between BMI groups. Subjects were recruited through advertising in media, flyers, and research registries—including the University of Pittsburgh Clinical and Translational Science Institute Research Participant Registry and Pitt+Me. All subjects were screened for the following exclusionary criteria: (1) any orthopedic or muscular disorders that would impede safe standing for prolonged periods, (2) lower extremity joint replacements, (3) pregnancy, (4) five or more X-rays in the past year, and (5) medical scans performed in the past ten days, such as a CT or bone scan. Written informed consent approved by the University of Pittsburgh Institutional Review Board was obtained prior to participation. If the subject met basic eligibility criteria assessed on the phone, the subject came in for an in-person screening and testing.

Table 5: Mean ± STD and range of subject demographics. An unpaired t-test was performed on age, height, weight, and BMI to confirm differences between groups. *$p < 0.0001$, *; $p > 0.05$, NS*

	Healthy Weight, HW (n = 16)	Obese, OB (n = 13)
Gender	6 M, 10 F	5 M, 8 F
Age, years [NS]	26.1 ± 3.4 (21.0 – 33.0)	28.5 ± 4.6 (21.0 – 35.0)
Height, cm [NS]	172.9 ± 7.6 (160.3 – 192.0)	175.5 ± 7.0 (162.9 – 185.1)
Weight, kg *	70.5 ± 11.0 (54.0 – 88.8)	112.3 ± 15.1 (89.1 – 134.5)
BMI, kg/m^2 *	23.5 ± 2.5 (19.7 – 28.5)	36.5 ± 4.7 (30.1 – 45.3)

3.2 Experimental Environment

Data collection was performed at two different locations: the Orthopaedic Biodynamics Laboratory (BDL, 3820 South Water Street, Pittsburgh, PA 15203) and the University of Pittsburgh Medical Center Mercy Hospital (Mercy Hospital, 1400 Locust St, Pittsburgh, PA 15219). All experimental testing was performed at the BDL. Equipment available at the BDL included a dual-stereo x-ray (DSX) system and a Bertec Instrumented Treadmill platform with two force plates (TM-07, 2500 Citygate Dr, Columbus, OH 43219). A continuous wave near-infrared spectroscopy acquisition device (NIRS-2, ISS, Inc., IL) was provided by Dr. Theodore Huppert (Associate Professor, Electrical and Computer Engineering, University of Pittsburgh). Surface electrodes (Delsys Trigno Wireless EMG, Delsys, Boston, MA) and subjective discomfort surveys (CR10-Borg, [96]) were provided by the Human Movement and Balance Laboratory at the University of Pittsburgh. Figure 9 displays a typical testing setup in which x-rays, force plates, NIRS, and EMG are labeled. The standing desk and harness system that were used during testing are also pictured. Computer tomography (CT) images of the knee—used for data analysis—were collected at Mercy Hospital.

The DSX system was designed and custom built by Dr. Scott Tashman (Director, Biomedical Engineering Program, Steadman Philippon Research Institute) to collect accurate *in vivo* skeletal kinematic data [97]. The DSX system emitted synchronized pulses, creating two radiographs that were used to determine an exact orientation of the knee. A 3D model of the knee, obtained from a CT scan, was processed with these x-rays to create a model of the knee. The average distance between the tibial plateaus and femoral condyles were derived from this data. This process has been validated for measuring gap distance at the knee joint, which is related to cartilage deformation [63, 97, 98].

Behavioral weight transfer characteristics of prolonged standing were measured using two force plates (one for each foot during standing). Force plates collected force and moment data from each leg to determine weight transfer changes over time [1]. Analyses only utilized the vertical force output from each force plate.

Muscular characteristics of prolonged standing were measured using EMG and NIRS. EMG was measured using surface electrodes to record electrical activity of the muscle tissue. Analysis of this electrical activity estimated muscle fatigue over time [2]. The NIRS device emitted low levels of infrared light at discrete wavelengths through a flexible fiber optic cable placed on the soleus muscle to measure circulatory characteristics of standing [77].

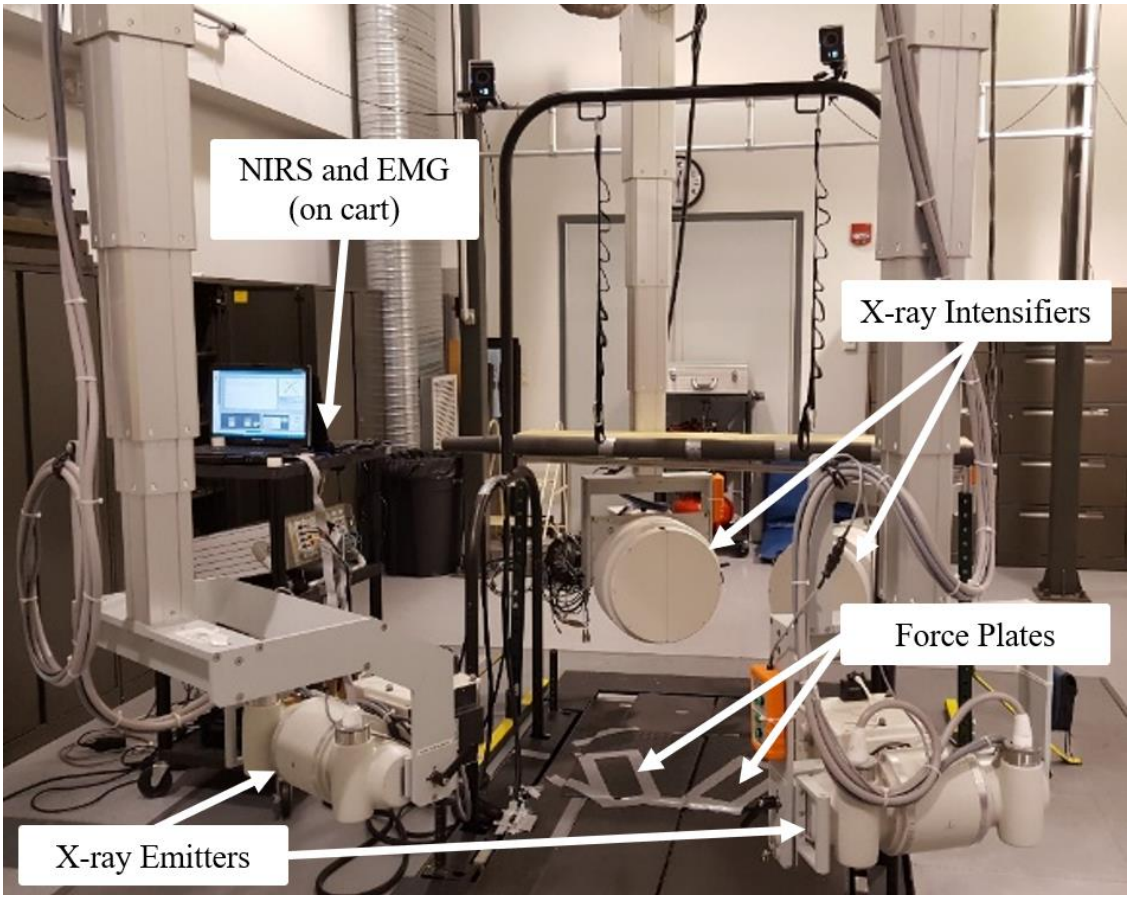

Figure 9: Typical testing setup at the Orthopaedic Biodynamics Laboratory. X-rays, force plates, NIRS, and EMG are labeled. Anti-fatigue mats with tape rectangles where a subject stood are sitting on top of the force plates. NIRS and EMG data acquisition devices sat on a cart near the subject. X-ray emitters and intensifiers were positioned such that there would not be interference by the harness system or the standing desk.

During standing, a tiredness and discomfort survey was administered every 30 minutes. Figure 10 displays the CR-10 Borg tiredness and discomfort survey that was administered [96]. Ratings of floor surface softness, overall tiredness, overall leg tiredness, and perceived discomfort of specific body segments (upper back, lower back, hips, upper legs, knees, lower legs, ankles, and feet) were collected. Separate answer sheets were given to each subject at each time point to self-report their answers. Answer sheets were immediately collected after completion. Subjects were not allowed to see their prior answers throughout the trial to minimize expectation bias.

I.

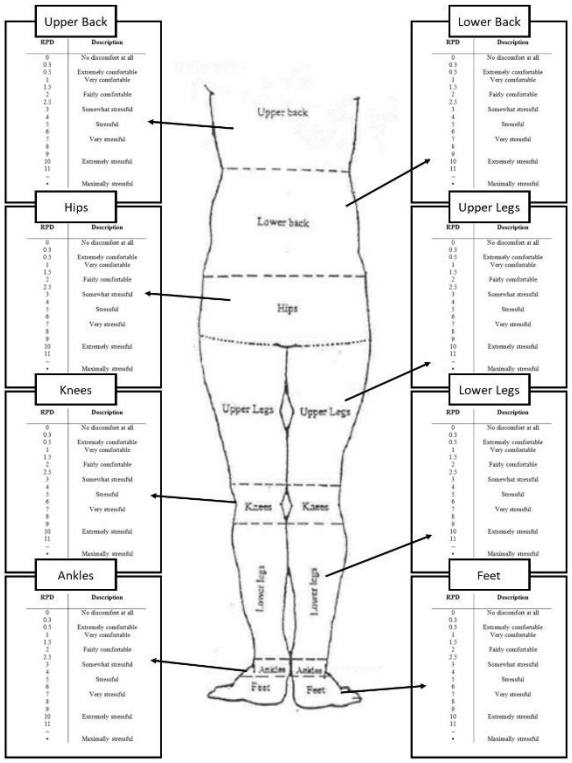

II.

RPD	Description
0	No discomfort at all
0.3	
0.5	Extremely comfortable
1	Very comfortable
1.5	
2	Fairly comfortable
2.5	
3	Somewhat stressful
4	
5	Stressful
6	
7	Very stressful
8	
9	
10	Extremely stressful
11	
~	
▪	Maximally stressful

Figure 10: I. Full document provided to subjects to complete their survey. II. Enlarged example of each scale used for separate body parts.

3.3 Experimental Protocol

3.3.1 Standing Visits

Each subject completed two standing visits. Subjects were instructed to refrain from participating in strenuous exercise 48 hours prior to their standing visits. All standing visits began between the hours of 6:00 AM and 9:00 AM to control for diurnal musculoskeletal or circulatory changes. Experimental testing duration was approximately four hours, including lab setup, subject setup, testing, and lab takedown. Subjects were provided the same shoes and socks to control for differences in shoe structure. Shore A hardness properties of the shoe sole have been previously reported as 61.0 [99]. Flooring conditions (hard floor, HF; anti-fatigue mat, MT) for each visit were randomly assigned, and the subject was informed of the flooring assignment during subject setup. The HF condition was a Bertec Instrumented Treadmill instrumented with a polyvinyl chloride belt with a material thickness of 4 mm. The MT condition was a standard diamond plated polyvinyl foam mat with a material thickness of 10 mm. Square sections of the MT (20 in. x 20 in.) were placed over the HF condition.

3.3.1.1 Subject Preparation

Subject preparation occurred in the following order and took approximately 30-45 minutes to complete.

1. Administration of a pregnancy test (females only)
2. Testing shoe selection
3. DSX alignment
4. Standing desk alignment

5. Reading of subject testing script
6. Safety harness outfitting
7. EMG electrode placement
8. NIRS probe placement

Due to radiation exposure experienced during testing, a pregnancy test was performed on all female participants. Those who tested negative were deemed eligible. Eligible subjects were supplied with black dress shoes (Figure 11) and socks. Shoe sizes were self-selected by subjects on their first visit and were consistent between visits.

To align the DSX and standing desk, the subject was asked to place each foot on a separate force plate in a self-selected "comfortable standing position," which was marked using tape. While standing in their "comfortable standing position," a standing desk was set to elbow height. Subjects were allowed to do computer work, reading, or watch TV/movies throughout the duration of testing. The activity of choice was not controlled between standing visits. X-ray emitters and image intensifiers were rotated about the subject to capture images of the right knee. After the DSX was positioned, a practice image was collected to ensure proper placement. An image of proper placement is displayed in Figure 12.

Figure 11: Shoes and socks used for testing. Subjects self-selected shoe size but all shoes were the same brand and model.

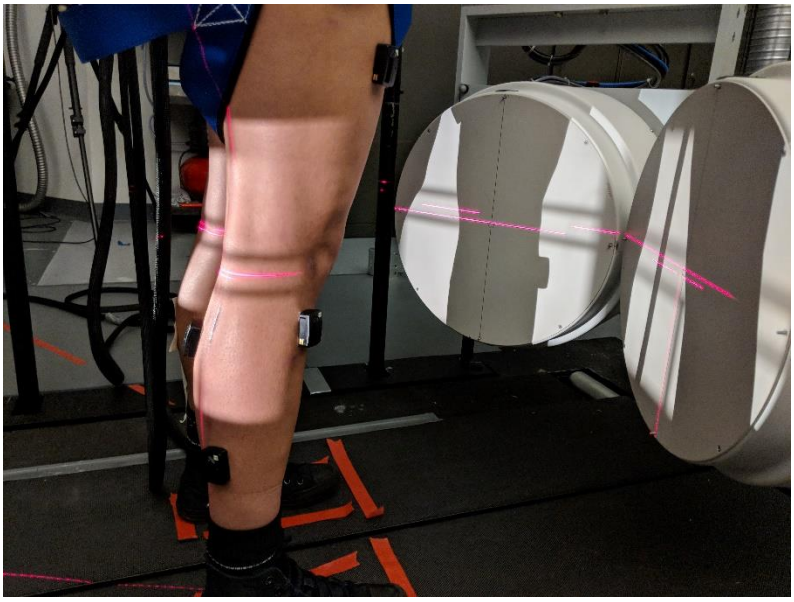

Figure 12: DSX placement to collect a radioscopic image of the right knee.

A script outlining the following main requirements, rules, and expectations of the study was read by the author or undergraduate researcher to each subject:

1. *Every 5-15 minutes today, we will ask you to stand up straight with equal weight on both legs. I will say 'stand up straight.' You will just stand still for 20 seconds during the x-ray. When I say relax, you can return to what you were doing.*
2. *Try to stand as still as you can with one foot on each plate, keeping both feet on the ground.*
3. *Do not lean on the desk in front of you. When you are using the computer or writing, you are allowed to put your arms on the desk as necessary without leaning.*
4. *You will also be asked to answer a short questionnaire every 30 minutes. The questionnaire will ask you to rate your fatigue or tiredness in different areas of your body.*
5. *We will come out every 30 minutes to take temperature readings of different areas of your legs, lower back, and elbow. During this time, just continue working on whatever you are doing, and we will direct you if we need to.*
6. *Please let us know immediately if you feel dizzy, lightheaded, clammy, or need water.*
7. *Bathroom breaks are highly difficult during testing, so we ask that you use the restroom before we start putting equipment on you. If you need a break though, please let us know.*

A harness was supplied for each subject in case of dizziness or lightheadedness. Subjects were outfitted in their harness and it was adjusted by a researcher for a secure fit.

Next, EMG surface electrodes and NIRS probes were placed on the subject. EMG electrodes were placed on the right leg, while NIRS probes were placed on the left leg. This was consistent for all subjects and was not dependent on their dominant leg. EMG electrodes were

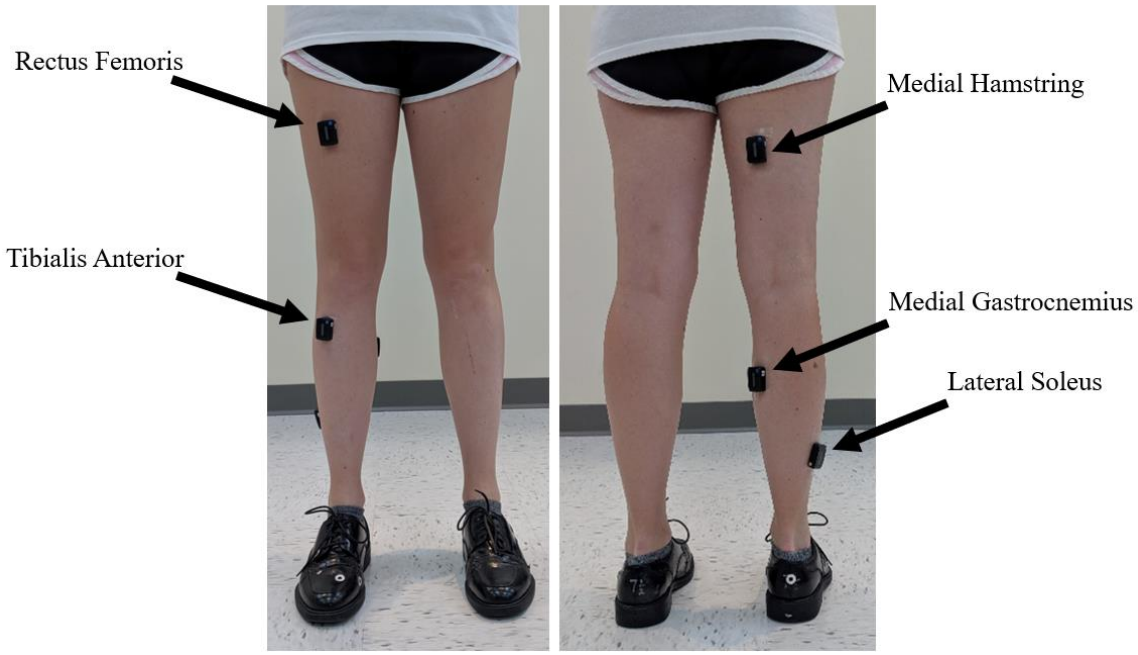

Figure 13: EMG placement on a typical subject. Following EMG placement, measurements were taken to maintain consistent placement between visits.

placed on the following muscles: rectus femoris, medial hamstring, tibialis anterior, medial gastrocnemius, and lateral soleus. EMG electrode placement was adapted from validated and published practices [2]. Prior to electrode placement, the subject's skin was shaved and cleaned using an alcohol swab. Once EMG electrodes were placed, distances between the EMG's to anatomical landmarks were recorded, to ensure accurate similar placement during the second visit. Figure 13 displays a diagram of EMG placement.

Table 6 displays the anatomical landmarks that were used for each EMG. A NIRS probe was placed on the left soleus muscle, and placement was analogous to that of the EMG. Placement of the NIRS probe on a subject soleus is displayed in Figure 14. Once subject preparation concluded, subjects completed a 30 minute seated rest prior to testing [38]. The purpose of this seated rest is to relax joint cartilage deformation and blood flow.

Table 6: Muscles measured using EMG's and accompanying anatomical landmarks. Distances were measured in centimeters to the center of the EMG to the center of the anatomical landmark. Anatomical landmarks were chosen based on the ability to access them for measurement while the subject was seated.

Muscle	Anatomical Landmark
Rectus Femoris (RF)	Patella
Tibialis Anterior (TA)	Tibial Tuberosity
Lateral Soleus (SOL)	Malleolus
Medial Gastrocnemius (GAS)	Popliteal Fossa
Medial Hamstrings (HAM)	Popliteal Fossa

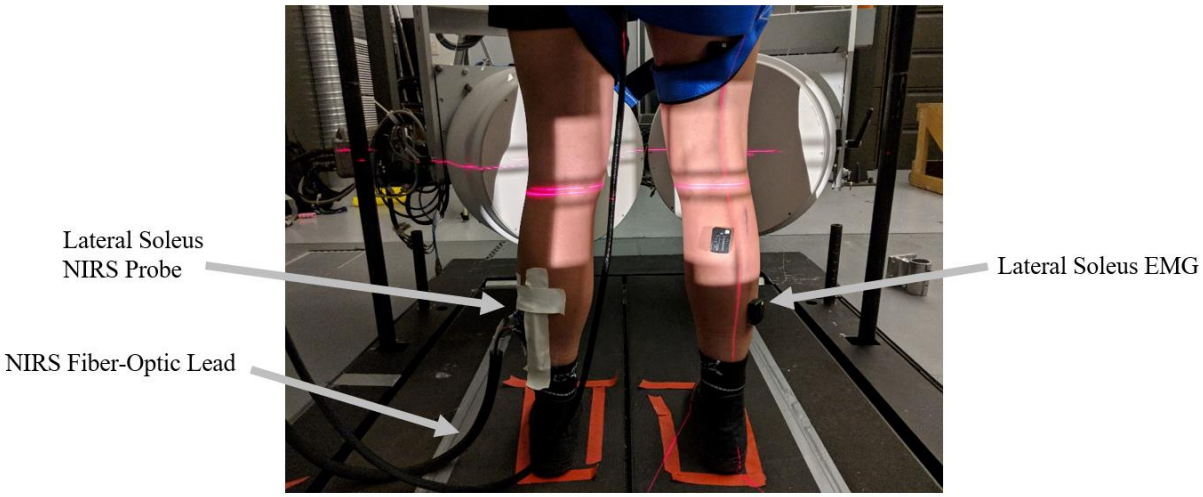

Figure 14: NIRS and EMG placement on a typical subject. The NIRS fiber-optic lead was lifted off the floor once standing and positioned away from the body as to avoid impeding natural movement.

3.3.1.2 Device Preparation

While the subject rested, devices were prepared for data collection. Force plates, NIRS, and EMG were started. An atomic clock was used to note the time of day that the force plates, NIRS, and EMG were started. Start times were recorded as the time of day in military time in the form hh:mm:ss. When asked to stand, the time of day that the subject stood was recorded. A

custom code was written to import start times for force plates, NIRS, and EMG and match with the time at which the subject stood to align each data type prior to analysis.

Each subject placed their feet in the marked foot locations (see Figure 9). Subjects were allowed to move without lifting their feet but were not directly instructed to do so. Furthermore, subjects were instructed not to put their weight on the standing desk in any way, other than naturally setting their arms on the desk when using a computer or writing. Once standing, subjects were harnessed as a safety precaution. The addition of a safety harness has not been shown to affect body sway during standing [100].

Subjects stood for two hours while data was collected. Force plate, NIRS, and EMG data were collected continuously. DSX image collection and discomfort survey administration were completed at discrete time points during testing. Collection frequency and times for each data type is displayed in Table 7.

Table 7: A list of devices and whether data was collected at discrete time points or continuously throughout the standing visit. If data was collected continuously, the collection frequency is noted.

Device	Collection Frequency or Times
DSX	0, 5, 10, 15, 20, 25, 30, 40, 50, 60, 75, 90, 105, and 120 minutes
Discomfort	0, 30, 60, 90, and 120 minutes
NIRS	200 Hz
EMG	2000 Hz
Force Plate	1000 Hz

3.3.2 CT Scan Visit

A single CT scan was completed by a radiologist or technician for each subject. The subject was free to obtain this CT scan anytime within two weeks of their standing visits. Axial images of the knee, hip, and ankle were recorded by radiologists and segmented at the Human Movement and Balance Lab using Mimics software (Materialise Inc., Ann Arbor, MI, USA) to create subject-specific bone models using a previously validated method [63, 101].

A slice through the hip and slice through the ankle were obtained to calculate knee joint kinematics using previously published joint coordinate system methods [102]. The slice through the hip occurred at the femoral head and the ankle slices were through the tibiotalar joint. Due to communication errors between radiologists and researchers, some hip slices were through the greater trochanter, and some ankle slices were through the tibiofibular joint. In these cases, the center of the trochanter and center of the tibiofibular joint were used for kinematics analysis. However, all kinematics analyses were conducted within subject and therefore makes no significant impact on analyses.

3.4 Data Processing and Analysis

3.4.1 Subjective Discomfort Measures

Tiredness and discomfort surveys were obtained for overall tiredness, legs tiredness, hips discomfort, upper legs discomfort, knees discomfort, lower legs discomfort, ankles discomfort, and feet discomfort throughout standing. While data for upper and lower back discomfort were

collected, it was not analyzed for the purposes of this study. Responses were transformed to a linear scale from 6 to 23, where a rating of 6 represented no discomfort reported by the subject [96]. For analysis, tiredness and discomfort ratings were normalized to the first survey response that was collected within the first minute of standing. A repeated measures mixed effects model was performed to determine the effects of time, BMI group, and flooring on tiredness and discomfort, with subject acting as a random effect. Time was considered a discrete variable for this analysis. Tukey HSD post-hoc analyses were performed to investigate effects that were deemed statistically significant by the mixed effects model.

3.4.2 Weight Transfer Measures

Vertical force data was collected from separate force plates simultaneously at 1000 Hz and low pass filtered with a cutoff frequency of 5 Hz. The resulting signal was resampled for analysis to 20 Hz. Proportion of bodyweight on the right foot (P_R) was calculated using Equation 3-1, in which Fz_R represents the amount of vertical force on the right force plate and Fz_L represents the amount of vertical force on the left force plate. P_R was analyzed using two previously published methods and a method proposed by the author.

$$P_R = \frac{Fz_R}{Fz_R + Fz_L} \quad \textbf{(3-1)}$$

All movement event counts were summed every five minutes for analysis. The first and last two minutes of standing were not considered for analysis.

3.4.2.1 Previously Published Method: Cham and Redfern, 2001

The method published by Cham and Redfern in 2001 (CWS) measured changes in lateral COP movement [1]. The average COP and total distance range for the trial were calculated [1]. Average COP was treated as "center," and any movement beyond average COP ± 5% the total distance range seen for the trial was counted as a weight shift [1]. For this study, P_R was used in lieu of COP data.

3.4.2.2 Previously Published Method: Wiggermann and Keyserling, 2013

The method published by Wiggermann and Keyserling in 2013 measured changes in P_R over time. A weight shift (WWS) occurred when P_R transitioned between any of the following three conditions: (a) greater than 0.8 bodyweight on the right foot, (b) less than 0.2 bodyweight on the right foot, or (c) simultaneously, at least 0.2 bodyweight on both feet. Changes between conditions must be withstood for at least 7.5 seconds. WWS were used to measure changes in behavioral responses to standing. Any change that did not last more than 7.5 seconds was considered part of a continuous motion to another weight shift. This method was used to measure WWS for each subject over two hours of standing.

3.4.2.3 New Proposed Method

Two different movement events that were displayed by subjects during testing were defined as standing strategies: shifts and fidgets. Shifts and fidgets occurred when P_R transitioned between any of the following three conditions: (a) greater than 0.63 bodyweight on the right foot, (b) less than 0.37 bodyweight on the right foot, or (c) simultaneously, at least 0.13 bodyweight on both feet. All changes between these groups were counted as events. Events were split into shifts and fidgets based on a temporal threshold. Any event that was maintained for at least 7.5 seconds

was considered a shift, and any event that occurred for less time was counted as a fidget. Therefore, performing a shift and fidget at the same time were mutually exclusive.

QQ plots were visually inspected, and a log(x+1) transformation was performed to achieve a normal distribution of residuals. This transformation—as opposed to a regular log transformation—was chosen to maintain degrees of freedom because many subjects performed 0 movement events. A repeated measures mixed effects model compared the fixed effects of flooring condition, BMI group, and time on shifts, fidgets, and total number of events (shifts + fidgets) with subject number as a random effect. Where time was a significant factor, a Dunnett's t-test was performed to identify change in shifts, fidgets, or total events at time points that were significantly different than those at zero minutes of standing. When interaction effects were significant, a Tukey HSD post hoc test was performed. Shifts, fidgets, and total events were correlated with tiredness and discomfort measures. The number of shifts, fidgets, and total events summed every five minutes were correlated with outcome measures associated with DSX, NIRS, and EMG.

3.4.3 Knee Joint Measures

The DSX system generated x-rays of the knee during standing trials with 1 ms pulsed exposures at 90 kV/125 mA. Source to detector distances were approximately 1.8 meters with an inter-beam angle of 60 degrees. However, source to detector distance and inter-beam angle varied slightly given subject preferred stance and the location of the standing desk. Synchronized x-ray pulses were emitted from two x-ray tubes, initiated by a sync pulse by two 4-megapixel, 14 bit digital video cameras (Phantom 10, Vision Research, Inc.). X-ray images were converted into visible light by each 40 cm image intensifier (Thales, Inc.). At each discrete collection time (Table

7), images were collected for 0.1 seconds at 100 Hz. A set of example x-rays taken during a single trial are displayed in Figure 15.

CT scan image specifications were as follows: slice thickness (1.22 ± 0.2 mm), resolution (2.26 ± 0.62 pixels/mm), distance above joint center (146.0 ± 19.5 mm), and distance below joint center (142.4 ± 18.4 mm). Subjects only received one CT scan. Commercially available software (PCXMC, STUK - Radiation and Nuclear Safety Authority, Helsinki, Finland; http://www.stuk.fi/pcxmc) was used to estimate total effective dose of 0.097 mSv for prolonged standing visits. Effective dose for the CT scans of each knee were estimated using the CT dosimetry reports (from the CT scanner) from previous knee studies performed in this lab. The average effective exposure from CT (based on 34 previous scans) is 0.98 mSv. Thus, effective dose estimate for the entire study is in the order of 1 mSv (100 mrem). This is well below the average exposure sustained by United States citizens per year from natural sources such as cosmic rays and radon gas, therefore study participation did not pose undue risk as a result of the radiation [103].

I. **II.**

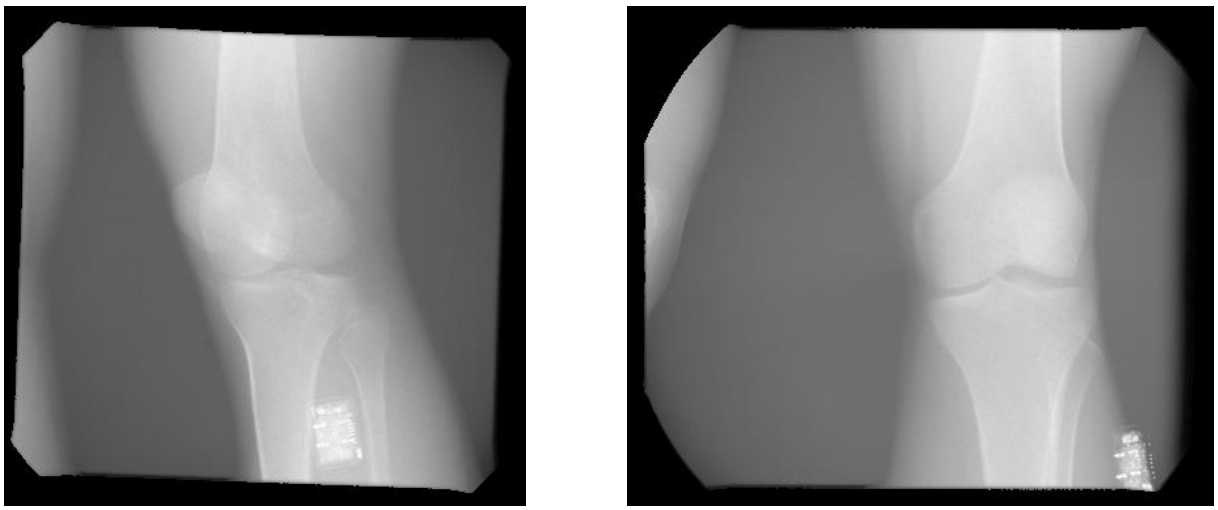

Figure 15: X-rays taken simultaneously of the right knee during a single trial. I. Image collected from the posterior-medial side of the knee. II. Image collected from the posterior and slightly lateral side of the knee.

I. II.

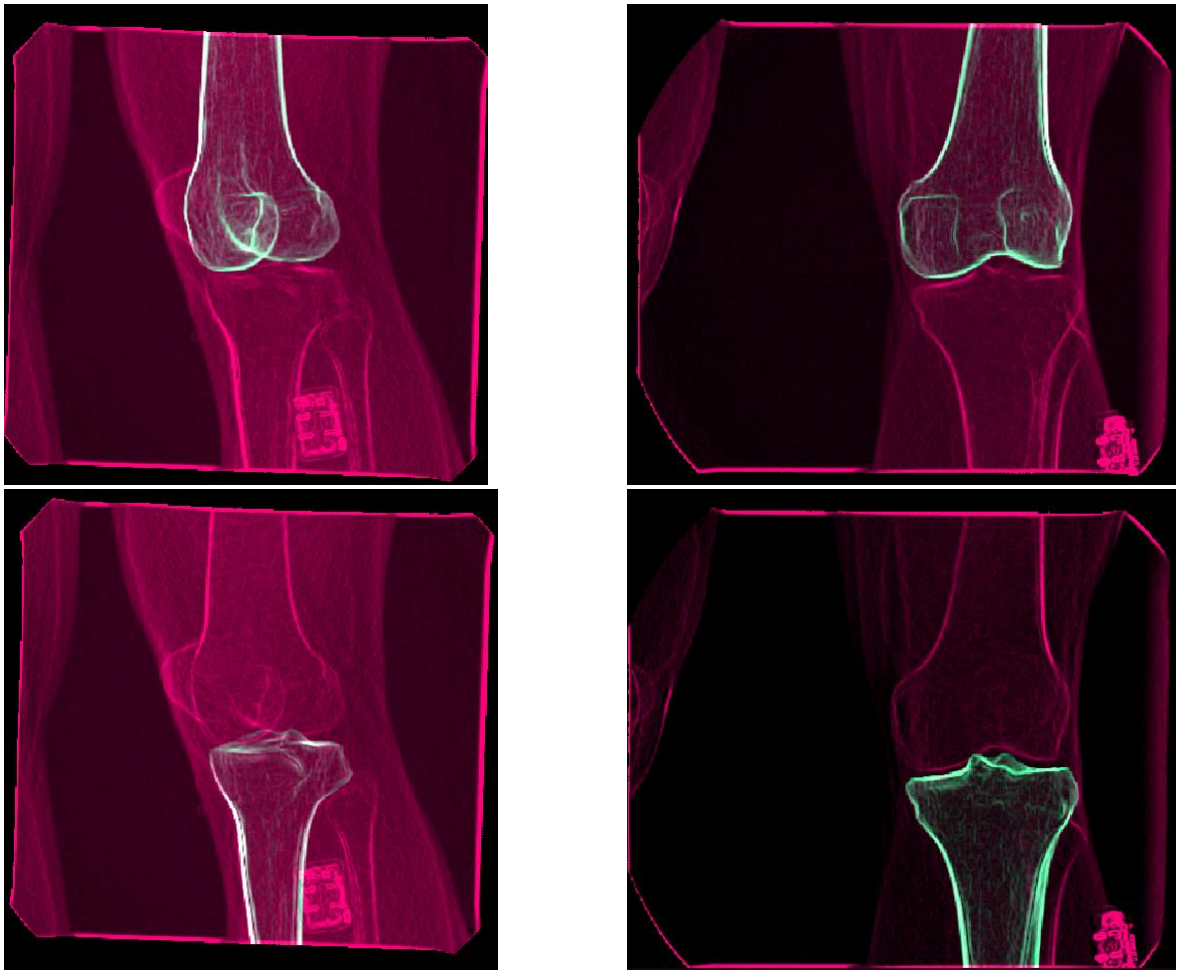

Figure 16: DRRs and x-ray renderings. Top row images are of the femur, and bottom row images are of the tibia. Images on the left (I) and right (II) sides were collected simultaneously using two x-rays.

Digitally reconstructed radiographs (DRRs) of segmented bone models were matched to radiographs collected during standing using custom software [63]. Images of these matched radiographs are displayed in Figure 16. Magenta contours are x-ray radiographs collected during standing trials. Green contours are of the bone model DRRs.

The researcher provided an initial placement guess within two adjacent frames that an algorithm manipulated to maximize correlations between DRRs and actual radiographs [63]. The two initial frames were then used as an initial guess for subsequent frames, the correlation maximization algorithm was repeated for all frames within a trial [63]. In situations in which EMG or border noise interfered with correlation, a mask was drawn around the source of the noise. The author visually checked each frame to confirm accurate placement. The results of this optimization were then projected into 3D space, allowing for measurement of motions and positions of the knee [63]. This method has been published extensively. Validation results for static poses are displayed in Table 8 [63].

Table 8: Model-based tracking accuracy and precision for individual bones and rotational measurements. Adapted from [63].

Axes Measurements (Mean ± STD)						
	Bias		Precision		rms Error	
	Femur	*Tibia*	*Femur*	*Tibia*	*Femur*	*Tibia*
x (mm)	-0.01 ± 0.51	-0.14 ± 0.47	0.07 ± 0.02	0.08 ± 0.04	0.18 ± 0.16	0.17 ± 0.06
y (mm)	-0.14 ± 0.18	0.14 ± 0.24	0.04 ± 0.02	0.03 ± 0.14	0.04 ±0.04	0.06 ± 0.05
z (mm)	-0.18 ± 0.54	-0.37 ± 0.13	0.04 ± 0.02	0.04 ± 0.01	0.23 ± 0.30	0.15 ± 0.10
Rotational Measurements (Mean ± STD)						
	Bias		Precision		rms Error	
F-E (°)	0.60 ± 1.03		0.21 ± 0.04		0.85 ± 0.76	
E-I (°)	0.31 ± 0.88		0.16 ± 0.09		0.67 ± 0.58	
Ab-d (°)	-0.30 ± 0.27		0.06 ± 0.03		0.28 ± 0.27	

The primary variables of interest collected include medial tibiofemoral gap (MTFG) and kinematic rotations of the knee in each anatomical plane. MTFG was collected from the central subregion of the medial tibial plateau due to the increased likelihood of OA development at this location [104]. Specifically, the minimum distance between the medial femoral condyle mesh and medial tibial plateau was located and the average gap distance was calculated within a 400 mm diameter of the minimum distance. Kinematics were calculated using methods described by Grood and Suntay [102]. Each trial included ten frames of data in which average values of MTFG and kinematics were calculated. An image of final knee rendering is displayed in Figure 17. Figure 17, I displays a rendering oriented from the posterior side viewing in the anterior direction. Figure 17, II displays an example rendering of the internal joint, with a color map detailing gap distance between the tibia and femur within the joint. MTFG was compared between flooring and BMI groups over time by comparing the coefficients of a fitted piecewise model, introduced in the results in section 4.3.3. Tukey HSD tests were performed to further investigate significant effects.

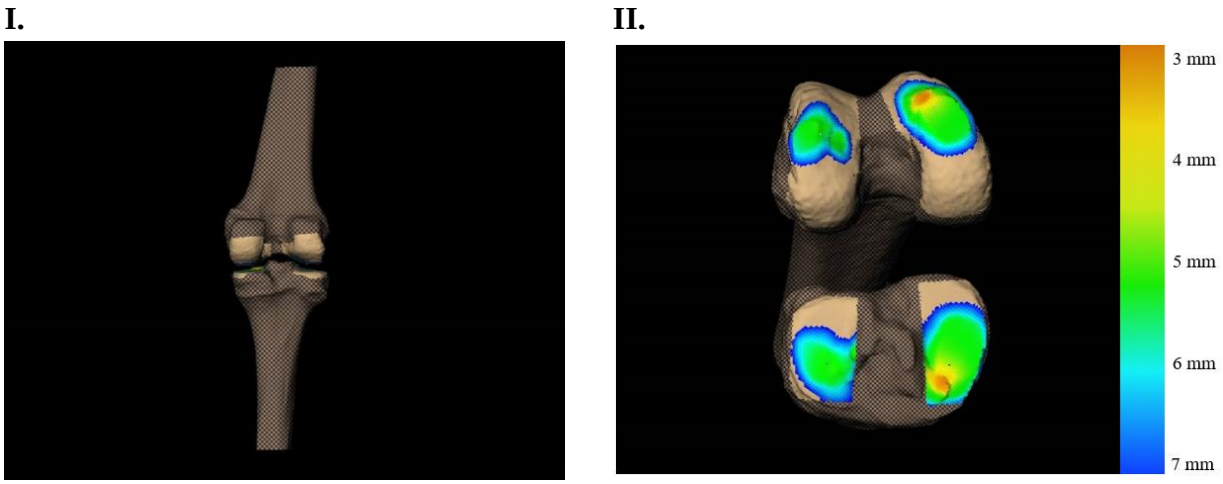

Figure 17: Final right knee rendering for a single subject. I. View is posterior to anterior. II. Color mapping indicates gap distance between the femoral condyles and tibial plateaus. Gap distance is less on the medial side than the lateral side.

3.4.4 Lower Extremity Muscle Measures

EMG and NIRS data were collected and analyzed following methods described in this section. Additionally, Pearson correlations were performed to compare EMG and NIRS data.

3.4.4.1 Electromyography

Surface EMGs collected electrical activity, measured in Volts, at 2000 Hz. Data was resampled to 20 Hz prior to analysis. Each subject's root mean square (RMS) and median power frequency (MPF) were calculated for each five-minute interval during testing [71]. RMS and MPF were analyzed for outliers using a Jackknife outlier analysis. Out of all data points (5,554), 2.5% were removed as outliers. RMS values were converted to percent change from RMS at 0 minutes of standing for each subject, where 100% represents the RMS value at 0 minutes of standing. Following outlier removal, residuals were analyzed using QQ plots and transformed to achieve normality. MPF residuals were normal for all muscles and did not need to be transformed. $RMS^{\%}$ data was transformed using a log transformation for all muscle types. MPF and $RMS^{\%}$ were analyzed using a repeated measures mixed effects model, setting MPF and $RMS^{\%}$ as dependent variables; flooring, BMI, and time as fixed effects; and subject as a random effect. Time was considered a discrete variable for the purposes of this analysis. The analysis was performed within each muscle separately. Where time was a significant factor, a Dunnett's test was performed to determine at what time points MPF and $RMS^{\%}$ were significantly different than at zero minutes of standing. Tukey HSD post hoc analyses were performed to further investigate significant differences between factors.

3.4.4.2 Near Infrared Spectroscopy

The NIRS device was outfitted with a linear probe specifically designed for the surface anatomy of the soleus muscle. The soleus probe is imaged in Figure 14. The probe was placed using double sided tape and medical tape. This provided a secure fit without the use of wrapping or elastics that may compress the leg and impede blood flow. Infrared light was emitted at two discrete wavelengths: 690 and 830 nm. Light attenuation was measured at 200 Hz and down sampled to 2 Hz for analysis. Light attenuation was converted using equations detailed in section 2.2.4 to calculate the following hemodynamic variables: concentration of oxygenated hemoglobin (HbO), concentration of deoxygenated hemoglobin (HHb), and total hemoglobin (HbT). These values were then be used to calculate flow, tissue oxygen saturation (StO_2) and pulmonary oxygen saturation (SpO2). Equations 3-2 through 3-4 display formulas for calculating Flow, StO_2, and SpO_2. These formulas have been previously published [105-107]. Flow was directly proportional to changes in blood volume and was represented as a proportional change from flow at baseline. StO_2 represents a proportion of HbT that is HbO. SpO_2 represents the proportional change in light transmission (R) throughout the cardiac cycle and is dependent on the extinction coefficients of the two wavelengths chosen during testing.

The units associated with changes in hemoglobin are changes in moles of hemoglobin per volume of muscle tissue μM. The concentration of hemoglobin in a set volume of blood was assumed for the purposes of this analysis to remain constant. Therefore, changes in volume of blood in a constant volume of tissue were reflected in changes of hemoglobin concentration. Flow, StO_2, and SpO_2 are unitless as they are proportional values.

A receiver operating characteristic (ROC) test indicated that a kurtosis filter with a spatial principal component analysis (PCA) was the most effective filter for each hemodynamic variable.

HbO, HHb, HbT, Flow, StO_2, and SpO_2 for each subject were averaged into five minute blocks. NIRS measurements are susceptible to heterogeneous noise throughout the population. To account for this noise, a Jackknife outlier analysis was performed on all NIRS data, resulting in approximately 3% of data points removed as outliers. Model residuals were normally distributed, according to visual inspection of normal quantile (QQ) plots. A repeated measures mixed effects model was run on HbO, HHb, HbT, Flow, StO_2, and SpO_2 setting flooring, BMI, and time as fixed effects and subject as a random effect. Time was considered a discrete variable for the purposes of this analysis. Where time was a significant factor, a Dunnett's test was performed to determine at what time points NIRS outcomes were significantly different from NIRS outcomes at zero minutes of standing. A Tukey HSD post hoc analysis was performed to further analyze any factors and interactions that were significant.

$$Flow = \frac{(Q - Q_0)}{Q_0} \qquad \textbf{(3-2)}$$

$$Q = -\frac{\delta I}{\delta t} \propto \frac{\delta HbT}{\delta t}$$

$$StO_2 = \frac{HbO}{HbO + HHb} \qquad \textbf{(3-3)}$$

$$R = \frac{(AC/DC)_1}{(AC/DC)_2} \qquad \textbf{(3-4)}$$

$$SpO_2 = \frac{\varepsilon_{d1} - R\varepsilon_{d2}}{R(\varepsilon_{02} - \varepsilon_{d2}) + R(\varepsilon_{d1} - \varepsilon_{01})}$$

4.0 Results

Results are introduced in the following order: tiredness and discomfort, weight transfer measures of prolonged standing, knee joint measures of prolonged standing, and lower extremity muscle measures of prolonged standing. Data representing statistically significant results are included in this section. Relevant subject specific data and figures representing non-statistically significant results are included in the Appendices.

4.1 Tiredness and Discomfort

Raw tiredness and discomfort data were transformed to a linear scale ranging from 6 – 23 and was normalized to survey data collected at the start of the standing trial [96]. A repeated measures mixed effects model was performed to measure the effects of time, flooring, and BMI group on tiredness and discomfort ratings (Table 9). Tiredness and discomfort over all body regions surveyed increased significantly with time (overall tiredness, $F_{1,213} = 35.78$, $p < 0.0001$; legs tiredness, $F_{1,213} = 61.49$, $p < 0.0001$; hips, $F_{1,213} = 30.75$, $p < 0.0001$; upper legs, $F_{1,213} = 36.86$, $p < 0.0001$; knees, $F_{1,213} = 28.26$, $p < 0.0001$; lower legs, $F_{1,213} = 50.33$, $p < 0.0001$; ankles, $F_{1,213} = 43.03$, $p < 0.0001$; and feet, $F_{1,213} = 97.80$, $p < 0.0001$).

Table 9: Full factorial within subjects repeated measures mixed effects analysis of tiredness and discomfort. Factors included are flooring (F), BMI (B), and time (T). ***p < 0.0001 ****, p < 0.001 ***, p < 0.01 **, p < 0.05 *, p > 0.05 NS***

	Overall Tiredness	**Legs Tiredness**
T	$F_{1,213} = 35.78$ ****	$F_{1,213} = 61.49$ ****
F	$F_{1,214} = 0.13$ NS	$F_{1,213} = 1.83$ NS
B	$F_{1,24} = 0.79$ NS	$F_{1,24} = 0.21$ NS
F x B	$F_{1,214} = 4.39$ *	$F_{1,213} = 0.09$ NS
F x T	$F_{1,213} = 0.16$ NS	$F_{1,213} = 0.94$ NS
B x T	$F_{1,213} = 0.69$ NS	$F_{1,213} = 0.41$ NS
F x B x T	$F_{1,213} = 1.18$ NS	$F_{1,213} = 0.51$ NS

	Hips	**Upper Legs**	**Knees**
T	$F_{1,213} = 30.75$ ****	$F_{1,213} = 36.86$ ****	$F_{1,213} = 28.26$ ****
F	$F_{1,213} = 3.00$ NS	$F_{1,213} = 0.05$ NS	$F_{1,213} = 4.13$ *
B	$F_{1,24} = 0.02$ NS	$F_{1,24} = 0.01$ NS	$F_{1,24} = 2.42$ NS
F x B	$F_{1,213} = 0.35$ NS	$F_{1,213} = 0.04$ NS	$F_{1,213} = 0.59$ NS
F x T	$F_{1,213} = 0.95$ NS	$F_{1,213} = 0.25$ NS	$F_{1,213} = 0.62$ NS
B x T	$F_{1,213} = 0.22$ NS	$F_{1,213} = 0.10$ NS	$F_{1,213} = 1.29$ NS
F x B x T	$F_{1,213} = 1.91$ NS	$F_{1,213} = 0.33$ NS	$F_{1,213} = 0.47$ NS
	Lower Legs	**Ankles**	**Feet**
T	$F_{1,213} = 50.33$ ****	$F_{1,213} = 43.03$ ****	$F_{1,213} = 97.80$ ****
F	$F_{1,213} = 1.37$ NS	$F_{1,213} = 1.44$ NS	$F_{1,213} = 16.66$ ****
B	$F_{1,24} = 1.63$ NS	$F_{1,24} = 0.32$ NS	$F_{1,24} = 1.79$ NS
F x B	$F_{1,213} = 0.02$ NS	$F_{1,213} = 0.41$ NS	$F_{1,213} = 6.61$ *
F x T	$F_{1,213} = 0.50$ NS	$F_{1,213} = 0.28$ NS	$F_{1,213} = 1.44$ NS
B x T	$F_{1,213} = 2.11$ NS	$F_{1,213} = 0.94$ NS	$F_{1,213} = 1.37$ NS
F x B x T	$F_{1,213} = 0.09$ NS	$F_{1,213} = 0.26$ NS	$F_{1,213} = 0.61$ NS

Figure 18 displays average tiredness and discomfort measures over time for each body region. A Tukey HSD post hoc analysis was performed to further investigate the time effect on all tiredness and discomfort measures. For all tiredness and discomfort measures, significant increases occurred within the first 30 – 60 minutes then continued to increase with time. Within Figure 18, different letter labels above each time point indicate significantly different time points.

A mixed effects model was performed to determine if change in discomfort after 120 minutes of standing differed between body region with subject number as a random effect. Body region was a statistically significant factor for change in discomfort after 120 minutes of prolonged standing ($F_{5,275} = 16.24$, $p < 0.0001$, Figure 19). The magnitude by which discomfort increased over two hours of standing became greater as the region of interest became more distal. In other words, the feet displayed the largest change in discomfort (7.75 ± 0.51) and were significantly higher than any other measures of discomfort. The hips (3.59 ± 0.51) and upper legs (4.04 ± 0.50) displayed the least. A t test was performed to compare legs tiredness and overall tiredness. Legs tiredness (6.92 ± 0.61) was significantly higher than overall tiredness (4.69 ± 0.59) ($t=4.07$, $p = 0.0001$). Lower case letters are labels for tiredness measures in Figure 19 that are significantly different.

Flooring was a significant effect for knees discomfort ($F_{1,213} = 4.13$, $p = 0.0433$) and feet discomfort ($F_{1,213} = 16.66$, $p < 0.0001$). In both cases, the MT condition (Knees, MT = 2.3 ± 0.3, Feet, MT = 4.4 ± 0.3) displayed significantly lower discomfort than the HF condition (Knees, HF = 2.9 ± 0.3, Feet, HF = 5.4 ± 0.4), displayed in Figure 20.

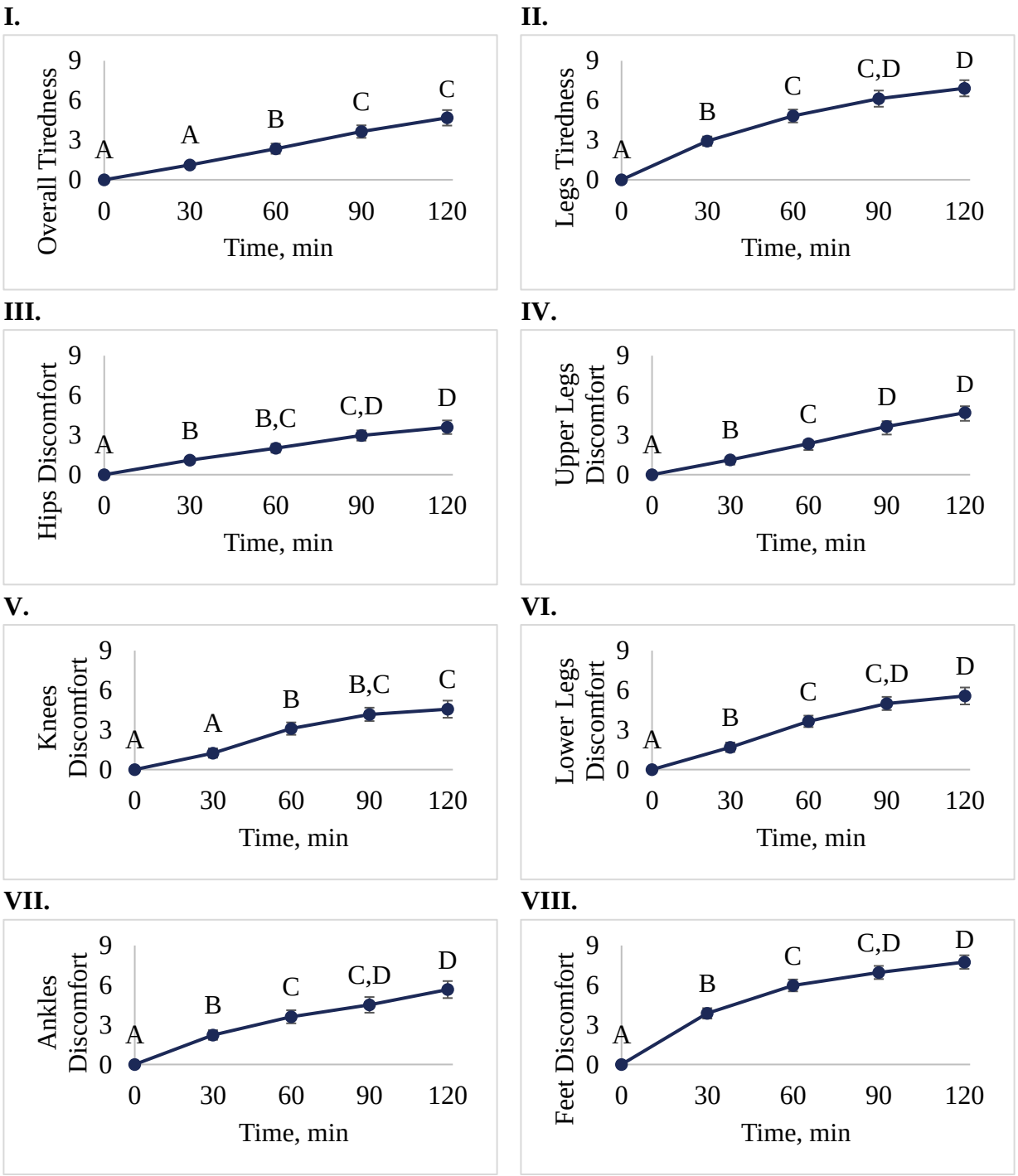

Figure 18: Change in I. Overall tiredness and II. Legs tiredness; and change in discomfort in III. Hips, IV. Upper Legs, V. Knees, VI. Lower Legs, VII. Ankles, and VIII. Feet from 0 minutes over time. Each point represents the average normalized value across subjects. Error bars represent standard error of the mean. Each measurement increased significantly with time. Time points labeled with different letters are significantly different.

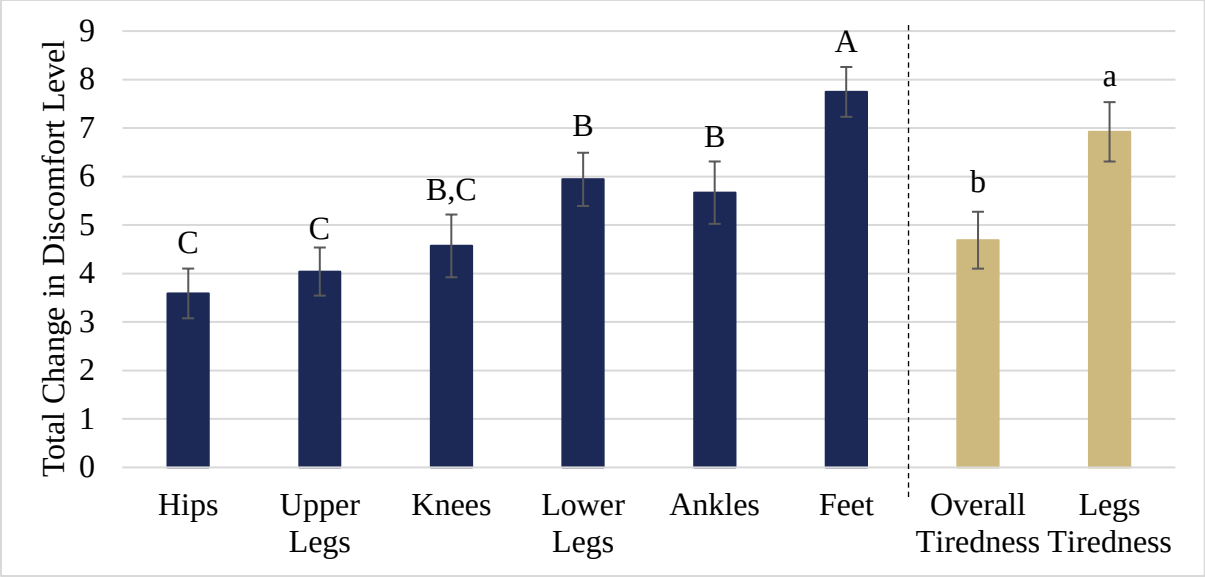

Figure 19: Total change in discomfort after 120 minutes of prolonged for all surveyed body segments. Changes in discomfort standing increased as distally across body segments.

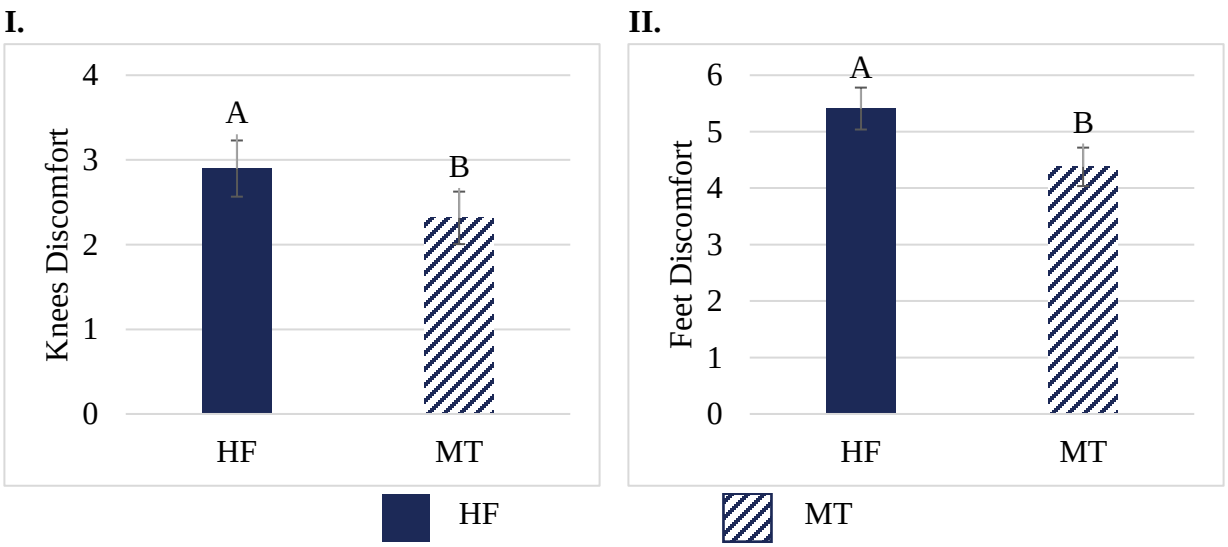

Figure 20: Average measurement of (I) knee discomfort and (II) foot discomfort across all time points and subjects standing on a hard floor (HF) or anti-fatigue mat (MT). Error bars indicate standard error of the mean. Standing on the MT resulted in significantly decreased knees and feet discomfort than on the HF overall. Bars not connected by the same letters are significantly different.

Figure 21 displays changes in tiredness and discomfort over time split between flooring conditions. Significant differences in knees and feet discomfort between the HF and MT condition were primarily observed as a result of diverging measurements over time after 30 minutes of standing. No other tiredness or discomfort measures displayed a significant flooring effect. This can also be observed in Figure 21, as overall tiredness, legs tiredness, hips, upper legs, lower legs, and ankles displayed very similar curves throughout two hours of standing between HF and MT conditions.

Tiredness and discomfort measurements did not display any significant differences due to BMI group. However, some trends are of note. Overall, tiredness and discomfort did increase over time within each BMI group (Figure 22). Interestingly, the OB group reported higher levels of overall tiredness over time, but lower levels of knees, lower legs, ankles, and feet discomfort. Differences between BMI groups became more apparent in knees, lower legs, ankles, and feet discomfort after 30 minutes of standing. There was little difference between BMI groups over time in reporting legs tiredness and hips and upper legs discomfort.

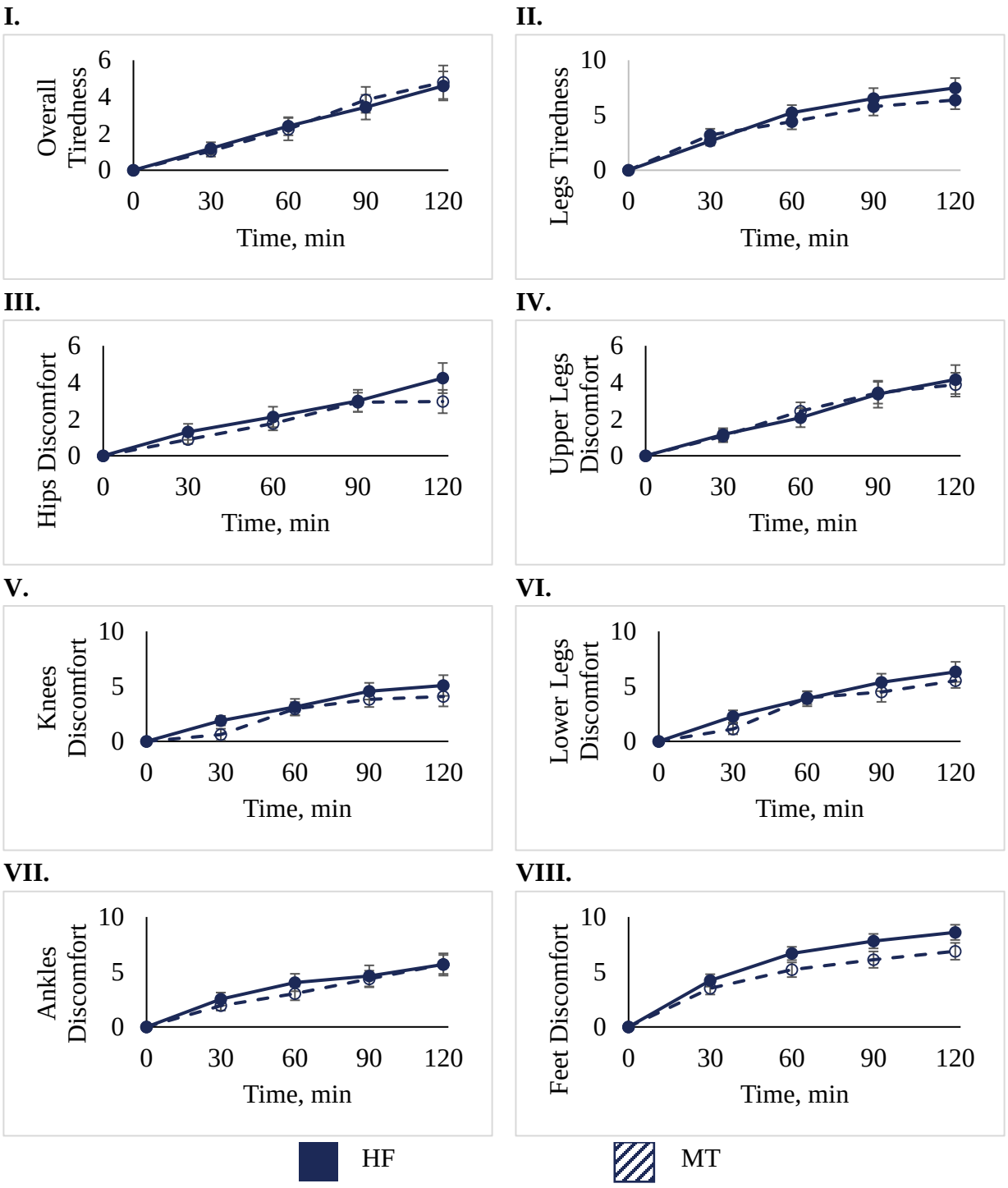

Figure 21: Change in I. Overall Tiredness and II. Legs Tiredness; and discomfort in III. Hips, IV. Upper Legs, V. Knees, VI. Lower Legs, VII. Ankles, and VIII. Feet from 0 minutes across time, split into flooring groups. Each point represents the average normalized value across subjects. Error bars represent standard error of the mean. No multiple comparisons between time points were performed, as the interaction effects did not indicate significant differences.

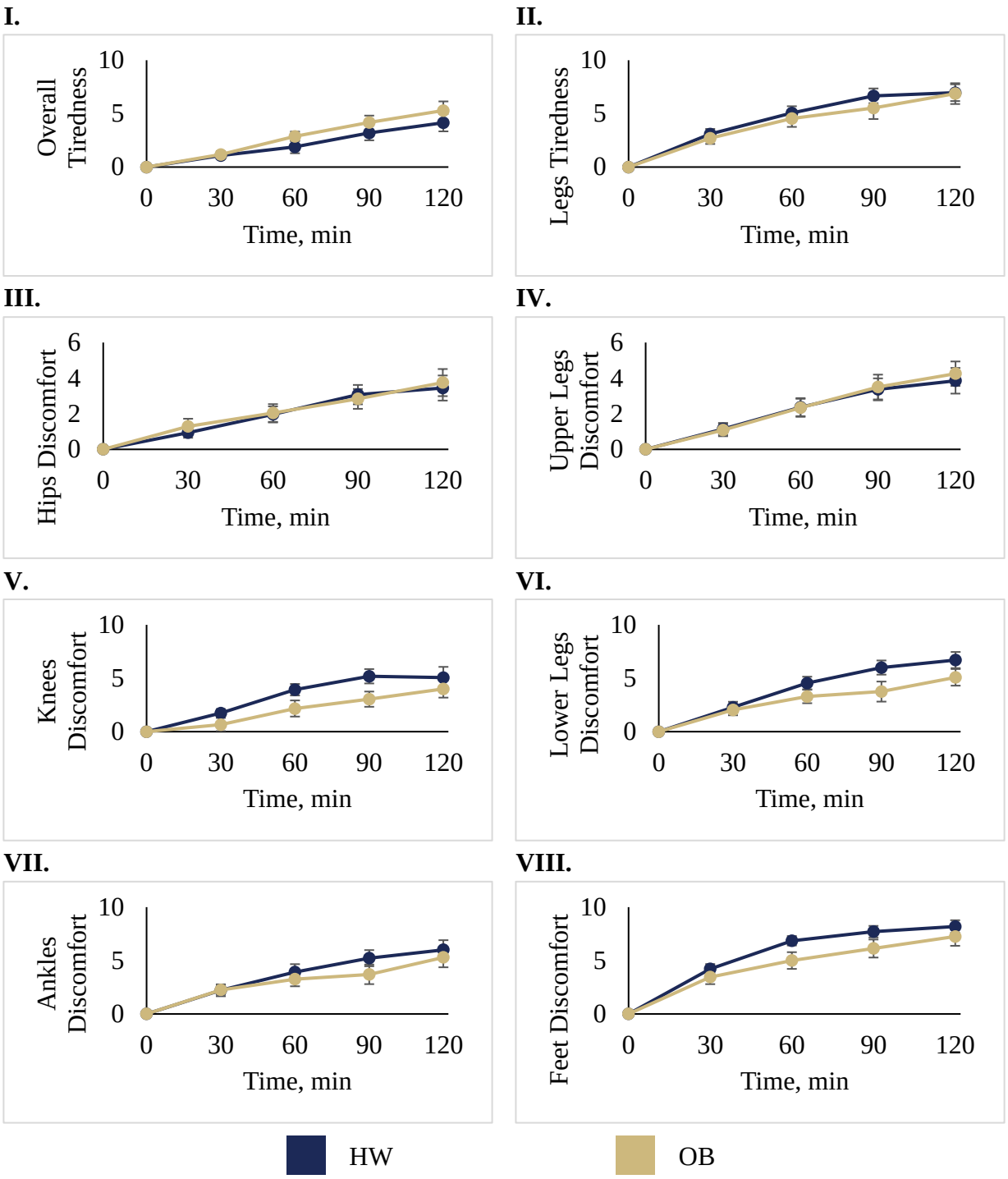

Figure 22: Change in I. Overall tiredness and II. Legs tiredness; and discomfort in III. Hips, IV. Upper Legs, V. Knees, VI. Lower Legs, VII. Ankles, and VIII. Feet from 0 minutes across time, split into BMI groups. Each point represents the average normalized value across subjects. Error bars represent standard error of the mean. No multiple comparisons between time points were performed, as the interaction effects did not indicate significant differences.

The interaction effect of flooring and BMI group was significant for overall tiredness ($F_{1,213}$ = 4.39, p = 0.0374, Figure 23). A Tukey HSD post hoc test was performed to investigate significant differences; however, no significant differences were measured indicating a lack of statistical power for multiple comparisons of overall tiredness data. A Dunnett's test also did not measure any statistically significant differences between the control group (HW, HF) and all other groups. In general, overall tiredness of the HW group slightly decreased on the MT condition in comparison with the HF condition by 0.5 ± 0.4. However, the inverse was true for the OB group: the MT condition increased overall tiredness in comparison with the HF condition by 0.7 ± 0.4.

While the interaction of time, flooring, and BMI group was not a significant factor for overall tiredness, Figure 24 displays how overall tiredness ratings changed over time for each flooring and BMI group. In each case, overall tiredness increased over time. On the HF, both HW and OB groups displayed very similar trends. The total change in overall tiredness over two hours of standing only differed between the HW and OB groups on the HF by 0.5 ± 1.10. When HW subjects stood on the MT condition versus the HF condition, change in overall tiredness over two hours of standing decreased by 1.3 ± 1.1. Alternatively, when the OB group stood on the MT condition versus the HF condition, change in overall tiredness over two hours of standing increased by 1.9 ± 1.1. Each of the four conditions displayed in Figure 24 did not seem to diverge until after 30 minutes of standing.

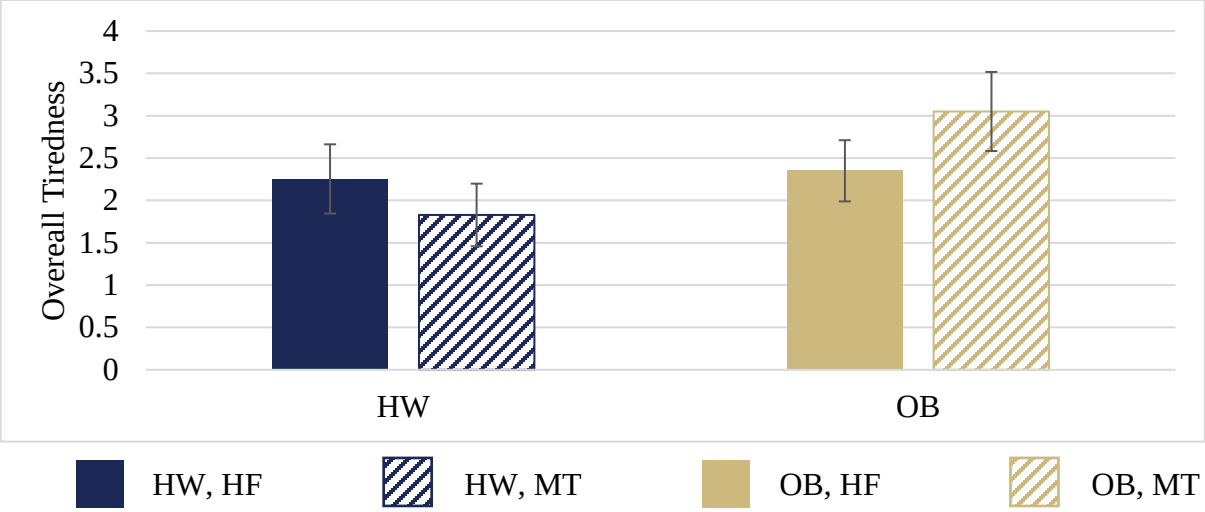

Figure 23: Average overall tiredness ratings across all time points and subjects, split into flooring and BMI groups are displayed. Error bars indicate standard error of the mean. The introduction of the MT condition displays an opposite effect for the HW group versus the OB group. While the main interaction effect was significant, no significant post hoc multiple comparisons were made.

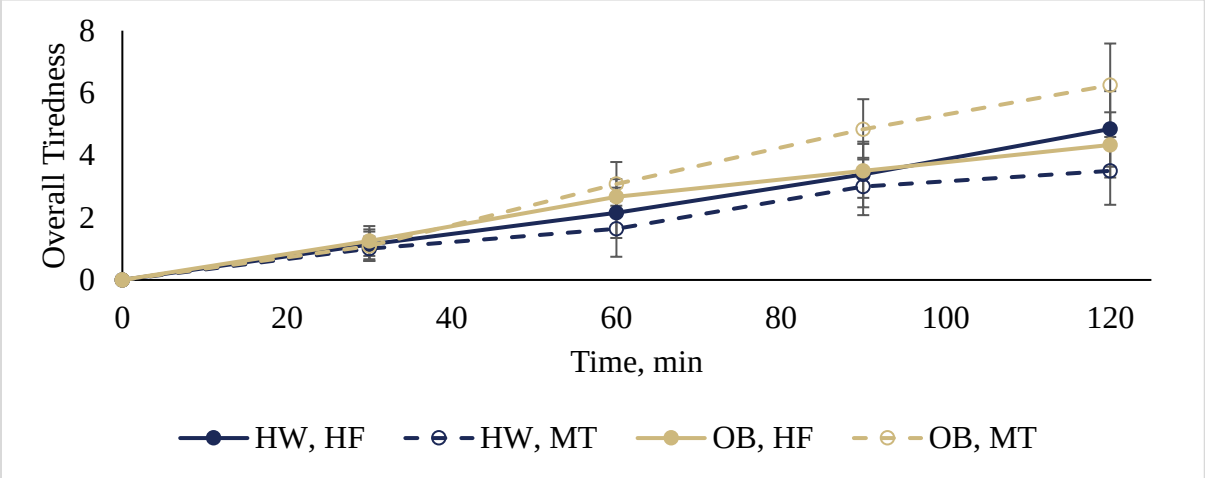

Figure 24: Overall tiredness ratings across subjects, split into flooring and BMI groups over time. Error bars indicate standard error of the mean. The interaction effect of time, flooring, and BMI group was not statistically significant. However, it seems that the MT condition begins to have an effect on overall tiredness after 30 minutes of standing. The MT condition tends to have an opposite effect on HW subjects versus OB subjects—decreasing overall tiredness for HW subjects and increasing overall tiredness for OB subjects.

The interaction effect of flooring and BMI group was significant for feet discomfort ($F_{1,213}$ = 6.61, p = 0.0108). Feet discomfort was significantly higher on the HF (5.30 ± 0.56) than on the MT (3.43 ± 0.52) for the OB BMI group. Within the HW group, the MT condition (5.19 ± 0.43) only slightly decreased feet discomfort in comparison with the HF condition (5.51 ± 0.50). Measures of feet discomfort displayed only a small difference of 0.21 ± 0.50 between HW and OB groups on the HF (Figure 25).

While the interaction effect of time, flooring, and BMI group was not significant for feet discomfort, the graph of each flooring and BMI group over time does display some interesting trends. On the HF, the HW and OB BMI groups display very similar measures of feet discomfort. After two hours of standing, the difference in change in feet discomfort between the HW and OB BMI groups was only 0.03 ± 1.10. When standing on the MT condition versus the HF condition, HW subjects only saw a small decrease in feet discomfort over two hours of standing (0.8 ± 0.87). However, the MT had a larger effect on the OB group—decreasing feet discomfort by 2.7 ± 1.10 after two hours of standing (Figure 26). This decrease begins to emerge by 30 minutes of standing.

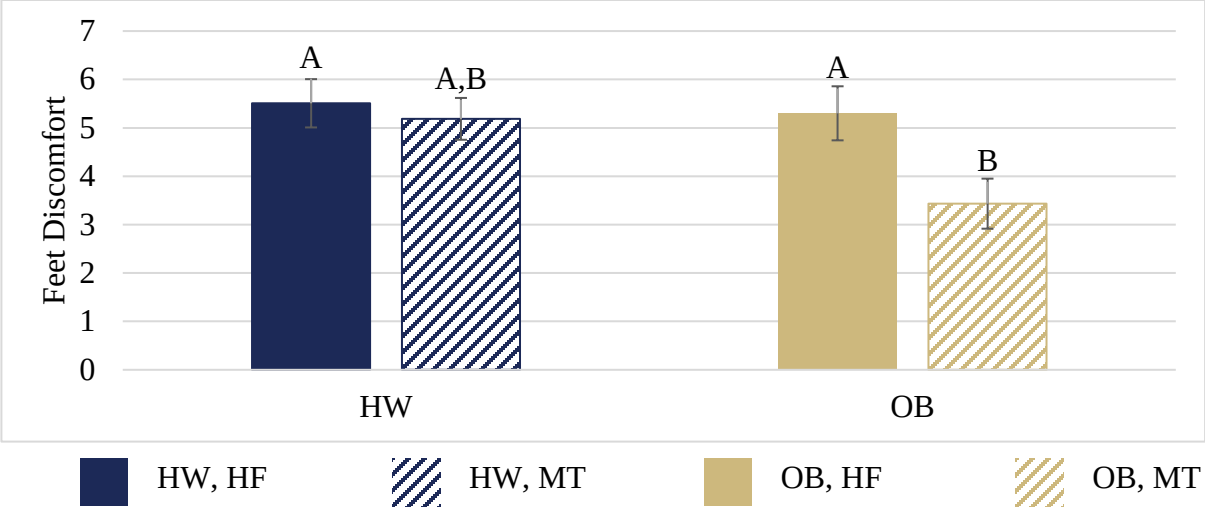

Figure 25: Average feet discomfort ratings across all time points and subjects, split into flooring and BMI groups are displayed. Error bars indicate standard error of the mean. The presence of the MT condition had a significant effect on foot discomfort within the OB group. This effect was not present within the HW group. Bars not connected by the same roman numerals are significantly different.

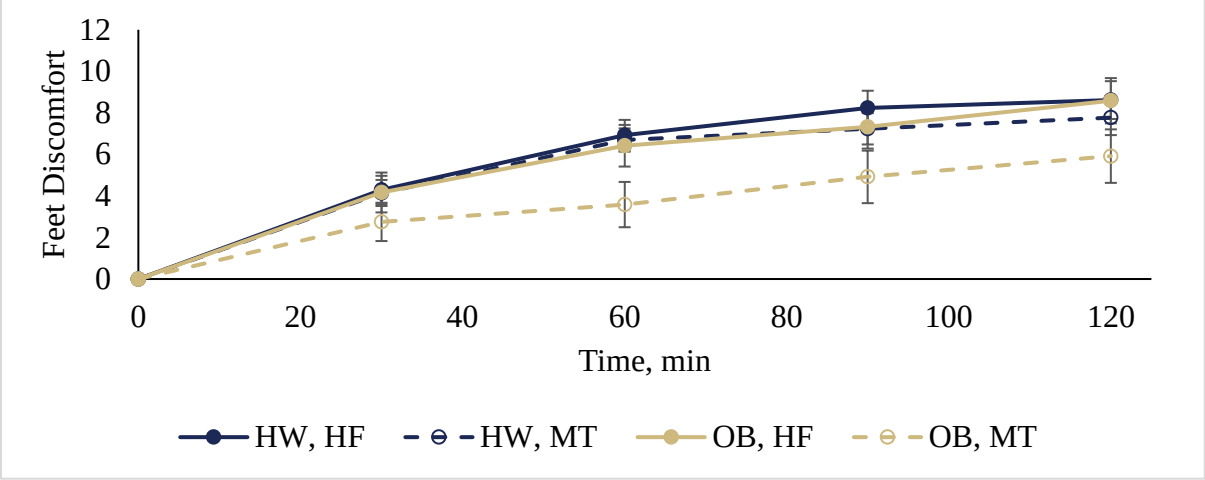

Figure 26: Feet discomfort ratings across subjects, split into flooring and BMI groups over time. Error bars indicate standard error of the mean. The interaction effect of time, flooring, and BMI group was not statistically significant. However, it seems that the MT condition begins to have an effect on feet discomfort for the OB group even by 30 minutes of standing. The MT condition does not seem to have the same effect on the HW group.

4.2 Weight Transfer Measures

4.2.1 Development of a New Method

It has been established that behavioral changes during standing may be related to physiological changes in the muscles and/or joints. The present study hypothesized that behavioral changes—in the form of transfers of weight from one foot to the other—take on different forms. As is explained in section 2.2.2, high frequency and high amplitude weight transfers from one leg to another may be associated with regulating blood flow and blood pooling in the muscles. Alternatively, joint pressure relief may be a function of force and time, due to the viscoelastic nature of cartilage. Therefore, low frequency movements may induce joint pressure relief. To determine if behavioral changes are related to physiological changes in NIRS, EMG, and MTFG, two different types of behaviors were measured: shifts and fidgets. The parameters used to determine when shifts and fidgets occur were informed by behavioral events measured by Cham and Redfern (CWS) and Wiggermann and Keyserling (WWS) [1, 11].

Proportion of bodyweight over the right foot (P_R) for a typical subject is displayed in Figure 27, I. The total number of CWS measured every five minutes of standing are displayed in Figure 27, II. Throughout 2 hours of standing, this subject performed a total of 3,652 CWS. The number of events increased over time, from 9 CWS from 0 - 5 minutes, to a maximum of 283 CWS occurring from 95 – 100 minutes. This translates to movements occurring at a frequency of 0.94 movements per second. Figure 27, III displays standing data for this subject between 95 and 97 minutes of standing. During this time, the subject continuously transferred weight between feet. For this subject, no WWS were measured throughout two hours of standing.

I.

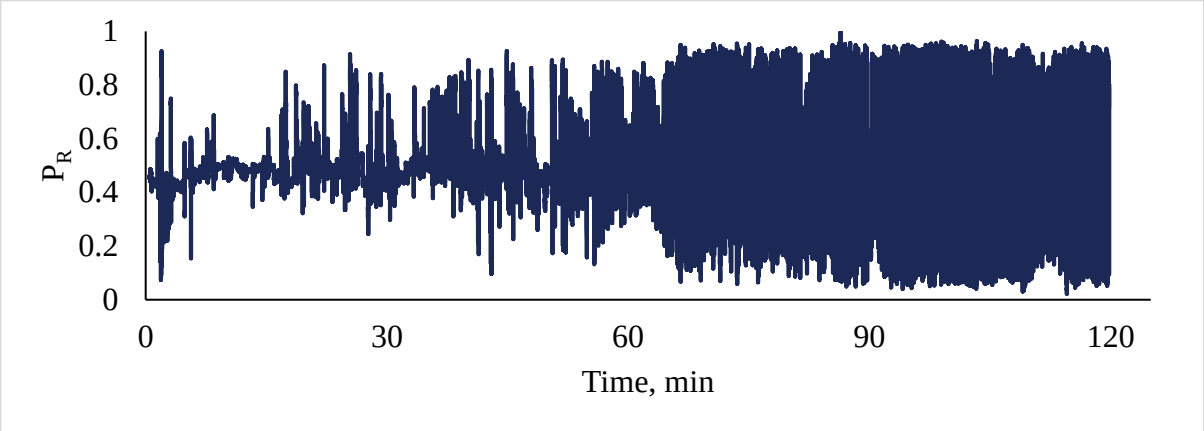

II.

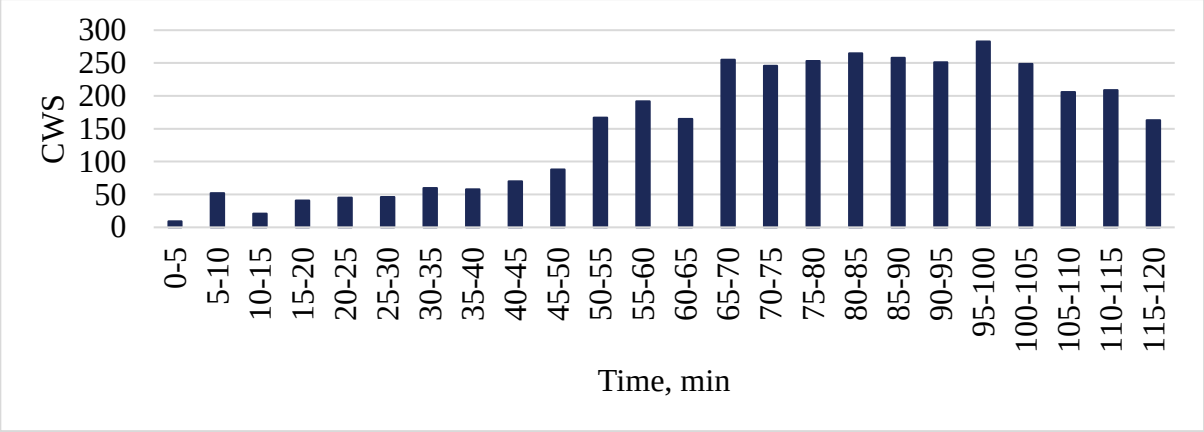

III.

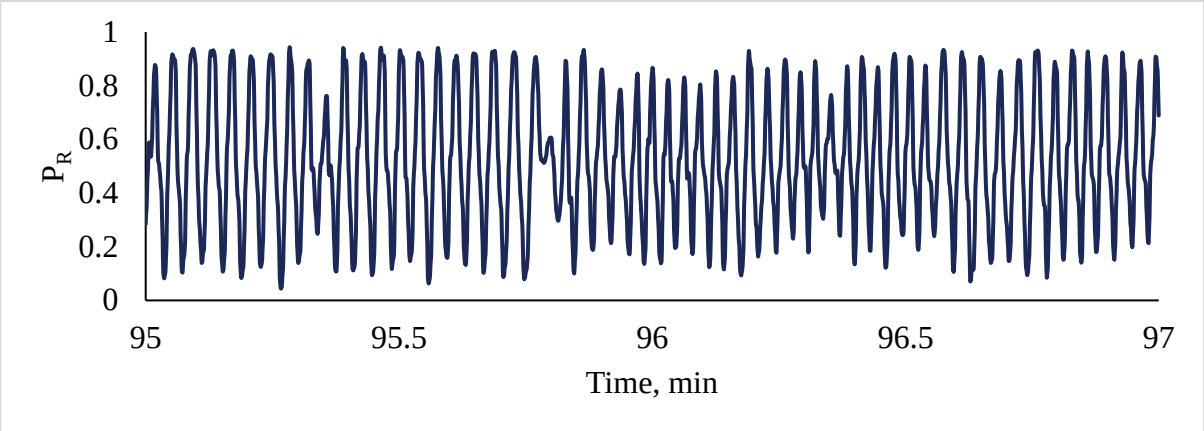

Figure 27: HW subject standing on a HF condition (S10). I. P_R data for two hours of standing. Movement amplitudes and frequencies seem to increase over time. II. CWS counted every five minutes over two hours of standing. The number of CWS over time tends to increase, with a maximum number of CWS occurring between 95 and 100 minutes (283 shifts). III. P_R between 95 and 97 minutes of standing. This subject continuously transferred weight between the right and left side.

Figure 28 displays data for another typical subject that showed a different movement pattern than that displayed in Figure 27. Figure 28, I displays P_R throughout two hours of standing. In comparison with the subject displayed in Figure 27, I, this subject maintained movement throughout the duration of standing. Furthermore, movement amplitudes and frequencies were not as high as those displayed by the subject in Figure 27, I. CWS and WWS are displayed in Figure 28, II and III, respectively. This subject performed 364 CWS, approximately 10% the number of CWS of the subject displayed in Figure 27. The number of CWS in Figure 28, II did not seem to increase over time. Figure 28, III displays the number of WWS over two hours of standing for this subject, which increased over time. Figure 29, I displays an example of the events that were measured as CWS and not WWS over two minutes of standing. The occurrence of CWS were at a much lower frequency (0.0075 movements per second) than those displayed in Figure 27, III. The CWS displayed in Figure 28, III were not registered as WWS because their amplitude of 0.8 bodyweight was not maintained for at least 7.5 seconds. In some cases, the amplitude did not reach 0.8 bodyweight at all. Figure 29, II displays an example of two WWS: a WWS to > 0.8 BW and another back to $0.2 < P_R < 0.8$.

I.

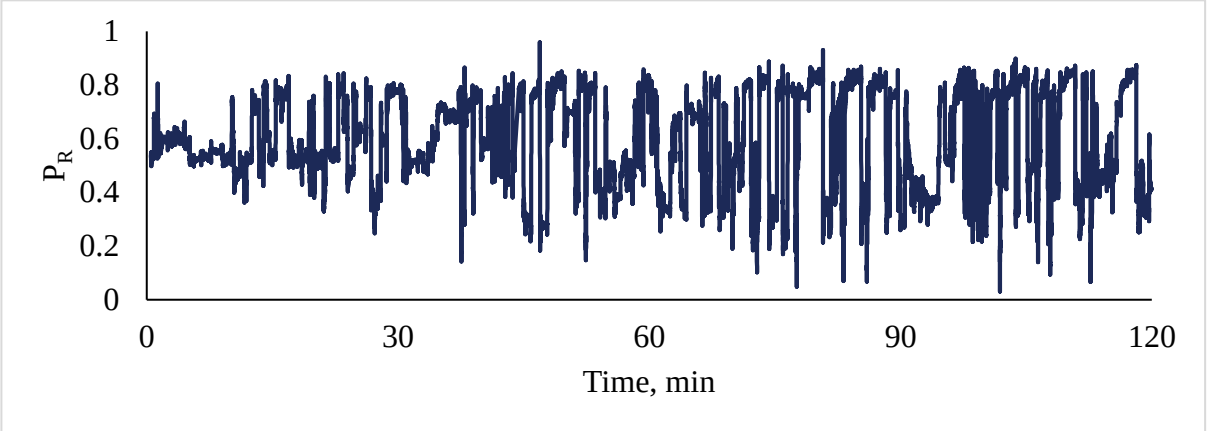

II.

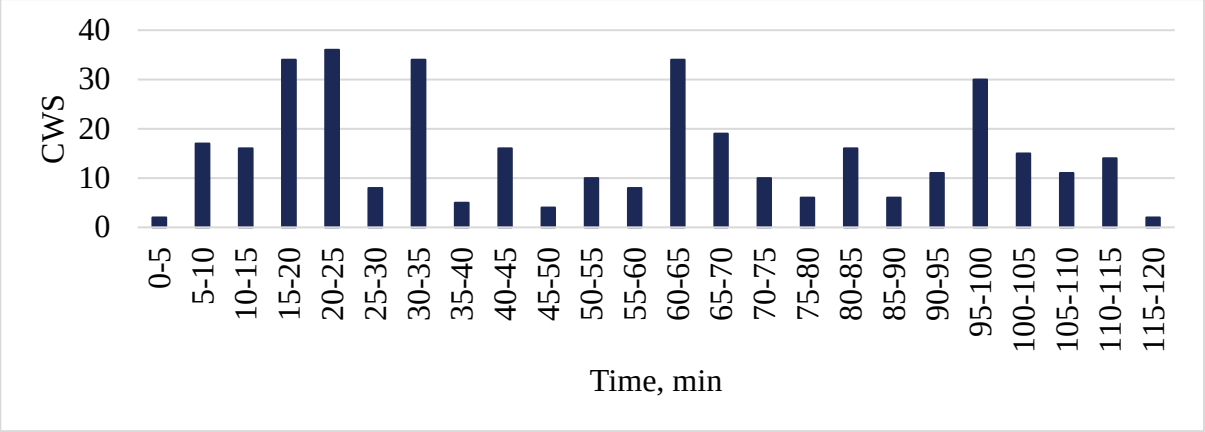

III.

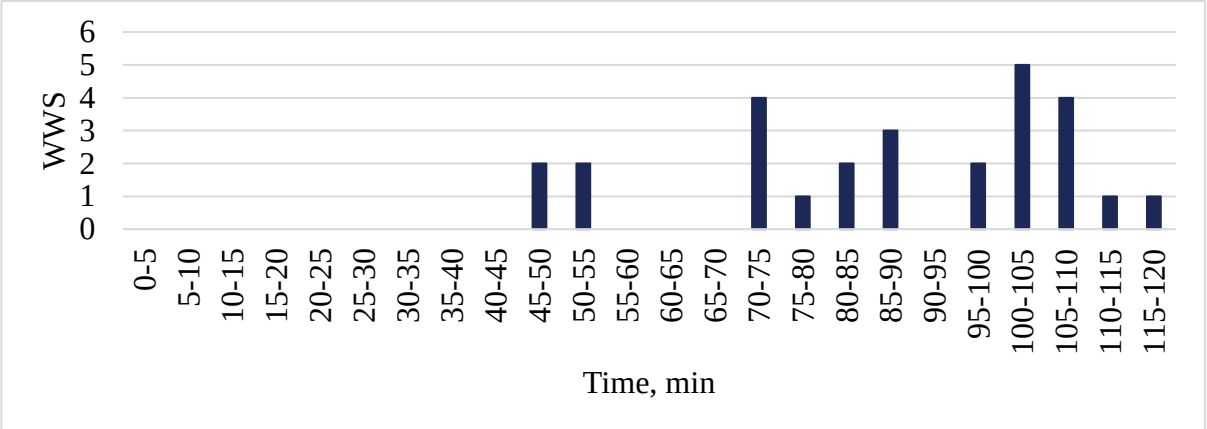

Figure 28: OB subject standing on a HF condition (S21). I. P_R data for two hours of standing. Movement amplitudes and frequencies do not seem to increase over time. II. CWS counted every 5 minutes over two hours of standing. The number of CWS does not seem to increase over time. III. WWS counted every 5 minutes over two hours of standing. The number of WWS increases over time for this subject.

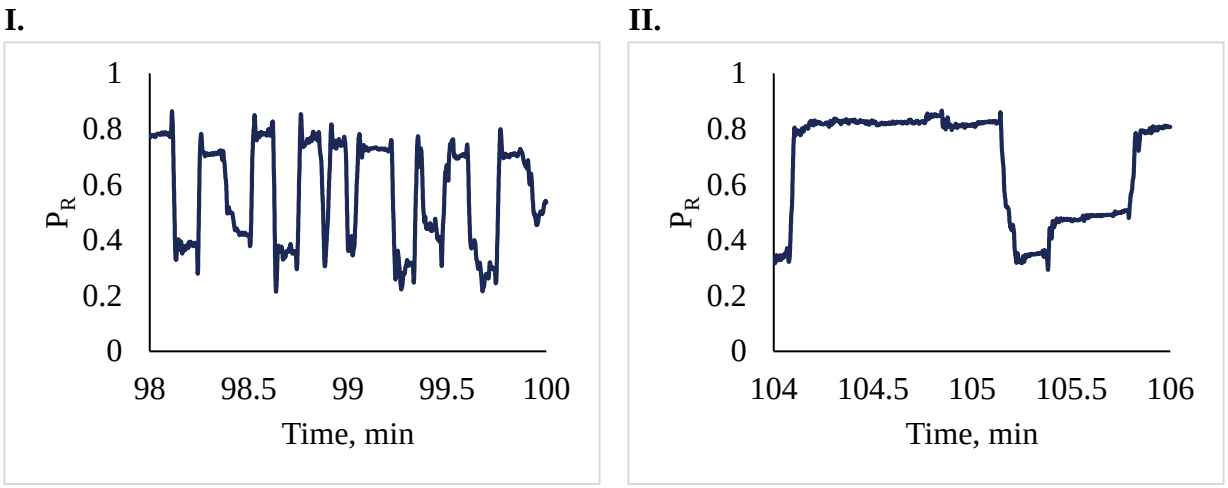

Figure 29: Selection of data from Figure 28. I. P_R over a 2 minute time period between 98 and 100 minutes of standing. Movements were recorded as CWS, but not as WWS. II. P_R over a 2 minute time period between 104 and 106 minutes of standing. This stepwise movement was registered as both a CWS and WWS.

Two types of behavioral strategies were measured during prolonged standing for the present study: shifts and fidgets. Occurrences of these strategies in time are referred to as events. Both strategies required measuring movement beyond predetermined force and temporal boundary conditions. Boundary conditions were informed by a combination of this study's data set and prior published research. The average mean P_R across all subjects was 0.50 ± 0.03 BW, with a minimum value of 0.43 and a maximum value of 0.60. "Center" was therefore set at the mean P_R across all subjects plus or minus a proportion of bodyweight, considered "boundaries," that was informed based on this study's data set. The range of BW that was considered "center" was informed by subject data through a process in which boundary conditions were iteratively changed and the number of events were determined and compared. The goal of this process was to determine what maximum boundary conditions were required to optimize the number of total events measured. Following determination of force boundary conditions, a temporal threshold was introduced to split events into shifts and fidgets.

Boundaries were set at 0.50 BW ± *y*, where *y* was 0 through 0.49 BW. The number of times a subject crossed these boundaries were counted every five minutes throughout two hours of standing (Figure 30, I). With boundaries at 0.50 ± 0 BW, 0 movements were recorded. When boundaries were low (between 0.01 – 0.05 BW), a large number of events were measured. This was expected, as the average range of COP (related to P_R) is approximately 20% of the total range, which translates to approximately 0.50 ± 0.10 BW [108]. As boundaries increased towards 0.49, the number of events measured flattened and eventually approached 0 again. To determine where the "flattening" region began, the slope of each line was calculated (Figure 30, II). Figure 30, III is Figure 30, II zoomed in on where slope approaches 0. Dunnett's t tests were performed to determine at which boundary condition the slope of time curves was significantly different from 0. The first boundary condition that was not significantly different from 0 was 0.13 BW. Because of this, 0.50 ± 0.13 BW was chosen as the boundary set for this project.

Once force boundary conditions were set, temporal thresholds were chosen to differentiate standing strategies. A fidget was defined as a movement out of or back into center that did not have a minimum time threshold associated with it. Any movement out of or back into center that lasted at least 7.5 seconds was considered a shift. The time threshold of 7.5 seconds was informed by the time threshold set by Wiggermann and Keyserling [11]. Therefore, fidgets and shifts at any single time point were mutually exclusive.

I.

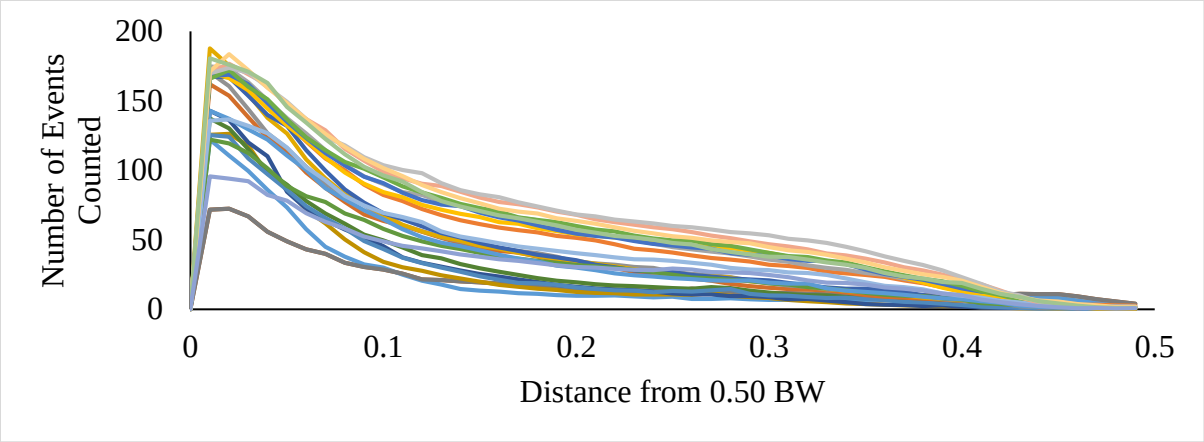

II.

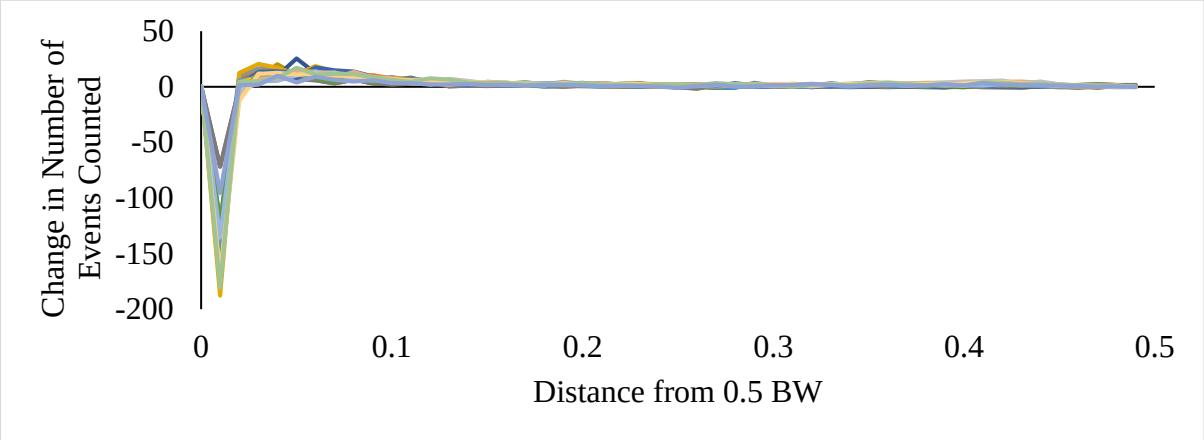

III.

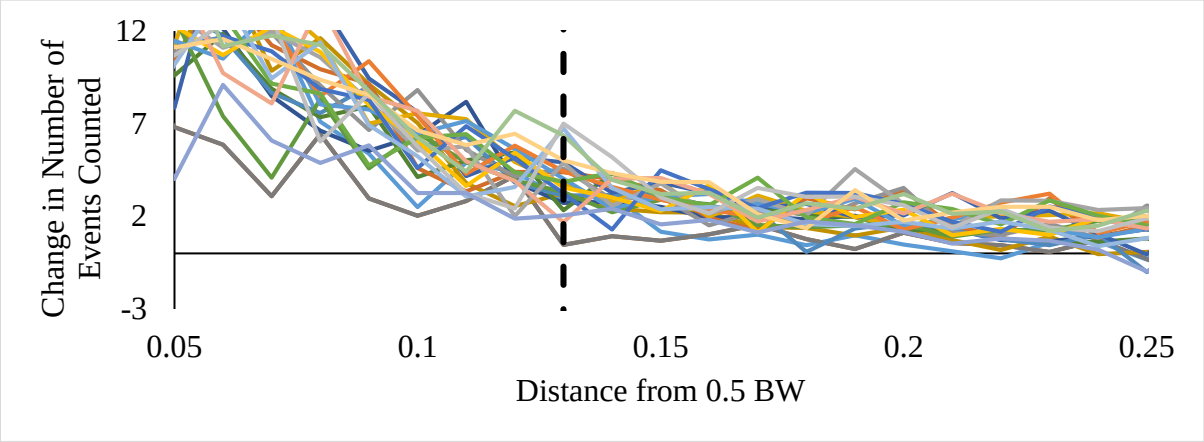

Figure 30: I. Each line represents the average number of events counted within a single five minute block of time across all subjects. This was performed iteratively for boundary conditions ranging from 0.01 BW to 0.49 BW. II. Slope of each line was calculated and plotted. III. The plot in II is zoomed in. at about 0.13 BW is where the slopes start to approach 0. This is where the amplitude boundary condition was set.

4.2.2 Comparison of Methods

Two sets of analyses were completed to determine if and how CWS, WWS, S, and F were related. A Pearson's correlation compared CWS, WWS, shifts, fidgets, and total events (Table 10). All methods were significantly correlated with one another. Interestingly, methods that have a time threshold (WWS and shifts) were negatively or more weakly correlated with those that don't have a time threshold (CWS and fidgets). The total events measured using the proposed method were highly positively correlated with methods that do not require a time threshold (CWS and fidgets) but were more weakly correlated with methods that have a time threshold (WWS and shifts).

Table 10: Pearson's correlation between methods of measuring behaviors during prolonged standing. *p* < *0.0001 **, *p* < *0.001 ***, *p* < *0.01 ****

	CWS	WWS	Shifts	Fidgets
CWS				
WWS	ρ = -0.0943 **			
Shifts	ρ = -0.1320 ****	ρ = 0.7927 ****		
Fidgets	ρ = 0.6210 ****	ρ = 0.1037 ***	ρ = -0.1003 ***	
Total Events	ρ = 0.6103 ****	ρ = 0.1434 ****	ρ = 0.1506 ****	ρ = 0.9987 ****

A one-way analysis of variance was performed to test if event counts produced by the different method types over two hours of standing were significantly different (CWS, WWS, shifts, fidgets, total events). Figure 31 displays average counts measured over two hours of standing by each method. CWS are significantly higher than all other methods (978.56 ± 87.40 CWS). WWS (11.63 ± 2.57 WWS) and shifts (22.20 ± 3.92 shifts) counted the least number of movement events

and were significantly different than the rest of the methods, but not each other. Fidgets (397.78 ± 83.66 fidgets) and total events (419.98 ± 84.16 events) were significantly different than the rest of the methods, but not each other.

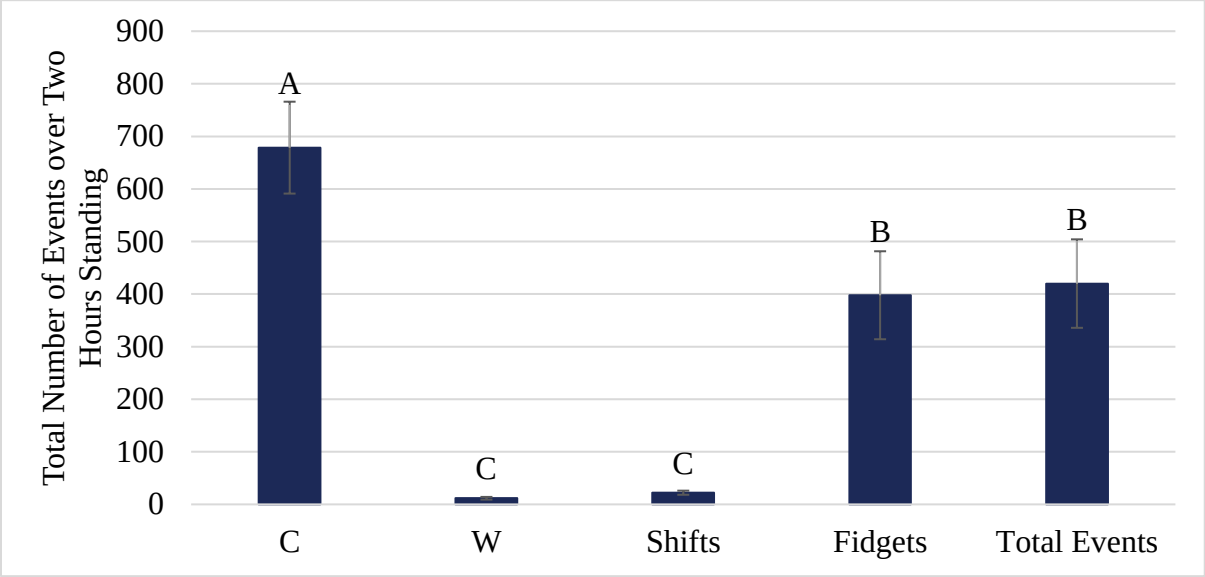

Figure 31: Average number of movement events registered every five minutes throughout two hours of standing. Each bar represents a single method. Error bars are standard error of the mean. Bars labeled with different letters are significantly different.

4.2.3 Standing Strategies during Prolonged Standing

A repeated measures mixed effects model was performed to determine if shifts, fidgets, and total events changed significantly with flooring condition, BMI group, and time (Table 11). A full factorial analysis was performed. First, numbers of shifts, fidgets, and total events were normalized to the number performed within the first five minutes of standing. Then normalized shifts, fidgets, and total events were transformed prior to analysis. Graphs representing statistically

significant results are included in this section, while graphs of non-significant results are included in the Appendix. Graphs represent the change in observed shifts, fidgets, and total events from the first block of time (prior to transformation). Total events and fidgets trends were very similar, given that there were a total number of 22,679 total events displayed throughout the whole study. Of those, 21,480 were fidgets and 1199 were shifts—this translates to 94.7% of total events being fidgets.

Shifts ($F_{23,958} = 7.23$, $p < 0.0001$), fidgets ($F_{23,851} = 24.08$, $p < 0.0001$), and total events ($F_{23,855} = 26.93$, $p < 0.0001$) changed significantly with time (Figure 32, I-III). A Dunnett's test was performed to determine which values are significantly different from zero minutes of standing. Average number of shifts were significantly different from 0 by 20 minutes of standing ($p = 0.0343$) and remained significantly different from 0 shifts for the remainder of the standing trial. Average number of fidgets and total events became significantly different from 0 by 5 minutes of standing ($p < 0.0001$).

Table 11: Results from repeated measures mixed effects model investigating the effects of flooring (F), BMI (B), and time (T) on shifts, fidgets, and total events performed during standing. ***p < 0.0001 ****, p < 0.001 ***, p < 0.01 **, p < 0.05 *, p > 0.05 NS***

	Log[Shifts+1]	Log[Fidgets+1]	Log[Total Events +1]
T	$F_{23,958} = 7.23$ ****	$F_{23,851} = 24.08$ ****	$F_{23,855} = 26.93$ ****
F	$F_{1,971} = 1.45$ NS	$F_{1,867} = 0.03$ NS	$F_{1,871} = 0.43$ NS
B	$F_{1,26} = 2.77$ NS	$F_{1,28} = 7.93$ **	$F_{1,28} = 8.19$ **
F x B	$F_{1,971} = 4.42$ *	$F_{1,867} = 0.03$ NS	$F_{1,871} = 0.01$ NS
F x T	$F_{23,958} = 0.64$ NS	$F_{23,851} = 0.54$ NS	$F_{23,855} = 0.48$ NS
B x T	$F_{23,958} = 1.68$ *	$F_{23,851} = 2.02$ **	$F_{23,855} = 1.79$ *
F x B x T	$F_{23,958} = 1.13$ NS	$F_{23,851} = 0.87$ NS	$F_{23,855} = 0.84$ NS

I.

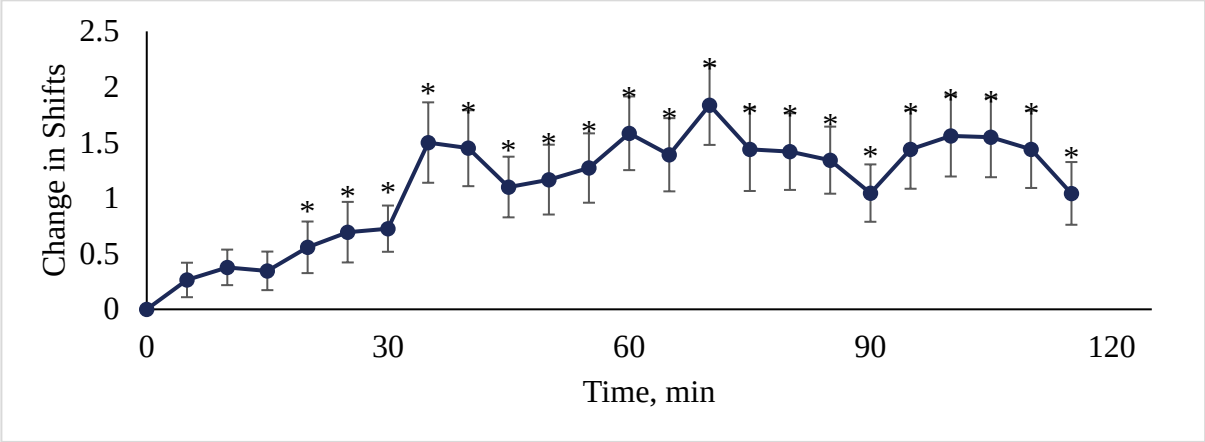

II.

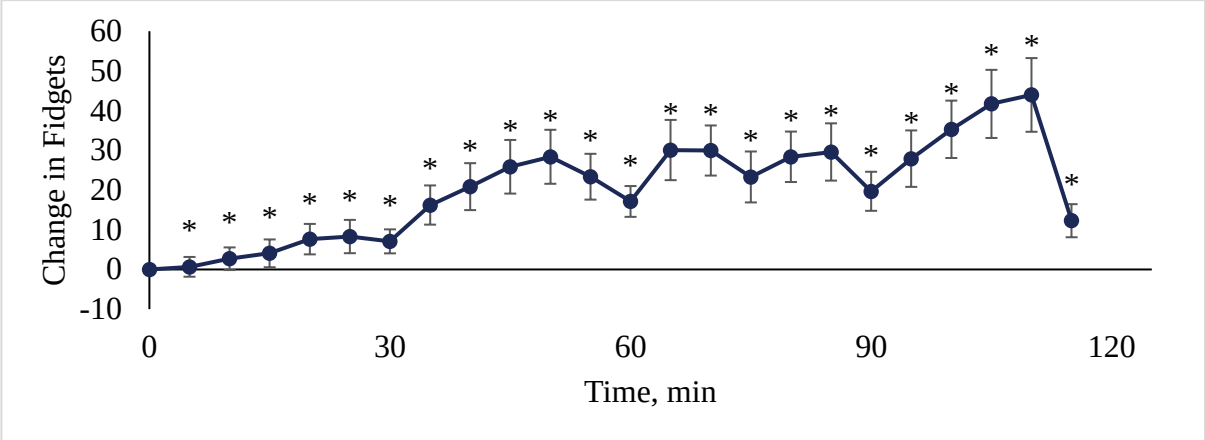

III.

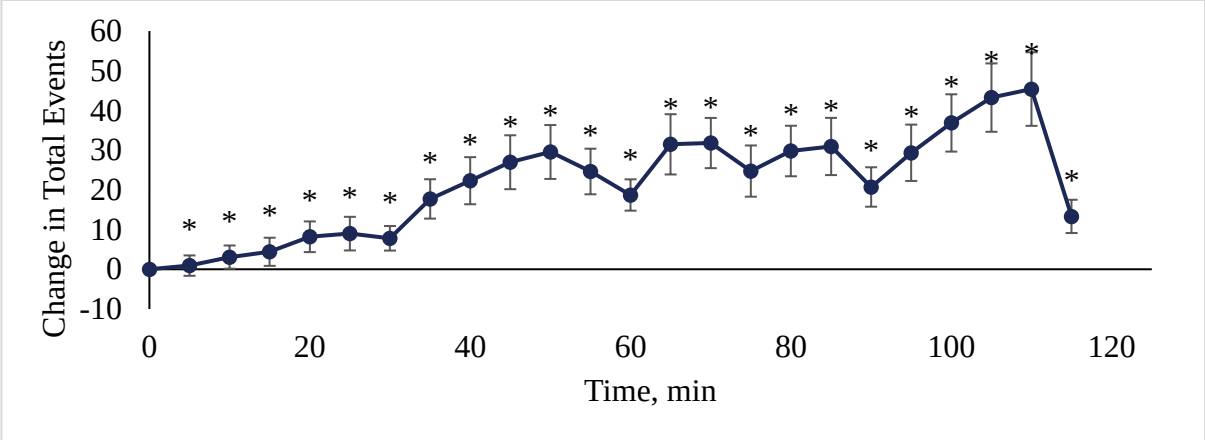

Figure 32: Time was a significant factor for I. Change in shifts, II. Change in Fidgets, and III. Change in total events. Error bars are standard error of the mean. Asterisks (*) represent time points that are significantly different from 0.

BMI group was a significant factor for fidgets ($F_{1,28} = 7.9310$, $p = 0.0088$) and total events ($F_{1,28} = 8.19$, $p = 0.0079$). Figure 33 I, II displays the average number of fidgets and total events, respectively, performed every five minutes across all subjects and time points, split into BMI groups. The number of fidgets (13.17 ± 1.06 fidgets) and total events (14.02 ± 1.07 events) performed by the HW group were significantly lower than those performed by the OB group (26.97 ± 2.27 fidgets, 28.32 ± 2.28 total events).

The interaction effect of flooring condition and BMI group was significant for shifts ($F_{1,971} = 4.42$, $p = 0.0358$, Figure 34). A Tukey HSD test was performed to determine significant differences between groups. No significant differences were found. However, a Dunnett's test was performed to compare all groups to the control group (HW, HF). According to this analysis, changes in shifts within the HW group on the MT condition (0.72 ± 0.10 shifts) are significantly less than on the HF condition (0.85 ± 0.11 shifts). This group is indicated in Figure 34 with an asterisk (*).

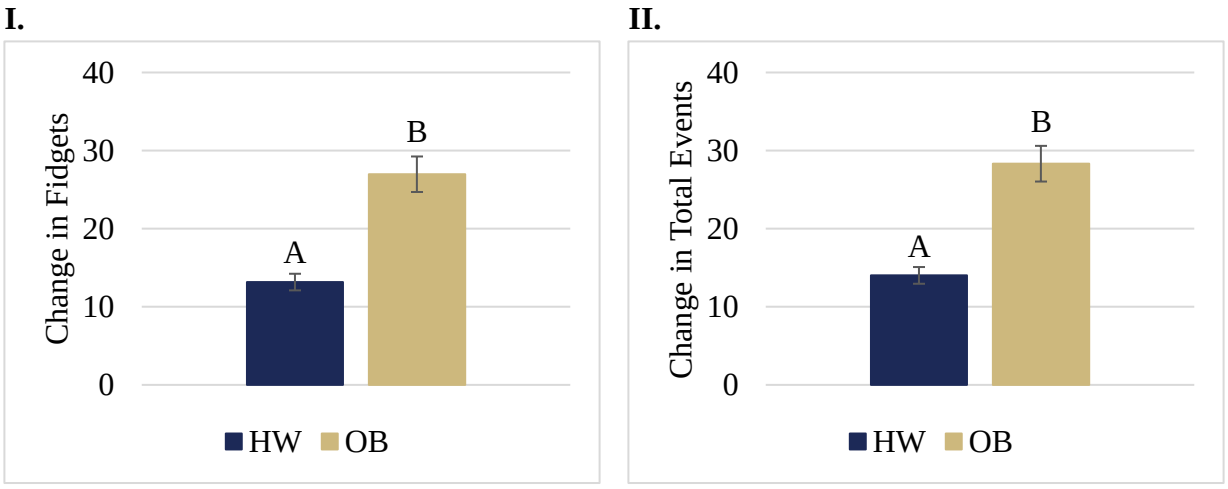

Figure 33: Average number of I. fidgets and II. Total events performed every 5 minutes across all flooring conditions and time points, split into BMI group. Error bars are standard error of the mean. Bars labeled with different letters are significantly different.

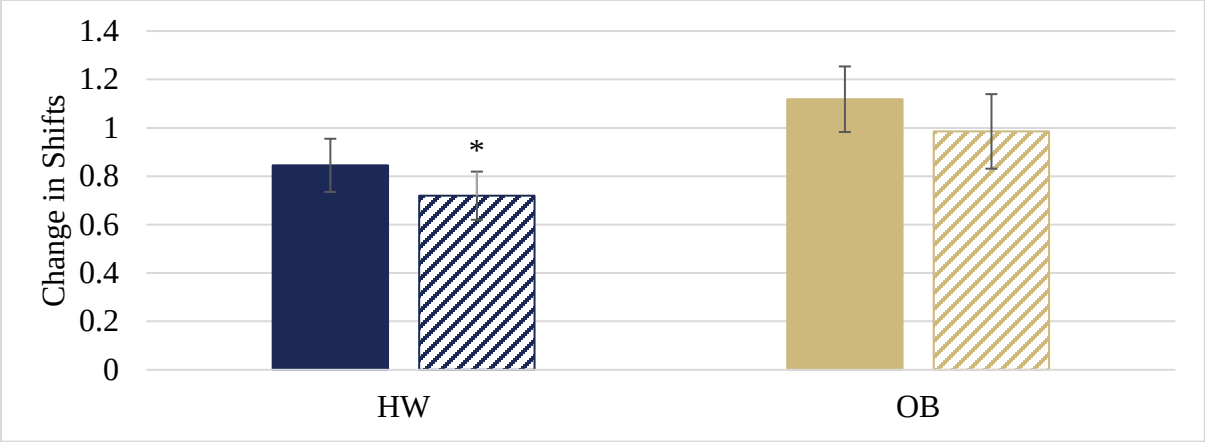

Figure 34: The interaction effect of flooring condition and BMI group is a significant factor for changes in shifts. Bars are the average change in shifts across all subjects and time points, split between BMI group and flooring conditions.

The interaction effect of BMI group and time was significant for changes in shifts ($F_{23,958}$ = 1.68, p = 0.0234), changes in fidgets ($F_{23,851}$ = 2.02, p = 0.0031), and changes in total events ($F_{23,855}$ = 1.79, p = 0.0129) (Figure 35, I-III). A Tukey HSD post hoc analysis of changes in shifts indicated that significant changes occurred over time within each BMI group. Change in shifts became significantly different from 0 at 50 minutes of standing for the HW group and 35 minutes for the OB group. Change in fidgets and total events were significantly different from those at zero minutes of standing at all time points. The point at which changes in shifts, fidgets, and total events became significantly different from 0 are labeled with A for the HW BMI group and B for the OB BMI group. No significant differences were found in changes in shifts, fidgets, and total events between BMI groups at each discrete time point. However, change in shifts, fidgets, and total events within the OB BMI group consistently displayed higher levels of shifts, fidgets, and total events throughout the course of standing than the HW group.

I.

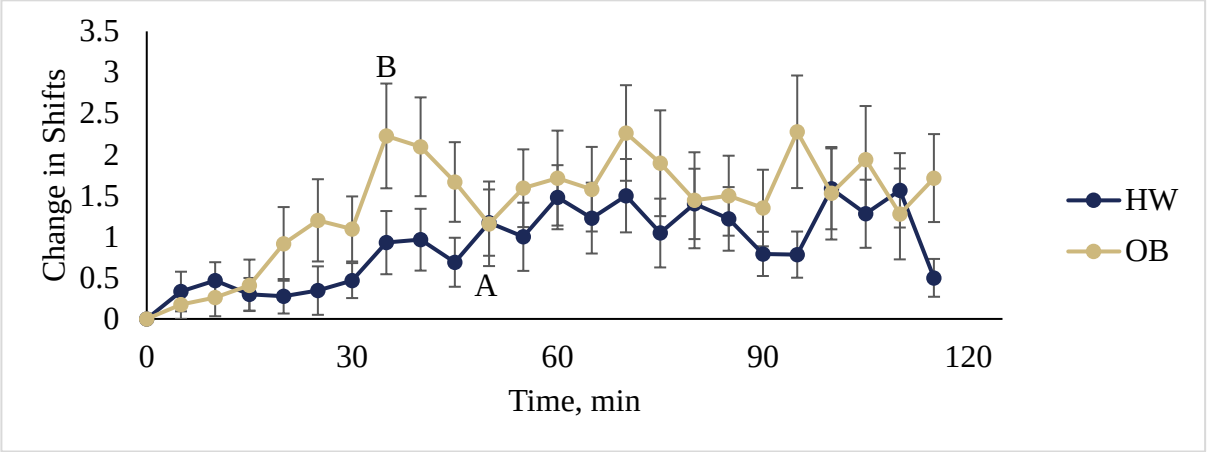

II.

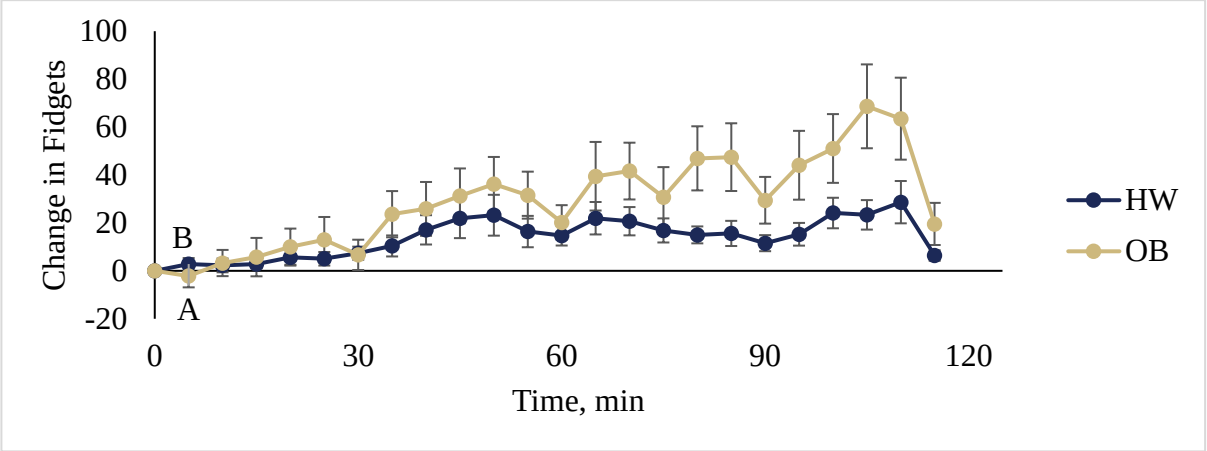

III.

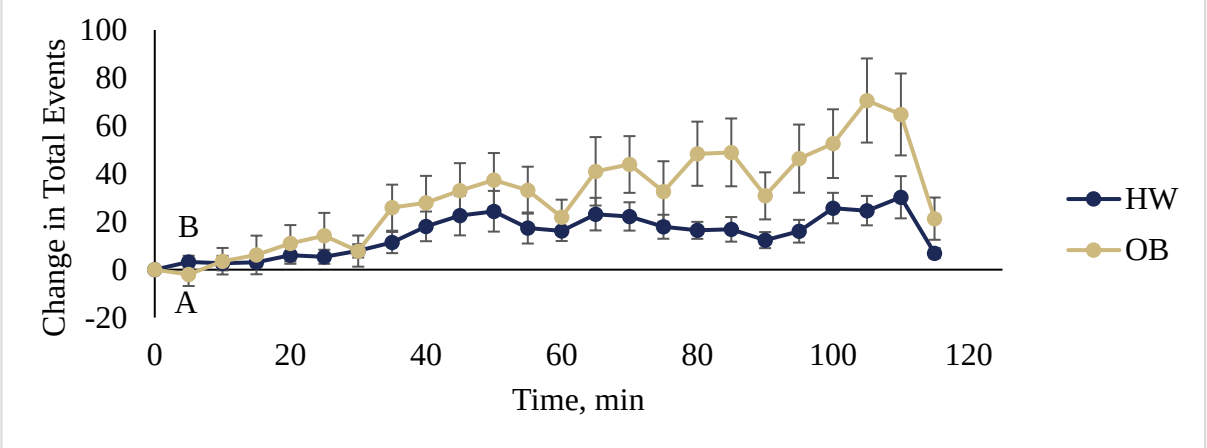

Figure 35: The interaction effect of flooring condition and BMI group is a significant factor for the change in I. Shifts, II. Fidgets, and III. Total events. Points represent average values across all subjects and flooring conditions split into BMI groups. Error bars are standard error of the mean. Letters represent time points that were significantly different from 0.

4.2.4 Standing Strategies and Subjective Tiredness and Discomfort

Pearson correlations compared standing strategies to tiredness and discomfort measures (Table 12). The total number of shifts and fidgets performed every 30 minutes were compared with subjective tiredness and discomfort measured every 30 minutes. Shifts were significantly correlated with hips ($p = 0.0008$) and upper legs ($p = 0.0408$). Fidgets were significantly correlated with overall tiredness ($p < 0.0001$), legs tiredness ($p < 0.0001$), upper legs ($p = 0.0012$), knees ($p = 0.0070$), lower legs ($p = 0.0404$), ankles ($p = 0.0444$), and feet ($p = 0.009$). Similarly, total events were significantly correlated with overall tiredness ($p < 0.0001$), legs tiredness ($p < 0.0001$), upper legs ($p = 0.0008$), knees ($p = 0.0052$), lower legs ($p = 0.0361$), ankles ($p = 0.0391$), and feet ($p = 0.0253$).

Table 12: Pearson correlations were performed to determine if tiredness and discomfort measures were related to standing strategies. ***p < 0.0001 ****, p < 0.001 ***, p < 0.01 **, p < 0.05 *, p > 0.05 NS***

	Shifts	Fidgets	Total Events
Overall Tiredness	$\rho = 0.1367^{NS}$	$\rho = 0.4073$ ****	0.4145 ****
Legs Tiredness	$\rho = -0.0027^{NS}$	$\rho = 0.3186$ ****	0.3198 ****
Hips	$\rho = 0.2364$ ***	$\rho = 0.0901^{NS}$	0.1003^{NS}
Upper Legs	$\rho = 0.1455$ *	$\rho = 0.2292$ **	0.2361 ***
Knees	$\rho = 0.0478^{NS}$	$\rho = 0.1913$ **	0.1979 **
Lower Legs	$\rho = 0.0644^{NS}$	$\rho = 0.1458$ *	0.1490 *
Ankles	$\rho = 0.0750^{NS}$	$\rho = 0.1431$ *	0.1467 *
Feet	$\rho = 0.0805^{NS}$	$\rho = 0.1589$ *	0.1629 *

4.3 Knee Joint Measures

4.3.1 Introduction to MTFG Data Analysis

Each trial, collected at a discrete time point during standing, contained approximately ten frames of images that could be used to measure MTFG and kinematics data. Kinematics measurements represent tibia movements in relation to the femur. Measured positive knee flexion is associated with flexion of the femur in relation to the tibia. Measured positive abduction is associated with adduction of the femur and a valgus rotation of the knee. Positive measured external rotation represents internal rotation of the femur over the tibia. Subjects were instructed to stand up straight when images were collected, but specific knee kinematics were not restricted during imaging. As such, changes in knee kinematics within subjects and between trials influenced MTFG data.

Figure 36 displays MTFG data for two subjects, which resulted in different trends in MTFG over two hours of standing. Each data point represents the average MTFG value collected for all frames at that time point. S10 (Figure 36, I) displays an expected decrease in MTFG, followed by an unexpected upwards trend in MTFG after 30 minutes of standing. S05 (Figure 36, II) displays no discernable trend in MTFG over time. Due to the variability displayed in MTFG data, a multistep process was performed to determine possible knee kinematic influences on MTFG data and fit a model to the data to measure changes in MTFG due to prolonged standing. Steps included: (1) exploration of a relationship between kinematics and MTFG as a possible source of error; (2) selection of a piecewise model to represent MTFG data for each standing visit; and (3) analysis of parameters derived from the piecewise model. Parameters derived from the piecewise model were terminal gap (G_T) and time at which terminal gap was reached (T_T).

I.

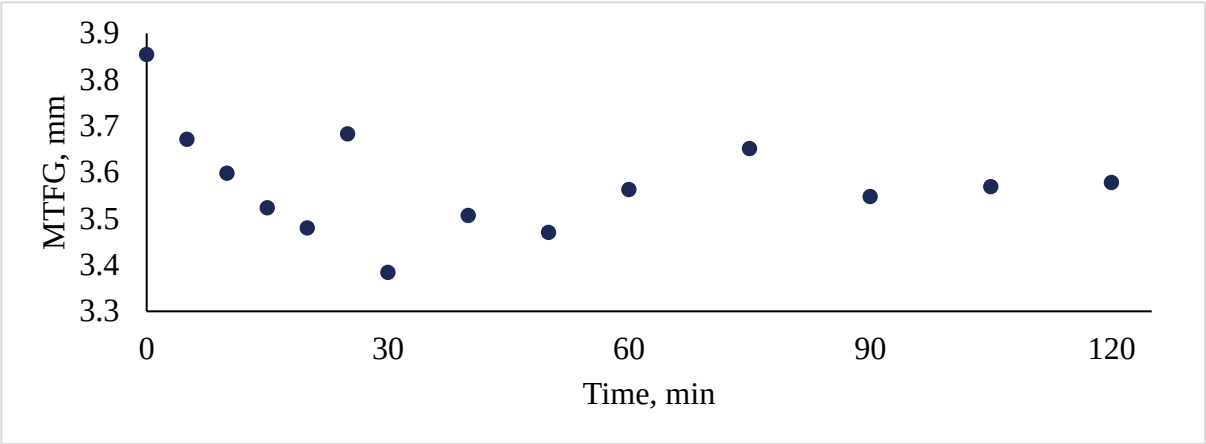

II.

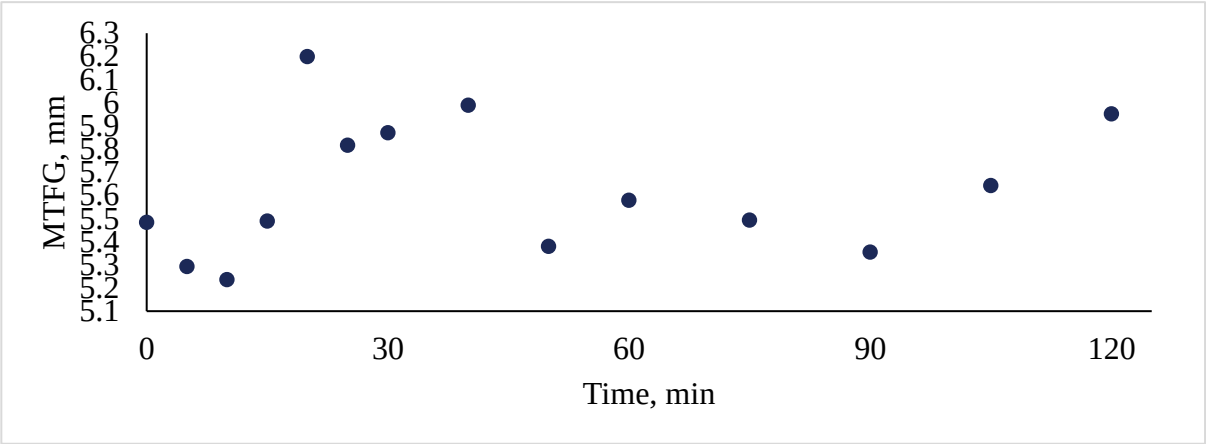

Figure 36: MTFG of two typical subjects. I. S10 (HF condition) MTFG seems to decrease over two hours of standing. However, MTFG unexpectedly increases again after 30 minutes of standing. II. S05 (HF condition) MTFG does not display any discernable changes in MTFG over time. These unexpected trends warranted an investigation of sources of variance in data, as well as development of a piecewise model to fit and analyze the data.

4.3.2 Exploration of the Relationship between MTFG and Kinematics during Prolonged Standing

Preliminary analysis of MTFG data indicated a relationship between knee kinematics and MTFG. A Pearson correlation was performed for all subjects comparing MTFG with knee flexion, abduction, and external rotation. Results of this overall Pearson correlation analysis are displayed in Table 13. Knee abduction and external rotation were significantly correlated with MTFG. Knee abduction was most highly correlated with MTFG, while knee flexion was least correlated with MTFG. However, the correlation coefficients were very low.

Table 13: Pearson correlation results comparing MTFG with flexion, abduction, and external rotation using all subject data. ***p < 0.0001 ****, p < 0.05 *, p > 0.05 NS***

	MTFG
Flexion	$\rho = 0.0076^{NS}$
Abduction	$\rho = 0.2111$ ****
External Rotation	$\rho = 0.1002$ *

Further inspection of the correlation between MTFG and knee kinematics was performed within each subject. This was warranted because the relationship between kinematics and MTFG has been shown to be related to knee morphology and other subject specific factors [63, 98]. For the purposes of these analyses, data from both visits were combined. Results from this analysis are displayed in Table 14. Subjects displayed different patterns of correlation between MTFG and knee flexion, abduction, and external rotation. Sixteen subjects displayed a significant correlation between MTFG and knee flexion. Out of those subjects, all but one was positively correlated with MTFG. Seven subjects displayed significant correlations between MTFG and knee abduction—

all of which were negatively correlated. Finally, six subjects displayed significant correlations between MTFG and knee external rotation all of which were positively correlated. Row-wise, the combination of significant and non-significant correlations within subjects did not show any distinct pattern. A multitude of subjects did not show any significant correlations between MTFG and kinematics (S03, S06, S07, S10, S15, S17, S26, S27, S29, S31). Some subjects (S05, S14, S22, S25) displayed significant correlations between MTFG and all knee kinematic rotations. Figure 37 contains a flow chart that displays an interpretation of these correlations and how they related to cartilage compression.

Two representative subjects are displayed in Figure 38. These are the same subjects that are included in Figure 36. Displayed for each subject are three scatter plots, which include MTFG versus knee flexion, abduction, and external rotation. Each data point represents a single trial collected at discrete time points during standing. Figure 38, I, III, and V displays data from subject S05. MTFG was significantly correlated with knee flexion, abduction, and external rotation for S05. Figure 38, II, IV, and VI displays data from subject S10, who alternatively did not display any significant correlations between MTFG and knee flexion, abduction, or external rotation.

Table 14: Correlation coefficients between MTFG and flexion, abduction, and external rotation by subject. Significant and non-significant probabilities are indicated. *p < 0.0001 ****, p < 0.001 ***, p < 0.01 **, p < 0.05 *, p > 0.05 NS*

Subject	Flexion	Abduction	External Rotation
S01	$\rho = 0.68$ ****	$\rho = -0.34^{NS}$	$\rho = 0.13^{NS}$
S03	$\rho = 0.16^{NS}$	$\rho = -0.17^{NS}$	$\rho = 0.30^{NS}$
S04	$\rho = 0.66$ ****	$\rho = -0.80$ ****	$\rho = 0.33^{NS}$
S05	$\rho = 0.92$ ****	$\rho = -0.76$ ****	$\rho = 0.90$ ****
S06	$\rho = 0.21^{NS}$	$\rho = -0.18^{NS}$	$\rho = 0.00^{NS}$
S07	$\rho = 0.26^{NS}$	$\rho = 0.00^{NS}$	$\rho = 0.22^{NS}$
S10	$\rho = 0.13^{NS}$	$\rho = -0.17^{NS}$	$\rho = 0.01^{NS}$
S12	$\rho = 0.76$ ****	$\rho = -0.62$ **	$\rho = -0.37^{NS}$
S13	$\rho = 0.77$ ****	$\rho = -0.12^{NS}$	$\rho = 0.19^{NS}$
S14	$\rho = 0.54$ *	$\rho = -0.66$ ***	$\rho = -0.58$ **
S15	$\rho = 0.36^{NS}$	$\rho = 0.11^{NS}$	$\rho = -0.17^{NS}$
S16	$\rho = 0.39$ *	$\rho = -0.22^{NS}$	$\rho = 0.14^{NS}$
S17	$\rho = 0.33^{NS}$	$\rho = -0.23^{NS}$	$\rho = 0.34^{NS}$
S19	$\rho = -0.95$ ****	$\rho = -0.96$ ****	$\rho = -0.11^{NS}$
S20	$\rho = 0.39$ *	$\rho = -0.05^{NS}$	$\rho = -0.11^{NS}$
S21	$\rho = 0.83$ ****	$\rho = 0.07^{NS}$	$\rho = 0.84$ ****
S22	$\rho = 0.60$ ***	$\rho = -0.46$ *	$\rho = 0.54$ **
S23	$\rho = 0.79$ ****	$\rho = -0.38^{NS}$	$\rho = 0.47$ *
S24	$\rho = 0.50$ *	$\rho = -0.28^{NS}$	$\rho = 0.32^{NS}$
S25	$\rho = 0.76$ ****	$\rho = -0.55$ **	$\rho = 0.56$ **
S26	$\rho = 0.32^{NS}$	$\rho = -0.31^{NS}$	$\rho = 0.31^{NS}$
S27	$\rho = 0.22^{NS}$	$\rho = 0.06^{NS}$	$\rho = 0.19^{NS}$
S28	$\rho = 0.43$ *	$\rho = 0.01^{NS}$	$\rho = 0.37^{NS}$
S29	$\rho = 0.39^{NS}$	$\rho = -0.03^{NS}$	$\rho = 0.21^{NS}$
S31	$\rho = 0.01^{NS}$	$\rho = 0.24^{NS}$	$\rho = -0.24^{NS}$
S32	$\rho = 0.89$ ****	$\rho = -0.36^{NS}$	$\rho = 0.22^{NS}$

I.

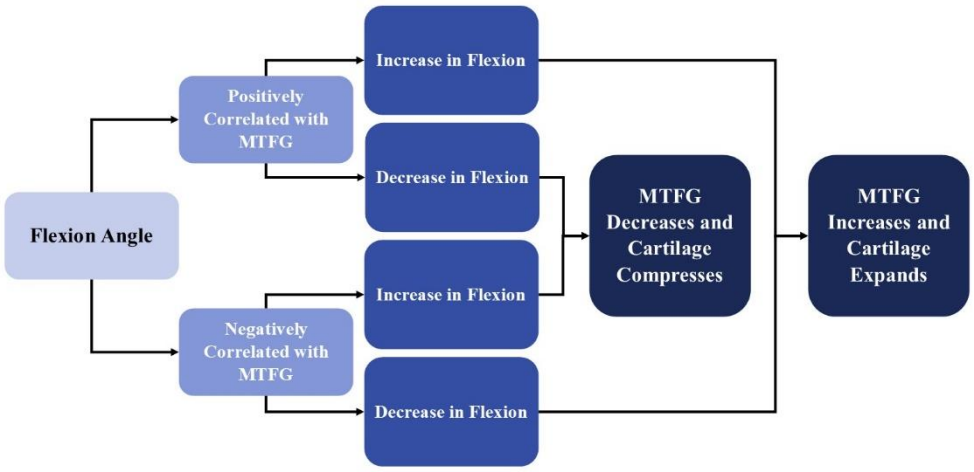

II.

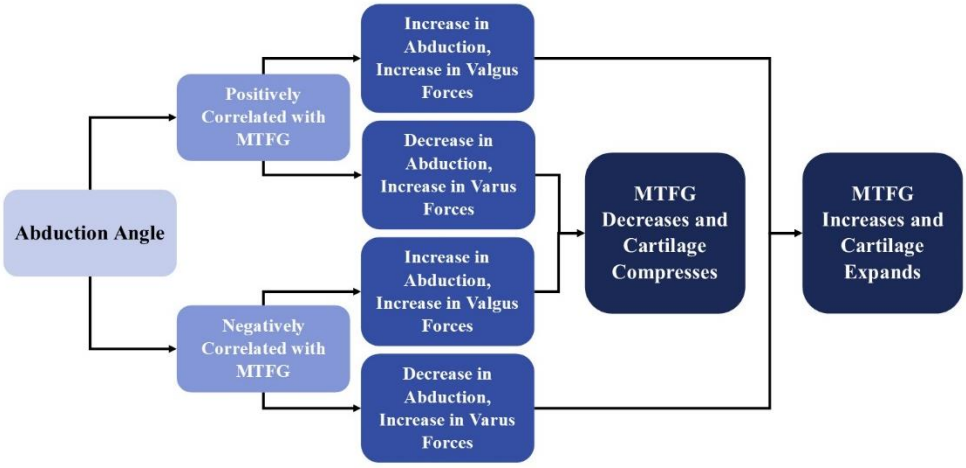

III.

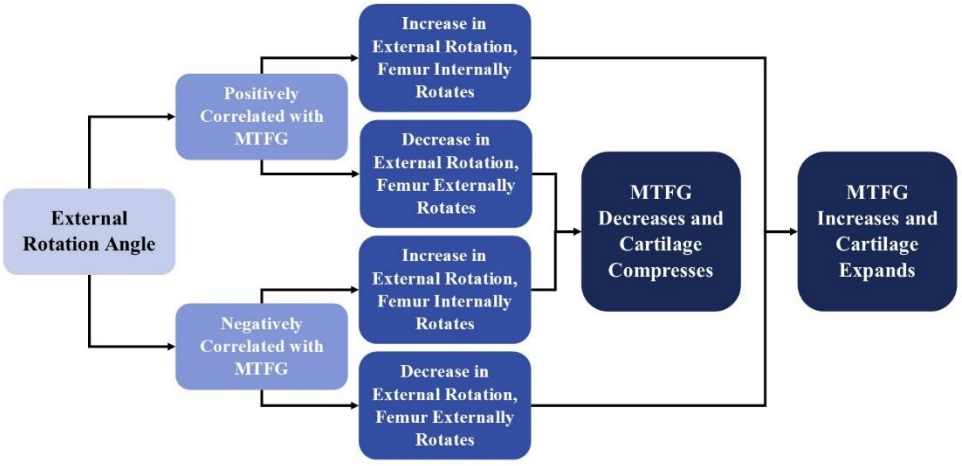

Figure 37: Flow charts describing how correlations for I. Flexion, II. Abduction, and III. External Rotation relate to changes in MTFG and cartilage compression.

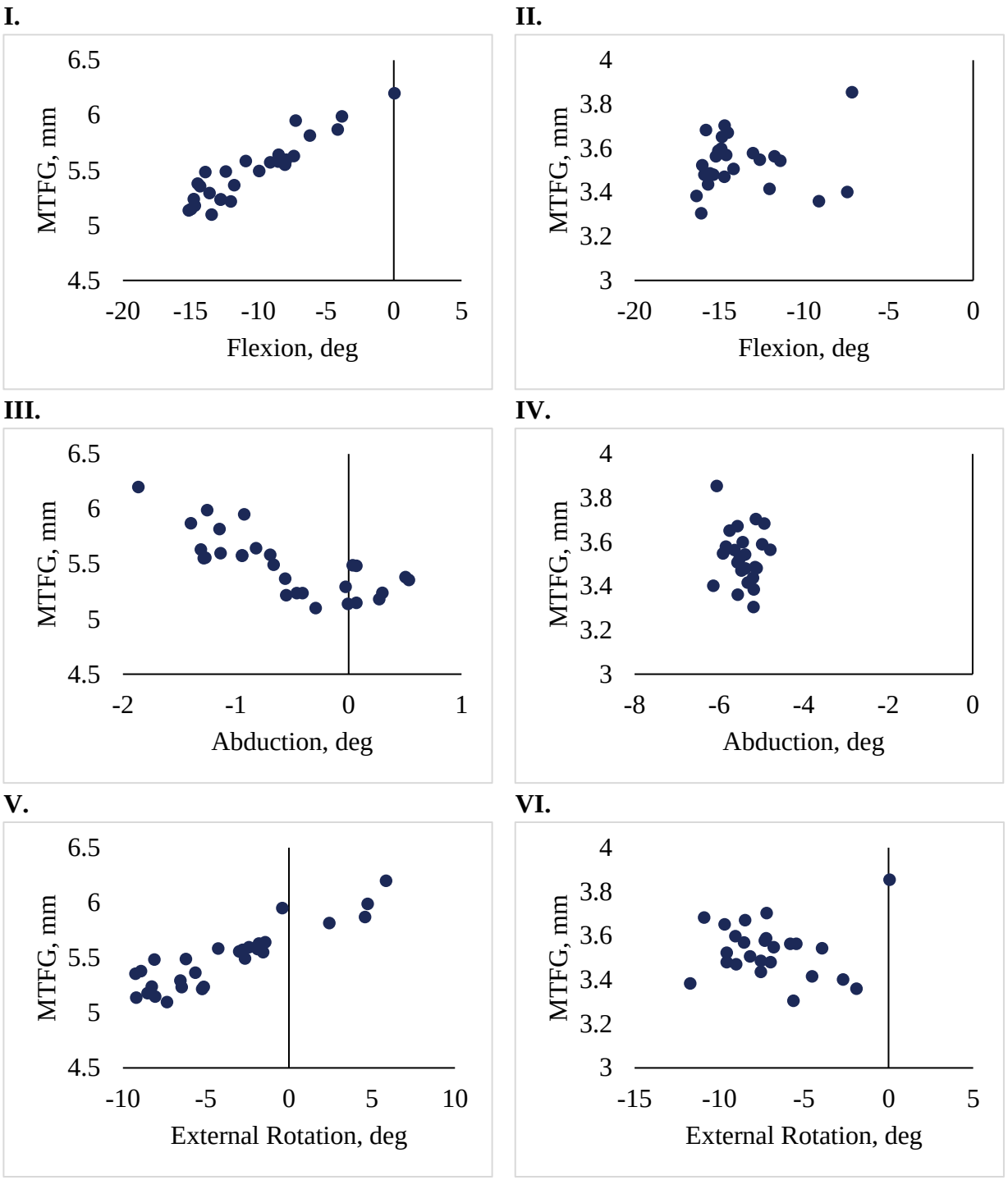

Figure 38: MTFG versus flexion, abduction, and external rotation for two subjects. I. S05 knee flexion is positively correlated with MTFG. II. S10 knee flexion is not correlated with MTFG. III. S05 knee abduction is negatively correlated with MTFG. IV. S10 knee abduction is not correlated with MTFG. V. S05 knee external rotation is positively correlated with MTFG. VI. S10 knee external rotation is not correlated with MTFG.

4.3.3 Development of a Piecewise Model for MTFG Data

The nature of possible variation in MTFG data over time is likely related to knee kinematics. However, this relationship is subject specific. Furthermore, many subjects did not display any relationship between knee kinematics and MTFG. For this reason, an empirically informed piecewise model was fit to the data on a subject and visit-by-visit basis to observe changes in MTFG over time. Based on previous literature introduced in section 2.2.3, changes in cartilage compression have displayed a fast elastic response to compression, followed by a slow creep response that behaves asymptotically with time. These changes have also been observed *in vivo* during walking and standing [38, 64, 66, 92].

Data for each subject was modeled twice: once for the HF condition, and once for the MT condition. The model was a quadratic function converged with a horizontal linear tail using average MTFG distances at each discrete time point. The statistical convergence was not constrained to a specific time frame. The coefficient describing the quadratic term in the quadratic equation was not constrained to be less than zero. In other words, the model allowed for a quadratic increase rather than decrease if the data displayed this type of relationship. The point at which each function converged was considered the "terminal point" in which a minimum MTFG was reached. The values describing the terminal point include terminal gap (G_T) and terminal gap time (T_T). MTFG at zero minutes of standing (G_0) was also noted for analyses.

Out of a total 26 subjects (51 visits) considered for this analysis, a total of 14 models did not converge. Six of these non-converging models occurred for HW subjects, while eight of them occurred for OB subjects. One subject (S05, HF) resulted in a modeled increase in gap distance over time and was excluded from further analysis. Most non-converging visits occurred on the MT condition (4 HF, 10 MT). A table of all subjects and visits that were run through the model

are listed in Table 15 and Table 16. These tables also include convergence information for each visit. Data that was not included in analyses is highlighted in grey.

Typical data that did not converge is displayed in Figure 39. This data is from an OB subject on the HF condition. Data that did not converge generally followed a horizontal trend and did not display any decrease in MTFG over time—especially between 0 minutes and 30 minutes.

Typical HW and OB subjects' MTFG and modeled MTFG on both flooring conditions are displayed in Figure 40 and Figure 41, respectively. Circular points represent MTFG data that was used to develop the model. The model is represented by a line overlaid with raw MTFG. Graphs containing blue points and lines are of the HW subject (Figure 40) and graphs containing gold points and lines are of the OB subject (Figure 41).

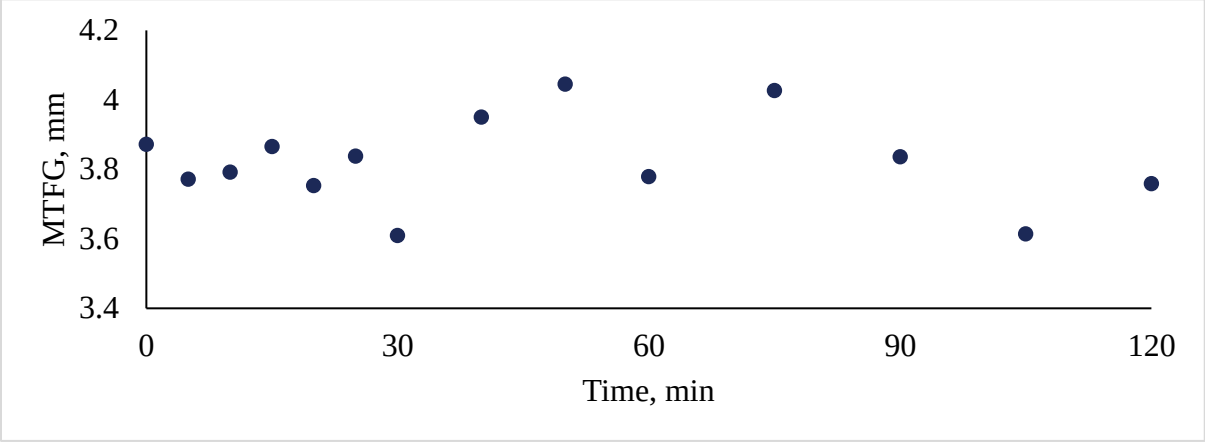

Figure 39: A typical subject that did not converge. Subject (S20) is from the obese subgroup and this data was collected while standing on the hard floor condition.

Table 15: All HW subject data, including subjects that did not converge or converged with errors. Values a, b, and c are coefficients for the quadratic piecewise equation, $at^2 + bt + c = g(t)$, where t is time in minutes, and g is predicted gap distance. G_0 is the intercept value at 0 minutes of standing. T_T and G_T are the values for terminal gap, where quadratic and linear functions converged. Data that was not included in analyses is shaded in light grey. Data was omitted if a convergence error occurred or if the quadratic fit modeled an increase in gap distance over time.

Subject	HF						MT					
	a x 10^{-4}	b x 10^{-2}	c, G_0	T_T	G_T	R^2	a x 10^{-4}	b x 10^{-2}	c, G_0	T_T	G_T	R^2
S01	125	-18.42	4.03	7.37	3.35	0.56	36.00	-6.20	3.79	8.61	3.52	0.26
S03	0.05	-0.17	2.43	155.88	2.29	0.06	Convergence Error					
S04	Convergence Error						0.30	-0.61	4.72	100.83	4.42	0.37
S05	-5.3	2.92	5.29	27.55	5.69	0.02	0.99	-1.39	5.69	70.20	5.20	0.76
S06	0.73	-0.62	3.27	42.12	3.14	0.86	7.35	-3.23	3.42	21.97	3.07	0.56
S07	4.12	-1.94	3.49	23.54	3.27	0.80	1.14	-0.81	3.48	35.48	3.34	0.46
S10	12.6	-3.94	3.85	15.63	3.54	0.28	Convergence Error					
S12	48.0	-11.05	4.81	11.51	4.18	0.08	Convergence Error					
S13	61.1	-8.35	3.68	6.83	3.39	0.08	0.22	-0.35	3.57	79.32	3.43	0.06
S14	Convergence Error						0.42	-0.42	3.03	49.76	2.92	0.04
S15	0.077	-0.21	3.89	134.33	3.75	0.38	5.92	-2.51	4.09	21.20	3.82	0.10
S16	46.3	-12.45	4.93	13.44	4.10	0.24	3.53	-1.93	4.37	27.34	4.10	0.36
S17	0.38	-0.43	3.86	56.97	3.73	0.51	Convergence Error					
S19	Subject did not complete protocol						-8.00	8.75	2.07	54.69	4.47	0.34

Table 16: All OB subject data, including subjects that did not converge or converged with errors. Data that was not included in analyses is shaded in light grey. Values a, b, and c are coefficients for the quadratic piecewise equation, $at^2 + bt + c = g(t)$, where t is time in minutes, and g is predicted gap distance. G_0 is the intercept value at 0 minutes of standing. T_T and G_T are the values for terminal gap, where quadratic and linear functions converged.

Subject	HF						MT					
	a x 10^{-4}	b x 10^{-2}	c	T_T	G_T	R^2	a x 10^{-4}	b x 10^{-2}	c	T_T	G_T	R^2
S20	Convergence Error						0.24	-0.62	4.11	128.33	3.71	0.65
S21	12.20	0.84	4.29	17.70	3.90	0.08	0.84	-1.16	4.43	69.05	4.03	0.42
S22	12.20	0.61	4.96	17.95	4.56	0.42	0.61	-0.71	4.82	58.44	4.61	0.52
S23	2.86	-1.29	3.45	22.55	3.30	0.63	Convergence Error					
S24	2.02	-1.04	3.59	25.74	3.46	0.32	1.28	-1.51	3.90	58.98	3.45	0.73
S25	7.38	-4.03	5.25	27.30	4.70	0.58	Convergence Error					
S26	4.01	-2.37	3.55	29.55	3.20	0.18	Convergence Error					
S27	1.91	-0.909	2.92	23.80	2.81	0.07	Convergence Error					
S28	Convergence Error						Convergence Error					
S29	5.15	-2.81	2.81	27.28	2.43	0.50	1.37	-1.12	2.79	40.88	2.56	0.39
S31	17.1	-4.65	5.22	13.60	4.91	0.40	4.24	-1.83	5.01	21.58	4.81	0.27
S32	2.36	-2.44	3.62	51.69	2.99	0.41	Convergence Error					

I.

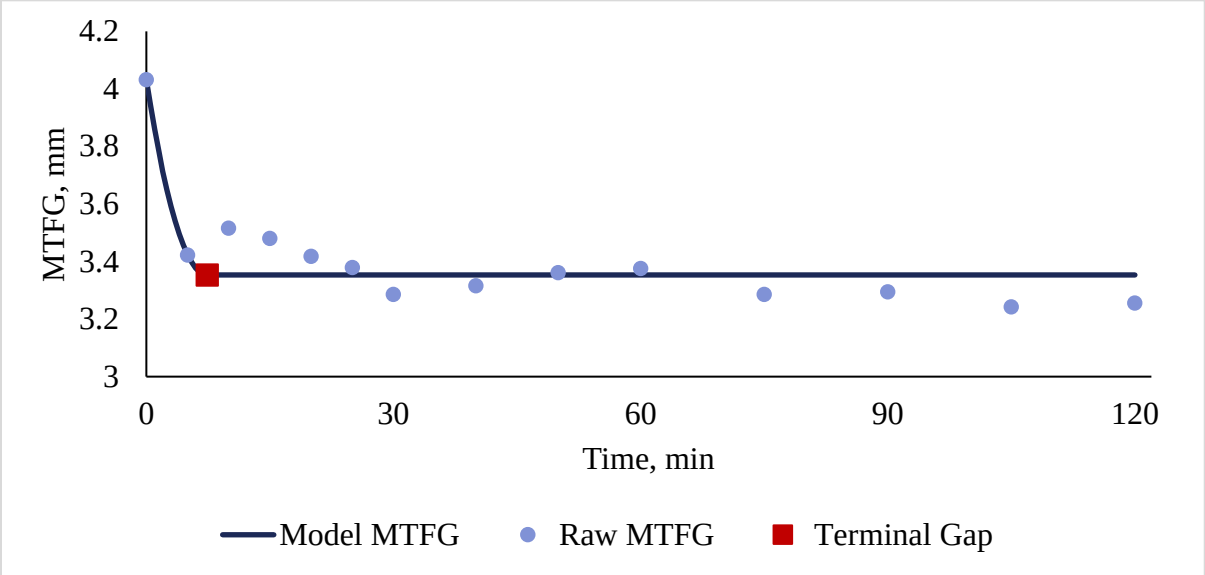

II.

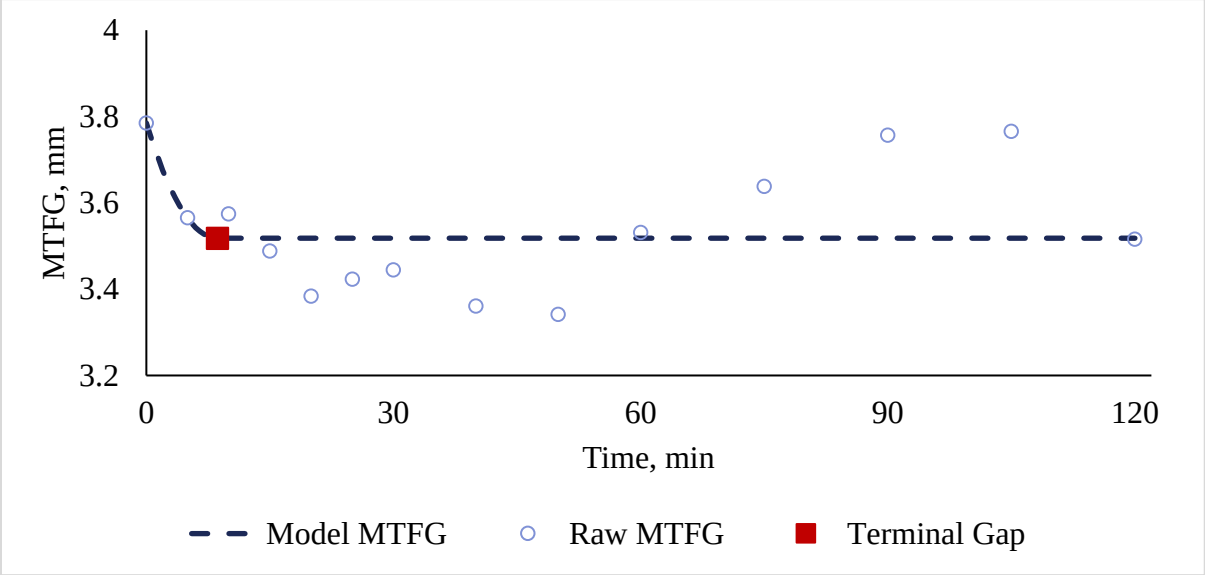

Figure 40: MTFG collected during 120 minutes of standing and model MTFG for a typical HW subject on the I. HF and II. MT conditions. Points represent the raw data used to develop the model values, displayed with a line. A red square denotes the location of terminal gap (T_T,G_T).

I.

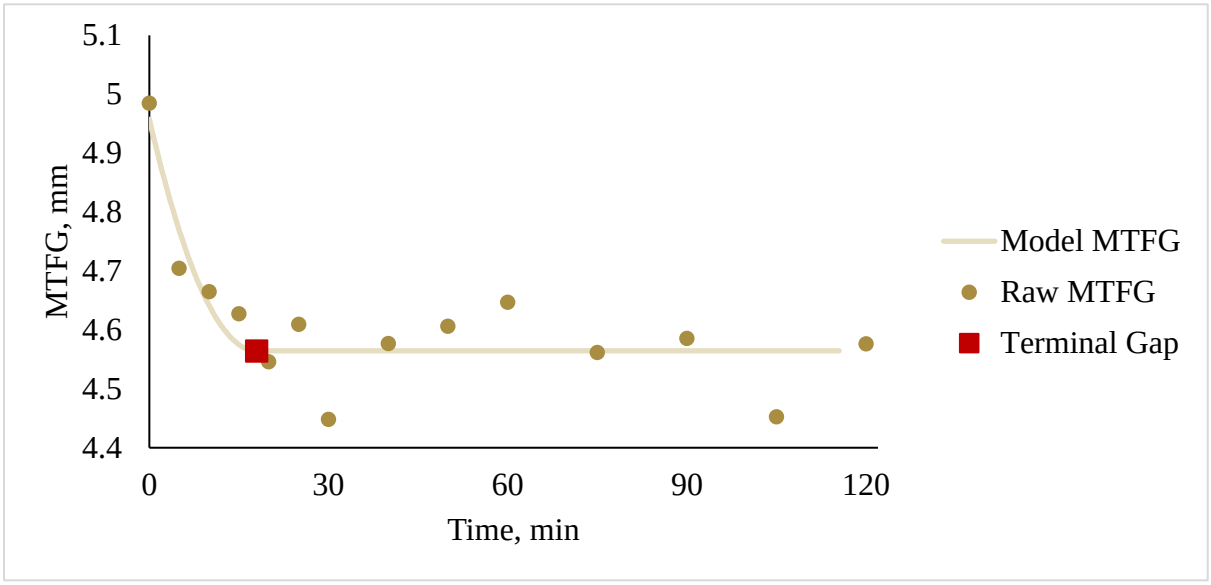

II.

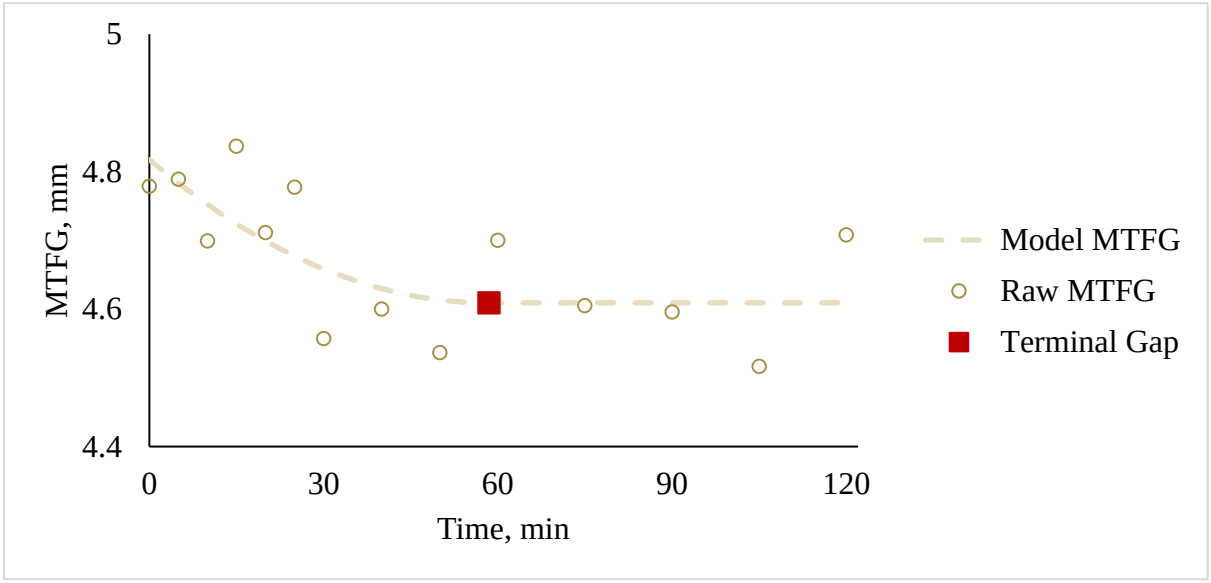

Figure 41: MTFG collected during 120 minutes of standing and model MTFG for a typical OB subject on the I. HF and II. MT conditions. Points represent the raw data used to develop the model values, displayed with a line. A red square denotes the location of terminal gap (T_T,G_T).

A two-way ANOVA was performed to compare the effects of BMI group and flooring on T_T, G_T, G_0, and G_T/G_0 using the data displayed in Table 15 and Table 16. No significant differences between flooring conditions or BMI groups were found. However, some general trends are noted. Figure 42, I displays MTFG at the start of the standing trial. There is very little change between flooring conditions within BMI groups (HW, 0.03 ± 0.3; OB, 0.01 ± 0.35 mm). The OB group displays slightly higher starting MTFG than the HW group (0.11 ± 0.31 mm). G_T values are displayed in Figure 42, II. These values show similar trends to those displayed in Figure 42, I. There is very little difference between flooring conditions within BMI group (HW, 0.03 ± 0.29; OB, -0.04 ± 0.4 mm). Likewise, the OB group displays a slightly higher G_T than the HW group (0.08 ± 0.36 mm). In Figure 42, III, G_T values were normalized for each subject to the starting gap value (G_T/G_0). G_T/G_0 is higher when both HW and OB groups stand on the MT condition, suggesting that MTFG decreased less on the MT condition than on the HF condition. The differences are very small, however (HW change, 2.13 ± 20.4 e^{-3}; OB change, 6.67 ± 15.43 e^{-3}). The most notable differences are displayed in Figure 42, IV. T_T only increased slightly for the HW group on the MT versus the HF (1.97 ± 13.5 min). However, flooring seemed to have a dramatic effect on T_T for obese subjects, increasing by 29.3 ± 5.5 min. T_T decreased between HW subjects and OB subjects on the HF condition (16.0 ± 9.7 min).

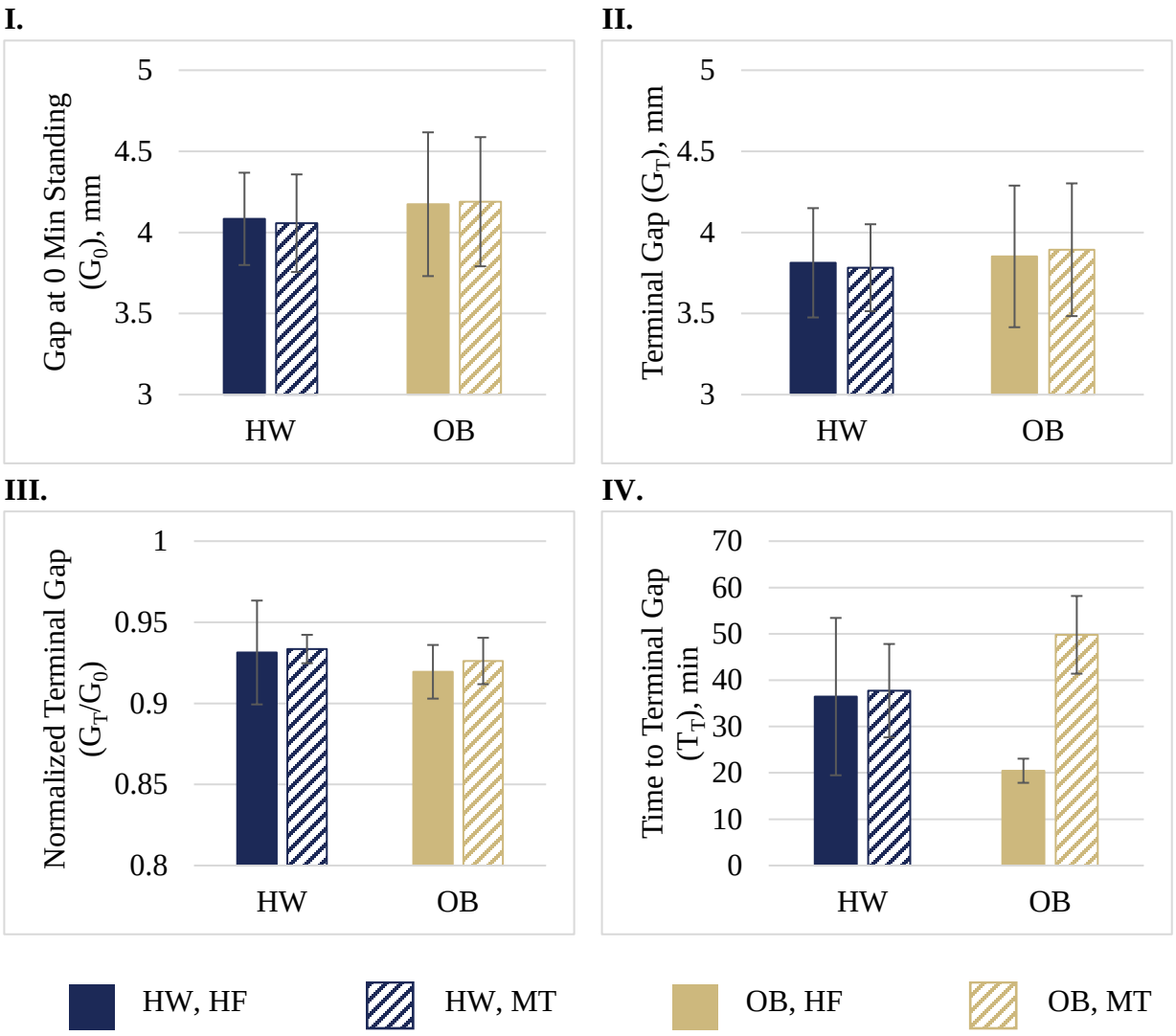

Figure 42: I. MTFG at start G_0 is similar within HW and OB groups when standing on different mats. G_0 may be slightly increased for the OB group versus the HW group. II. G_T calculated by the piecewise model. There is no discernable difference between flooring or BMI groups. III. Terminal gap normalized to start (G_T/G_0) may be slightly increased on the MT versus the HF. In other words, MTFG compressed less on the MT versus the HF. IV. Time to terminal gap (T_T) did not change within the HW group between flooring conditions. However, T_T did increase on the MT versus the HF for the OB group.

4.3.4 Knee Joint Measures and Subjective Tiredness and Discomfort

Pearson correlations of T_T, G_T, G_0, and G_T/G_0 with changes in overall tiredness, legs tiredness, hips discomfort, upper legs discomfort, knees discomfort, lower legs discomfort, ankles discomfort, and feet discomfort over two hours of standing were performed. Only T_T was significantly correlated with feet discomfort. No other correlations between MTFG outcomes and tiredness and discomfort outcomes were statistically significant. All correlation values are displayed in Table 17.

Table 17: Pearson correlation results comparing MTFG outcome variables and subjective tiredness and discomfort. Only T_T was significantly correlated with feet discomfort. ** Denotes significance ($p < 0.05$), NS denotes non-significance.*

	T_T	G_T	G_0	G_T/G_0
Overall Tiredness	$\rho = -0.26^{NS}$	$\rho = 0.13^{NS}$	$\rho = 0.13^{NS}$	$\rho = -0.02^{NS}$
Legs Tiredness	$\rho = -0.31^{NS}$	$\rho = -0.08^{NS}$	$\rho = -0.02^{NS}$	$\rho = -0.07^{NS}$
Hips	$\rho = -0.14^{NS}$	$\rho = 0.12^{NS}$	$\rho = 0.17^{NS}$	$\rho = -0.05^{NS}$
Upper Legs	$\rho = -0.18^{NS}$	$\rho = 0.24^{NS}$	$\rho = 0.26^{NS}$	$\rho = 0.01^{NS}$
Knees	$\rho = -0.02^{NS}$	$\rho = 0.10^{NS}$	$\rho = 0.03^{NS}$	$\rho = 0.11^{NS}$
Lower Legs	$\rho = -0.24^{NS}$	$\rho = 0.02^{NS}$	$\rho = 0.03^{NS}$	$\rho = 0.02^{NS}$
Ankles	$\rho = -0.15^{NS}$	$\rho = 0.03^{NS}$	$\rho = 0.03^{NS}$	$\rho = -0.01^{NS}$
Feet	$\rho = -0.42$ *	$\rho = 0.01^{NS}$	$\rho = 0.06^{NS}$	$\rho = -0.04^{NS}$

4.3.5 Knee Joint Measures and Standing Strategies

Pearson correlations compared the total number of shifts and fidgets performed over two hours of standing with knee joint measures (Table 18). No significant relationships were found.

Further analysis was performed to determine if a lack of convergence was related to the number of shifts or fidgets performed during the trial. Figure 43 displays a graph of P_R and MTFG on two axes. This single subject (S20, HF condition) did not converge. Visual observation of the graph suggests that as the number of higher amplitude movements increase, MTFG variance tends to increase and points become more spread out. To test this theory, a chi square test of independence was performed to examine the relation between the total change in shifts, fidgets, and total events and convergence/non-convergence of the piecewise model. No significant relationships were found.

Table 18: Pearson correlations comparing standing behaviors and MTFG outcome variables. No significant correlations were found. *p > 0.05 NS*

	T_T	G_T	G_0	G_T/G_0
Shifts	$\rho = -0.0438^{NS}$	$\rho = 0.3287^{NS}$	$\rho = 0.2055^{NS}$	$\rho = 0.2016^{NS}$
Fidgets	$\rho = -0.1214^{NS}$	$\rho = -0.2736^{NS}$	$\rho = -0.1933^{NS}$	$\rho = -0.1290^{NS}$
Total Events	$\rho = -0.1246^{NS}$	$\rho = -0.2603^{NS}$	$\rho = -0.1852^{NS}$	$\rho = -0.1204^{NS}$

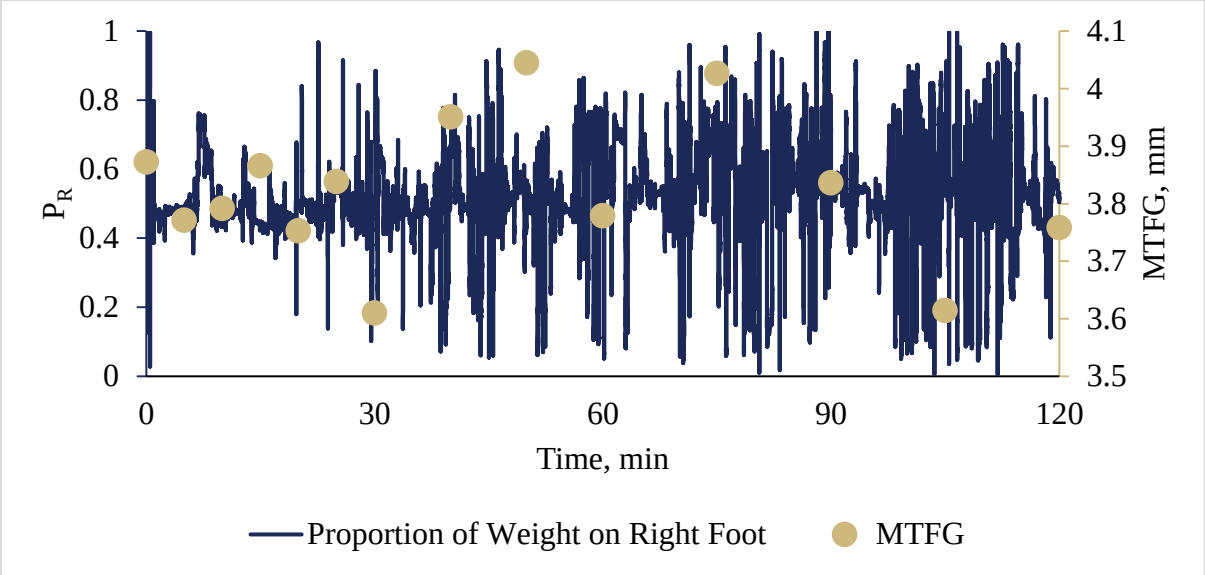

Figure 43: Raw MTFG and proportion of bodyweight over the right leg overlaid for a single subject visit (S20, HF). As the number of events increase over time, MTFG variance increases and MTFG becomes more spread out.

4.4 Lower Extremity Muscle Measures

Analyses of muscle related outcome variables (EMG and NIRS) are performed in this section. While both EMG and NIRS are both related to muscular outcomes, they are introduced in separate subsections as to not imply that they are necessarily dependent on one another. Graphs explaining all statistically significant effects are included in this section. Appendix D contains all other graphs.

4.4.1 Electromyography

EMG outcome variables of fatigue—MPF and $RMS^{\%}$—were analyzed using repeated measures mixed effects models in which time, flooring, and BMI group were treated as factors. Analyses were performed by muscle. MPF values displayed a normal distribution of residuals, so MPF data was not transformed prior to analyses. RMS values were converted to percent change from RMS at time 0, where RMS at time 0 was 100%. These values were then transformed prior to analysis (described in section 3.4.4.1). Graphs represent MPF values (Hz) and percent $RMS^{\%}$ values (%). EMG analyses were run separately for each muscle and are introduced by muscle.

4.4.1.1 Tibialis Anterior

Table 19 displays results of repeated measures mixed effects models run on TA MPF and TA $RMS^{\%}$. Time was a significant effect for TA MPF ($F_{23,936} = 1.80$, $p = 0.0117$). Flooring was a significant effect for TA $RMS^{\%}$ ($F_{1,951} = 6.03$, $p = 0.0142$). TA MPF and $RMS^{\%}$ displayed no other significant effects.

Table 19: Tibialis anterior MPF and $RMS^{\%}$ results from repeated measures mixed effects model investigating the effects of flooring (F), BMI (B), and time (T). ***p < 0.0001 ****, p < 0.001 ***, p < 0.01 **, p < 0.05 *, p > 0.05 NS***

	MPF	**$RMS^{\%}$**
T	$F_{23,936} = 1.80$ *	$F_{23,936} = 1.32$ NS
F	$F_{1,950} = 0.71$ NS	$F_{1,951} = 6.03$ *
B	$F_{1,24} = 0.35$ NS	$F_{1,24} = 0.15$ NS
F x B	$F_{1,950} = 0.27$ NS	$F_{1,951} = 0.17$ NS
F x T	$F_{23,936} = 0.88$ NS	$F_{23,936} = 0.64$ NS
B x T	$F_{23,936} = 0.38$ NS	$F_{23,936} = 0.23$ NS
F x B x T	$F_{23,936} = 0.75$ NS	$F_{23,936} = 0.33$ NS

Time was a significant factor for TA MPF ($F_{23,936} = 1.80$, p = 0.0117, Figure 44). A Dunnett's post hoc test was performed to determine if any time points in Figure 44 were significantly different from TA MPF at 0 minutes. No significant differences were observed. A Tukey HSD post hoc analysis was performed to analyze specific differences between all time points. Only TA MPF measured at 30 minutes (68.44 ± 3.79 Hz) was significantly different from TA MPF measured at 55 minutes of standing (83.65 ± 3.32 Hz). These points are labeled A and B in Figure 44, respectively. The maximum increase in TA MPF over the course of standing occurred at 55 minutes and was by 6.38 ± 3.40 Hz. All other factors and interaction effects did not result in statistically significant differences in TA MPF.

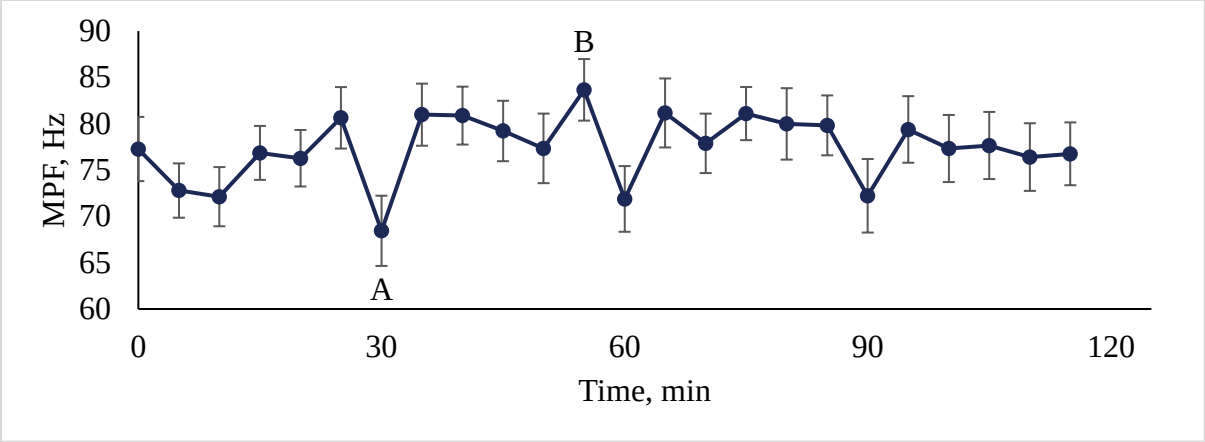

Figure 44: TA MPF changed significantly with time. Data points represent the average MPF value measured across all subjects at that time point. Error bars represent the standard error of the mean. No TA MPF values were significantly different from TA MPF at 0 minutes. However, TA MPF at 30 minutes and 55 minutes were significantly different from one another (labeled A and B, respectively).

TA $RMS^{\%}$ changed significantly with flooring condition ($F_{1,951} = 6.03$, $p = 0.0142$, Figure 45). In both flooring cases, TA $RMS^{\%}$ increased, as TA $RMS^{\%}$ is higher than 100% for both HF (108.52 ± 2.83 %) and MT (115.18 ± 4.25 %) conditions. However, TA $RMS^{\%}$ significantly increased more on the MT than the HF condition (6.66 ± 3.54 %). Figure 45, II displays average TA $RMS^{\%}$ over all time points throughout the duration of standing. The interaction effect of flooring condition and time was not statistically significant. All other factors and interaction effects did not result in statistically significant differences in TA $RMS^{\%}$.

I.

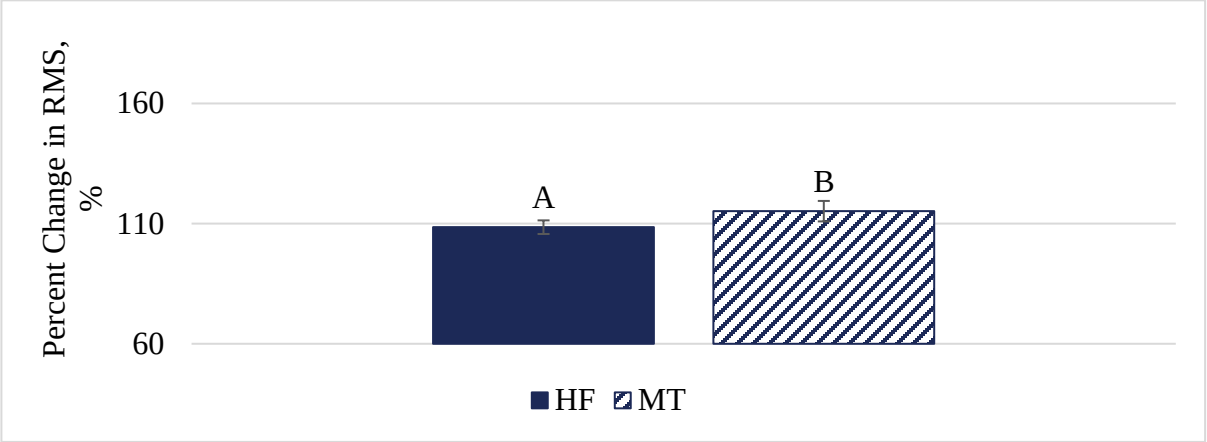

II.

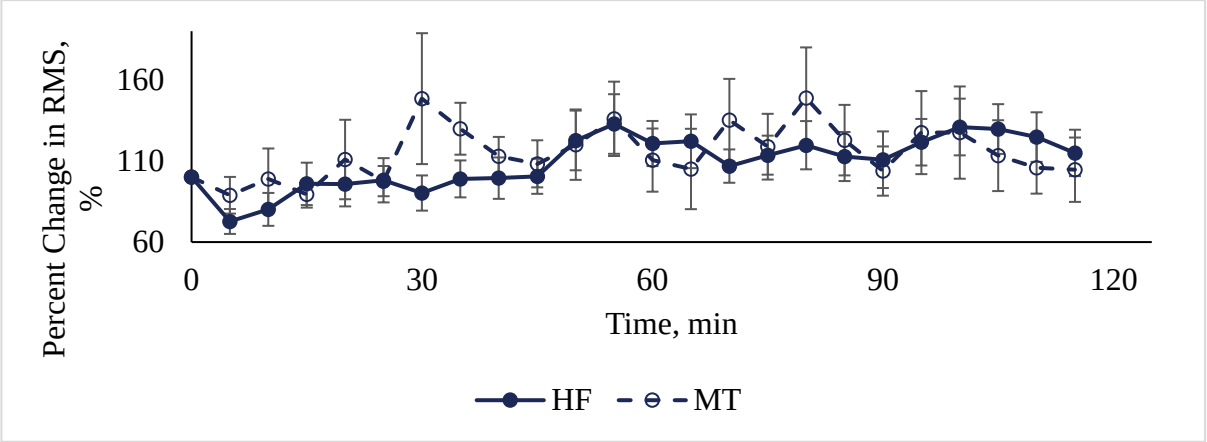

Figure 45: TA RMS$^{\%}$ changed significantly with flooring condition. I. Average TA RMS$^{\%}$ split into HF and MT groups. Bars with different letter labels are significantly different. Error bars represent standard error of the mean. II. The interaction effect of flooring with time was not a significant factor for TA RMS$^{\%}$. Differences between overall flooring conditions may be due to spikes in MT data occurring at 30, 70, and 80 minutes of standing.

4.4.1.2 Gastrocnemius

Table 20 displays results of repeated measures mixed effects models run on GAS MPF and GAS $RMS^{\%}$. The interaction effect of flooring with BMI group were significant for both GAS MPF ($F_{1,1019} = 33.17$, $p < 0.0001$) and GAS $RMS^{\%}$ ($F_{1,1019} = 16.70$, $p < 0.0001$). BMI group was also a significant effect for GAS MPF ($F_{1,25} = 4.87$, $p = 0.0367$). Flooring was a significant effect for GAS $RMS^{\%}$ ($F_{1,1019} = 66.91$, $p < 0.0001$). No other significant effects were measured for GAS MPF or GAS $RMS^{\%}$.

BMI group was a significant factor for GAS MPF ($F_{1,25} = 4.87$, $p = 0.0367$). Figure 46 displays average GAS MPF over all time points, split into HW and OB BMI groups. Average GAS MPF was less for the OB group (86.05 ± 0.91 Hz) than the HW group (96.64 ± 0.65 Hz) over two hours of standing. The difference between HW and OB GAS MPF was displayed throughout the duration of the standing trial. Figure 47 displays average GAS MPF over time, split between BMI groups. Though the interaction effect of time and BMI group was not statistically significant, the OB BMI group displayed a visibly lower GAS MPF throughout the duration of standing.

Table 20: Gastrocnemius MPF and $RMS^{\%}$ results from repeated measures mixed effects model investigating the effects of flooring (F), BMI (B), and time (T). ***p < 0.0001 ****, p < 0.001 ***, p < 0.01 **, p < 0.05 *, p > 0.05 NS***

	MPF	**$RMS^{\%}$**
T	$F_{23,1010} = 0.84^{NS}$	$F_{23,1010} = 0.70^{NS}$
F	$F_{1,1019} = 0.14^{NS}$	$F_{1,1019} = 66.91$ ****
B	$F_{1,25} = 4.87$ *	$F_{1,25} = 0.16^{NS}$
F x B	$F_{1,1019} = 33.17$ ****	$F_{1,1019} = 16.70$ ****
F x T	$F_{23,1010} = 0.68^{NS}$	$F_{23,1010} = 0.37^{NS}$
B x T	$F_{23,1010} = 0.46^{NS}$	$F_{23,1010} = 0.48^{NS}$
F x B x T	$F_{23,1010} = 0.62^{NS}$	$F_{23,1010} = 0.43^{NS}$

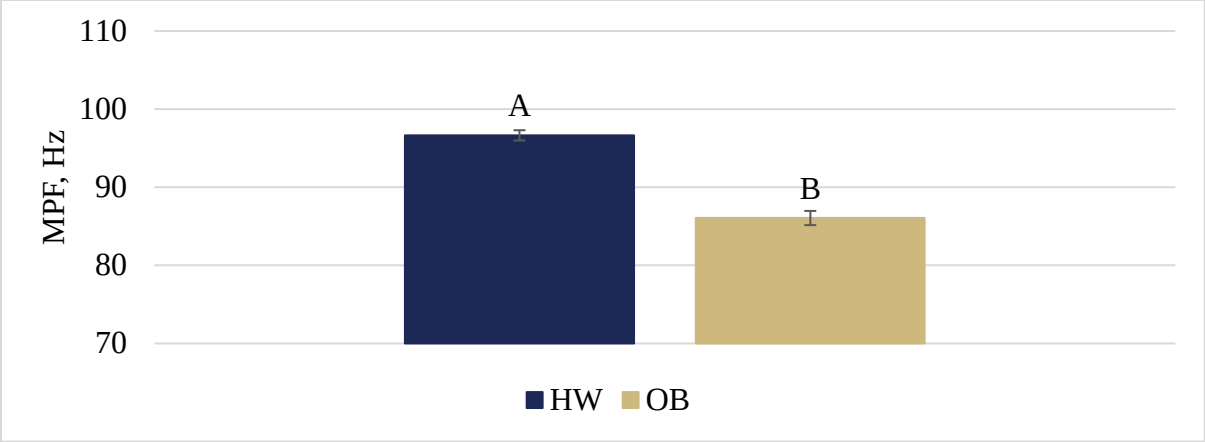

Figure 46: Average GAS MPF over all time points and flooring conditions, split into BMI groups. OB GAS MPF was significantly lower than the HW group. Error bars represent standard error of the mean.

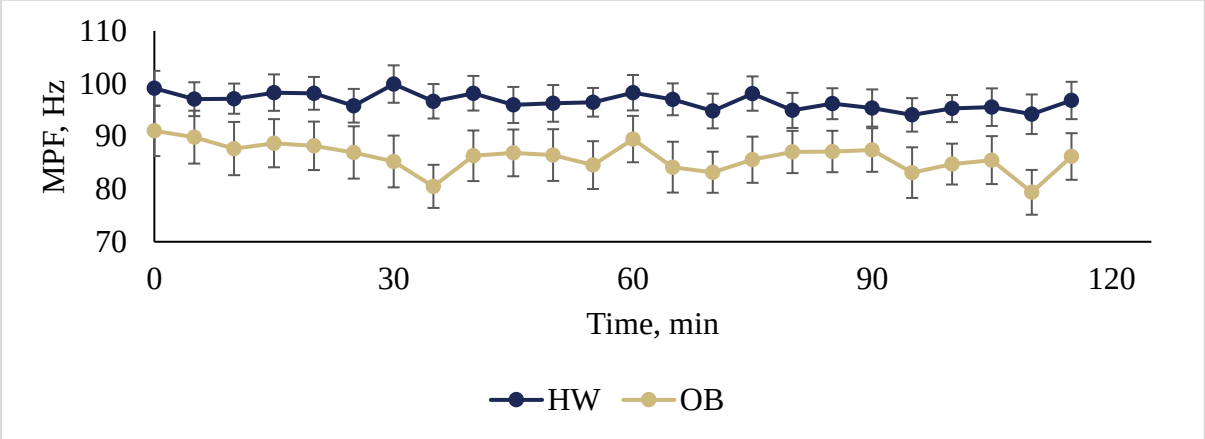

Figure 47: GAS MPF split into BMI groups over time. The interaction effect of time and BMI group was not statistically significant for GAS MPF. However, BMI group as an effect on its own was significant—and this graph displays the OB group's decreased GAS MPF throughout the duration of standing.

The interaction effect of BMI group and flooring was a significant factor for GAS MPF ($F_{1,1019}$ = 33.17, p < 0.0001, Figure 48). On the HF condition, the HW and OB groups display statistically significant differences in GAS MPF (14.40 ± 1.21 Hz). Interestingly, the MT had an opposite effect on the HW and OB BMI groups. When the HW group was exposed to the MT condition, GAS MPF decreased significantly (5.67 ± 0.09 Hz). However, when the OB group was exposed to the MT condition, GAS MPF increased significantly (4.21 ± 1.35 Hz).

Flooring condition was significantly related to GAS $RMS^{\%}$ ($F_{1,1019}$ = 66.91, p < 0.0001, Figure 49, I). Overall, GAS $RMS^{\%}$ increased from baseline on the HF condition (116.40 ± 2.72 %), while GAS $RMS^{\%}$ decreased slightly from baseline on the MT condition (97.17 ± 2.43 %). The difference in percent change between flooring conditions is 19.23 ± 2.43 %. Figure 49, II displays GAS $RMS^{\%}$ throughout the course of the standing trial, the interaction effect of flooring and time was not statistically significant.

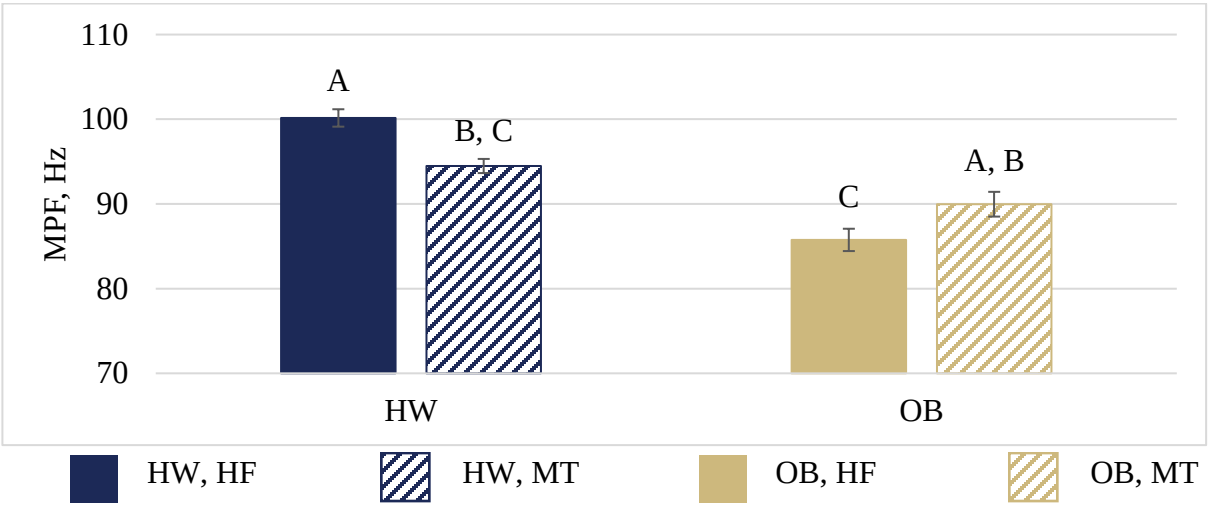

Figure 48: The interaction effect of flooring and BMI group was statistically significant for GAS MPF. GAS MPF was significantly less for the OB group than the HW group. The HW group on the MT condition was significantly less than on the HF condition. Alternatively, the OB group on the MT condition was significantly more than on the HF condition.

I.

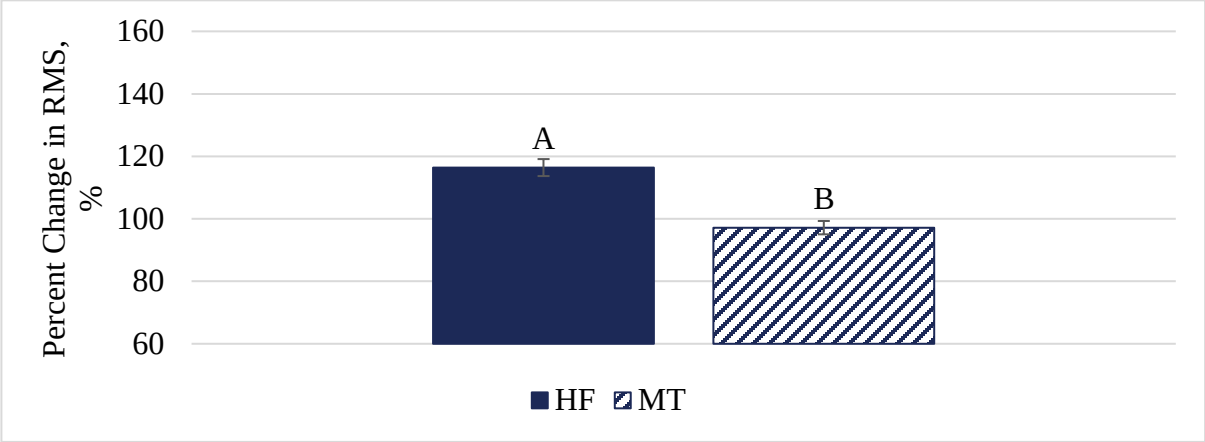

II.

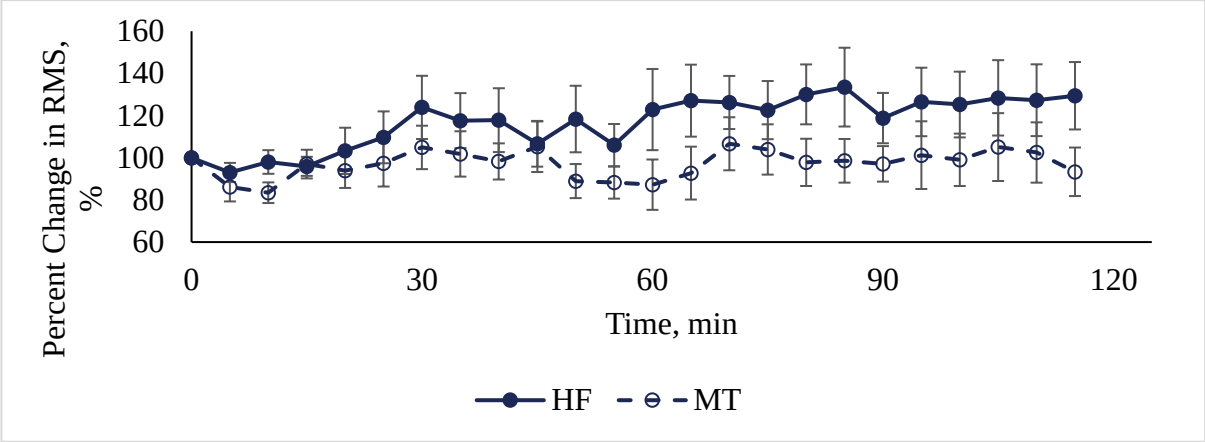

Figure 49: I. Flooring was a significant factor for GAS RMS$^{\%}$. Bars represent average GAS RMS$^{\%}$ across all subjects and time points, split into HF and MT conditions. Bars labeled with different letters are significantly different. Error bars are standard error of the mean. II. Flooring with time is not a significant factors for GAS RMS$^{\%}$. The overall difference between HF and MT is observed throughout the time course, as HF GAS RMS$^{\%}$ is larger than MT GAS RMS$^{\%}$.

The interaction effect of flooring and BMI group was significant for GAS RMS$^{\%}$ ($F_{1,1019}$ = 16.70, $p < 0.0001$, Figure 50). For both BMI groups, standing on the HF condition increased GAS RMS$^{\%}$ from baseline (HW, 123.53 ± 3.82 %; OB, 112.01 ± 3.19 %). The introduction of the MT condition (HW, 95.71 ± 3.08 %; OB, 101.71 ± 2.21 %) significantly decreased GAS RMS$^{\%}$ relative to the HF condition for both the HW and OB groups, respectively. In respect to baseline, the GAS RMS$^{\%}$ saw no significant change on the MT condition.

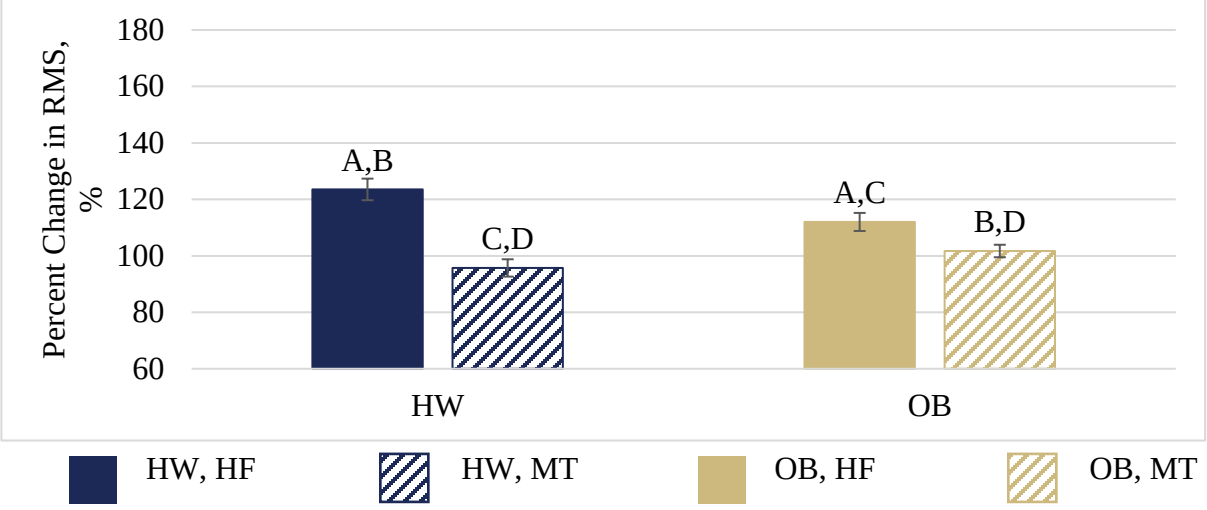

Figure 50: The interaction effect of flooring condition and BMI group was a significant factor for GAS RMS$^{\%}$. Bars represent GAS RMS$^{\%}$ averaged across all time points for each flooring condition and BMI group. Bars labeled with different letters are significantly different. Error bars are standard error of the mean.

4.4.1.3 Soleus

Table 21 displays results of repeated measures mixed effects models run on SOL MPF and SOL RMS$^{\%}$. Flooring was a significant factor for both SOL MPF ($F_{1,999}$ = 14.13, p = 0.0002) and SOL RMS$^{\%}$ ($F_{1,1010}$ = 13.56, p = 0.0002). No other significant factors were found for SOL MPF.

The interaction effect of flooring and BMI group was a significant factor for SOL $RMS^{\%}$ ($F_{1,1010} = 76.20$, $p < 0.0001$). No other significant effects were measured for SOL $RMS^{\%}$.

Table 21: Soleus MPF and $RMS^{\%}$ results from repeated measures mixed effects model investigating the effects of flooring (F), BMI (B), and time (T). ***p < 0.0001 ****, p < 0.001 ***, p < 0.01 **, p < 0.05 *, p > 0.05 NS***

	MPF	**$RMS^{\%}$**
T	$F_{23,994} = 1.03$ NS	$F_{23,994} = 0.63$ NS
F	$F_{1,999} = 14.13$ ***	$F_{1,1010} = 13.56$ ***
B	$F_{1,26} = 1.58$ NS	$F_{1,26} = 1.20$ NS
F x B	$F_{1,999} = 0.46$ NS	$F_{1,1010} = 76.20$ ****
F x T	$F_{23,994} = 0.33$ NS	$F_{23,994} = 0.44$ NS
B x T	$F_{23,994} = 0.82$ NS	$F_{23,994} = 0.40$ NS
F x B x T	$F_{23,994} = 0.54$ NS	$F_{23,994} = 0.59$ NS

Flooring condition was a significant factor for SOL MPF ($F_{1,999} = 14.13$, $p = 0.0002$). SOL MPF increased significantly (5.32 ± 1.25 Hz) when standing on the MT condition, as opposed to the HF condition (Figure 51, I). While the interaction of flooring condition and time was not statistically significant for SOL MPF, Figure 51, II displays average SOL MPF over time, split into flooring conditions.

Flooring was a significant factor for SOL $RMS^{\%}$ ($F_{1,1010} = 13.56$, $p = 0.0002$, Figure 52). The HF condition resulted in an overall slight increase in SOL $RMS^{\%}$ in comparison with baseline (104.90 ± 2.37 %), while the MT condition resulted almost no increase from baseline (101.98 ± 4.93 %).

I.

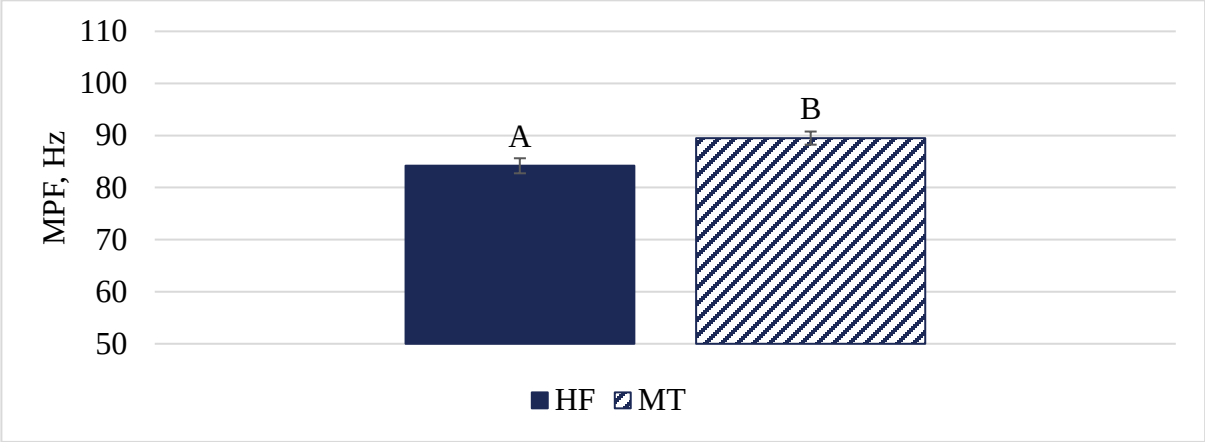

II.

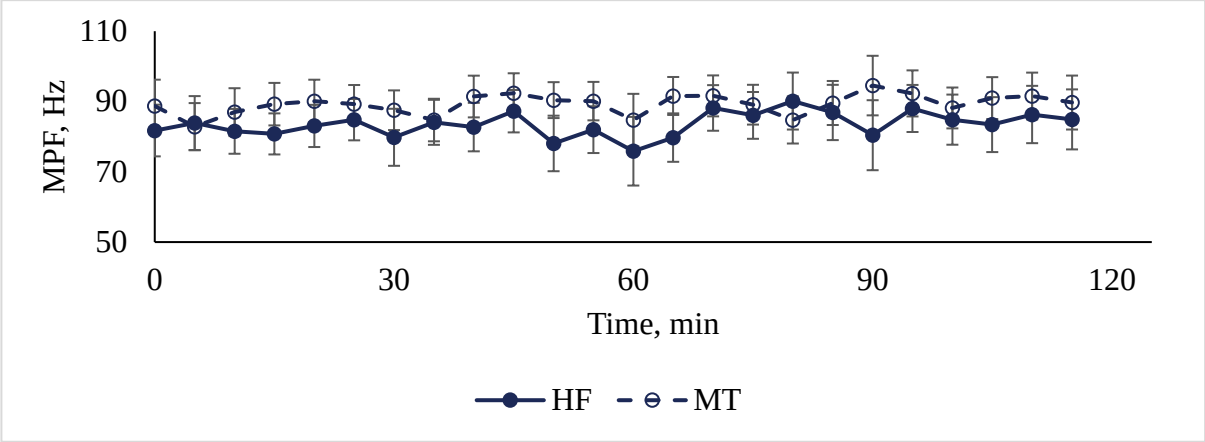

Figure 51: SOL MPF changed significantly with flooring condition. I. SOL MPF, across all time points and BMI groups, split into flooring conditions. Bars not labeled with the same letter are significantly different. Error bars represent standard error the mean. II. SOL MPF averaged within each time point, split into flooring conditions. Throughout the course of standing, the MT condition displayed a higher level of SOL MPF.

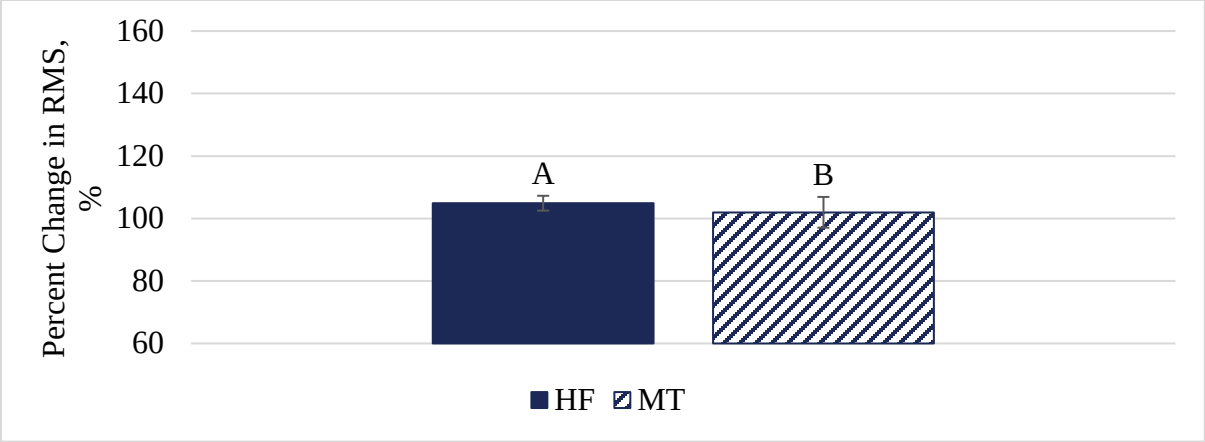

Figure 52: Flooring was a significant factor for SOL RMS$^{\%}$. All SOL RMS$^{\%}$ values, averaged across subjects and time, split into flooring conditions. Bars labeled with different letters are significantly different. Error bars are standard error of the mean. Both the HF and MT condition increased from baseline.

Significant differences in SOL RMS$^{\%}$ were found due to the interaction effect of flooring and BMI group ($F_{1,1010} = 76.20$, $p < 0.0001$, Figure 53). The introduction of the MT condition for both the HW and OB group had a significant—but opposite—effect. Within the HW group, the HF condition resulted in an overall increase from baseline by 8.02 ± 3.25 %. However, the introduction of the MT condition decreased SOL RMS$^{\%}$ by 28.92 ± 2.29 % from baseline (resulting in an overall difference between HF and MT conditions of 36.94 ± 2.77 %). Alternatively, SOL RMS$^{\%}$ did not change from baseline significantly when standing on the HF (100.54 ± 3.39 %). However, standing on the MT condition increased SOL RMS$^{\%}$ significantly, in respect to the HF condition, to 145.07 ± 10.61 %. There were no significant differences between HW and OB groups while standing on the HF condition.

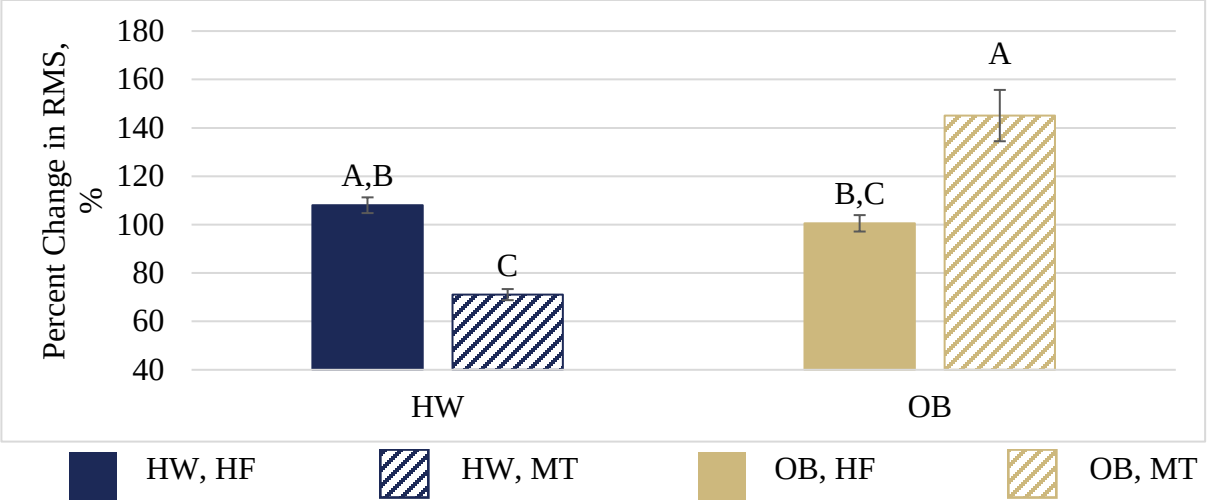

Figure 53: SOL RMS$^{\%}$ changed significantly due to the interaction effect of flooring condition and BMI group. Bars represent average SOL RMS$^{\%}$ values across all time points, split into BMI group and flooring conditions. Bars not connected by the same letter are significantly different. Error bars are standard error of the mean.

4.4.1.4 Rectus Femoris

Table 22 displays results of repeated measures mixed effects models run on RF MPF and RF RMS$^{\%}$. Time was a significant factor for RF MPF ($F_{23,882}$ = 1.56, p = 0.0449). The interaction effect of flooring and BMI group was a significant factor for both RF MPF ($F_{1,903}$ = 7.67, p = 0.0058) and RF RMS$^{\%}$ ($F_{1,898}$ = 59.77, p < 0.0001). No other significant effects were measured for RF MPF or RF RMS$^{\%}$.

Time was significant factor for RF MPF ($F_{23,882}$ = 1.56, p = 0.0449, Figure 54). Time points that were significantly different from RF MPF at 0 minutes are marked with asterisks (*). RF MPF at 75 minutes (68.27 ± 1.76 Hz) and 85 minutes (69.87 ± 1.99 Hz) increased significantly from RF MPF at 0 minutes (60.21 ± 2.38 Hz) of standing.

Table 22: Rectus femoris MPF and RMS$^{\%}$ results from repeated measures mixed effects model investigating the effects of flooring (F), BMI (B), and time (T). ***p < 0.0001 ****, p < 0.001 ***, p < 0.01 **, p < 0.05 *, p > 0.05 NS***

	MPF	**RMS$^{\%}$**
T	$F_{23,882} = 1.56$ *	$F_{23,883} = 0.63$ NS
F	$F_{1,903} = 1.84$ NS	$F_{1,898} = 3.40$ NS
B	$F_{1,26} = 1.53$ NS	$F_{1,27} = 0.60$ NS
F x B	$F_{1,903} = 7.66$ **	$F_{1,898} = 59.77$ ****
F x T	$F_{23,882} = 0.31$ NS	$F_{23,883} = 0.27$ NS
B x T	$F_{23,882} = 0.93$ NS	$F_{23,883} = 0.57$ NS
F x B x T	$F_{23,882} = 0.57$ NS	$F_{23,883} = 0.28$ NS

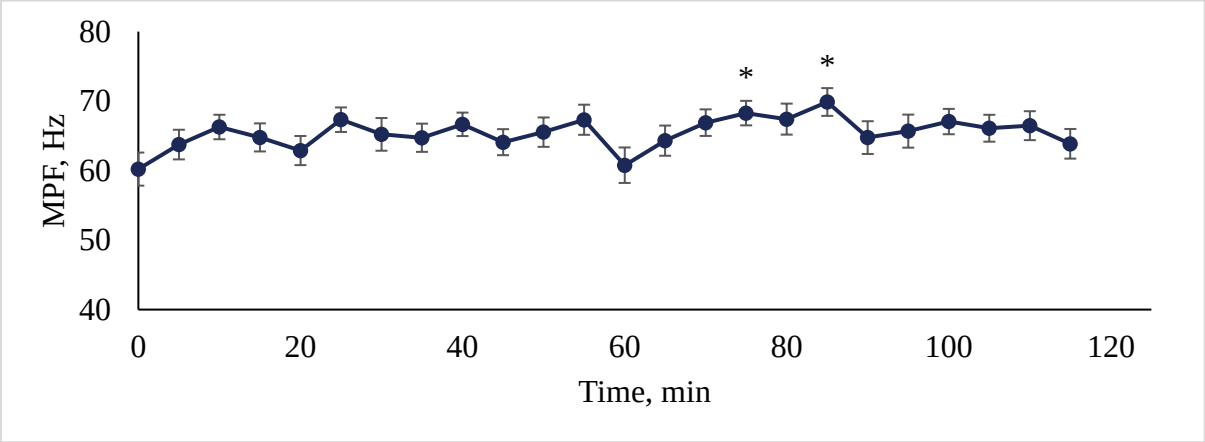

Figure 54: Time was a significant factor for RF MPF. Points represent average RF MPF data across all subjects and flooring conditions. Error bars are standard error of the mean. Significant differences from 0 minutes of standing are denoted with asterisks (*) at 75 and 85 minutes of standing.

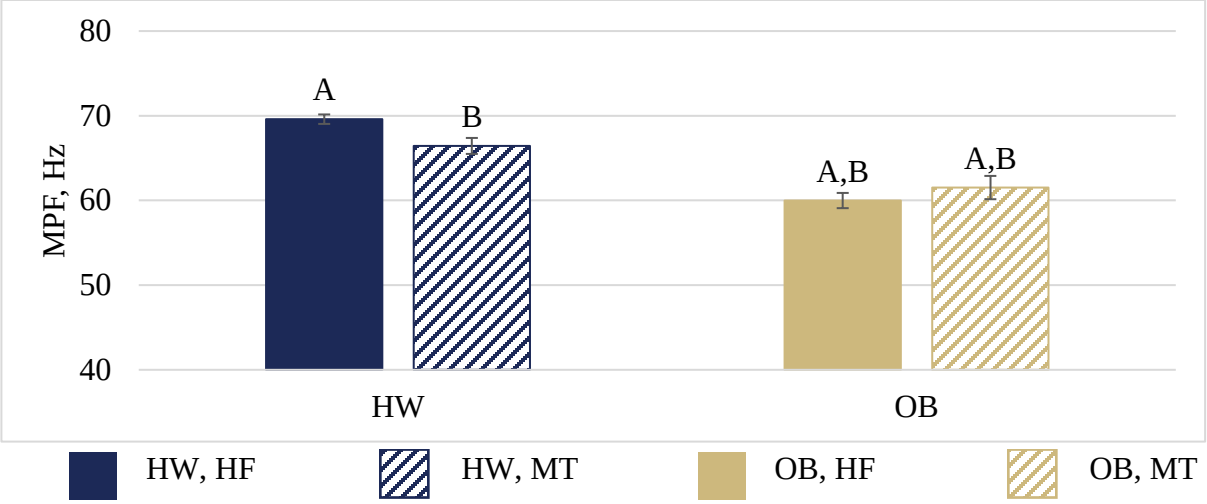

Figure 55: RF MPF changed significantly due to the interaction effect of flooring and BMI group. Bars represent average RF MPF values across all subjects, split into BMI group and flooring conditions. Bars labeled with different letters are significantly different. Error bars are standard error of the mean.

The interaction effect of flooring condition and BMI group was significant for RF MPF ($F_{1,903}$ = 7.66, p = 0.0058, Figure 55). RF MPF of the HW group decreased significantly when standing on the MT condition as opposed to the HF condition (3.16 ± 0.75 Hz). Though RF MPF was lower on the HF condition for the OB group than the HW group, the difference was not statistically significant (9.61 ± 0.72 Hz).

The interaction effect of flooring condition and BMI group were significant factors for RF $RMS^{\%}$ ($F_{1,898}$ = 59.77, p < 0.0001, Figure 56). Under all conditions, RF $RMS^{\%}$ decreased from baseline. RF $RMS^{\%}$ changed significantly for both the HW group and OB group due to flooring. On the HF, the HW group hovered around baseline (99.63 ± 2.00 %). However, the MT condition (91.51 ± 3.86 %) significantly decreased RF $RMS^{\%}$ from the HF condition. RF $RMS^{\%}$ for the OB group on the HF (75.63 ± 3.58 %) was well below baseline and was significantly less on the MT condition (72.89 ± 3.75 %).

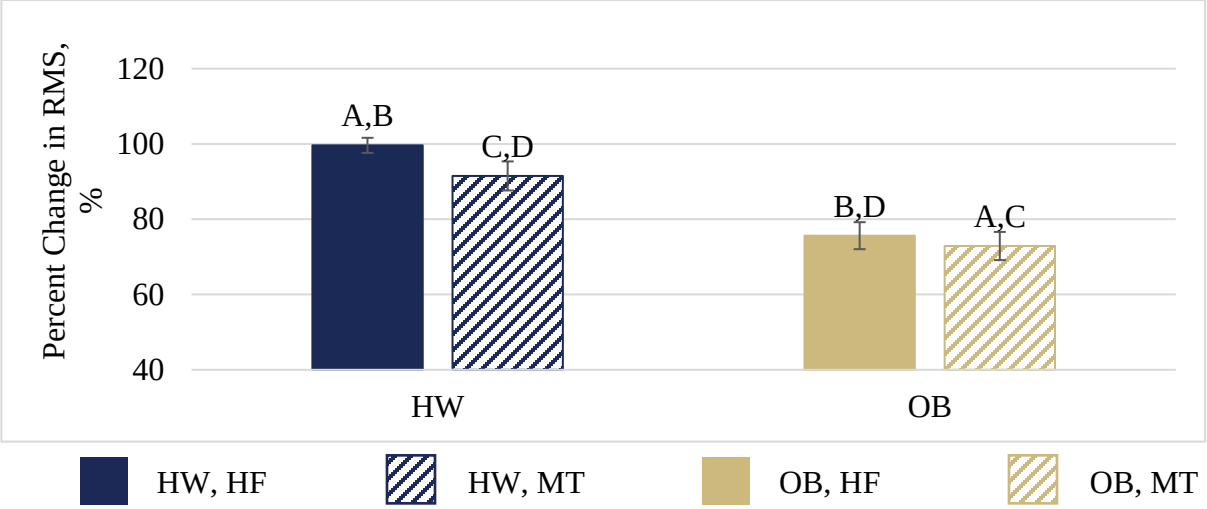

Figure 56: RF RMS$^{\%}$ changed significantly due to the interaction effect of flooring and BMI group. Bars represent the average percent change across all subjects and time points, split into flooring and BMI groups. Error bars are standard error of the mean. RMS$^{\%}$ changed significantly between flooring conditions within BMI group.

4.4.1.5 Hamstring

Table 23 displays results of repeated measures mixed effects models run on HAM MPF and HAM RMS$^{\%}$. Flooring was a significant factor for HAM MPF ($F_{1,1080} = 4.42$, $p = 0.0357$) and HAM RMS$^{\%}$ ($F_{1,1081} = 5.76$, $p = 0.0165$). The interaction effect of flooring and BMI group was a significant factor for HAM MPF ($F_{1,1080} = 6.51$, $p = 0.0108$). No other significant effects were measured for HAM MPF or HAM RMS$^{\%}$.

HAM MPF changed significantly with flooring condition ($F_{1,1080} = 4.42$, $p = 0.0357$, Figure 57). Standing on the MT versus the HF decreased HAM MPF significantly (2.36 ± 0.77 Hz). This difference was not necessarily consistent throughout the course of the standing trial. Figure 57, II displays the average HAM MPF at each time point, split into flooring conditions. The interaction effect of flooring condition and time was not statistically significant.

Table 23: Hamstring MPF and RMS$^{\%}$ results from repeated measures mixed effects model investigating the effects of flooring (F), BMI (B), and time (T). ***p < 0.0001 ****, p < 0.001 ***, p < 0.01 **, p < 0.05 *, p > 0.05 NS***

	MPF	**RMS$^{\%}$**
T	$F_{23,1074} = 0.86^{NS}$	$F_{23,1074} = 0.62^{NS}$
F	$F_{1,1080} = 4.42$ *	$F_{1,1078} = 5.76$ *
B	$F_{1,27} = 0.15^{NS}$	$F_{1,26} = 0.45^{NS}$
F x B	$F_{1,1080} = 6.51$ *	$F_{1,1078} = 2.30^{NS}$
F x T	$F_{23,1074} = 0.71^{NS}$	$F_{23,1074} = 0.32^{NS}$
B x T	$F_{23,1074} = 0.87^{NS}$	$F_{23,1074} = 0.23^{NS}$
F x B x T	$F_{23,1074} = 0.26^{NS}$	$F_{23,1074} = 0.39^{NS}$

HAM MPF changed significantly with the interaction effect of flooring condition and BMI group ($F_{1,1080} = 6.51$, $p = 0.0108$, Figure 58). HAM MPF decreased significantly on the MT condition versus the HF condition for the HW group (4.63 ± 1.07 Hz). Flooring condition did not have a significant effect on HAM MPF for the OB BMI group. No significant differences were found between the HW and OB BMI groups on the HF condition.

I.

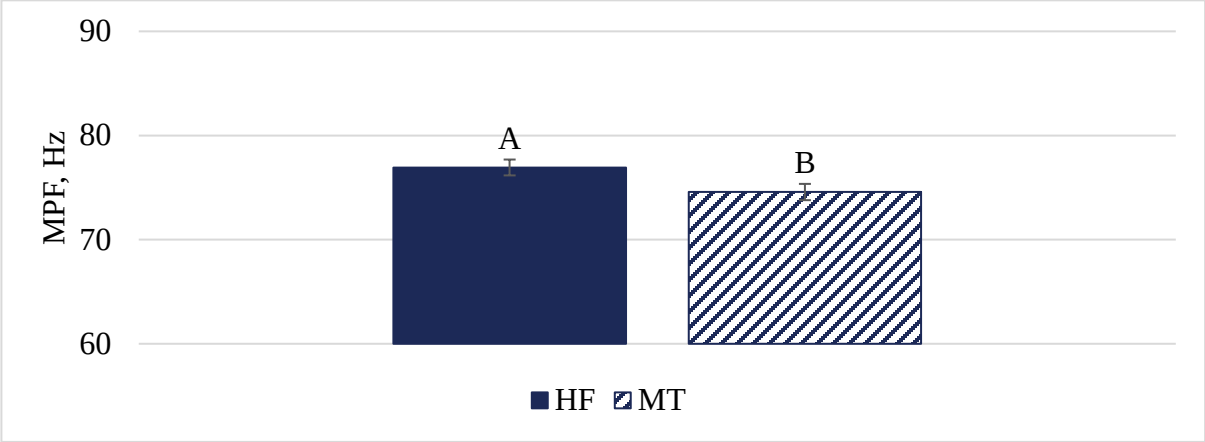

II.

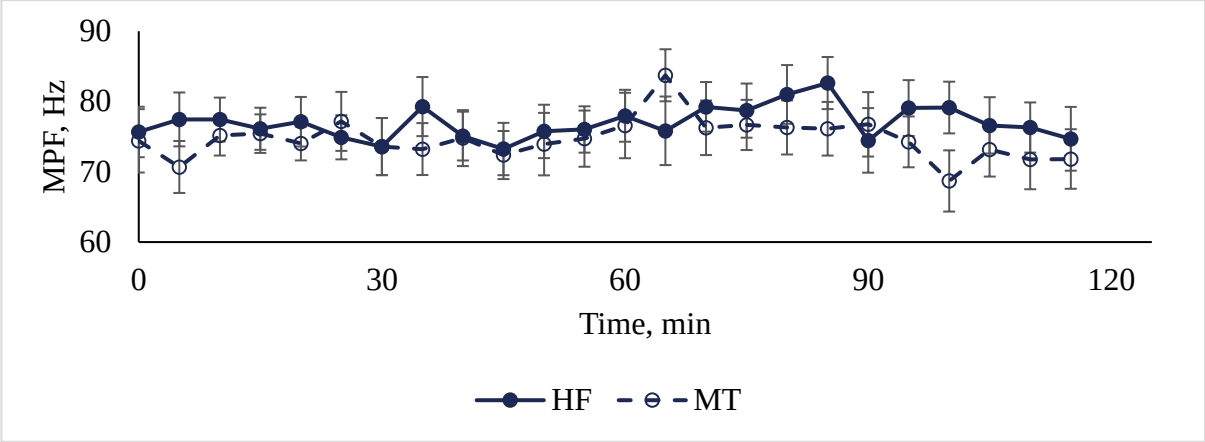

Figure 57: I. HAM MPF on the HF condition was significantly different than on the MT condition. Bars represent the average HAM MPF value averaged across all time points and subjects, split into flooring conditions. Error bars are standard error of the mean. Bars not connected by the same letter are significantly different. II. The time and flooring condition interaction effect was not a significant factor for HAM MPF. However, the difference seen in I. may have occurred as a result of slight increases in HAM MPF on the HF after 80 minutes of standing.

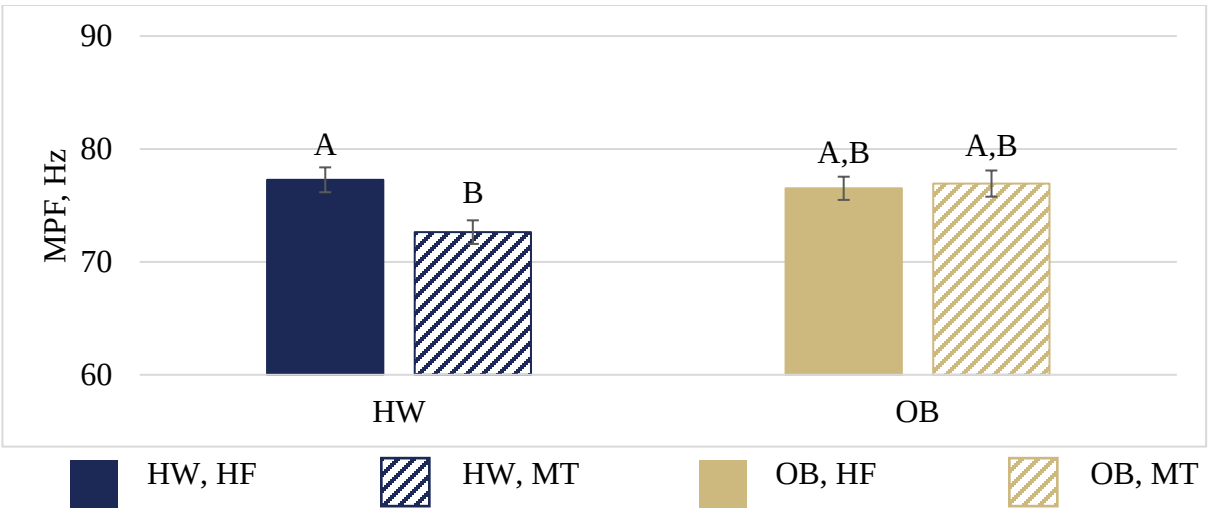

Figure 58: HAM MPF changed significantly with the interaction effect of flooring and BMI group. Bars labeled with the same letter are not significantly different. Error bars represent standard error of the mean.

Flooring was a significant factor for HAM $RMS^{\%}$ ($F_{1,1081} = 5.76$, $p = 0.0165$, Figure 59, I). Overall, HAM $RMS^{\%}$ on both flooring conditions were less than the starting baseline value of 100%. The HF condition displayed a significantly higher HAM $RMS^{\%}$ (91.14 ± 1.74 %) than the MT condition (89.66 ± 1.85 %). While the interaction effect of flooring and time was not significant, Figure 59, II displays the average HAM $RMS^{\%}$ across all subjects for each time point, split into flooring condition.

I.

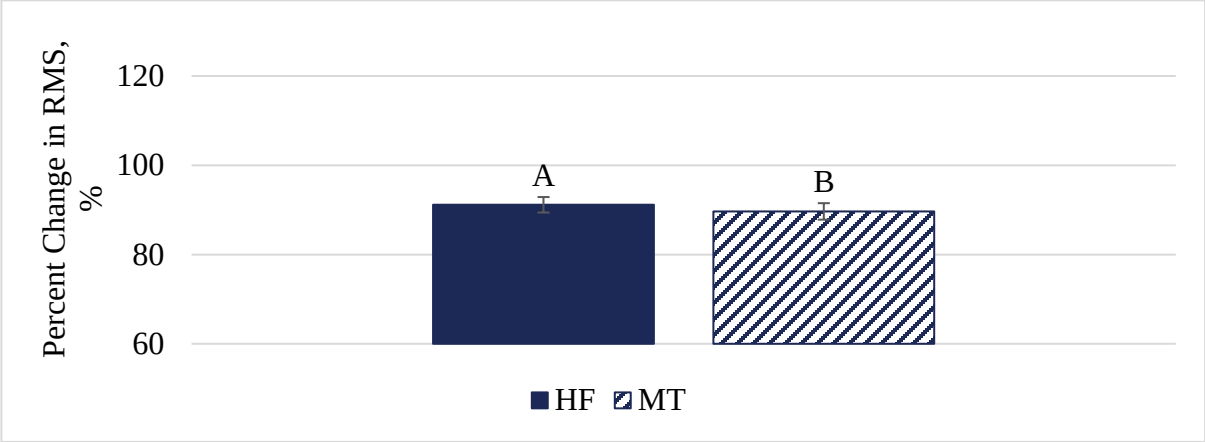

II.

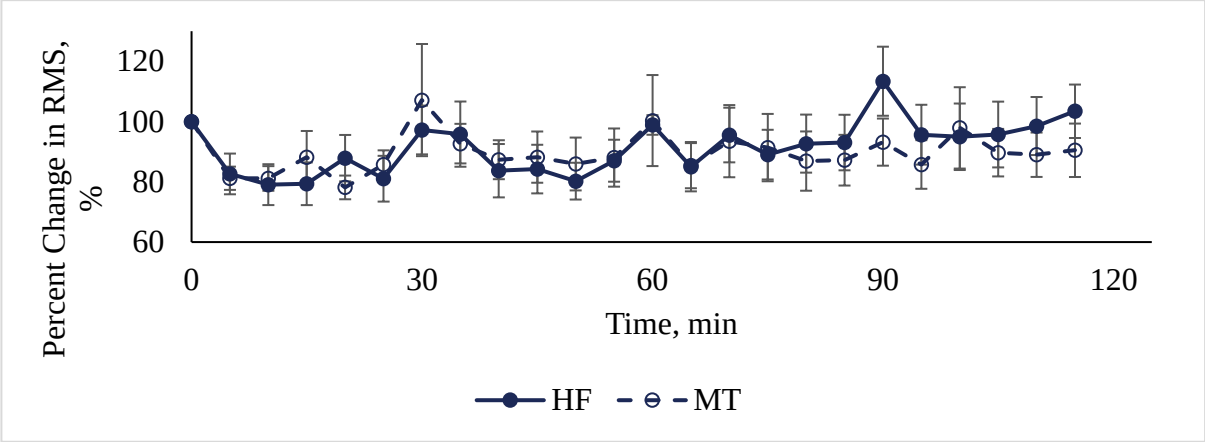

Figure 59: I. Flooring was a significant factor for HAM RMS$^{\%}$. Bars are the average HAM RMS$^{\%}$ value across all subjects and time points, split into flooring conditions. Bars connected by different letters are significantly different. Error bars are standard error of the mean. II.

4.4.1.6 Electromyography Measures and Subjective Tiredness and Discomfort

Pearson correlations were performed to compare MPF and $RMS^{\%}$ of all muscles with tiredness and discomfort measures (Table 24). Discomfort measures collected every 30 minutes were compared with EMG measures observed within the 5 minute period directly preceding the time at which discomfort and tiredness measures were collected. RF MPF was significantly correlated with overall tiredness and legs tiredness. No significant correlations were found between TA MPF, GAS MPF, SOL MPF, and HAM MPF with tiredness and discomfort measures. SOL $RMS^{\%}$ was significantly correlated with legs tiredness, upper legs, knees, and feet discomfort. HAM $RMS^{\%}$ was significantly correlated with hips, knees, and ankles discomfort. TA $RMS^{\%}$, GAS $RMS^{\%}$, and RF $RMS^{\%}$ were not significantly correlated with any tiredness or discomfort measures.

4.4.1.7 Electromyography Measures and Standing Strategies

Pearson correlations were performed to compare MPF and $RMS^{\%}$ of all muscles to standing strategies at each five minute interval (Table 25). Measurements of MPF and $RMS^{\%}$ of all muscles were significantly correlated with one or more standing strategies. GAS, RF, and HAM MPF were negatively correlated with shifts. Likewise, TA, SOL, and HAM MPF were negatively correlated with fidgets and total events. $RMS^{\%}$ was significantly correlated with fidgets and total events. TA, GAS, RF, and HAM $RMS^{\%}$ were positively correlated with fidgets and total events. However, SOL $RMS^{\%}$ was negatively correlated with fidgets and total events. HAM $RMS^{\%}$ weakly and negatively correlated with shifts.

Table 24: Pearson correlation results comparing EMG outcome variables and subjective tiredness and discomfort. ***p < 0.0001 ****, p < 0.001 ***, p < 0.01 **, p < 0.05 *, p > 0.05 NS***

MPF					
	TA	GAS	SOL	RF	HAM
Overall Tiredness	$\rho = -0.0846^{NS}$	$\rho = -0.0118^{NS}$	$\rho = 0.0404^{NS}$	$\rho = 0.2690$ ***	$\rho = -0.0930^{NS}$
Legs Tiredness	$\rho = -0.0606^{NS}$	$\rho = -0.0034^{NS}$	$\rho = -0.0443^{NS}$	$\rho = 0.2721$ ***	$\rho = -0.0318^{NS}$
Hips	$\rho = -0.0596^{NS}$	$\rho = -0.0784^{NS}$	$\rho = -0.0305^{NS}$	$\rho = -0.0747^{NS}$	$\rho = -0.0249^{NS}$
Upper Legs	$\rho = 0.0094^{NS}$	$\rho = -0.0756^{NS}$	$\rho = -0.1246^{NS}$	$\rho = 0.0347^{NS}$	$\rho = 0.0147^{NS}$
Knees	$\rho = -0.1413^{NS}$	$\rho = -0.0224^{NS}$	$\rho = -0.0011^{NS}$	$\rho = -0.0216^{NS}$	$\rho = -0.0991^{NS}$
Lower Legs	$\rho = -0.0585^{NS}$	$\rho = -0.0123^{NS}$	$\rho = 0.0835^{NS}$	$\rho = 0.1032^{NS}$	$\rho = 0.0260^{NS}$
Ankles	$\rho = -0.0496^{NS}$	$\rho = 0.0061^{NS}$	$\rho = 0.0598^{NS}$	$\rho = 0.0522^{NS}$	$\rho = 0.0570^{NS}$
Feet	$\rho = -0.1527^{NS}$	$\rho = -0.0634^{NS}$	$\rho = -0.0010^{NS}$	$\rho = 0.1425^{NS}$	$\rho = -0.0326^{NS}$
$RMS^{\%}$					
	TA	GAS	SOL	RF	HAM
Overall Tiredness	$\rho = 0.0204^{NS}$	$\rho = -0.0848^{NS}$	$\rho = -0.0606^{NS}$	$\rho = -0.0773^{NS}$	$\rho = -0.0635^{NS}$
Legs Tiredness	$\rho = 0.0833^{NS}$	$\rho = -0.0702^{NS}$	$\rho = -0.1864$ *	$\rho = 0.1149^{NS}$	$\rho = 0.0080^{NS}$
Hips	$\rho = 0.1036^{NS}$	$\rho = 0.0398^{NS}$	$\rho = -0.0858^{NS}$	$\rho = 0.0459^{NS}$	$\rho = -0.1604$ *
Upper Legs	$\rho = 0.0979^{NS}$	$\rho = -0.0216^{NS}$	$\rho = -0.1863$ *	$\rho = 0.1266^{NS}$	$\rho = -0.1263^{NS}$
Knees	$\rho = 0.0896^{NS}$	$\rho = 0.0096^{NS}$	$\rho = -0.1776$ *	$\rho = 0.0999^{NS}$	$\rho = -0.1567$ *
Lower Legs	$\rho = 0.0751^{NS}$	$\rho = -0.0807^{NS}$	$\rho = -0.1025^{NS}$	$\rho = 0.1543^{NS}$	$\rho = -0.1296^{NS}$
Ankles	$\rho = 0.0414^{NS}$	$\rho = -0.0872^{NS}$	$\rho = -0.0976^{NS}$	$\rho = 0.0560^{NS}$	$\rho = -0.1819$ *
Feet	$\rho = 0.0188^{NS}$	$\rho = -0.0420^{NS}$	$\rho = -0.1804$ *	$\rho = 0.0835^{NS}$	$\rho = -0.1340^{NS}$

Table 25: Pearson correlation results comparing EMG outcome variables and subjective tiredness and discomfort. ***p < 0.0001 ****, p < 0.001 ***, p < 0.01 **, p < 0.05 *, p > 0.05 NS***

MPF					
	TA	GAS	SOL	RF	HAM
Shifts	ρ = -0.0029 ^{NS}	ρ = -0.2194 ****	ρ = -0.0007 ^{NS}	ρ = -0.0860 **	ρ = -0.1002 ***
Fidgets	ρ = -0.1508 ****	ρ = 0.0128 ^{NS}	ρ = -0.1996 ****	ρ = 0.0211 ^{NS}	ρ = -0.2061 ****
Total Events	ρ = -0.1512 ****	ρ = 0.0037 ^{NS}	ρ = -0.2000 *	ρ = 0.0174 ^{NS}	ρ = -0.2108 ****
RMS$^{\%}$					
	TA	GAS	SOL	RF	HAM
Shifts	ρ = 0.0301 ^{NS}	ρ = 0.0559 ^{NS}	ρ = -0.0580 ^{NS}	ρ = -0.0242 ^{NS}	ρ = -0.0904 **
Fidgets	ρ = 0.2922 ****	ρ = 0.0610 *	ρ = -0.1276 ****	ρ = 0.2206 ****	ρ = 0.1431 ****
Total Events	ρ = 0.2940 ****	ρ = 0.0635 *	ρ = -0.1303 ****	ρ = 0.2199 ****	ρ = 0.1396 ****

4.4.2 Near Infrared Spectroscopy

A repeated measures mixed effects model was performed setting time, flooring, and BMI group as fixed effects; and subject as a random effect (Table 26). Graphs of observed means representing significant factors are included in this section. Plots of BMI group and flooring condition over time (observed averages and t statistics) are included in the appendix.

Time was a significant factor for HbO ($F_{23,940} = 1.96$, $p = 0.0045$), HHb ($F_{23,935} = 3.26$, $p < 0.0001$), and HbT ($F_{23,935} = 3.28$, $p < 0.0001$) (Figure 60 I-III). Dunnett's test was performed separately for each Hb type to compare all time points to the first time block, which was the average Hb value from 0 to 5 minutes. Time points that were significantly different from the first time block are labeled with asterisks (*). HbO and HHb both significantly increased with time. Both HbO and HHb contributed to the significant increase in HbT that occurs over time. StO_2 did not change significantly with time, suggesting that the amount of Hb that HbO and HHb contribute to HbT over time does not change proportionally over time. While HbO increased significantly from 0 minutes of standing by 35 minutes of standing, HHb was significantly different from 0 quickly—at 5 minutes of standing. After 20 minutes of standing, HbT was consistently significantly different from 0.

Time was a significant factor for Flow ($F_{23,927} = 12.54$, $p < 0.0001$, Figure 61). Flow was proportional to the change in HbT over time. Therefore, an increase in change in flow indicates an increase in the rate of HbT entering the tissue region of interest. Values are reported as percent changes from 0 minutes of standing. A Dunnett's post hoc test indicated that significant differences in flow occurred by 35 minutes of standing and leveled off.

Table 26: NIRS results from repeated measures mixed effects model investigating the effects of flooring (F), BMI (B), and time (T). ***p < 0.0001 ****, p < 0.001 ***, p < 0.01 **, p < 0.05 *, p > 0.05 NS***

	HbO	**HHb**	**HbT**
T	$F_{23,940} = 1.96$ **	$F_{23,935} = 3.26$ ****	$F_{23,935} = 3.28$ ****
F	$F_{1,956} = 11.51$ ***	$F_{1,944} = 0.47^{NS}$	$F_{1,950} = 7.05$ **
B	$F_{1,24} = 0.05^{NS}$	$F_{1,24} = 0.89^{NS}$	$F_{1,24} = 0.41^{NS}$
F x B	$F_{1,956} = 4.09$ *	$F_{1,944} = 0.02^{NS}$	$F_{1,950} = 3.52^{NS}$
F x T	$F_{23,940} = 0.25^{NS}$	$F_{23,935} = 0.18^{NS}$	$F_{23,935} = 0.28^{NS}$
B x T	$F_{23,940} = 0.29^{NS}$	$F_{23,935} = 0.46^{NS}$	$F_{23,935} = 0.39^{NS}$
F x B x T	$F_{23,940} = 0.35^{NS}$	$F_{23,935} = 0.66^{NS}$	$F_{23,935} = 0.44^{NS}$
	Flow	**SpO_2**	**StO_2**
T	$F_{23,927} = 12.54$ ****	$F_{23,883} = 0.55^{NS}$	$F_{23,901} = 0.36^{NS}$
F	$F_{1,936} = 7.99$ **	$F_{1,902} = 3.55^{NS}$	$F_{1,919} = 12.55$ ***
B	$F_{1,24} = 3.06^{NS}$	$F_{1,24} = 0.40^{NS}$	$F_{1,24} = 0.00^{NS}$
F x B	$F_{1,936} = 7.59$ **	$F_{23,883} = 0.02^{NS}$	$F_{23,901} = 5.65$ *
F x T	$F_{23,927} = 0.76^{NS}$	$F_{23,883} = 0.70^{NS}$	$F_{23,901} = 0.22^{NS}$
B x T	$F_{23,927} = 1.18^{NS}$	$F_{23,883} = 0.99^{NS}$	$F_{23,901} = 0.24^{NS}$
F x B x T	$F_{23,927} = 0.73^{NS}$	$F_{23,883} = 0.23^{NS}$	$F_{23,901} = 0.67^{NS}$

I.

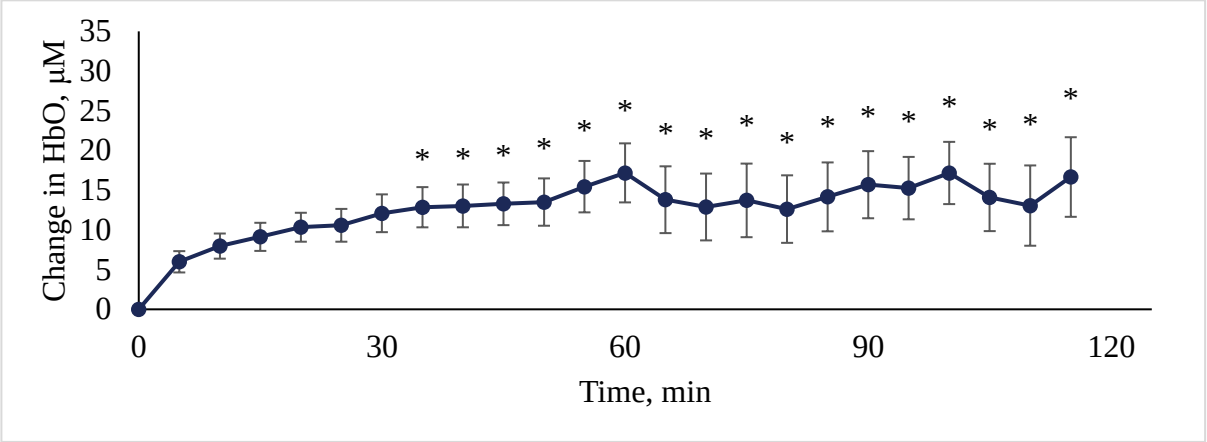

II.

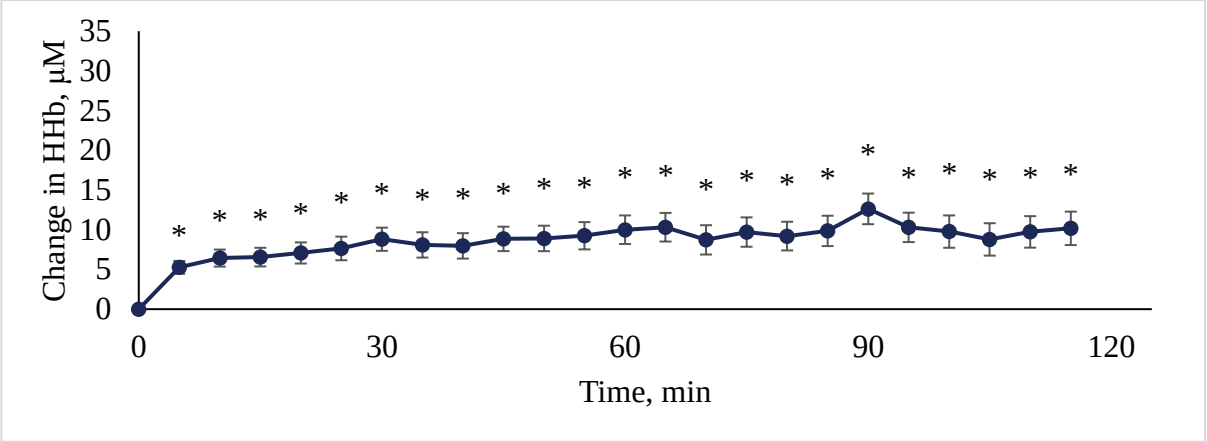

IV.

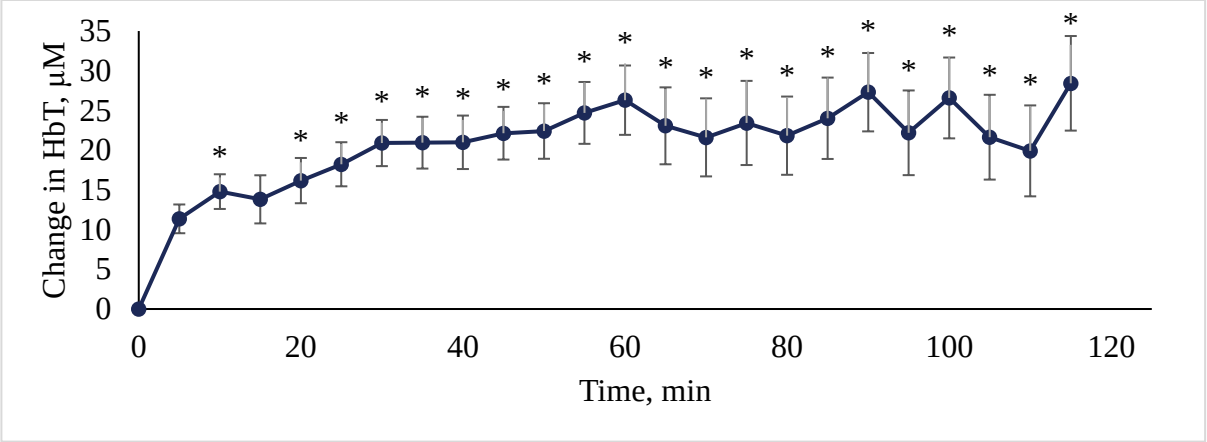

Figure 60: Change in I. HbO, II. HHb, and III. HbT over time. All data points represent average Hb values across all subjects and both flooring conditions at that time point. Error bars represent standard error of the mean. Values that are significantly different from the first time point (0) are labeled with asterisks (*).

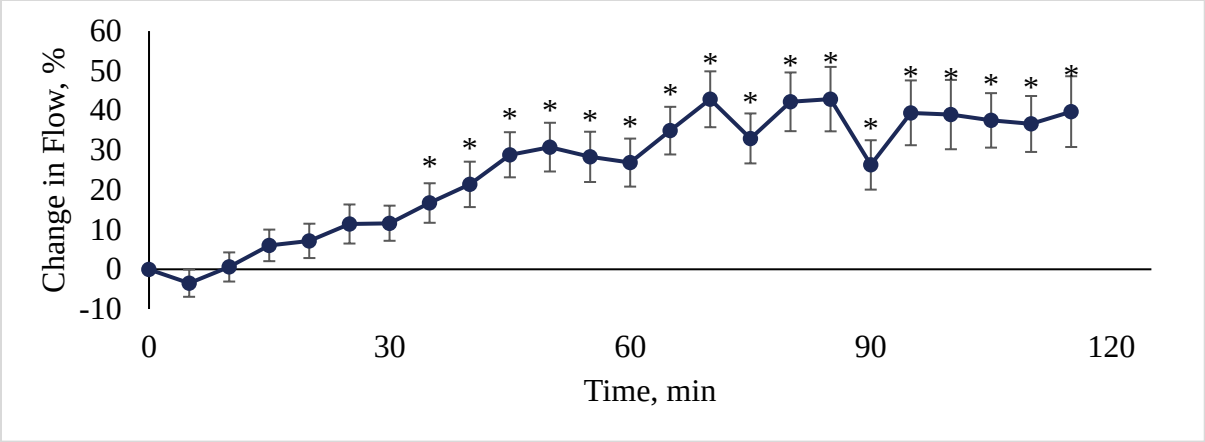

Figure 61: Change in flow over time. Points represent averages of all subjects standing on both flooring conditions every five minutes. Error bars represent standard error of the mean. Flow became significantly different from flow at time 0 by 35 minutes of standing, and continued to remain significantly different from 0 for the remainder of the standing trial. Values that are significantly different from 0 are labeled with asterisks (*).

Flooring was a significant factor for HbO ($F_{1,956}$ = 11.51, p = 0.0007), HbT ($F_{1,950}$ = 7.05 p = 0.0081), Flow ($F_{1,936}$ = 7.99, p = 0.0048), and StO2 ($F_{1,919}$ = 12.55, p = 0.0004). Flooring was trending towards significance for SpO2 ($F_{1,902}$ = 3.55, p = 0.0598). Bar graphs comparing HF and MT conditions are displayed in Figure 62, I-V. HbO increased significantly more on the HF condition (12.86 ± 1.03 μM) than on the MT condition (9.60 ± 0.99 μM). Similarly, change in HbT was significantly higher on the HF (19.63 ± 1.14 μM) than on the MT (17.43 ± 1.26 μM). The difference between HF HbO and MT HbO (3.25 ± 1.00 μM) is similar to the difference in HF HbT and MT HbT (2.19 ± 1.20 μM), confirming the non-significant difference between flooring conditions for HHb. Change in Flow was significantly higher for the HF condition (29.72 ± 1.97 %) than the MT condition (23.80 ± 1.93 %). This indicates that HbT not only increased more on the HF than on the MT condition, but the rate of change was higher overall on the HF condition

than the MT condition. Percent change in StO_2 represents the percent of HbT that is HbO. On the HF condition, this change was only slightly negative (-0.05 ± 0.07 %). However, percent change of StO_2 on the MT condition was significantly lower (-0.40 ± 0.07 %). Change in SpO_2 was not significantly different between flooring conditions. However, change in SpO_2 on the HF (0.46 ± 0.54 %) was lower than that on the MT condition (2.25 ± 0.41 %).

The interaction effect of flooring condition and BMI group was significant for HbO ($F_{1,956}$ = 4.09 p = 0.0434), Flow ($F_{1,936}$ = 7.59, p = 0.0060), and StO_2 ($F_{23,901}$ = 5.65, p = 0.0177). Figure 63, I displays observed HbO means, split into BMI group and flooring conditions. HbO increased during sanding from time 0 for all groups. Standing on the HF condition resulted in a significantly larger increase in HbO (10.52 ± 1.65 μM) than on the MT condition (8.56 ± 1.00 μM) A similar trend occurred within Flow. No significant differences were found between flooring conditions within the HW BMI group. However, the MT (28.77 ± 2.72 %) condition significantly decreased Flow within the OB group (OB HF, 40.70 ± 2.46 %, Figure 63, II). While no significant difference was found between flooring conditions within the HW BMI group, StO2 changed significantly between flooring conditions for the OB group. On the HF condition (0.07 ± 0.10 %), StO_2 was slightly positive. However, on the MT condition StO_2 became negative (-0.51 ± 0.09, Figure 63, III).

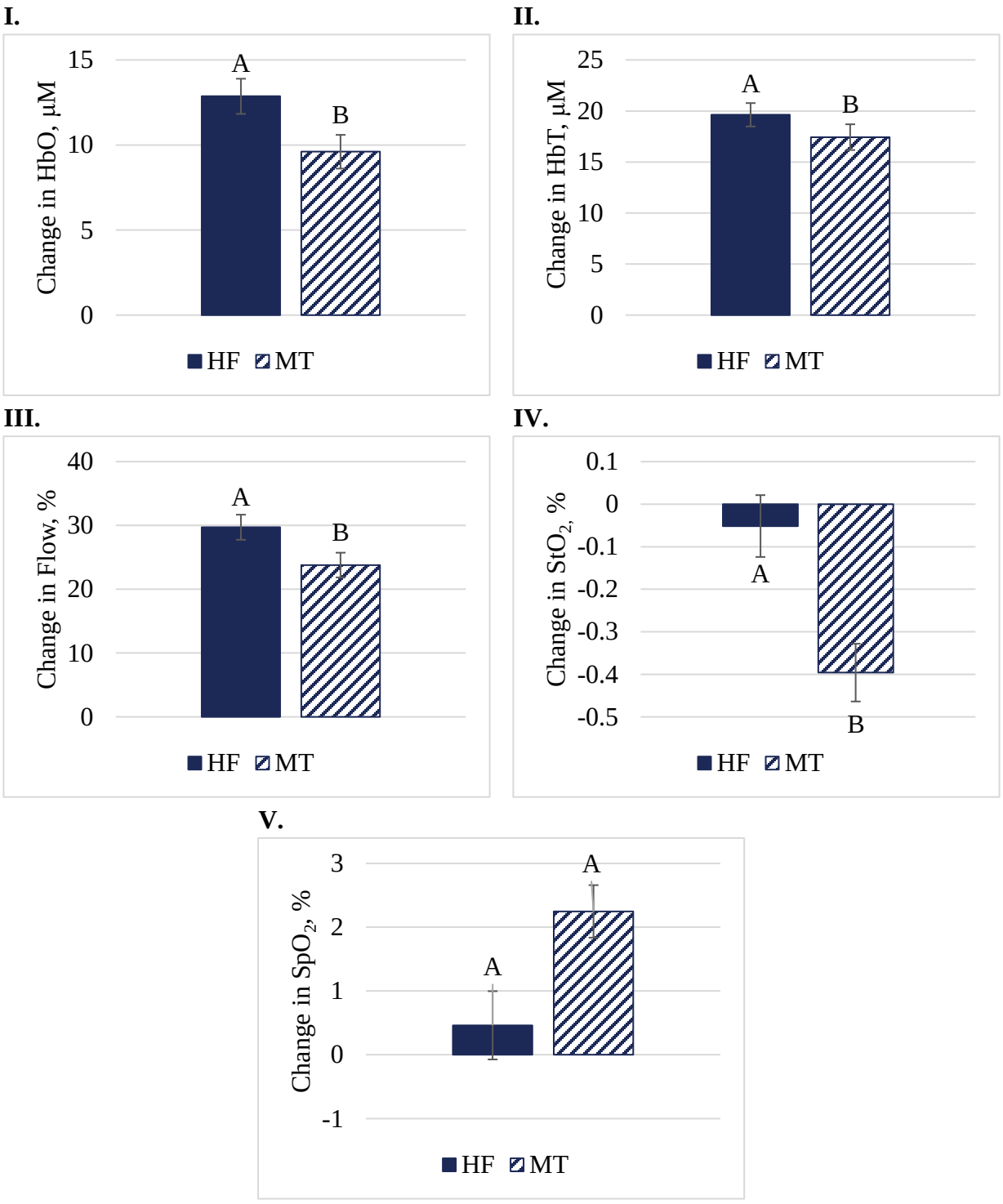

Figure 62: I. HbO, II. HbT, III. Flow, and IV. StO_2 changed significantly with flooring condition. SpO_2 did not change significantly, but was trending towards significance, so is included. Bars are average values across all subjects and all time points, split into flooring conditions. Bars are standard error of the mean. Bars labeled with different letters are significantly different.

I.

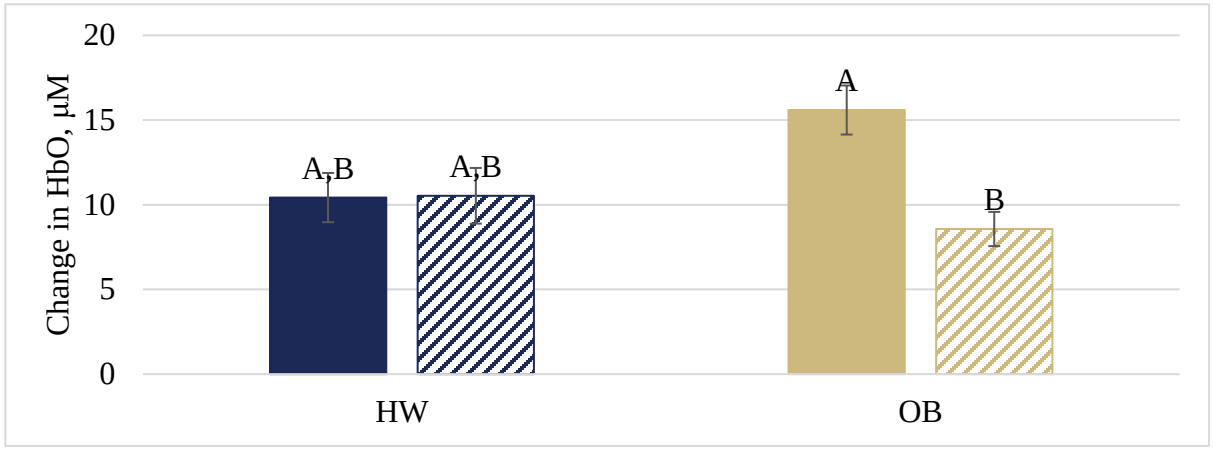

II.

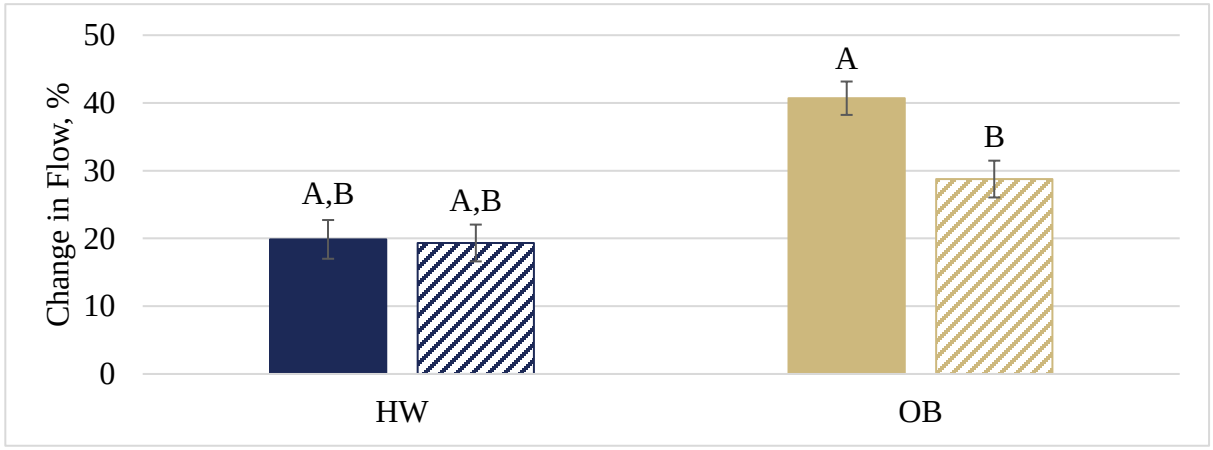

III.

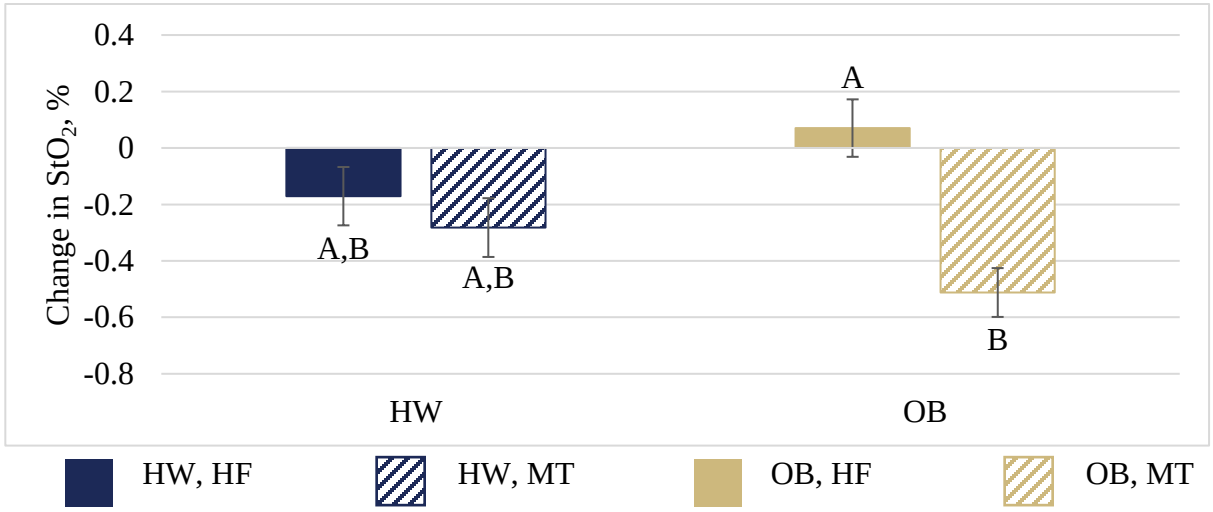

Figure 63: The interaction effect of flooring condition and BMI group was significant for I. HbO, II. Flow, and III. StO_2. Each bar represents average values, across all time points, split into BMI group and flooring conditions. Bars labeled with different letters are significantly different.

4.4.2.1 Near Infrared Spectroscopy Measures and Subjective Tiredness and Discomfort

Pearson correlations were performed comparing tiredness and discomfort measures every 30 minutes with the corresponding NIRS outcome measures from the 5 minutes period preceding the discomfort measure. Table 27 displays results from each correlation. HbO, HHb, HbT, Flow, and SpO_2 were positively correlated with tiredness and discomfort measures. Correlations between Flow and all tiredness and discomfort measures were most strongly correlated, in comparison with other NIRS outcome measures. StO_2 was negatively correlated with overall tiredness and hips discomfort.

Table 27: Pearson correlation results comparing NIRS outcome measures and subjective tiredness and discomfort. All six NIRS outcome measures were significantly correlated with tiredness and discomfort measures. ***p < 0.0001 ****, p < 0.001 ***, p < 0.01 **, p < 0.05 *, p > 0.05 NS***

	HbO	HHb	HbT
Overall Tiredness	$\rho = 0.0651^{NS}$	$\rho = 0.2679$ ****	$\rho = 0.1369$ *
Legs Tiredness	$\rho = 0.1185^{NS}$	$\rho = 0.2836$ ****	$\rho = 0.1850$ **
Hips	$\rho = 0.1048^{NS}$	$\rho = 0.2523$ ***	$\rho = 0.1690$ *
Upper Legs	$\rho = 0.0618^{NS}$	$\rho = 0.2010$ **	$\rho = 0.1201^{NS}$
Knees	$\rho = 0.1442$ *	$\rho = 0.2086$ **	$\rho = 0.1938$ **
Lower Legs	$\rho = 0.1571$ *	$\rho = 0.2574$ ***	$\rho = 0.2271$ **
Ankles	$\rho = 0.1670$ *	$\rho = 0.1683$ *	$\rho = 0.1910$ **
Feet	$\rho = 0.1435$ *	$\rho = 0.2684$ ****	$\rho = 0.2238$ **
	Flow	SpO_2	StO_2
Overall Tiredness	$\rho = 0.4985$ ****	$\rho = 0.2297$ **	$\rho = -0.1874$ **
Legs Tiredness	$\rho = 0.4558$ ****	$\rho = 0.1391^{NS}$	$\rho = -0.1042^{NS}$
Hips	$\rho = 0.2981$ ****	$\rho = 0.1118^{NS}$	$\rho = -0.1663$ *
Upper Legs	$\rho = 0.3847$ ****	$\rho = 0.0706^{NS}$	$\rho = -0.0929^{NS}$
Knees	$\rho = 0.3770$ ****	$\rho = 0.1844$ **	$\rho = 0.0105^{NS}$
Lower Legs	$\rho = 0.4034$ ****	$\rho = 0.2020$ **	$\rho = -0.0780^{NS}$
Ankles	$\rho = 0.3580$ ****	$\rho = 0.0564^{NS}$	$\rho = -0.0213^{NS}$
Feet	$\rho = 0.3804$ ****	$\rho = 0.0874^{NS}$	$\rho = -0.1084^{NS}$

4.4.2.2 Standing Strategies and Near Infrared Spectroscopy Measures

Pearson correlations were performed to compare NIRS outcome measures with standing strategies for every 5 minute period (Table 28). Fidgets and total events were significantly positively correlated with Flow. HHb was very weakly correlated with total events. Likewise, HbT and SpO_2 were very weakly correlated with shifts. No correlations were measured between HbO and StO_2 and standing strategies.

Table 28: Pearson correlation results comparing NIRS outcome measures and standing strategies. ***p < 0.0001 ****, p < 0.001 ***, p < 0.01 **, p < 0.05 *, p > 0.05 NS***

	HbO	HHb	HbT
Shifts	$\rho = 0.0523^{NS}$	$\rho = 0.0611^{NS}$	$\rho = 0.0625$ *
Fidgets	$\rho = -0.0307^{NS}$	$\rho = 0.0612^{NS}$	$\rho = -0.0126^{NS}$
Total Events	$\rho = -0.0286^{NS}$	$\rho = 0.0639$ *	$\rho = -0.0101^{NS}$
	Flow	SpO_2	StO_2
Shifts	$\rho = 0.0546^{NS}$	$\rho = 0.0161$ ***	$\rho = -0.1083^{NS}$
Fidgets	$\rho = 0.1978$ ****	$\rho = -0.0299^{NS}$	$\rho = -0.0385^{NS}$
Total Events	$\rho = 0.2007$ ****	$\rho = -0.0293^{NS}$	$\rho = -0.0431^{NS}$

4.4.3 Correlations of Electromyography and Near Infrared Spectroscopy Data

Pearson correlations were performed to compare EMG and NIRS outcome variables. Table 29 displays results of this analysis. Significant results were found. However, all correlations were weak. The largest correlation coefficient was 0.275 (TA $RMS^{\%}$ and Flow). TA MPF was weakly and negatively correlated with HbO, HbT, and Flow. TA $RMS^{\%}$ displayed stronger correlations with HHb, Flow, and StO_2. TA $RMS^{\%}$ was weakly correlated with HbT. GAS MPF was significantly, weakly, and negatively correlated with HbO and Flow. GAS $RMS^{\%}$ was significantly correlated with HbO, Flow, and StO_2 and more strongly correlated with SpO_2. SOL MPF was significantly correlated with SpO_2 and StO_2. SOL $RMS^{\%}$ was significantly correlated with HbO and HbT, and more strongly correlated with HHb. RF MPF was significantly correlated with HHb, HbT, and SpO_2. RF $RMS^{\%}$ was significantly correlated with HHb and StO_2. HAM MPF was significantly correlated with all NIRS outcome measures. HAM $RMS^{\%}$ was significantly correlated with SpO_2 and StO_2.

Table 29: Pearson correlations between EMG and NIRS outcome variables. ***p < 0.0001 ****, p < 0.001 ***, p < 0.01 **, p < 0.05 *, p > 0.05 NS***

	TA		GAS	
	MPF	$RMS^{\%}$	MPF	$RMS^{\%}$
HbO	ρ = -0.113 *	ρ = -0.002	ρ = -0.130 **	ρ = 0.095 *
HHb	ρ = -0.086	ρ = -0.236 ****	ρ = 0.097 *	ρ = -0.044
HbT	ρ = -0.116 *	ρ = -0.094 *	ρ = -0.057	ρ = 0.052
Flow	ρ = -0.129 **	ρ = 0.275 ****	ρ = -0.122 **	ρ = -0.126 **
SpO_2	ρ = 0.085	ρ = -0.034	ρ = -0.061	ρ = -0.249 ****
StO_2	ρ = 0.016	ρ = 0.246 ****	ρ = -0.270 ****	ρ = 0.142 **
	SOL		**RF**	
	MPF	$RMS^{\%}$	MPF	$RMS^{\%}$
HbO	ρ = -0.079	ρ = -0.126 **	ρ = 0.077	ρ = -0.038
HHb	ρ = -0.016	ρ = -0.227 ****	ρ = 0.092 *	ρ = -0.147 **
HbT	ρ = -0.064	ρ = -0.181 ****	ρ = 0.093 *	ρ = -0.086
Flow	ρ = 0.049	ρ = 0.023	ρ = 0.011	ρ = 0.076
SpO_2	ρ = 0.177 ****	ρ = -0.002	ρ = 0.114 *	ρ = 0.038
StO_2	ρ = -0.130 **	ρ = 0.052	ρ = -0.028	ρ = 0.100 *
	HAM			
	MPF	$RMS^{\%}$		
HbO	ρ = -0.094 *	ρ = 0.041		
HHb	ρ = -0.131 **	ρ = -0.037		
HbT	ρ = -0.120 **	ρ = 0.015		
Flow	ρ = -0.107 *	ρ = 0.078		
SpO_2	ρ = -0.091 *	ρ = -0.104 *		
StO_2	ρ = 0.093 *	ρ = 0.111 *		

5.0 Discussion

5.1 Tiredness and Discomfort

All recorded tiredness and discomfort measures increased significantly with time. Initiation of significant increases in tiredness and discomfort ratings occurred between 30 and 60 minutes of standing for all regions of interest. These findings agree with prior studies that measured subjective outcomes of prolonged standing over time [3, 5, 6, 21, 39, 42, 43, 45]. The magnitude of the change in tiredness and discomfort ratings at the end of two hours of standing were greater as the region of interest became more distal. Discomfort at the feet was significantly higher than any other body region. Similarly, legs tiredness was significantly higher than overall tiredness. This finding is also in agreement with previous literature and support by epidemiological evidence [3, 5, 9, 21, 39, 42, 43, 45, 46]. Epidemiological studies measuring musculoskeletal symptoms due to prolonged standing repeatedly cite disorder manifestation in the feet, ankles, and lower legs [17, 19, 20].

Measures of knees and feet discomfort were higher on the HF condition than the MT condition. No other tiredness or discomfort regions changed significantly due to flooring condition. Prior literature has measured decreased ratings of tiredness and discomfort on flooring interventions in comparison to a control hard floor [1, 3-6, 9, 11, 43, 45, 46]. Cham and Redfern found significant differences in tiredness and discomfort between the control hard floor and all anti-fatigue mat interventions [1]. These differences did not appear until after the second hour of testing. Considering these results, more differences between HF and MT conditions may exist, but subjects may not have stood long enough to observe statistically significant differences in more

body regions. Wiggermann and Keyserling found that flooring surface only had a significant effect on lower leg discomfort [11]. However, subjects were allowed to lift their feet. The protocol for the present study required that subjects maintain foot contact with the floor and did not lift their heels off the floor. This could make a marked impact on tiredness and discomfort measures over time. In most occupational applications, workers are able to lift their feet when standing. This not only increases blood flow and allows cartilage to relax— which may narrow the differences between the anti-fatigue mat and hard floor condition.

No significant differences in tiredness and discomfort measures due to BMI group were found. This nonsignificant trend was unexpected. Those within the OB group carry more weight—and therefore more joint and muscle forces during standing. It was expected then that they would report higher levels of tiredness and discomfort. Epidemiological studies have found that high BMI is linked to a higher likelihood of leg, foot, and knee pain from standing at work [19] and those with obesity are more likely to develop OA [86]. Additional research, a larger sample size, and recording for a longer period of time may clarify these trends.

The interaction effect of flooring condition and BMI group was significant for overall tiredness and feet discomfort. In both cases, the application of the MT condition within BMI group had different effects. The MT condition had very little effect on overall tiredness for the HW group, while the MT condition increased overall tiredness for the OB group. Prior literature suggests that an anti-fatigue mat increases overall torques on the ankle, which induce more small movements during standing [90]. These movements are likely very small and would not have been measured using the standing strategy methods. The MT condition may have exacerbated their predisposition to low stability [88-90]. This lack of stability may also suggest why overall tiredness was higher overall within the OB BMI group than the HW group. Alternatively, feet

discomfort decreased significantly for the OB group on the MT condition in comparison to the HF condition—suggesting that the load absorption qualities of the MT condition may have decreased discomfort, but increased engagement of stability mechanisms, which lead to increased tiredness over time. This phenomenon—in which the MT condition had different effects on each BMI group—is explored further throughout the discussion section.

5.2 Weight Transfer Measures

For this study, standing strategies were categorized based on underfoot force and temporal characteristics. This resulted in a novel method that determined two weight shift strategies, termed here fidgets and shifts. It has been hypothesized that a feedback loop exists where behavioral changes are utilized to mitigate negative physiological changes of prolonged standing [10, 11, 14]. Possible physiological changes during prolonged standing were split into two groups: changes in joint compression and changes in muscular fatigue. These two changes were chosen based on epidemiological evidence of development of both muscular/circulatory and joint related pathologies [25, 28, 29]. Compression of cartilage between the joints is associated with the compressive force applied to the joint, as well as the amount of time that force is applied. Muscular fatigue is generally associated with blood pooling and muscle use. The calf pump mechanism has been cited as a way to increase blood flow away from the lower extremities and back towards the heart [73]. To initiate this mechanism, the calf muscle must contract to develop pressure gradients that force blood against gravity. Therefore, any fast and strong movement may be related to muscular fatigue.

The two weight transfer strategies identified here may be related to different physiological mechanisms of prolonged standing. A fidget was defined as a movement out of or back into center that did not have a minimum time threshold associated with it. Any movement out of or back into center that lasted at least 7.5 seconds was considered a shift. The number of shifts, fidgets, and total events performed increased over time. Shifts increased significantly from 0 by 20 minutes of standing. Fidgets and total events increased significantly after only 5 minutes of standing. These results agree with prior literature despite many different methods being used to measure changes in weight transfers over time [11, 42-44].

Various methods have been used to measure weight transfers over time. Previous research has found that the frequency of medial-lateral transfers of COP and vertical force change over time [1, 6, 8, 11, 42-44]. The measurement methods chosen within each study were informed by the overall goals and rationale of the study, which can make interpretation across studies difficult at times. Comparisons between two previously published methods and the method used in the present study were performed [1, 11]. Overall, all measures (CWS, WWS, shifts, fidgets, and total events) were significantly correlated.

Shifts were most highly and positively correlated to WWS, as was expected. WWS were developed by Wiggermann and Keyserling to determine if "behavioral changes" occurred over time and between standing surfaces [11]. It was hypothesized that behavioral changes during standing manifested themselves when the distribution of vertical force between each foot transitioned between the following conditions: "(1) At least 20% of total body weight being supported by both the right and left foot, (2) >80% total body weight being supported by the right foot, or (3) >80% body weight being supported by the left foot" and the time spent in the condition was at least 7.5 seconds. Transitions between conditions that did not last 7.5 seconds were

considered part of a continuous motion and did not indicate changes in behavior over time. Shifts measured in this study maintained the same temporal threshold as WWS, but condition boundaries were 47% and 63% bodyweight.

Changes made to Wiggermann and Keyserling's methods were justified because of (1) an objective to measure changes in the use of stabilographic strategies and (2) differences in standing protocol between the study and the present study. Preliminary visual observation of force plate data indicated that subjects rarely transferred weight in which a single foot supported > 80% bodyweight. In fact, on average subjects only moved between the conditions defined by Wiggermann and Keyserling 11.63 ± 2.57 times over 2 hours of standing. Wiggermann and Keyserling allowed subjects to lift their feet. The subjects in the present study were not allowed to lift their feet or heels off the floor at any point during standing. If a subject is permitted to completely lift his or her foot off the ground during standing, 100% of their bodyweight must be placed on the other foot. Therefore, allowing subjects to lift their feet may lead to sustained and high amplitude changes in P_R over time and, possibly, a change in how the subjects respond to standing for prolonged times.

High force threshold did not capture sustained—but lower level—transfers in weight between legs. While this high threshold worked within Wiggermann and Keyserling's study, subjects in the present study could not lift their feet [11]. For this reason, an iterative process using all P_R data collected for this study was performed. This iterative process determined the minimum proportion in bodyweight that could be used to optimize the number of weight transfers performed over time. This value was calculated at 0.50 ± 0.13 BW. Using this force boundary condition instead of the boundary conditions set by Wiggermann and Keyserling doubled the average

number of shifts measured over two hours of standing, though both methods still significantly increased with time.

Fidgets were highly correlated with CWS. The standing protocol required for the study published by Cham and Redfern was very similar to the present study—in that subjects were not allowed to lift their feet [1]. It was hypothesized that lateral COP movement would indicate attempts to decrease discomfort and fatigue during standing. For the present study, P_R was used instead of lateral COP to measure CWS. P_R is the proportion of the total vertical force from the right and left feet that is on the right foot. COP measures the location where the ground reaction force would act [50, 51]. Equation 5-1 – Equation 5-7 describe how lateral COP is calculated when a subject is standing on two force plates (one foot on each plate). First, the COP (x_p) for each separate force plate are calculated using a ratio of the height of the force plate (h), lateral force (F_x), and moment about the y axis (M_y) with vertical force (F_z). This ratio is then corrected based on the location of the feet on the force plate (a). If the subject's feet are situated at the origin point on the force plate, then a goes to zero. This is performed for each force plate separately (Equation 5-1 and Equation 5-2). Then, these COP values are combined using a ratio of vertical force on the right (F_z^R) and left (F_z^L) force plates and total combined vertical force (F_t) as weighting values. Net COP (COP_{net}), according to a combination of Equation 5-1 – Equation 5-7, can be written in terms of the P_R. As P_R increases, the expression representing the right side is weighted proportionally higher than the left side. When P_R decreases, P_L increases and the expression representing the left side is weighted proportionally higher than the right side. Equation 5-7 describes net COP as a function of the location of each foot in space, proportion of weight on the right leg, vertical force, lateral force, and moment about the y axis on each force plate. Using P_R instead of COP to measure stabilographic changes due to prolonged standing omits differences

$$x_p^R = \frac{-h * (F_x^R - M_y^R)}{F_z^R} + a^R \quad \textbf{(5-1)}$$

$$x_p^L = \frac{-h * (F_x^L - M_y^L)}{F_z^L} + a^L \quad \textbf{(5-2)}$$

$$COP_{net} = \left(\frac{x_p^R * F_z^R}{F_t}\right) + \left(\frac{x_p^L * F_z^L}{F_t}\right) \quad \textbf{(5-3)}$$

$$F_t = F_z^R + F_z^L \quad \textbf{(5-4)}$$

$$P_R = \frac{F_z^R}{F_z^R + F_z^L} \quad \textbf{(5-5)}$$

$$P_L = \frac{F_z^L}{F_z^R + F_z^L} \quad \textbf{(5-6)}$$

$$COP_{net} = \left(\left(\frac{-h * \left(F_x^R - M_y^R\right)}{F_t * P_R} + a^R\right) * P_R\right) + \left(\left(\frac{-h * \left(F_x^L - M_y^L\right)}{\left(F_t * (1 - P_R)\right)} + a^L\right) * (1 - P_R)\right) \quad \textbf{(5-7)}$$

in lateral force and moment about the y axis, which will change—especially when transferring weight laterally.

Figure 88 (displayed in Appendix B.1) displays five minutes of COP and P_R for a single subject collected from a previous study performed at the Human Movement and Balance Laboratory [43]. COP is on the left vertical axis, while P_R is on the right vertical axis. Positive COP is movement towards the right side of the body, while negative COP is movement towards the left side of the body. Likewise, a value of $> 0.5\ P_R$ is movement towards the right side of the body, and a value of $< 0.5\ P_R$ is movement towards the left side of the body. CWS was calculated using the five minutes of both COP and P_R data to compare outcome variables. In both cases, the average value was used as "center," and a weight shift was counted when the subject moved beyond the average value ± 5% of the total range observed during standing. Using COP, 31 weight shifts were measured. Using P_R, 15 weight shifts were measured. This suggests that using P_R will underestimate the number of weight shifts in comparison with using COP. It is likely that the number of events measured by Cham and Redfern were much higher than those measured here. However, it is also likely that the overall trends were the same given the similarity in overall shapes of the curves, based on the analysis of data portrayed in Figure 88.

Shifts were weakly positively correlated with total events. Positive correlation is expected given the total number of events is a sum of fidgets and shifts. The weak correlation may be due to the disproportion of shifts performed in comparison to fidgets. Considering the total number of movements measured over two hours of standing, subjects performed more fidgets overall than shifts. This is expected, as the minimum time threshold set for shifts limits the number of shifts performed during two hours of standing to 960 shifts— assuming that each shift was performed sequentially and for exactly 7.5 seconds. This translates to 40 shifts every 5 minutes. In some

cases, subjects performed over 100 fidgets in a 5 minute period. It is unknown if the time threshold—adapted from Wiggermann and Keyserling—represents actual physiological differences in behaviors [11]. However, it is clear that low frequency and high frequency strategies exist.

Shifts were negatively correlated with fidgets. Across all subjects, shifts and fidgets both increased over time. However, a negative correlation between shifts and fidgets suggests that, on a subject level, when a subject increases the number of shifts performed, they are not necessarily increasing the number of fidgets. A visual observation of the change in shifts and change in fidgets on a subject by subject level indicated that approximately 12 subjects increased both standing strategies, shifts and fidgets, over time. Eight subjects increased fidgets over time, five subjects increased shifts over time, and two subjects displayed no discernable changes over time. A preliminary analysis was performed to group subjects with similar characteristics of fidgets and shifts throughout two hours of standing. More details about this analysis are included in Appendix B.3.

No significant differences in shifts, fidgets, or total events were found due to flooring condition. This is in disagreement with some prior literature, in which standing on the anti-fatigue mat decreased overall movement in comparison with the hard floor condition [1, 3, 6, 11]. Standing studies that found significant differences in movement due to standing surfaces may have had slightly different protocols—such as allowing subjects to lift their feet or their heels [11]. Alternatively, subjects stood for at least four hours and changes were only found after two hours of standing [1, 5, 11]. However, a study performed by Haney utilized the same anti-fatigue mat as this study for 6 hours of standing [43]. Both this previous study and the present study did not find significant differences in stabilographic events between floors. This suggests that standing

for a longer period of time may not show a difference in stabilographic events with the mat used. However, different flooring surfaces may induce different movements. Cham and Redfern measured mechanical properties of multiple mats and determined that standing on an anti-fatigue mat with greater elasticity, greater stiffness, and lower energy absorption significantly decreases CWS [1].

Differences in discomfort, EMG measures, and NIRS measures occurred due to flooring condition. However, no significant differences in shifts, fidgets, or total events were found due to flooring condition. The metrics and thresholds chosen to measure stabilographic strategies may not have been sensitive enough to measure changes due to the MT condition. Alternatively, standing strategies may be subject specific. In other words, the kinds of standing strategies that a person performs during prolonged standing may not be affected by environmental factors such as the MT condition. To determine if standing strategies are subject specific, a large cohort of subjects are needed so that clusters of similar groups may be formed.

The number fidgets and total events was higher for the OB group than the HW group. COP speed, displacements, and postural sway were found in prior literature to increase with BMI during quiet standing [88-90]. While small stabilographic changes are likely not registered as standing strategies, this lack of stability may have led to a greater need for more movement within OB as tiredness increased, manifesting itself in higher numbers of fidgets. Unexpectedly, changes in shifts due to BMI group were not significantly different. Those with obesity carry more mass and therefore, it was expected that higher levels of cartilage compression may occur. Further analysis may be needed to pinpoint temporal differences in weight transfer behaviors in groups to optimize this method. Other future directions should be considered. Subjects could stand for longer periods of time to determine if shifting behavior is exhibited later during prolonged standing. It may also

be the case that OB subjects' cartilage was already adapted to added weight during standing. To examine this, results from OB subjects could be compared to a controlled test in which MTFG data is collected from healthy weight subjects wearing weight vests while standing.

As time increased, OB adults demonstrated significantly more shifts, fidgets, and total events than their HW counterparts. Prior literature also confirms that during quiet stance, postural sway increases significantly over time with increasing BMI [90]. While no significant differences were found between BMI group at each discrete time point, visual observation of the graphs (Figure 35) indicate that the OB BMI group displayed higher numbers of shifts, fidgets, and total events over time in comparison to the HW group. The lack of statistical significance may be due to a lack of power comparing 24 time points between 2 groups within the Tukey HSD comparison tests. It is known that those with obesity have higher likelihoods of development of joint and circulatory disorders [10, 85, 86]. It is likely that higher numbers of shifts and fidgets seen as time spent standing increased may be to relieve the effects of added weight over the lower extremities and known physiological differences in obese adults.

The interaction effect of BMI group and flooring condition was significant for change in shifts. Change in shifts within the HW BMI group decreased significantly when standing on the MT versus the HF condition. The MT condition may have had a protective effect on joint compression. However, no significant differences in MTFG or T_T were measured due to flooring within the HW BMI group. Shifts as a standing strategy may be related to other physiological changes. No change in shifts was confirmed between flooring conditions for the OB BMI group.

5.3 Knee Joint Measures

MTFG was highly influenced by knee kinematics that varied across subjects. Studies measuring MTFG and kinematics during gait, running, and squatting determined that knee kinematics affect MTFG during these dynamic activities [63, 65, 66, 68]. In studies measuring *in vivo* tibiofemoral cartilage compression, knee kinematics were controlled throughout the study [38, 64, 66]. This was much easier in prior literature that measured compression over a maximum of ten minutes. Allowing subjects to stand more freely during the present study introduced kinematics as a source of variability. These differences in kinematics made it very difficult to measure changes in MTFG over two hours of standing.

Due to variability caused by differences in kinematics, time was not directly measured as a fixed effect of MTFG. Instead, an empirical piecewise model was fit to the data in which a quadratic function converged with a linear tail. This model was informed by prior research in which *in vivo* and *ex vivo* cartilage compression followed similar trends [53, 55-58, 64, 68]. Out of a total 51 visits to be modeled, 14 visits did not converge. One visit converged but resulted in an increase in MTFG over time. The abundance of models that resulted in a decrease in MTFG over time suggests that MTFG does likely decrease due to prolonged standing.

The effect of time on MTFG was measured by calculating the time at which terminal gap was reached (T_T). This value is the time point during each two-hour visit where the quadratic minimum value and linear tail converged. This time was not constrained, meaning that the time leading to the best fit was found—even if that time was greater than 120 minutes. T_T as a metric was not directly measured by Paranjape et. al. when investigating the effects of prolonged walking on cartilage strain [68]. However, visual inspection of the graphs included in the study (and replicated in Figure 4) indicate that group level “terminal gap distance” may be reached between

10 and 60 minutes of walking [68]. This is somewhat consistent with the present study, where mean T_T across all subjects was 42.53 ± 5.71 minutes, ranging from 6.83 to 155.88 minutes. More research needs to be done to determine what other factors affect T_T. However, these values could be used to inform best practices in the workplace. Currently, the United States Department of Labor mandates a 30 minute break after 4.5 hours of working [15]. For those that stand all day at work, T_T values suggest that tibiofemoral cartilage is likely completely compressing during this time. This may explain why continual and repeated exposure to prolonged standing at work is linked to increased risk of OA [24]. Before any changes in workplace culture are mandated, more convergence studies across a longer period of standing time should be performed.

The large quantity of visits that did not converge begged whether or not standing strategies may influence the lack of convergence. For this reason, the likelihood of convergence was investigated based on the total number of shifts, fidgets, and total events performed during two hours of standing for each visit. These relationships were not statistically significant. This may be due a few reasons. The model chosen may not be appropriate for prolonged standing data. An exponential decay formula or other formula more informed by viscoelastic models of cartilage compression could be used [56, 58, 68]. Over 2 hours of standing, there were a total of 14 data points collected. A more controlled study may be required in which images are collected through the full motion of a shift or fidget.

No significant changes in knee joint measures were found due to flooring condition. It was hypothesized that differences in standing strategies may be related to changes in knee joint measures. However, standing strategies were not significantly different due to flooring condition. Lack of significance in both measures makes it difficult to determine if there is a relationship between knee joint measures and standing strategies on different flooring conditions.

While no statistically significant interaction effects were found, the most interesting knee joint measures results suggest a change in T_T due to the MT condition within the OB group. Because a number of visits were removed due to a lack of convergence, a lack of statistical findings may be due to a lack of statistical power. Between flooring conditions, T_T was noticeably larger on the MT (29.3 ± 5.5 min) versus the HF (16.0 ± 9.7 min) condition for the OB group. No discernable changes occurred for the HW group between flooring conditions. A larger T_T value indicates that the MT condition may have delayed onset of full cartilage compression during standing, according to the model. The load bearing properties of the MT condition may have helped slow cartilage compression for the OB group. The clinical and human factors implications of these results are important to note. Findings that the MT condition may delay onset of full cartilage compression for the OB BMI group and not the HW group suggest that the MT intervention may be more effective for those with obesity. These findings also provide evidence that ergonomic interventions should be studied across different demographic groups to determine how interventions should be designed and implemented across groups. A more controlled study, in which more images of subjects are collected and movements are more controlled may shed light on this phenomena.

5.4 Lower Extremity Muscle Measures

5.4.1 Electromyography

Time was a significant factor for TA MPF and RF MPF. However, in both cases, no clear trends of changes with time were measured. It is expected that MPF will decrease with time as

muscle fatigue increases [50]. TA MPF displayed significant differences between time points at 30 and 55 minutes. Neither of these time points were significantly different than TA MPF at 0 minutes. RF MPF also did not display any obvious trends with time. However, RF MPF at 75 and 85 minutes were significantly larger than RF MPF at 0 minutes of standing. This may indicate a trend towards an increase in RF MPF over time, but no other evidence for this trend exists. No other measurements of MPF or $RMS^{\%}$ changed significantly with time.

Most prolonged standing studies utilized EMG to compare the effects of anti-fatigue mats or other interventions. No prolonged standing studies found by the author discovered significant differences in MPF or RMS with time during standing [1, 6, 43, 45]. Similarly, it was found here that the flooring and time interaction effect had a no significant effect on MPF or $RMS^{\%}$ over time. In maximum voluntary contraction (MVC) studies, MPF and RMS are monitored over time as indicators of muscle fatigue [50]. MVC results in decreased MPF and increased RMS over time. It is possible that these metrics are not as effective in measuring effects of the low intensity, prolonged contractions and slow fatiguing experienced during prolonged standing.

Changes in MPF are related to changes in signal amplitude and duration. When fatiguing occurs, MPF is expected to decrease due to increasing duration and decreasing amplitude. Analysis of flooring effects compared overall averages of MPF and $RMS^{\%}$ across all time points and subjects and split these groups into flooring conditions. No significant differences in MPF or $RMS^{\%}$ were associated with flooring condition over time. However, some overall average MPF and $RMS^{\%}$ values were significantly different between flooring conditions. Overall, SOL MPF was higher on the MT condition than on the HF condition. Throughout the duration of standing, SOL MPF on the MT was consistently higher than on the HF condition. However, no distinct changes occurred due to time. These differences therefore may be due to differences in EMG

placement. HAM MPF was lower on the MT condition than the HF condition. The plot of HAM MPF over time between flooring conditions does display a slight decreasing trend in MPF on the MT condition over time. However, this flooring and time interaction was not significant.

$RMS^{\%}$ is a measure of muscle activity of regional muscle fibers. Posterior muscles (HAM, GAS, and SOL) $RMS^{\%}$ was significantly lower on the MT condition than the HF condition. This difference did not occur significantly with time. However, plots of HAM, GAS, and SOL $RMS^{\%}$ over time do display a slight decreasing trend in $RMS^{\%}$ on the MT condition after approximately 60 minutes of standing. The HF condition does not display the same trend. Interestingly, TA $RMS^{\%}$ (anterior muscle) was significantly higher on the MT condition than on the HF condition. Over time, TA $RMS^{\%}$ on the HF and MT condition showed the same trends. However, throughout standing TA $RMS^{\%}$ was slightly higher. This is consistent with Madeleine et. al., in which soleus RMS was less on the soft surface, and tibialis anterior RMS was higher on the soft surface, in comparison to the hard surface control [6]. During standing, subjects were permitted to utilize a standing desk set at elbow height in front of them. Subjects were instructed to not lean on the desk or put their bodyweight on the desk. Our subjects had to work in tight quarters because due to the required configuration of the x-ray system and standing desk. For this reason, the standing desk may have been too close to the subject. In fact, some subjects (especially from the OB group) mentioned this during testing. This would require subjects to lean slightly backwards, which would initiate engagement of the tibialis anterior to maintain stance. The differences in $RMS^{\%}$ between flooring conditions may reflect the interaction of the load bearing capabilities of the MT and the muscle systems used to maintain stance. It is important to note, though, that RMS data is difficult to interpret because (1) it only measures muscle activity in a small region of interest, and (2) there are many muscles that participate in stance maintenance that were not measured.

Significant flooring condition and BMI group interactions indicate that the MT condition may impact BMI groups differently. SOL MPF of the HW group was significantly lower on the MT condition than the HF condition. Instead, SOL MPF of the OB group was significantly higher on the MT condition than on the HF condition. Within the HW group, HAM MPF was significantly lower on the MT—but there was no significant change in HAM MPF between flooring conditions within the OB group. Only these two muscle groups displayed significant differences associated with the interaction of flooring and BMI group. SOL, GAS, and RF $RMS^{\%}$ significantly decreased within the HW group on the MT condition. However, the MT condition had different effects on each muscle within the OB group. SOL $RMS^{\%}$ significantly increased, GAS $RMS^{\%}$ significantly decreased, and HAM $RMS^{\%}$ showed no significant differences on the MT condition within the OB group.

These findings suggest that muscular adaption to the MT condition may be different between HW and OB BMI groups. It has already been established that those with higher BMI display less stability during quiet stance. The introduction of the MT condition likely disrupts this stability even more. The HW and OB BMI groups may displays different methods of dealing with this instability. Because SOL $RMS^{\%}$ increased on the MT, the OB group may prefer an ankle strategy to maintain stance, while the HW group may use a strategy that utilizes multiple muscles or other muscles that were not measured. Many muscles were not recorded that could have also played a role in maintaining stance during prolonged standing.

5.4.2 Near Infrared Spectroscopy

The primary circulatory pathologies associated with prolonged standing include chronic venous insufficiency, carotid atherosclerosis, and varicose veins. Each of these pathologies are

associated with repeated exposure to high blood volume changes in the lower extremities [10]. Because of this, the most important metric to monitor during prolonged standing may be HbT. HbT increased with time, and HbT was significantly different from 0 between 5 and 10 minutes of standing. In agreement with previous research, HbT tends to increase rapidly and then displays a tendency to level off after approximately 30 minutes of standing [73]. It is known that compliance of venous structures is higher than arterial structures [73-75]. Therefore, it is likely that the majority of changes in Hb over time resided in the capillaries and venous structures [74]. According to hemodynamics research, HbT increases while capillaries and veins expand until internal hydrostatic pressure and external hydrostatic pressure equalize—at which point HbT levels off [73]. The velocity that this occurs and the time at which HbT levels off may be related to a person's likelihood for the development of circulatory pathologies due to prolonged standing.

Most prolonged standing studies did not directly measure circulatory effects. Previous studies have reported changes in leg/foot volume and temperature as indicators of blood pooling. Some studies measured significant differences in leg/foot volume and skin surface temperature over time [3, 5, 42]. Assuming that changes in leg/foot volume and skin surface temperature are induced by increases in blood volume in the lower extremities, these studies agree with increased levels of HbT over time. This is a good assumption for the healthy subjects in this study. However, interstitial fluid also settles in the lower extremities due to prolonged standing. For those with edema or other similar pathologies, changes in leg/foot volume due to interstitial fluid will be higher [109]. Madeleine et. al. did not find any significant differences in volume or surface temperature with time [6]. However, no details of standing constraints were mentioned for this study [6]. If subjects were allowed to perform calf raises or lift their feet during standing, changes in leg volume and skin surface temperature may have been mitigated [6].

HbT is comprised of HbO and HHb, both of which increased significantly with time. HbO was significantly different from 0 by 35 minutes of standing. HHb was significantly different from 0 by just the first 5 minutes of standing. Arterial oxygen saturation for healthy individuals is approximately 96-98% and venous oxygen saturation is approximately 75% of the total Hb binding sites available [110]. Therefore, it was expected that changes in HHb over time were less than changes in HbO over time. Flow, a measurement of the rate of change of arterial blood volume over time, also increased with time. Expectedly, then, significant changes in HbO occurred within the same 5 minute time block that significant increases in flow occurred (35 minutes).

It has been hypothesized that muscle fatiguing that occurs during prolonged standing is due to a lack of oxygen available for muscles [42]. However, it is clear from these results that not only does HbT increase over time, but HbO also increases. Garcia et. al. found similar results in which HbT and StO_2 increased over time [42]. StO_2, which is a measurement of the proportion of HbT and HbO, and the relationship between these factors are included in section 3.4.4.2. Therefore, it is likely that fatiguing during a low intensity, long duration task may be due to an imbalance of other metabolic substrates or slowing of oxygen diffusion through the muscle [42, 73]. Haney measured changes in HbT and StO_2 over time, but did not find any significant differences [43]. The study performed by Haney required six hours of standing. Within each hour, increases in HbT and StO_2 were found. However, there were seated breaks every hour—which may have mitigated changes in circulatory effects enough to lose statistical significance.

No changes in StO_2 and SpO_2 were found due to time. StO_2 is the proportion of HbT that is HbO. While both measurements increased over time, a lack of significant differences in StO_2 suggest that these changes increased proportionally. SpO_2 measures arterial oxygenation, which is approximately 96 – 98% at baseline [110]. Large changes in SpO_2 occur most often due to

increased metabolism (for example, due to exercise) or circulatory pathologies [110]. Prolonged standing is not a high energy activity. Therefore, changes in SpO_2 are not expected.

HbO, HbT, Flow, and StO_2 changed significantly due to flooring condition. HbO, HbT, and Flow were significantly lower on the MT condition in comparison with the HF condition. StO_2 decreased significantly more on the MT condition than on the HF condition. These significant differences did not occur over time. Rather, they are indicative of circulatory patterns in response to the MT condition at all time points. Haney measured differences in HbT and SpO_2 due to different flooring conditions. No significant differences between flooring conditions were found. However, studies that indirectly measured circulatory changes due to standing found significant differences due to flooring effects. Cham and Redfern found that skin surface temperature was significantly higher on the HF condition than on any of the anti-fatigue mat conditions during the fourth hour of testing. No significant differences were found during the first three hours. Lin et. al. found that shank circumference was significantly higher on the HF condition for the first two hours of standing.

Flow measures the rate at which blood volume (HbT) moves through the arteries over time. The majority of blood passed through the arteries is oxygenated. Because of a decrease in Flow on the MT condition, smaller changes in HbT (and therefore HbO) were measured on the MT condition during standing. StO_2 is a measure of the proportion of HbT that is HbO. Therefore, if the changes in StO_2 are negative, then the proportion of HbO went down when standing on the MT condition. This proportional decrease may be due to decreased Flow into the region, or increased metabolism. Higher levels of metabolism would be required if muscle contractions increase. Anti-fatigue mats are designed to increase small torques on the ankle to induce tiny movements to

maintain stance. The soleus muscle is highly involved in this process. Therefore, higher metabolism may have been required to maintain stance.

These results indicate that the use of an anti-fatigue mat may decrease Flow and consequentially decrease HbT. These results, while statistically significant, their clinical impact is unclear. In other words, it is unknown if a decrease in HbT, HbO, and Flow results in more positive outcomes and less circulatory pathologies over time. It is also unknown if these differences are maintained for over a two-hour standing period. Additional research should be performed to determine how these differences progress beyond two hours of standing. This is especially important given that workers tend to stand for over 4.5 hours at a time at work [15].

Similar to EMG findings, each BMI group had different responses to the MT flooring condition. HbO and Flow similarly saw no significant differences between flooring conditions within the HW group. HbO and flow for the OB group were more similar to Flow within the HW group when standing on the MT condition. However, these values increased significantly when standing on the HF condition. StO_2 displayed similar trends, in which the MT condition did not have a significant effect within the HW group. However, change in StO_2 was negative on the MT condition, but slightly positive on the HF condition. This means that the overall proportion of HbO was lower on the MT condition than the HF condition [90]. This may again be related to increased torques on the ankle and resultant small movements which increase metabolism and use more oxygen.

5.4.3 Correlations of Electromyography and Near Infrared Spectroscopy

Prior prolonged standing studies have speculated that muscle fatigue is linked to ischemia [2, 11]. MPF and RMS have been used repeatedly in prior literature to assess muscle fatigue during prolonged standing [1, 6, 43]. To investigate the relationship between NIRS and EMG measures, Pearson correlations were performed. MPF and $RMS^{\%}$ were significantly correlated with NIRS outcome variables within each muscle region of interest. All correlations were low, suggesting that any relationships are weak and may require further analysis.

Some assumptions regarding interpretation of correlations between EMG and NIRS measures are important to note. The NIRS probe was placed on the soleus muscle on the left leg. All EMG devices were placed on the right leg. Any relationships between NIRS and EMG measurements therefore are under the assumption that subjects treat each leg the same. Furthermore, the circulatory system is a closed loop system in which changes in the soleus muscle may be linked to changes in other muscle regions. Therefore, significant correlations between NIRS outcome measures and EMG measures of the HAM, RF, TA, or GAS may be due to unknown interdependent circulatory effects.

SOL $RMS^{\%}$ was significantly and negatively correlated with all blood volume measures (HbO, HHb, and HbT). In other words, increases in muscle activity were related to lower blood volume levels. When muscles contract and release, a pressure differential is formed. This pressure differential creates a pumping mechanism that moves blood through the muscle and towards the heart. Therefore, negative correlations may reflect this phenomenon.

SOL MPF was significantly correlated with SpO_2 and StO_2. Both correlations were low. SpO_2 was positively correlated with SOL MPF and StO_2 was negatively correlated with SOL MPF. It is expected that decreasing MPF values are linked to increases in muscle fatigue. Similarly,

decreases in oxygen are linked to increases in muscle fatigue. The positive correlation between SpO_2 and SOL MPF are therefore expected. However, StO_2 displayed a negative correlation with SOL MPF. These findings suggest that the manner in which oxygenated blood is measured (pulsatile, SpO_2; tissue saturation, StO_2) may influence how fatigue is interpreted.

5.5 Correlations with Discomfort and Tiredness

Correlations were performed to examine if a relationship between discomfort and tiredness, standing strategies, and physiological outcomes of prolonged standing. They do not justify causation, and therefore significant relationships should not be misconstrued as such. This is especially true as both discomfort and tiredness and stabilographic strategies increased significantly with time. Therefore, correlations may be significant due to time acting as a covariate between groups. However, relationships are still worth noting.

All tiredness and discomfort measures are significantly and positively correlated with fidgets and total events. Likewise, hips and upper legs discomfort are significantly correlated with shifting behavior. All three of these measures increased with time. It is interesting to note though that shifts were *only* correlated with hips and upper legs. Because subjects were not allowed to lift their feet during standing, a shift involved single knee flexion (leg 1) combined with hip adduction of the contralateral leg (leg 2). The majority of bodyweight is maintained by leg 2 while leg 1 relaxes. Shifts have a minimum time requirement, which means subjects shift and then temporarily stop moving. To shift again, they have to build up momentum to move. Fidgets on the other hand are a more continuous rocking motion between legs. This indicates that shifts may be more related to proximal lower extremity discomfort and fidgets may be more related to total lower extremity discomfort. There is some epidemiological evidence of hips osteoarthritis associated with prolonged standing at work. More work may need to be done in the area of measuring cartilage deformation at the hips, as well as the knees, during prolonged standing.

T_T was significantly and positively correlated with feet discomfort. These two outcomes, while not intuitively connected, may be linked by changes in movement. Feet discomfort, the

discomfort region that was most sensitive to time spent standing, may initiate more movement, which could relieve joint pressures resulting in changes in T_T.

EMG measures were correlated with discomfort and tiredness. RF MPF was only positively correlated with overall tiredness and legs tiredness. Because MPF is an indicator of muscle fatigue, it is expected that fatigue and discomfort should be positively related. SOL $RMS^{\%}$ was significantly correlated with legs tiredness, upper legs, knees, and feet discomfort. Similarly, HAM $RMS^{\%}$ was significantly correlated with hips, knees, and ankles discomfort. $RMS^{\%}$ and tiredness and discomfort measures were negatively correlated in all cases. It is expected that continued muscle activity may lead to increases in discomfort. Alternatively, increases in discomfort may initiate recruitment of different muscle systems leading to a decrease in muscle activity in these areas. The fact that *only* these three measures (RF MPF, SOL $RMS^{\%}$, and HAM $RMS^{\%}$) were correlated with tiredness and discomfort measures suggests that these EMG outcome variables may not be a sensitive enough measurement tool for evaluating small changes in fatigue over long periods of time.

HbO, HHb, HbT, Flow, and SpO_2 were significantly and positively correlated with discomfort and tiredness measures. HbO was significantly correlated with knees, lower legs, ankles, and feet. HHb and Flow were significantly correlated with all measures of tiredness and discomfort. Because tiredness and discomfort, HbO, HHb, HbT, and Flow all increased with time, it is expected that positive correlations would arise. Interestingly, SpO_2 was significantly correlated with overall tiredness, knees, and lower legs—despite not changing significantly with time. SpO_2 is a measure of the percentage of HbO that resides in arterial structures. This value normally changes due to changes in metabolism. Higher metabolism is linked to muscle usage and therefore tiredness and discomfort. Therefore, a positive change SpO_2 may be related to a

metabolic need. However, more research in this area should be completed to understand these relationships, given that SpO_2 did not significantly change with time.

StO_2 was negatively correlated with overall tiredness and hips discomfort. StO_2 measures the amount of HbT in muscle tissue that is HbO. This means that as overall tiredness and hips discomfort increased, StO_2 decreased—or the proportion of oxygenated blood decreased. This is most interesting in the context of the overall tiredness measure. Overall tiredness is a subjective measure of fatigue, which may be due to a lack of adequate oxygen for metabolism. More research would need to be performed to determine how localized increases in oxygen use (such as in the lower extremities) affects other regions in the body and how it is related to subjective measures of tiredness.

5.6 Correlations with Standing Strategies

No significant correlations between standing strategies and DSX measurements were found. This may be due to a lack of statistical power. It may also be related to how correlations for this aim were performed. Correlations for this aim were calculated slightly differently than the rest of the outcome variables of this study because of the necessity to a model to determine DSX measures. Correlations were performed between DSX outcome variables and the total number of shifts and fidgets that were performed during standing. Alternatively, the number of shifts and fidgets before and after T_T may differentiate the relationship between shifting and fidgeting and MTFG prior to when G_T is reached.

Standing strategies require movement, which is initiated by muscle contractions. Interestingly, all MPF measures were significantly and negatively correlated with shifts, fidgets,

and/or total events. As previously stated, decreasing MPF is an indication of muscle fatigue. While MPF across all muscles and subjects did not display significant changes with time, row-wise correlations suggest that when subjects moved more, their MPF measures were lower. TA $RMS^{\%}$, GAS $RMS^{\%}$, RF $RMS^{\%}$, and HAM $RMS^{\%}$ were significantly and positively correlated with fidgets and total events, suggesting that increased muscle activation in these regions are related to increased fidgeting and total events. SOL $RMS^{\%}$ was significantly and negatively correlated with fidgets and total events. The soleus muscle is a deep, slow twitch muscle that maintains stance—whereas the tibialis anterior, gastrocnemius, rectus femoris, and hamstrings all are powerful muscles that create stronger movements. Therefore, it is expected that these muscles would be positively correlated with movements, while the soleus muscle would be negatively correlated with movements.

NIRS outcomes were also significantly and positively correlated with standing strategies. It was hypothesized that fidgets would be the standing strategy more related to changes in circulatory mechanisms during standing. Most interestingly, Flow was significantly (and very highly) correlated with fidgets and total events. HHb was significantly and positively correlated with total events. HbT and SpO_2 were significantly and positively correlated with shifts. It is still unknown how standing strategies are related to circulatory outcomes of prolonged standing. However, these findings indicate that there is a positive relationship between movement and circulatory effects of standing. Therefore, certain aspects of NIRS outcomes may be a promising device for measuring the circulatory and fatiguing effects of prolonged standing.

6.0 Limitations

The overall goal of this study was to investigate physiological changes that occur due to prolonged standing. A subject cohort of 29 healthy adults—ranging from 21 to 35 years of age—were enrolled. The rationale for choosing young and healthy subjects was to determine a baseline for future research endeavors. However, this means that the results collected in this study are not necessarily representative of the broader working population. In 2019, the median age of the working population in the United States was 42.3 years old [111]. Results collected during this study are not externally valid for middle-aged or older workers with predispositions to musculoskeletal or circulatory effects, who may exhibit more extreme knee joint, muscle, and circulatory effects due to prolonged standing.

Four subjects did not complete the entire testing protocol. Furthermore, there were some miscommunications between Mercy Hospital and the researchers—resulting in the loss of one subject's CT scan data. All of these subjects were HW subjects and female. This affected statistical power for the HW group.

Some limitations of this study were due to nuances of testing and testing protocols. During the standing trial, subjects were instructed to not lift their feet or heels off the floor. Subjects were allowed to transfer weight between legs but were not directly instructed to do so. The purpose of controlling feet movement was to control for varied movements between subjects. This does not reflect a real world situation in which workers are able to lift and shake out their feet. Only one anti-fatigue mat was tested for this study. Physiological outcomes of standing measured during this study are limited to the effects of this specific mat only. Previous research has shown that

differences in flooring do impact outcomes measures during prolonged standing [1]. Therefore, the same study performed on a different flooring surface may lead to different results.

Subjects were allowed to perform "office work" during standing. The kind of work was not specified by the researcher and was not controlled for between standing trials. If work during one visit was less engaging than work performed during the second visit, subjective tiredness and discomfort measures may have been impacted.

When DSX images were collected, subjects were instructed to "stand up straight with equal weight on both legs." This normally only lasted a few seconds. However, if a subject was shifted to the far right or left, this could have impacted his or her standing strategies measures. This was completed the same number of times and at the same intervals for each subject. Therefore, this should not impact weight transfer differences between flooring condition or BMI group. However, because most DSX measures were taken early during the visit, the total number of events performed early in the standing trial may be slightly skewed, though results showed a significant increase with time.

A limitation of the primary knee joint measures was that kinematics measurements are subject specific and cannot be compared across subjects or generalized to a larger population. Due to differences in technicians at Mercy Hospital, hip slices were either the femoral head or greater trochanter. Ankle slices were either the tibiotalar joint or the very distal tibia. Because of this, kinematics may only be used within subject and are only representative of a trend. Resolution and accuracy of the DSX imaging device should also be considered. Changes in MTFG that are less than bias of the machine in the z direction (0.37 mm) may not be accurately registered. A total of 24 visits out of 51 displayed an overall range of MTFG data less than 0.37 mm. To mitigate this,

multiple frames were collected at each time point and averaged together. However, this does suggest that changes in MTFG less than 0.37 mm may not be true changes.

Early in this study, an attempt was made to use knee flexion trials to correct for differences in kinematics during prolonged standing. These flexion trials were collected at 0, 60, and 120 minutes of standing for 22 subjects. Instead of collecting a static standing trial, the subject was asked to perform a closed chain knee flexion exercise. This exercise looked like a small, shallow squat. It was determined that these flexion trials would not be adequate to correct for differences in kinematics. Because of this, the maximum and minimum flexion during all static standing trials were calculated and only the frames of the flexion trials that occurred within the "range of static standing trials" were used. This unfortunately eliminated some data points for some visits. A relationship between subjects with missing data points and model non-convergence was not found.

The model itself that was chosen is a limitation of this study. The model was empirically informed but was not necessarily a "line of best fit" for the data. Because of this, a different model might be better suited for prolonged standing data. However, a more controlled study with higher resolution of kinematic and MTFG changes during the beginning of the trial is necessary to develop a data driven model.

Both NIRS and EMG sensors are highly sensitive to probe placement. Therefore, changes between standing visits may have been due to differences in probe placement. However, the researchers mitigated this by measuring probe placement during the first visit to replicate it during the second visit. Also, the order of flooring conditions was picked at random to defeat any bias in probe placement due to visit number.

The strongest limitation for NIRS measurements is the estimate of DPF. Incorrectly estimating DPF leads to different concentration values of HbO, HHb, and HbT. Overall trends are

the same, but actual concentration values may vary. Therefore, it is best to use NIRS measurements as trend indicators and not exact changes in hemoglobin concentration. NIRS measurements are also susceptible to accumulation of heterogeneous noise throughout the trial. Published NIRS studies used various weighting structures and robust statistics to mitigate this noise. For this study, outlier and distribution analyses indicated that averaging NIRS outcome measures every five minutes of standing was enough to handle noise concerns.

7.0 Conclusion

This research investigated the underlying mechanisms of physiological changes due to prolonged standing using methods novel to the field of prolonged standing research. Additionally, differences between BMI groups were investigated for the first time. This research confirmed that prolonged standing leads to increased levels of tiredness and discomfort, cartilage compression, and blood volume in the lower extremities. Furthermore, these results were affected by BMI and flooring condition. The effect of the MT condition was not the same across BMI groups. Feet discomfort and overall tiredness displayed significant changes due to flooring condition, but only for the OB group.

A method was developed to measure differences in standing strategies over time. It was hypothesized that people perform different strategies when standing to mitigate different kinds of negative physiological outcomes during standing. Fast movements, fidgets, were hypothesized to be related to muscular fatigue and circulatory mechanisms during standing. Slower movements, shifts, were hypothesized to be related to relaxing cartilage between the joints. Categorizing weight transfers in this way allowed differences in movements between BMI groups and even on a subject level to be noted. Between BMI groups, the OB group displayed higher levels of both strategies over time. Flooring did not affect these strategies. Observation of results on a subject-by-subject basis revealed that some subjects performed primarily fidgets, some performed primarily shifts, and some performed a mix of strategies. While the number of subjects in this study was too low to statistically group subjects based on strategy type, findings from this research opens the door to investigating the kinds of strategies and behaviors people perform during standing. Investigating different kinds of strategies and how these strategies are related to

physiological outcomes of standing has never been done before. Understanding what strategies link to the best physiological outcomes could inform future intervention designs and worker regulations and training.

Measuring gap distance and kinematics using DSX technology is well established in the field of gait analysis and other dynamic movements. However, prior research using DSX technology to measure the effects of time on cartilage compression over time have been over a short duration. This study measured decreases in tibiofemoral gap distance over two hours of standing. Models suggest a decrease in MTFG over time. The MT condition may also have a beneficial effect on cartilage compression for the OB adults. Standard interventions may impact those of different populations in different ways such that one group may benefit while another group may not. Therefore, design of interventions—such as anti-fatigue mats—should consider human factors, such as BMI, age, pregnancy, or diseases (such as diabetes) when testing intervention effectiveness.

Circulatory measures of muscle fatigue were more sensitive to prolonged standing than traditional EMG fatigue measures. NIRS has proven to be an effective method to measure changes in circulatory parameters during prolonged standing. HbO, HHb, HbT, and Flow all increased with time. For the OB group, the MT condition seemed to have a protective effect on circulatory mechanisms, in which overall blood volume, Flow, and StO_2 was lower across all time points. Development of circulatory pathologies in turn caused by prolonged standing are largely the result of repeated exposure to capillary and venous dilation due to increased volume and pressure changes. Therefore, measures of HbT and Flow (the rate of change of arterial HbT) may be the most important metrics relating circulatory effects to development of pathologies. Anti-fatigue

mats and other interventions that are designed to decrease these metrics may minimize the likelihood of circulatory pathology developments, especially in obese adults.

Subjective discomfort and EMG measures may not adequately detect changes due to human or environmental factors during prolonged standing indicating a need for new or improved metrics. Muscular and circulatory related pathologies associated with prolonged standing stem from blood pooling and deviations from normal circulatory behavior. Because of this, NIRS may more directly measure physiological changes that contribute to pathologies related to occupational standing. DSX may also assist in explaining the epidemiological relationships between prolonged standing and OA development. This research has shown that adults with obesity demonstrate different physiological responses to flooring characteristics, suggesting interventions may not impact workers of different demographics in the same way. Future research should include human factors, such as BMI, age, gender, pregnancy, and disease conditions, when investigating occupational injuries associated with prolonged standing. These human factors should also be considered when evaluating the effectiveness of ergonomic interventions and designing new interventions that will then benefit populations that are at a higher risk of occupational injuries.

Appendix A Tiredness and Discomfort

All graphs of discomfort data are included in this section. Graphs represent relationships between flooring condition, BMI group, and time. Overall tiredness, legs tiredness, and discomfort of the hips, upper legs, knees, lower legs, ankles, and feet are included. Each measurement was normalized to 0 minutes of standing and was analyzed using methods described in section 3.4.1. Only graphs are included in this section. Statistical and analysis information is included in section 4.1.

Appendix A.1 Overall Tiredness

I.

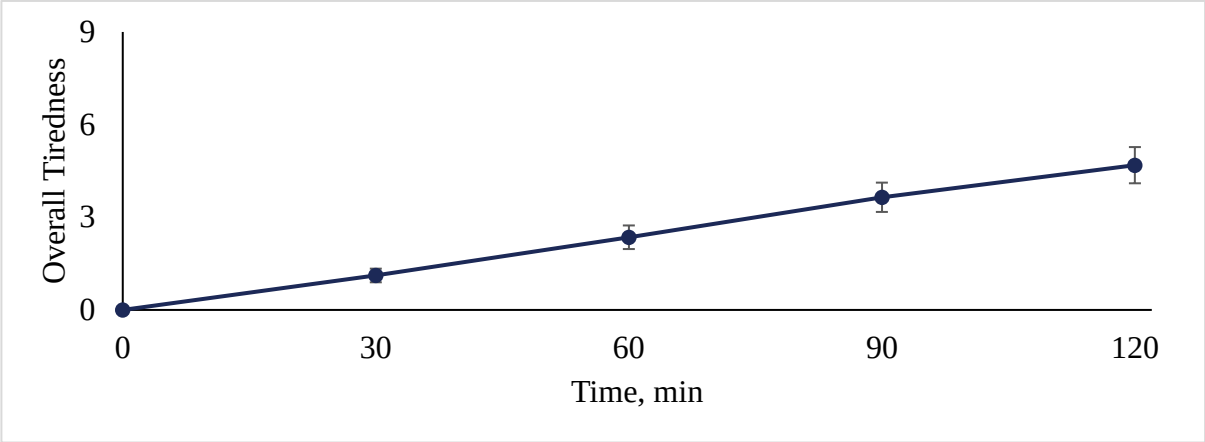

II.

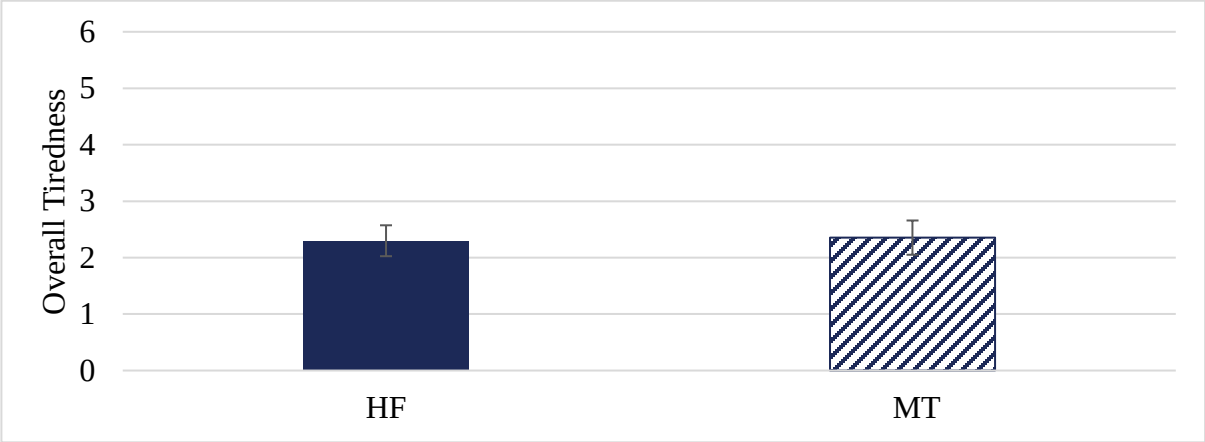

III.

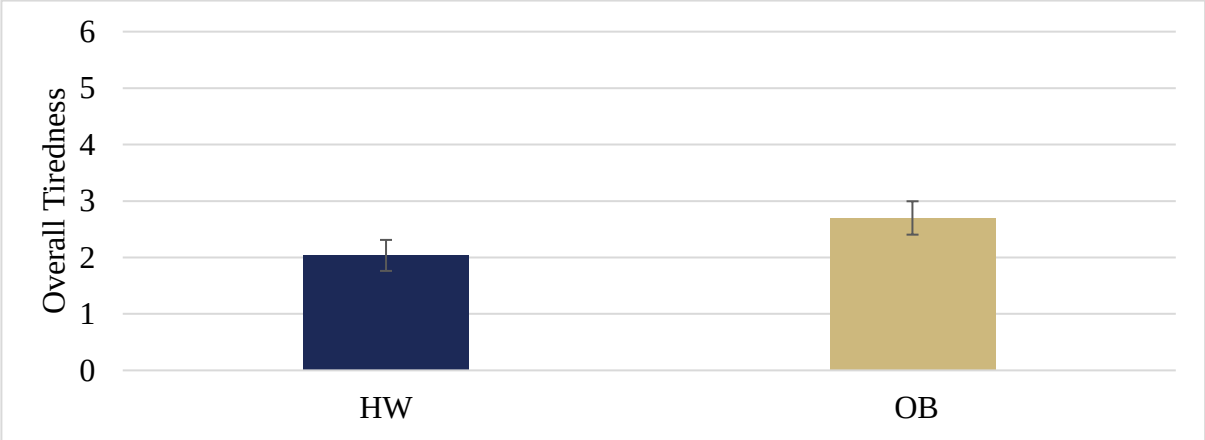

Figure 64: Overall Tiredness over time (I) and between flooring conditions (II) and BMI groups (III). Error bars are standard error of the mean.

I.

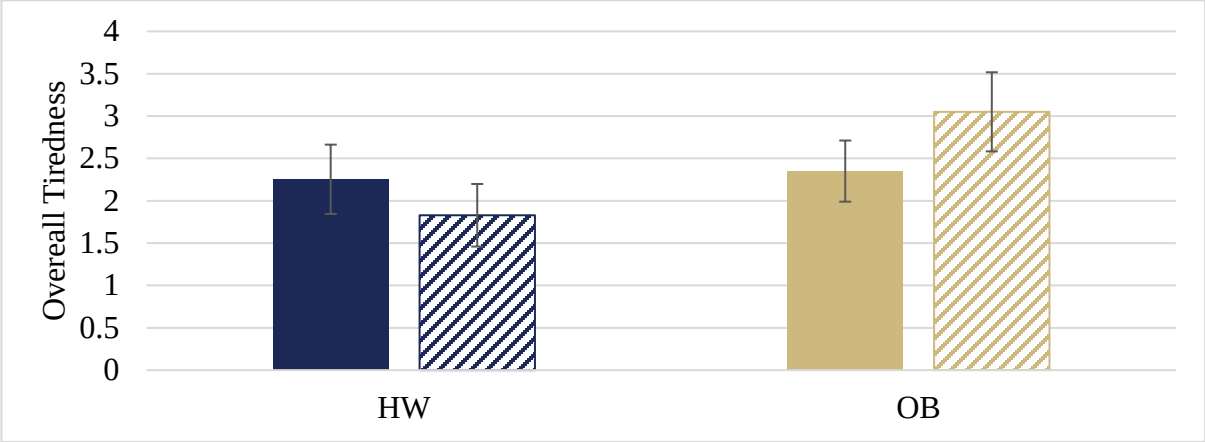

II.

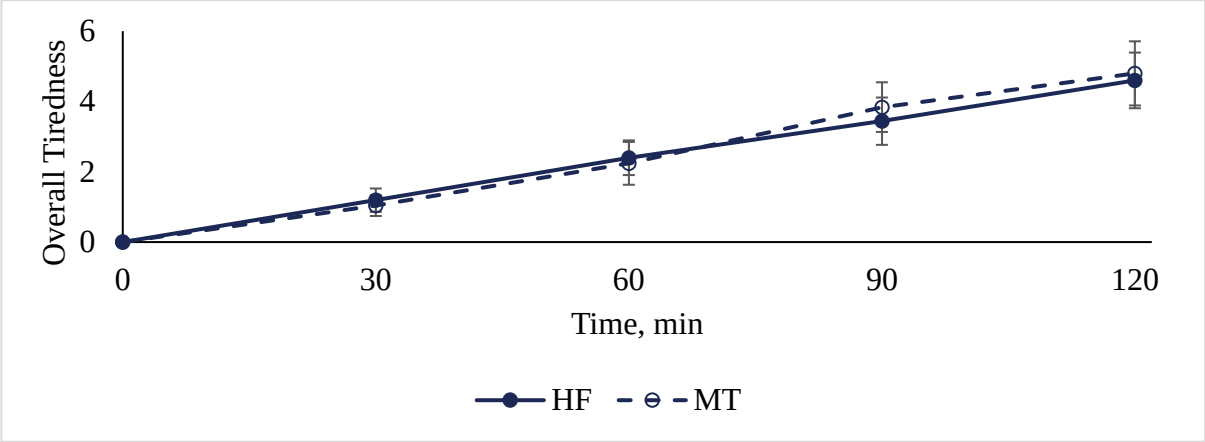

III.

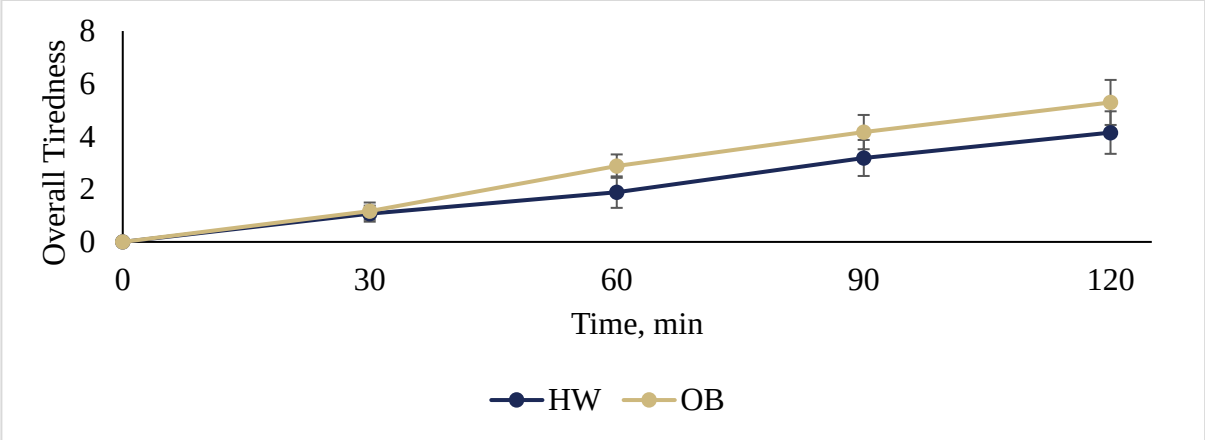

Figure 65: Overall Tiredness between BMI groups, split into flooring conditions (I), and over time, split between flooring conditions (II) and BMI groups (III). Error bars are standard error of the mean.

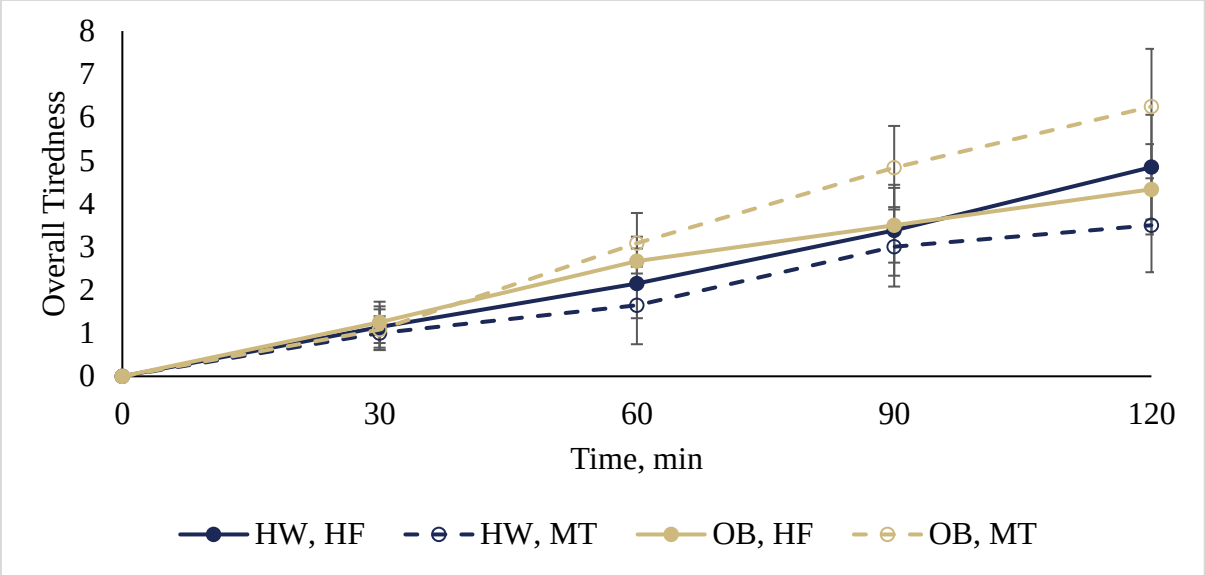

Figure 66: Overall Tiredness over time, split between BMI groups and flooring conditions. Error bars are standard error of the mean.

Appendix A.2 Legs Tiredness

I.

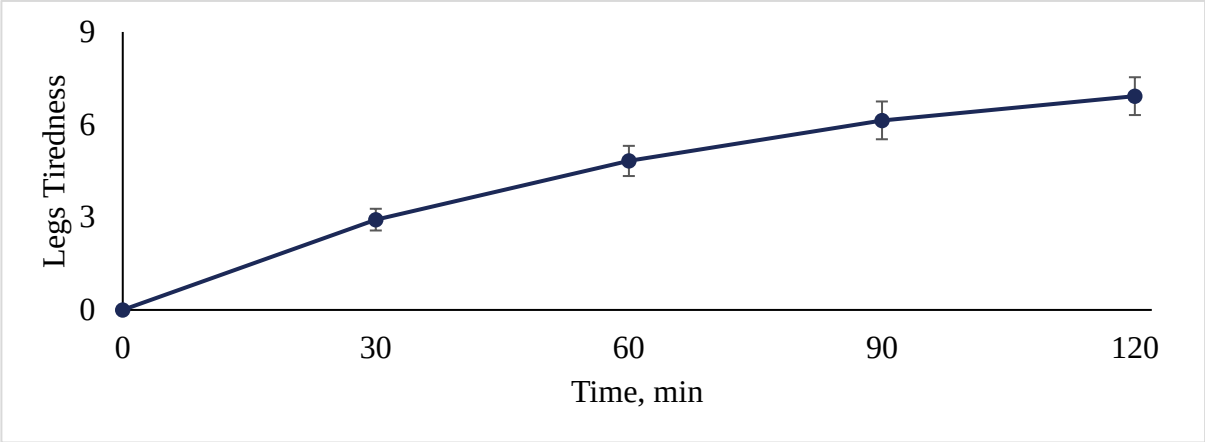

II.

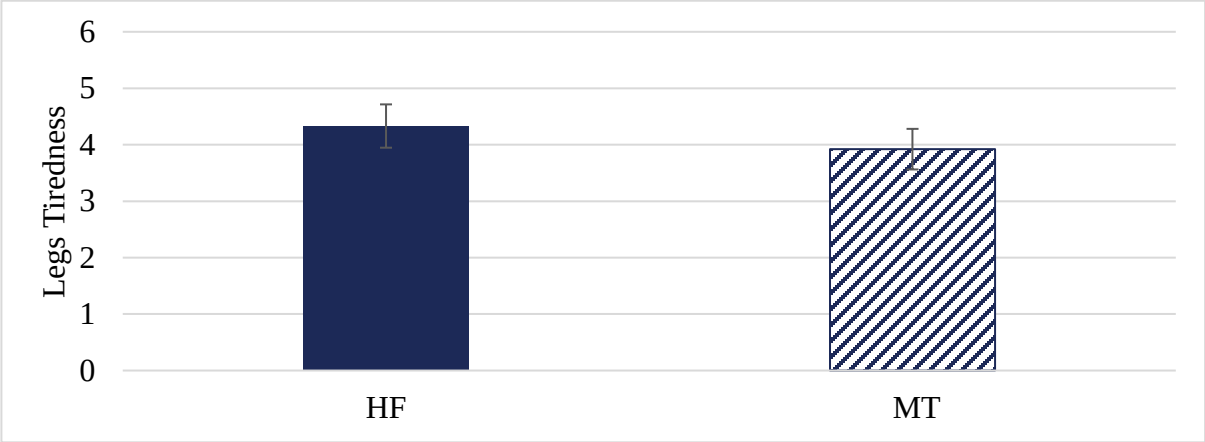

III.

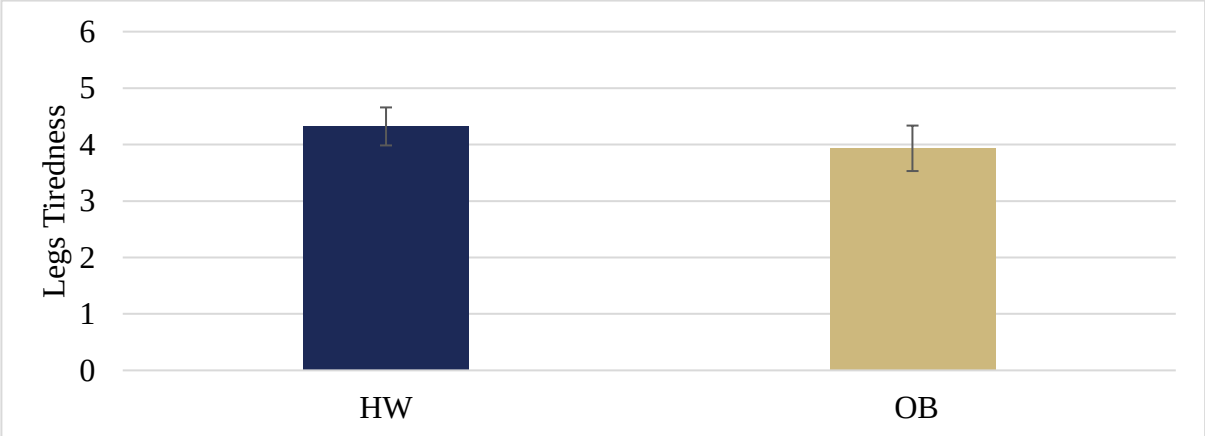

Figure 67: Legs Tiredness over time (I) and between flooring conditions (II) and BMI groups (III). Error bars are standard error of the mean.

I.

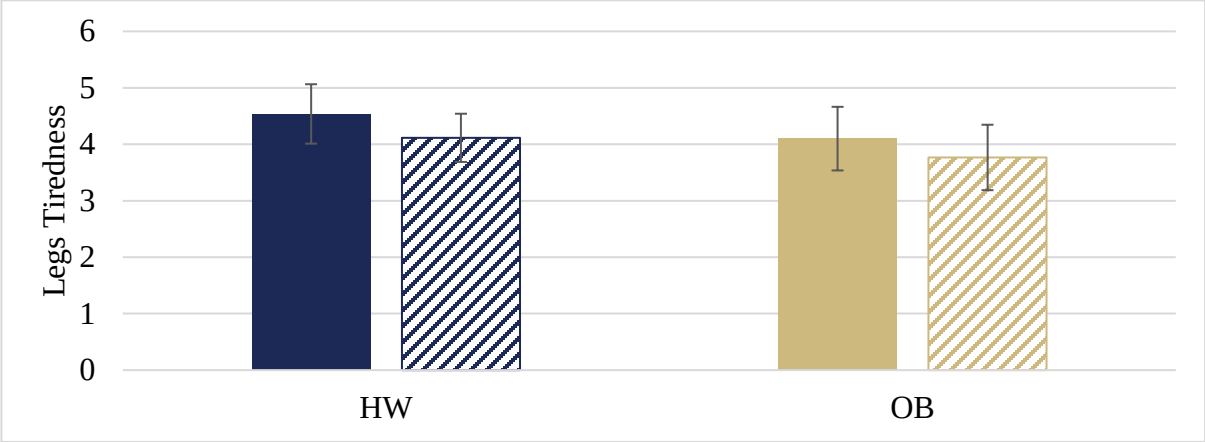

II.

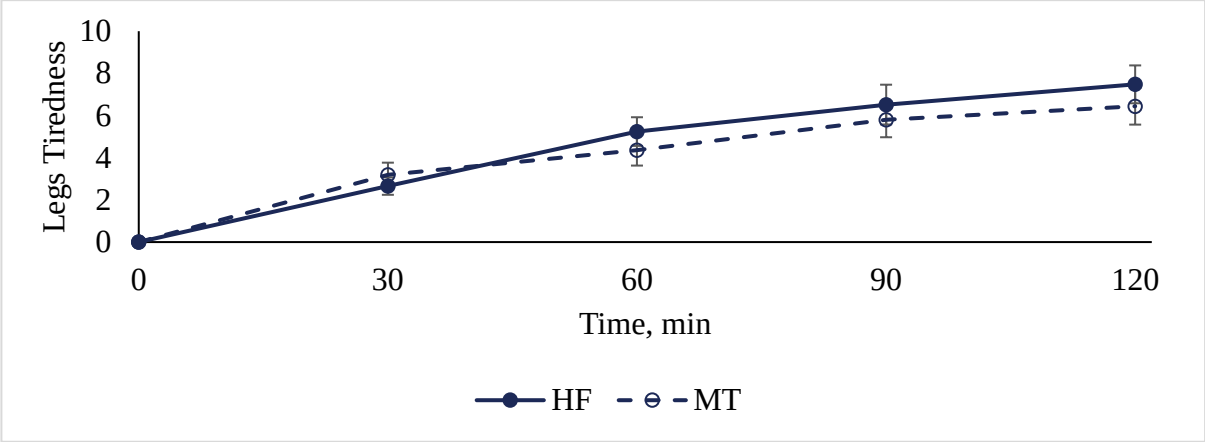

III.

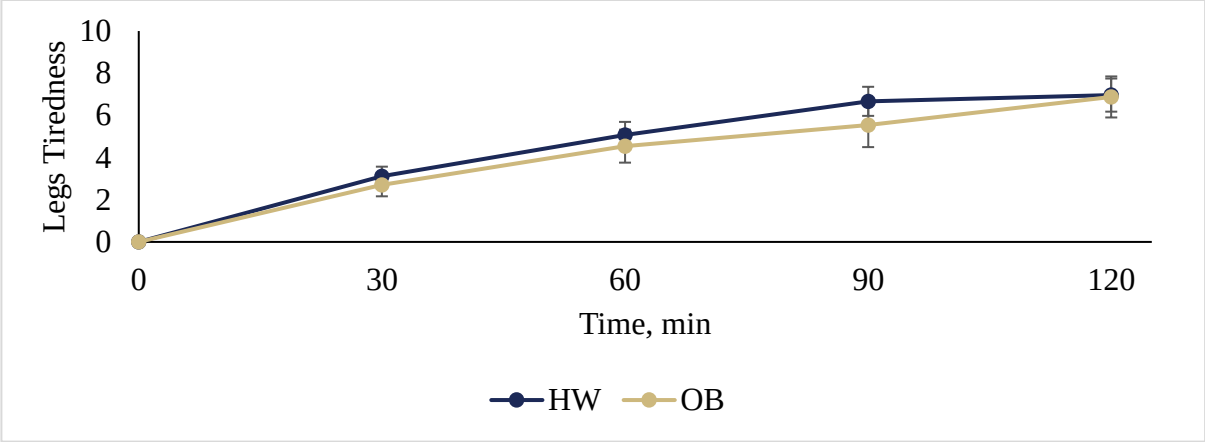

Figure 68: Legs Tiredness between BMI groups, split into flooring conditions (I), and over time, split between flooring conditions (II) and BMI groups (III). Error bars are standard error of the mean.

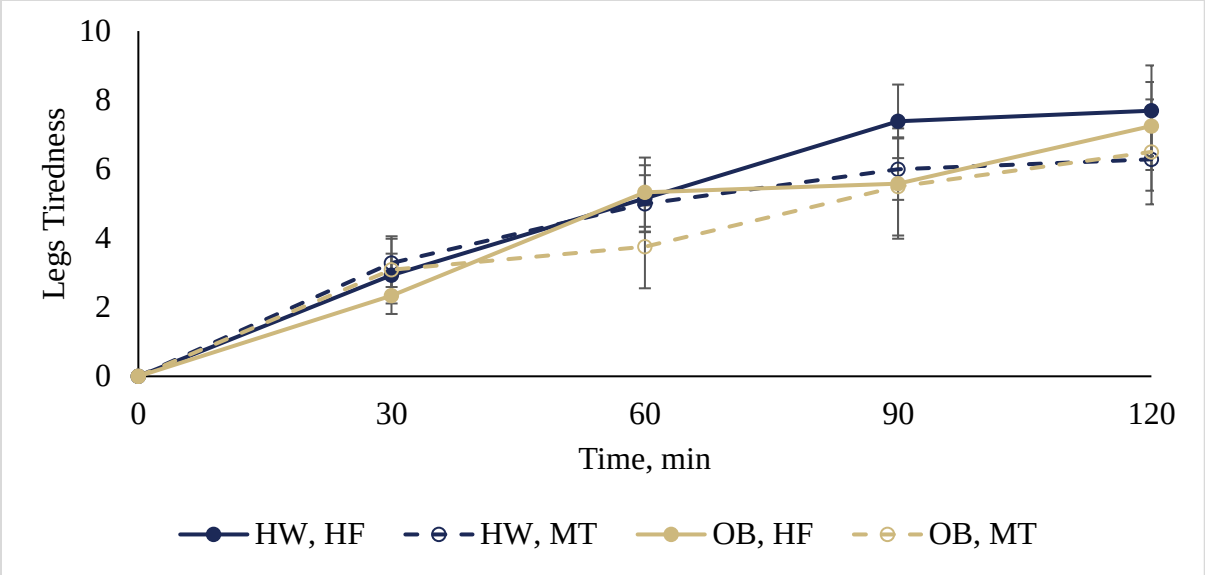

Figure 69: Legs Tiredness over time, split between BMI groups and flooring conditions. Error bars are standard error of the mean.

Appendix A.3 Hips

I.

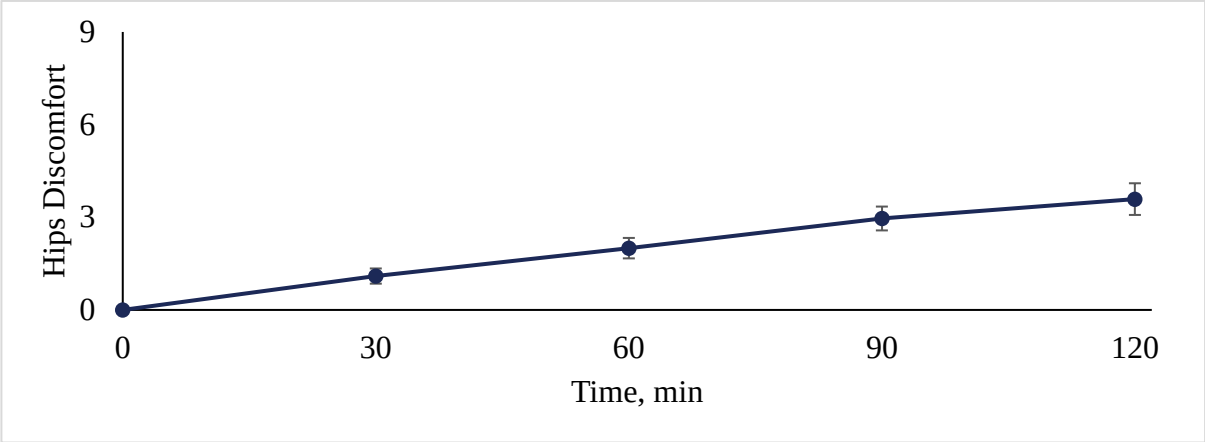

II.

III.

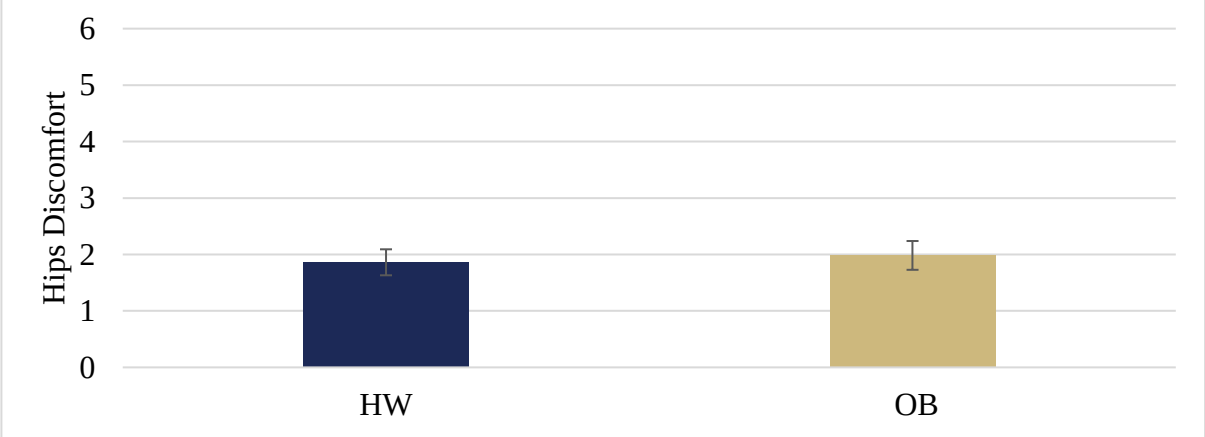

Figure 70: Hips discomfort over time (I) and between flooring conditions (II) and BMI groups (III). Error bars are standard error of the mean.

I.

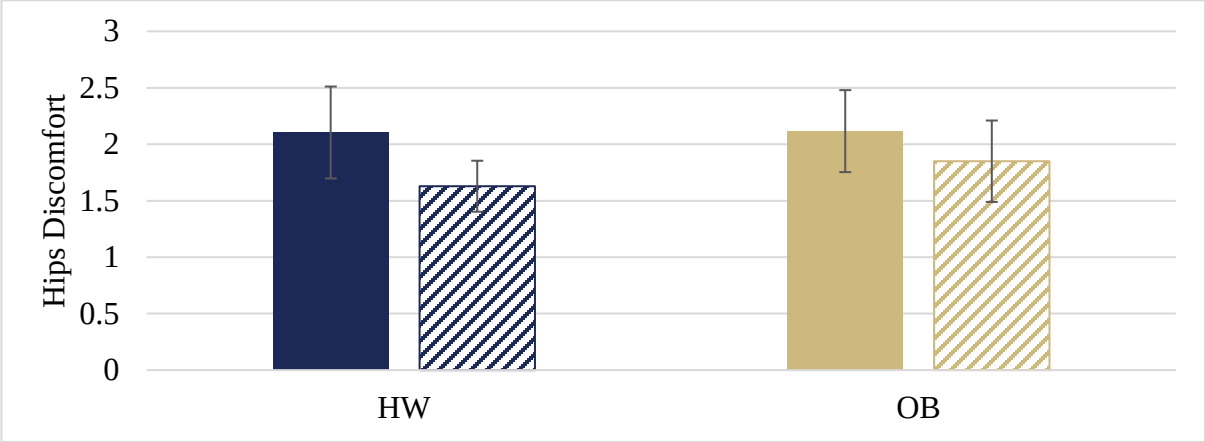

II.

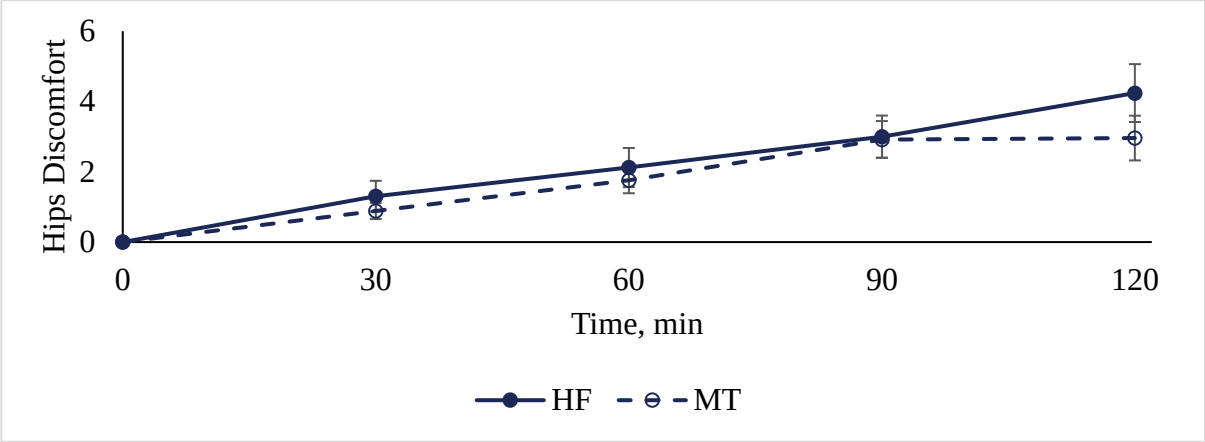

III.

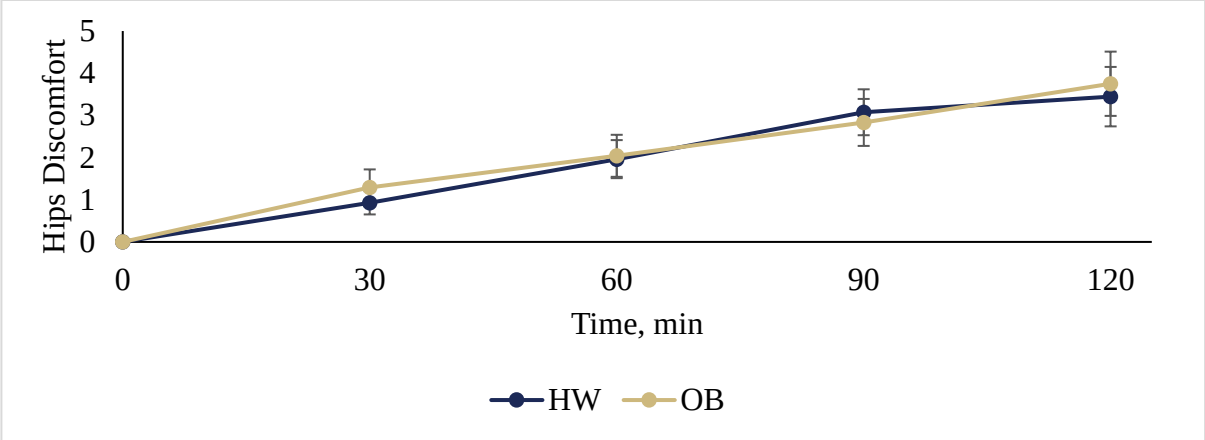

Figure 71: Hips discomfort between BMI groups, split into flooring conditions (I), and over time, split between flooring conditions (II) and BMI groups (III). Error bars are standard error of the mean.

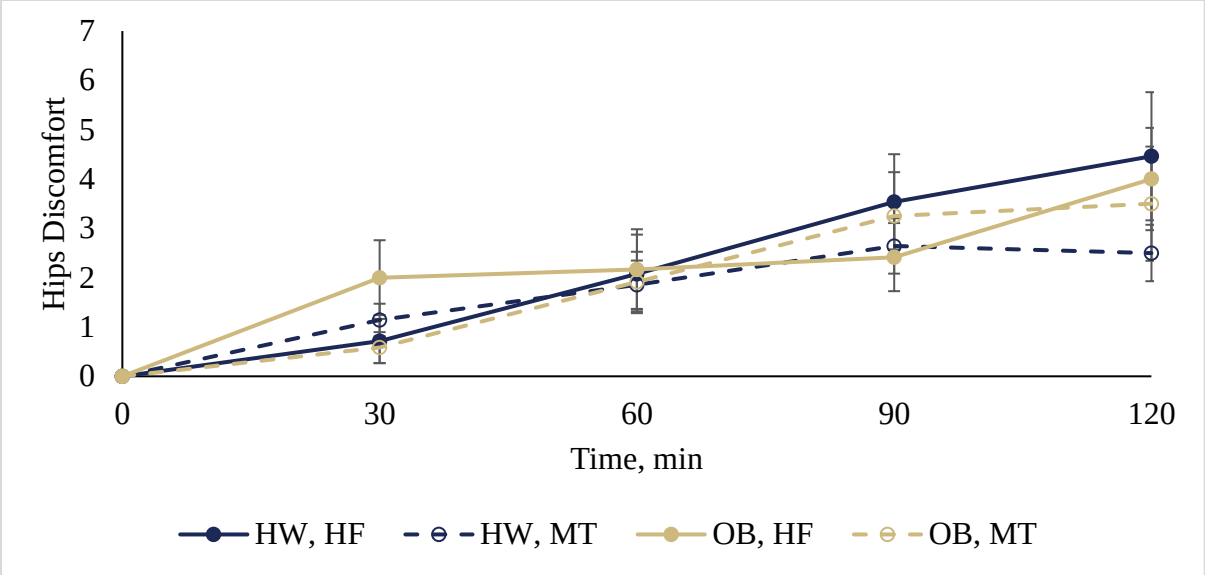

Figure 72: Hips discomfort over time, split between BMI groups and flooring conditions. Error bars are standard error of the mean.

Appendix A.4 Upper Legs

I.

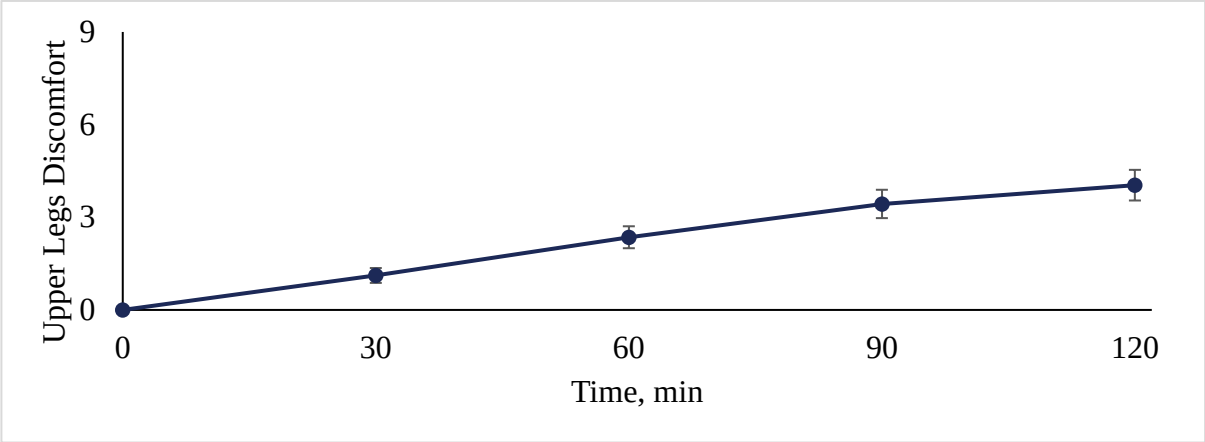

II.

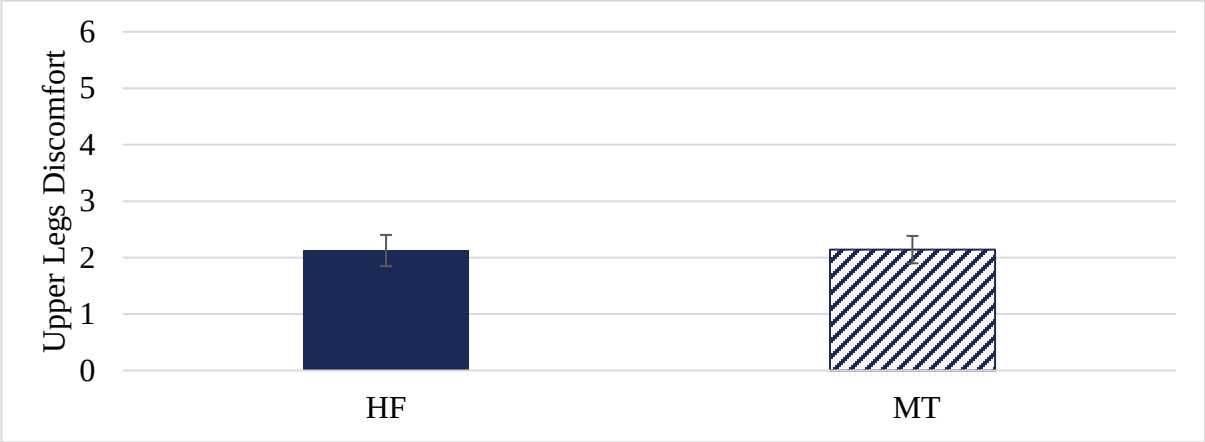

III.

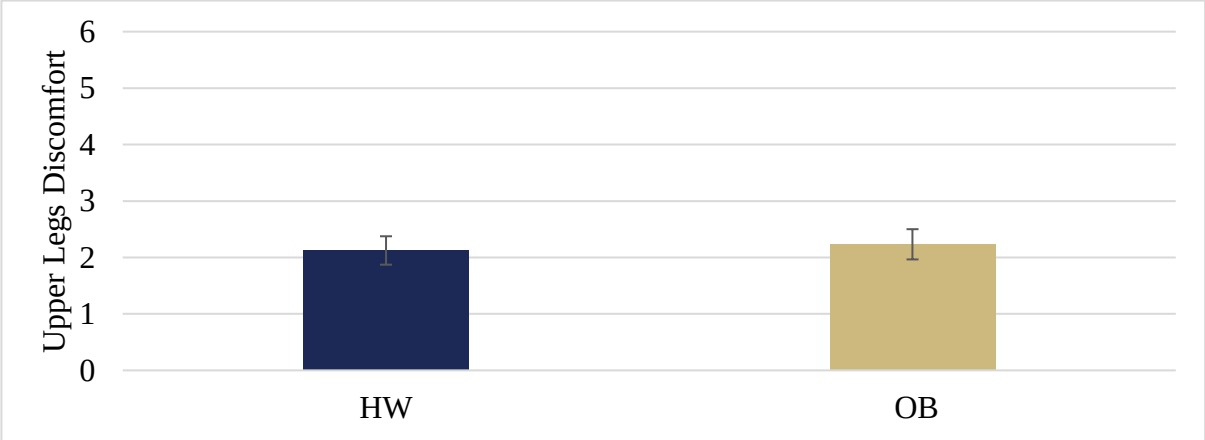

Figure 73: Upper Legs over time (I) and between flooring conditions (II) and BMI groups (III). Error bars are standard error of the mean.

I.

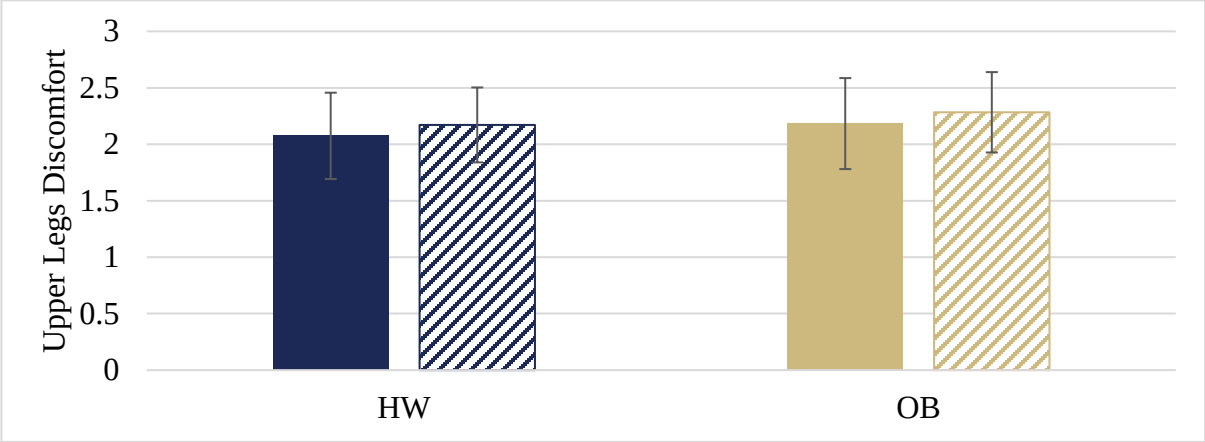

II.

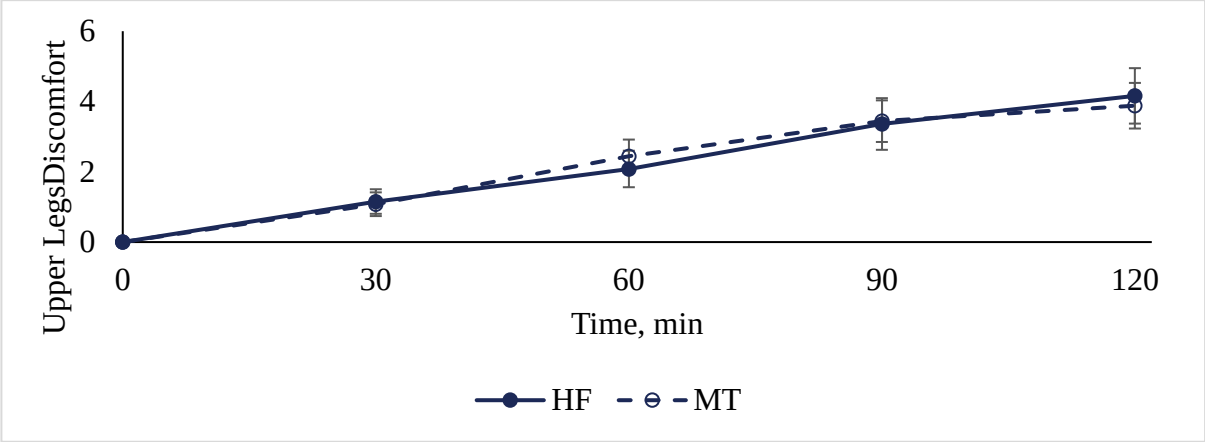

III.

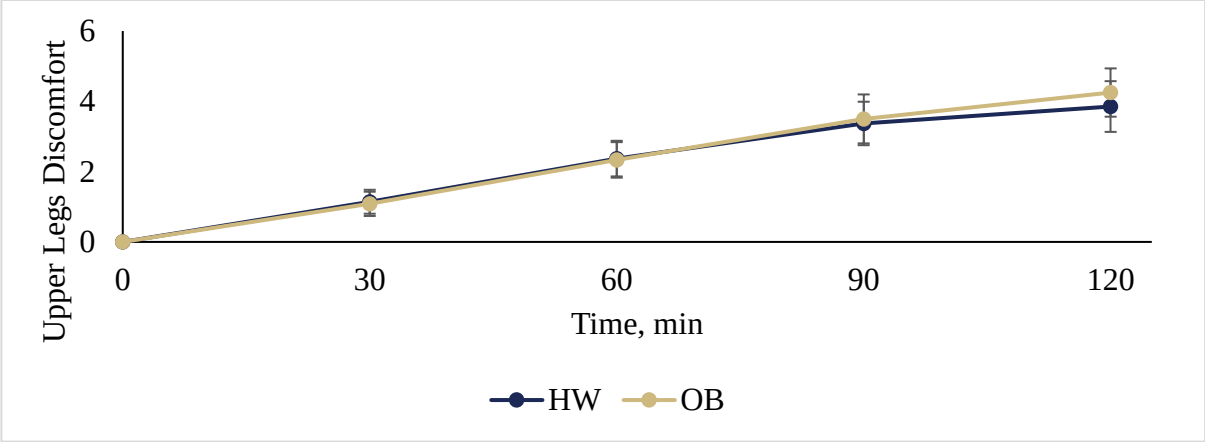

Figure 74: Upper Legs discomfort between BMI groups, split into flooring conditions (I), and over time, split between flooring conditions (II) and BMI groups (III). Error bars are standard error of the mean.

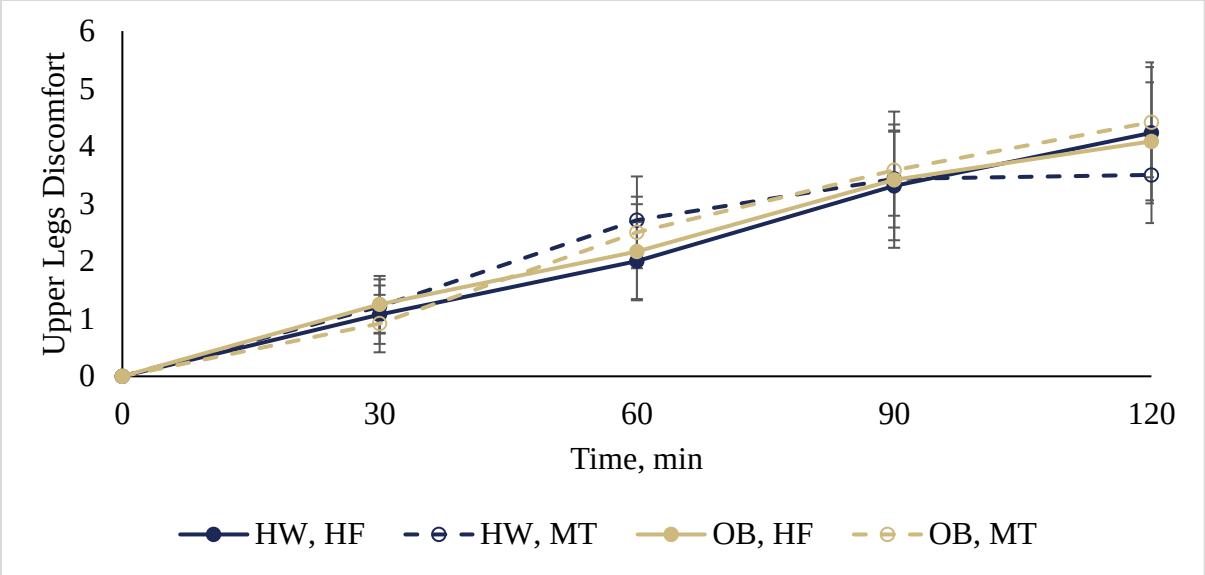

Figure 75: Upper Legs discomfort over time, split between BMI groups and flooring conditions. Error bars are standard error of the mean.

Appendix A.5 Knees

I.

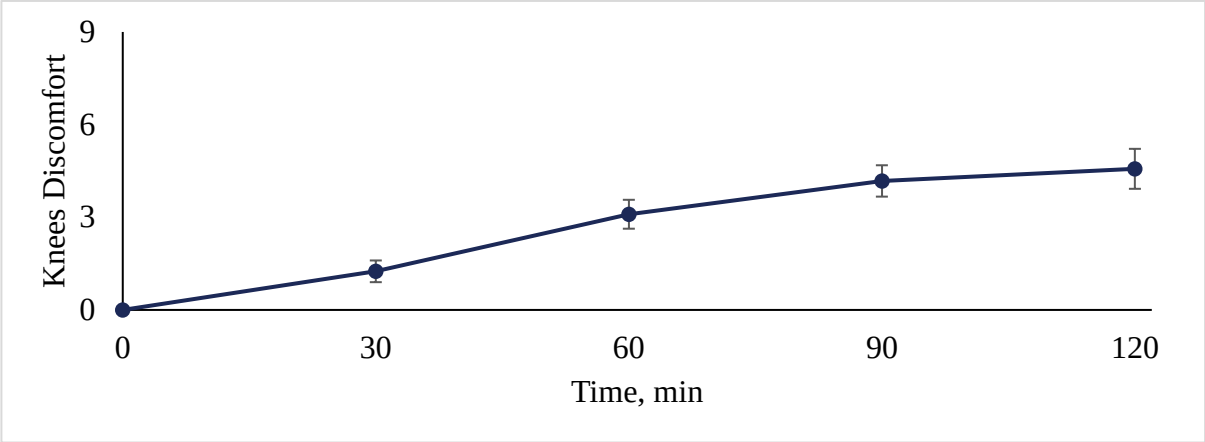

II.

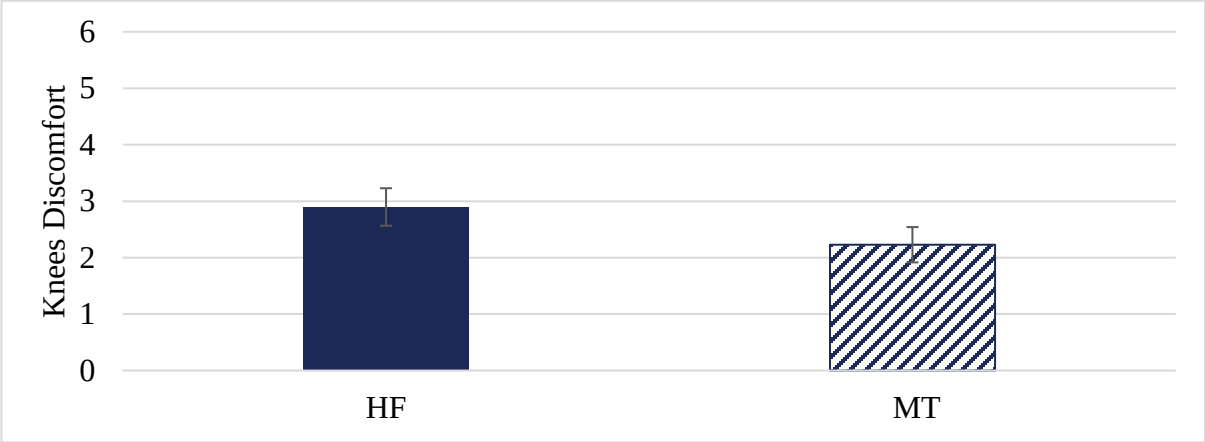

III.

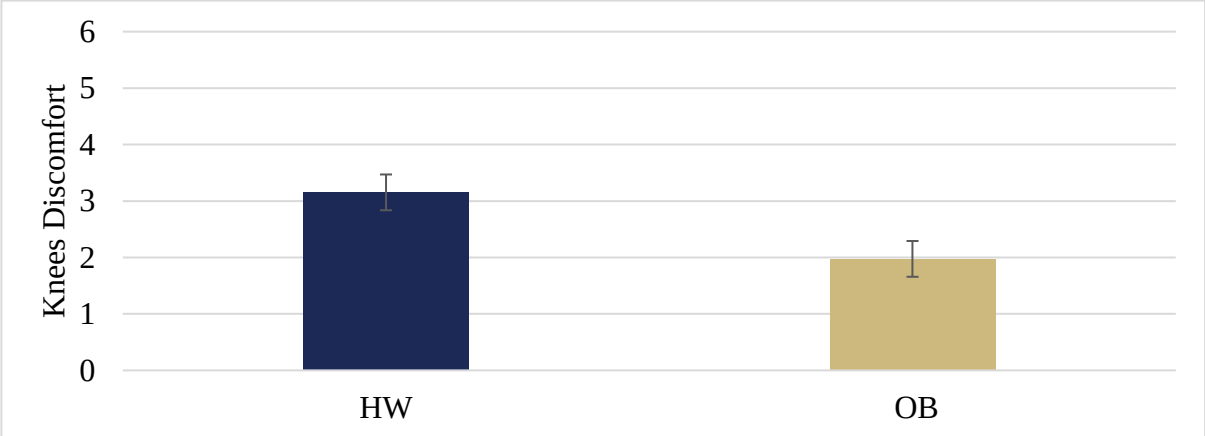

Figure 76: Knees over time (I) and between flooring conditions (II) and BMI groups (III). Error bars are standard error of the mean.

I.

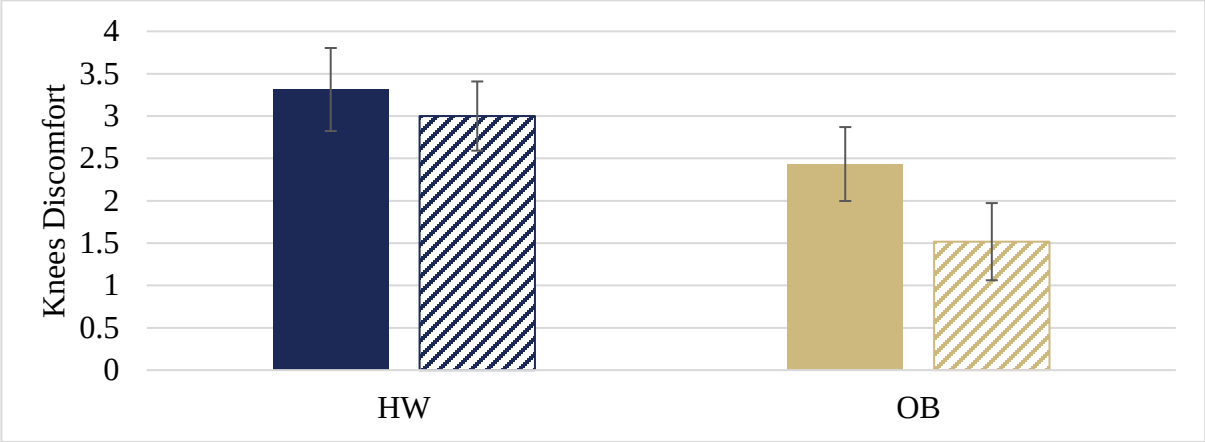

II.

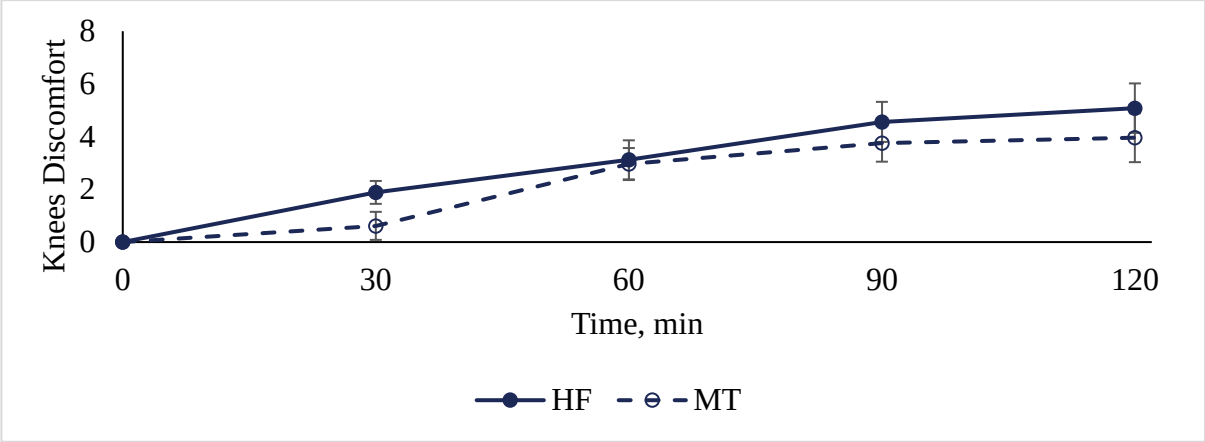

III.

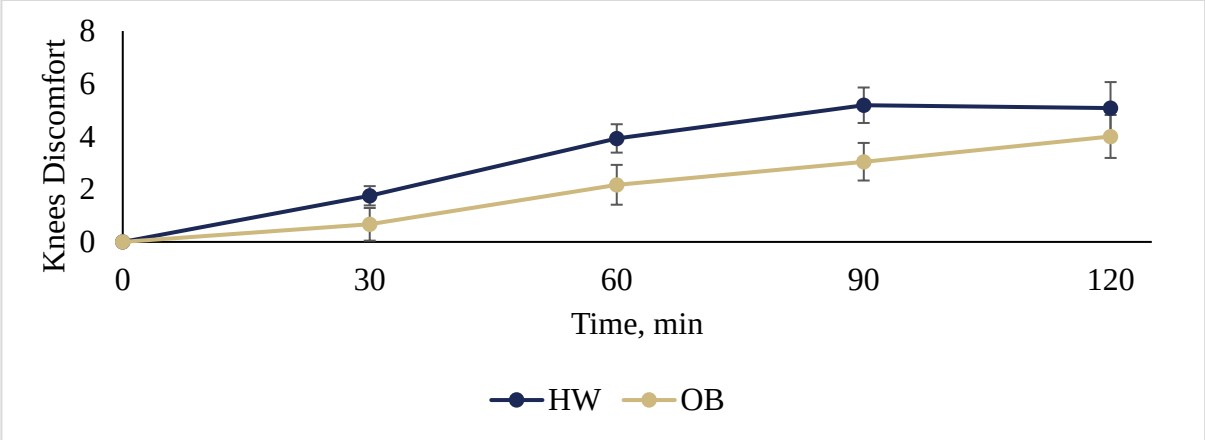

Figure 77: Knees discomfort between BMI groups, split into flooring conditions (I), and over time, split between flooring conditions (II) and BMI groups (III). Error bars are standard error of the mean.

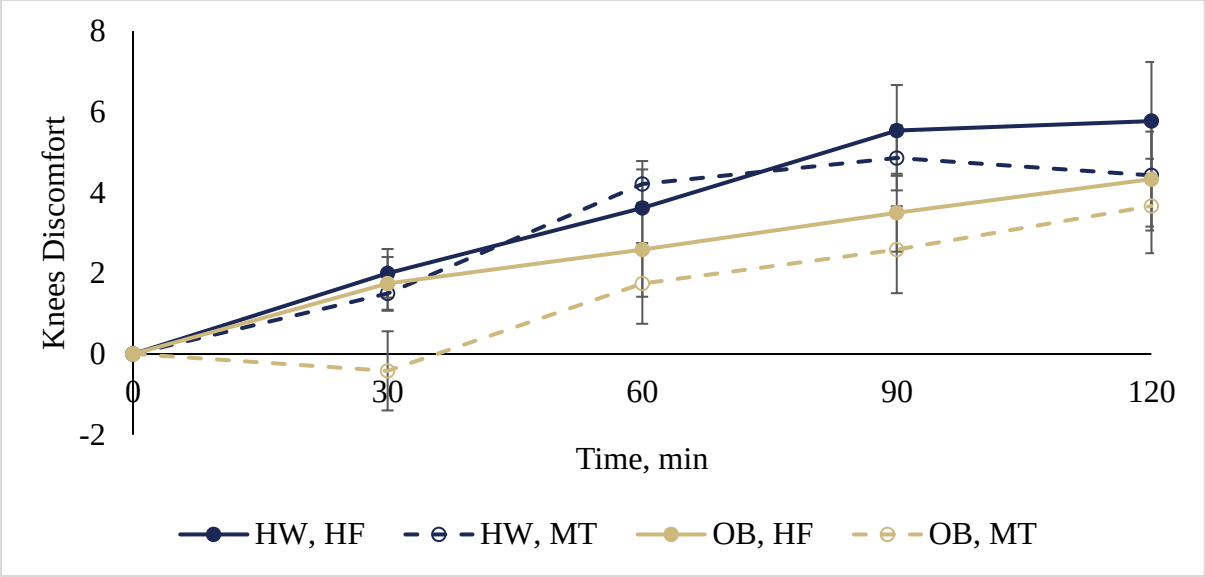

Figure 78: Knees discomfort over time, split between BMI groups and flooring conditions. Error bars are standard error of the mean.

Appendix A.6 Lower Legs

I.

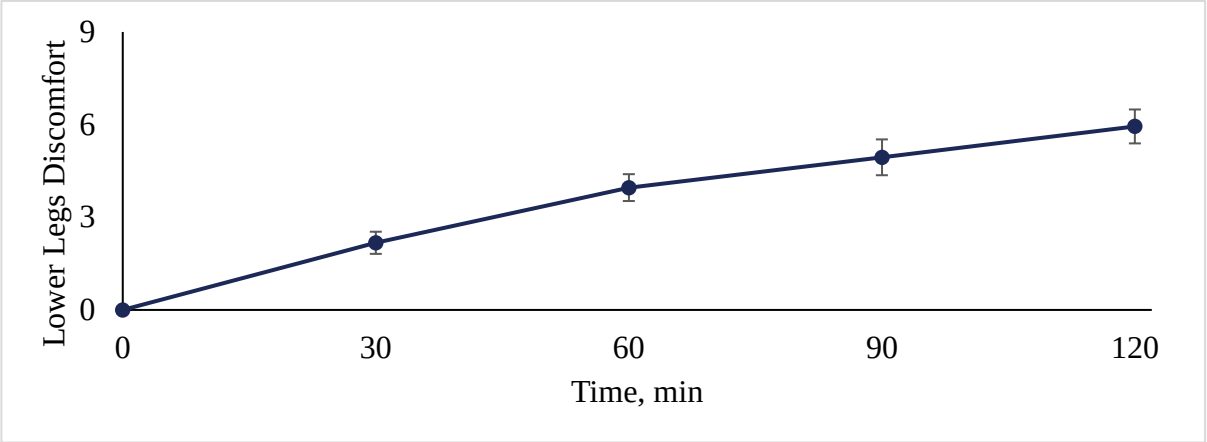

II.

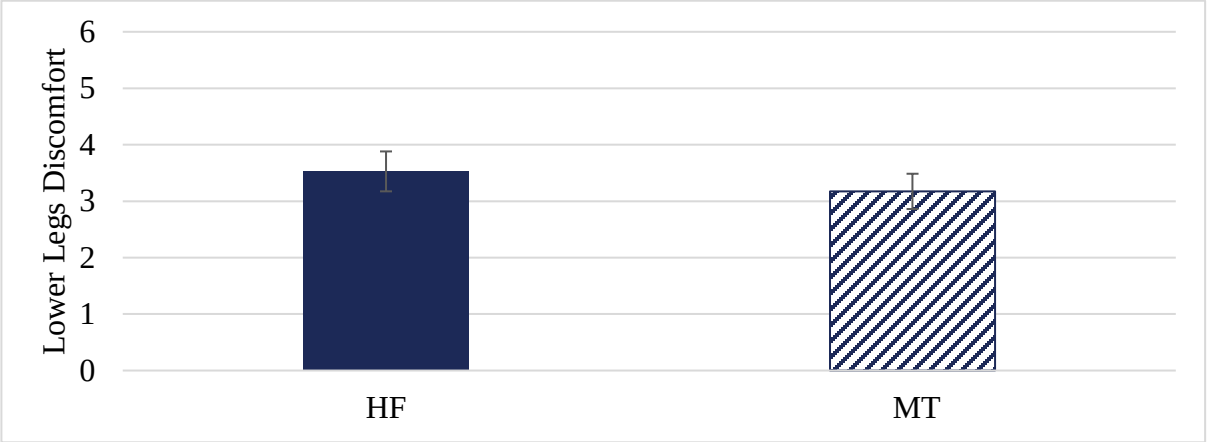

III.

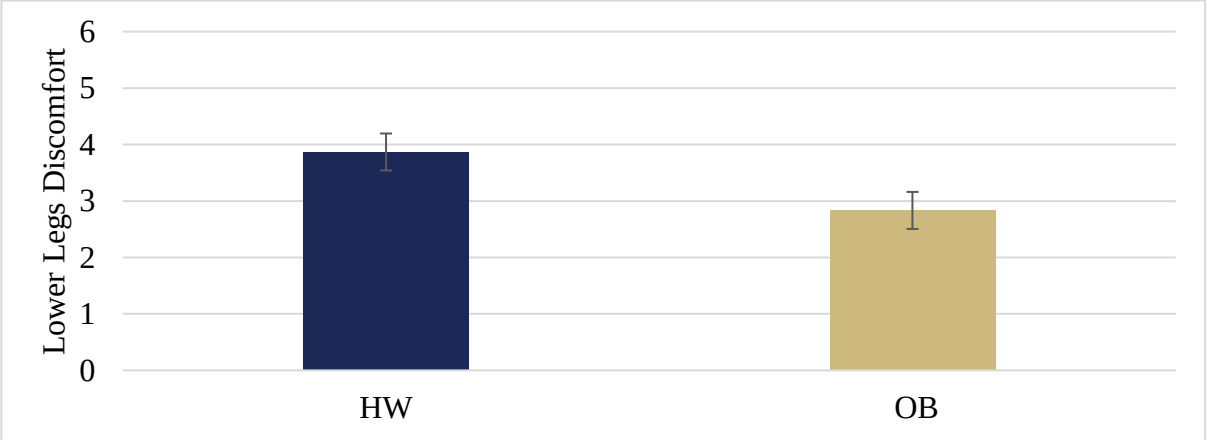

Figure 79: Lower Legs over time (I) and between flooring conditions (II) and BMI groups (III). Error bars are standard error of the mean.

I.

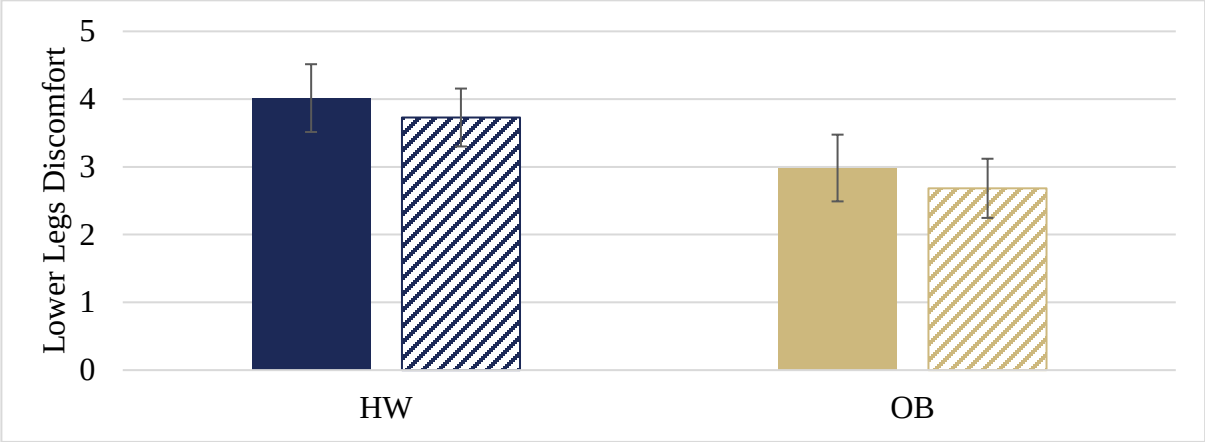

II.

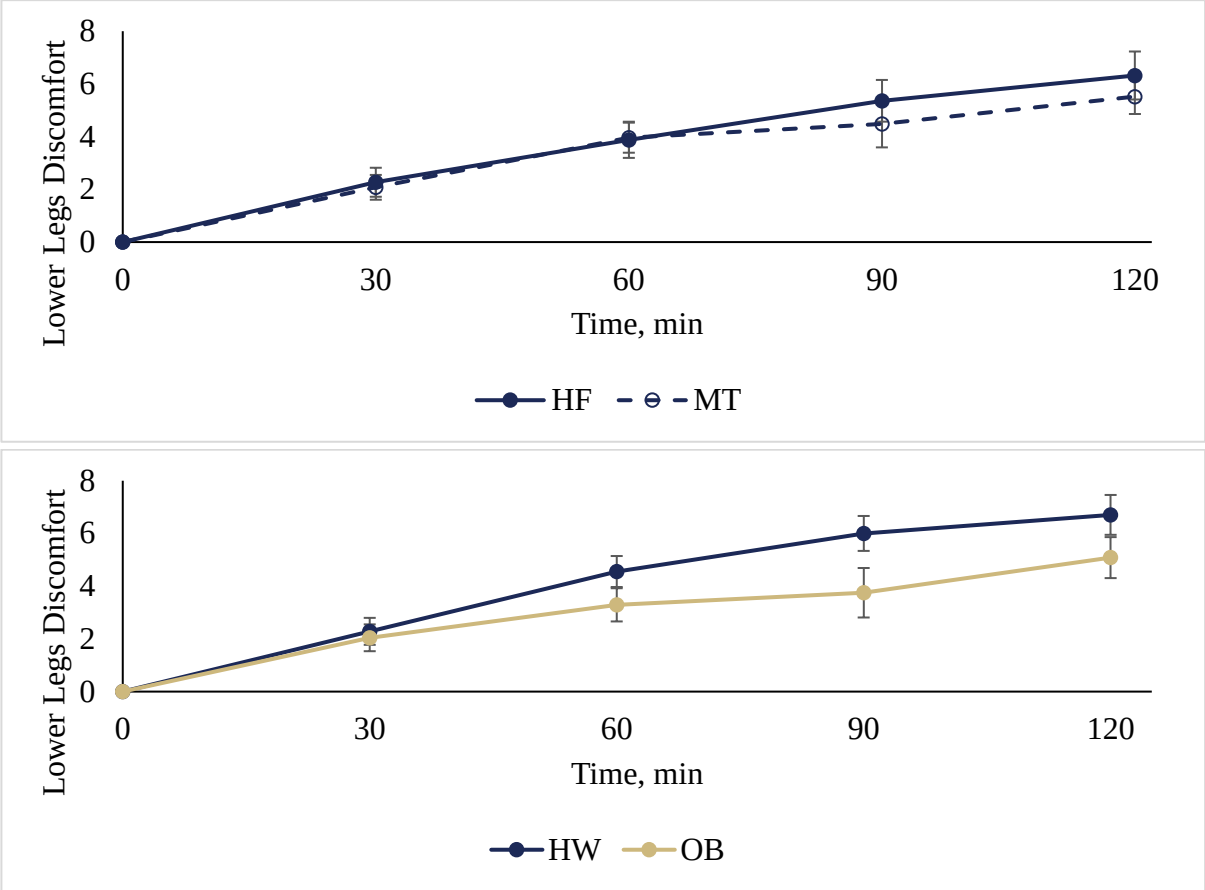

Figure 80: Lower Legs discomfort between BMI groups, split into flooring conditions (I), and over time, split between flooring conditions (II) and BMI groups (III). Error bars are standard error of the mean.

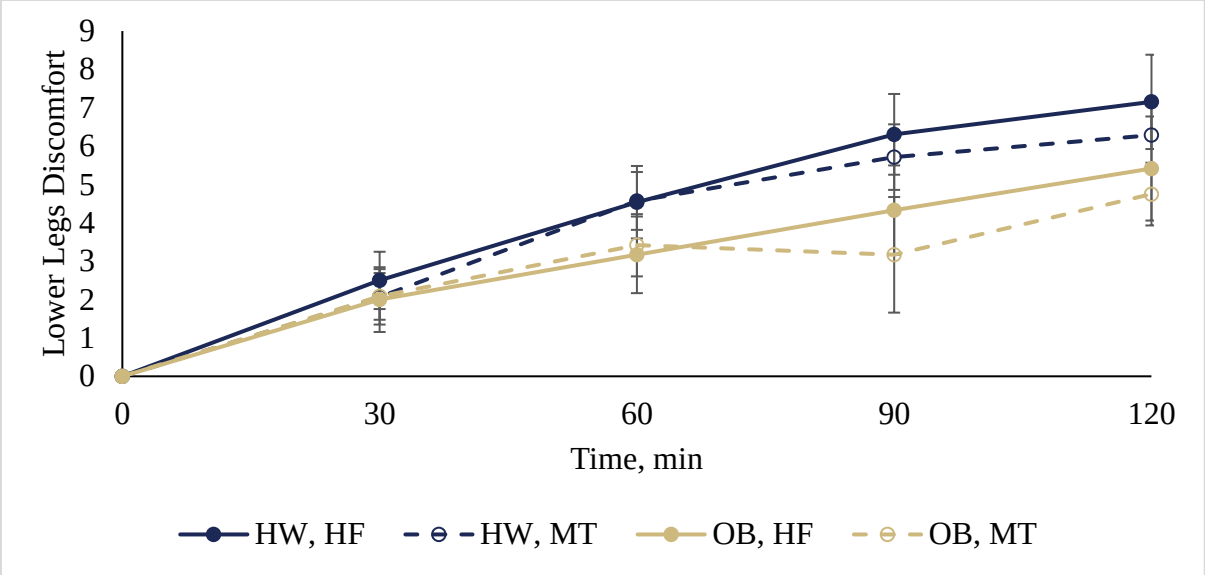

Figure 81: Lower Legs discomfort over time, split between BMI groups and flooring conditions. Error bars are standard error of the mean.

Appendix A.7 Ankles

I.

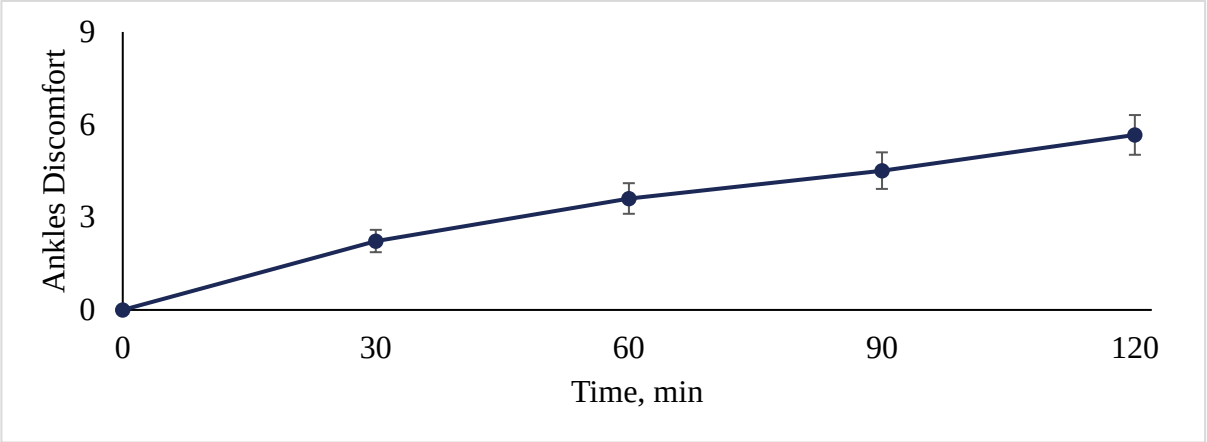

II.

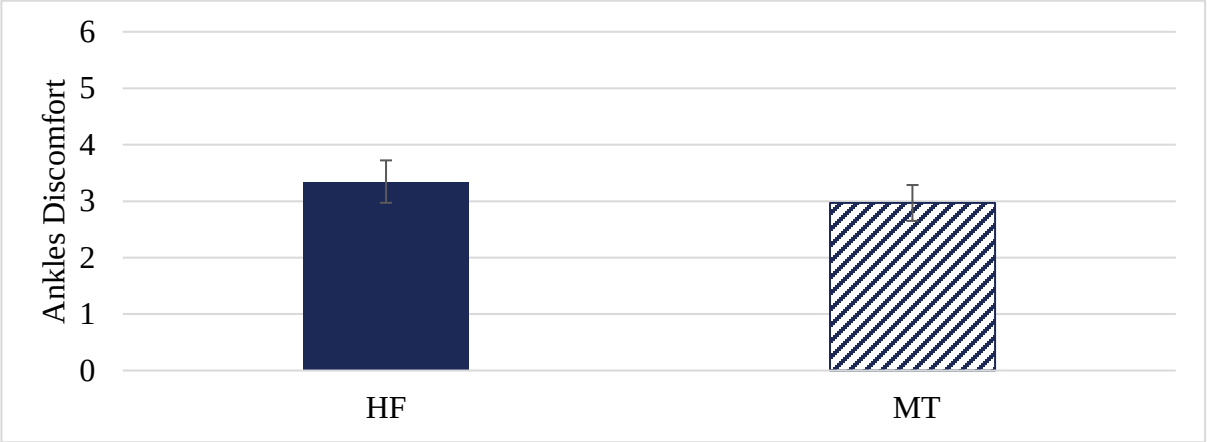

III.

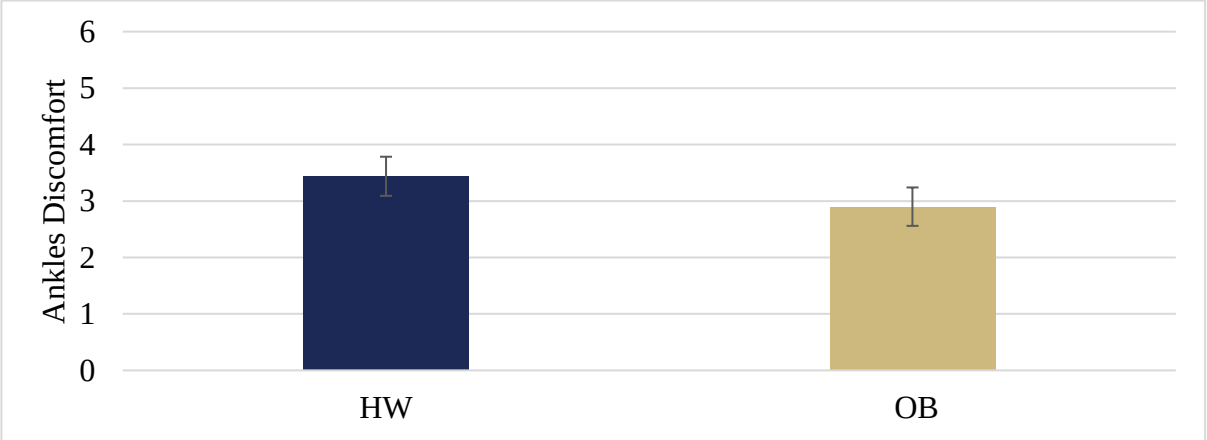

Figure 82: Ankles discomfort over time (I) and between flooring conditions (II) and BMI groups (III). Error bars are standard error of the mean.

I.

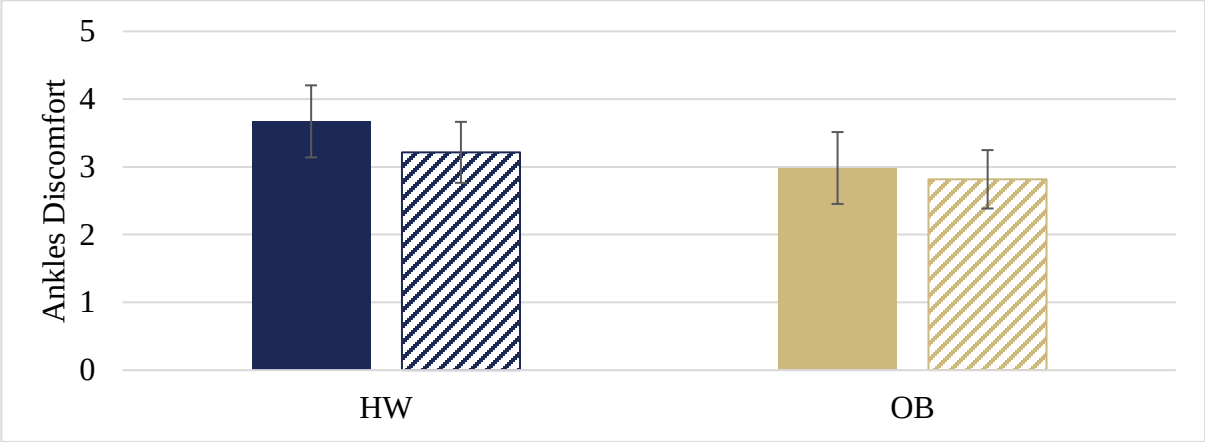

II.

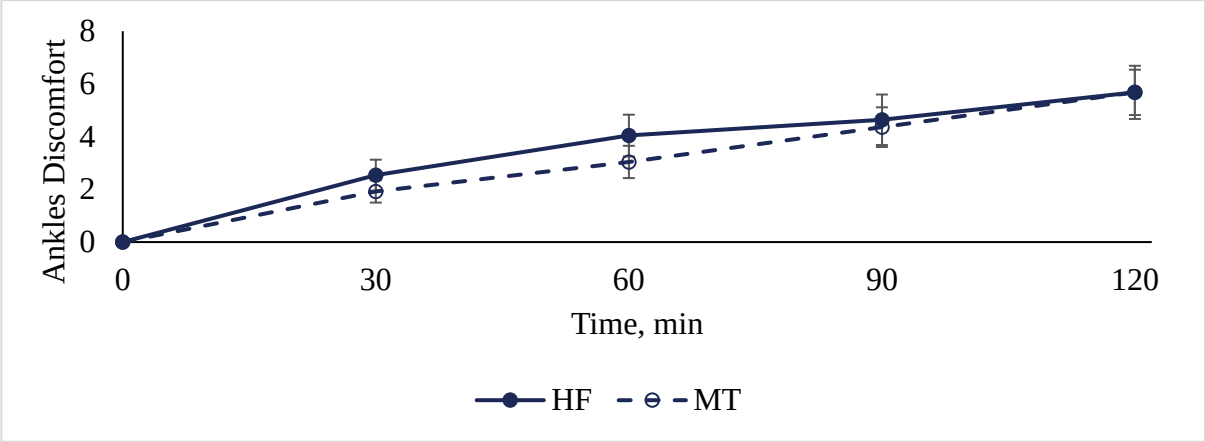

III.

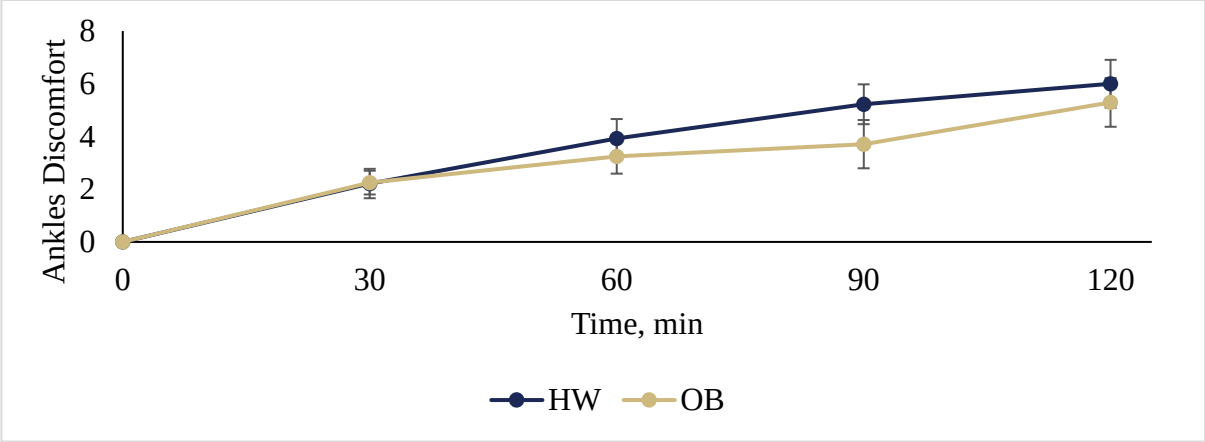

Figure 83: Ankles discomfort between BMI groups, split into flooring conditions (I), and over time, split between flooring conditions (II) and BMI groups (III). Error bars are standard error of the mean.

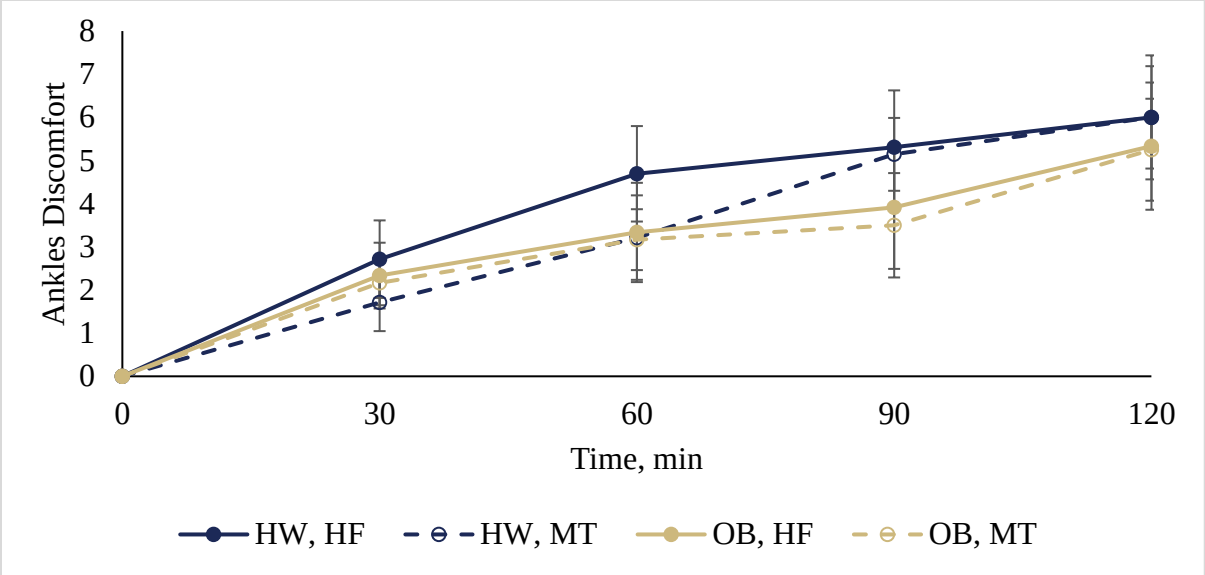

Figure 84: Ankles discomfort over time, split between BMI groups and flooring conditions. Error bars are standard error of the mean.

Appendix A.8 Feet

I.

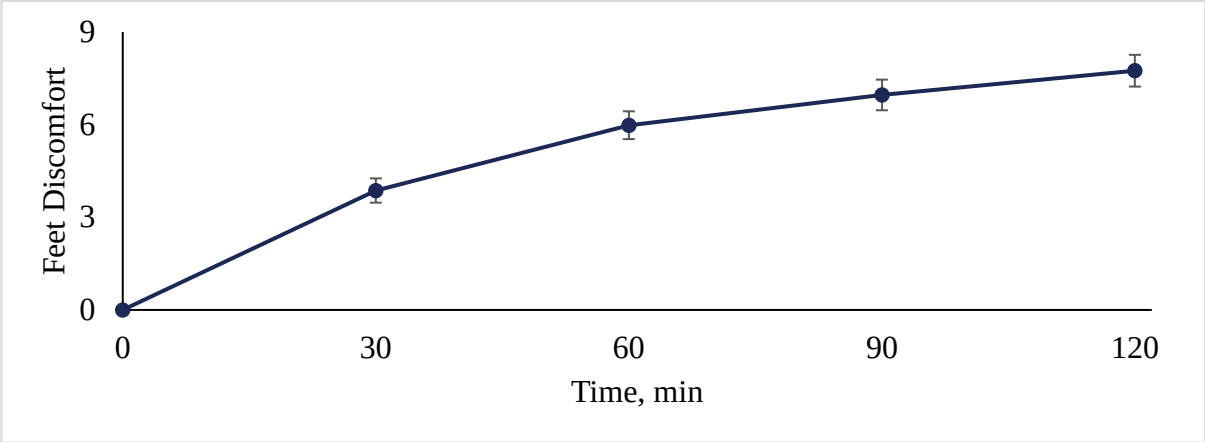

II.

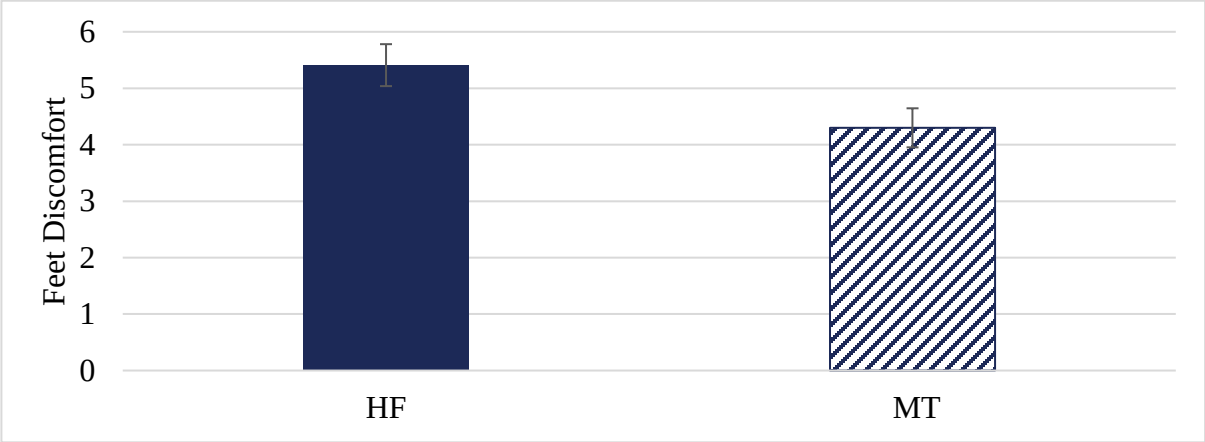

III.

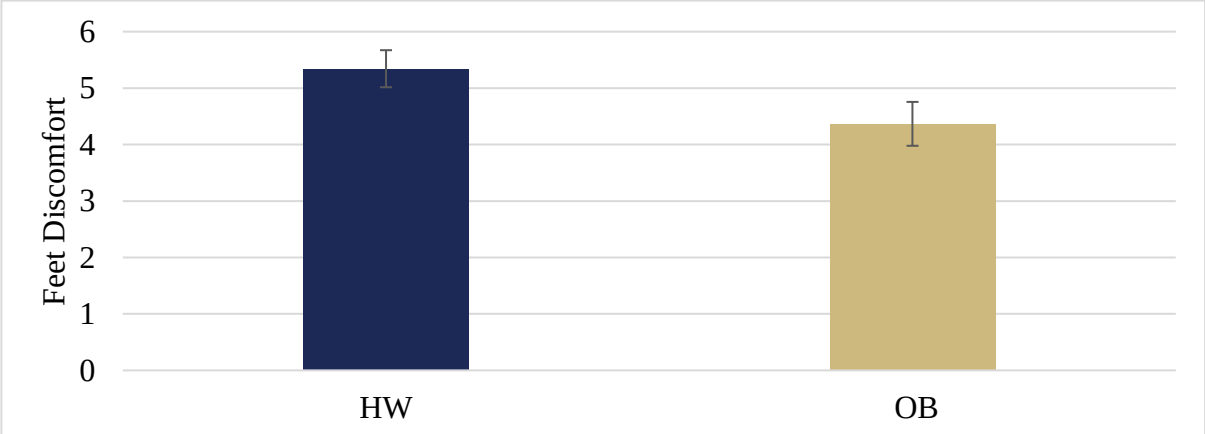

Figure 85: Feet discomfort over time (I) and between flooring conditions (II) and BMI groups (III). Error bars are standard error of the mean.

I.

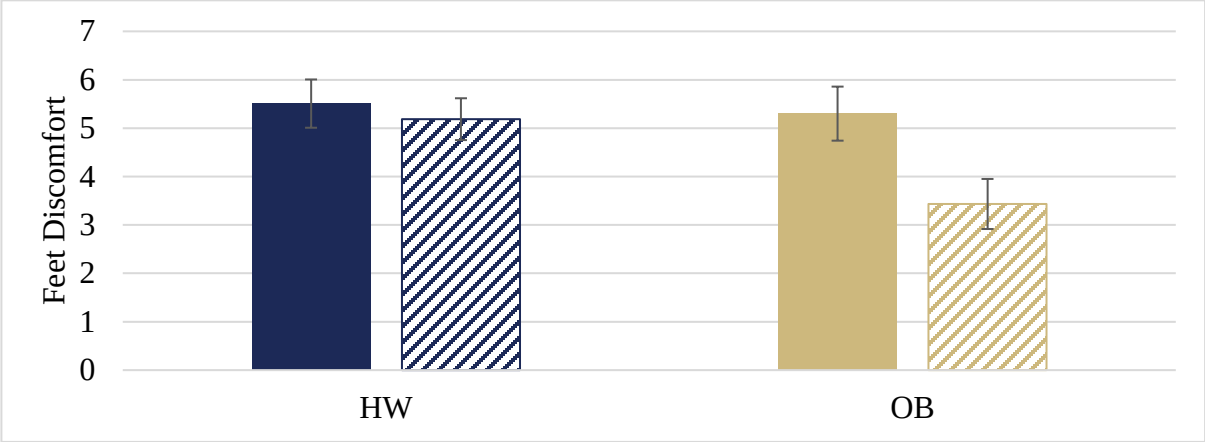

II.

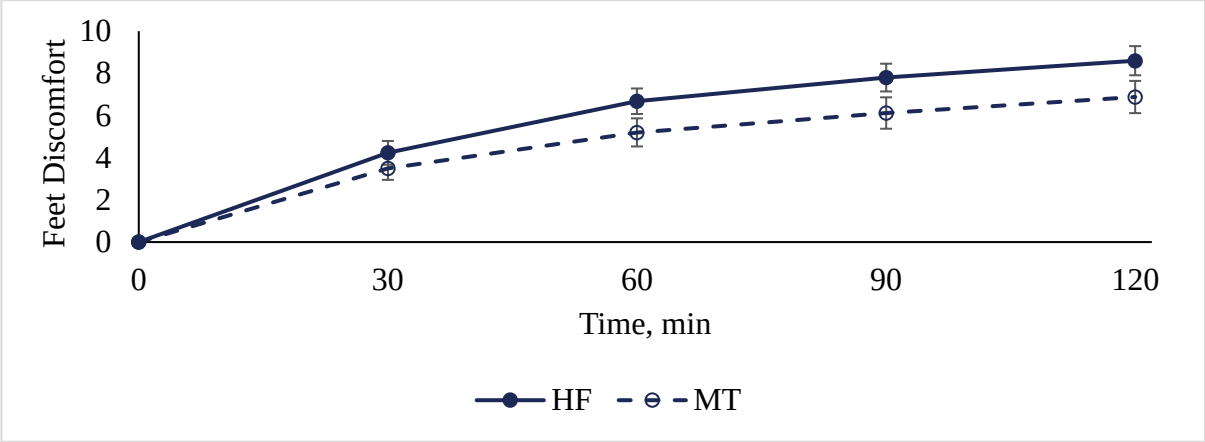

III.

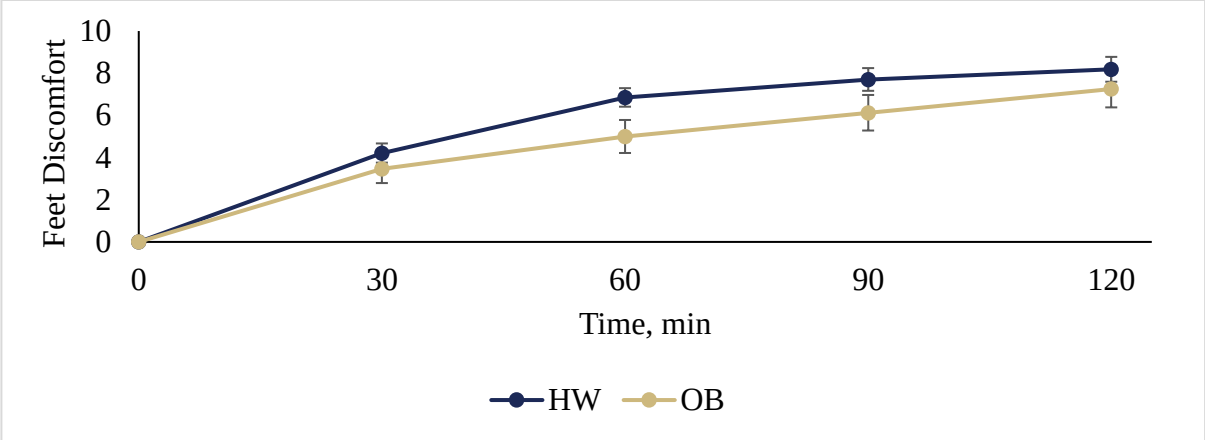

Figure 86: Feet discomfort between BMI groups, split into flooring conditions (I), and over time, split between flooring conditions (II) and BMI groups (III). Error bars are standard error of the mean.

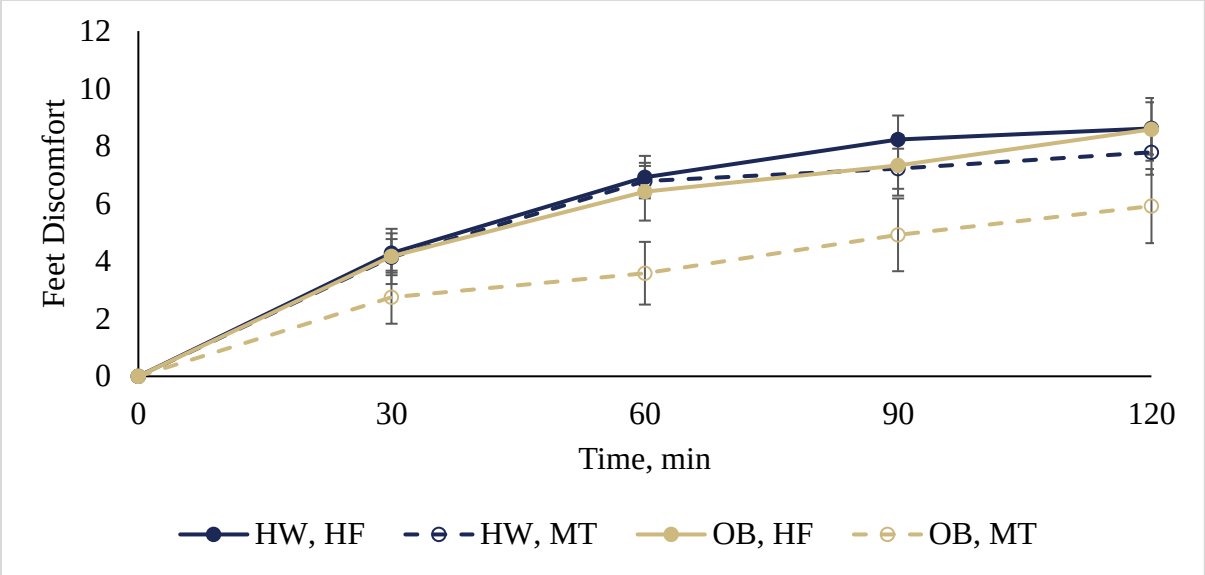

Figure 87: Feet discomfort over time, split between BMI groups and flooring conditions. Error bars are standard error of the mean.

Appendix B Weight Transfer Measures

This section includes details of weight transfer analysis measures, including a comparison of COP and P_R data (briefly discussed in section 5.2), all graphs of shift and fidget data representing relationships between flooring condition, BMI group, and time factors, and further discussion of strategy usage.

Appendix B.1 Comparison of COP and P_R Data

In section 5.2, the relationship between COP and proportion of underfoot vertical force on the right foot (P_R) was discussed. Prior literature indicated that changes in COP are partially due to changes in P_R—and are also a function of My, Fx, and the location of each foot in respect to the origin (Equation 5-7). A visual representation of the differences between COP and P_R over five minutes of standing data is displayed in Figure 88. General weight transfer patterns were similar between COP and P_R. However, amplitude differs between methods.

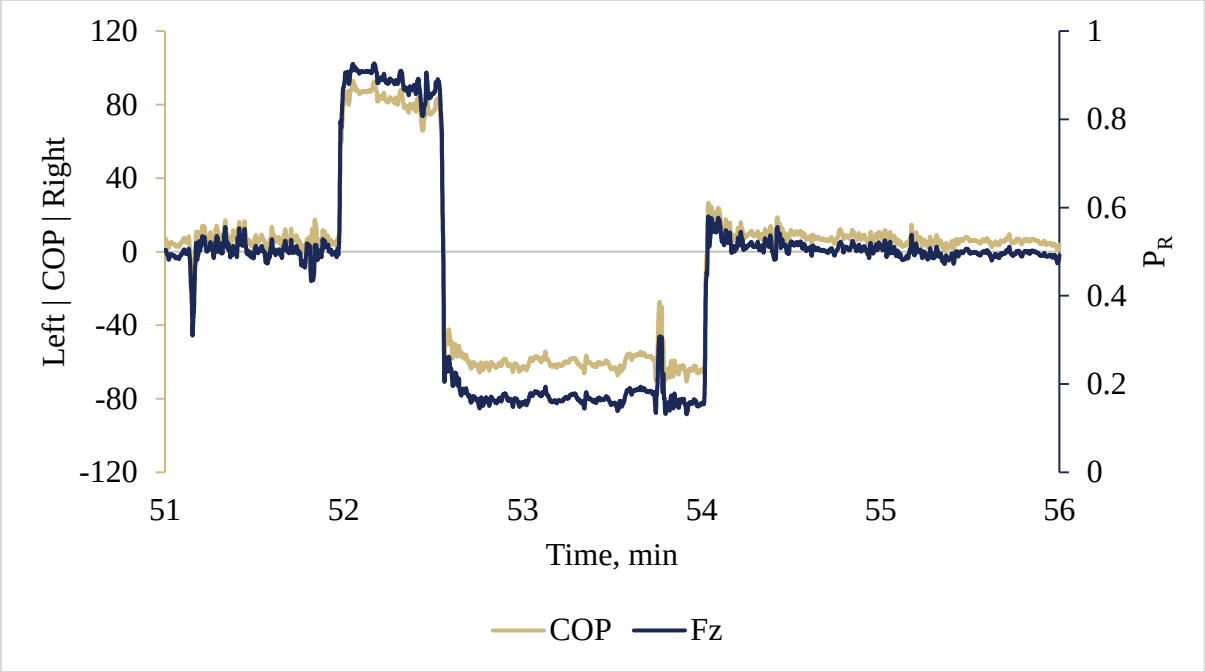

Figure 88: Comparison of COP (gold) and P_R (navy). Fz and COP are related and show similar curves. Differences between COP and P_R are due to, Fx, My, and the location of the feet.

The number of weight shifts measured over the displayed five minute period, as measured by Cham and Redfern [1] were 31 and 15 weight shifts for COP and P_R, respectively. This indicates that COP may be measuring more smaller deviations in weight transfers than P_R. The overall goal of measuring weight transfers for this study was inspired by the potential relationship between the amount of force applied to the legs, discomfort, and objective joint and muscle measures. Therefore, the scope of this research justifies the use of P_R rather than COP for the analysis of weight transfers during prolonged standing.

Appendix B.2 Shift and Fidget Data

Appendix B.2.1 Shifts

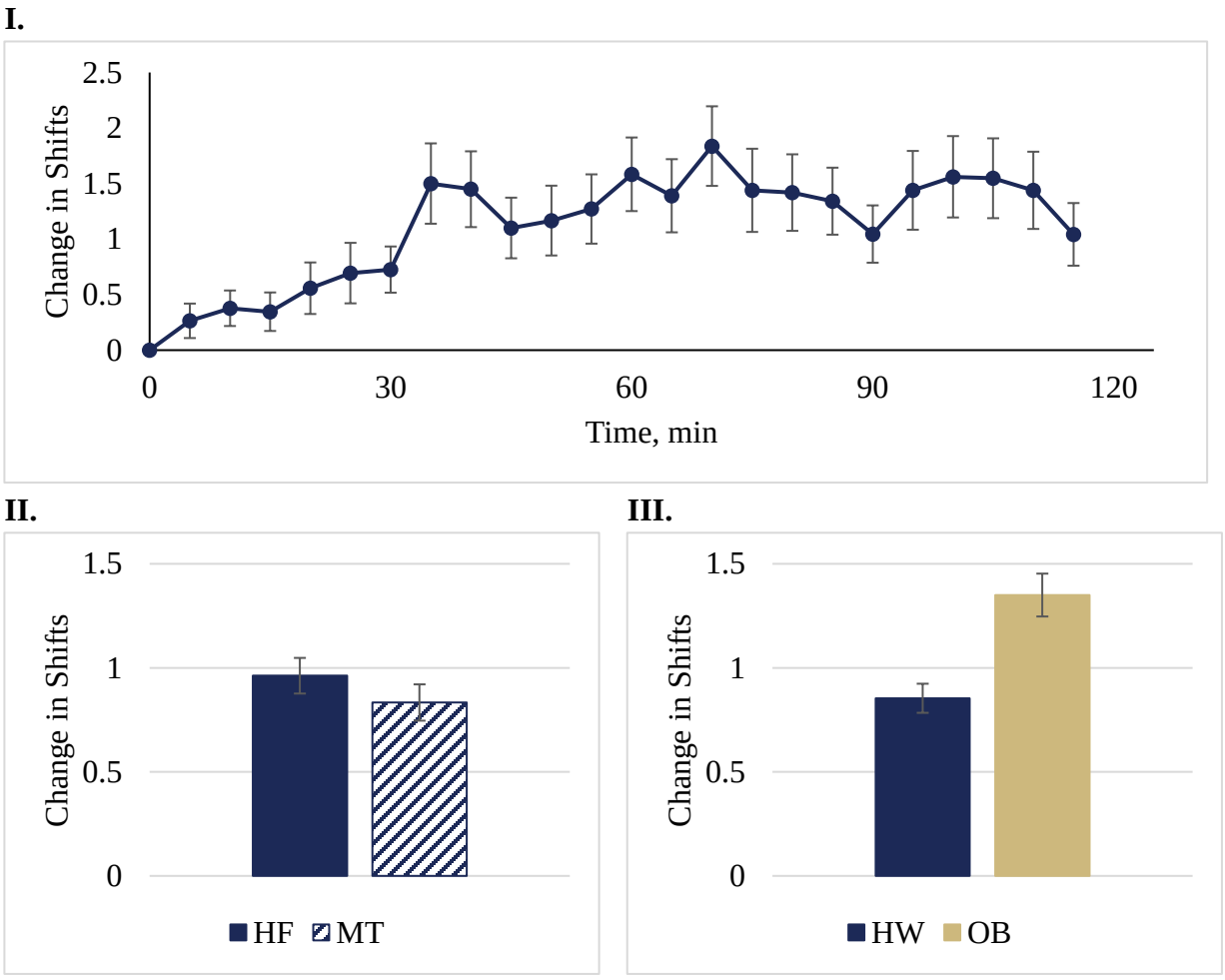

Figure 89: Change in Shifts over time (I) and between flooring conditions (II) and BMI groups (III). Error bars are standard error of the mean.

I.

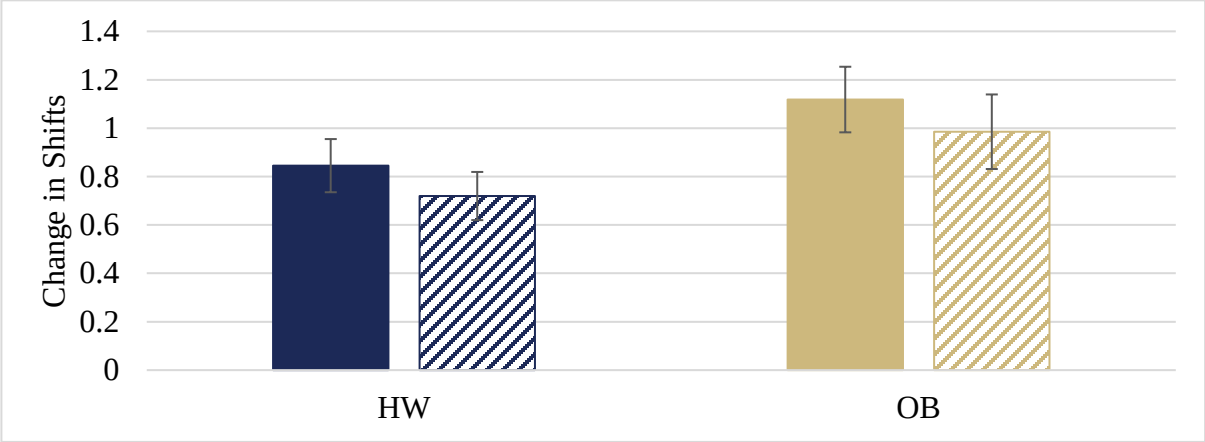

II.

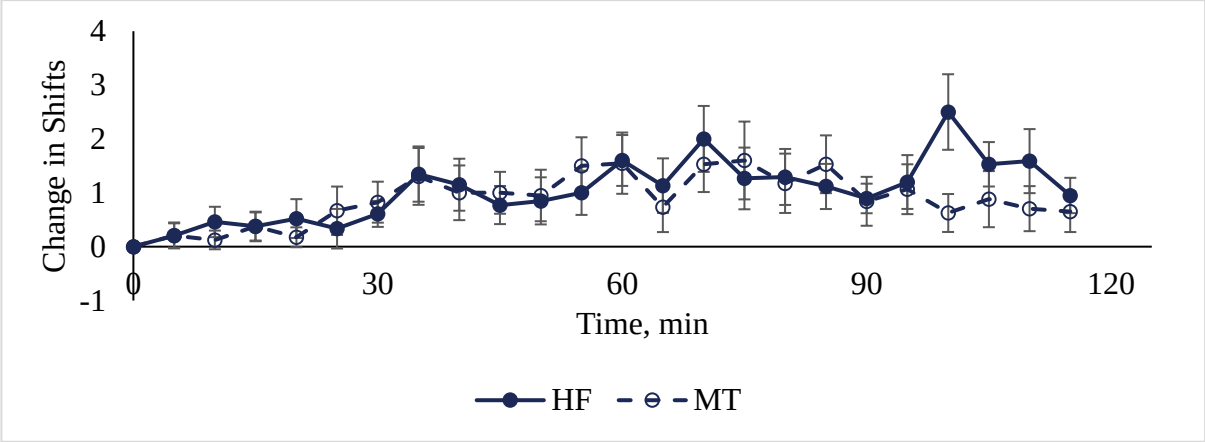

III.

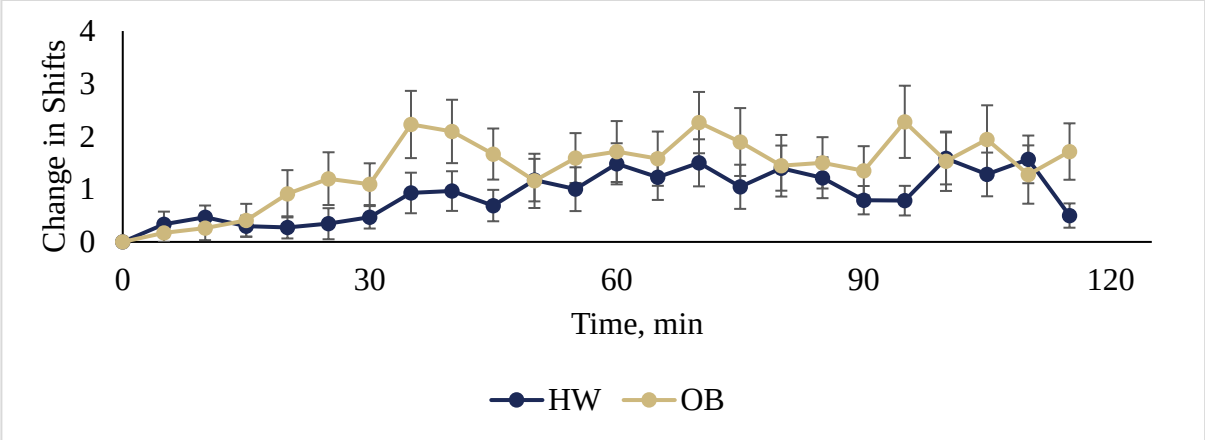

Figure 90: Change in Shifts between BMI groups, split into flooring conditions (I), and over time, split between flooring conditions (II) and BMI groups (III). Error bars are standard error of the mean.

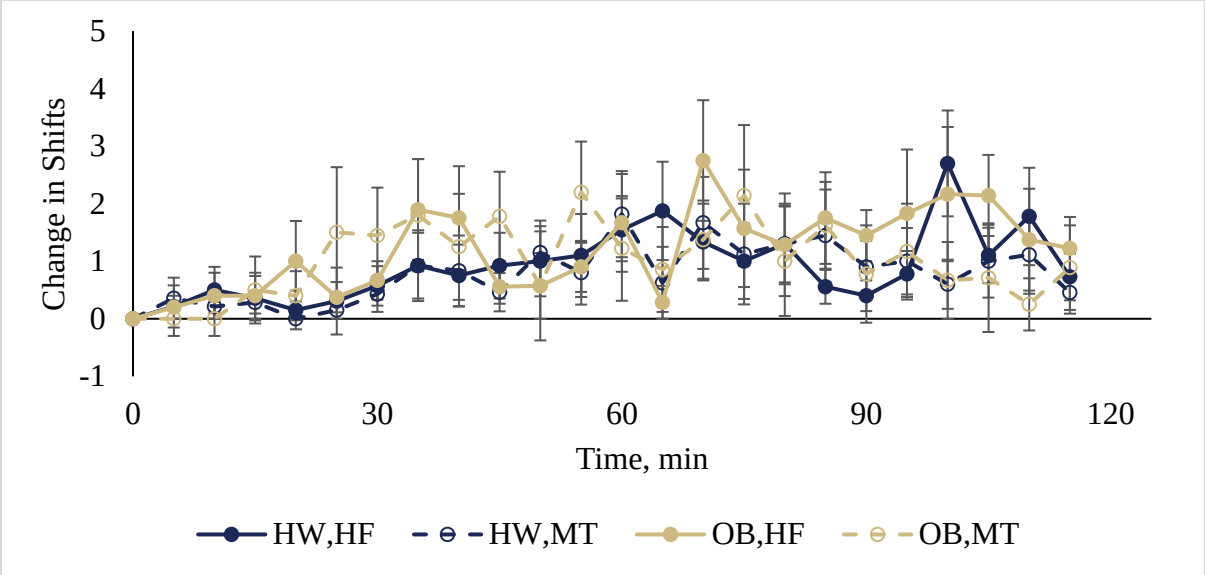

Figure 91: Change in Shifts over time, split between BMI groups and flooring conditions. Error bars are standard error of the mean.

Appendix B.2.2 Fidgets

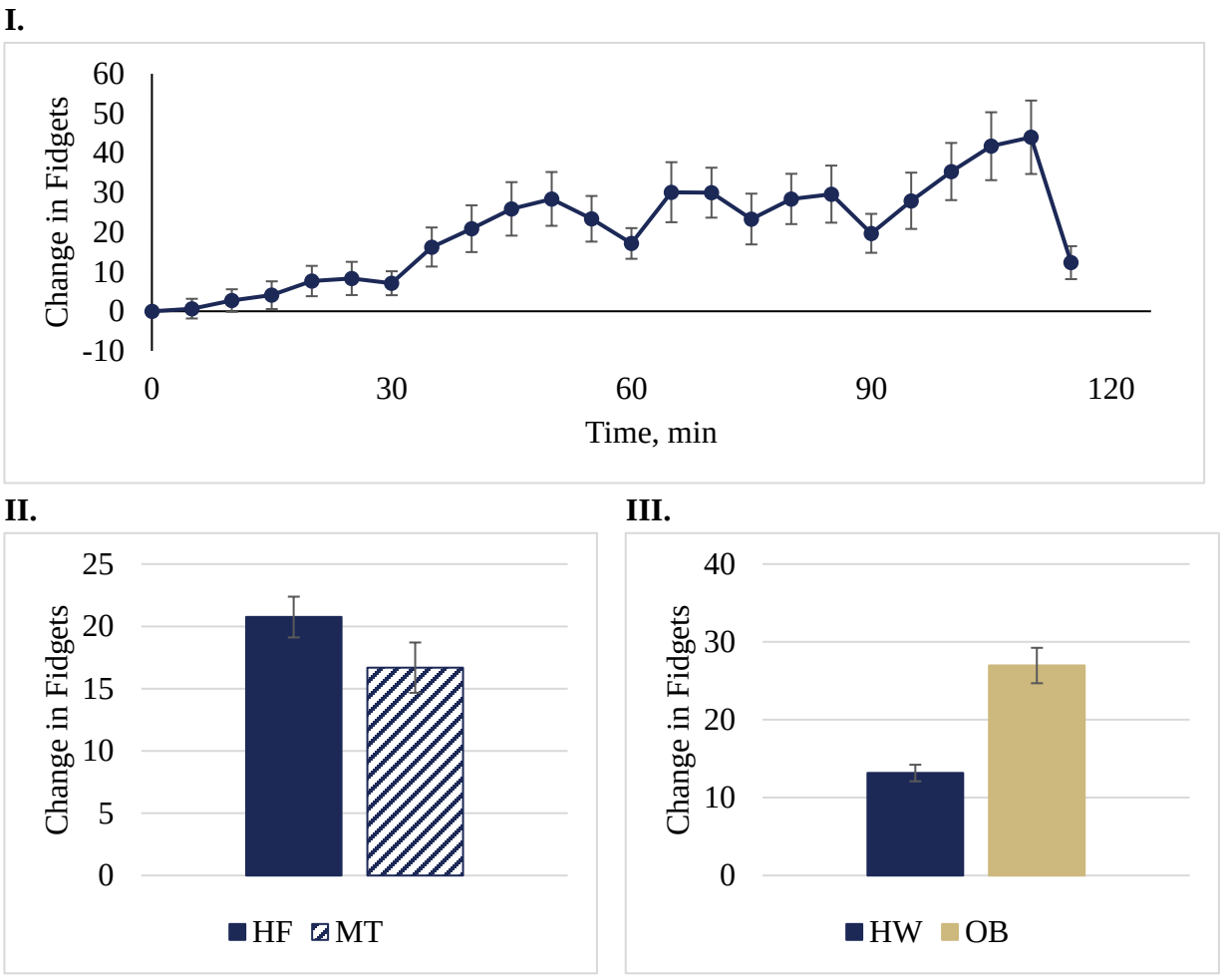

Figure 92: Change in Fidgets over time (I) and between flooring conditions (II) and BMI groups (III). Error bars are standard error of the mean.

I.

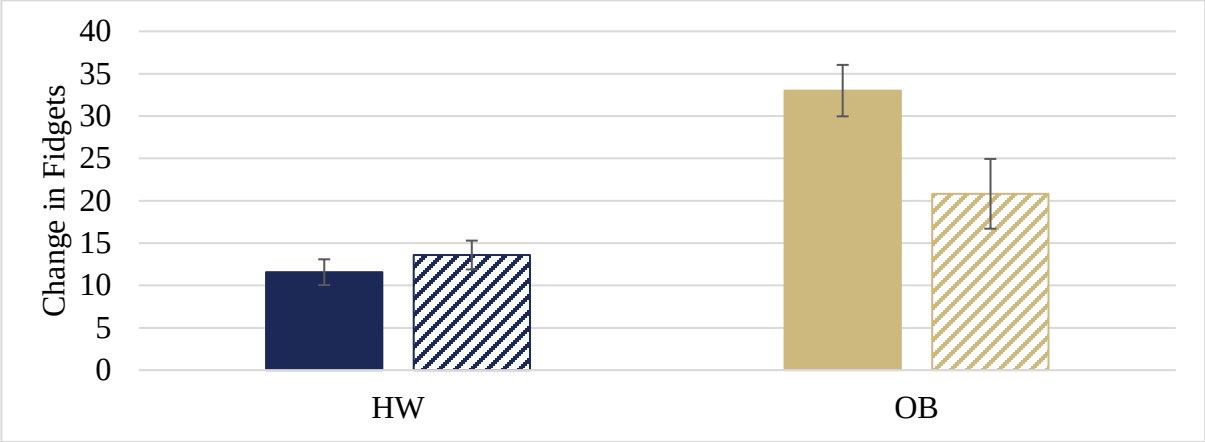

II.

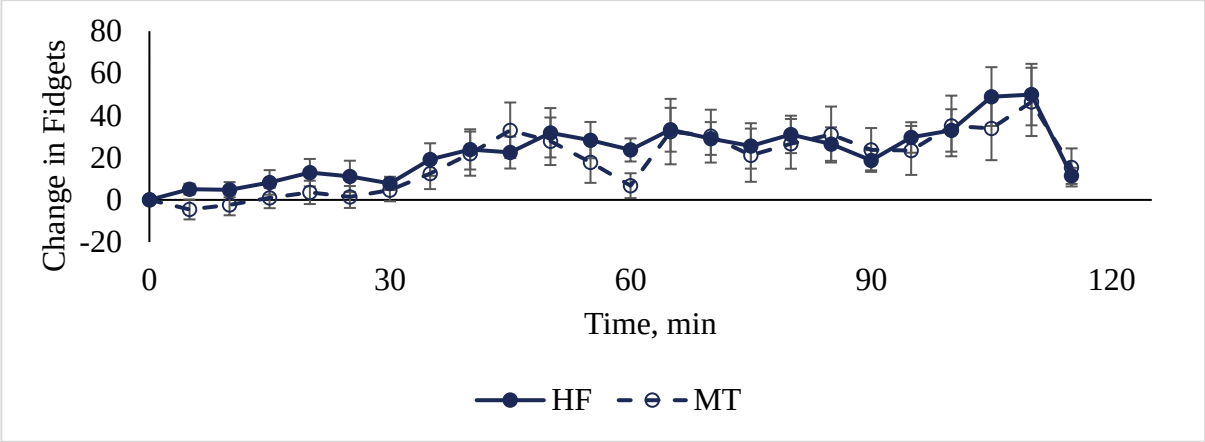

III.

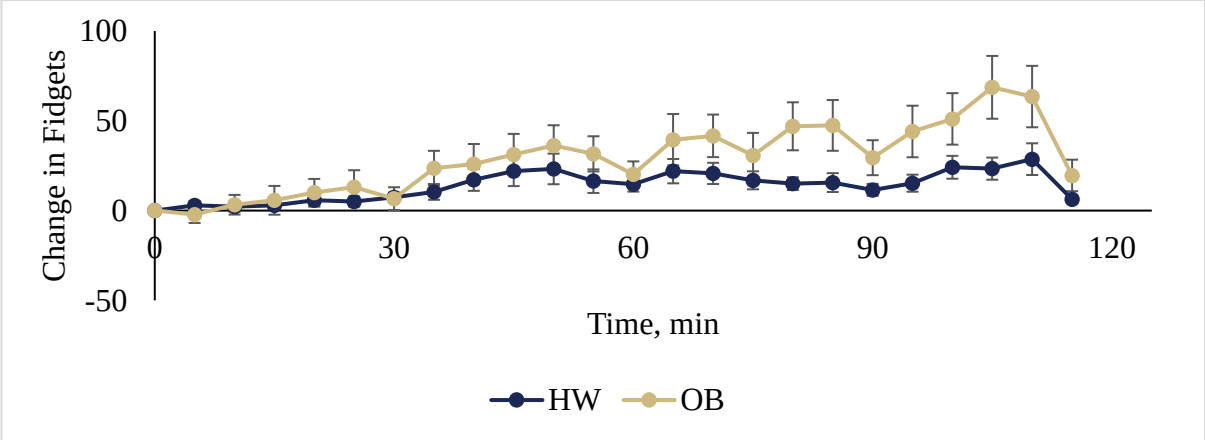

Figure 93: Change in Fidgets between BMI groups, split into flooring conditions (I), and over time, split between flooring conditions (II) and BMI groups (III). Error bars are standard error of the mean.

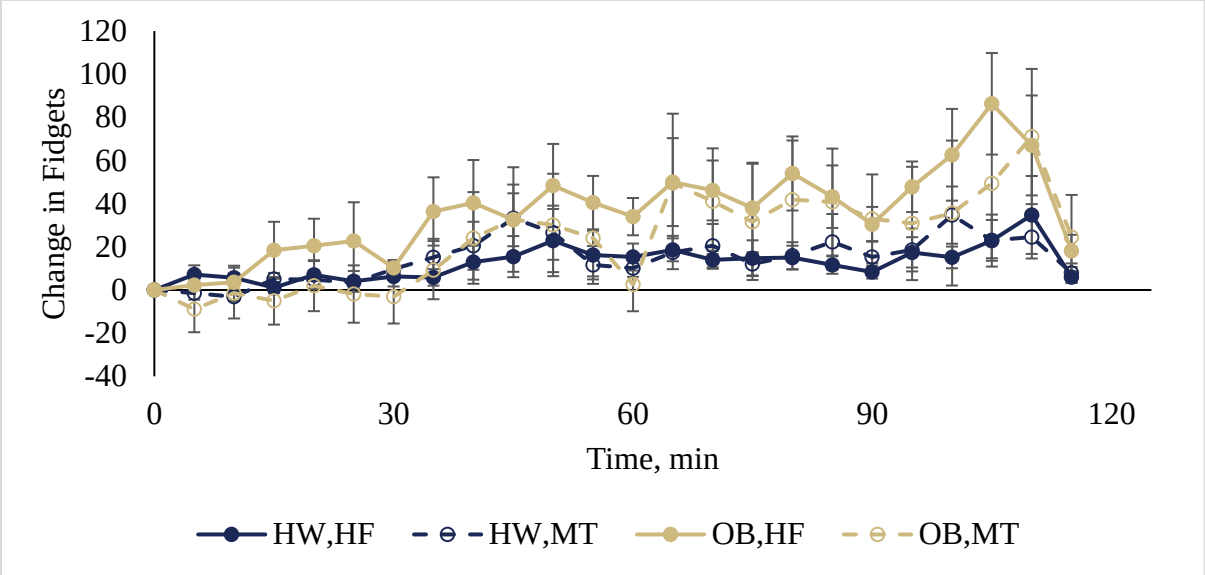

Figure 94: Change in Fidgets over time, split between BMI groups and flooring conditions. Error bars are standard error of the mean.

Appendix B.2.3 Total Events

I.

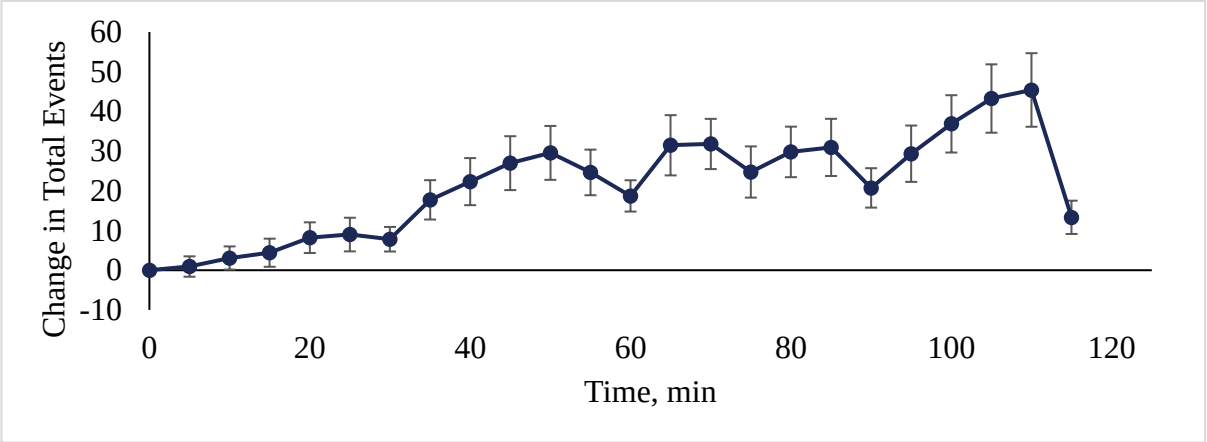

II.

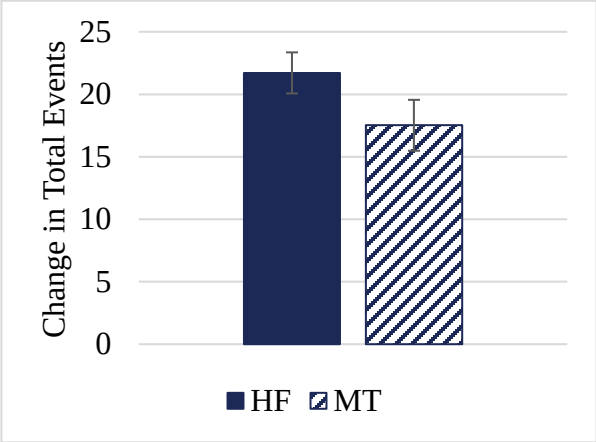

III.

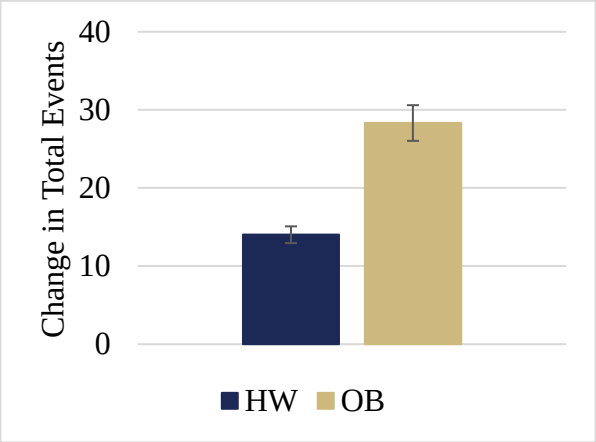

Figure 95: Change in Total Events over time (I) and between flooring conditions (II) and BMI groups (III).

Error bars are standard error of the mean.

I.

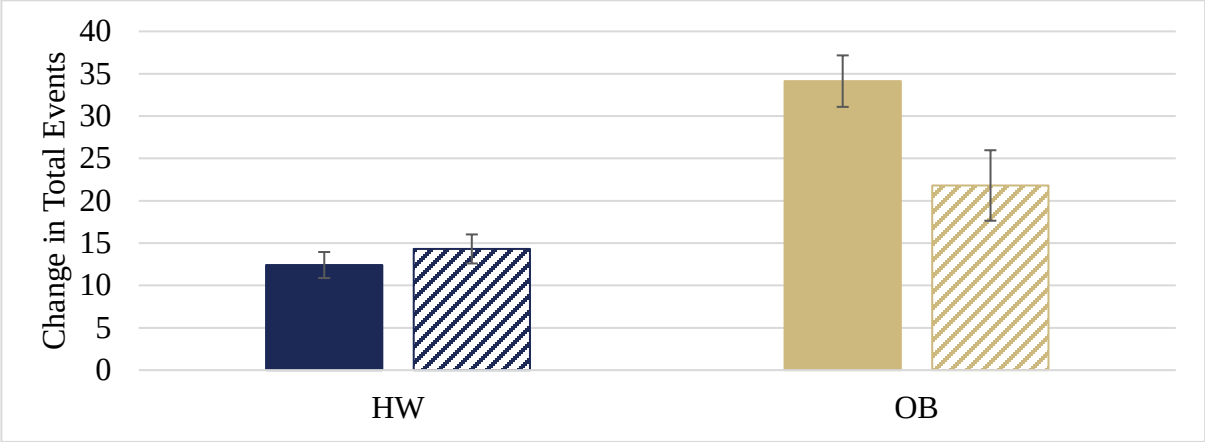

II.

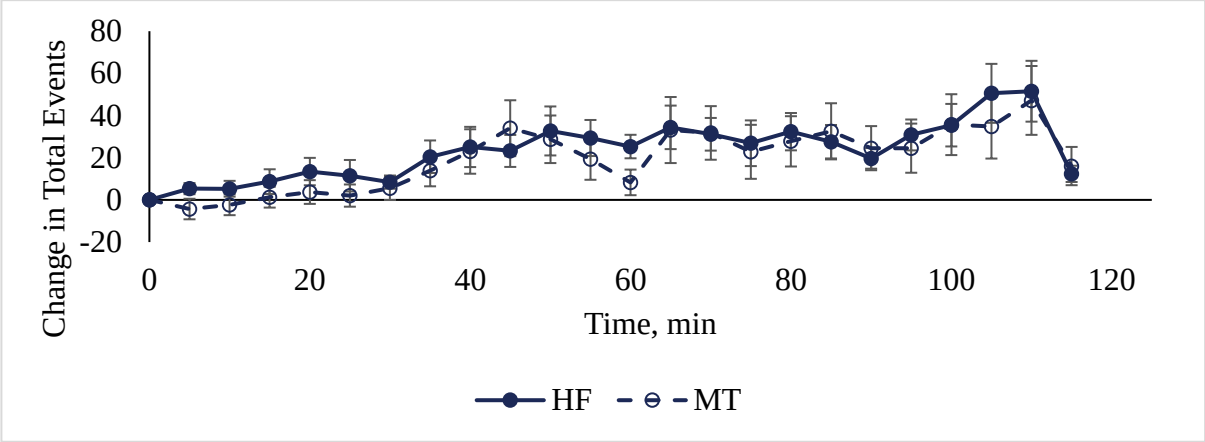

III.

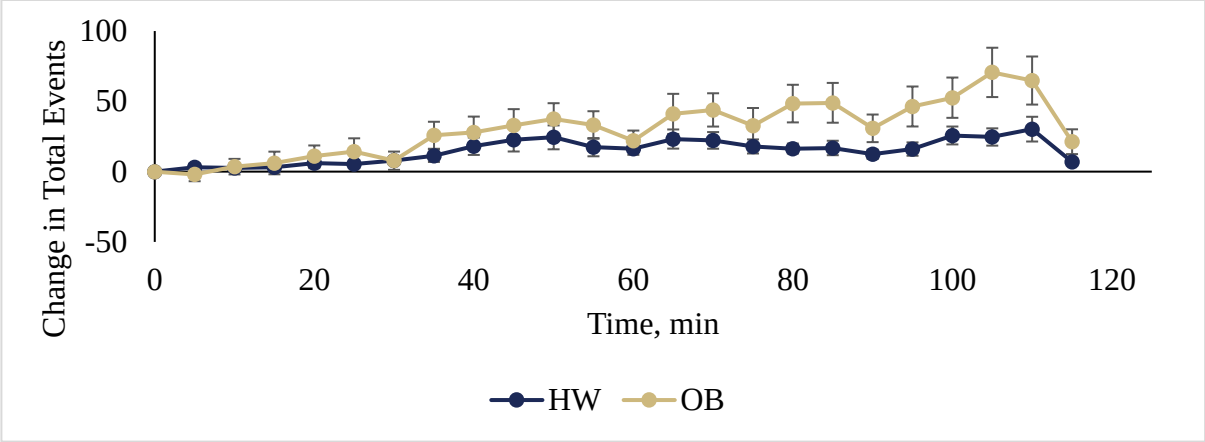

Figure 96: Change in Total Events between BMI groups, split into flooring conditions (I), and over time, split between flooring conditions (II) and BMI groups (III). Error bars are standard error of the mean.

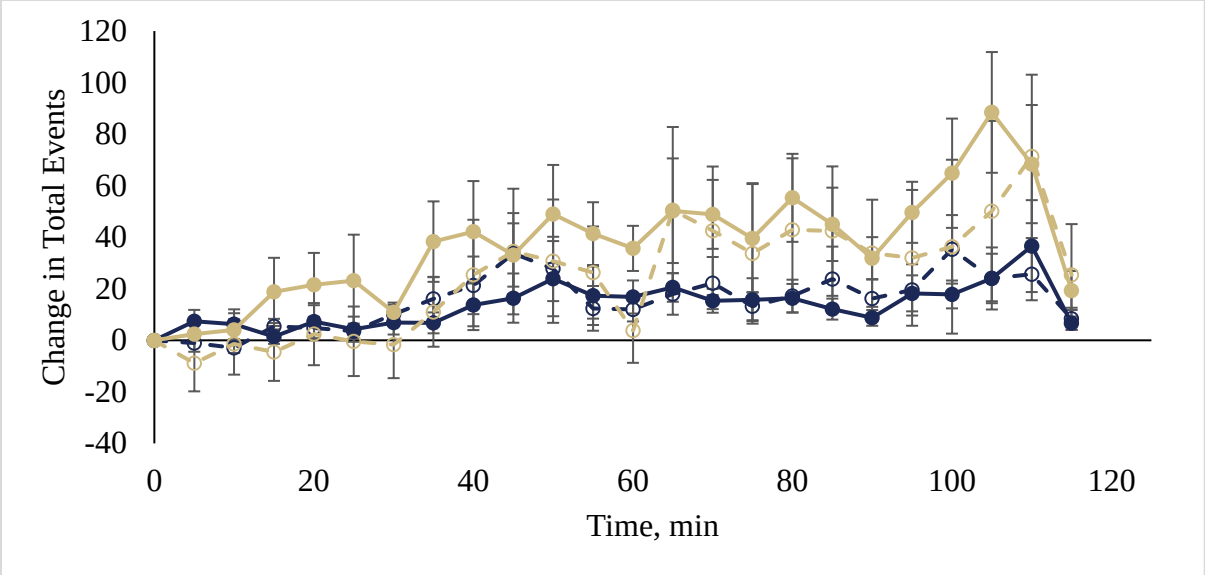

Figure 97: Change in Total Events over time, split between BMI groups and flooring conditions. Error bars are standard error of the mean.

Appendix B.3 Investigation of Strategy Usage

In section 3.4.2.3, standing strategies—shifts and fidgets—were introduced as methods by which subjects may move during prolonged standing. It was hypothesized that these movements may be related to discomfort and physiological changes that occur during prolonged standing. Another interpretation of standing strategies was investigated, in which standing strategies did not define a single movement, but an overall pattern of movements displayed by a subject.

An effort was made to separate subjects based on their tendency to primarily shift, primarily fidget, or display a mixed set of strategies. First, the number of shifts, fidgets, and ratios of shifts and fidgets were calculated for each subject. Shifts and fidgets are displayed in Figure 98 - Figure 125. A visual observation of each subject's shifts and fidgets over time was performed to determine if any patterns existed. Specifically, the ratios calculated are displayed in Equation B-

1 and Equation B-2. It was expected that ratios may reveal subject tendencies towards primarily fidgeting strategies or shifting strategies. However, many subjects displayed zero shifts or fidgets. Ratios resulted in zero, NaN, INF values, which were difficult to interpret. Therefore, ratio values are not included in this section.

$$R_1 = \frac{S}{F} \tag{B-1}$$

$$R_2 = \frac{F}{(F+S)} \tag{B-2}$$

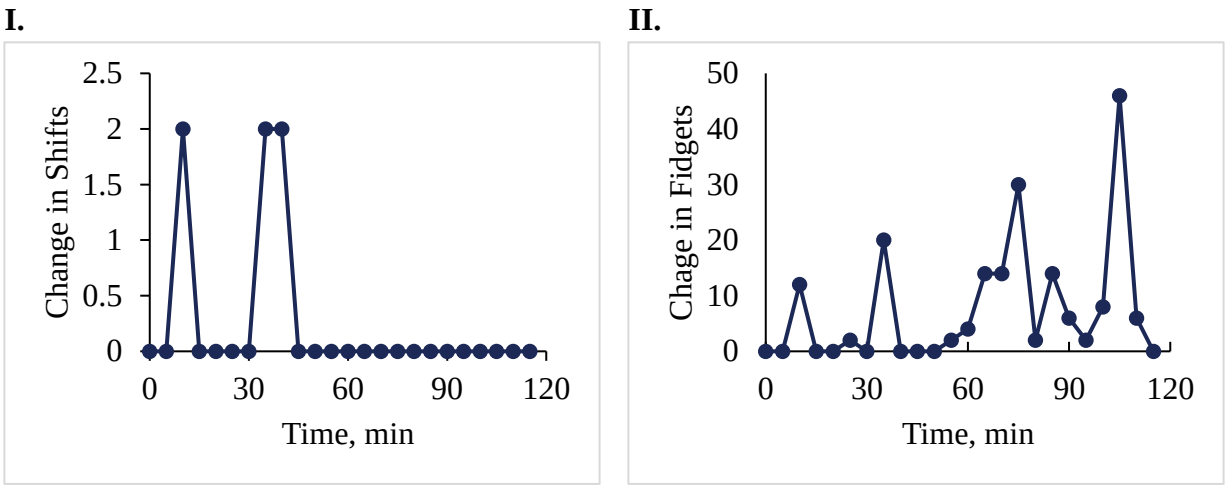

Figure 98: Subject S01 weight transfer events counted every five minutes during standing. I. Change in Shifts and II. Change in Fidgets on the HF condition. S01 force plate data on the MT condition was not included for analyses.

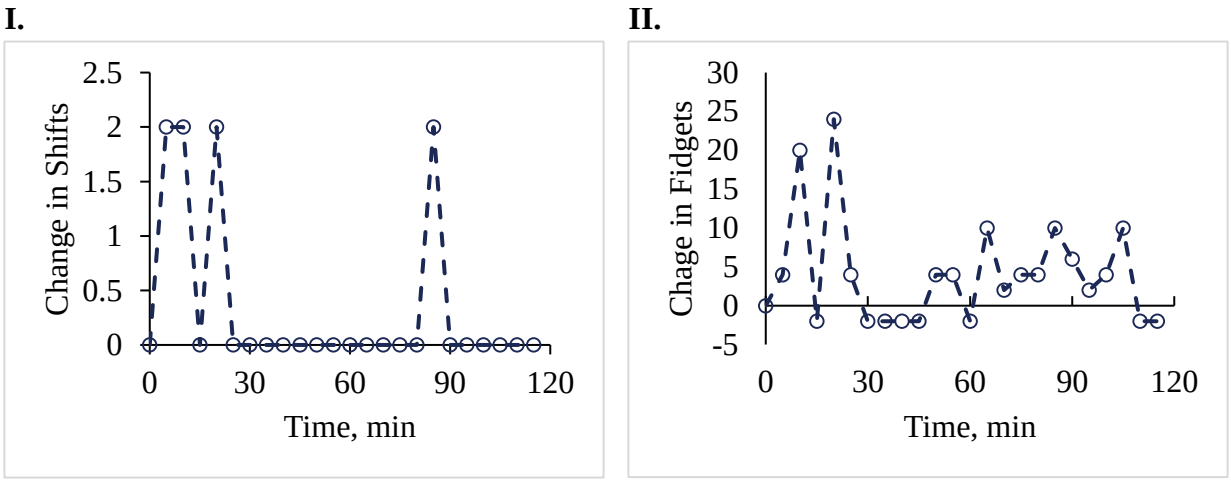

Figure 99: Subject S02 weight transfer events counted every five minutes during standing. I. Change in Shifts and II. Change in Fidgets on the MT condition. S02 did not complete the standing protocol, and therefore only MT data is available.

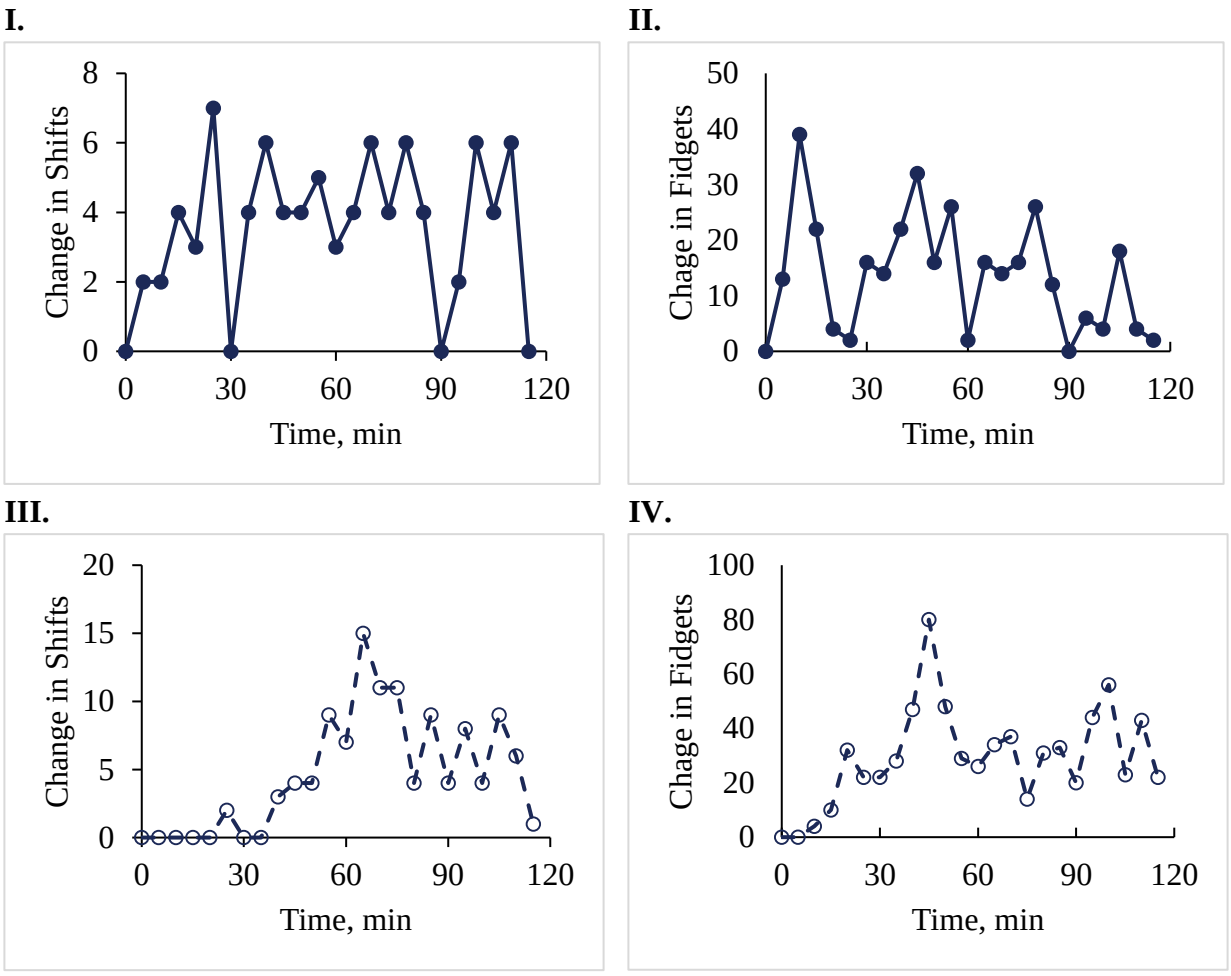

Figure 100: Subject S03 weight transfer events counted every five minutes during standing. I. Change in Shifts and II. Change in Fidgets on the HF condition. III. Change in Shifts and IV. Change in Fidgets on the MT condition.

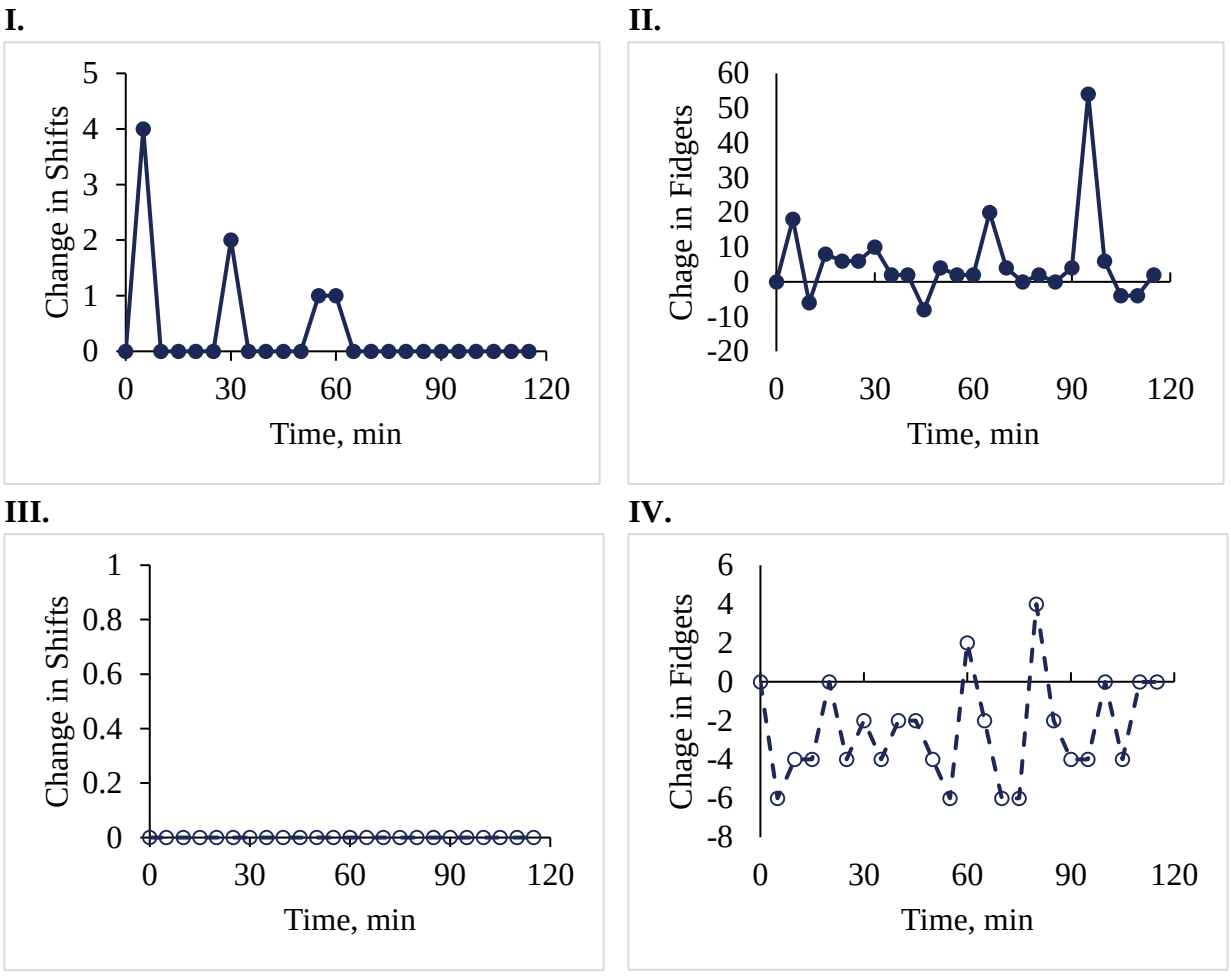

Figure 101: Subject S04 weight transfer events counted every five minutes during standing. I. Change in Shifts and II. Change in Fidgets on the HF condition. III. Change in Shifts and IV. Change in Fidgets on the MT condition.

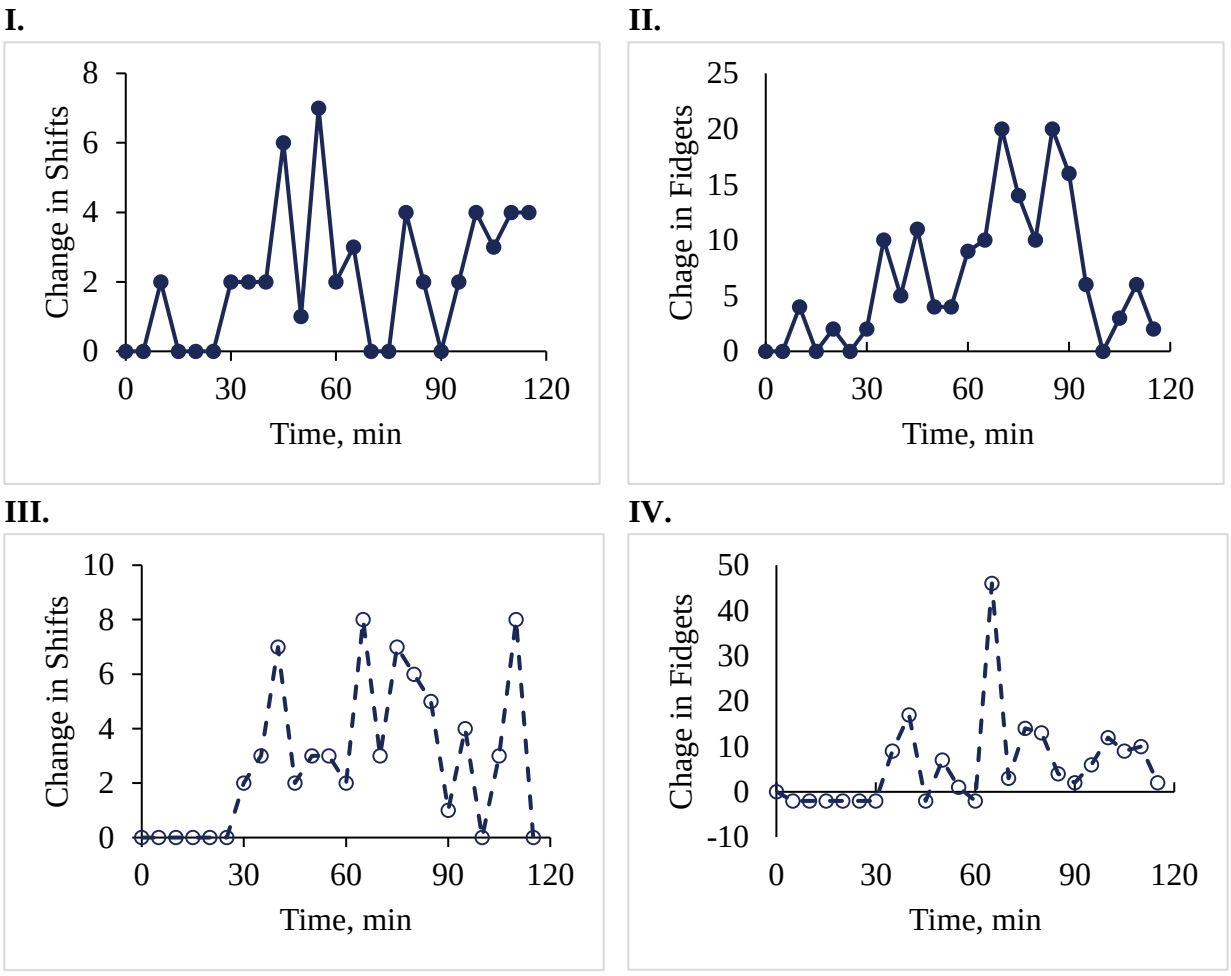

Figure 102: Subject S05 weight transfer events counted every five minutes during standing. I. Change in Shifts and II. Change in Fidgets on the HF condition. III. Change in Shifts and IV. Change in Fidgets on the MT condition.

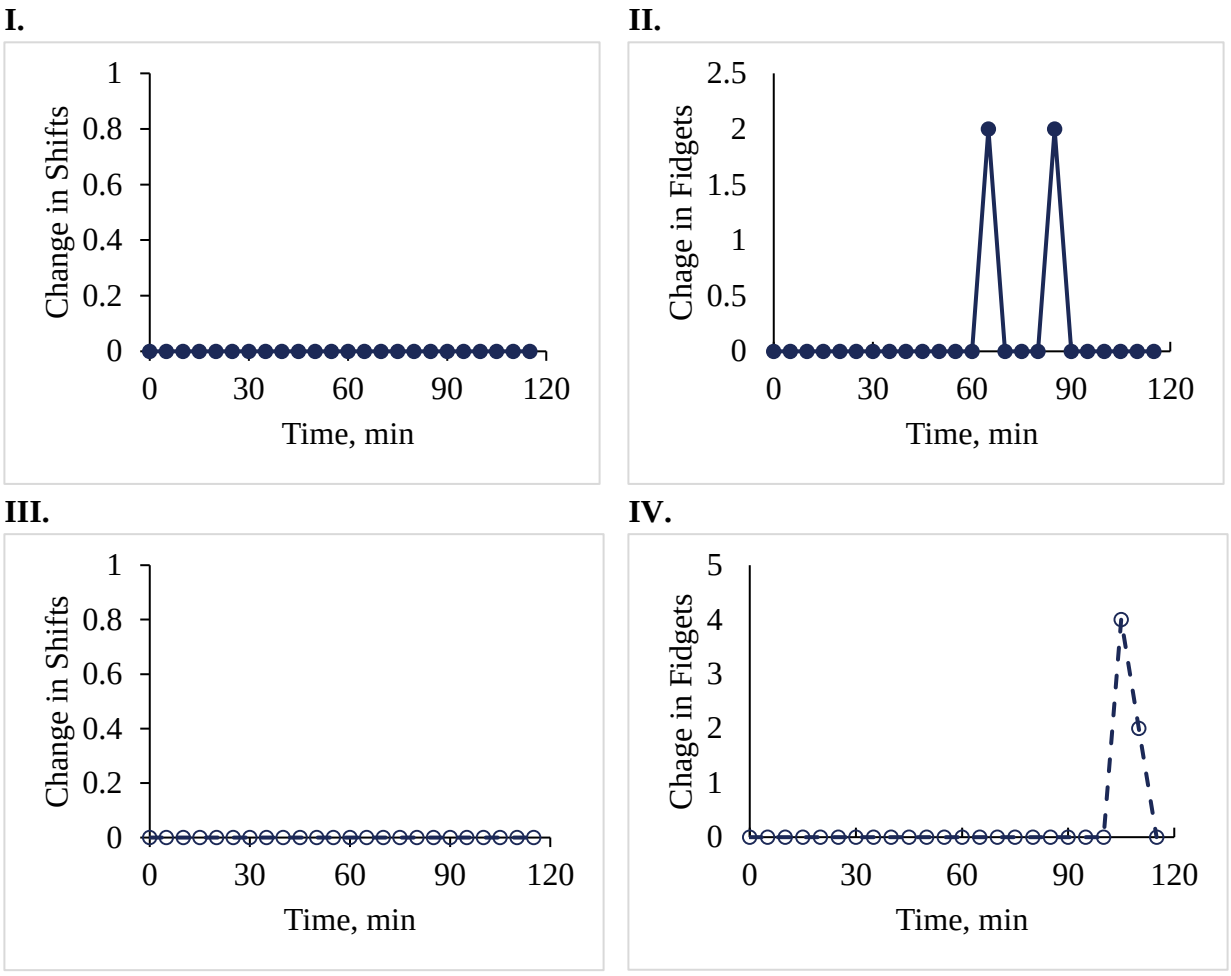

Figure 103: Subject S06 weight transfer events counted every five minutes during standing. I. Change in Shifts and II. Change in Fidgets on the HF condition. III. Change in Shifts and IV. Change in Fidgets on the MT condition.

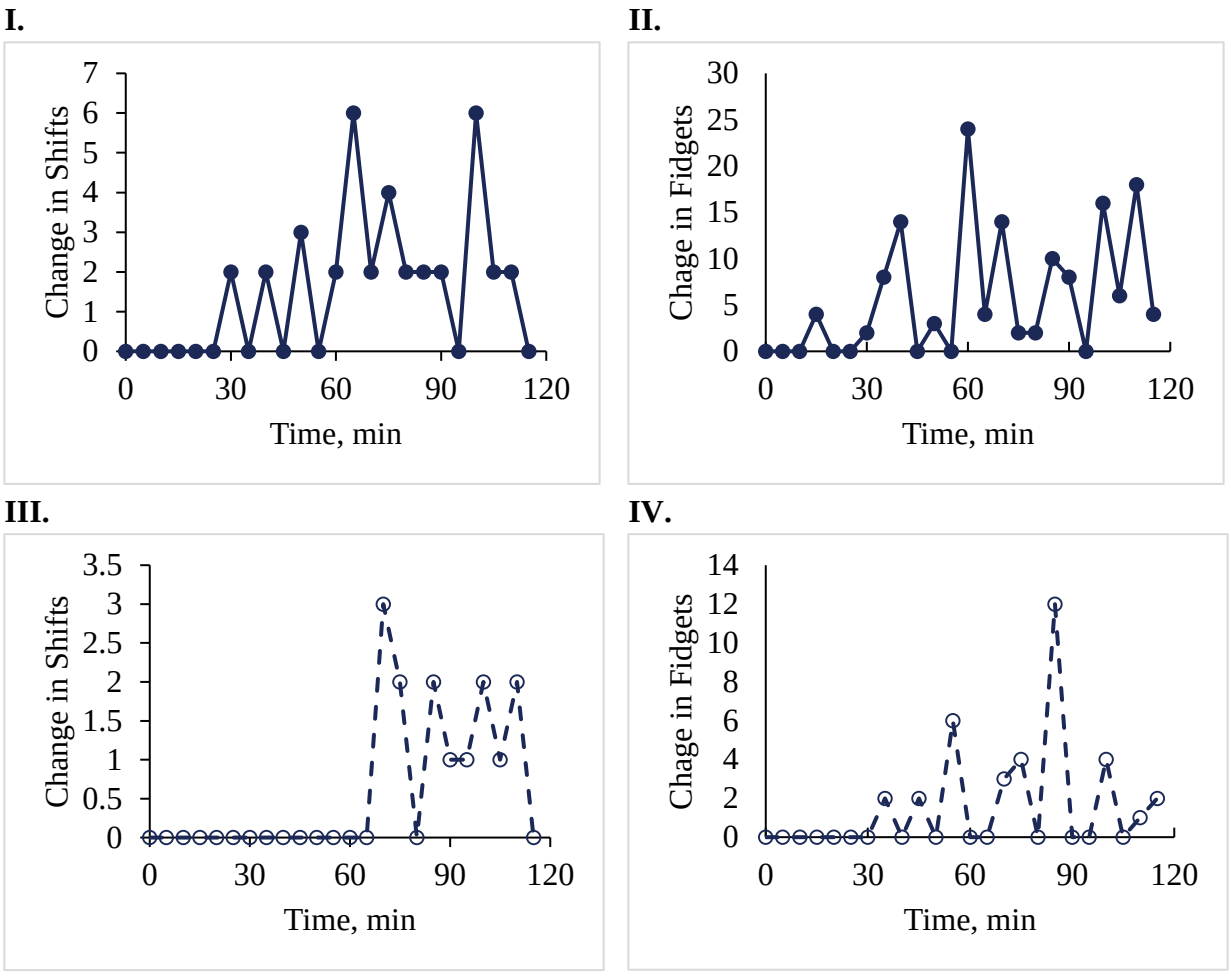

Figure 104: Subject S07 weight transfer events counted every five minutes during standing. I. Change in Shifts and II. Change in Fidgets on the HF condition. III. Change in Shifts and IV. Change in Fidgets on the MT condition.

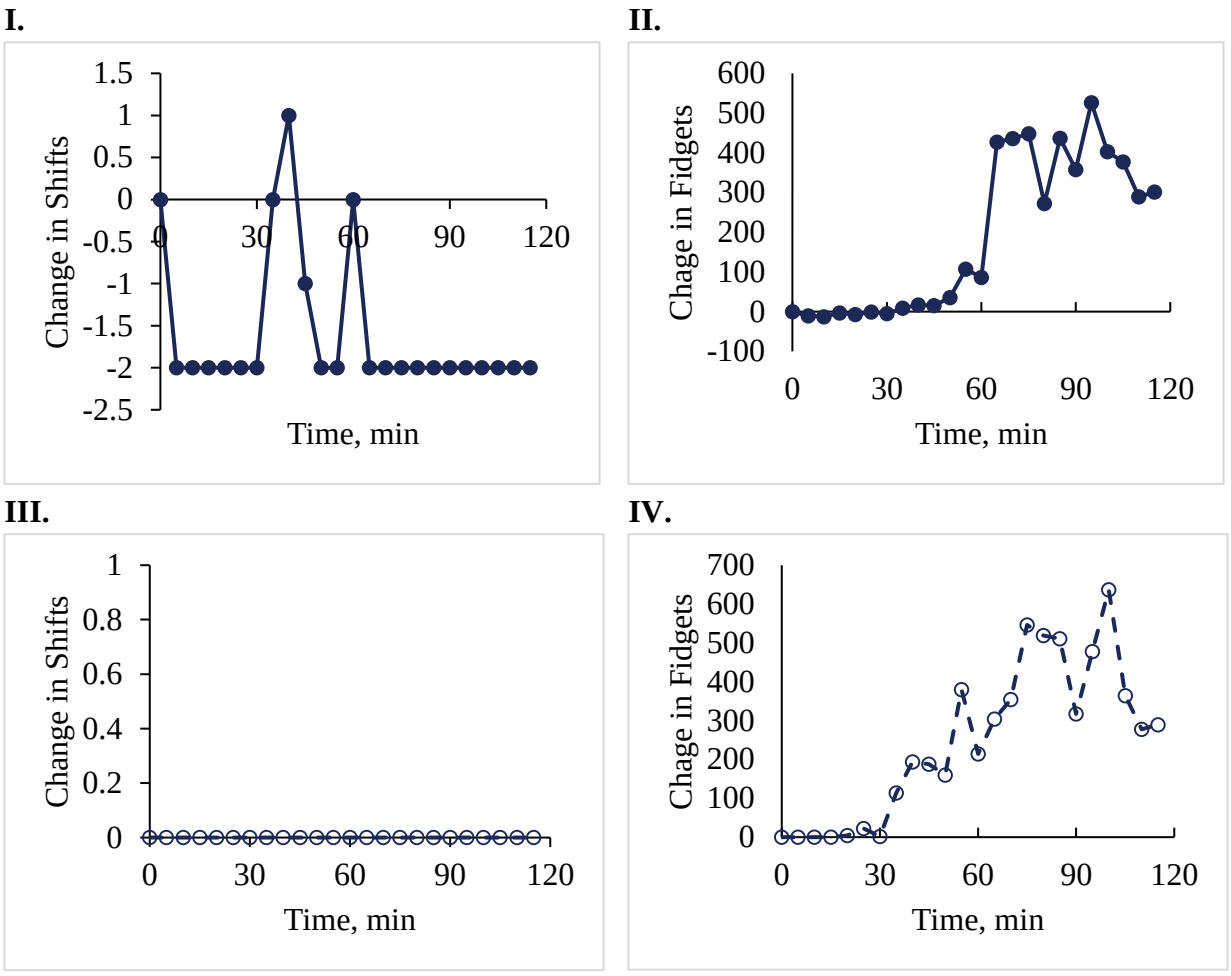

Figure 105: Subject S10 weight transfer events counted every five minutes during standing. I. Change in Shifts and II. Change in Fidgets on the HF condition. III. Change in Shifts and IV. Change in Fidgets on the MT condition.

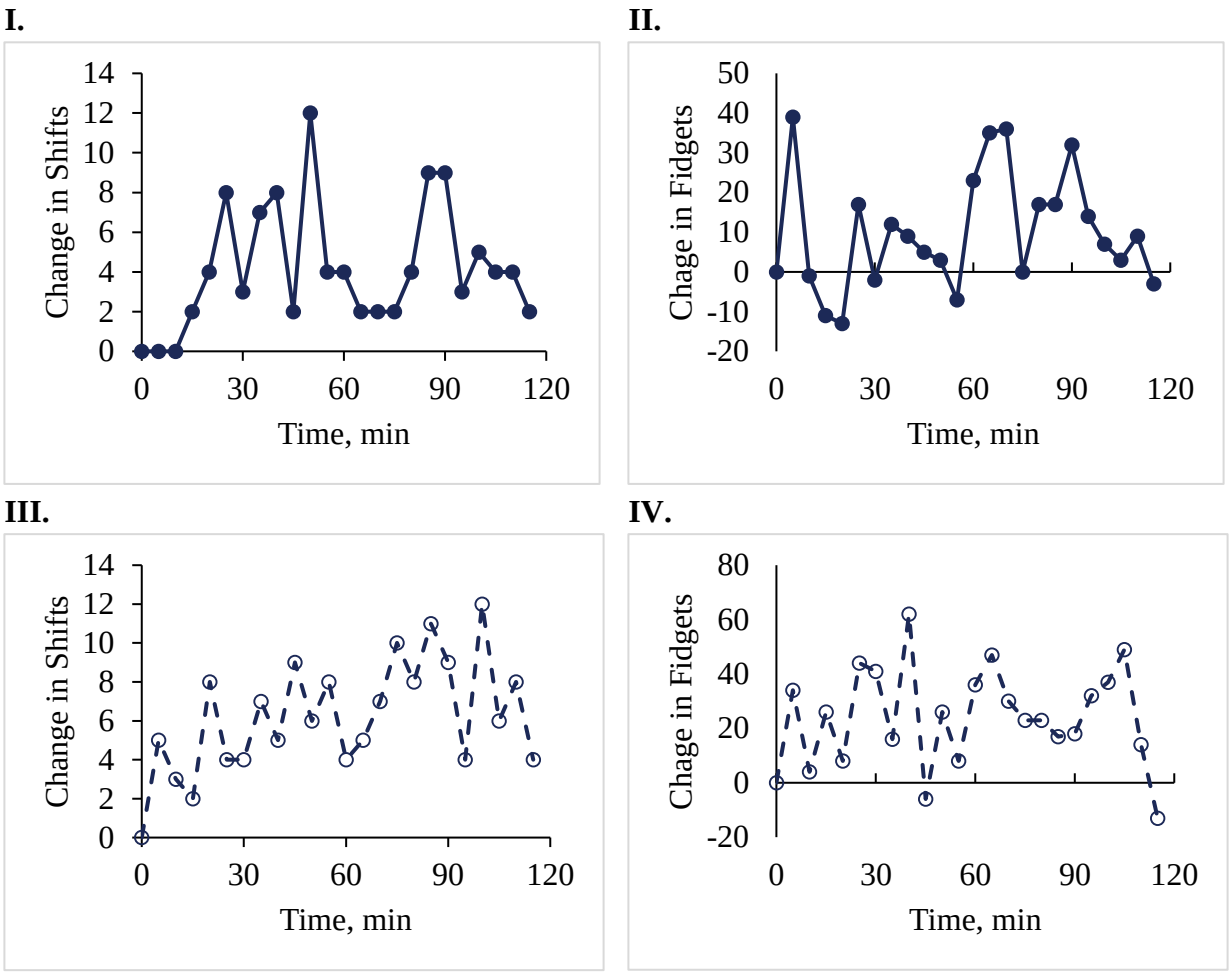

Figure 106: Subject S11 weight transfer events counted every five minutes during standing. I. Change in Shifts and II. Change in Fidgets on the HF condition. III. Change in Shifts and IV. Change in Fidgets on the MT condition.

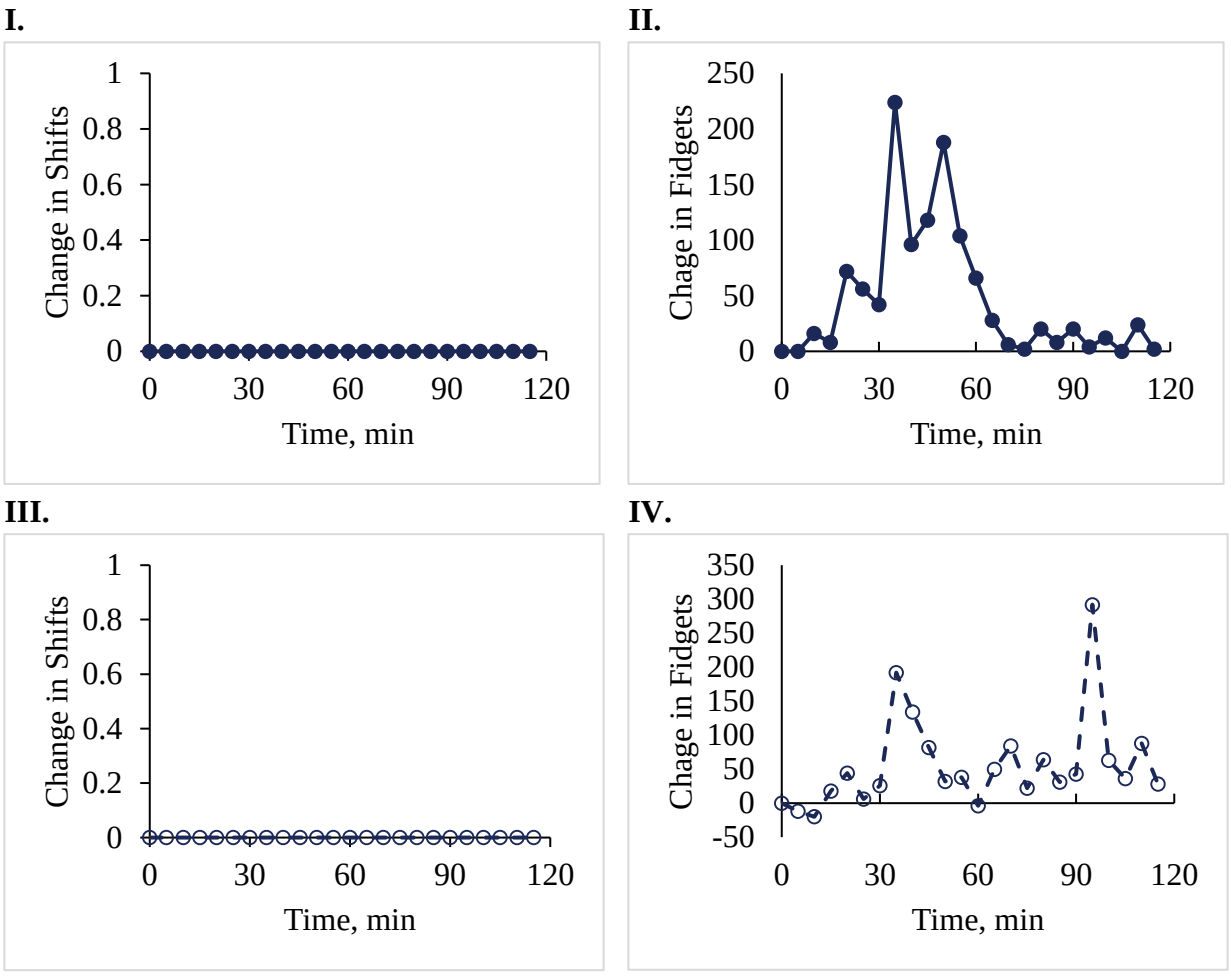

Figure 107: Subject S12 weight transfer events counted every five minutes during standing. I. Change in Shifts and II. Change in Fidgets on the HF condition. III. Change in Shifts and IV. Change in Fidgets on the MT condition.

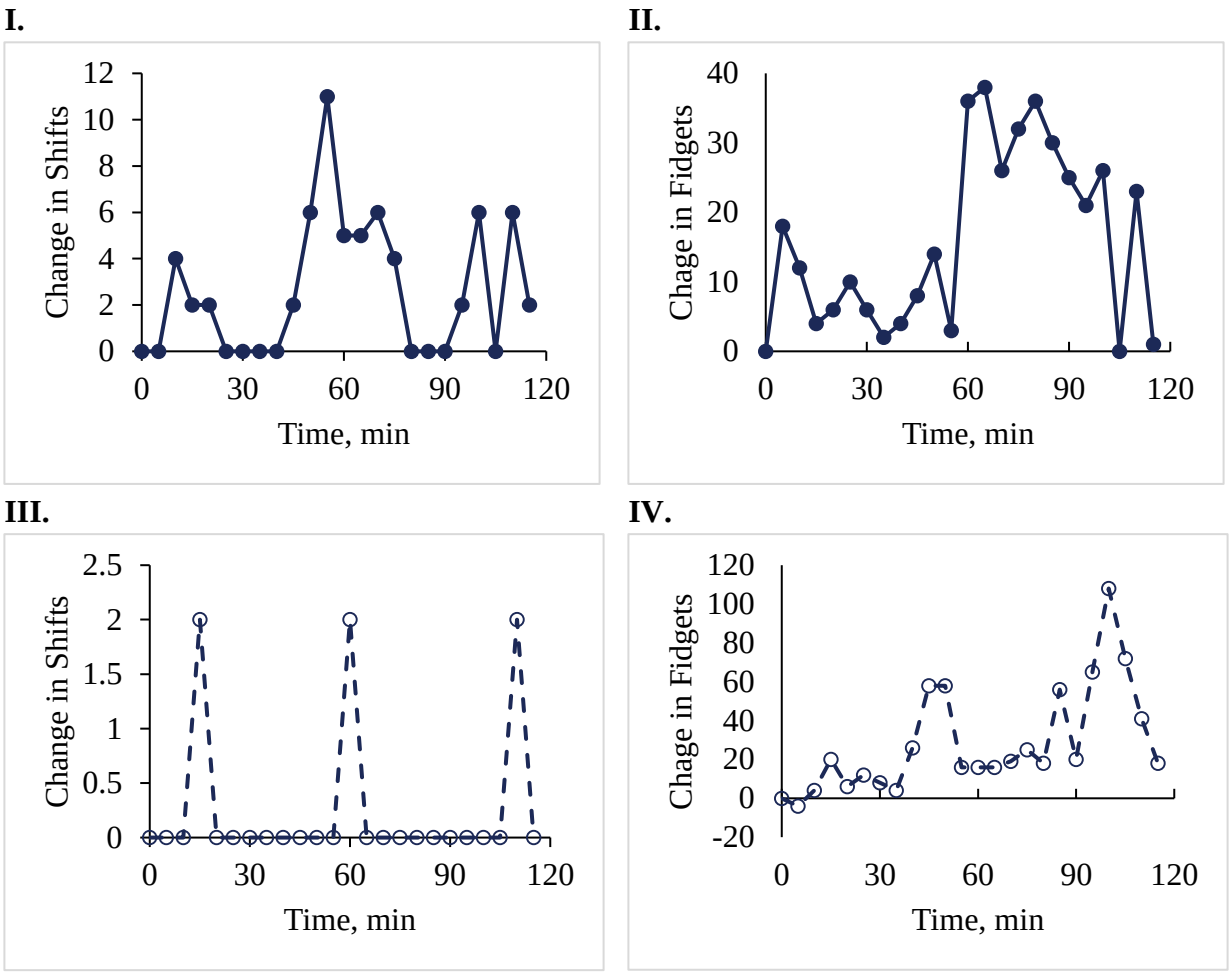

Figure 108: Subject S13 weight transfer events counted every five minutes during standing. I. Change in Shifts and II. Change in Fidgets on the HF condition. III. Change in Shifts and IV. Change in Fidgets on the MT condition.

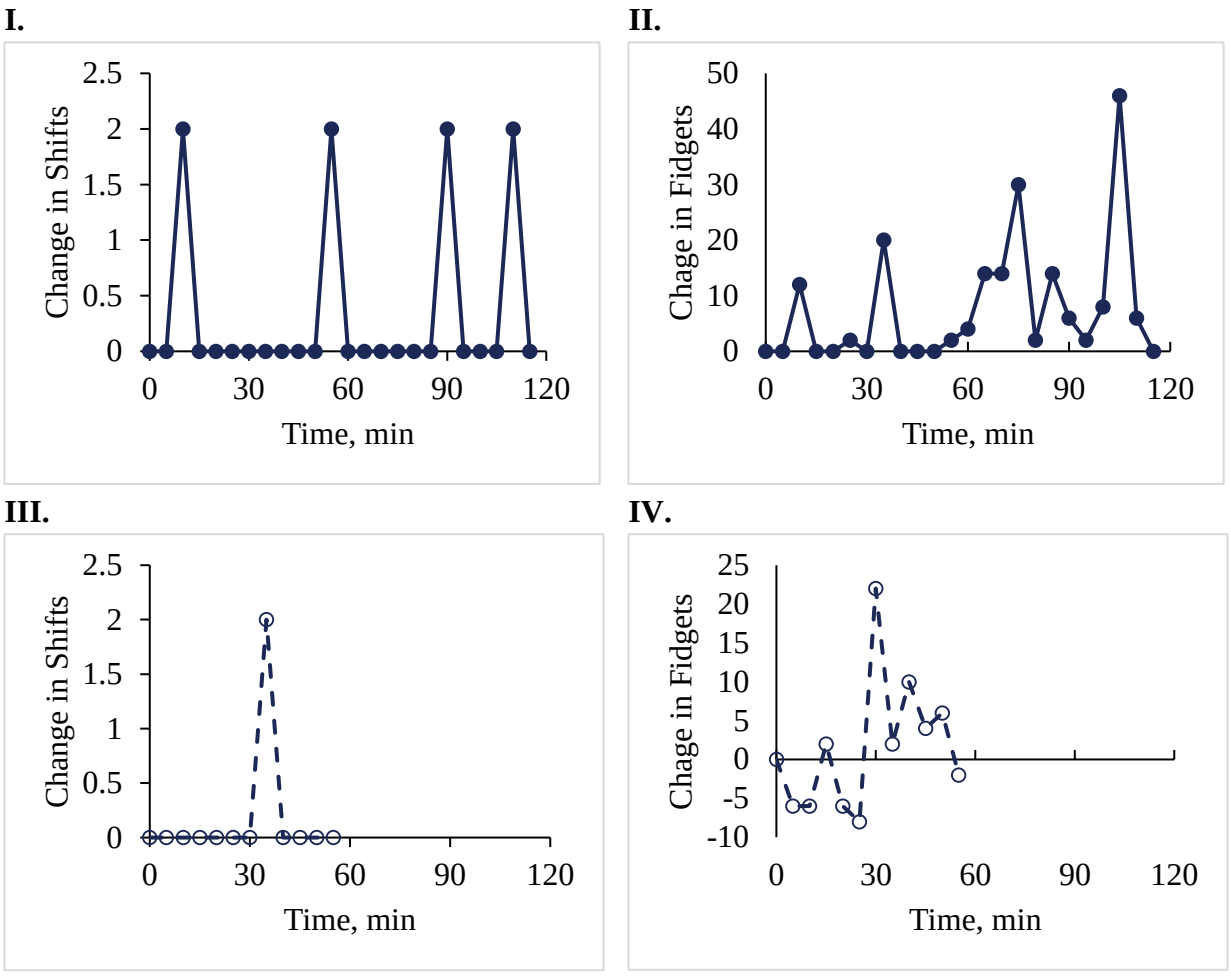

Figure 109: Subject S14 weight transfer events counted every five minutes during standing. I. Change in Shifts and II. Change in Fidgets on the HF condition. III. Change in Shifts and IV. Change in Fidgets on the MT condition.

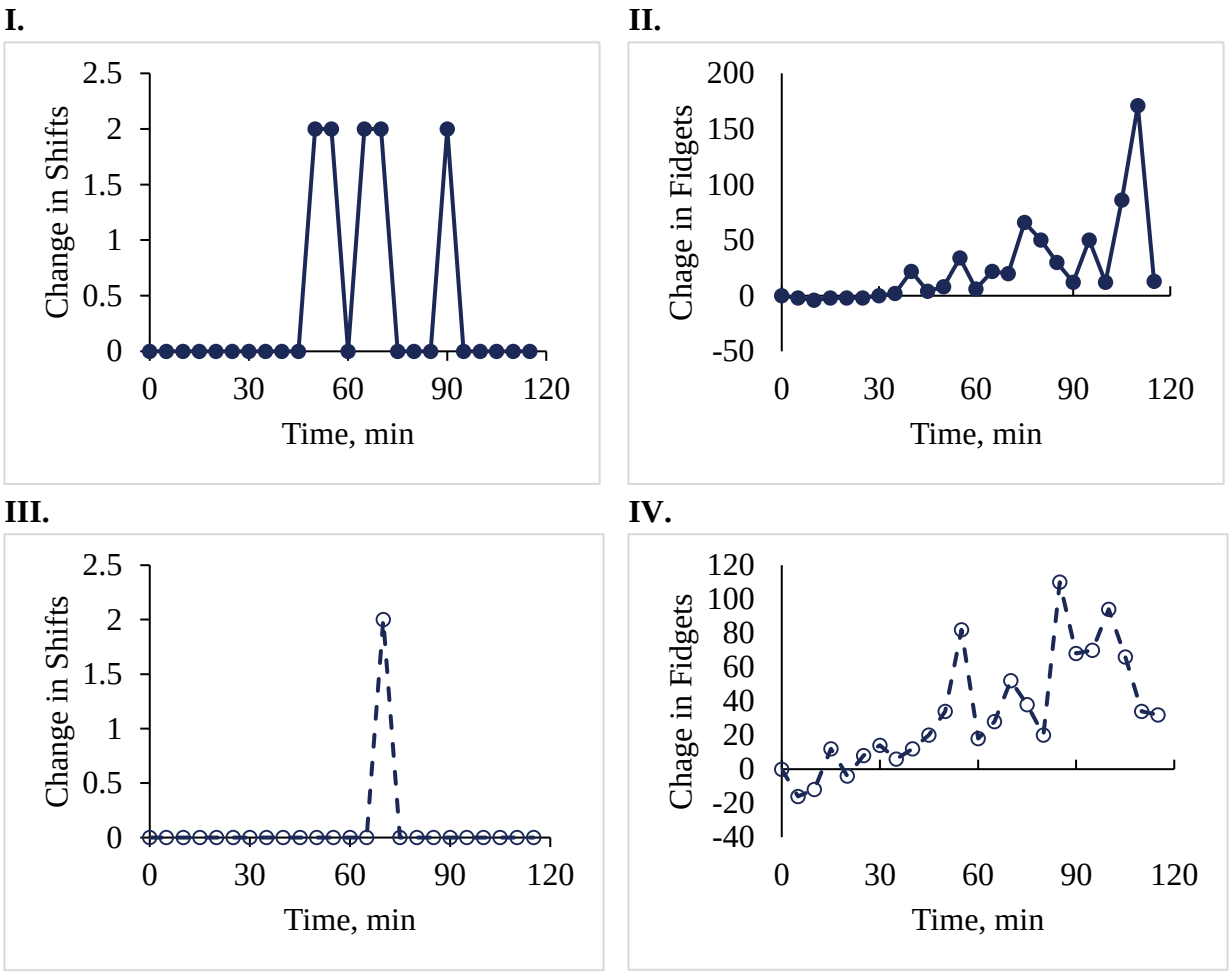

Figure 110: Subject S15 weight transfer events counted every five minutes during standing. I. Change in Shifts and II. Change in Fidgets on the HF condition. III. Change in Shifts and IV. Change in Fidgets on the MT condition.

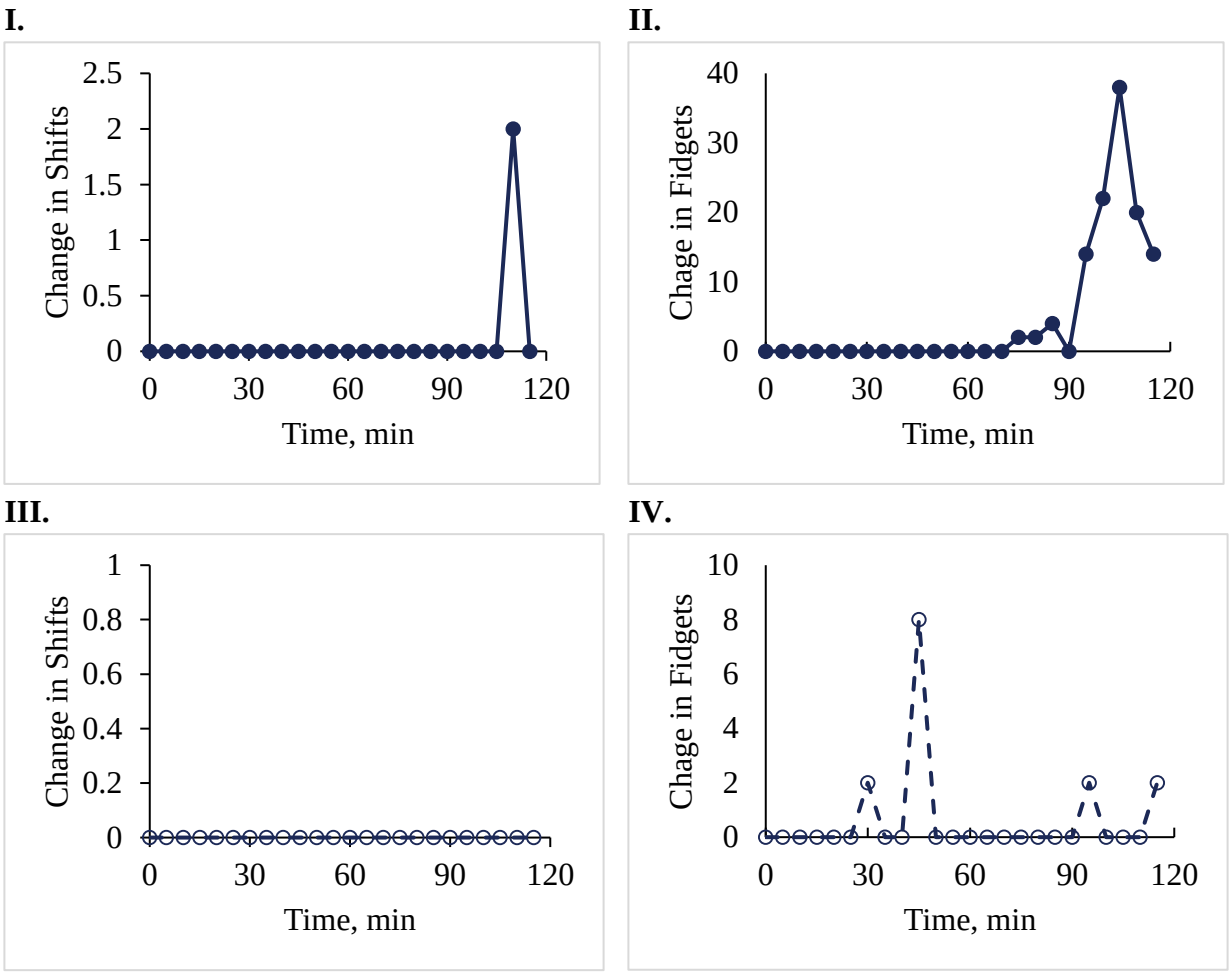

Figure 111: Subject S16 weight transfer events counted every five minutes during standing. I. Change in Shifts and II. Change in Fidgets on the HF condition. III. Change in Shifts and IV. Change in Fidgets on the MT condition.

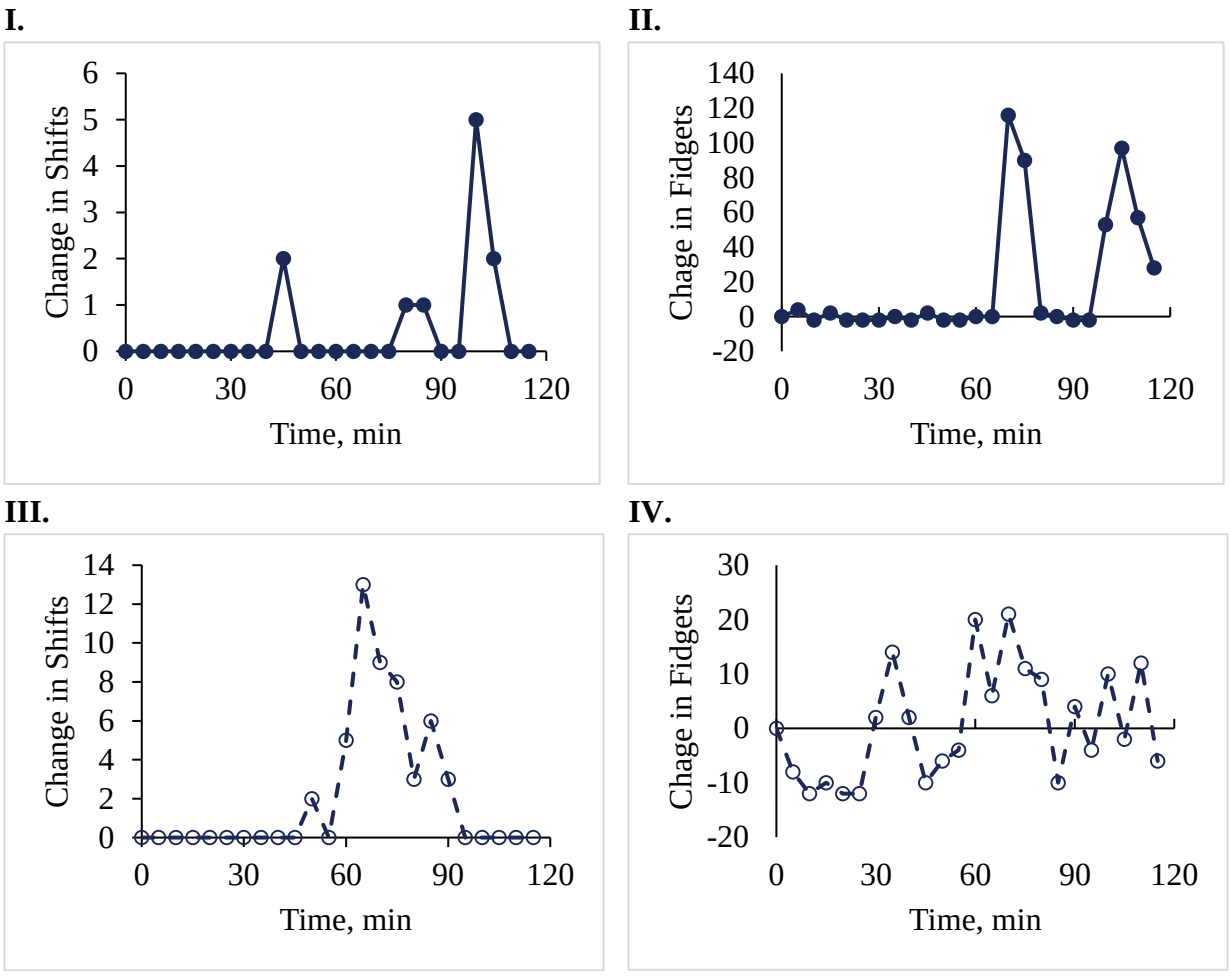

Figure 112: Subject S17 weight transfer events counted every five minutes during standing. I. Change in Shifts and II. Change in Fidgets on the HF condition. III. Change in Shifts and IV. Change in Fidgets on the MT condition.

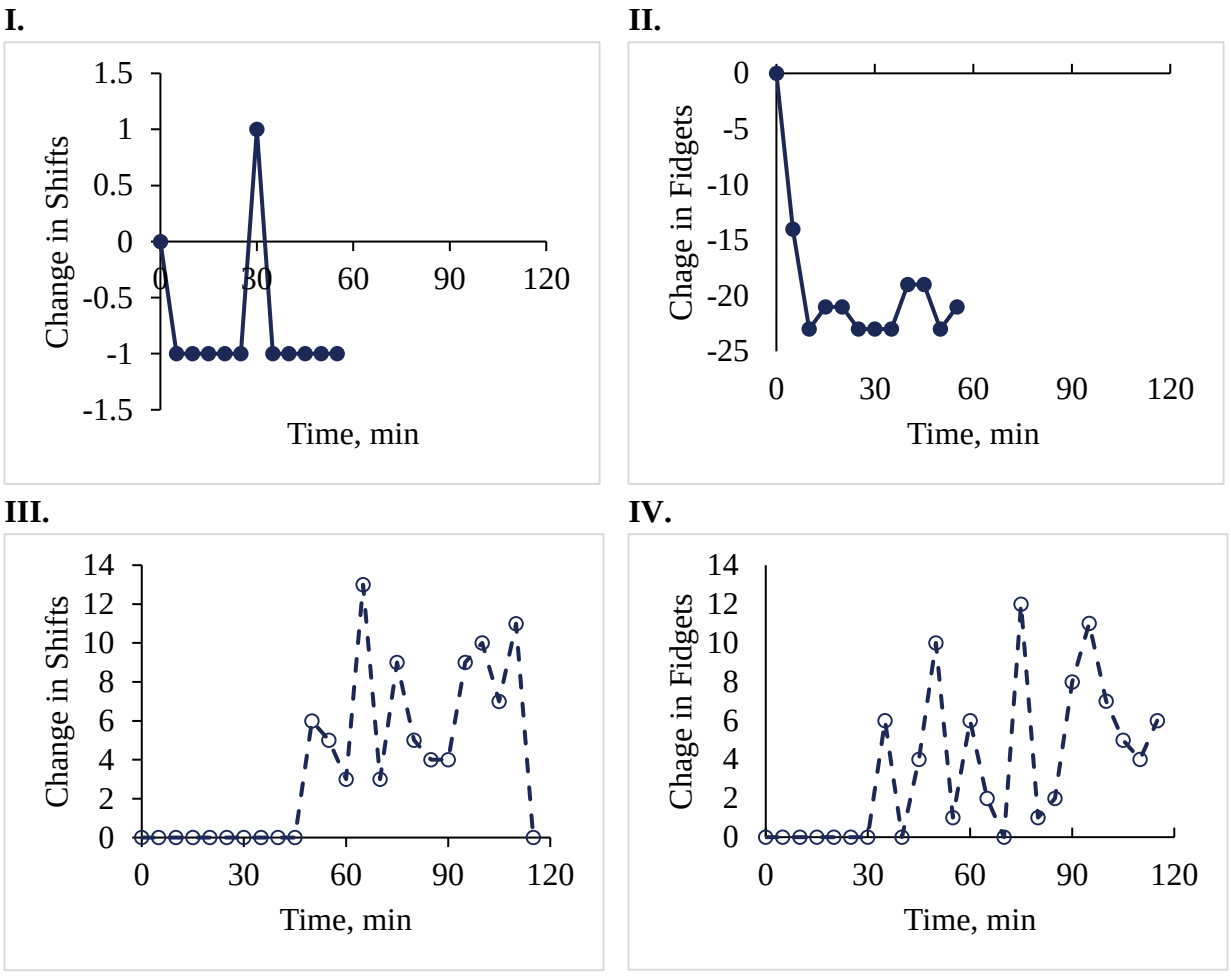

Figure 113: Subject S19 weight transfer events counted every five minutes during standing. I. Change in Shifts and II. Change in Fidgets on the HF condition. III. Change in Shifts and IV. Change in Fidgets on the MT condition.

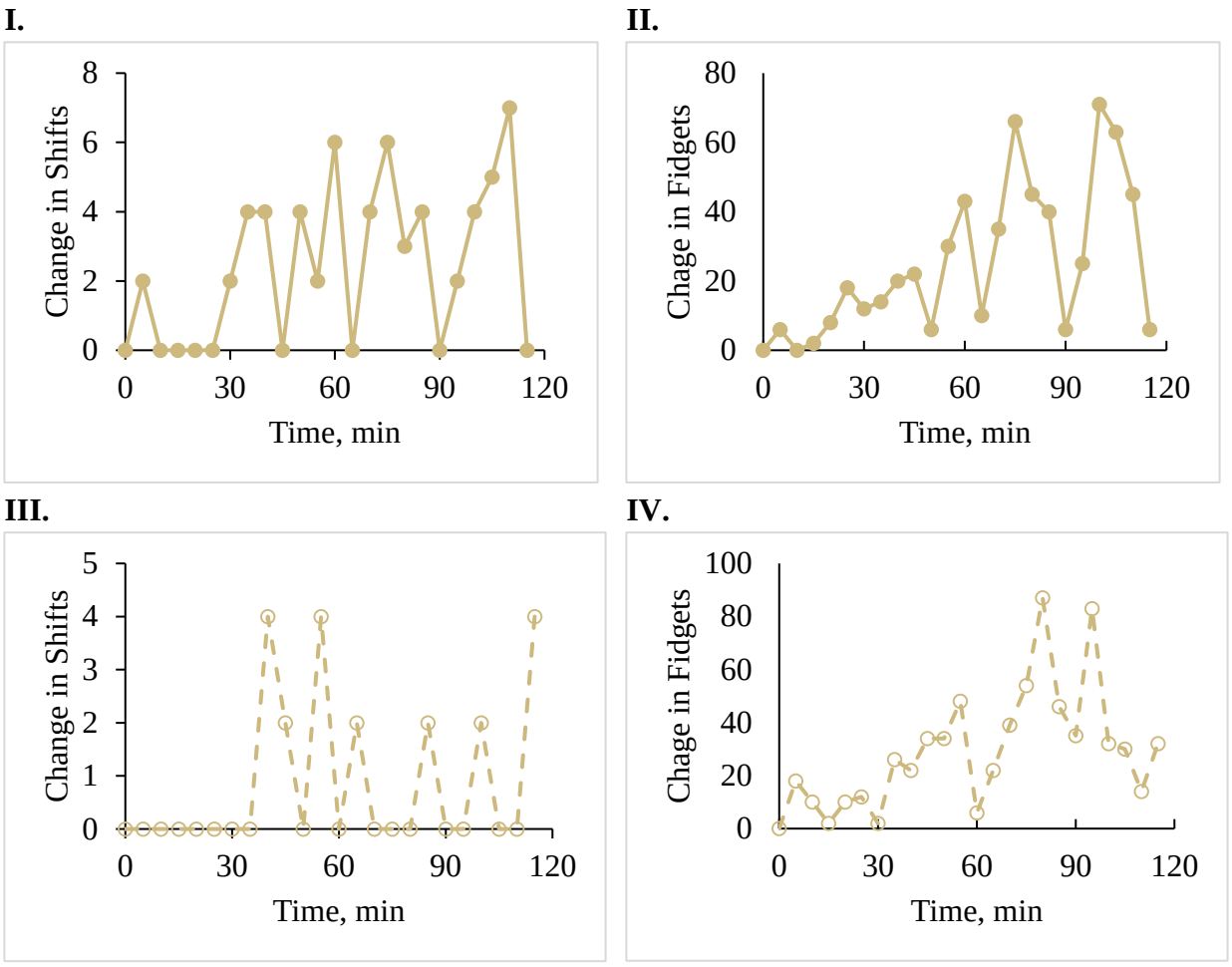

Figure 114: Subject S20 weight transfer events counted every five minutes during standing. I. Change in Shifts and II. Change in Fidgets on the HF condition. III. Change in Shifts and IV. Change in Fidgets on the MT condition.

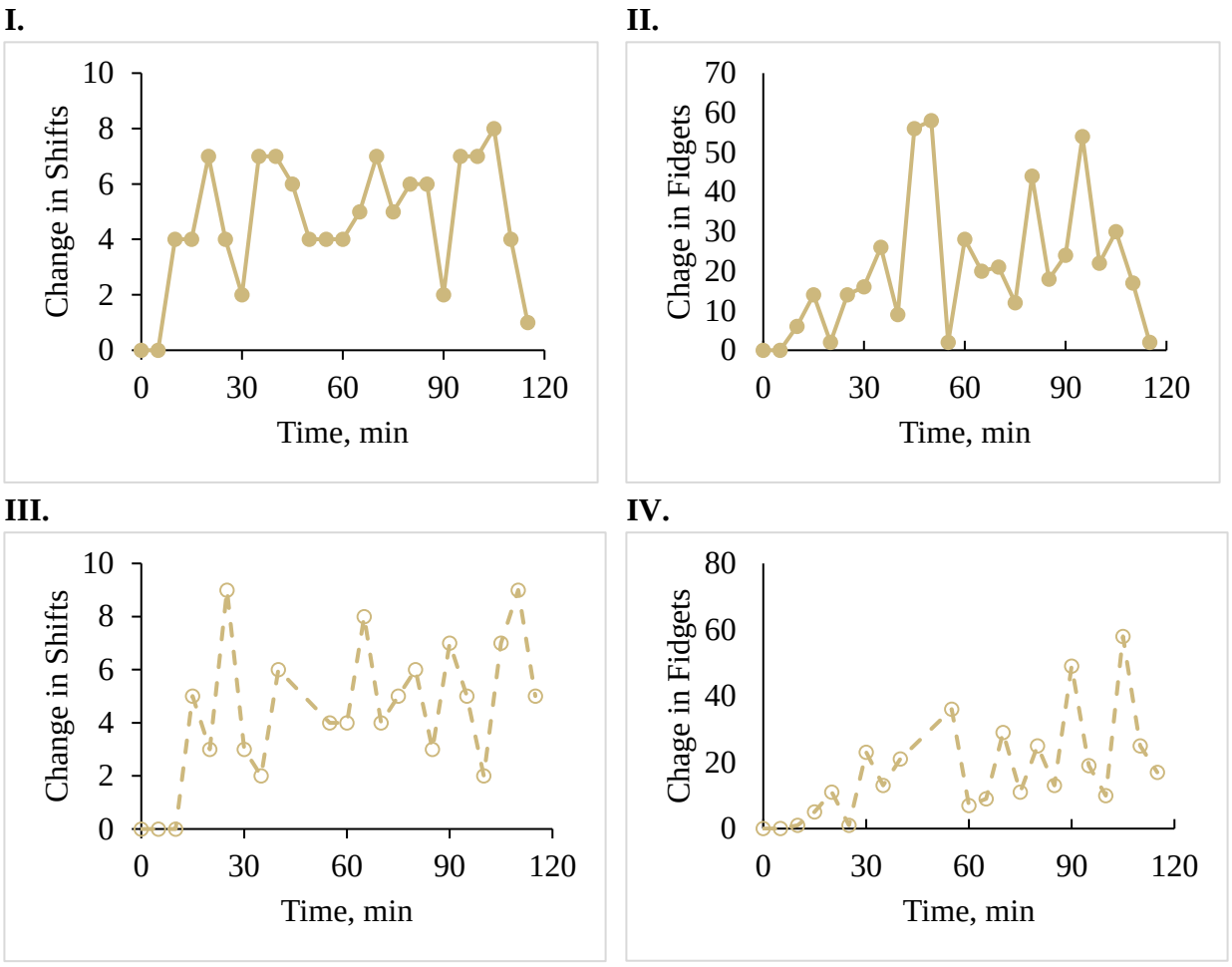

Figure 115: Subject S21 weight transfer events counted every five minutes during standing. I. Change in Shifts and II. Change in Fidgets on the HF condition. III. Change in Shifts and IV. Change in Fidgets on the MT condition.

I. **II.**

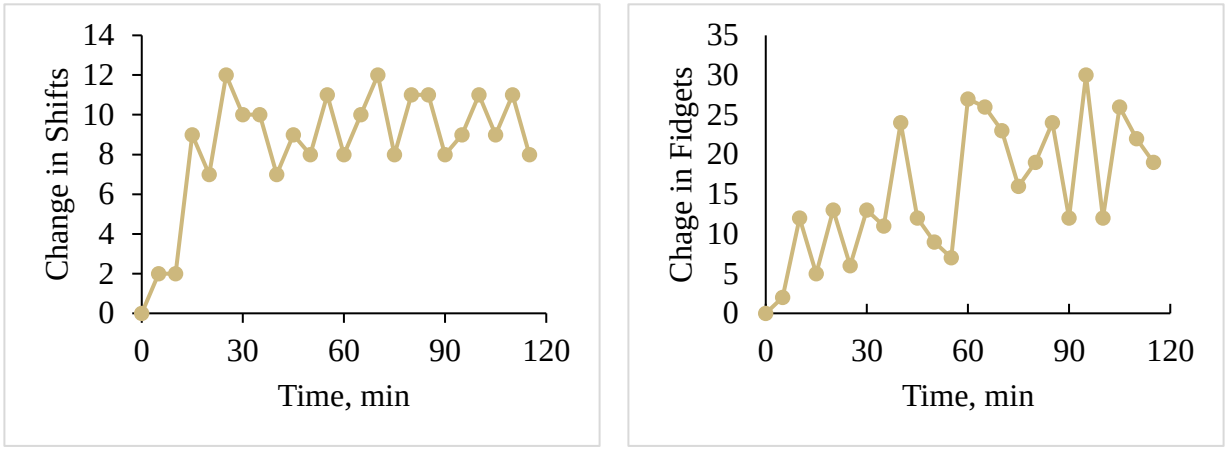

Figure 116: Subject S22 weight transfer events counted every five minutes during standing. I. Change in Shifts and II. Change in Fidgets on the HF condition. Data for the MT condition was not included in analyses.

I. **II.**

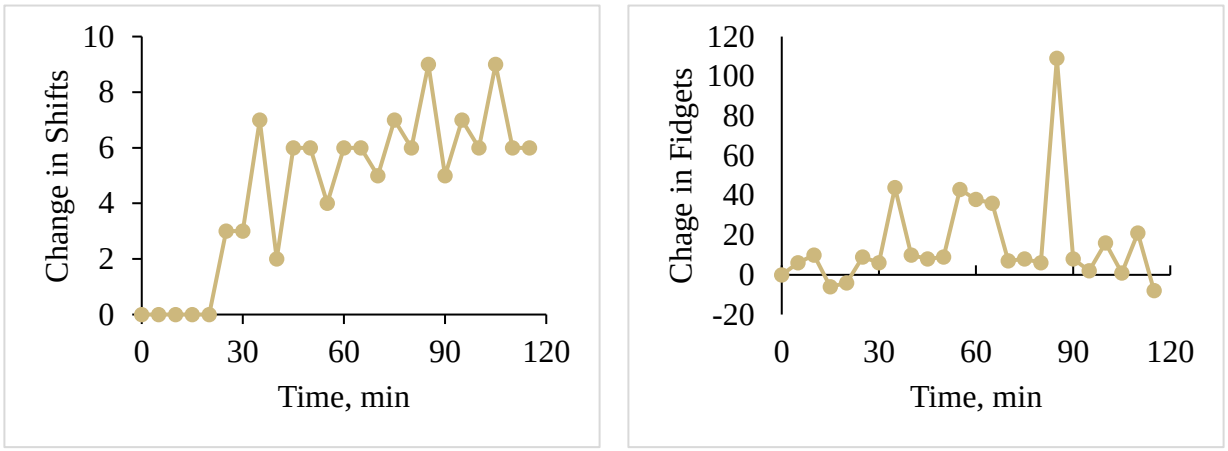

Figure 117: Subject S23 weight transfer events counted every five minutes during standing. I. Change in Shifts and II. Change in Fidgets on the HF condition. III. Data for the MT condition was not included in analyses.

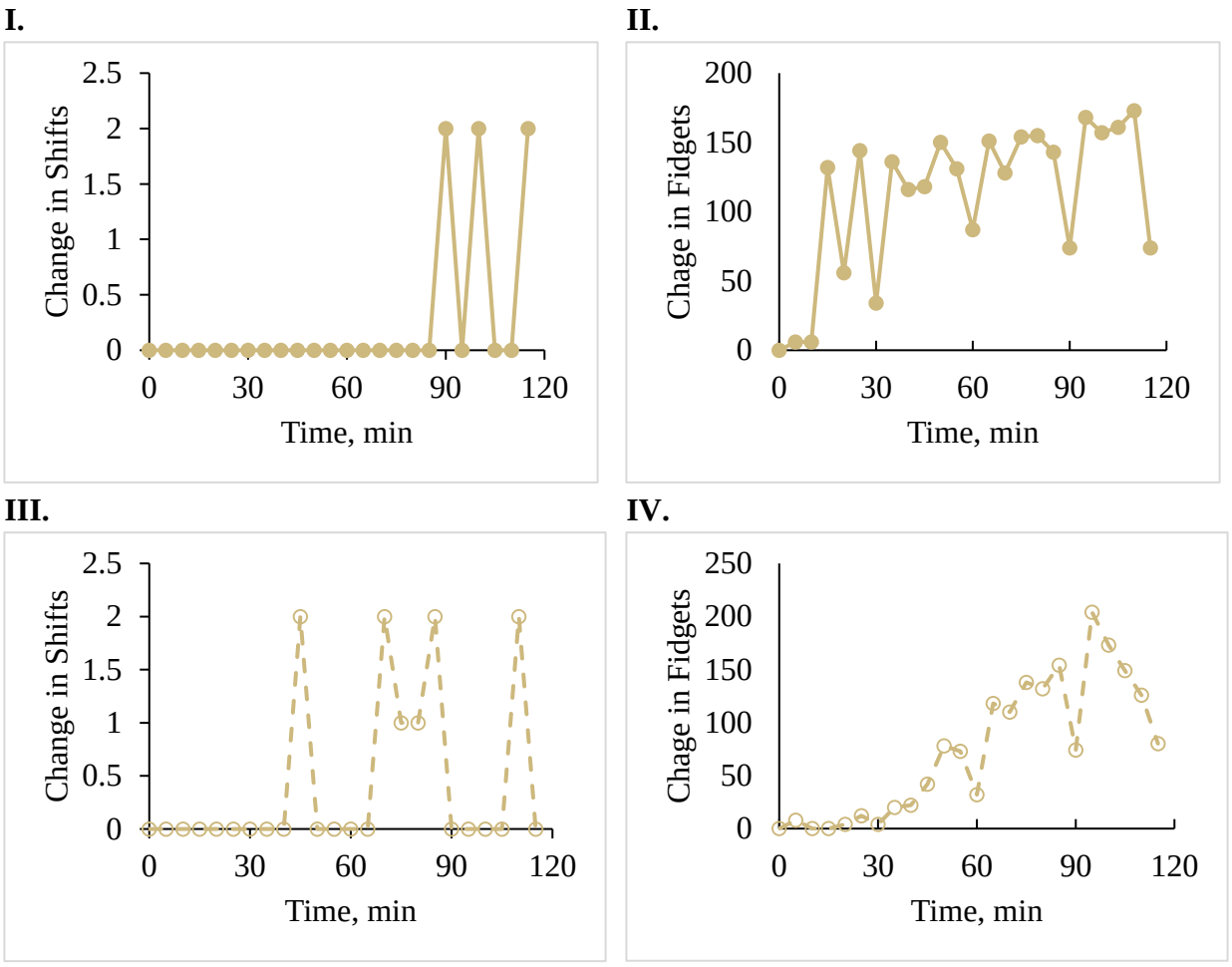

Figure 118: Subject S24 weight transfer events counted every five minutes during standing. I. Change in Shifts and II. Change in Fidgets on the HF condition. III. Change in Shifts and IV. Change in Fidgets on the MT condition.

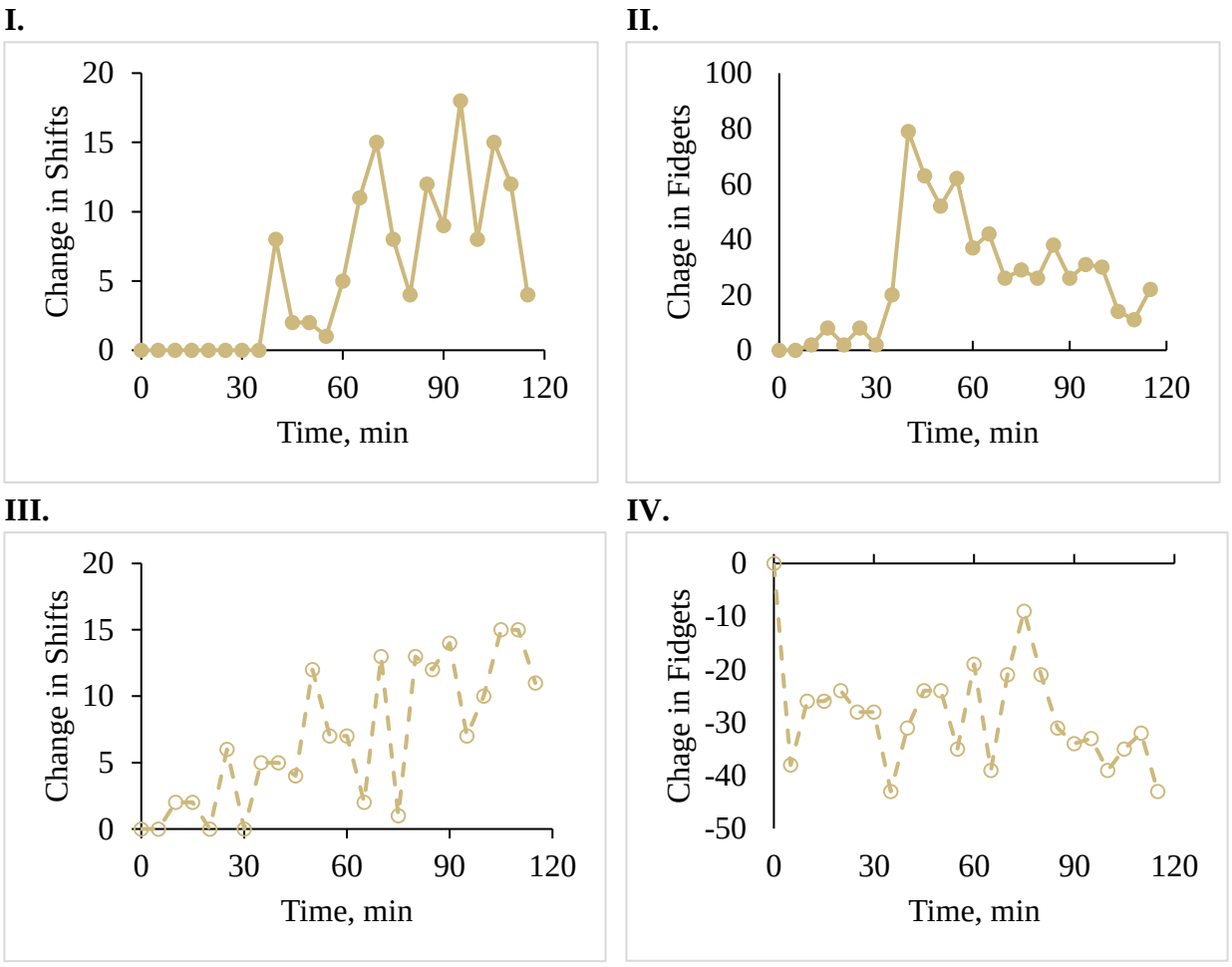

Figure 119: Subject S25 weight transfer events counted every five minutes during standing. I. Change in Shifts and II. Change in Fidgets on the HF condition. III. Change in Shifts and IV. Change in Fidgets on the MT condition.

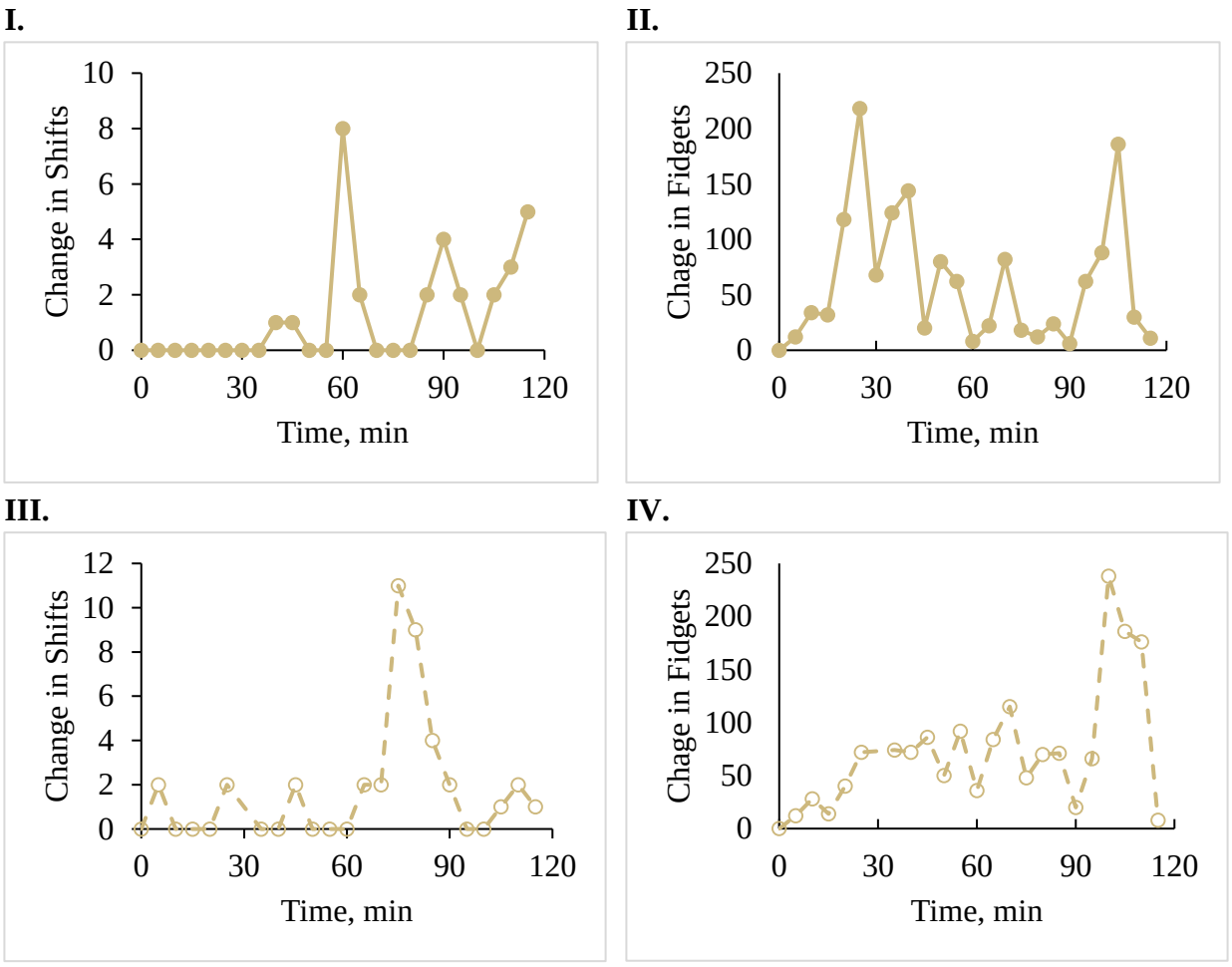

Figure 120: Subject S26 weight transfer events counted every five minutes during standing. I. Change in Shifts and II. Change in Fidgets on the HF condition. III. Change in Shifts and IV. Change in Fidgets on the MT condition.

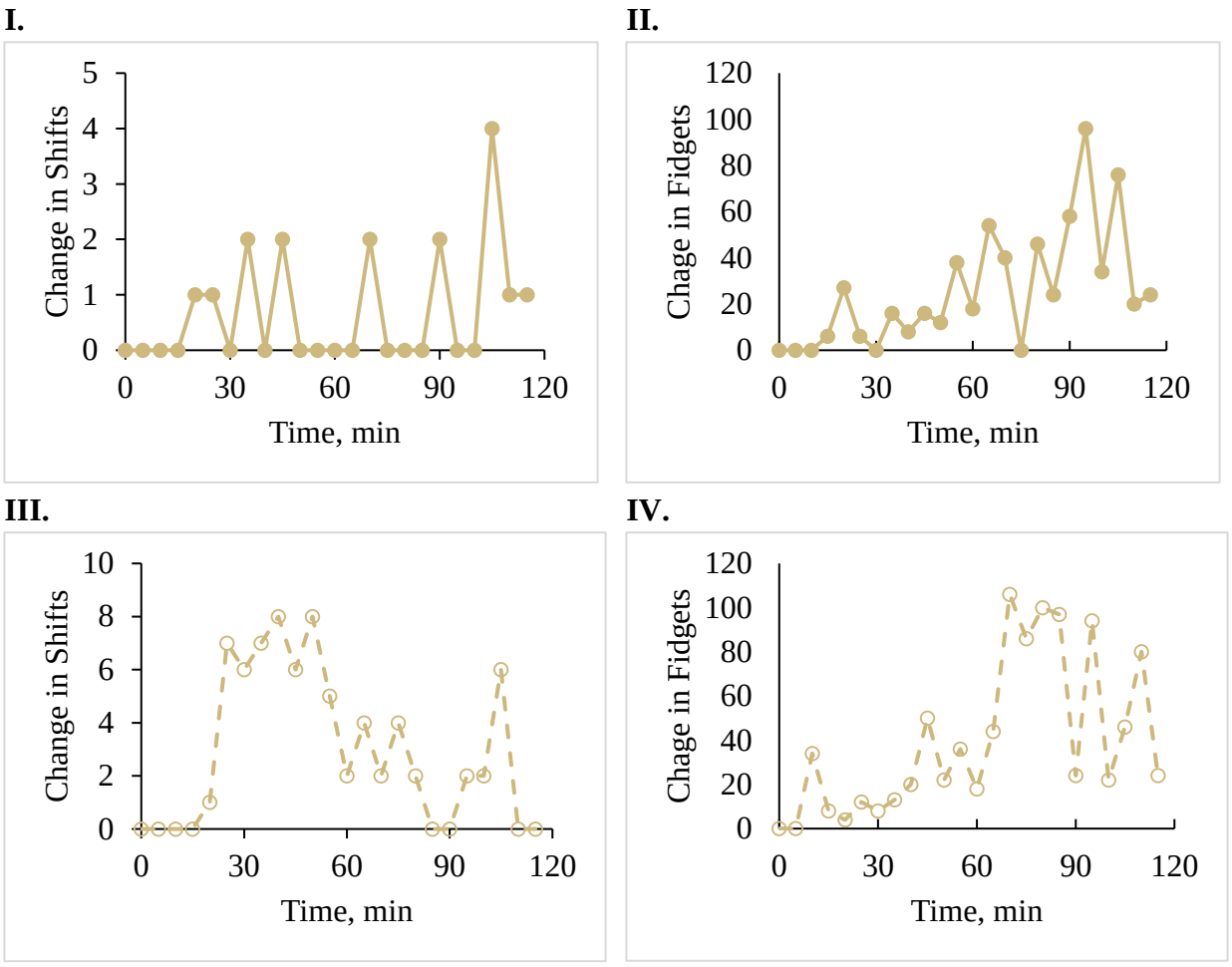

Figure 121: Subject S27 weight transfer events counted every five minutes during standing. I. Change in Shifts and II. Change in Fidgets on the HF condition. III. Change in Shifts and IV. Change in Fidgets on the MT condition.

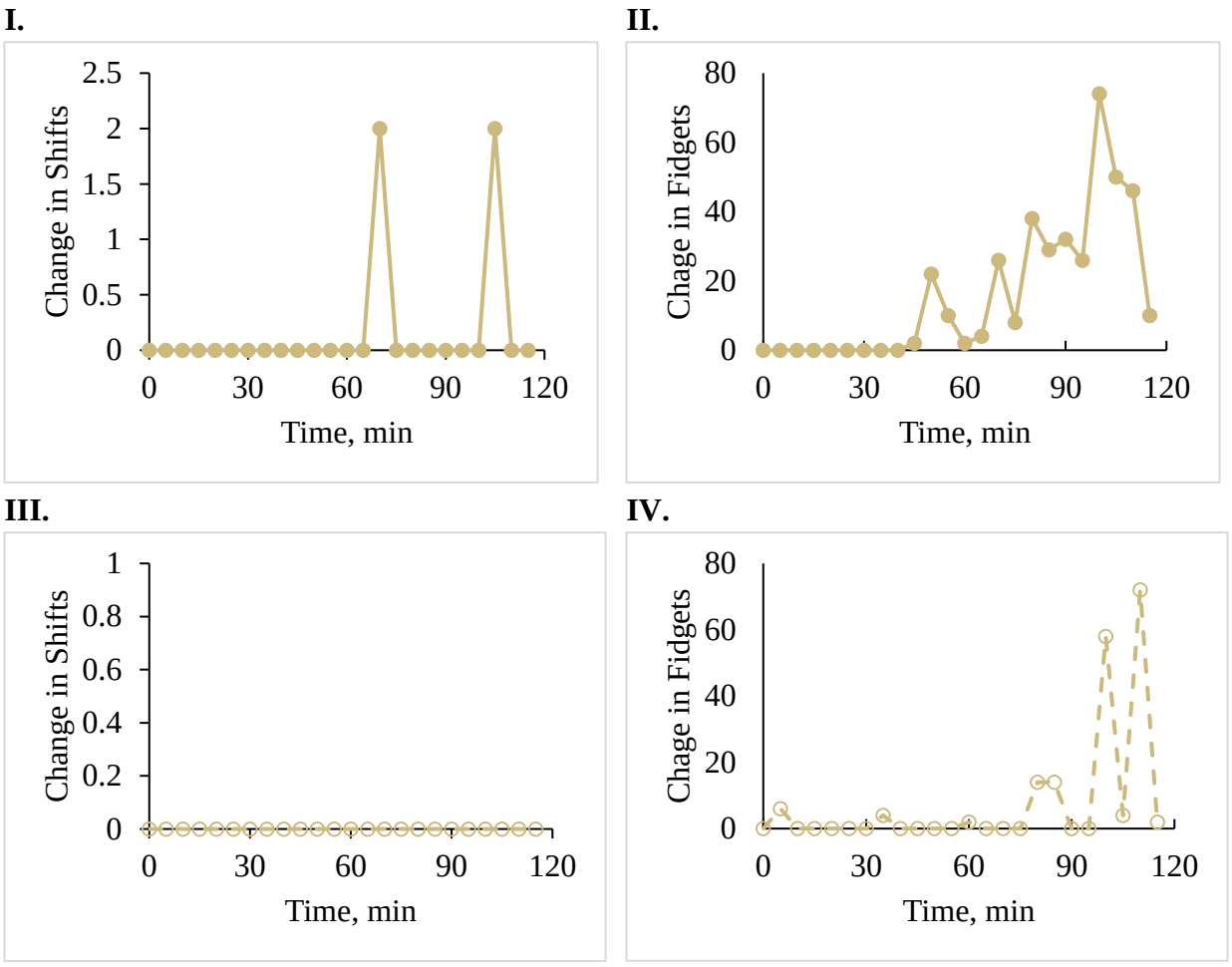

Figure 122: Subject S28 weight transfer events counted every five minutes during standing. I. Change in Shifts and II. Change in Fidgets on the HF condition. III. Change in Shifts and IV. Change in Fidgets on the MT condition.

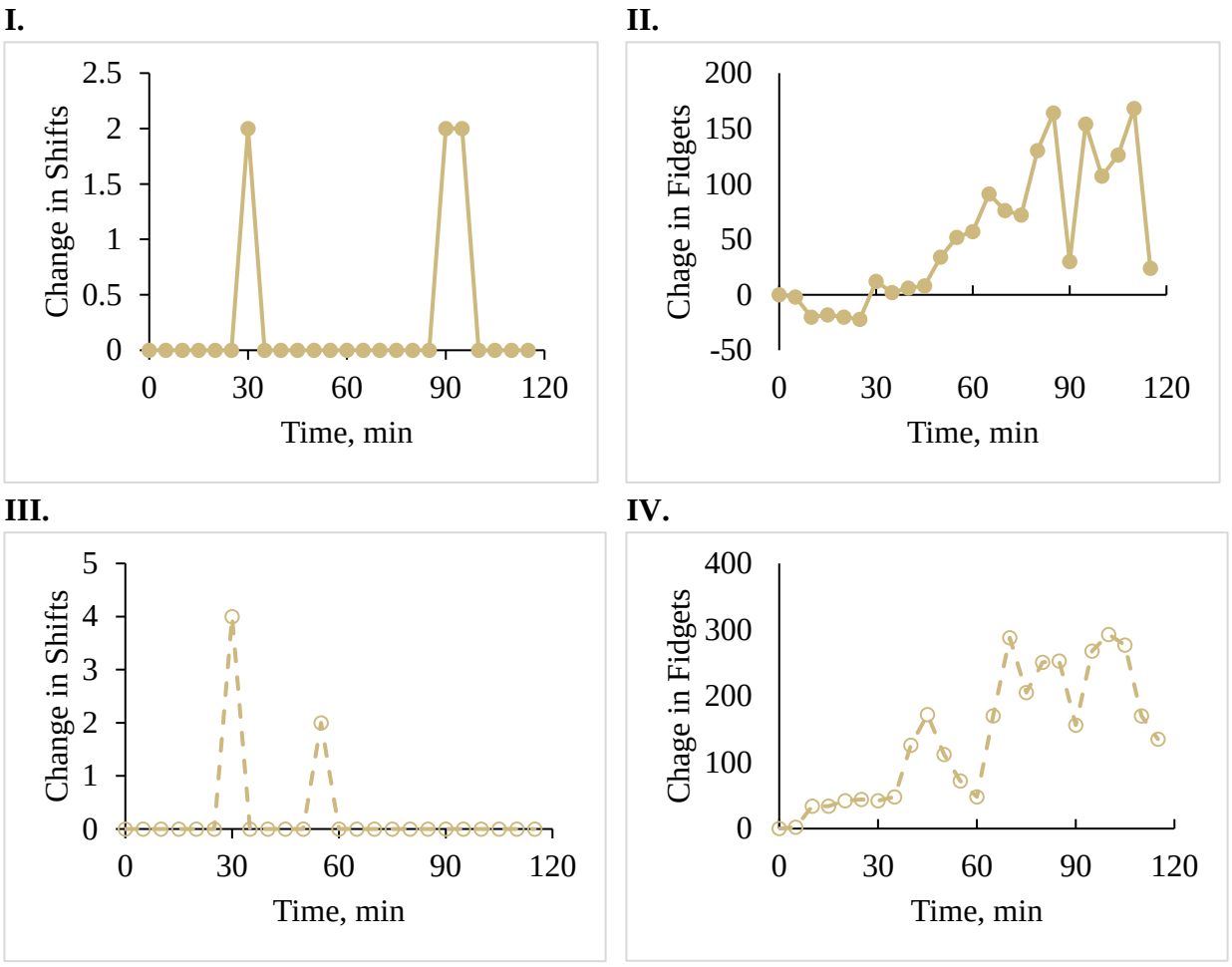

Figure 123: Subject S29 weight transfer events counted every five minutes during standing. I. Change in Shifts and II. Change in Fidgets on the HF condition. III. Change in Shifts and IV. Change in Fidgets on the MT condition.

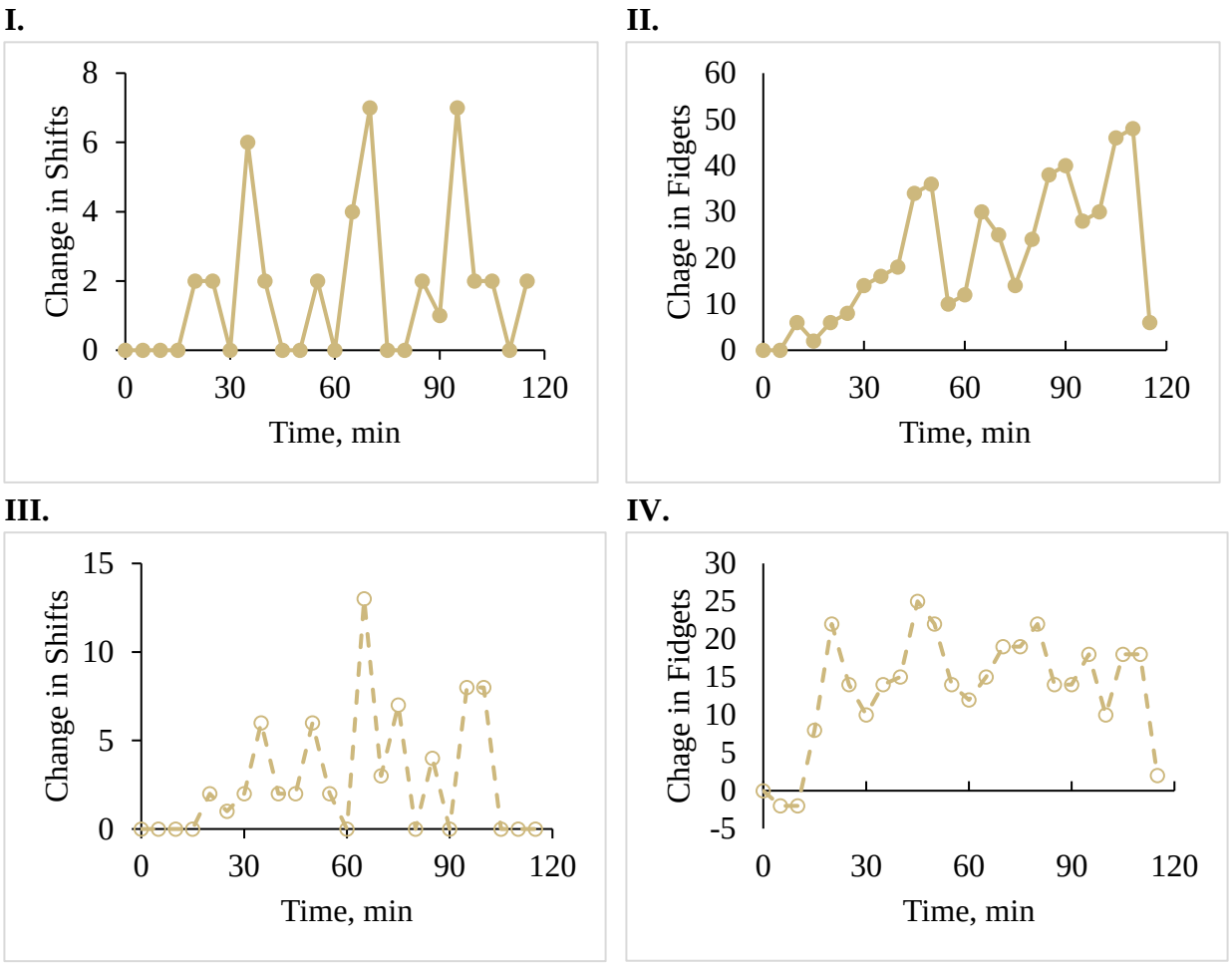

Figure 124: Subject S31 weight transfer events counted every five minutes during standing. I. Change in Shifts and II. Change in Fidgets on the HF condition. III. Change in Shifts and IV. Change in Fidgets on the MT condition.

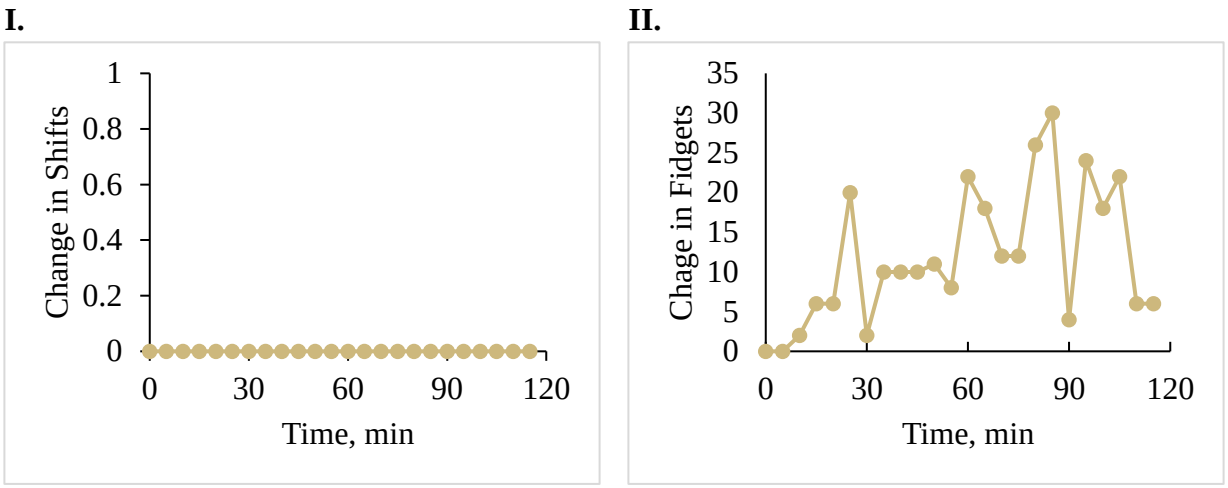

Figure 125: Subject S32 weight transfer events counted every five minutes during standing. I. Change in Shifts and II. Change in Fidgets on the HF condition. Data for the MT condition was not included in analyses.

Instead of analyzing ratios of raw numbers of shift and fidgets, the following steps were followed:

1. Total number of shifts and fidgets performed by each subject were calculated for each visit separately.
2. Total shifts and fidgets for each visit were ranked in ascending order. A rank of 1 was assigned to the visit with the least number of shifts or fidgets. The highest rank was assigned to the visit with the most shifts or fidgets. If visits displayed the same number of shifts and fidgets, they were assigned the same number.
3. A ratio of ranks was calculated (Equation B-3).
4. Visits were split into three groups, displayed in Equation B-4. Primary fidgeters were the first group (G=1), primary shifters were the third group (G=3), and mixed method were the second group (G=2).

$$RankRatio = \frac{Rank(Shifts)}{Rank(Fidgets)} \quad \textbf{(B-3)}$$

$$\begin{cases} G = 1 & 0 < RankRatio \leq 0.33 \\ G = 2 & 0.33 < RankRatio \leq 0.66 \\ G = 3 & 0.66 < RankRatio \leq 1 \end{cases} \quad \textbf{(B-4)}$$

Table 30 - Table 32 display total shifts, fidgets, rank, and RankRatio data for each subject and each visit. A two-way ANOVA was performed to determine if RankRatio changed significantly with flooring condition or BMI group. No statistically significant differences were found. Therefore, it is likely that each subject's tendency to perform shifts or fidgets is likely unaffected by the flooring condition or BMI.

Figure 126, I displays the number of shifts performed by each standing strategy group. Figure 126, II displays the number of fidgets performed by each standing strategy group. The mixed method and primary shifter groups are more similar than the primary fidgeter group. Figure 127 displays the number of fidgets versus shifts performed by each subject, during each visit, every five minutes. This plot also indicates that mixed method and primary shifter groups are more similar than the primary fidgeter group.

Based on these results, it is likely that subjects may perform different movements during prolonged standing. These different movements may be subject specific. However, this research was not designed to investigate this hypothesis. A larger cohort of subjects is required to statistically determine if subject specific standing strategy usage during prolonged standing occurs.

Table 30: Subjects included in Group 1. These subjects were ranked higher based on total fidgets displayed during standing, and lower based on total shifts displayed during standing. RankRatio was calculated using Equation B-3.

Subject	Flooring	BMI	Shifts	Rank(Shifts)	Fidgets	Rank(Fidgets)	RankRatio
S10	MT	HW	0	1	5875	50	0.01961
S12	HF	HW	0	2	1116	39	0.04878
S12	MT	HW	0	3	1820	45	0.0625
S15	MT	HW	2	10	1170	40	0.2
S24	HF	OB	6	14	2655	47	0.22951
S29	MT	OB	6	15	3260	48	0.2381
S32	HF	OB	0	4	288	14	0.22222
S29	HF	OB	6	16	1781	44	0.26667
S10	HF	HW	10	21	4815	49	0.3
S13	MT	HW	6	17	784	36	0.32075

Table 31: Subjects included in Group 2. These subjects were ranked similarly based on total fidgets displayed during standing and total shifts displayed during standing. RankRatio was calculated using Equation B-3.

Subject	Flooring	BMI	Shifts	Rank(Shifts)	Fidgets	Rank(Fidgets)	RankRatio
S24	MT	OB	10	22	1764	43	0.338
S28	MT	OB	0	5	176	11	0.312
S28	HF	OB	4	12	380	21	0.363
S26	HF	OB	30	28	1845	46	0.378
S15	HF	HW	10	23	696	32	0.418
S26	MT	OB	43	31	1725	42	0.424
S04	MT	HW	0	6	84	5	0.545
S20	MT	OB	20	27	702	33	0.45
S27	HF	OB	16	26	620	30	0.464
S32	MT	OB	4	13	301	15	0.464
S17	HF	HW	11	24	481	25	0.489
S27	MT	OB	72	38	949	37	0.506
S11	HF	HW	100	41	1033	38	0.518
S04	HF	HW	8	19	322	17	0.527
S31	HF	OB	41	30	495	26	0.535
S11	MT	HW	149	48	1488	41	0.539
S20	HF	OB	59	34	593	29	0.539
S23	MT	OB	106	42	780	35	0.545
S03	MT	HW	111	45	753	34	0.569
S01	HF	HW	6	18	182	12	0.6
S25	HF	OB	134	47	631	31	0.602
S16	HF	HW	2	11	116	7	0.611
S23	HF	OB	109	44	572	28	0.611
S13	HF	HW	63	35	381	22	0.614
S21	HF	OB	111	46	495	27	0.630
S21	MT	OB	107	43	460	23	0.651

Table 32: Subjects included in Group 2. These subjects were ranked lower based on total fidgets displayed during standing, and higher based on total shifts displayed during standing. RankRatio was calculated using Equation B-3.

Subject	Flooring	BMI	Shifts	Rank(Shifts)	Fidgets	Rank(Fidgets)	RankRatio
S17	MT	HW	49	32	303	16	0.666
S31	MT	OB	67	36	371	18	0.666
S25	MT	OB	163	49	471	24	0.671
S03	HF	HW	86	39	374	19	0.672
S02	MT	HW	8	20	144	9	0.689
S22	HF	OB	203	50	375	20	0.714
S16	MT	HW	0	7	14	3	0.7
S05	MT	HW	67	37	187	13	0.74
S05	HF	HW	50	33	158	10	0.767
S06	MT	HW	0	8	6	2	0.8
S07	HF	HW	37	29	139	8	0.783
S07	MT	HW	14	25	36	4	0.862
S19	MT	HW	89	40	85	6	0.869
S06	HF	HW	0	9	4	1	0.9

I.

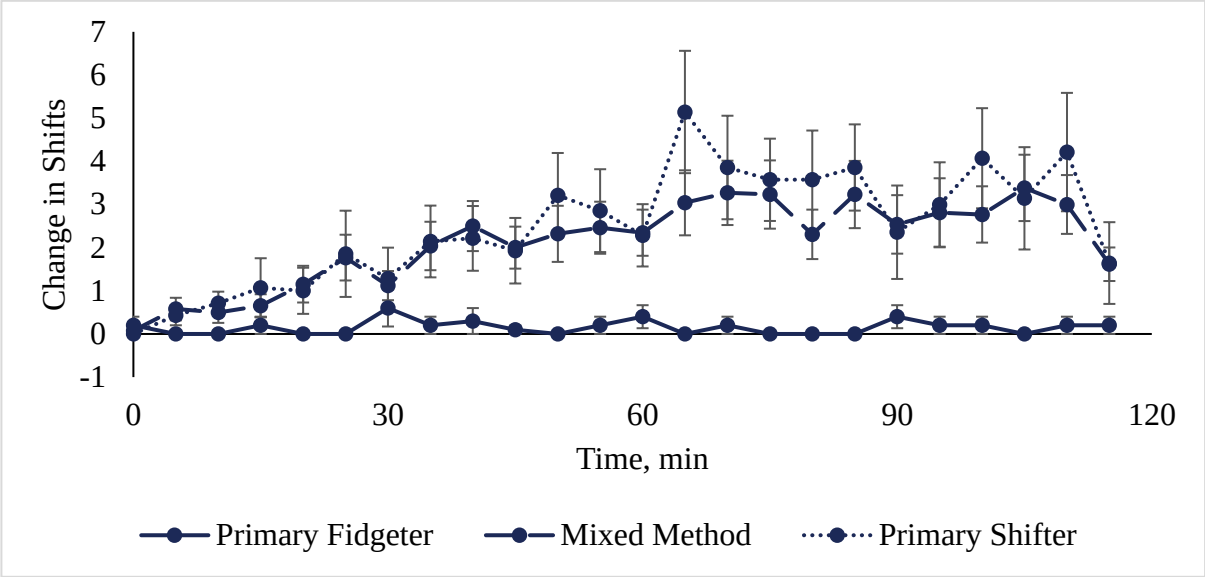

II.

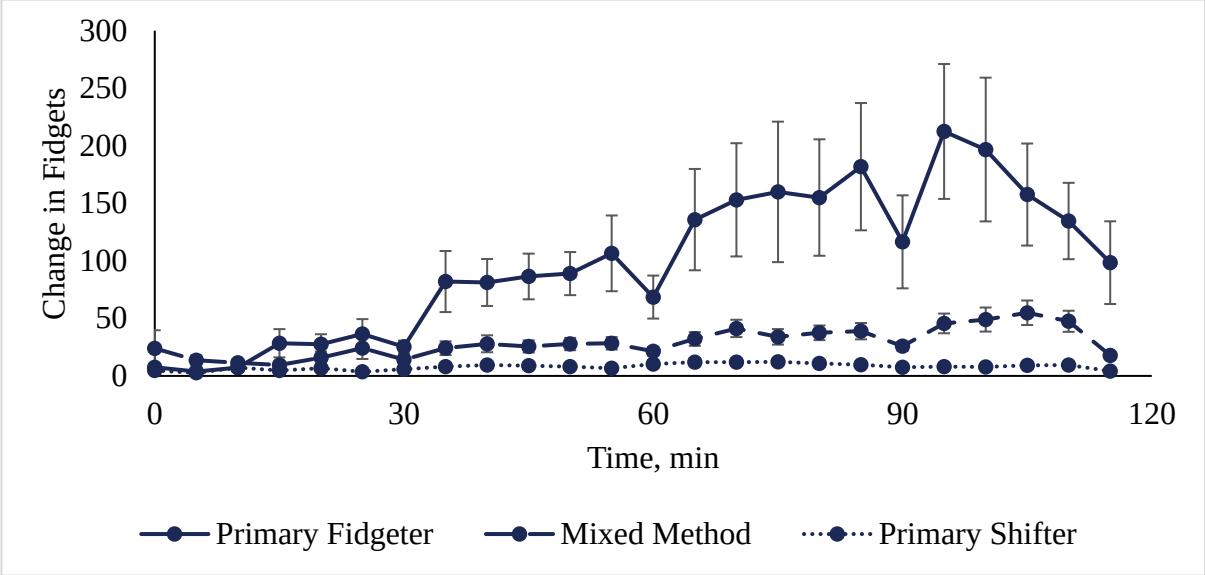

Figure 126: Average change in shifts (I) and change in fidgets (II) split into strategy groups. Error bars are standard error of the mean.

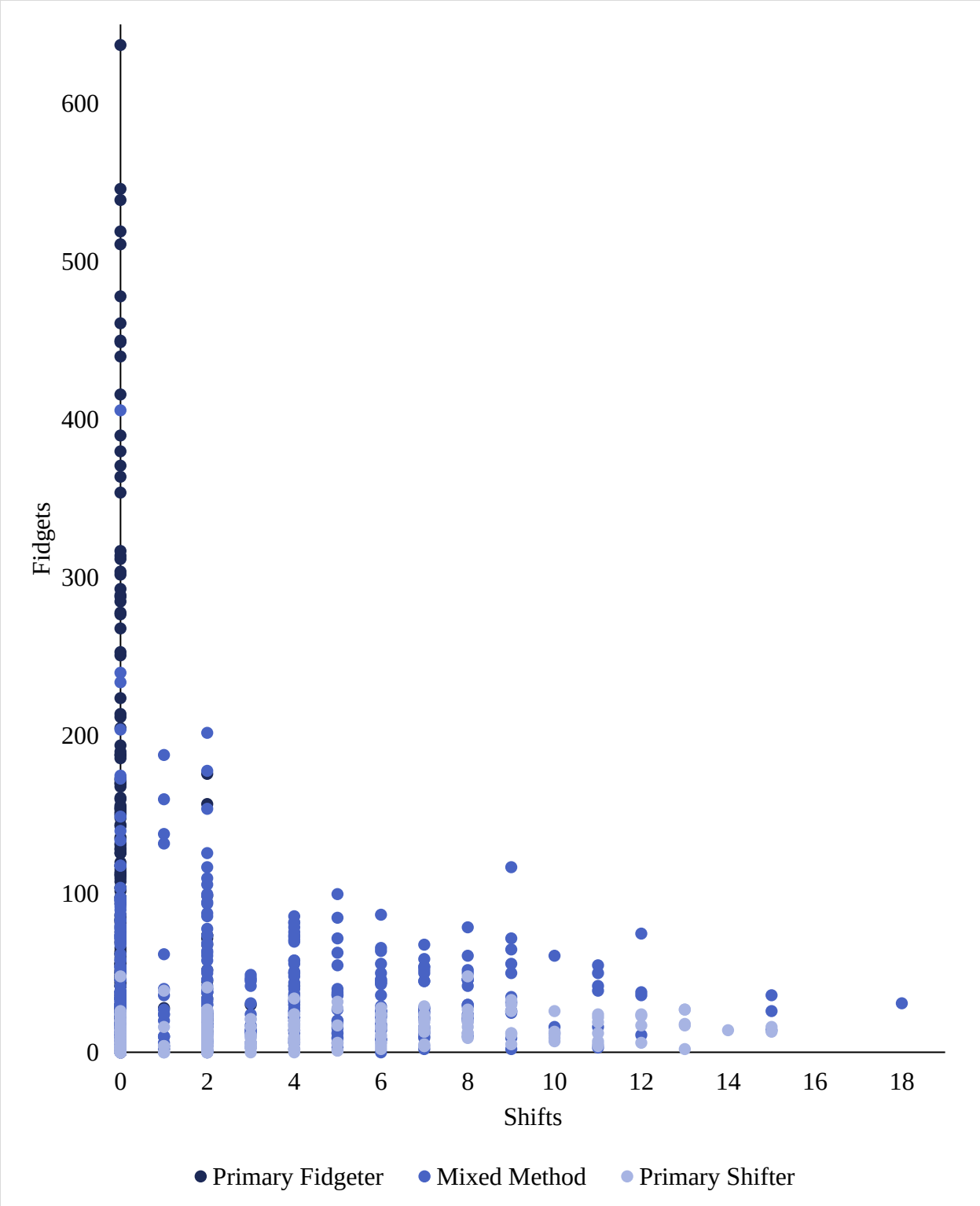

Figure 127: Scatter plot of fidgets versus shifts every five minutes for all subjects and visits.

Appendix C Knee Joint Measures

This section includes two subsections. The first section contains graphs of all subject MTFG versus kinematics data. This data was used to perform correlation analyses, reported in Table 14. The first section also contains graphs of raw MTFG over time for all subjects. If a converging piecewise model occurred, the result of the model are also plotted with raw MTFG data. Details of this piecewise model are introduced in section 3.4.3 and detailed in section 4.3.3. The original protocol for this study required standing for four hours rather than two hours. For the seven subjects that completed the four hour protocol, the piecewise model was performed on the first two hours of standing as well as the full four hours of standing. The second section of Appendix C contains tables comparing differences in model output between these sets of data.

Appendix C.1 MTFG and Kinematics Data

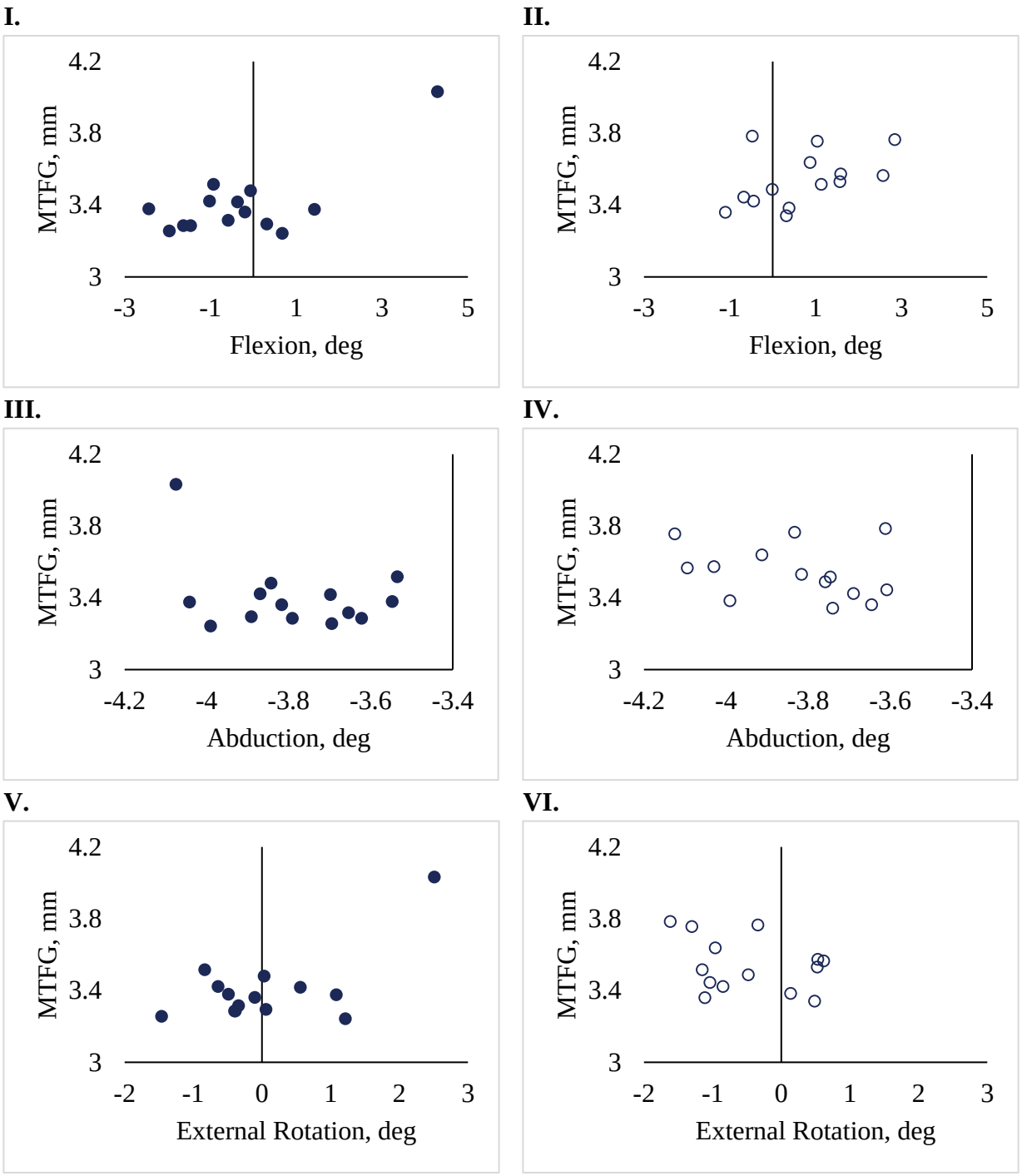

Figure 128: Subject S01 MTFG and kinematics data for all collected trials. On the HF condition: Flexion (I), Abduction (III), and External Rotation (V). On the MT condition: Flexion (II), Abduction (IV), and External Rotation (VI).

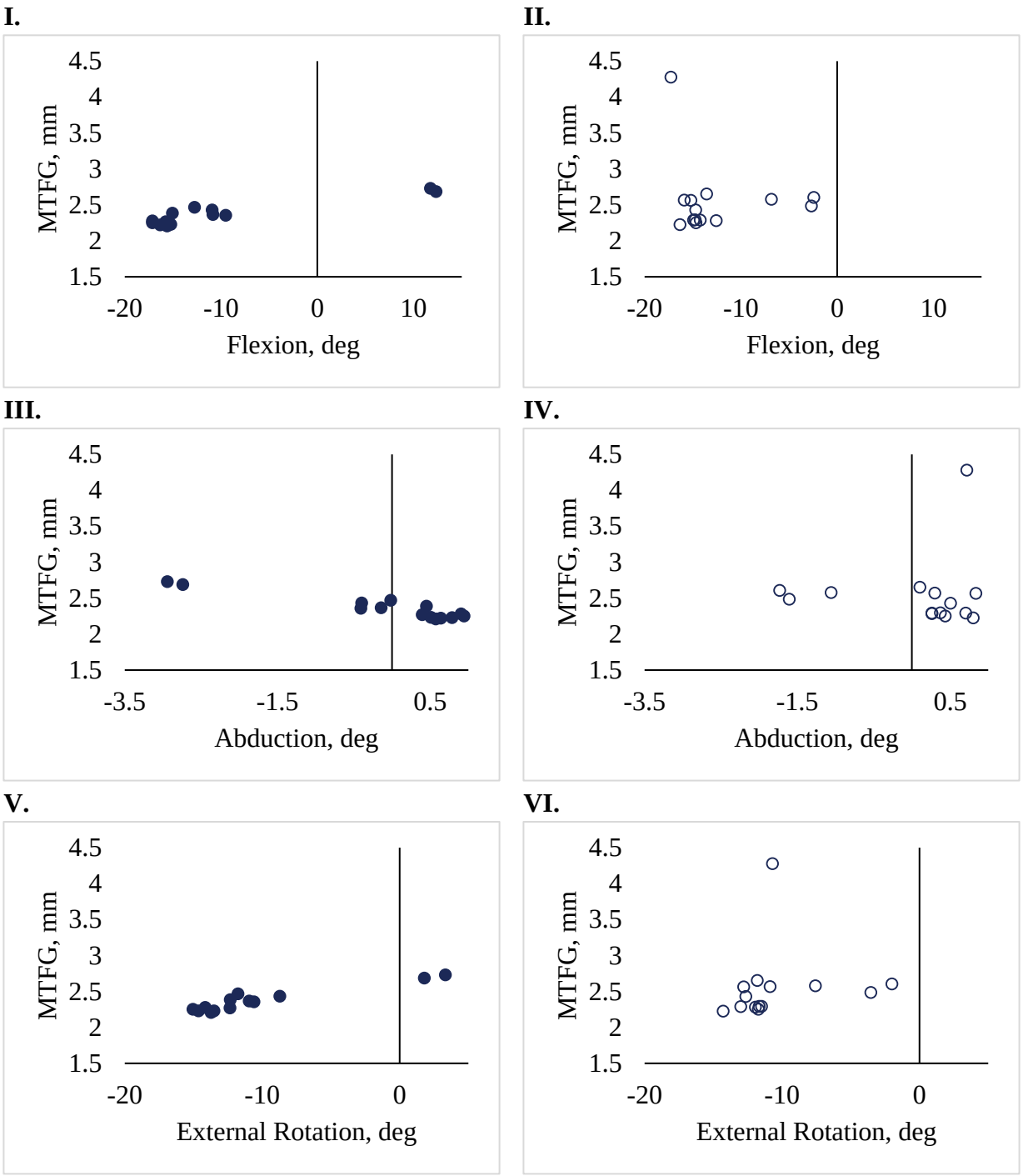

Figure 129: Subject S03 MTFG and kinematics data for all collected trials. On the HF condition: Flexion (I), Abduction (III), and External Rotation (V). On the MT condition: Flexion (II), Abduction (IV), and External Rotation (VI).

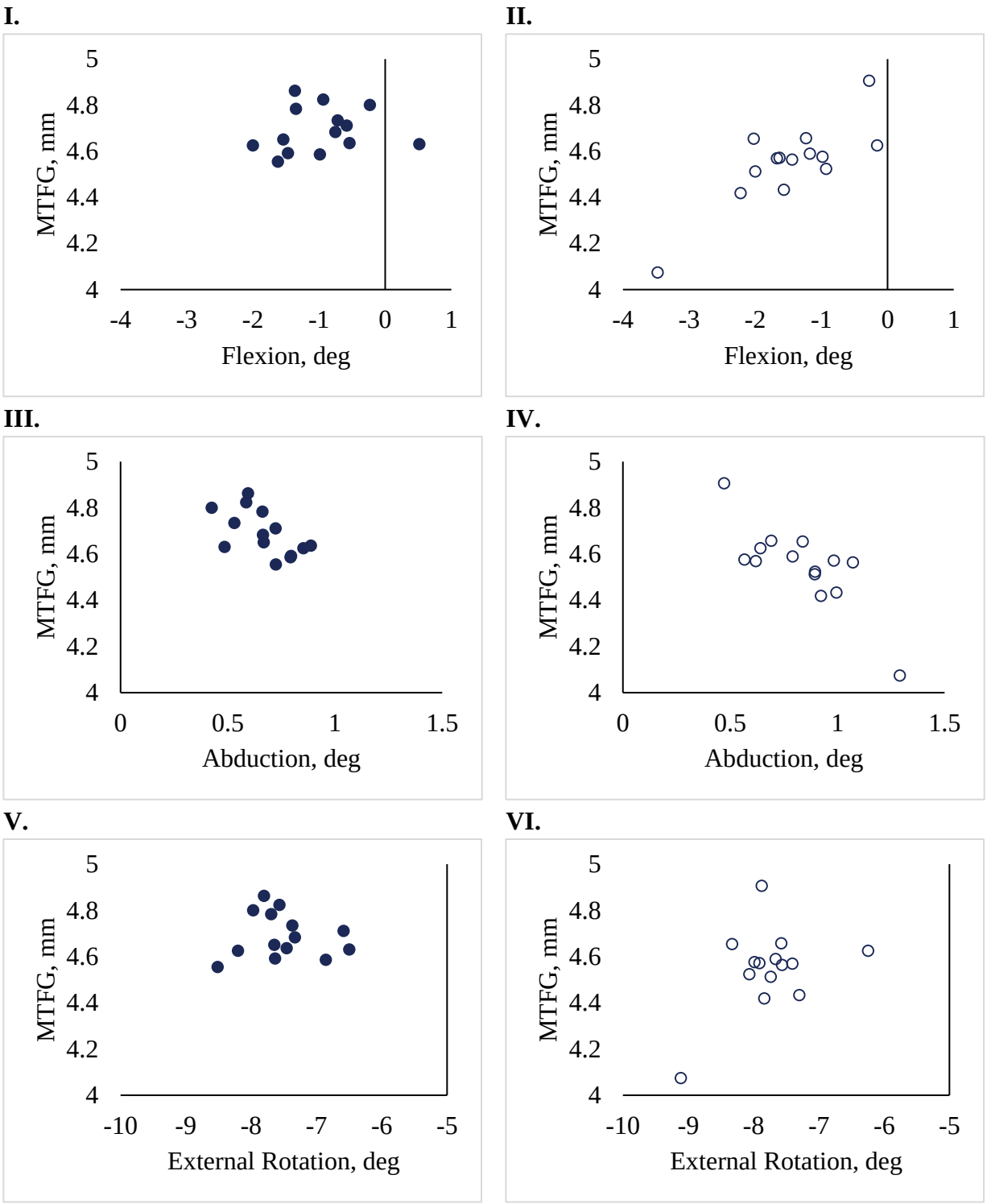

Figure 130: Subject S04 MTFG and kinematics data for all collected trials. On the HF condition: Flexion (I), Abduction (III), and External Rotation (V). On the MT condition: Flexion (II), Abduction (IV), and External Rotation (VI).

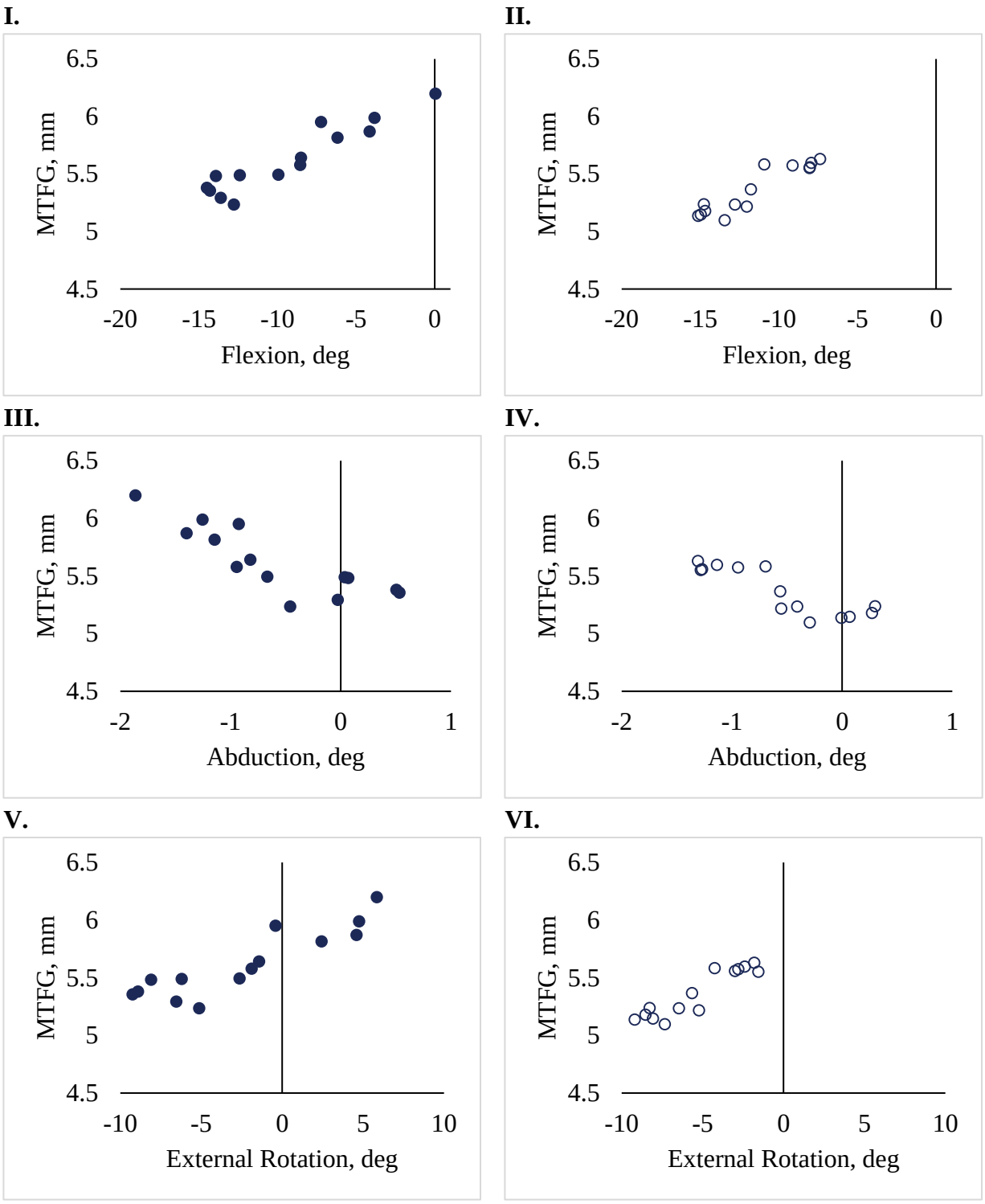

Figure 131: Subject S05 MTFG and kinematics data for all collected trials. On the HF condition: Flexion (I), Abduction (III), and External Rotation (V). On the MT condition: Flexion (II), Abduction (IV), and External Rotation (VI).

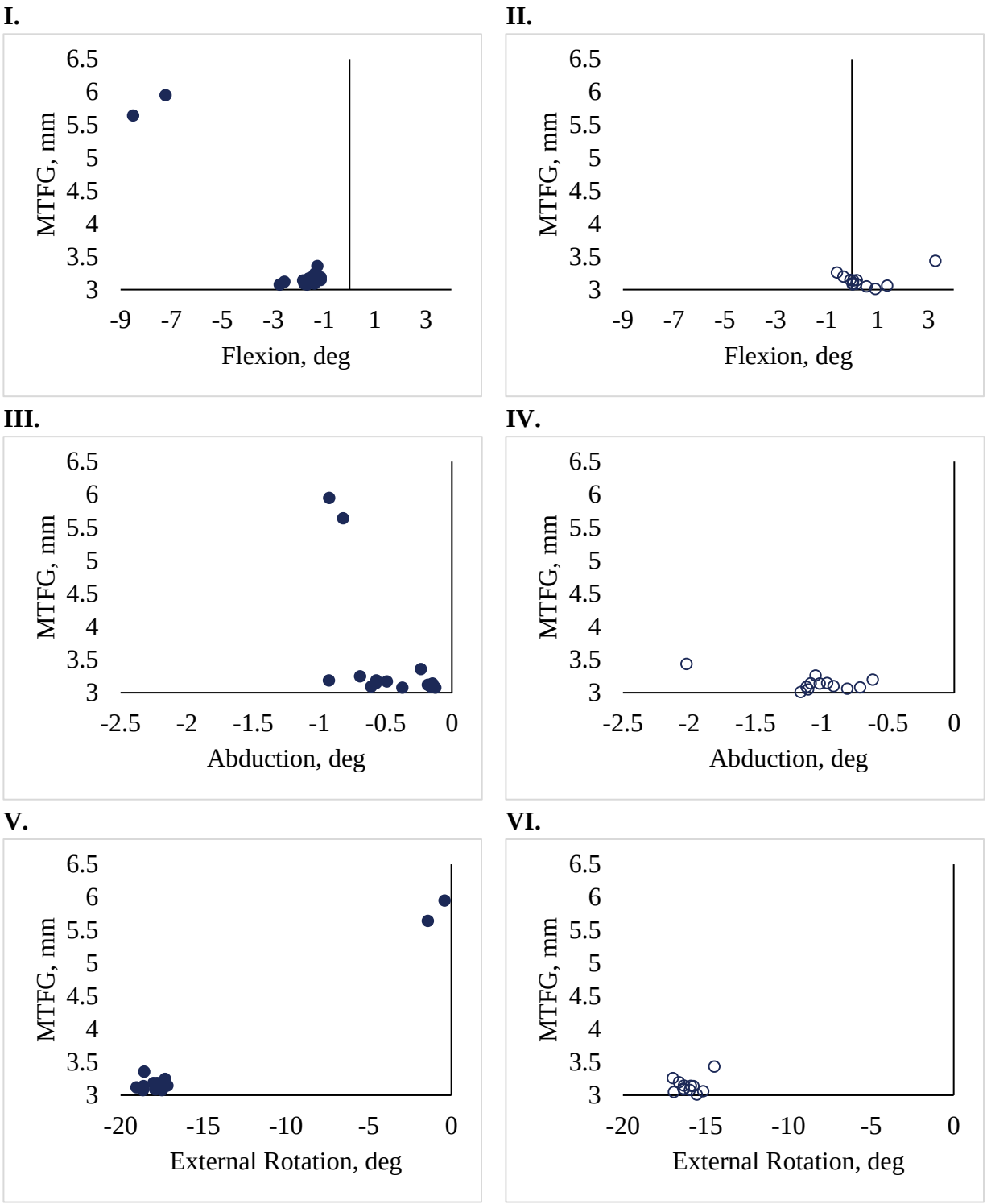

Figure 132: Subject S06 MTFG and kinematics data for all collected trials. On the HF condition: Flexion (I), Abduction (III), and External Rotation (V). On the MT condition: Flexion (II), Abduction (IV), and External Rotation (VI).

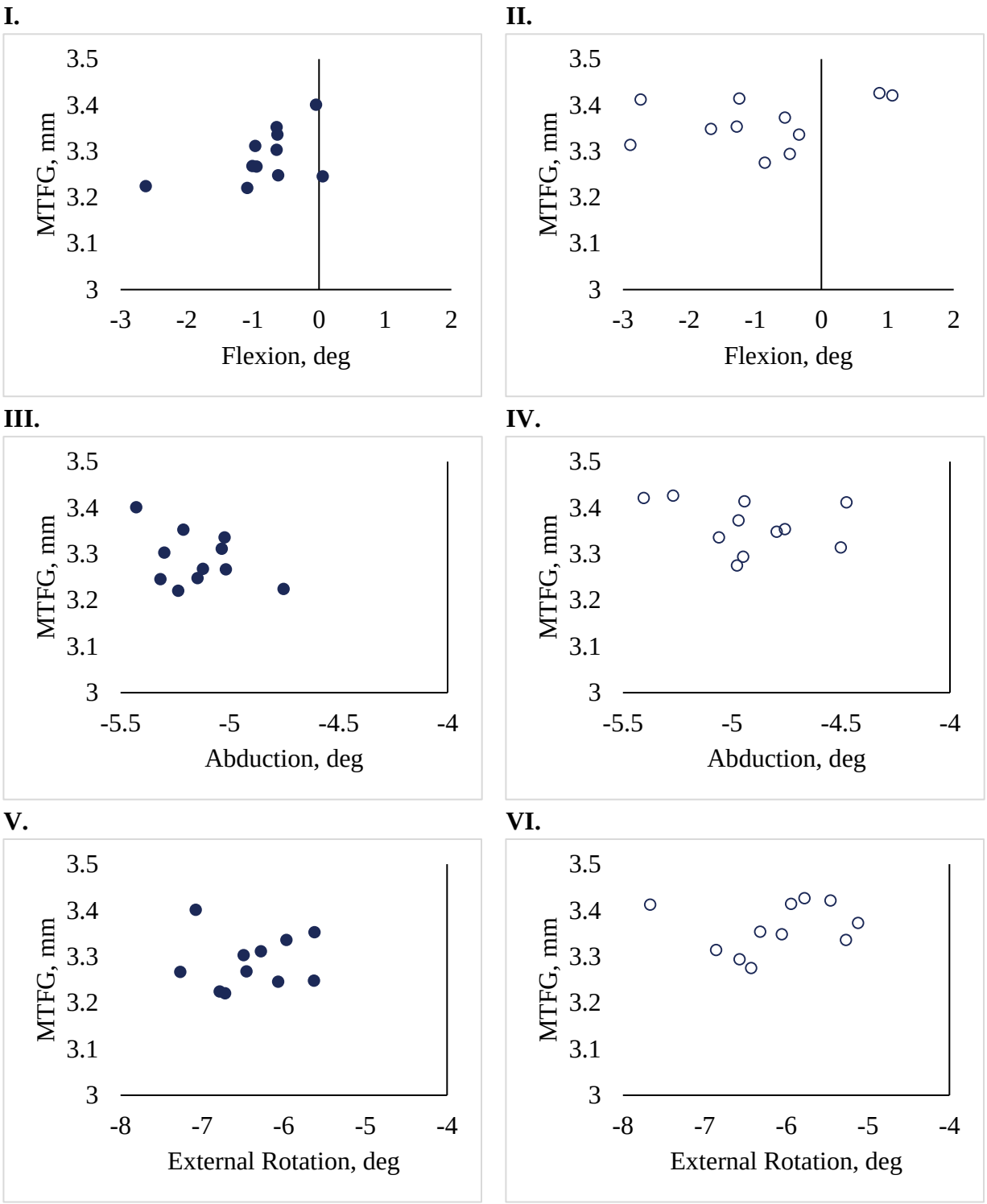

Figure 133: Subject S07 MTFG and kinematics data for all collected trials. On the HF condition: Flexion (I), Abduction (III), and External Rotation (V). On the MT condition: Flexion (II), Abduction (IV), and External Rotation (VI).

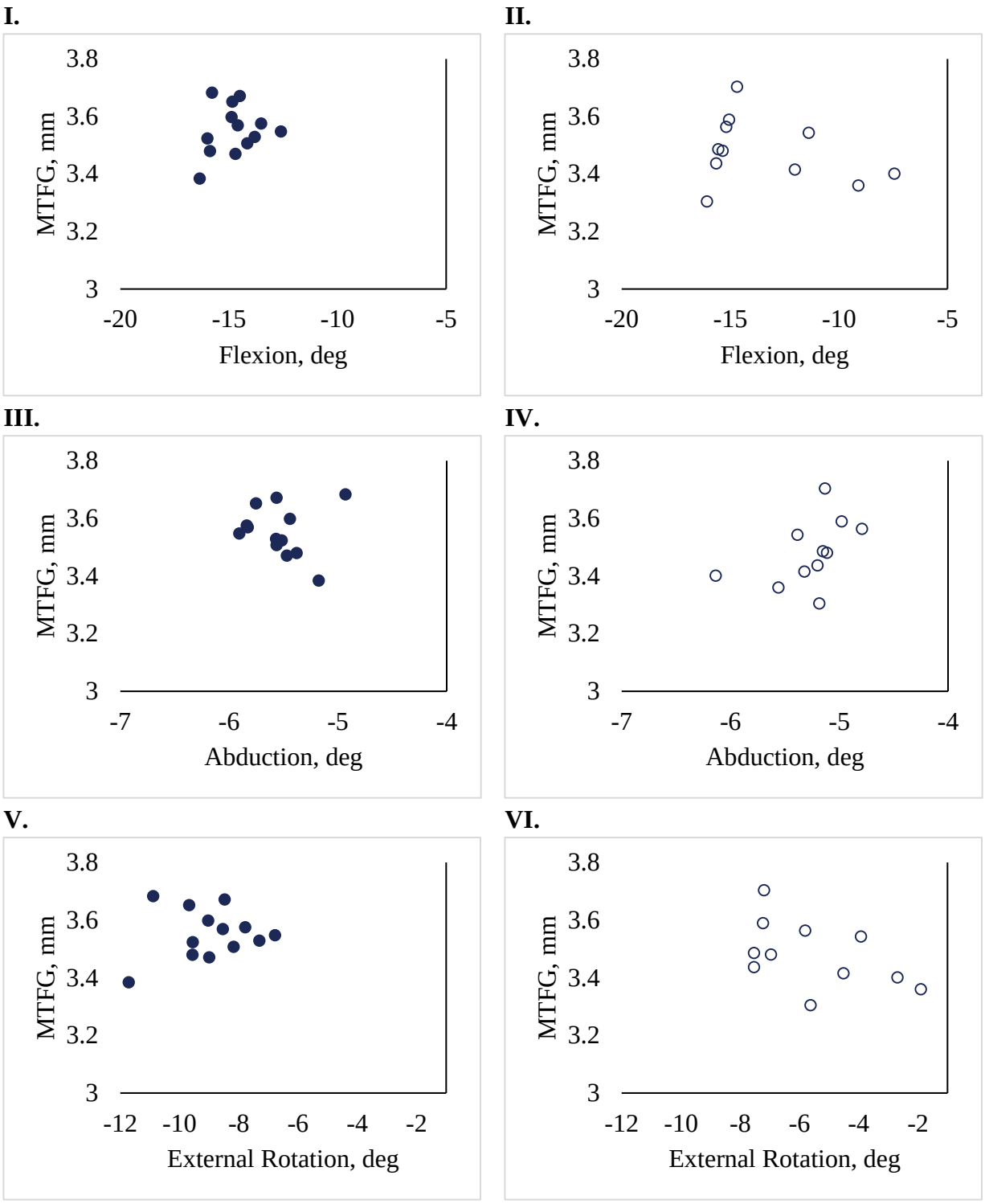

Figure 134: Subject S10 MTFG and kinematics data for all collected trials. On the HF condition: Flexion (I), Abduction (III), and External Rotation (V). On the MT condition: Flexion (II), Abduction (IV), and External Rotation (VI).

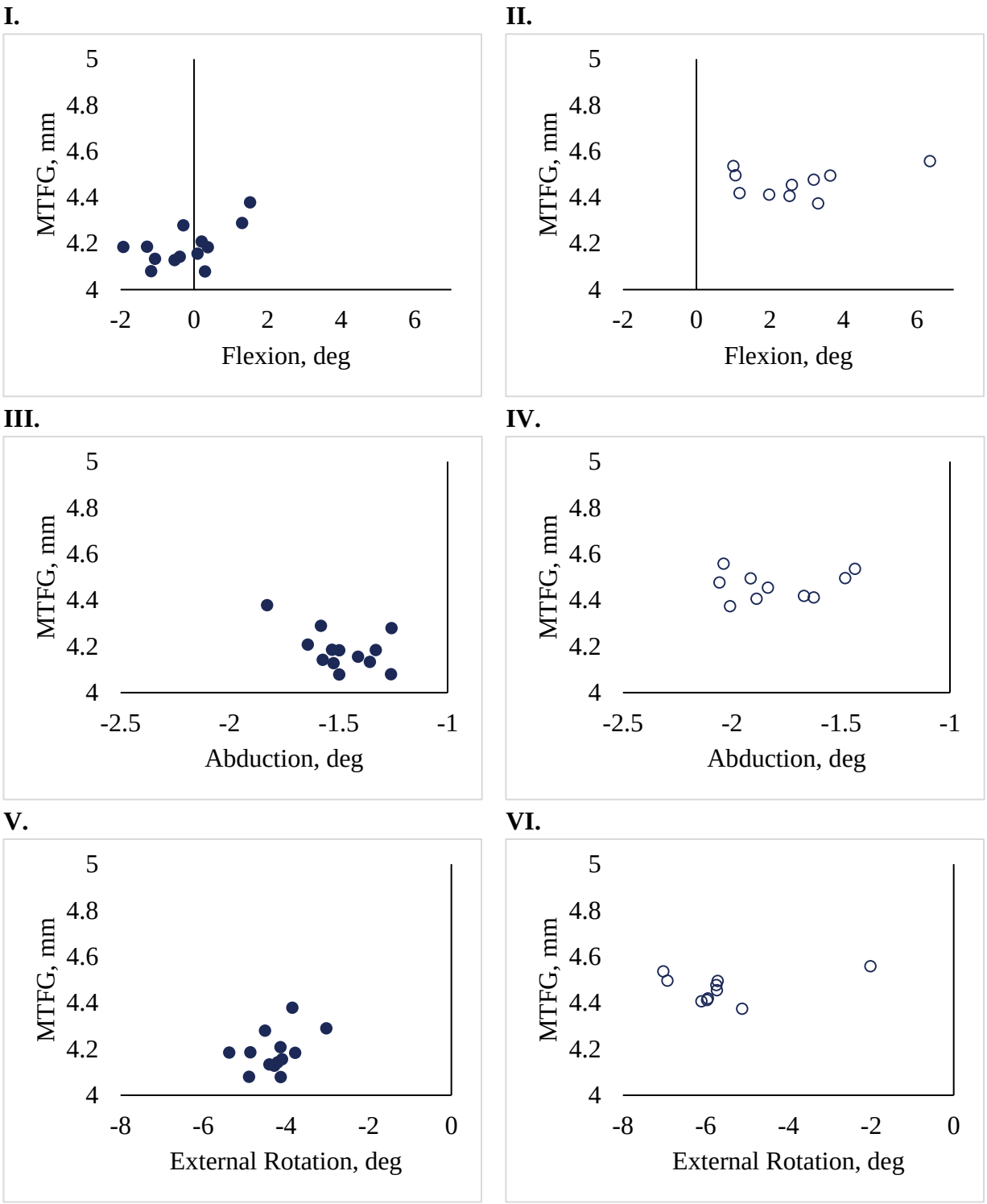

Figure 135: Subject S12 MTFG and kinematics data for all collected trials. On the HF condition: Flexion (I), Abduction (III), and External Rotation (V). On the MT condition: Flexion (II), Abduction (IV), and External Rotation (VI).

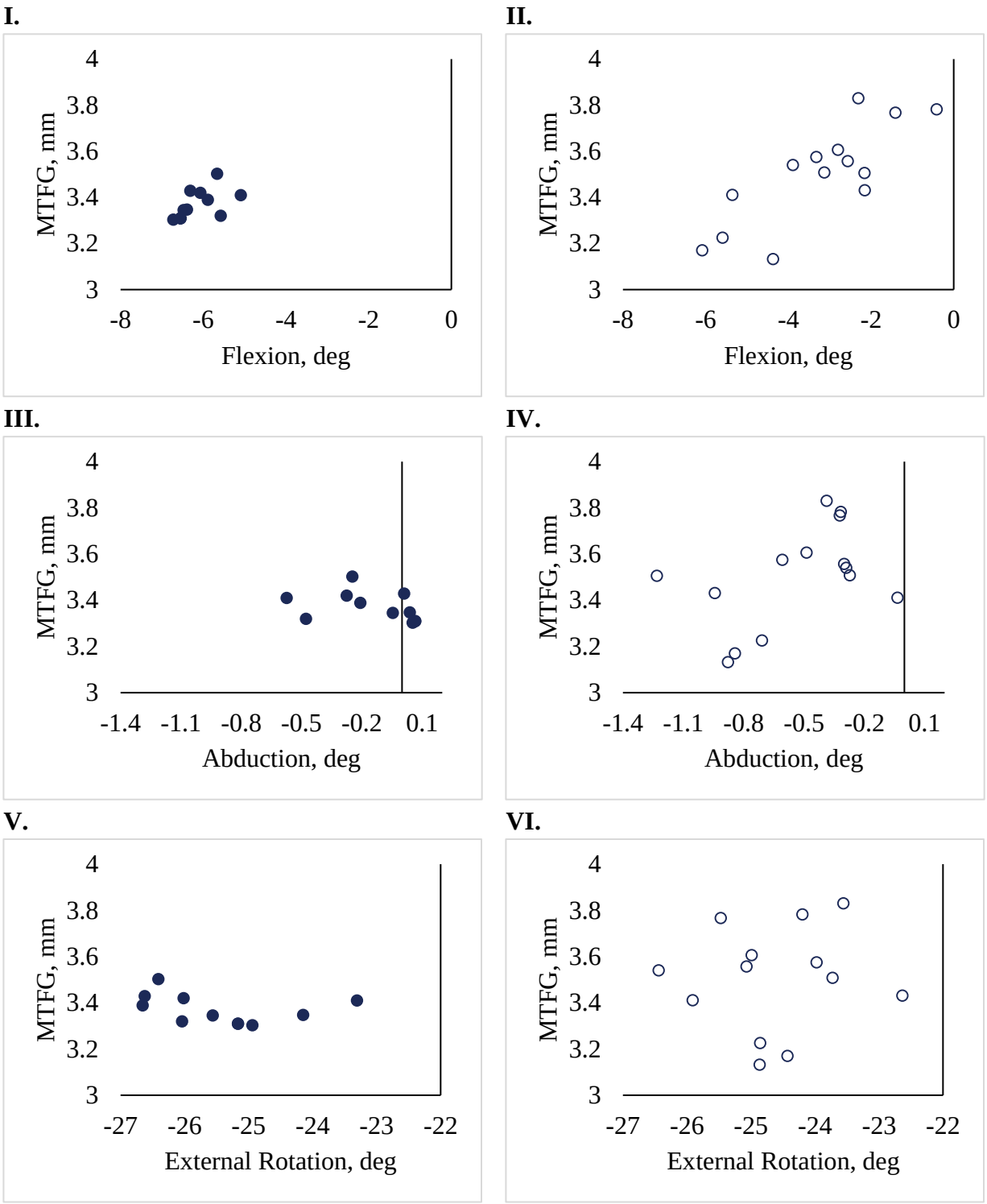

Figure 136: Subject S13 MTFG and kinematics data for all collected trials. On the HF condition: Flexion (I), Abduction (III), and External Rotation (V). On the MT condition: Flexion (II), Abduction (IV), and External Rotation (VI).

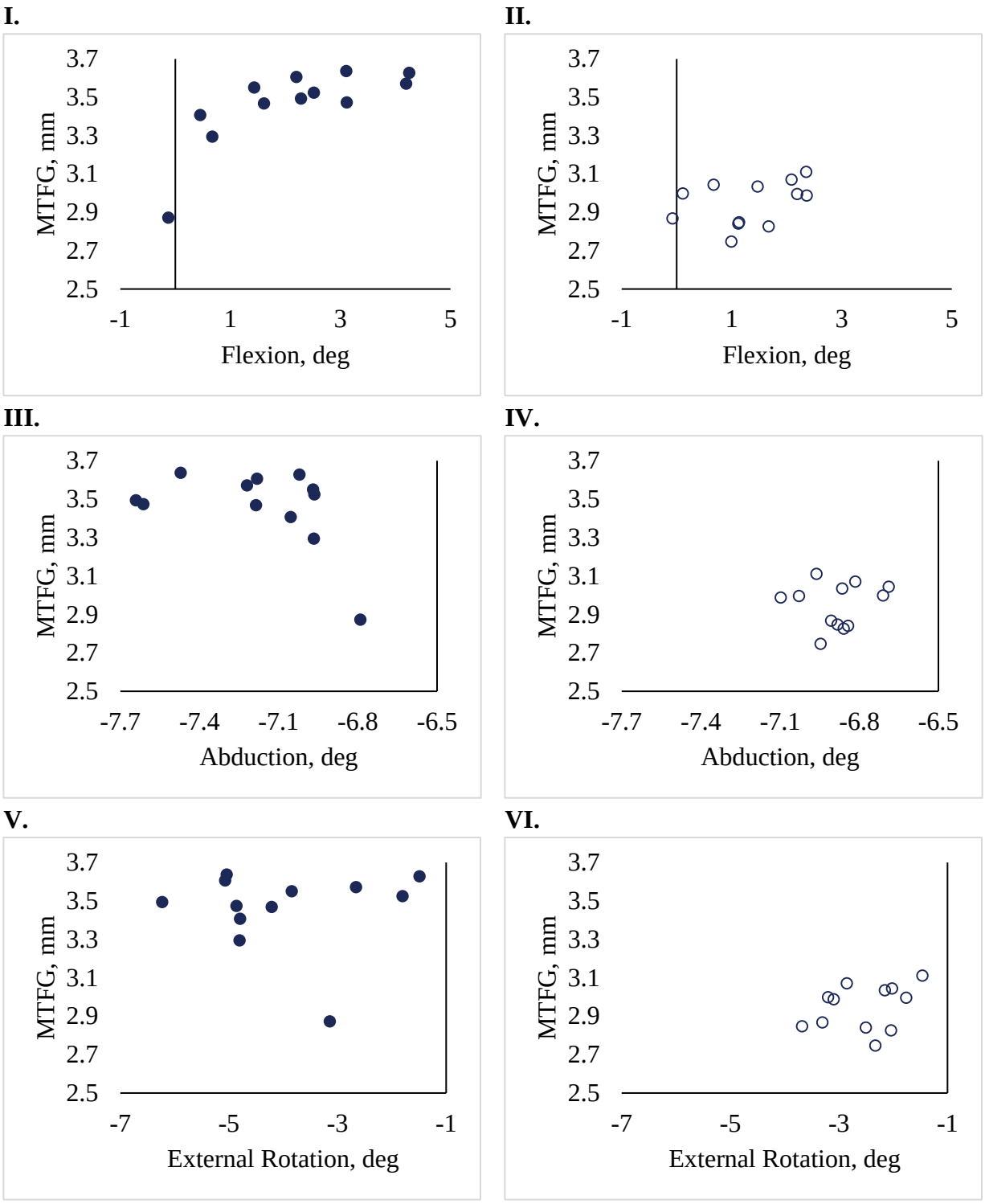

Figure 137: Subject S14 MTFG and kinematics data for all collected trials. On the HF condition: Flexion (I), Abduction (III), and External Rotation (V). On the MT condition: Flexion (II), Abduction (IV), and External Rotation (VI).

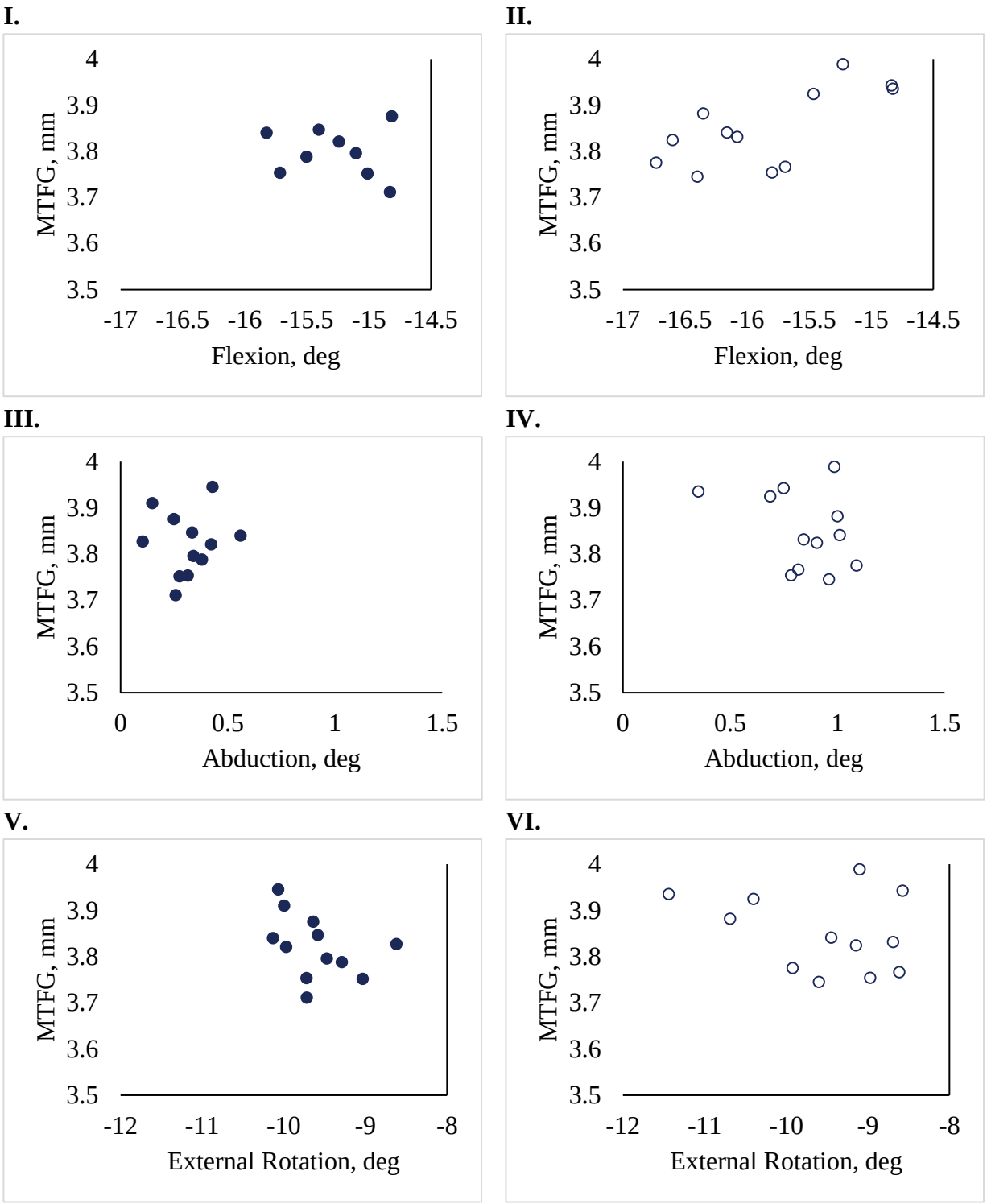

Figure 138: Subject S15 MTFG and kinematics data for all collected trials. On the HF condition: Flexion (I), Abduction (III), and External Rotation (V). On the MT condition: Flexion (II), Abduction (IV), and External Rotation (VI).

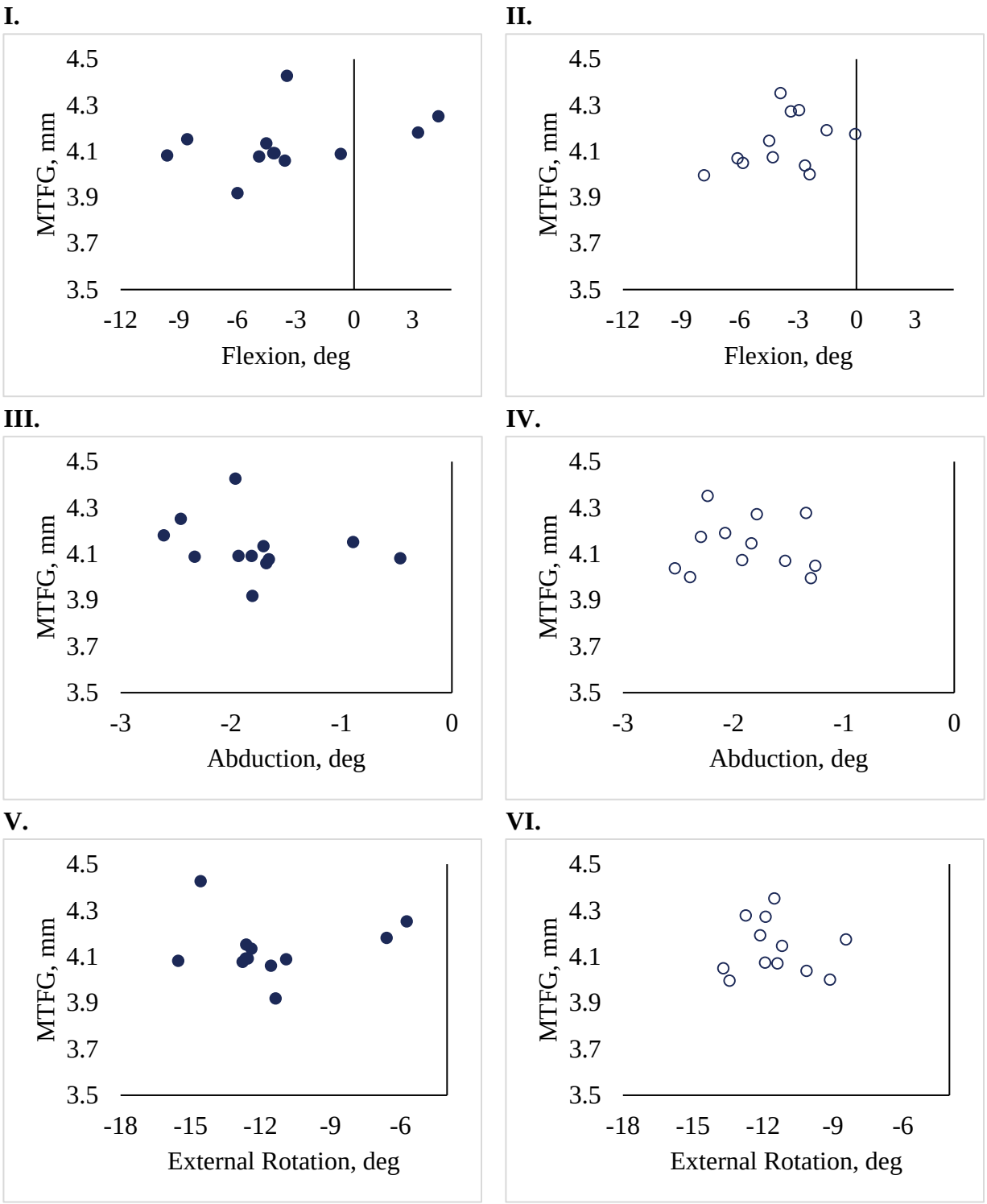

Figure 139: Subject S16 MTFG and kinematics data for all collected trials. On the HF condition: Flexion (I), Abduction (III), and External Rotation (V). On the MT condition: Flexion (II), Abduction (IV), and External Rotation (VI).

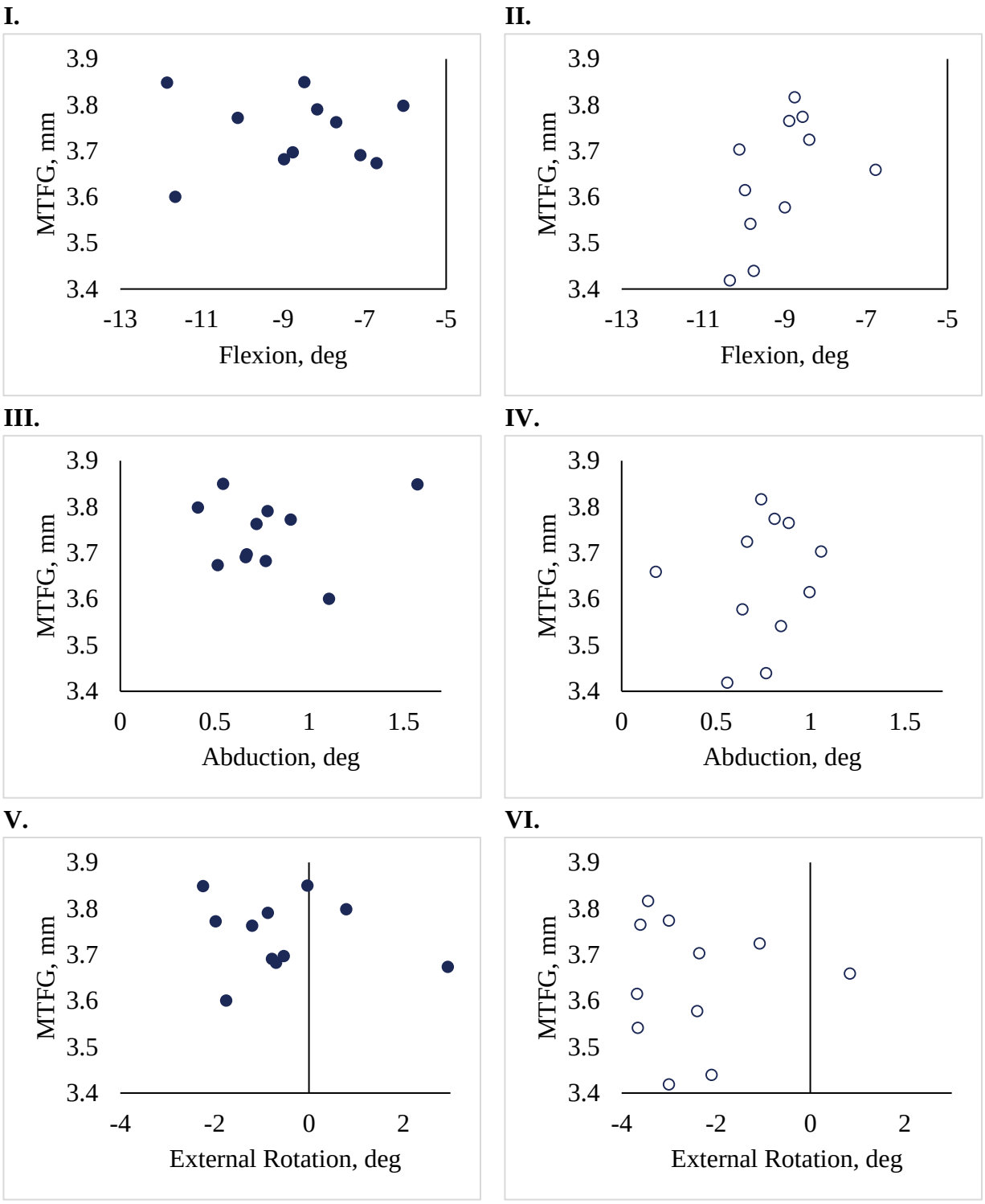

Figure 140: Subject S17 MTFG and kinematics data for all collected trials. On the HF condition: Flexion (I), Abduction (III), and External Rotation (V). On the MT condition: Flexion (II), Abduction (IV), and External Rotation (VI).

I.

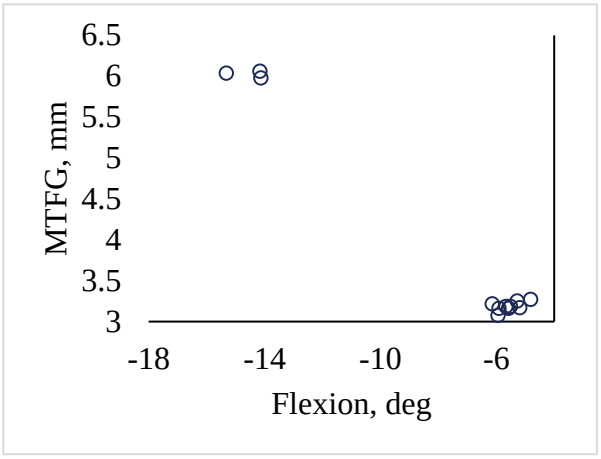

II.

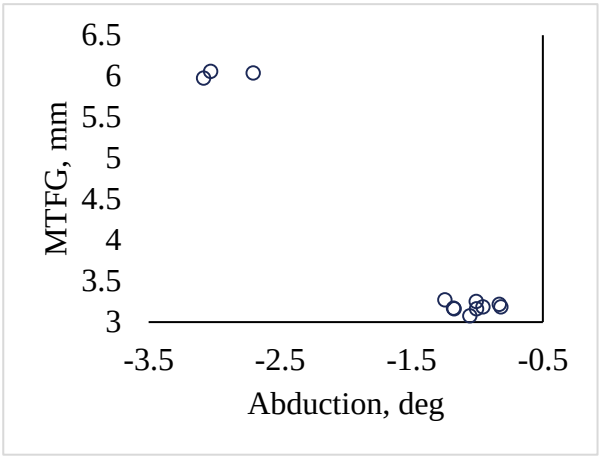

III.

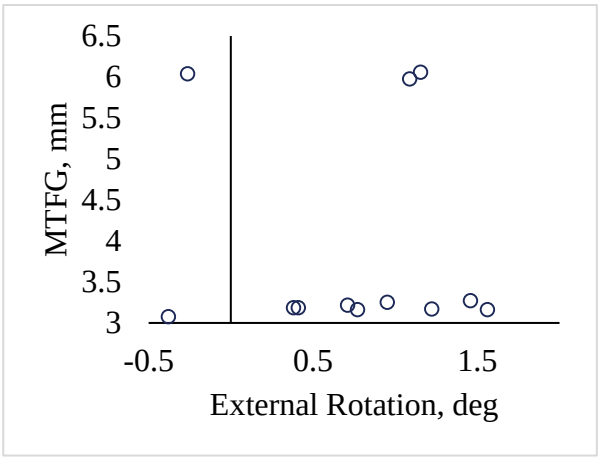

Figure 141: Subject S19 MTFG and kinematics data for all collected trials. On the MT condition: Flexion (I), Abduction (II), and External Rotation (III). No HF data is displayed, as the subject did not complete the HF visit.

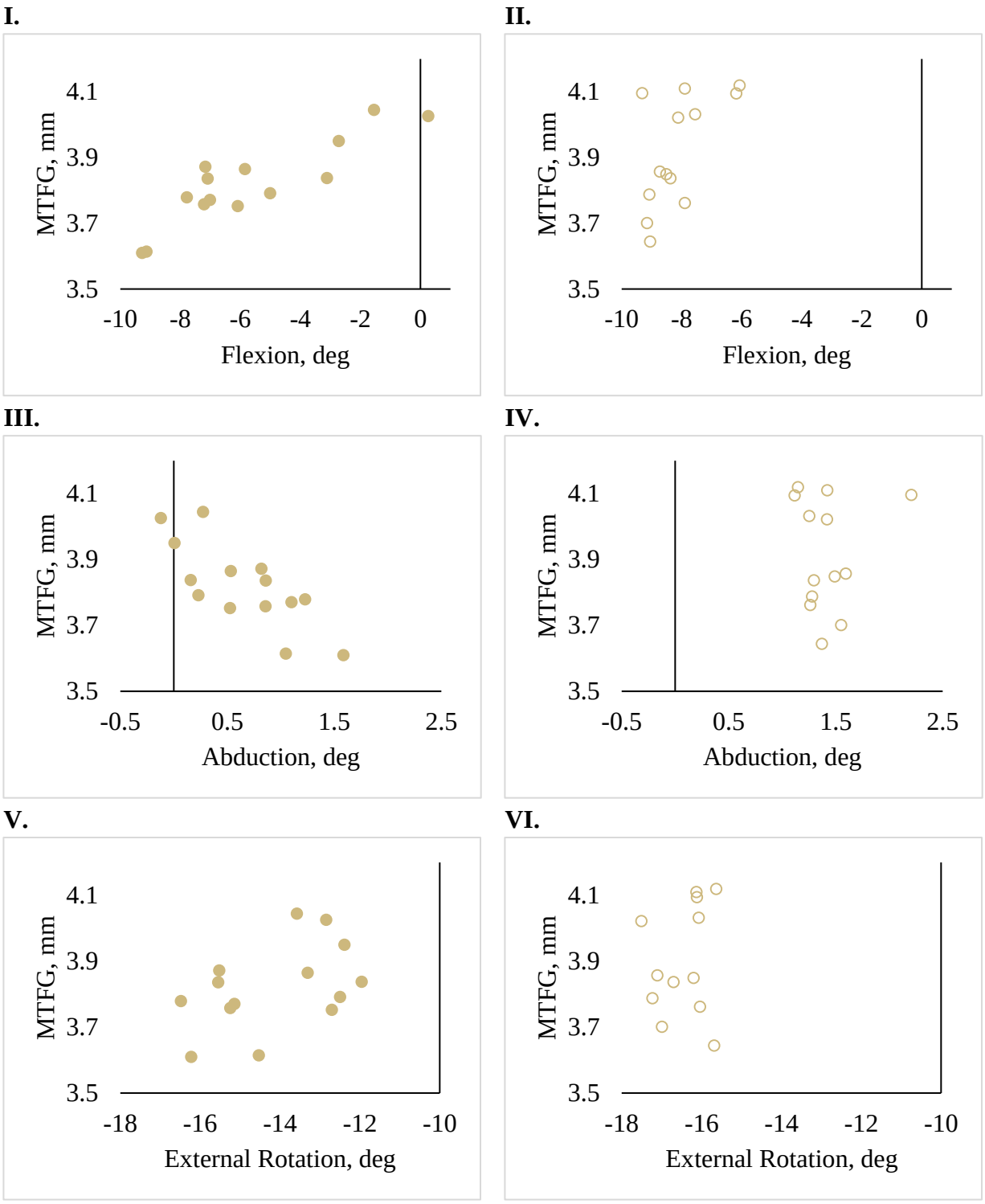

Figure 142: Subject S20 MTFG and kinematics data for all collected trials. On the HF condition: Flexion (I), Abduction (III), and External Rotation (V). On the MT condition: Flexion (II), Abduction (IV), and External Rotation (VI).

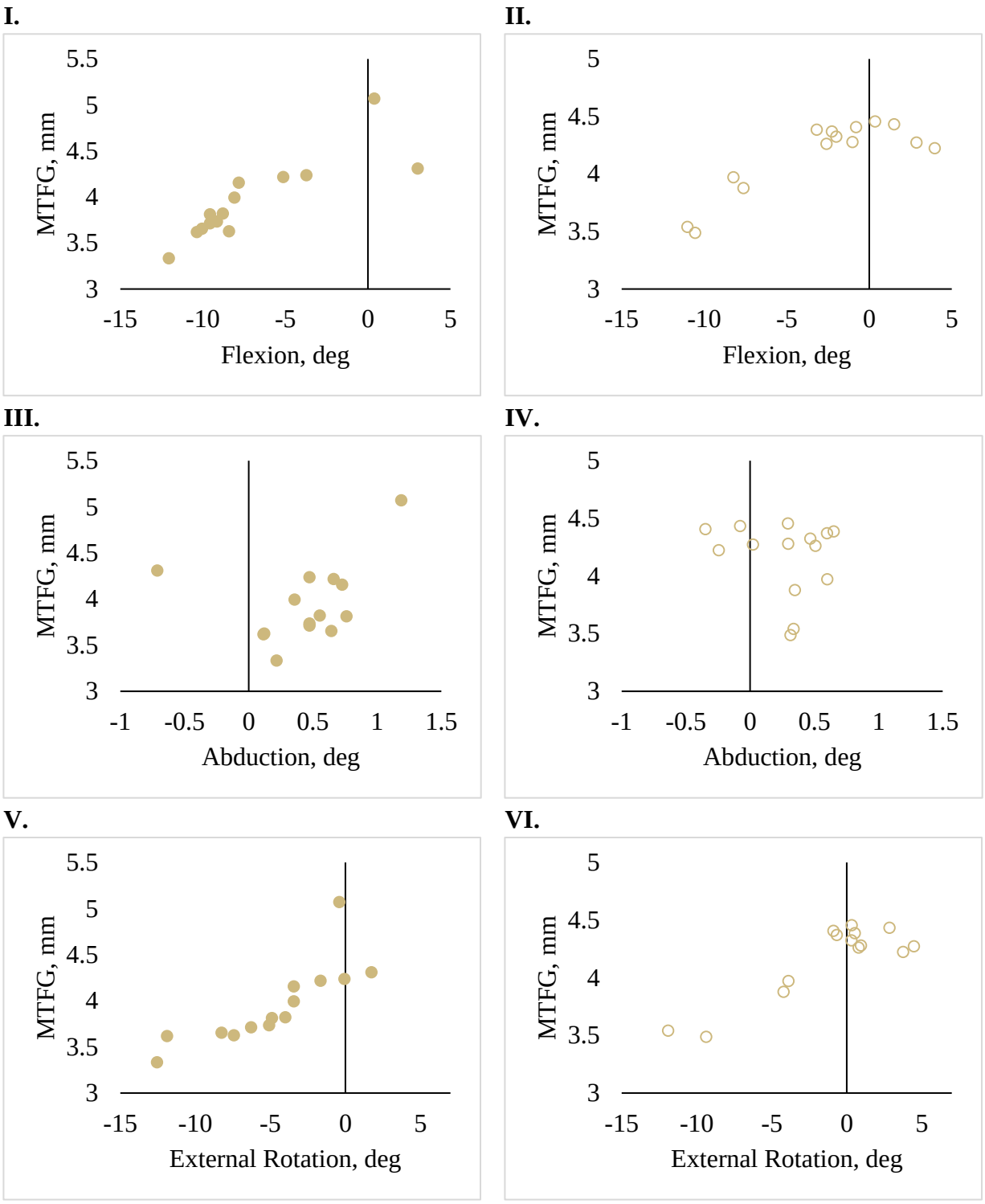

Figure 143: Subject S21 MTFG and kinematics data for all collected trials. On the HF condition: Flexion (I), Abduction (III), and External Rotation (V). On the MT condition: Flexion (II), Abduction (IV), and External Rotation (VI).

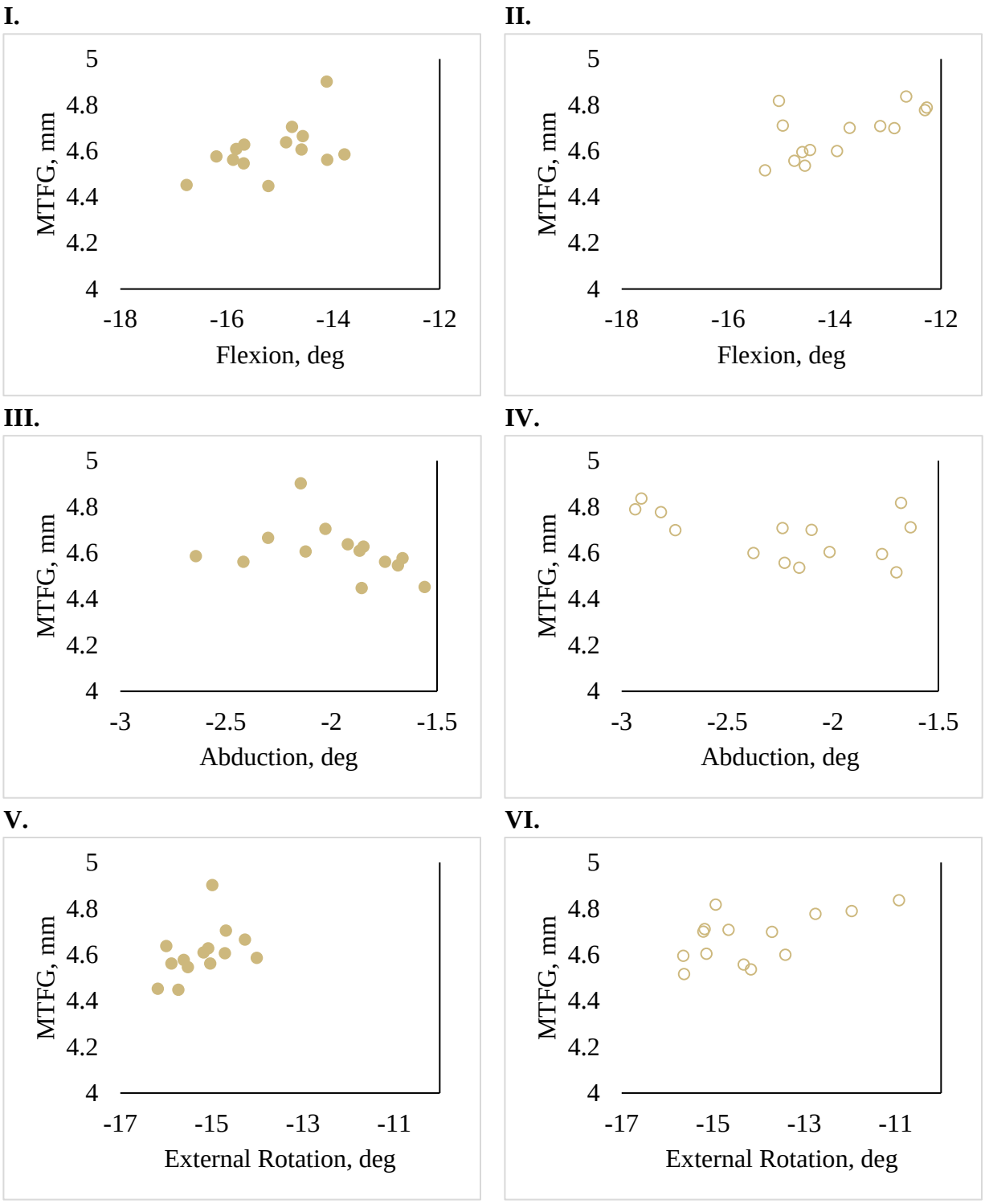

Figure 144: Subject S22 MTFG and kinematics data for all collected trials. On the HF condition: Flexion (I), Abduction (III), and External Rotation (V). On the MT condition: Flexion (II), Abduction (IV), and External Rotation (VI).

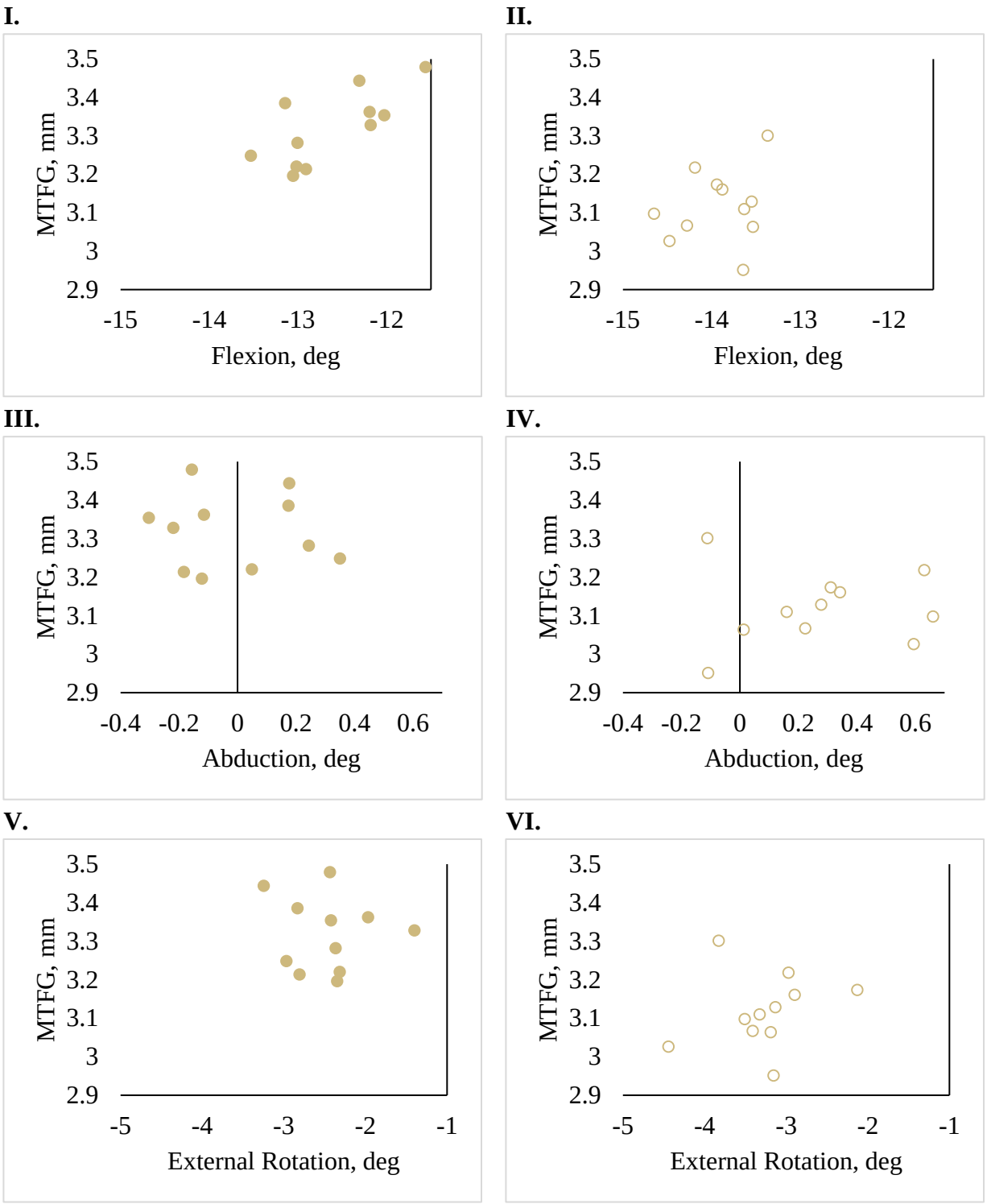

Figure 145: Subject S23 MTFG and kinematics data for all collected trials. On the HF condition: Flexion (I), Abduction (III), and External Rotation (V). On the MT condition: Flexion (II), Abduction (IV), and External Rotation (VI).

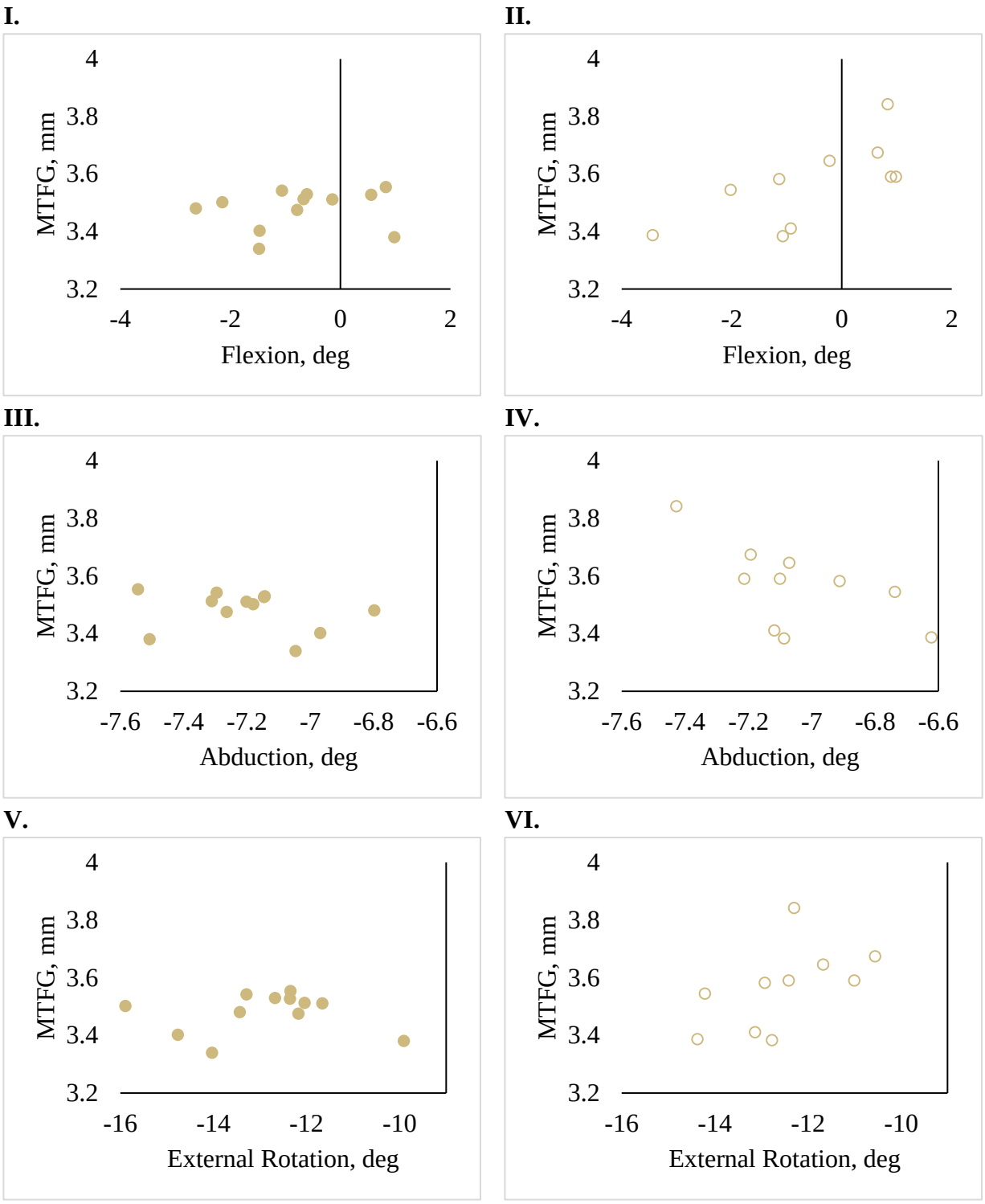

Figure 146: Subject S24 MTFG and kinematics data for all collected trials. On the HF condition: Flexion (I), Abduction (III), and External Rotation (V). On the MT condition: Flexion (II), Abduction (IV), and External Rotation (VI).

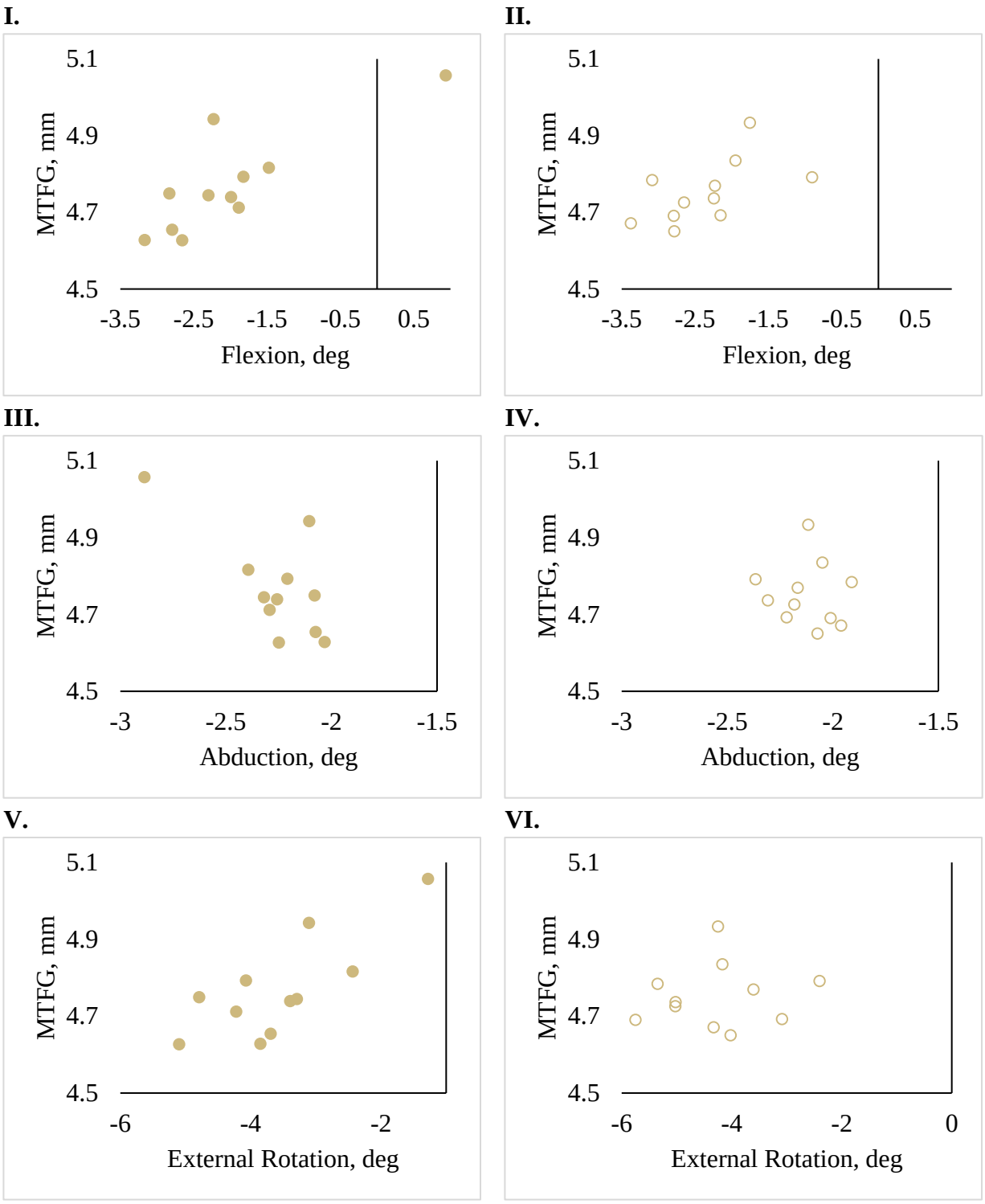

Figure 147: Subject S25 MTFG and kinematics data for all collected trials. On the HF condition: Flexion (I), Abduction (III), and External Rotation (V). On the MT condition: Flexion (II), Abduction (IV), and External Rotation (VI).

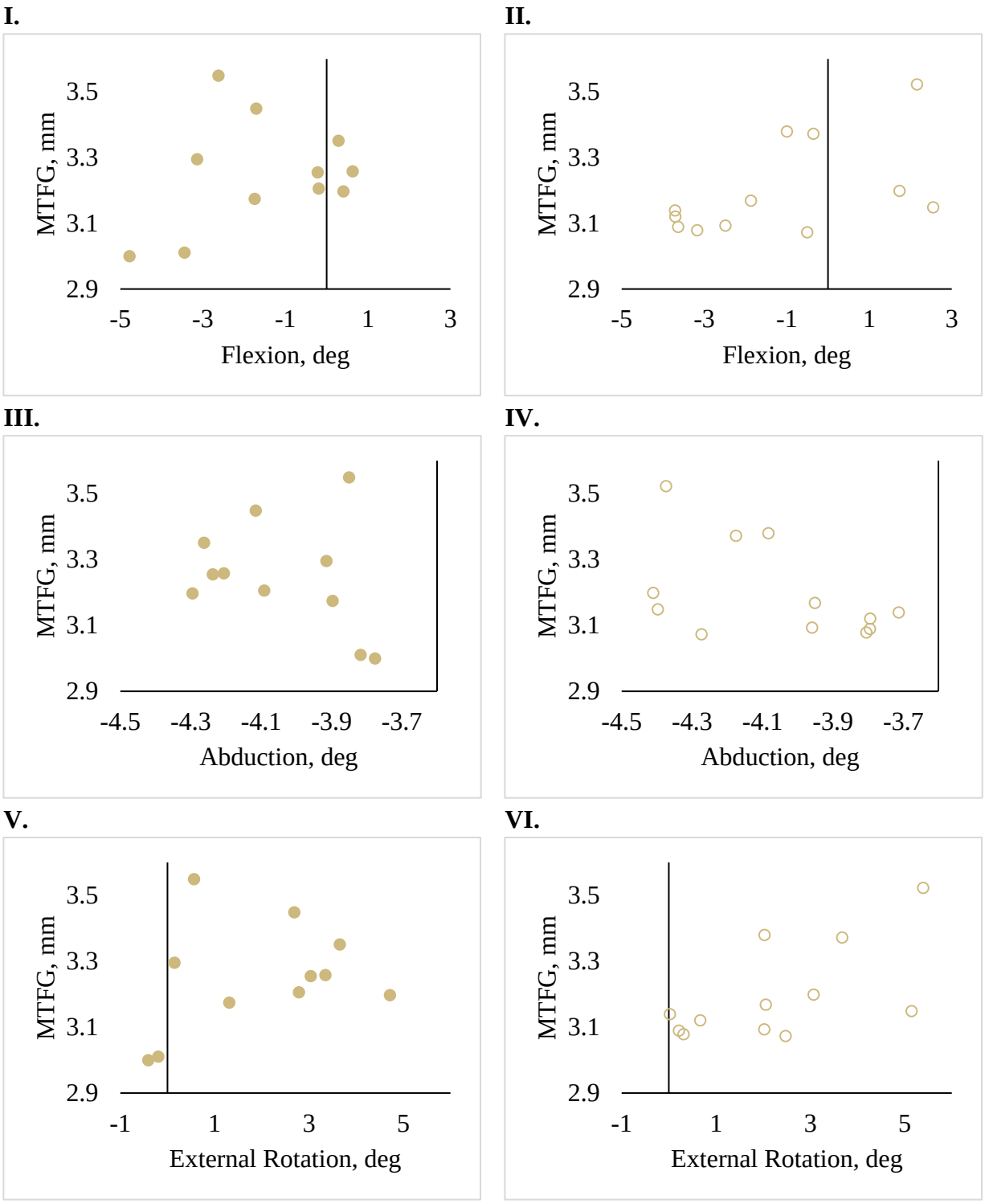

Figure 148: Subject S26 MTFG and kinematics data for all collected trials. On the HF condition: Flexion (I), Abduction (III), and External Rotation (V). On the MT condition: Flexion (II), Abduction (IV), and External Rotation (VI).

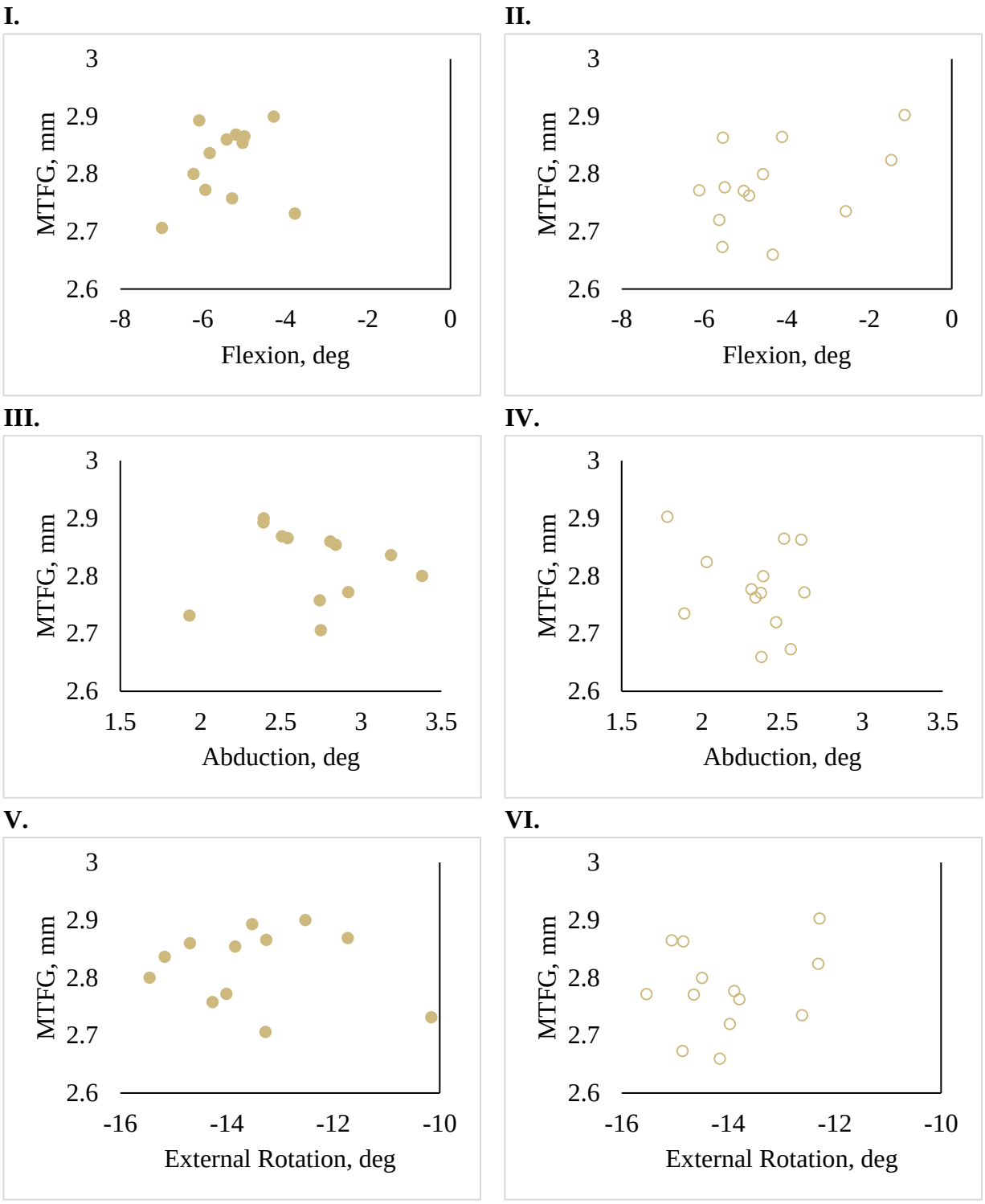

Figure 149: Subject S27 MTFG and kinematics data for all collected trials. On the HF condition: Flexion (I), Abduction (III), and External Rotation (V). On the MT condition: Flexion (II), Abduction (IV), and External Rotation (VI).

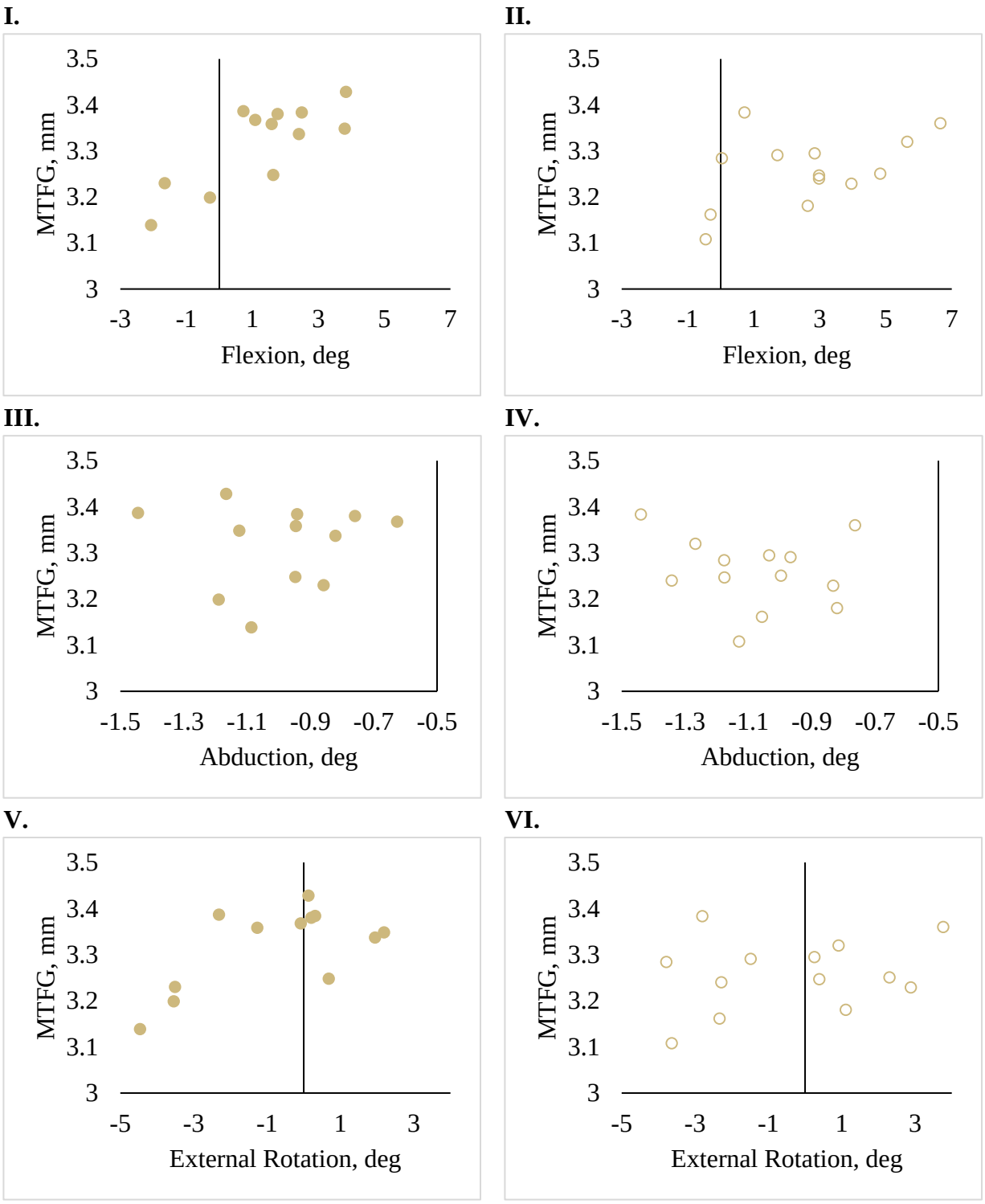

Figure 150: Subject S28 MTFG and kinematics data for all collected trials. On the HF condition: Flexion (I), Abduction (III), and External Rotation (V). On the MT condition: Flexion (II), Abduction (IV), and External Rotation (VI).

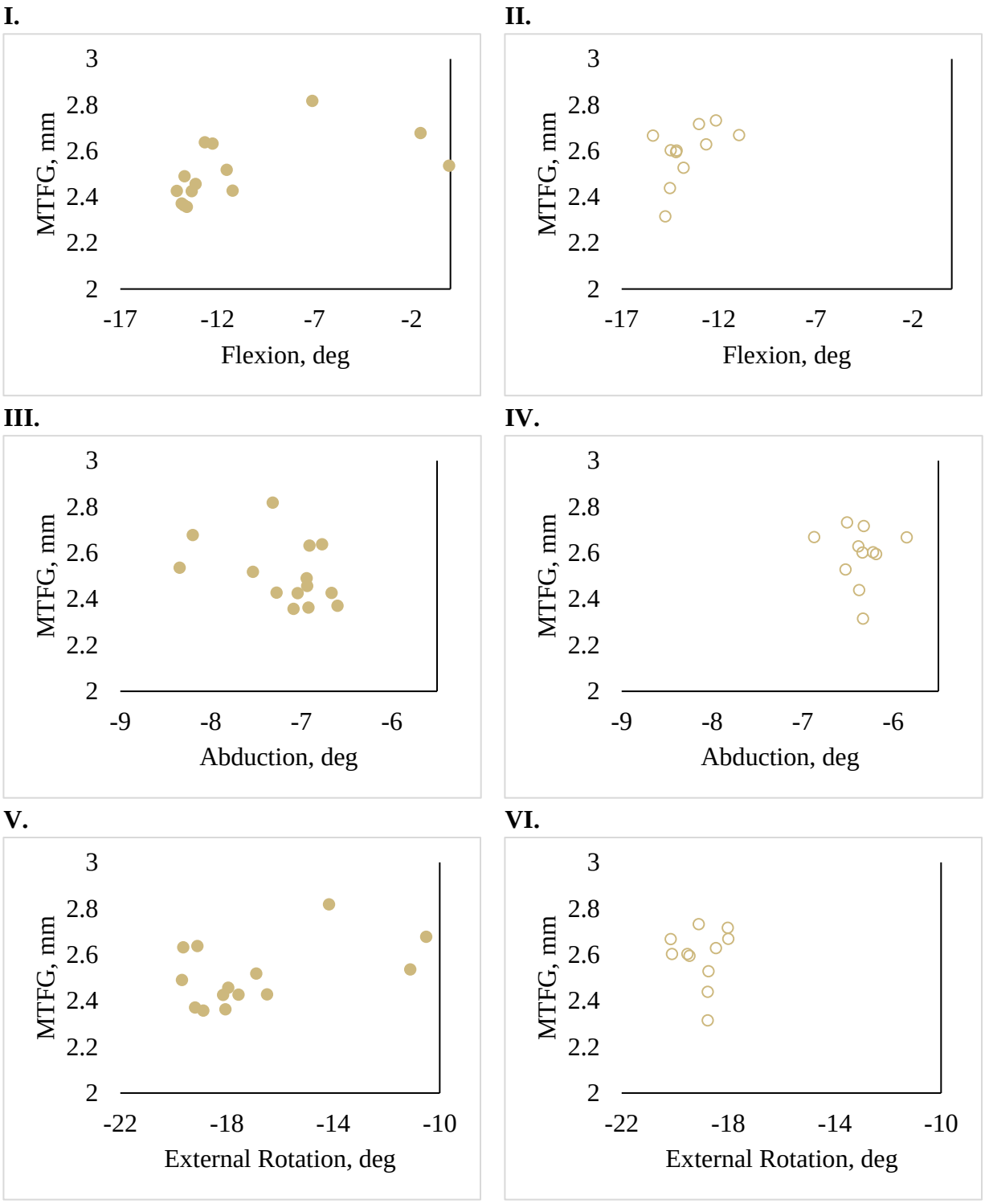

Figure 151: Subject S29 MTFG and kinematics data for all collected trials. On the HF condition: Flexion (I), Abduction (III), and External Rotation (V). On the MT condition: Flexion (II), Abduction (IV), and External Rotation (VI).

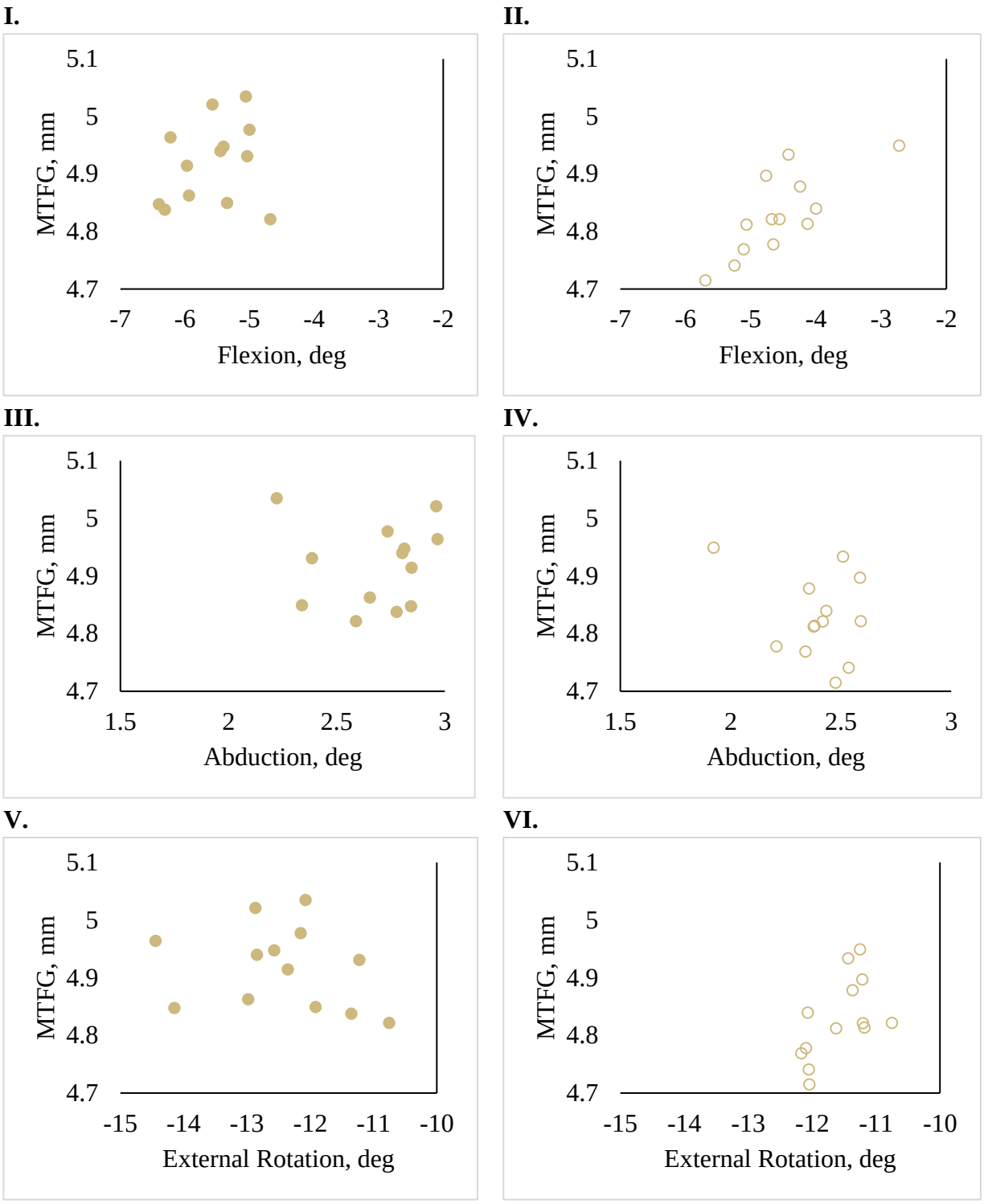

Figure 152: Subject S31 MTFG and kinematics data for all collected trials. On the HF condition: Flexion (I), Abduction (III), and External Rotation (V). On the MT condition: Flexion (II), Abduction (IV), and External Rotation (VI).

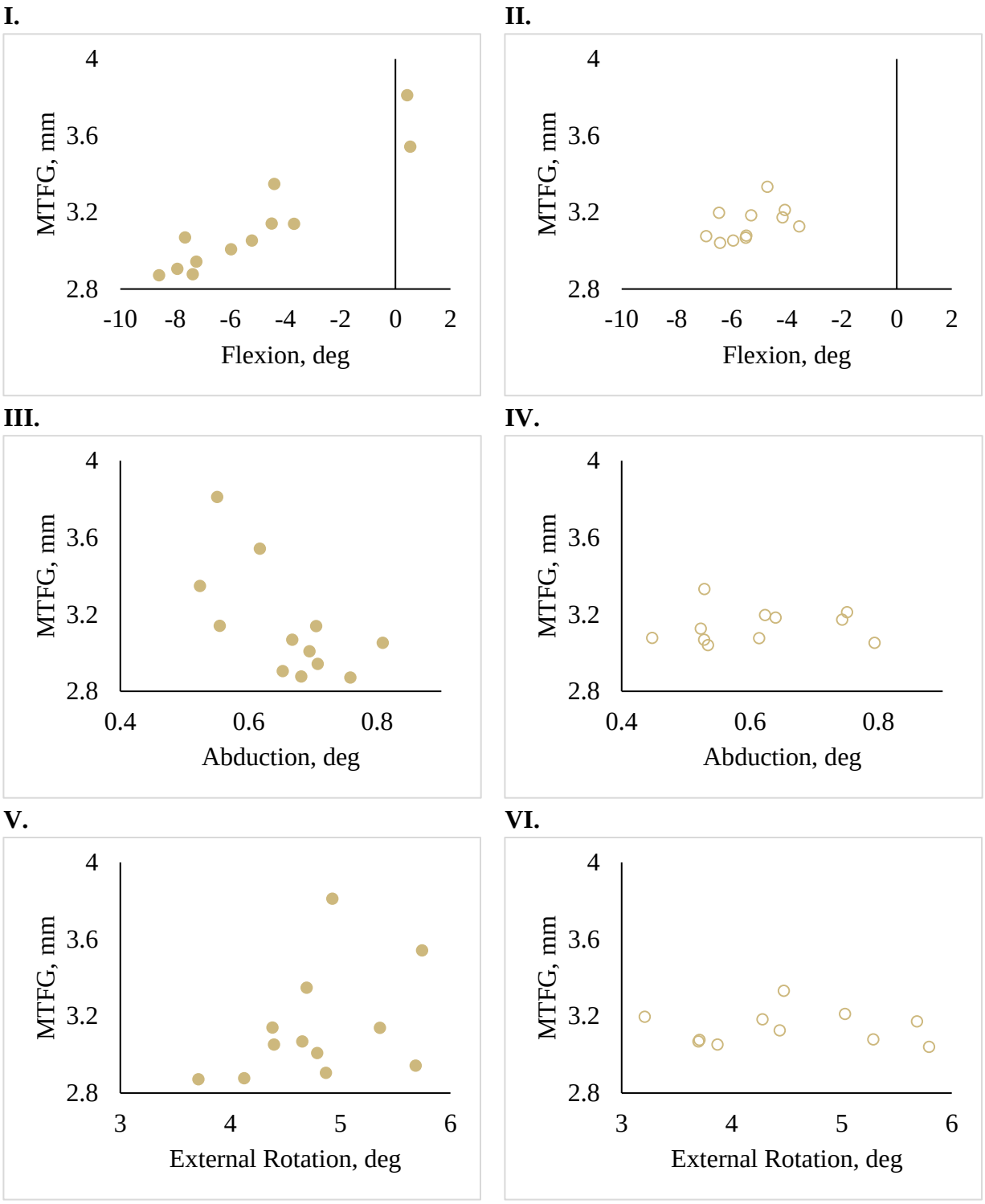

Figure 153: Subject S32 MTFG and kinematics data for all collected trials. On the HF condition: Flexion (I), Abduction (III), and External Rotation (V). On the MT condition: Flexion (II), Abduction (IV), and External Rotation (VI).

Appendix C.2 Comparison of Models using Two and Four Hours of Data

Table 33: MTFG model coefficients, T_T, and G_T for seven subjects (five HW and two OB) standing on the HF condition.

Subject	Healthy Weight											
	Two Hours						Four Hours					
	a x 10^{-4}	b x 10^{-2}	c, G_0	T_T	G_T	R^2	a x 10^{-4}	b x 10^{-2}	c, G_0	T_T	G_T	R^2
S01	125	-18.42	4.03	7.37	3.35	0.56	143	-19.34	4.03	6.76	3.38	0.29
S03	0.05	-0.17	2.43	155.88	2.29	0.06	0.28	-0.24	2.43	47	2.63	0.21
S04	Convergence Error						Convergence Error					
S05	-5.3	2.92	5.29	27.55	5.69	0.02	-5.2	2.76	5.30	26.54	5.67	0.01
S06	0.73	-0.62	3.27	42.12	3.14	0.86	8.28	-2.48	3.35	14.98	3.16	0.06
	Obese											
	Two Hours						Four Hours					
	a x 10^{-4}	b x 10^{-2}	c, G_0	T_T	G_T	R^2	a x 10^{-4}	b x 10^{-2}	c, G_0	T_T	G_T	R^2
S20	Convergence Error						-0.007	0.22	3.77	162.0	3.95	0.05
S21	12.20	0.84	4.29	17.70	3.90	0.08	-4.32e^{-2}	0.17	3.91	196.76	4.07	0.03

Table 34: MTFG model coefficients, T_T and G_T for seven subjects (five HW and two OB) standing on the MT condition.

Subject	Healthy Weight											
	Two Hours						Four Hours					
	a x 10^{-4}	b x 10^{-2}	c, G_0	T_T	G_T	R^2	a x 10^{-4}	b x 10^{-2}	c, G_0	T_T	G_T	R^2
S01	36.00	-6.20	3.79	8.61	3.52	0.26	Convergence Error					
S03	Convergence Error						-0.9	0.85	2.43	47	2.63	0.008
S04	0.30	-0.61	4.72	100.83	4.42	0.37	26.7	-6.15	4.90	11.52	4.55	0.12
S05	0.99	-1.39	5.69	70.20	5.20	0.76	1.25	-1.27	5.67	50.8	5.34	0.11
S06	7.35	-3.23	3.42	21.97	3.07	0.56	21.6	-4.85	3.44	11.23	3.17	0.35
	Obese											
	Two Hours						Four Hours					
	a x 10^{-4}	b x 10^{-2}	c, G_0	T_T	G_T	R^2	a x 10^{-4}	b x 10^{-2}	c, G_0	T_T	G_T	R^2
S20	0.24	-0.62	4.11	128.33	3.71	0.65	$1.63e^{-2}$	-0.09	4.00	276.07	3.87	0.05
S21	0.84	-1.16	4.43	69.05	4.03	0.42	0.82	-1.01	4.41	61.59	4.10	0.05

Appendix D Lower Extremity Muscle Measures

Appendix D.1 Electromyography Data

All graphs of EMG data are included in this section. Each subsection includes graphs for each specific region of interest (tibialis anterior, gastrocnemius, soleus, rectus femoris, and hamstring). Within each muscle, MPF is displayed first and RMS is displayed second. Methods by which MPF and RMS were measured and calculated are included in section 3.4.4.1. No analyses of graphs are included in this section. Analyses of significant EMG findings are included in section 4.4.1.

Appendix D.1.1 Tibialis Anterior MPF

I.

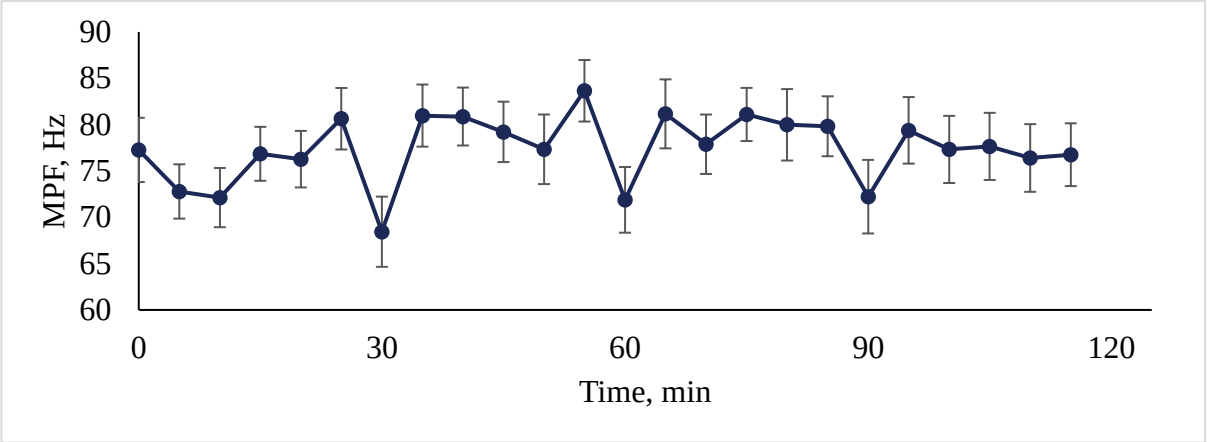

II.

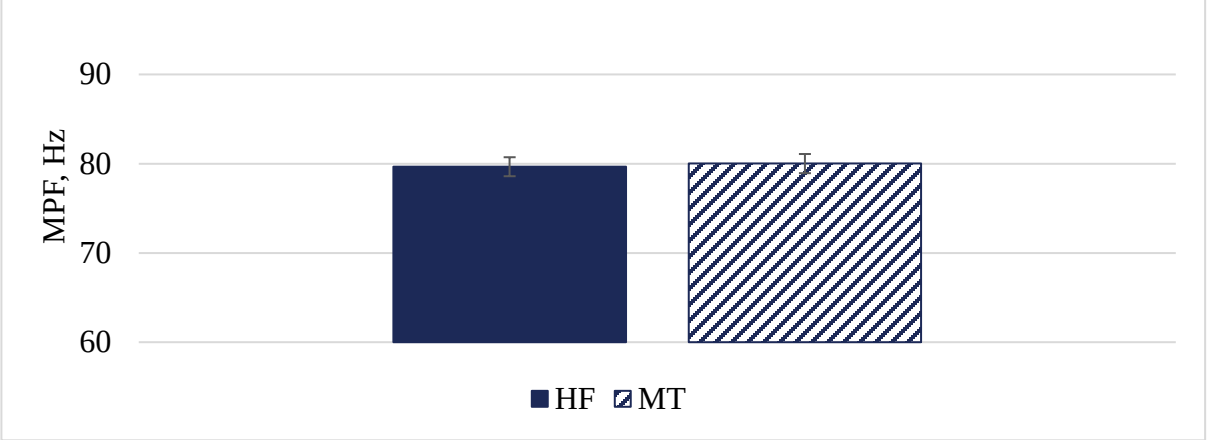

III.

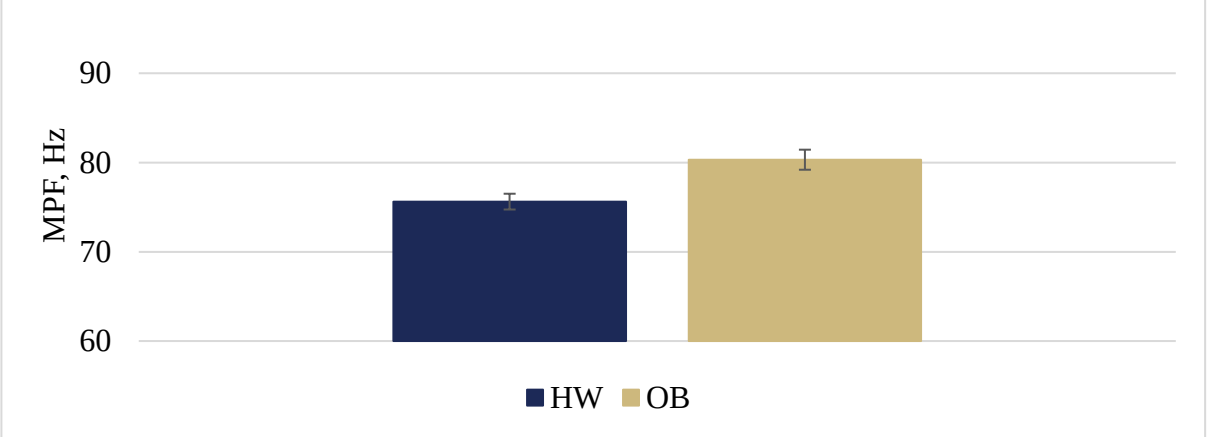

Figure 154: Tibialis Anterior MPF over time (I) and between flooring conditions (II) and BMI groups (III). Error bars are standard error of the mean.

I.

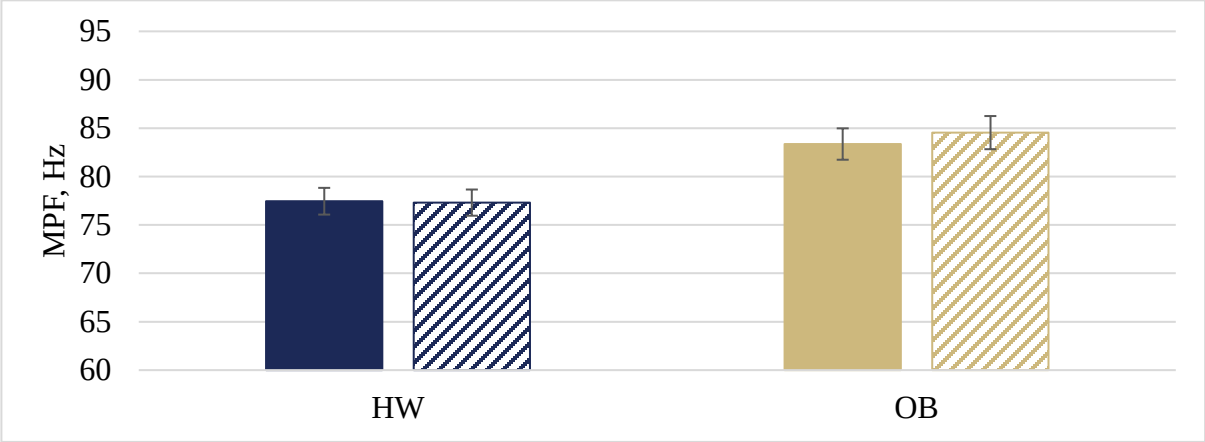

II.

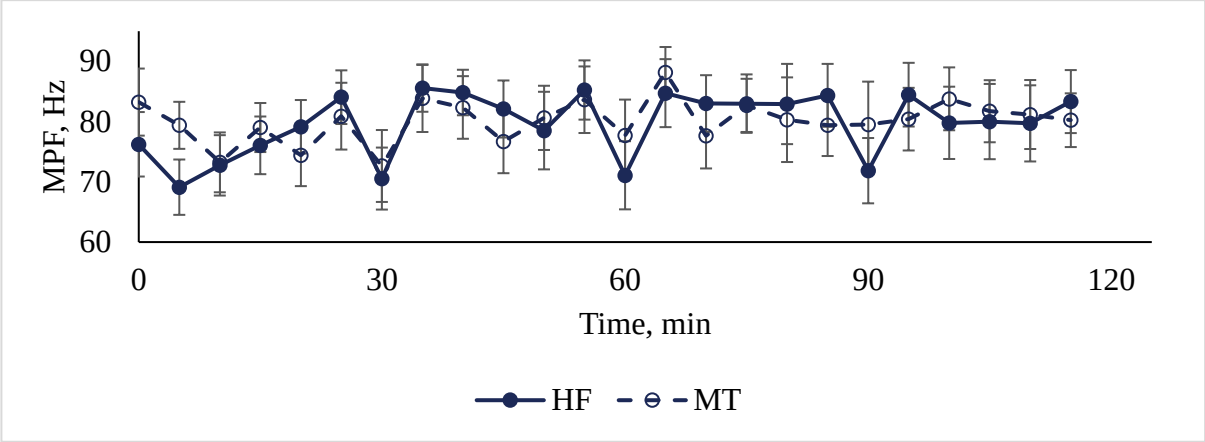

III.

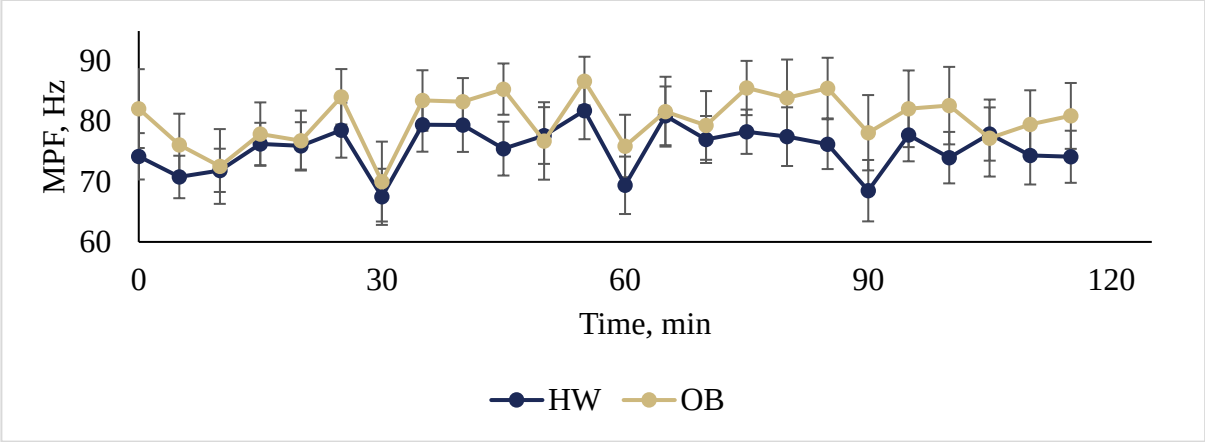

Figure 155: Tibialis Anterior MPF between BMI groups, split into flooring conditions (I), and over time, split between flooring conditions (II) and BMI groups (III). Error bars are standard error of the mean.

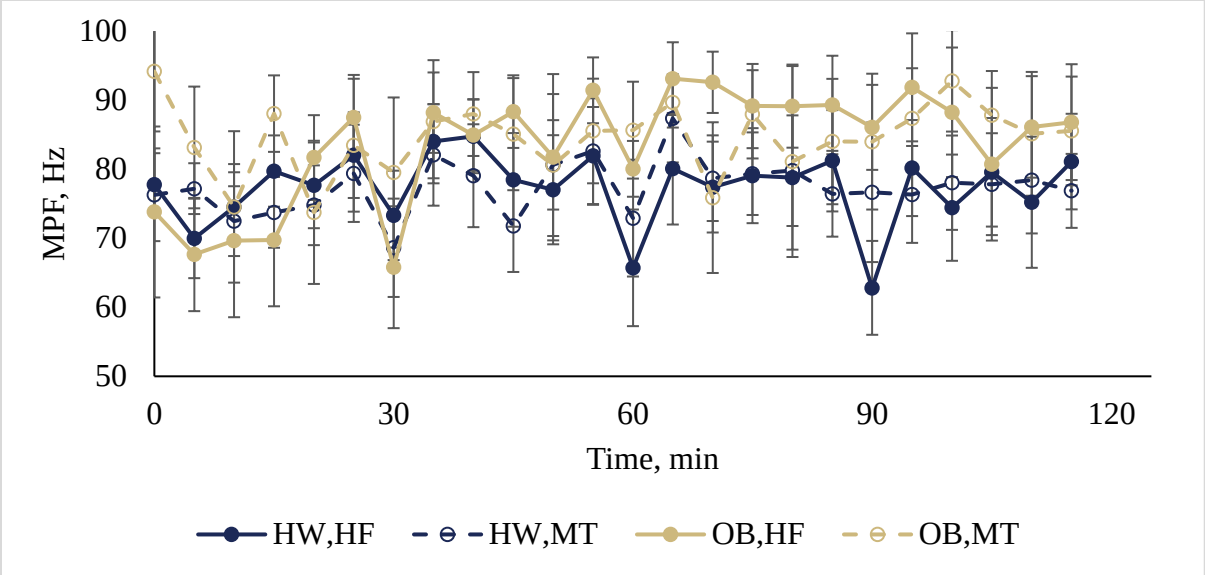

Figure 156: Tibialis Anterior MPF over time, split between BMI groups and flooring conditions. Error bars are standard error of the mean.

Appendix D.1.2 Tibialis Anterior RMS

I.

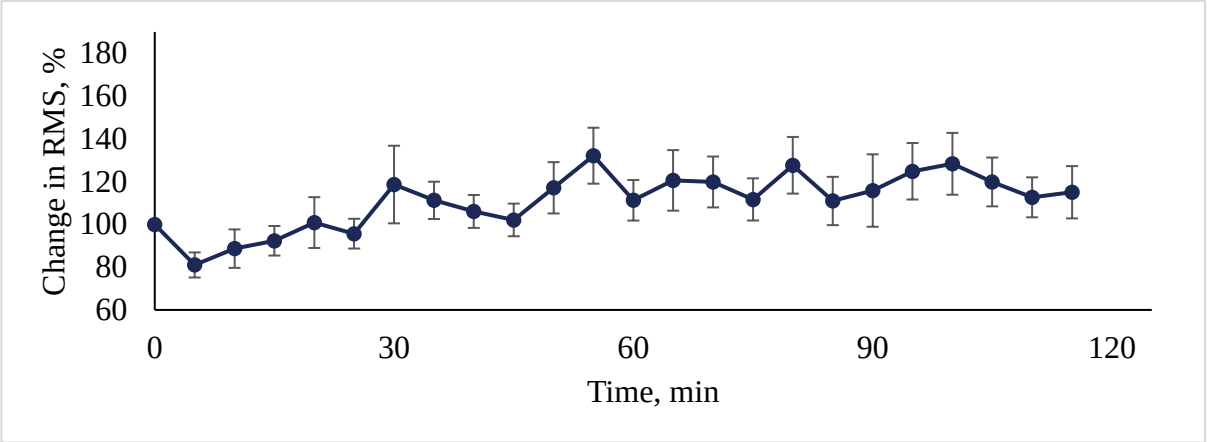

II.

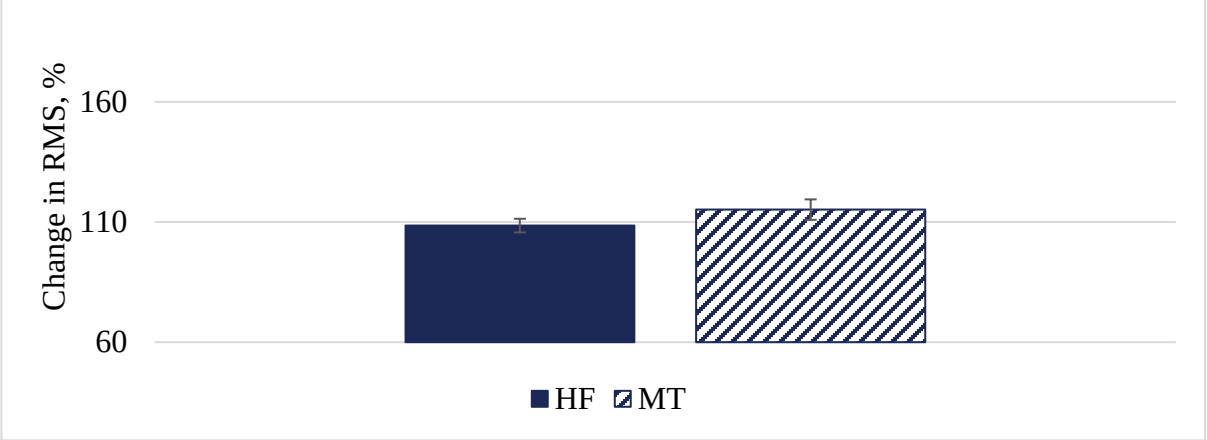

III.

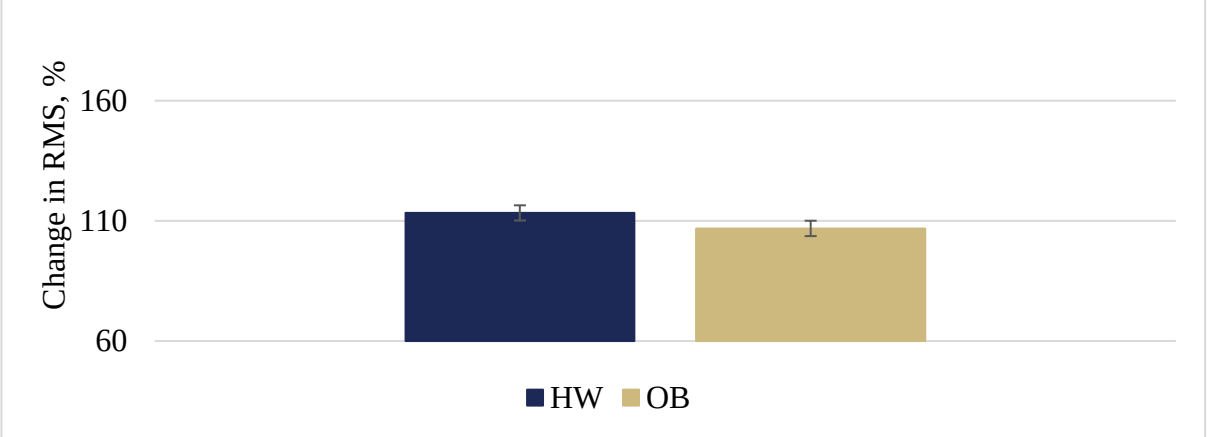

Figure 157: Tibialis Anterior RMS over time (I) and between flooring conditions (II) and BMI groups (III).

Error bars are standard error of the mean.

I.

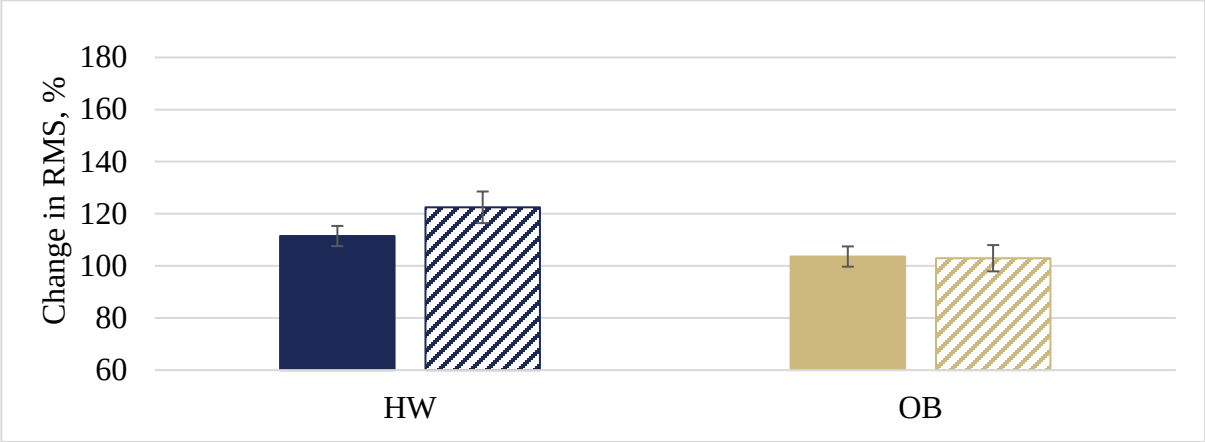

II.

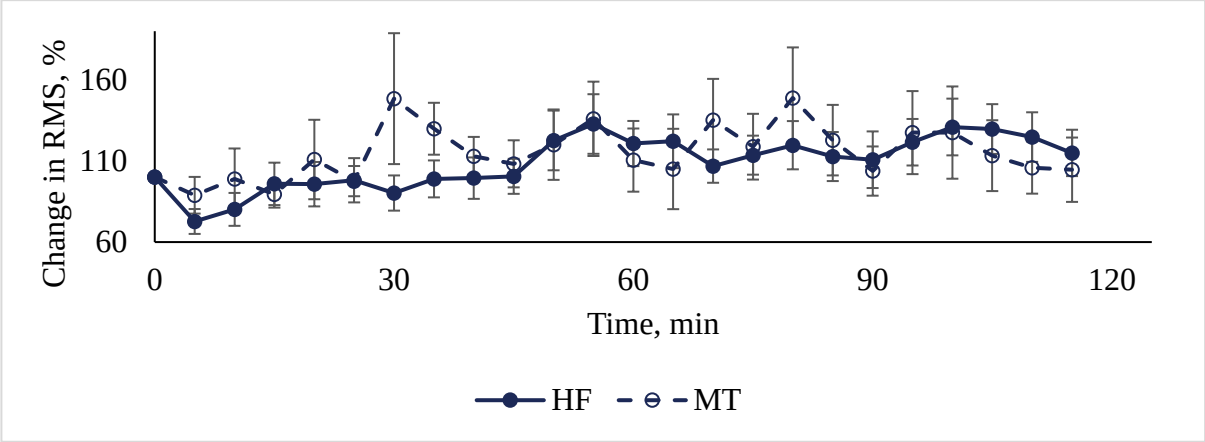

III.

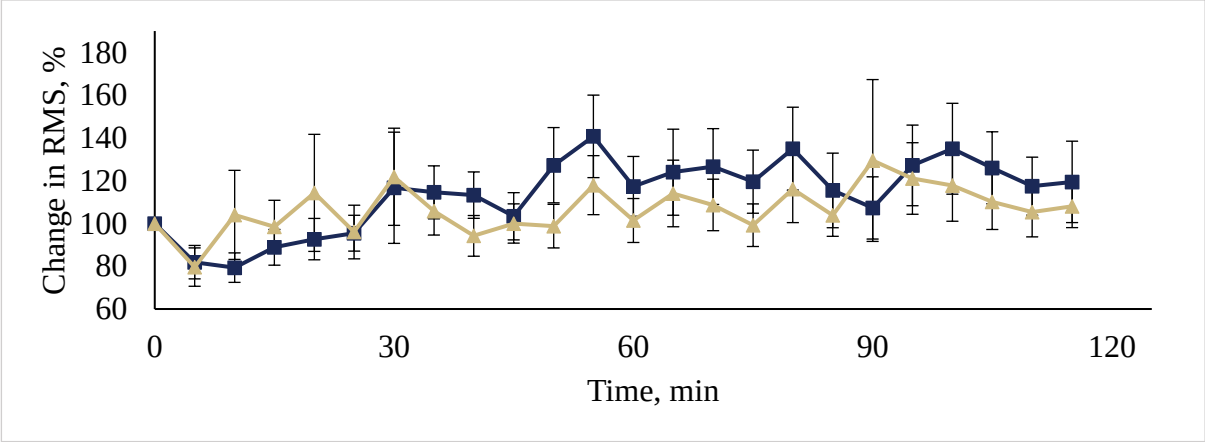

Figure 158: Tibialis Anterior RMS between BMI groups, split into flooring conditions (I), and over time, split between flooring conditions (II) and BMI groups (III). Error bars are standard error of the mean.

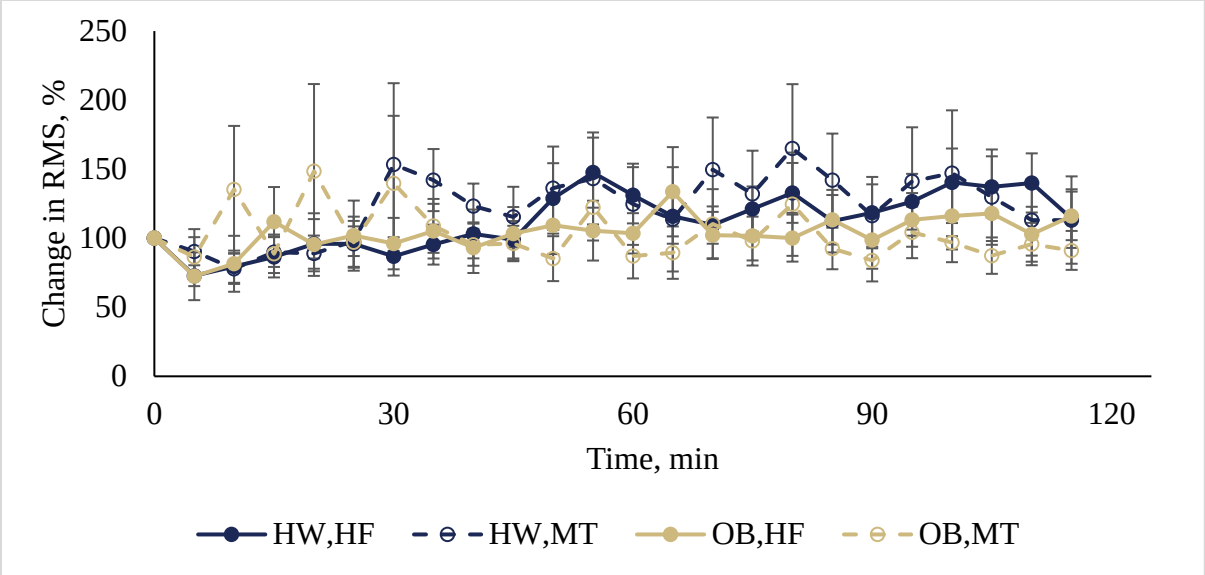

Figure 159: Tibialis Anterior RMS over time, split between BMI groups and flooring conditions. Error bars are standard error of the mean.

Appendix D.1.3 Gastrocnemius MPF

I.

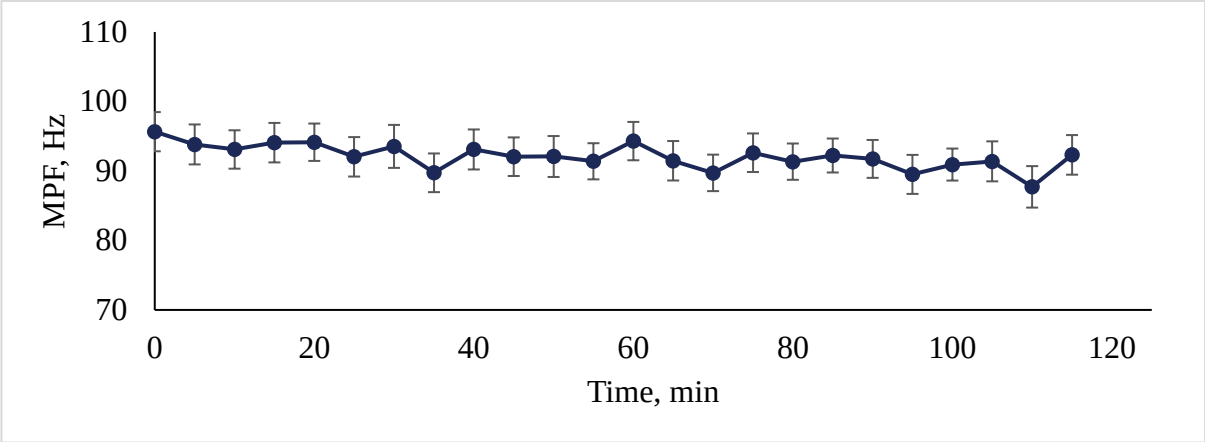

II.

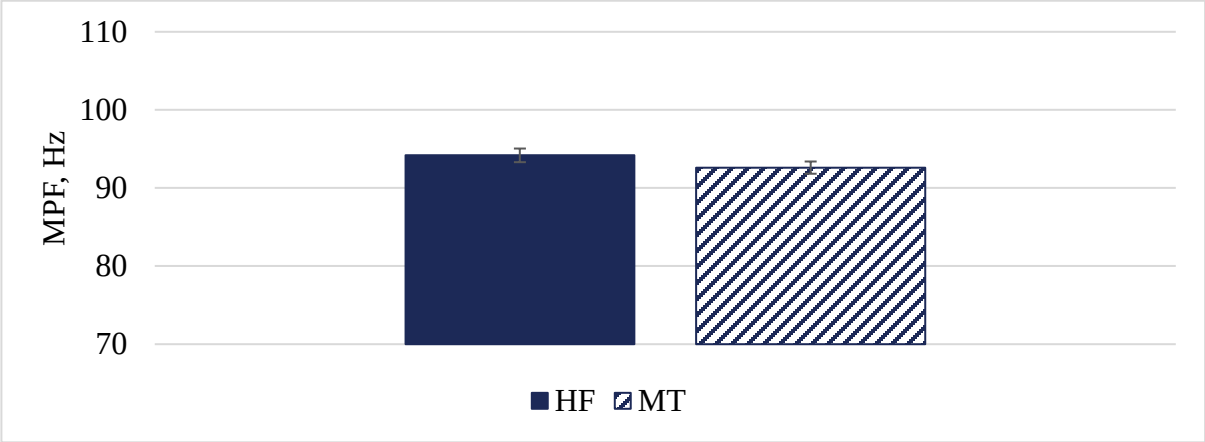

III.

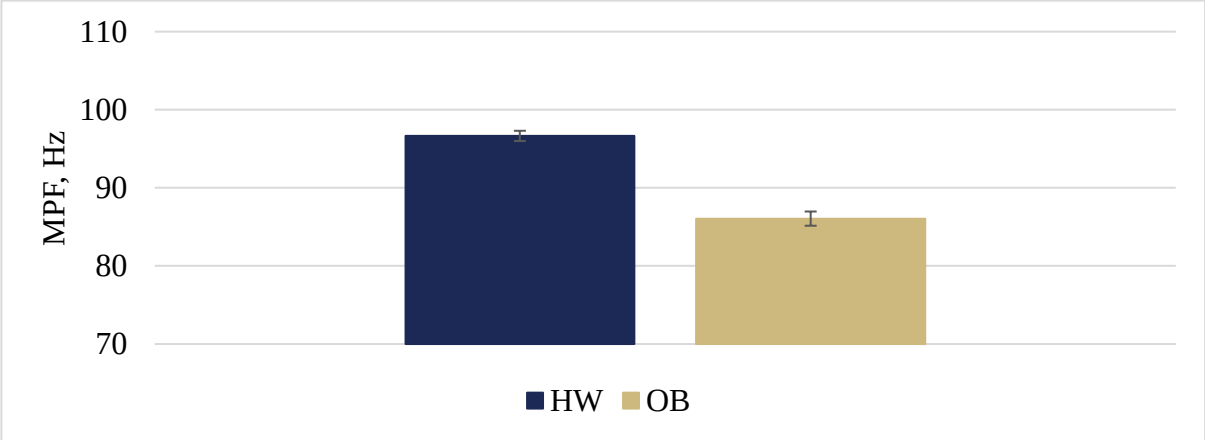

Figure 160: Gastrocnemius MPF over time (I) and between flooring conditions (II) and BMI groups (III). Error bars are standard error of the mean.

I.

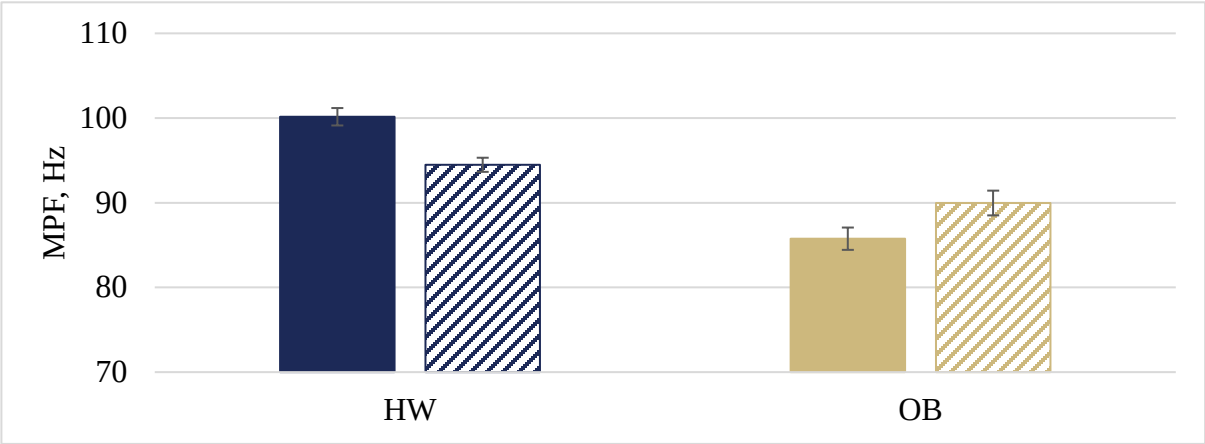

II.

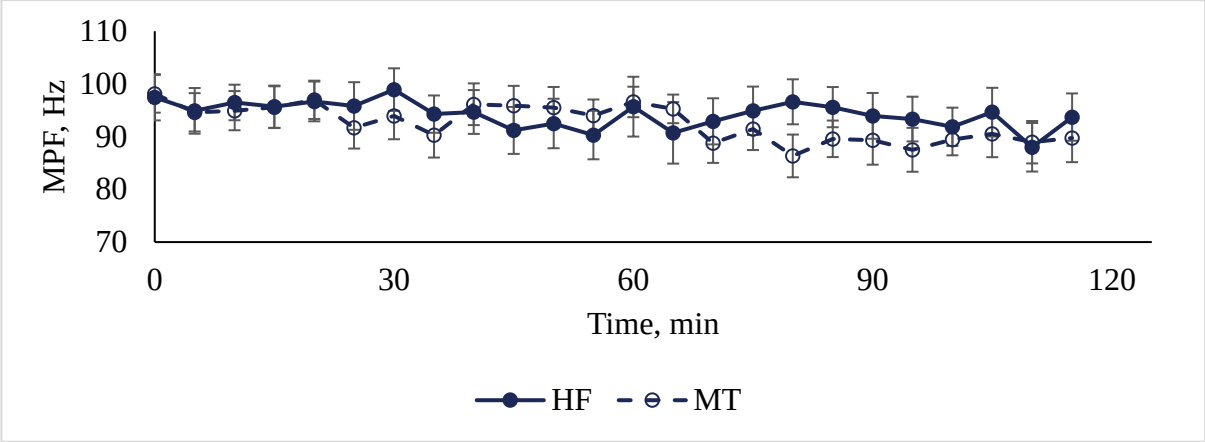

III.

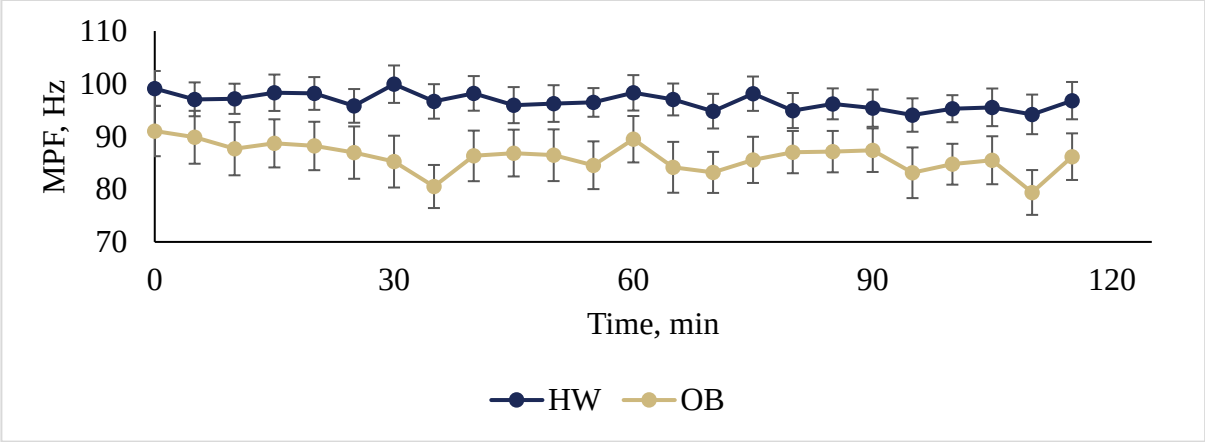

Figure 161: Gastrocnemius MPF between BMI groups, split into flooring conditions (I), and over time, split between flooring conditions (II) and BMI groups (III). Error bars are standard error of the mean.

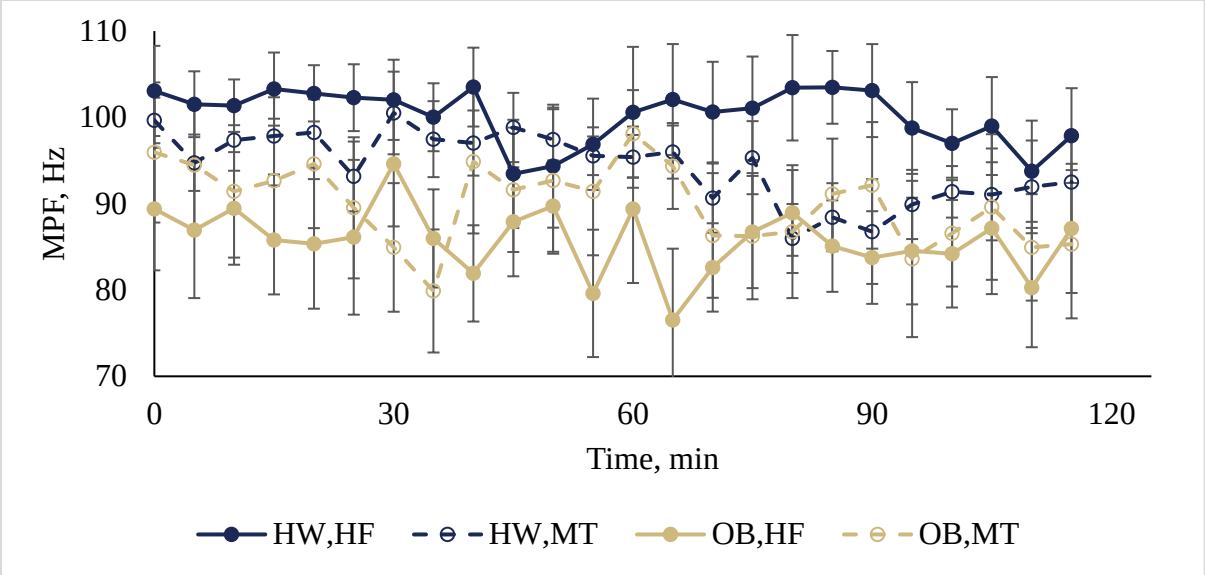

Figure 162: Gastrocnemius MPF over time, split between BMI groups and flooring conditions. Error bars are standard error of the mean.

Appendix D.1.4 Gastrocnemius RMS

I.

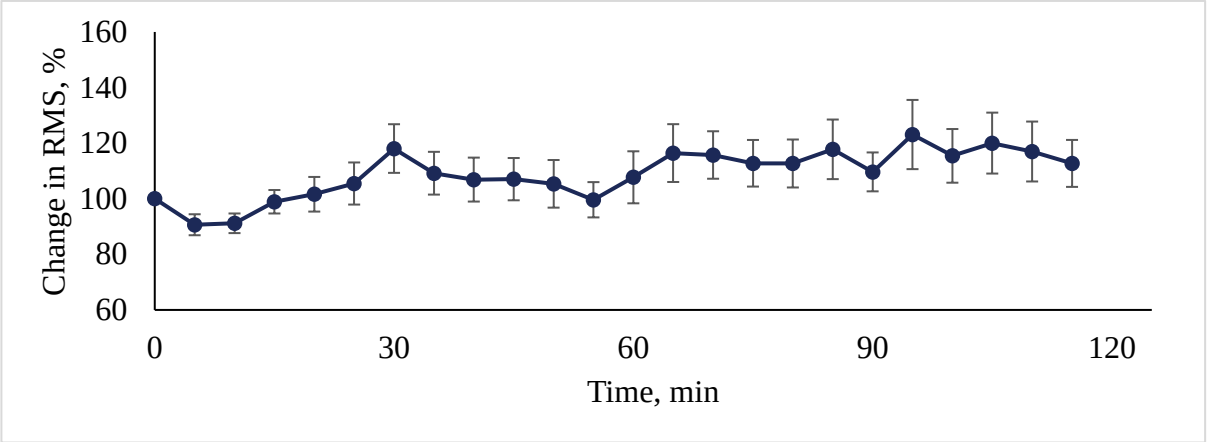

II.

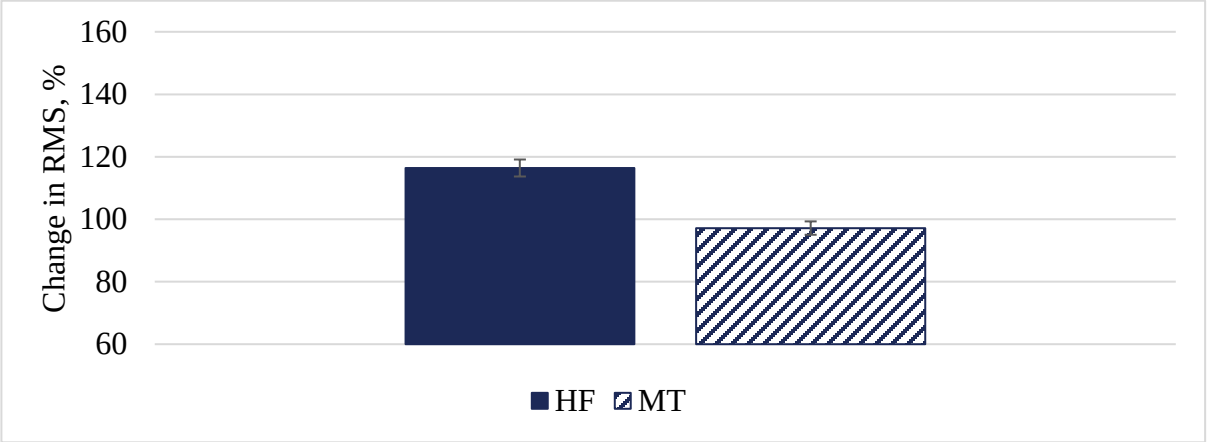

III.

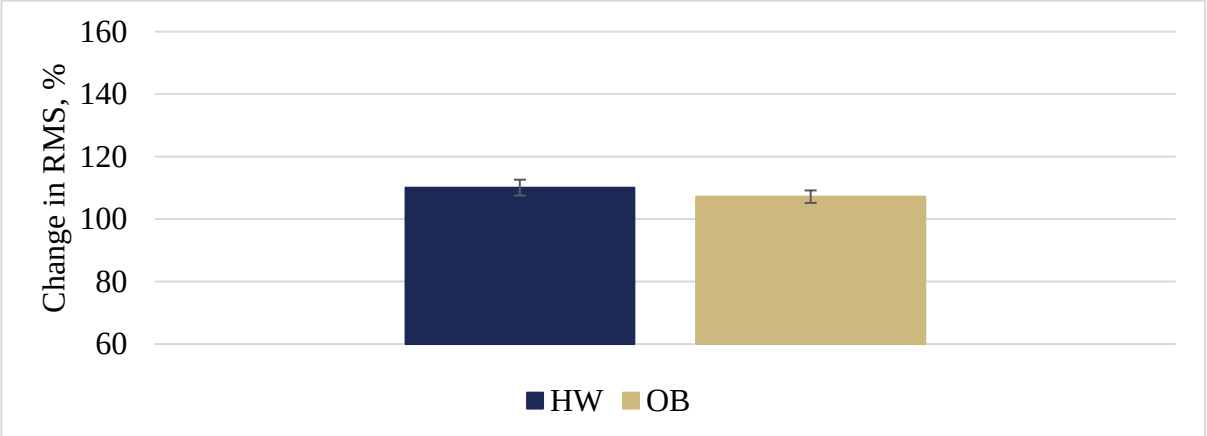

Figure 163: Gastrocnemius RMS over time (I) and between flooring conditions (II) and BMI groups (III). Error bars are standard error of the mean.

I.

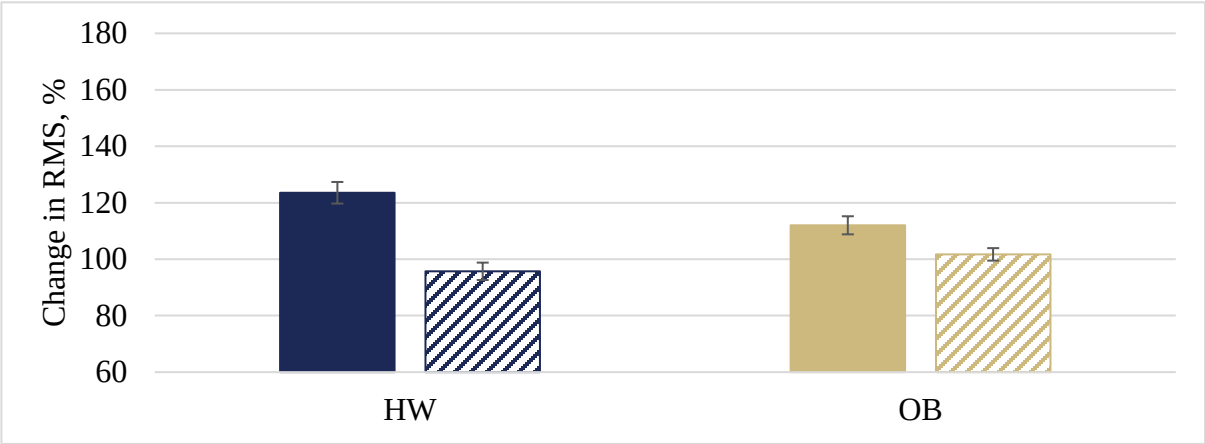

II.

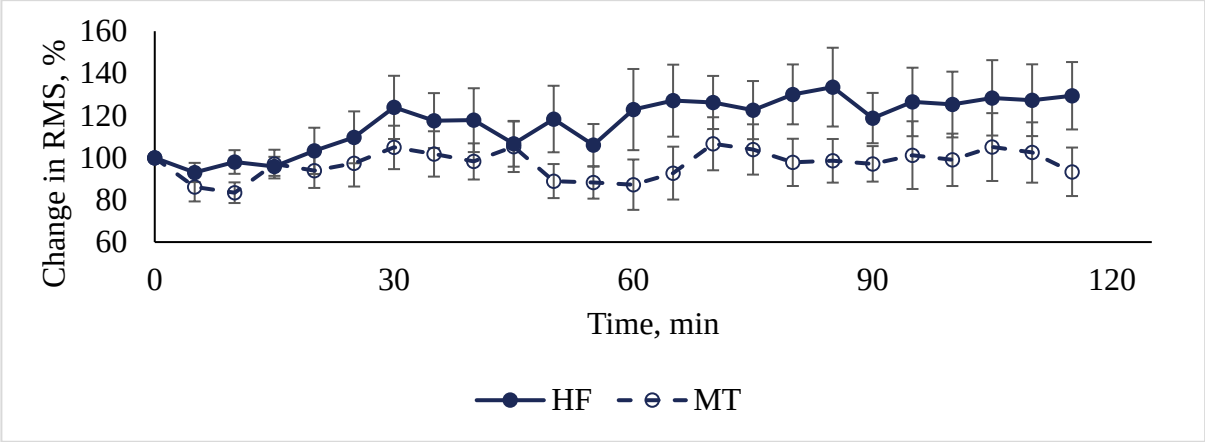

III.

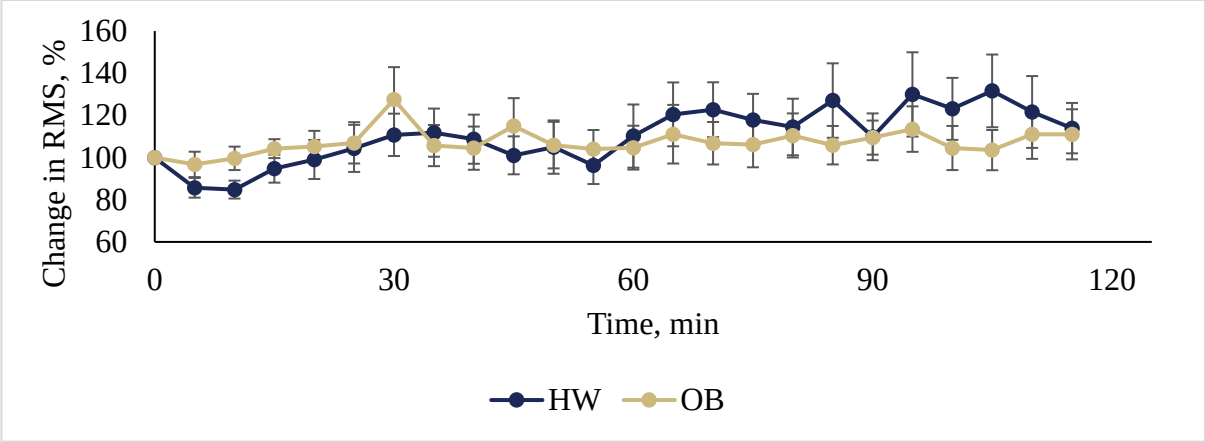

Figure 164: Gastrocnemius RMS between BMI groups, split into flooring conditions (I), and over time, split between flooring conditions (II) and BMI groups (III). Error bars are standard error of the mean.

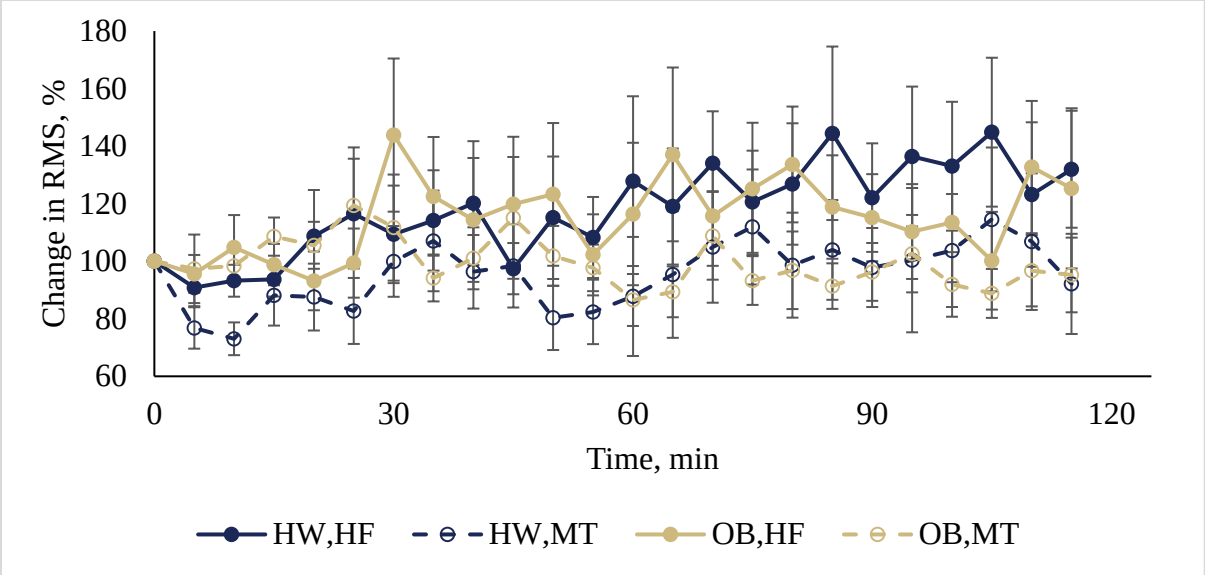

Figure 165: Gastrocnemius RMS over time, split between BMI groups and flooring conditions. Error bars are standard error of the mean.

Appendix D.1.5 Soleus MPF

I.

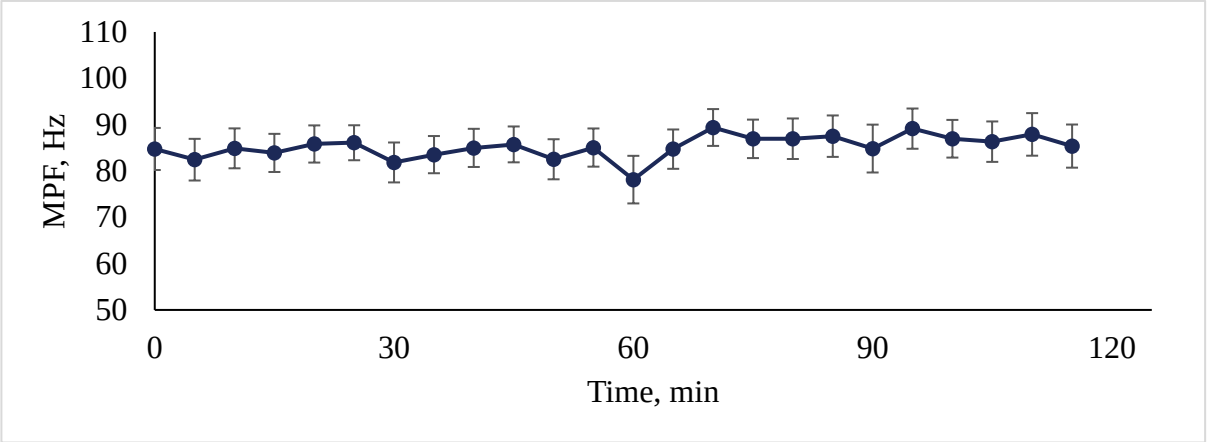

II.

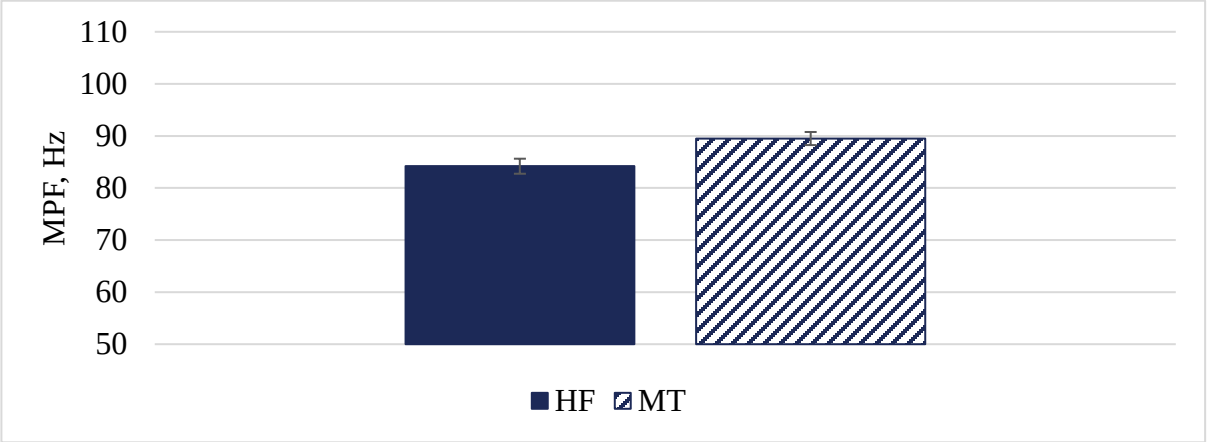

III.

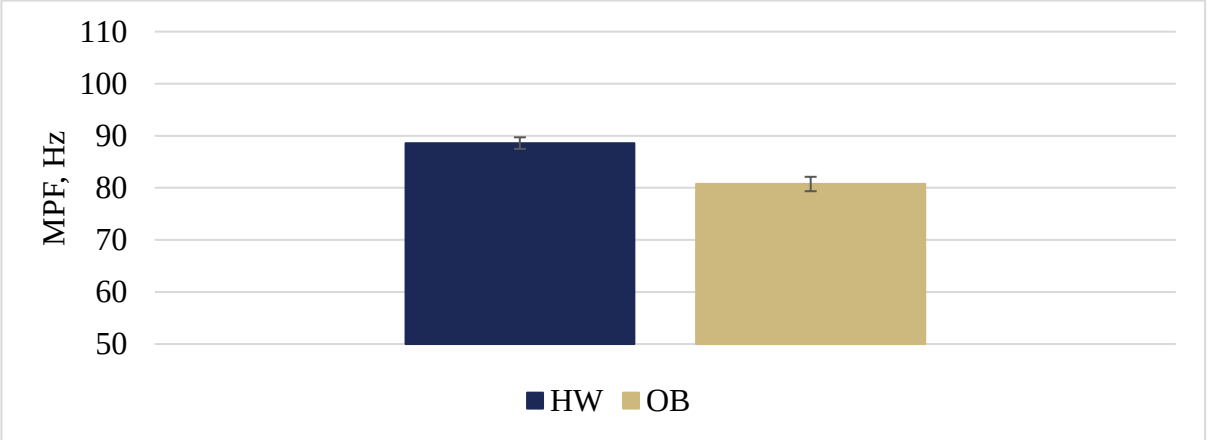

Figure 166: Soleus MPF over time (I) and between flooring conditions (II) and BMI groups (III). Error bars are standard error of the mean.

I.

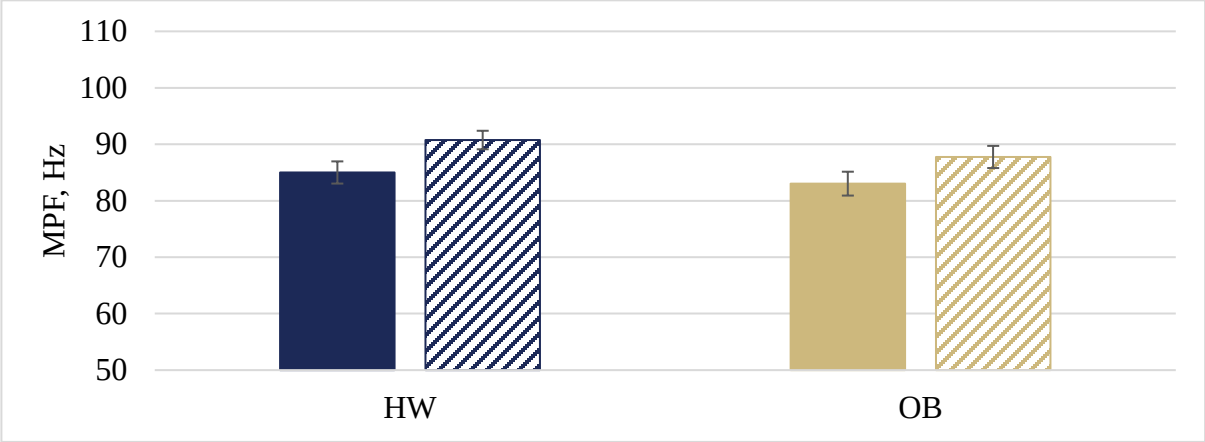

II.

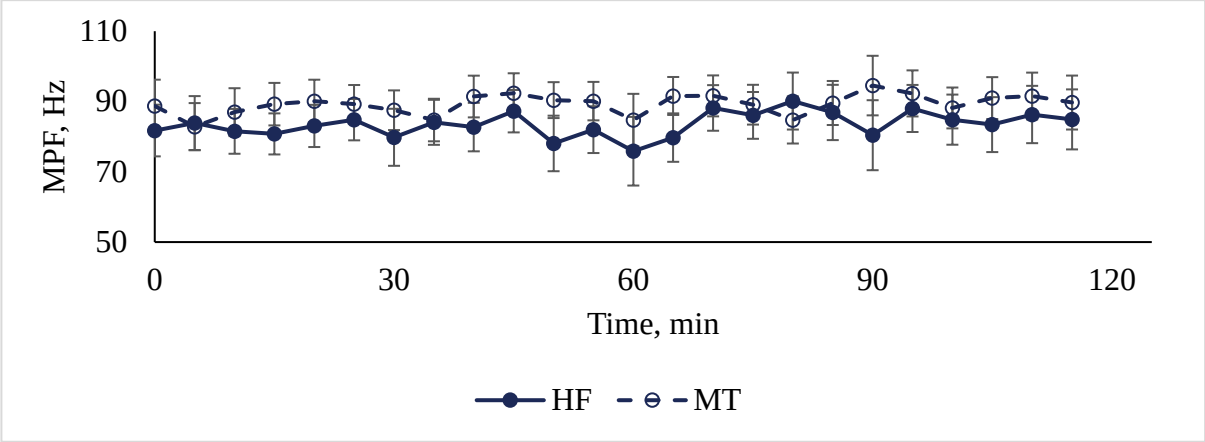

III.

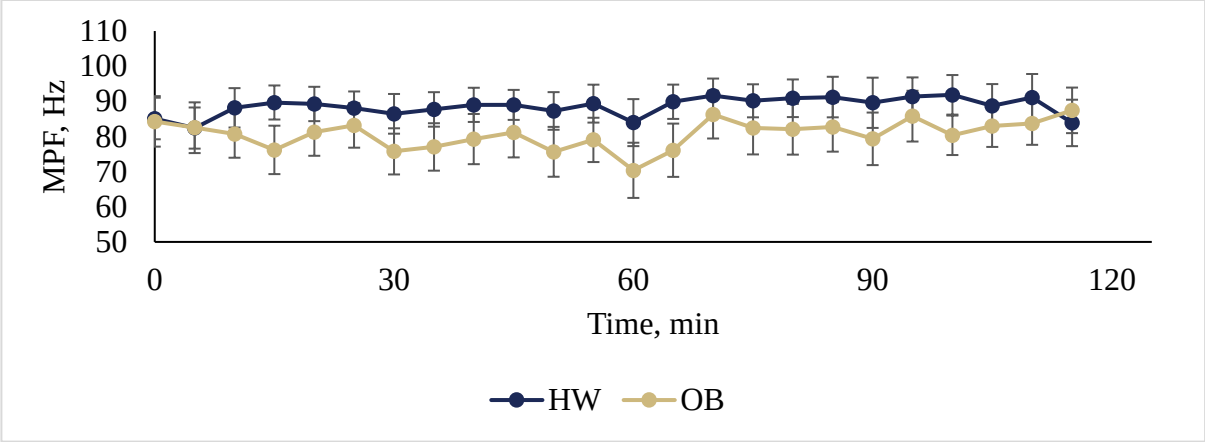

Figure 167: Soleus MPF between BMI groups, split into flooring conditions (I), and over time, split between flooring conditions (II) and BMI groups (III). Error bars are standard error of the mean.

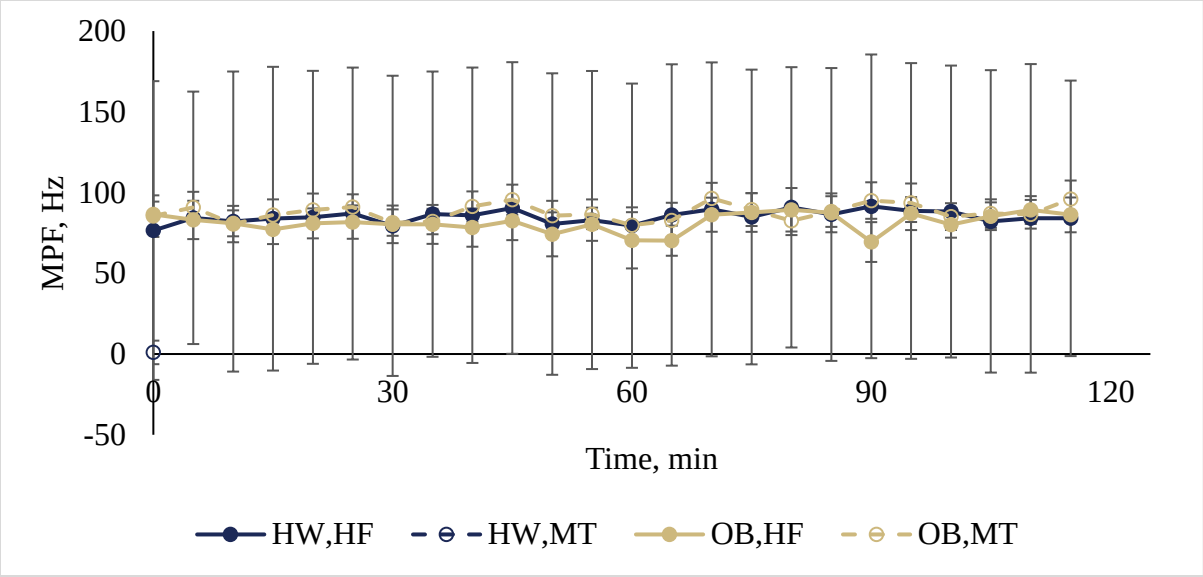

Figure 168: Soleus MPF over time, split between BMI groups and flooring conditions. Error bars are standard error of the mean.

Appendix D.1.6 Soleus RMS

I.

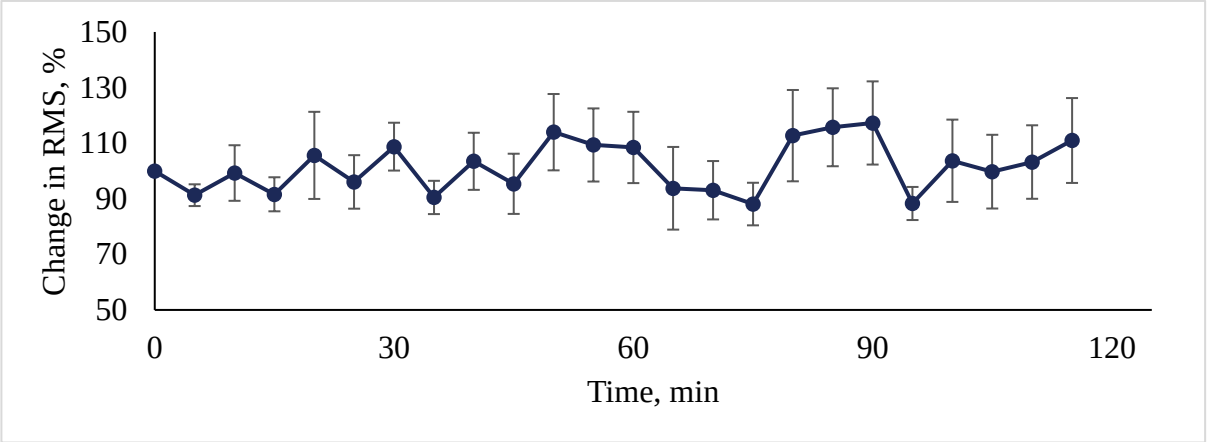

II.

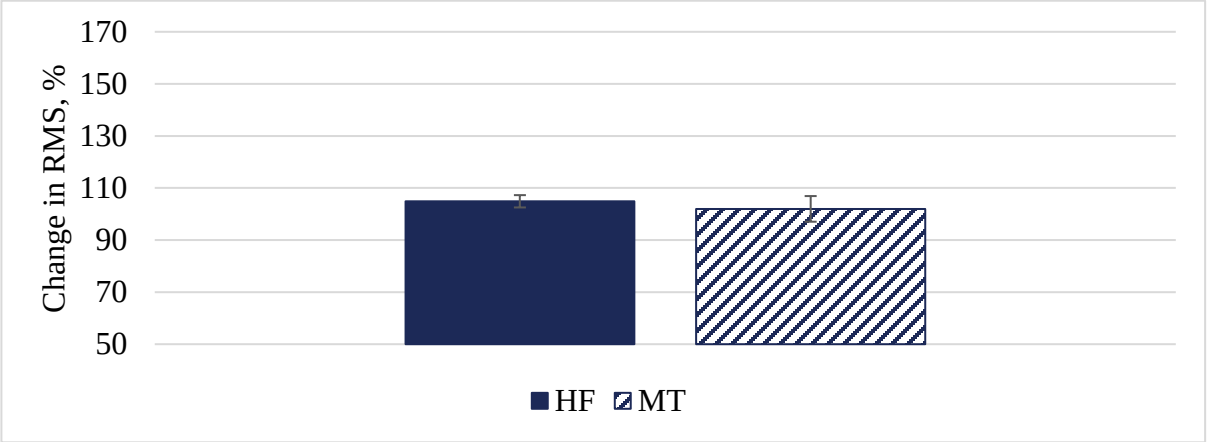

III.

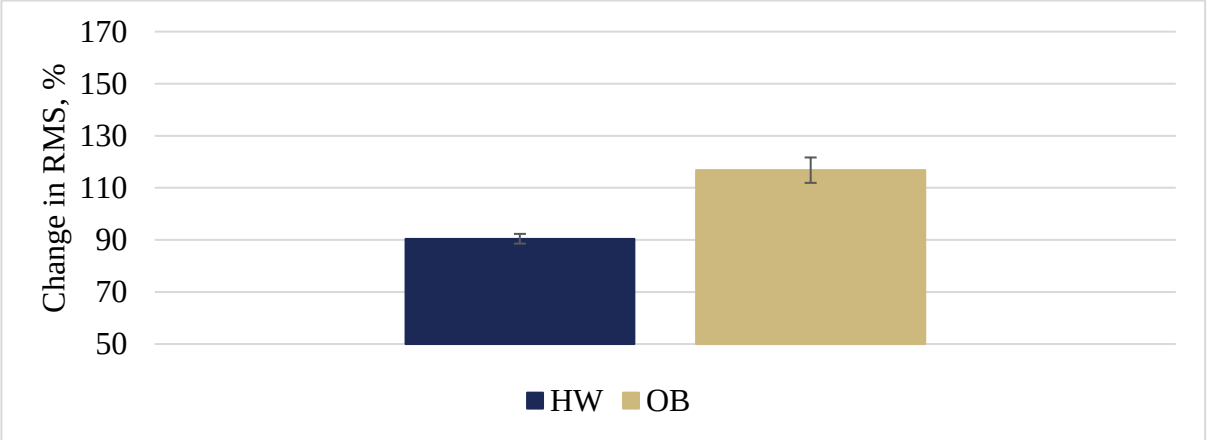

Figure 169: Soleus RMS over time (I) and between flooring conditions (II) and BMI groups (III). Error bars are standard error of the mean.

I.

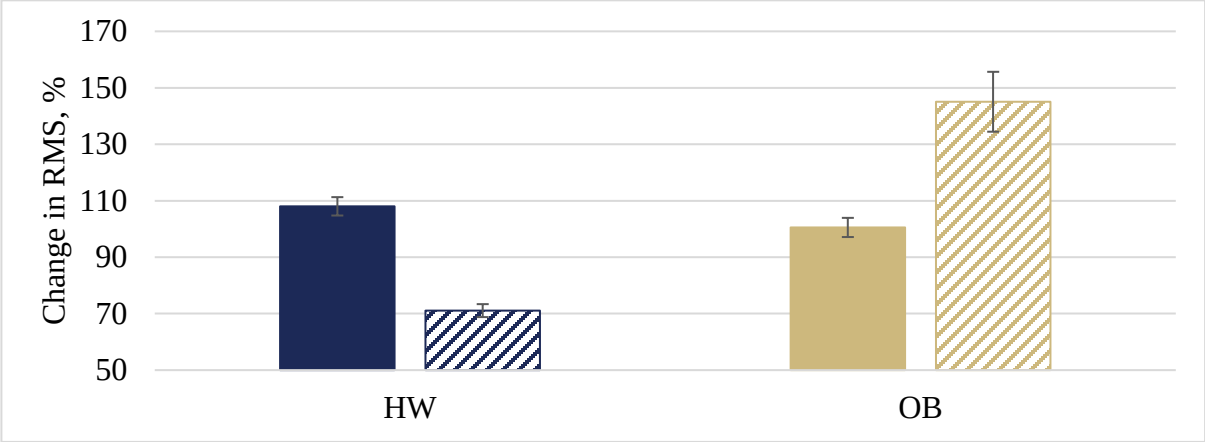

II.

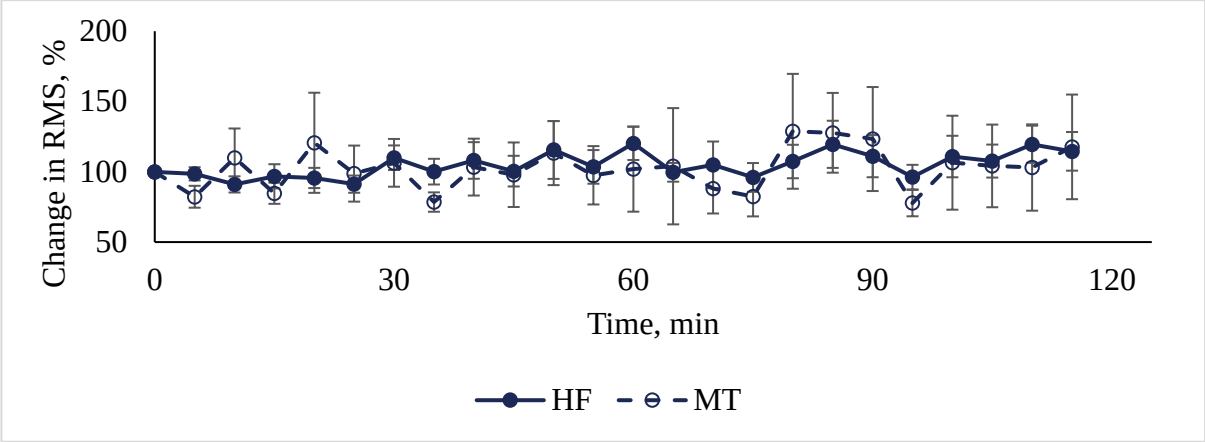

III.

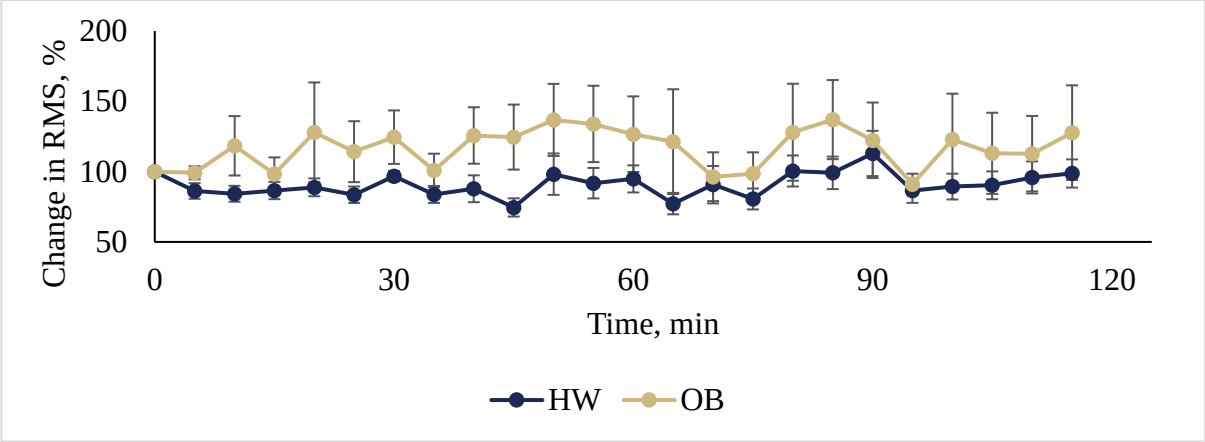

Figure 170: Soleus RMS between BMI groups, split into flooring conditions (I), and over time, split between flooring conditions (II) and BMI groups (III). Error bars are standard error of the mean.

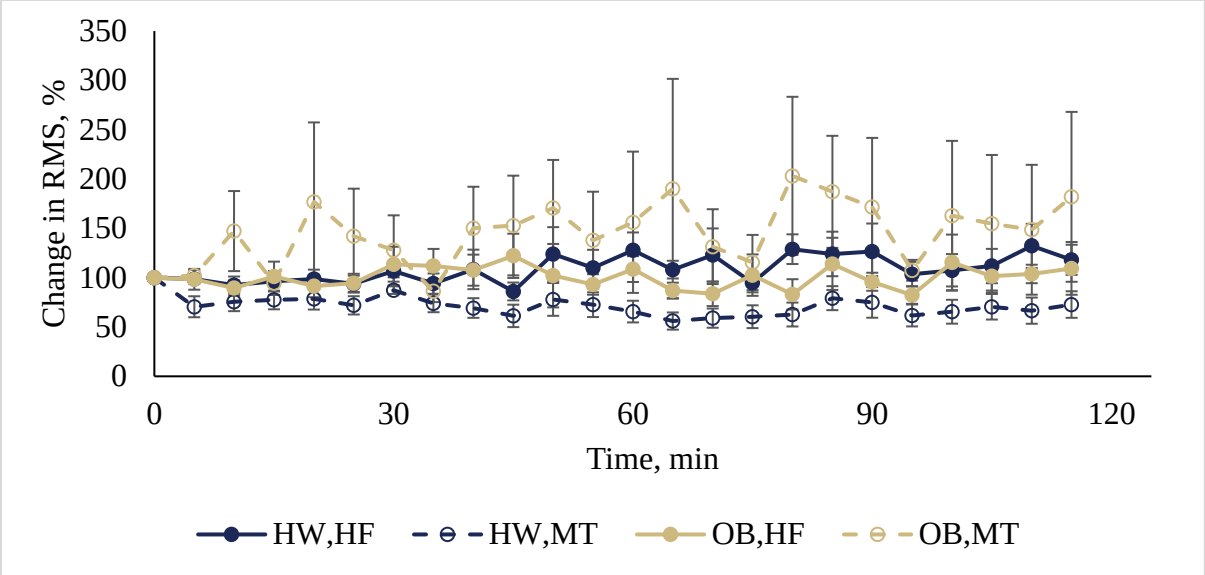

Figure 171: Soleus RMS over time, split between BMI groups and flooring conditions. Error bars are standard error of the mean.

Appendix D.1.7 Rectus Femoris MPF

I.

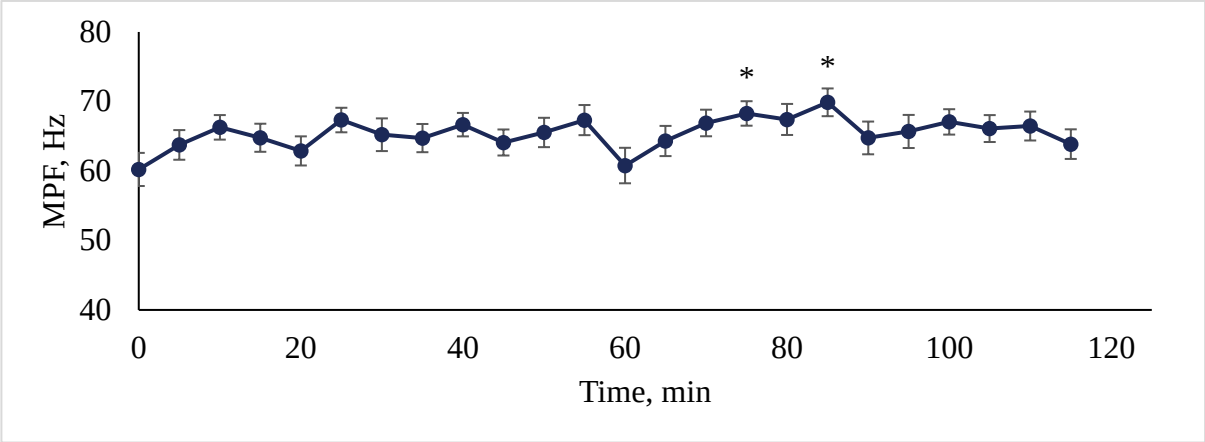

II.

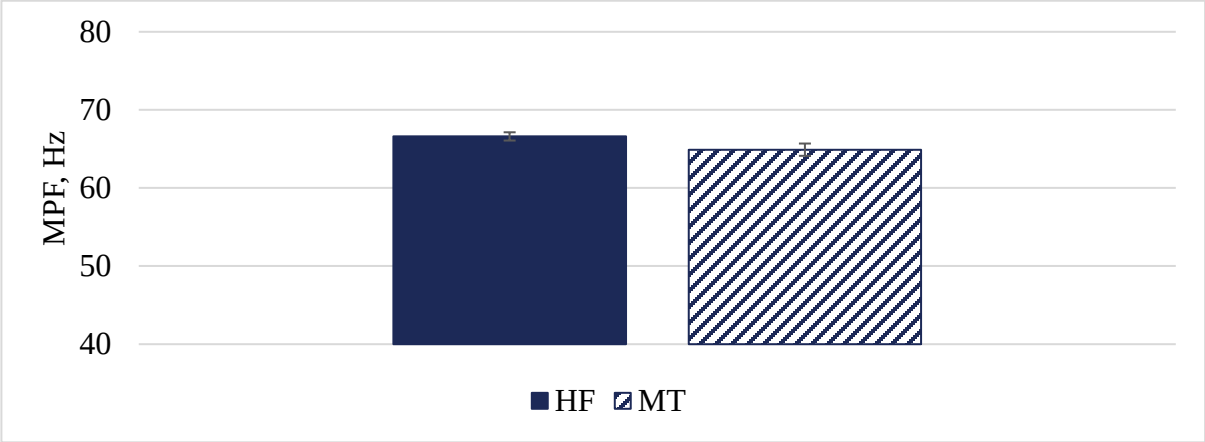

III.

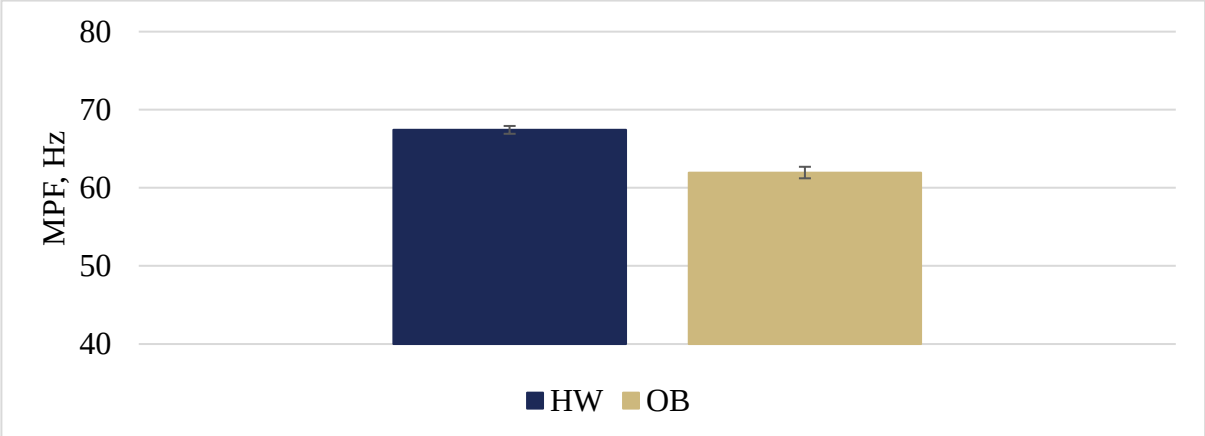

Figure 172: Rectus Femoris MPF over time (I) and between flooring conditions (II) and BMI groups (III). Error bars are standard error of the mean.

I.

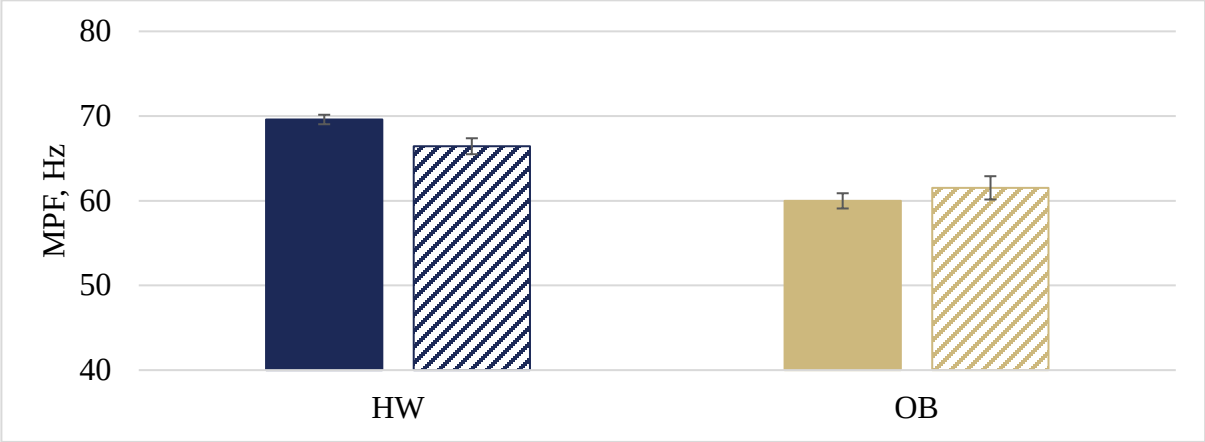

II.

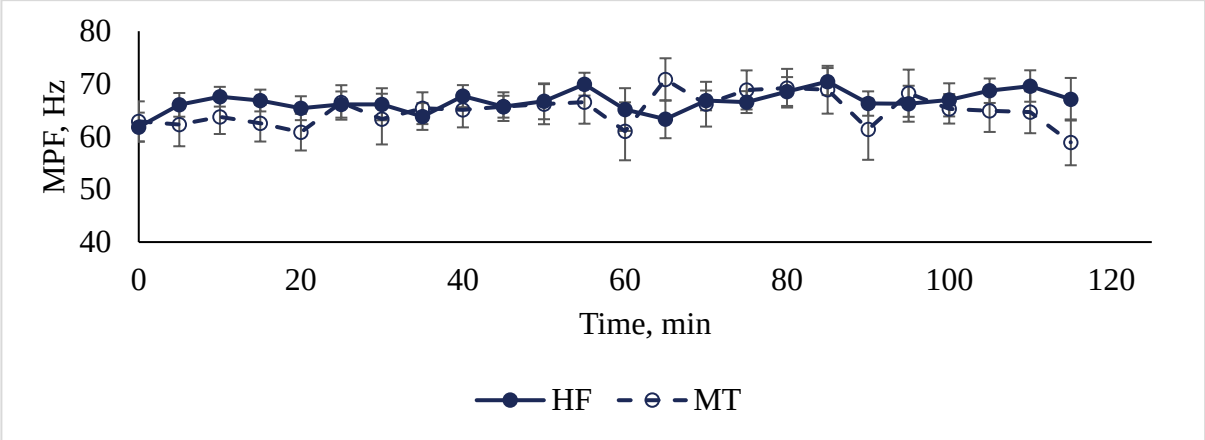

III.

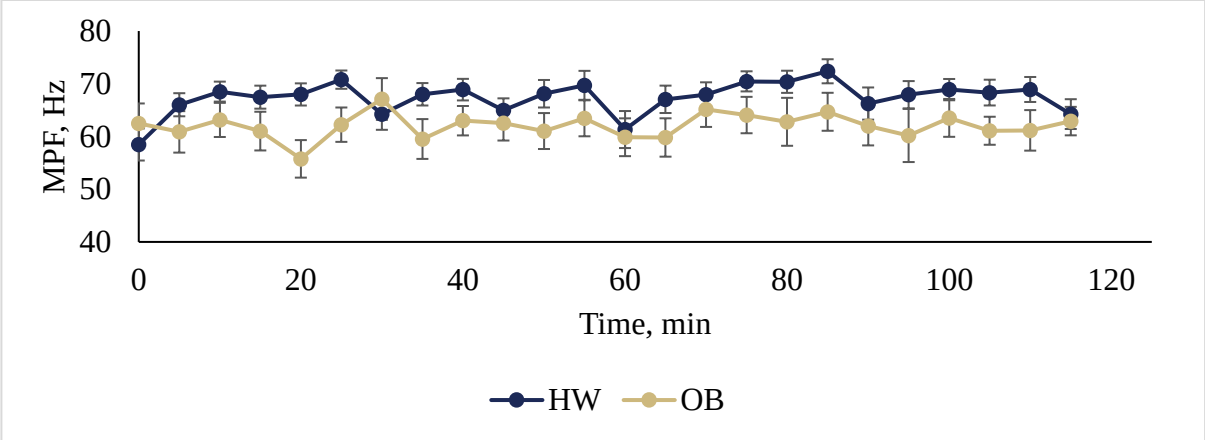

Figure 173: Rectus Femoris MPF between BMI groups, split into flooring conditions (I), and over time, split between flooring conditions (II) and BMI groups (III). Error bars are standard error of the mean.

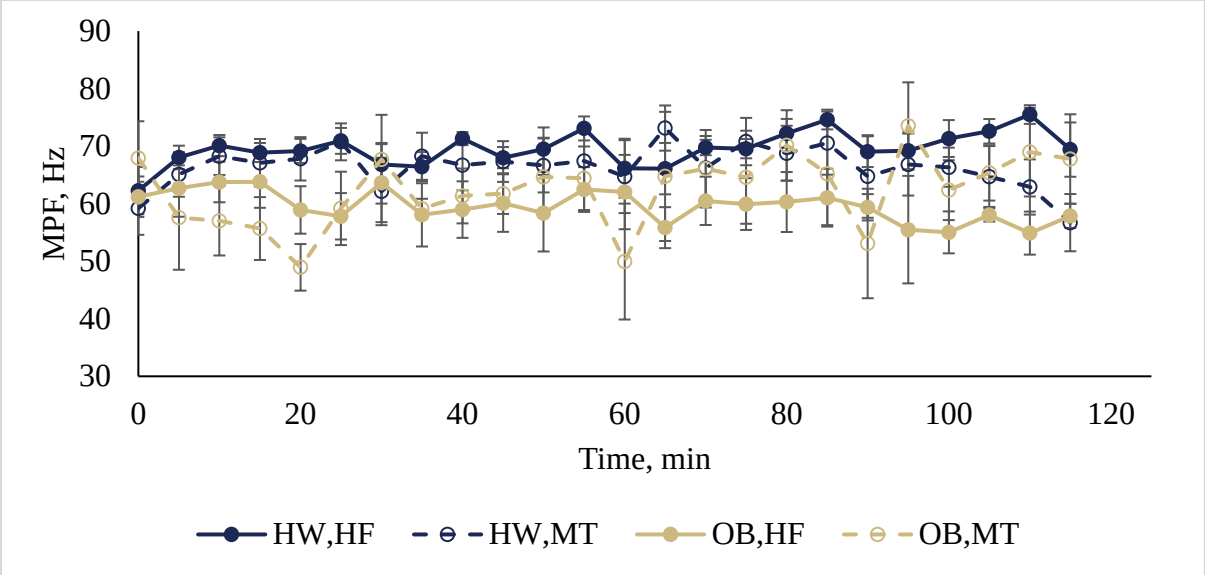

Figure 174: Rectus Femoris MPF over time, split between BMI groups and flooring conditions. Error bars are standard error of the mean.

Appendix D.1.8 Rectus Femoris RMS

I.

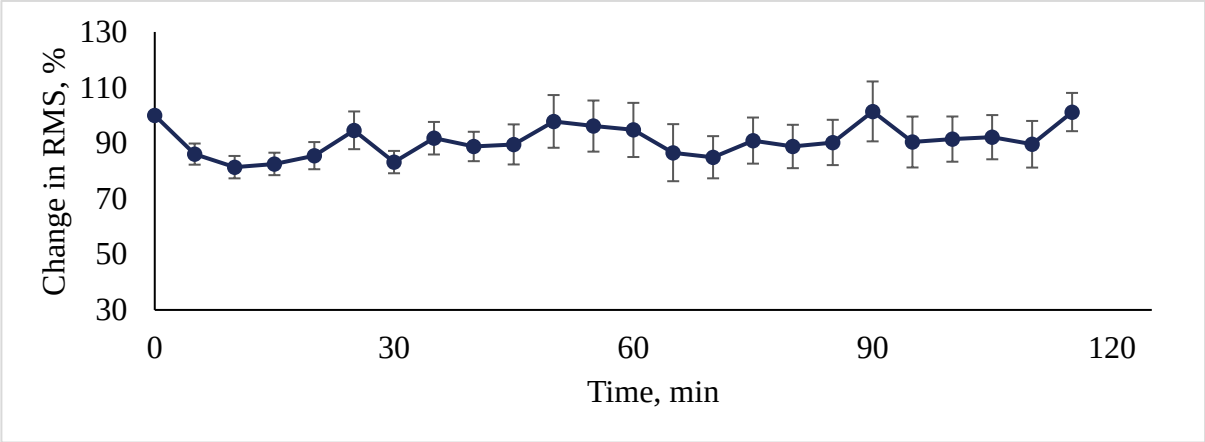

II.

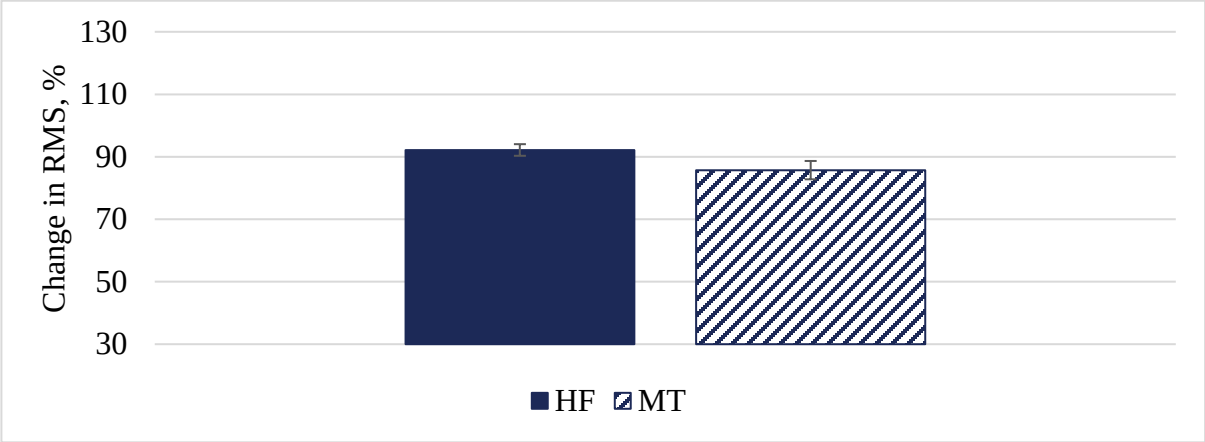

III.

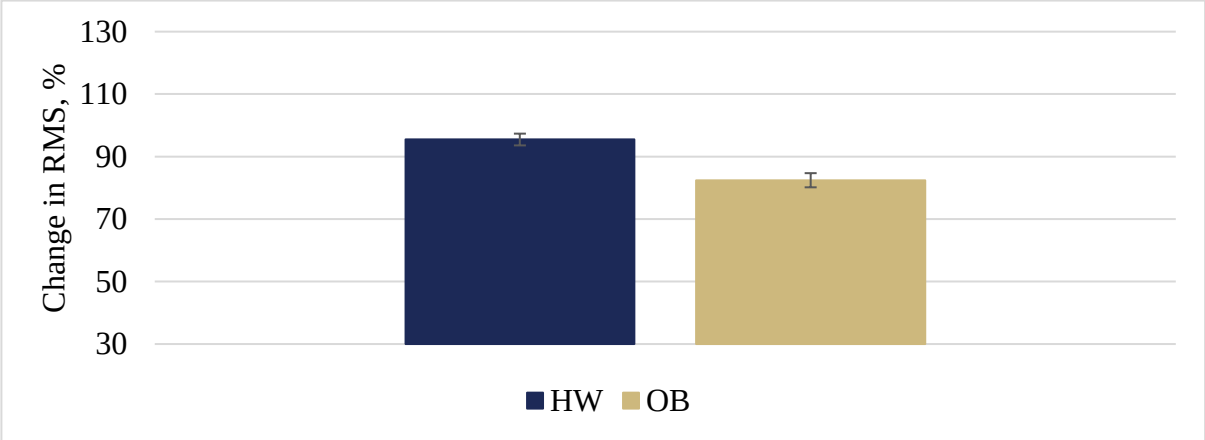

Figure 175: Rectus Femoris RMS over time (I) and between flooring conditions (II) and BMI groups (III). Error bars are standard error of the mean.

I.

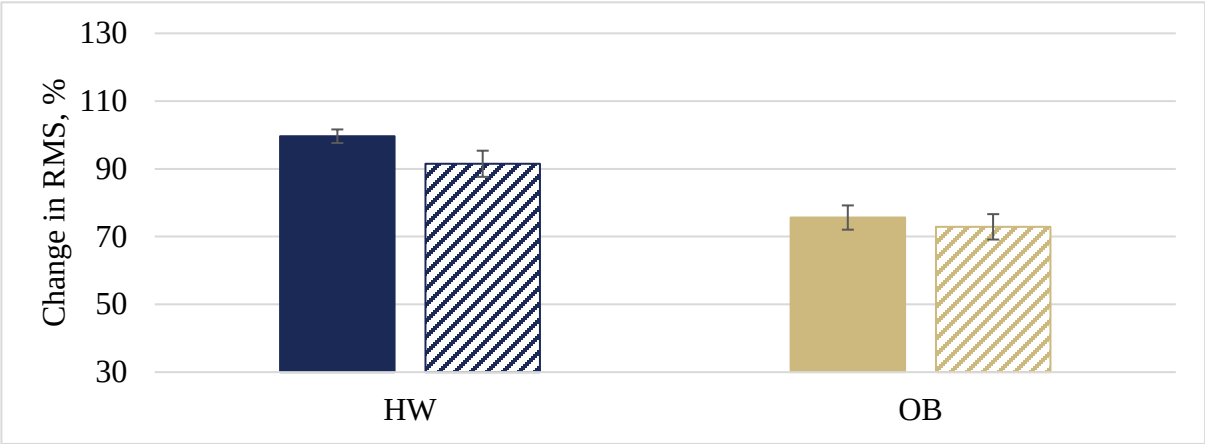

II.

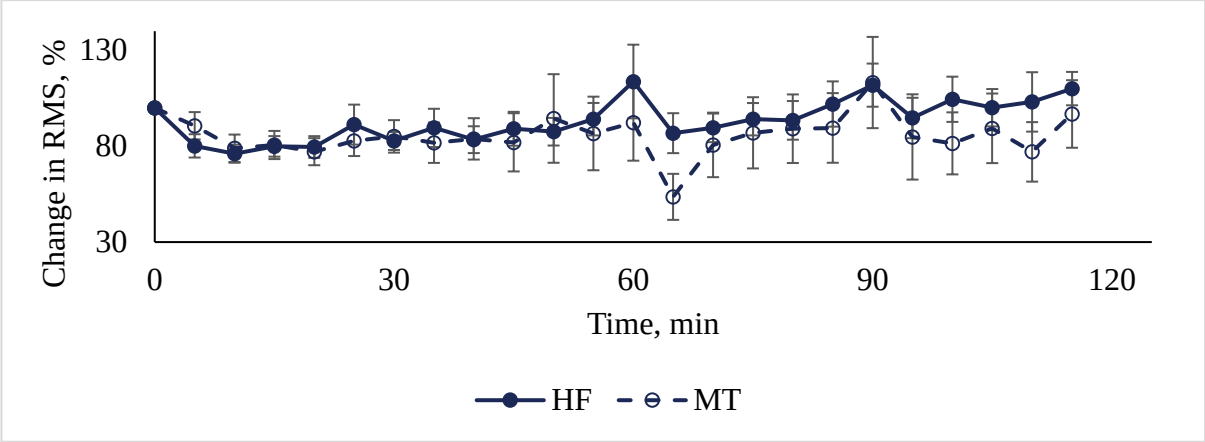

III.

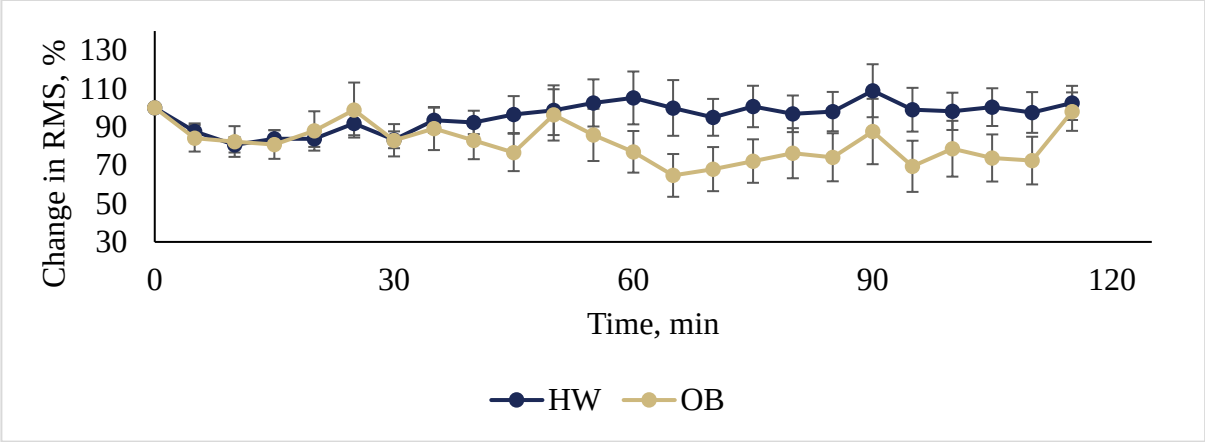

Figure 176: Rectus Femoris RMS between BMI groups, split into flooring conditions (I), and over time, split between flooring conditions (II) and BMI groups (III). Error bars are standard error of the mean.

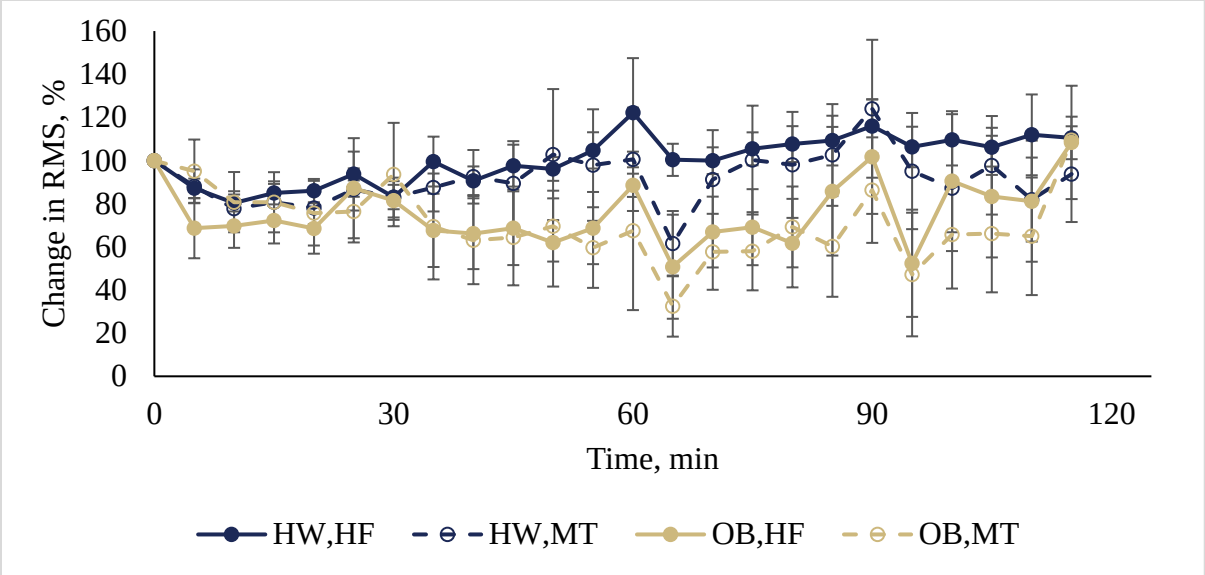

Figure 177: Rectus Femoris RMS over time, split between BMI groups and flooring conditions. Error bars are standard error of the mean.

Appendix D.1.9 Hamstring MPF

I.

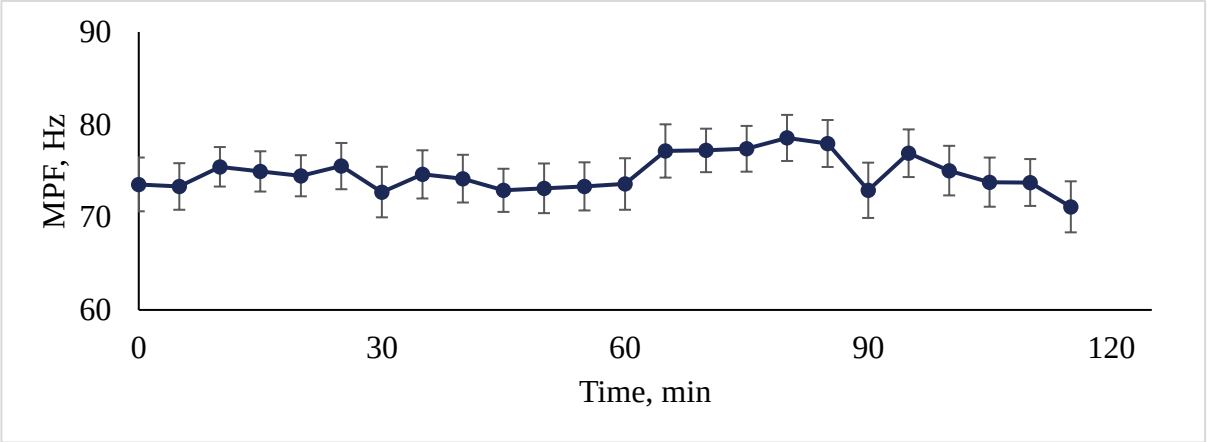

II.

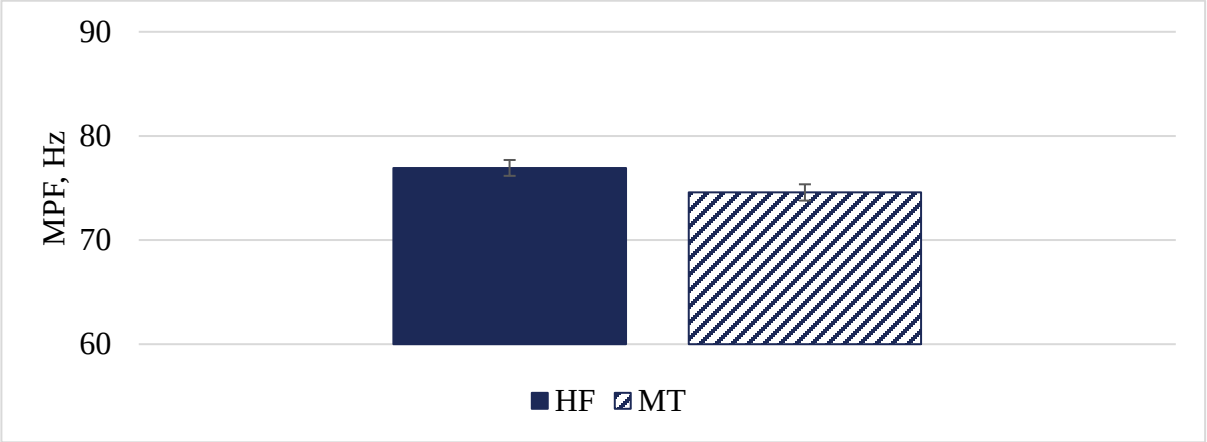

III.

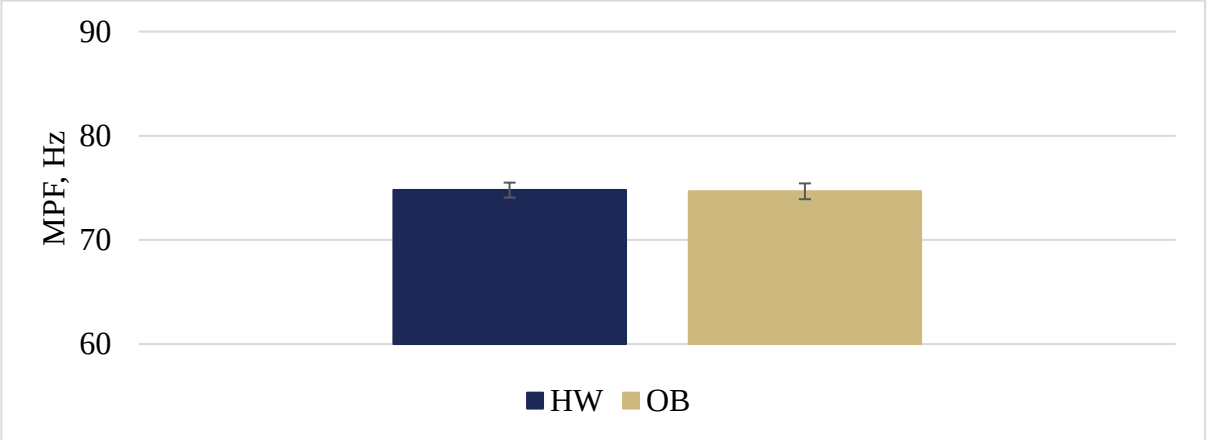

Figure 178: Hamstring MPF over time (I) and between flooring conditions (II) and BMI groups (III). Error bars are standard error of the mean.

I.

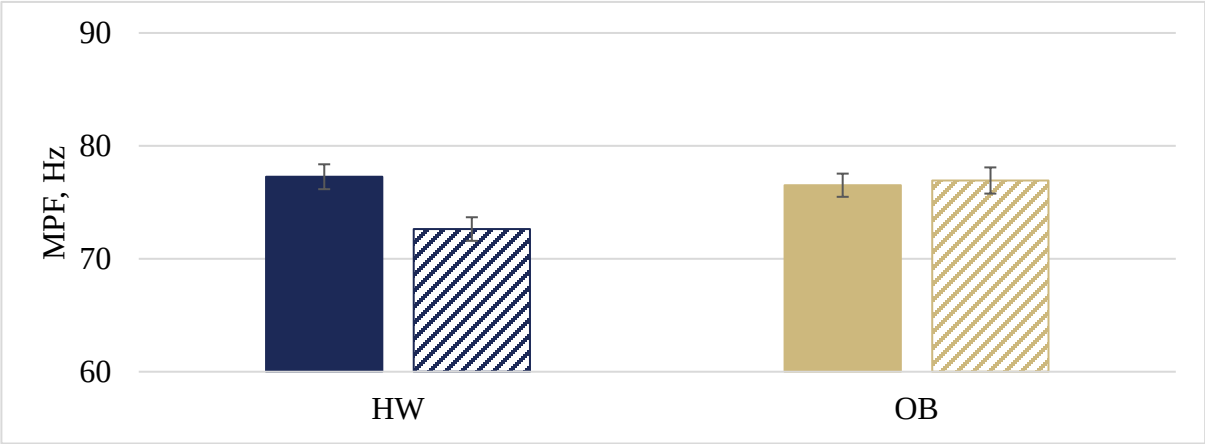

II.

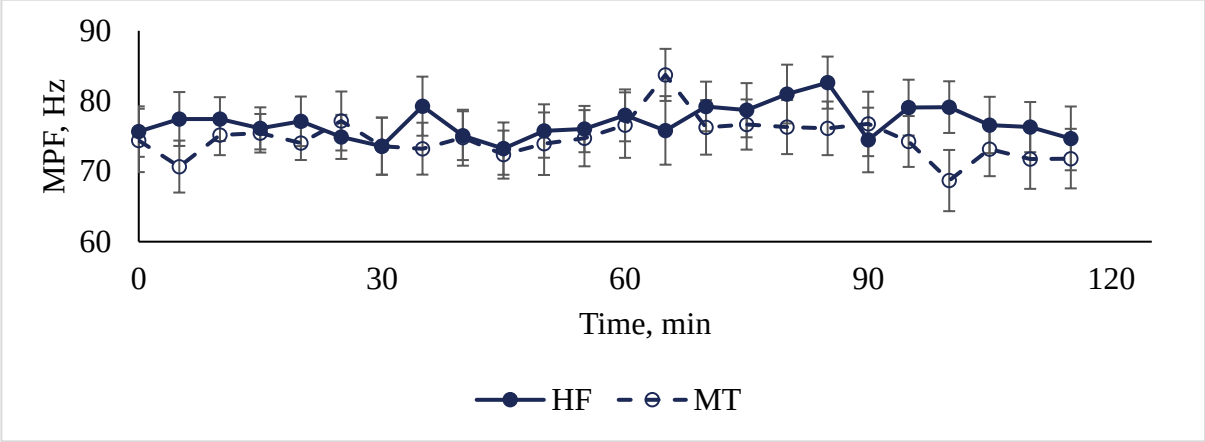

III.

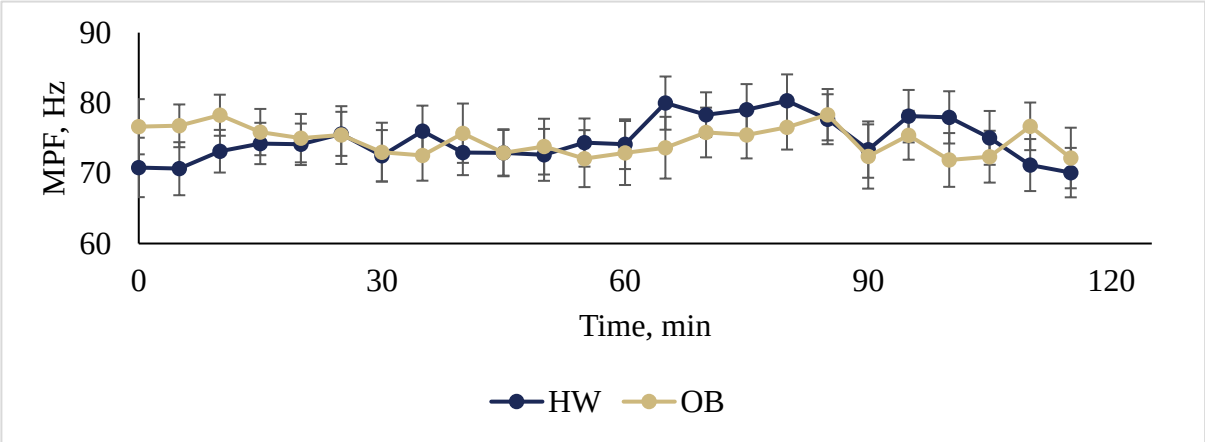

Figure 179: Hamstring MPF between BMI groups, split into flooring conditions (I), and over time, split between flooring conditions (II) and BMI groups (III). Error bars are standard error of the mean.

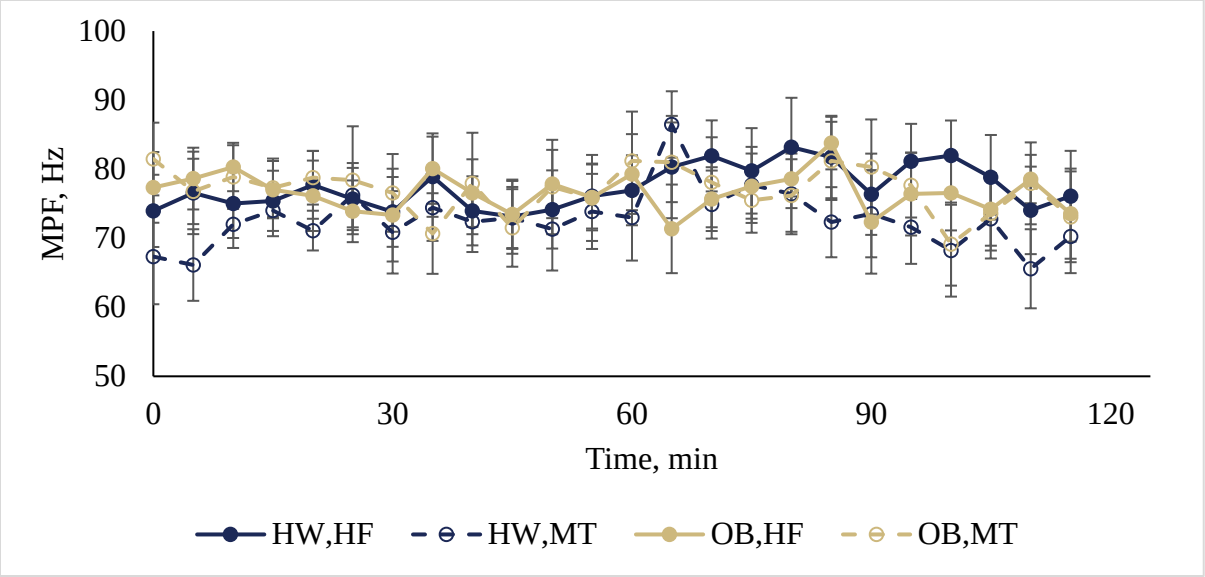

Figure 180: Hamstring MPF over time, split between BMI groups and flooring conditions. Error bars are standard error of the mean.

Appendix D.1.10 Hamstring RMS

I.

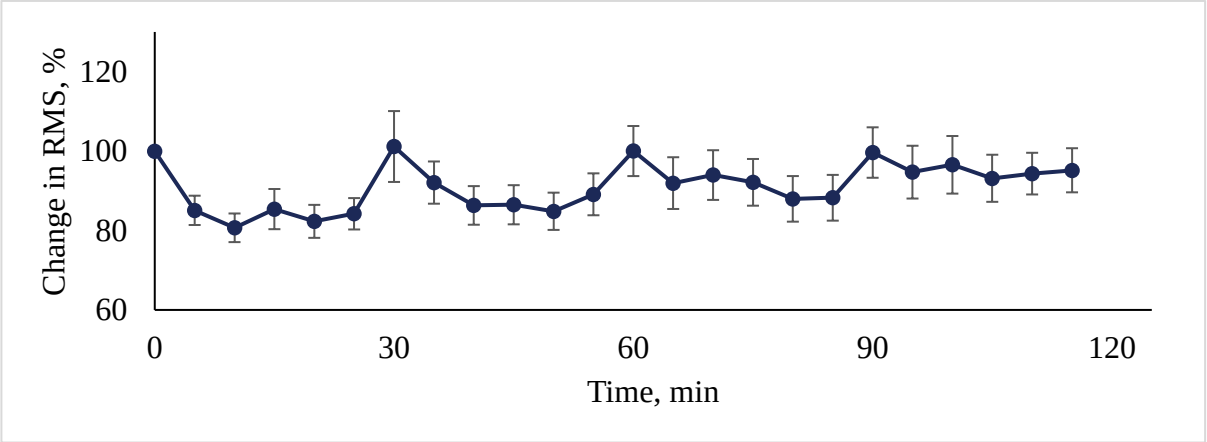

II.

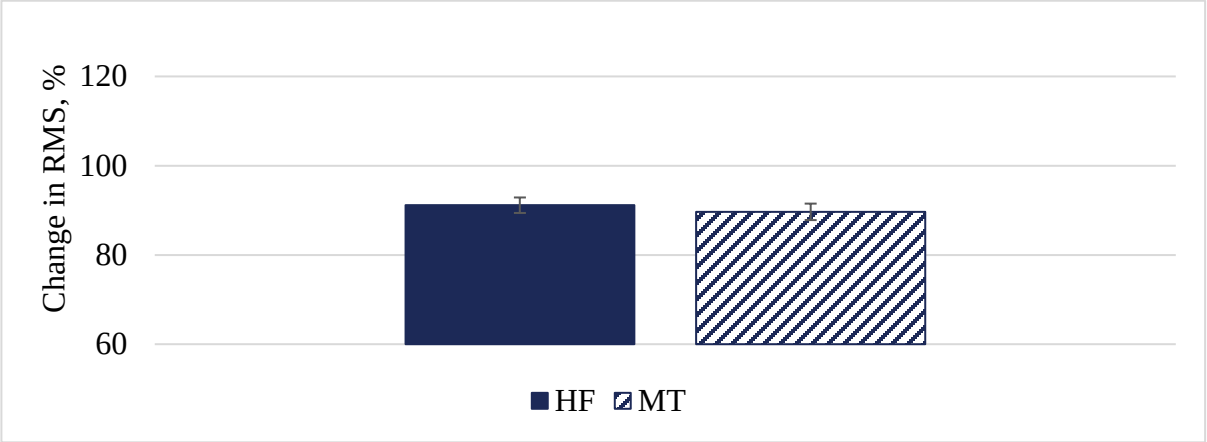

III.

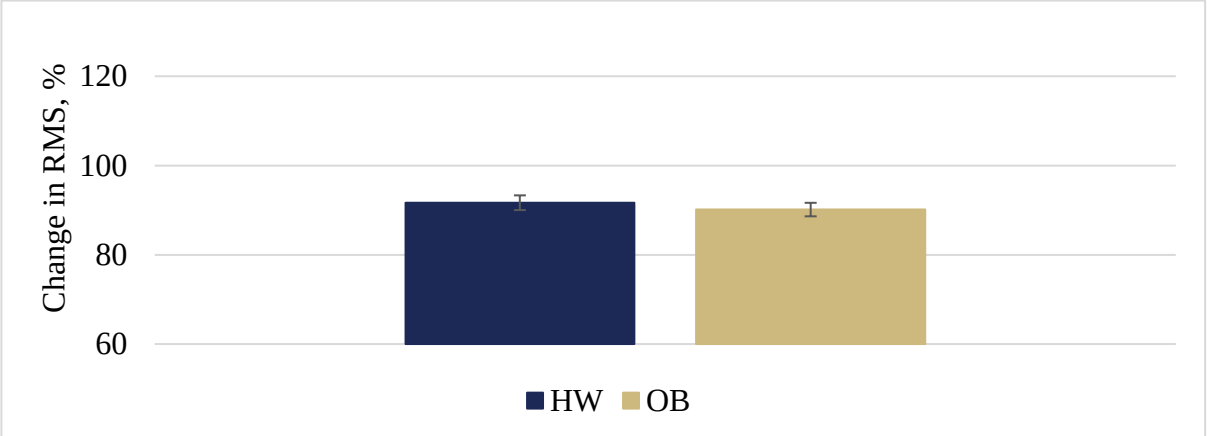

Figure 181: Hamstring RMS over time (I) and between flooring conditions (II) and BMI groups (III). Error bars are standard error of the mean.

I.

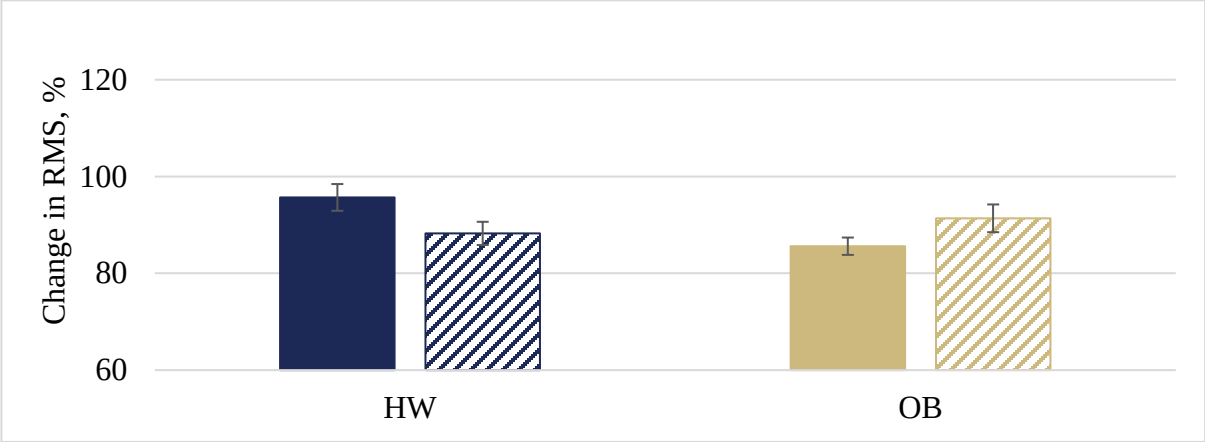

II.

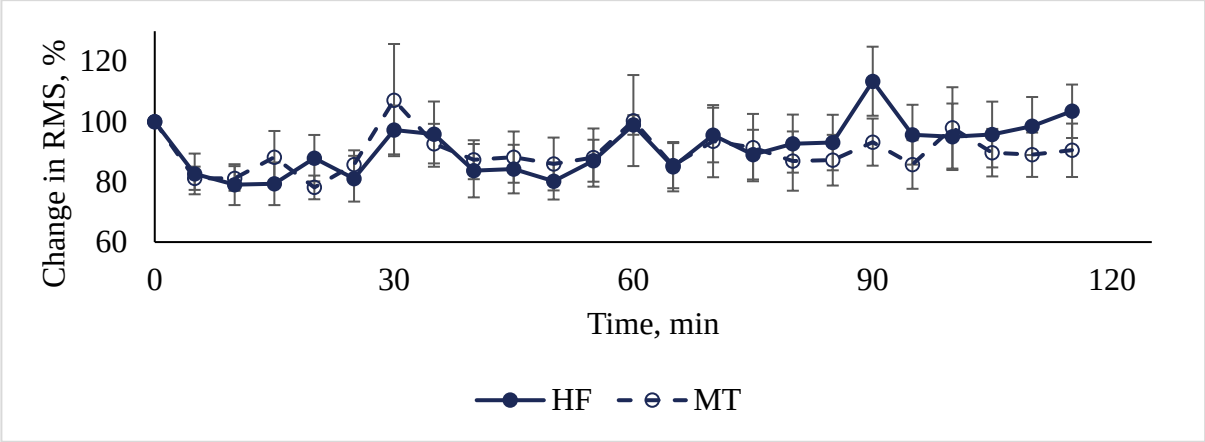

III.

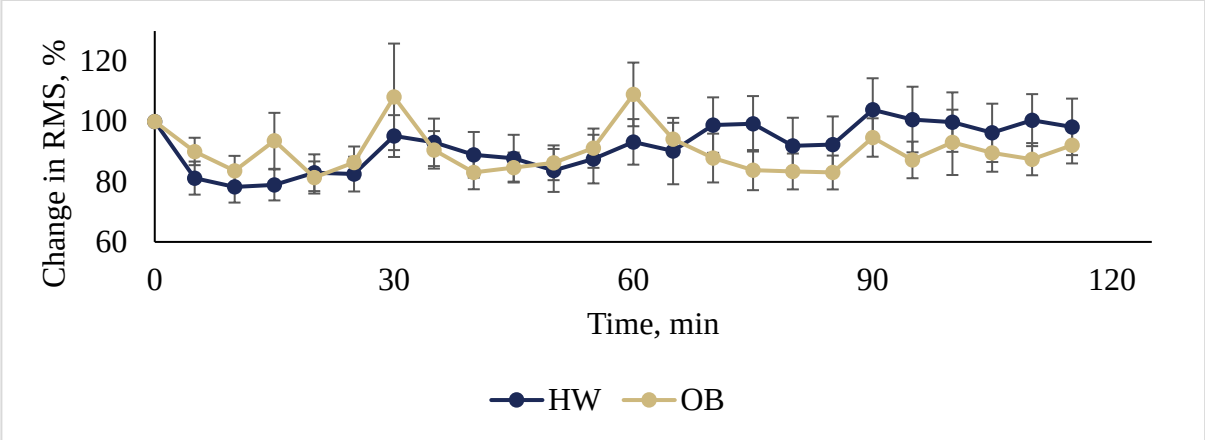

Figure 182: Hamstring RMS between BMI groups, split into flooring conditions (I), and over time, split between flooring conditions (II) and BMI groups (III). Error bars are standard error of the mean.

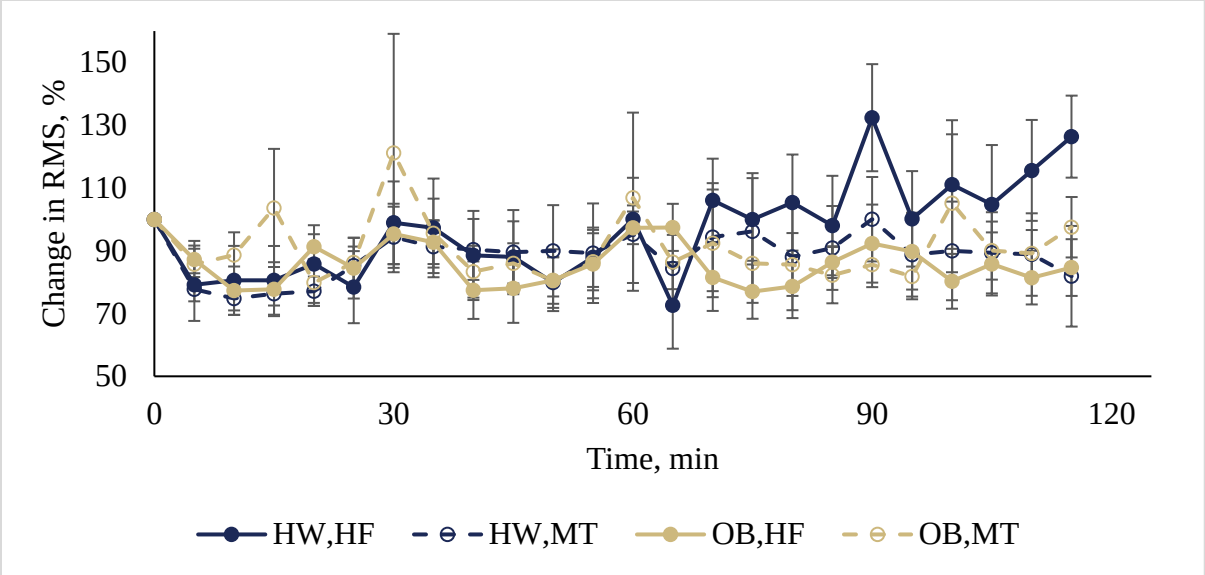

Figure 183: Hamstring RMS over time, split between BMI groups and flooring conditions. Error bars are standard error of the mean.

Appendix D.2 Near Infrared Spectroscopy Data

All graphs of NIRS data are included in this section. Each subsection includes graphs for each outcome measurement (HbO, HHb, HbT, Flow, StO_2, and SpO_2). Graphs displaying the effect of flooring condition, BMI group, and time as effects of each outcome measurement are included. Tukey HSD tests were performed to investigate the interaction effects of flooring condition and time, as well as BMI group and time, which resulted in t statistics for each comparison. Comparisons at each time point between flooring conditions and BMI groups are graphed as well. Methods by which NIRS measures were calculated are included in section 3.4.4.2. No analyses of graphs are included in this section. Analyses of significant NIRS findings are included in section 4.4.2.

Appendix D.2.1 Oxy-Hemoglobin

I.

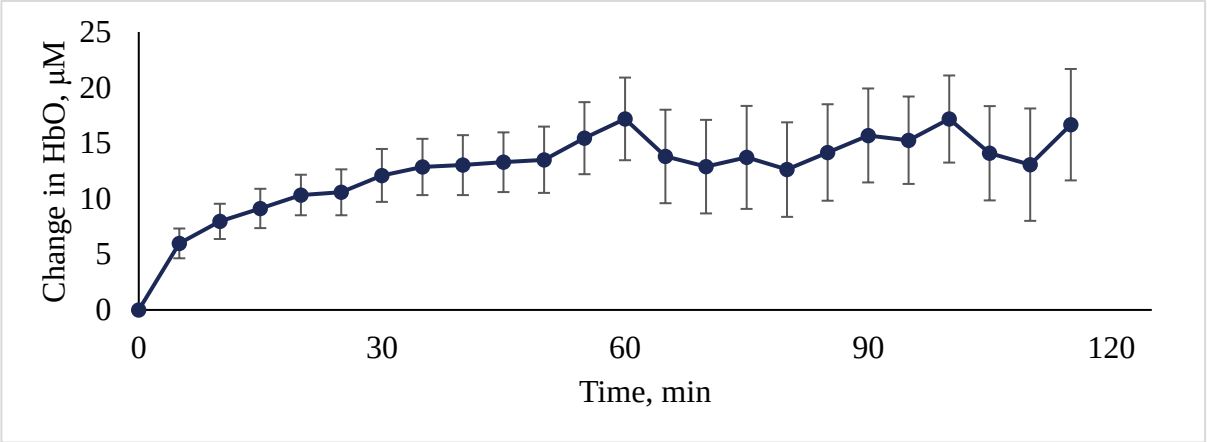

II.

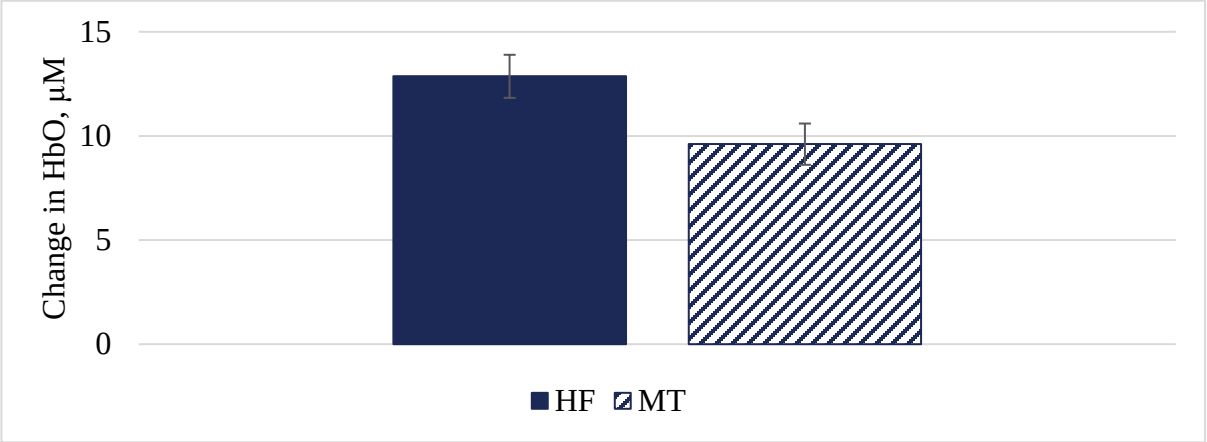

III.

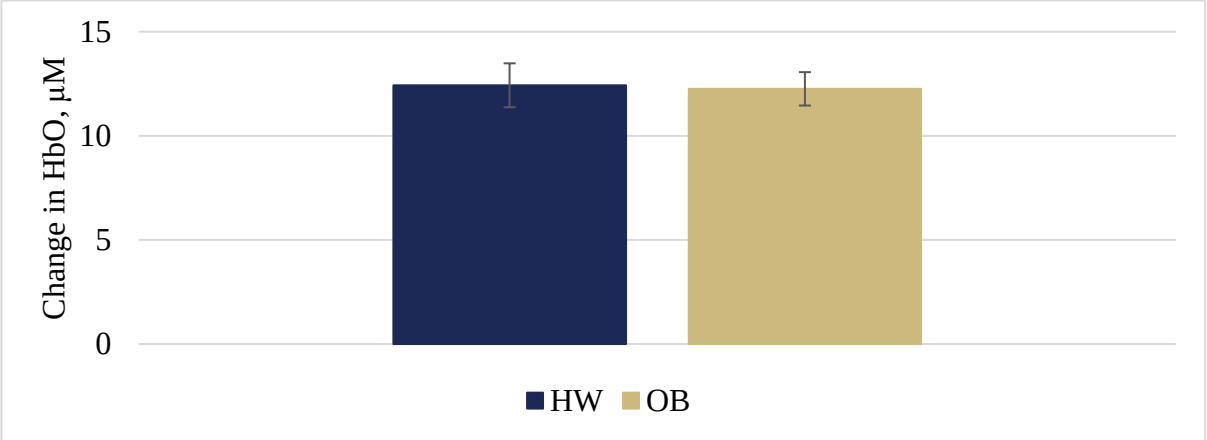

Figure 184: Change in HbO over time (I) and between flooring conditions (II) and BMI groups (III). Error bars are standard error of the mean.

I.

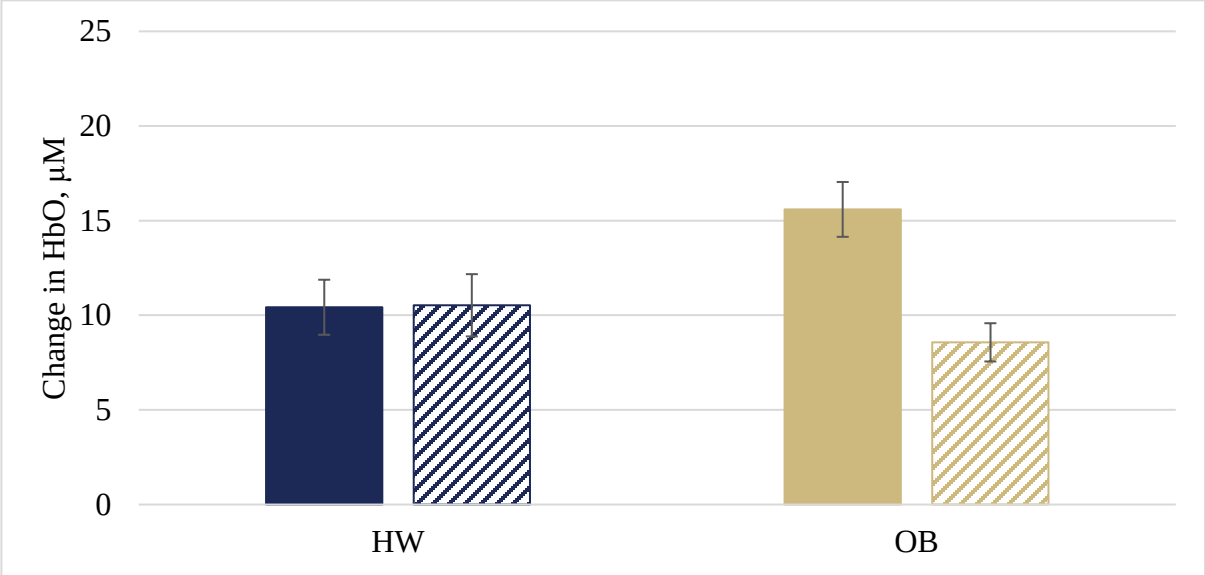

II.

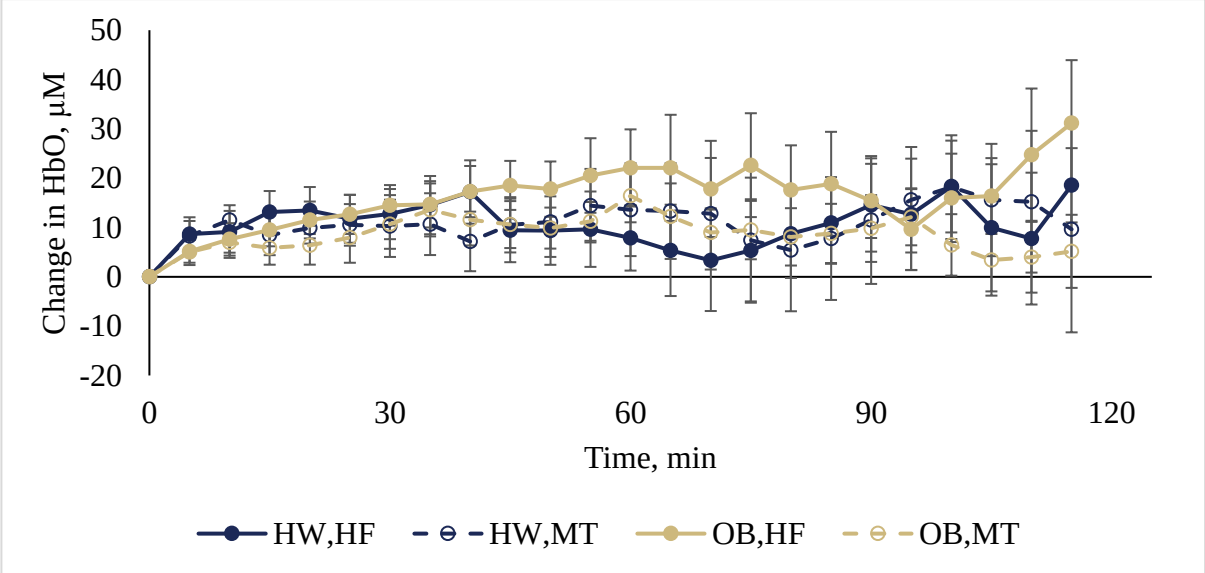

Figure 185: I. Change in HbO split into BMI group and flooring condition and II. Change in HbO split into BMI group and flooring condition displayed over time. Error bars are standard error of the mean.

I.

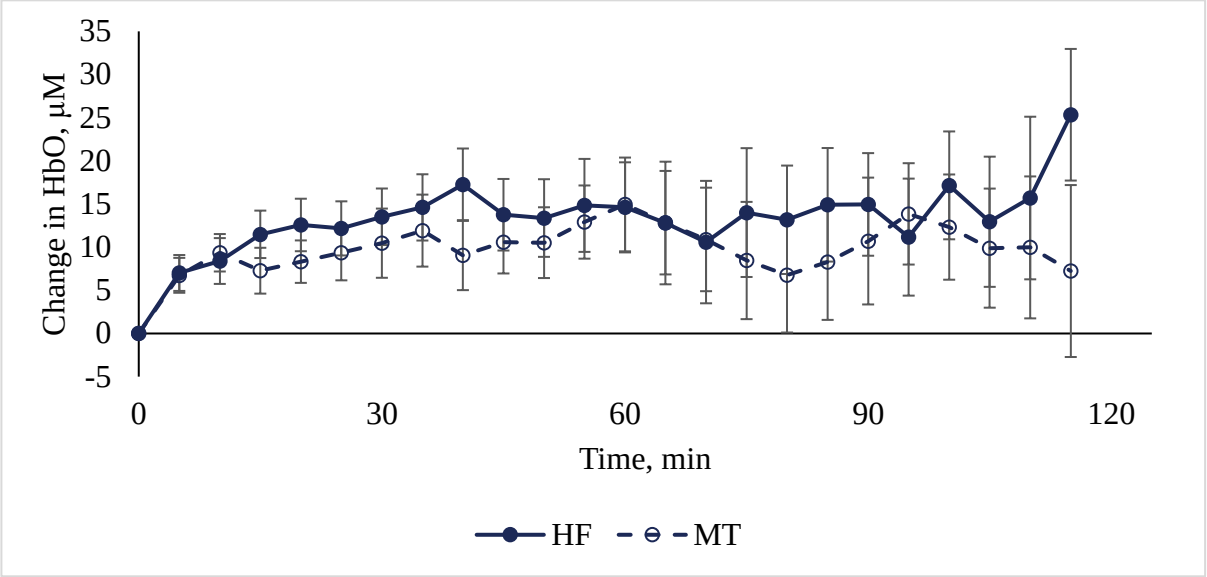

II.

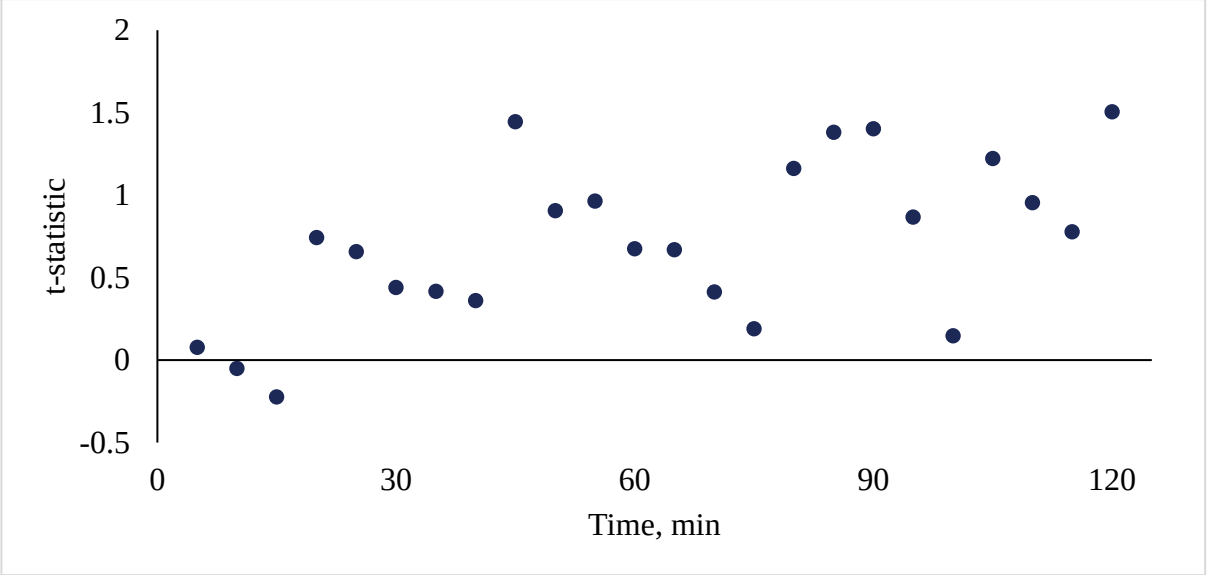

Figure 186: I. Change in HbO split into HF and MT flooring conditions and plotted over time. Error bars are standard error of the mean. II. Tukey HSD t statistic comparing mean change in HbO between flooring conditions at each five minute time interval.

I.

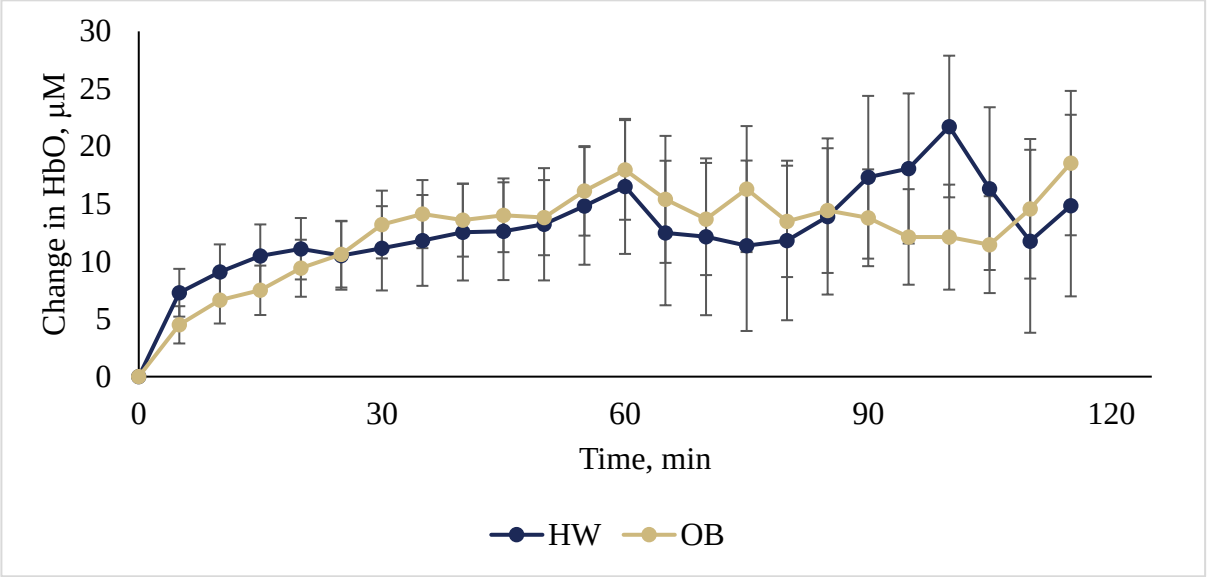

II.

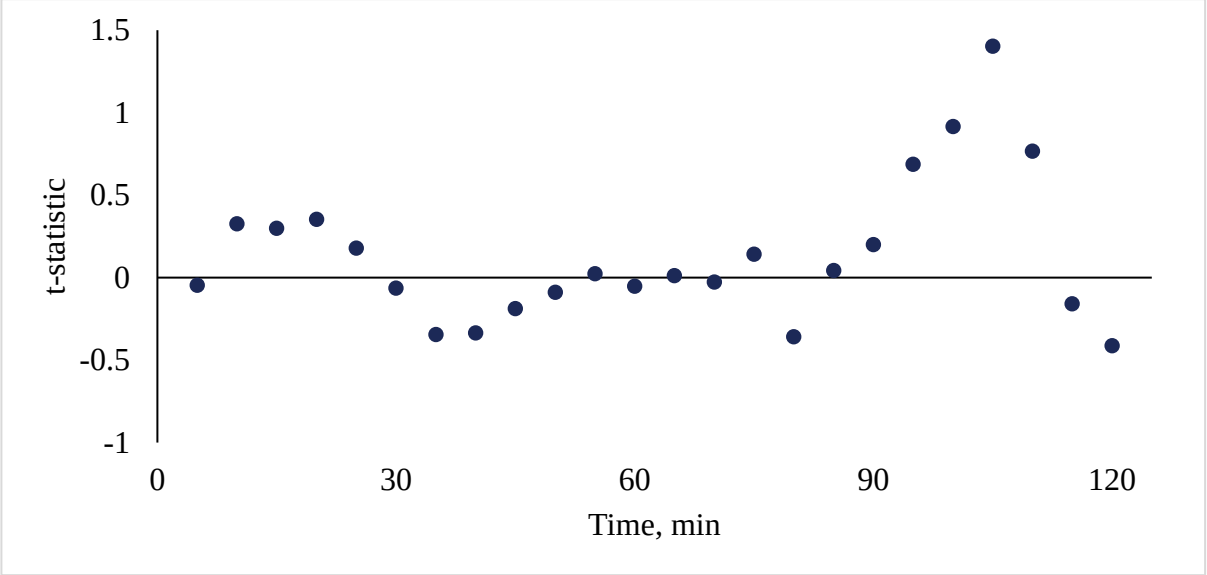

Figure 187: I. Change in HbO split into BMI groups and plotted over time. Error bars are standard error of the mean. II. Tukey HSD t statistic comparing mean change in HbO between BMI groups at each five minute time interval.

Appendix D.2.2 Deoxy-Hemoglobin

I.

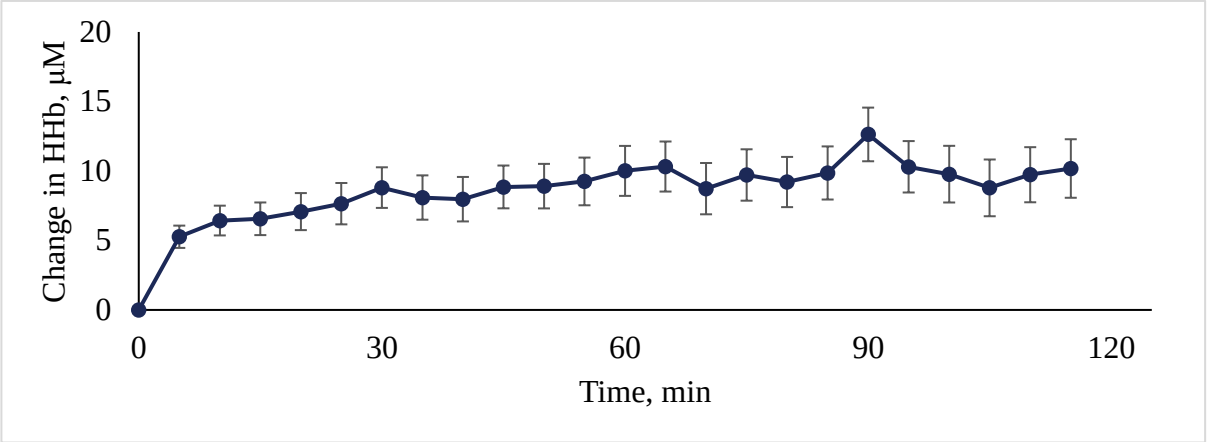

II.

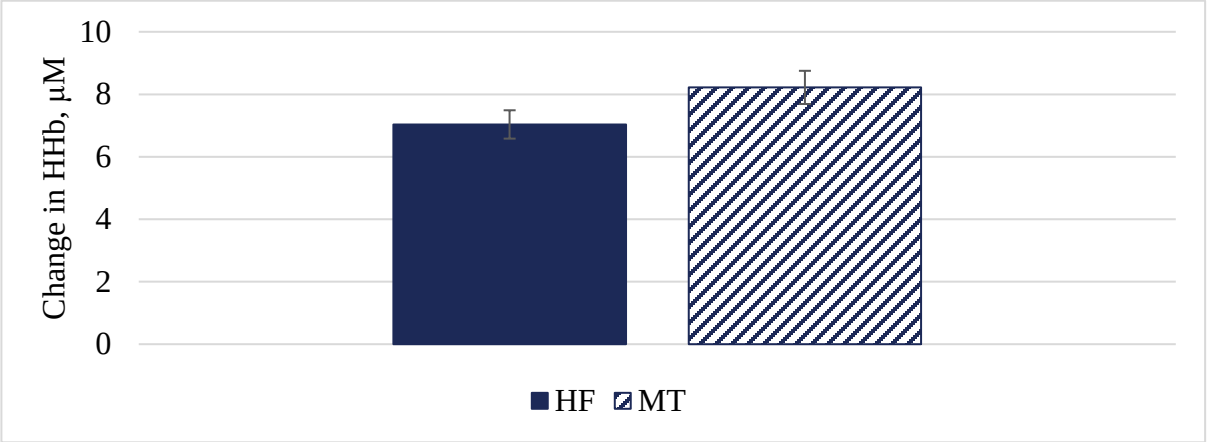

III.

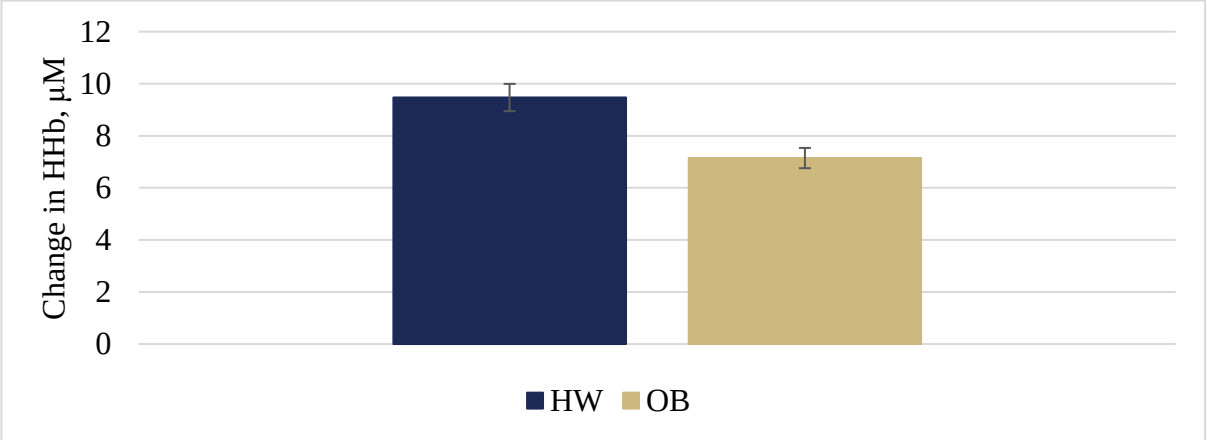

Figure 188: Change in HHb over time (I) and between flooring conditions (II) and BMI groups (III). Error bars are standard error of the mean.

I.

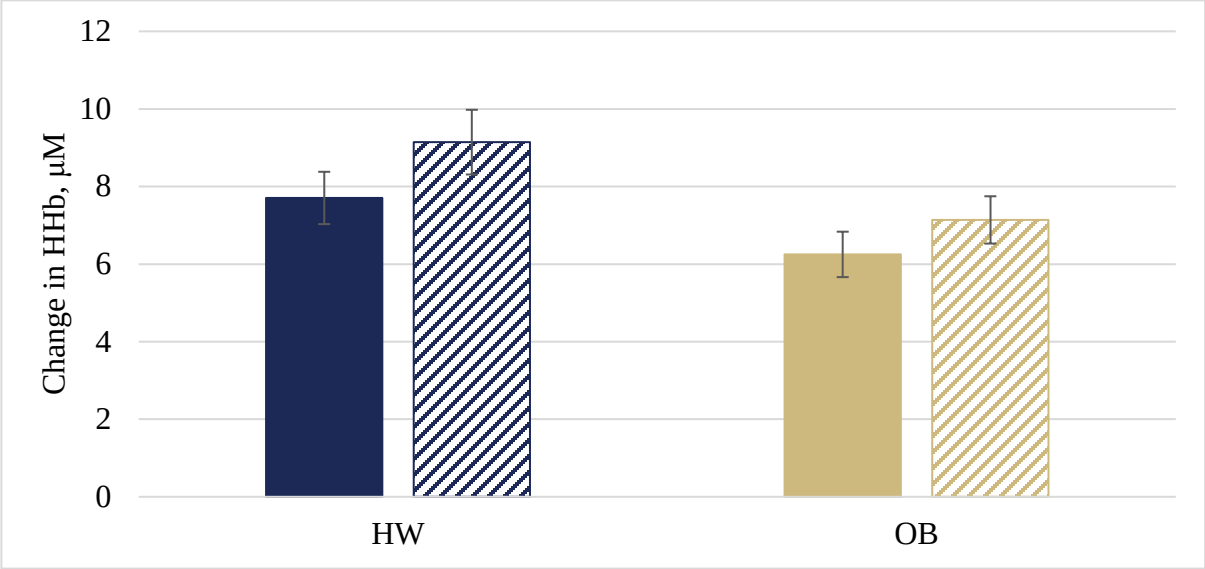

II.

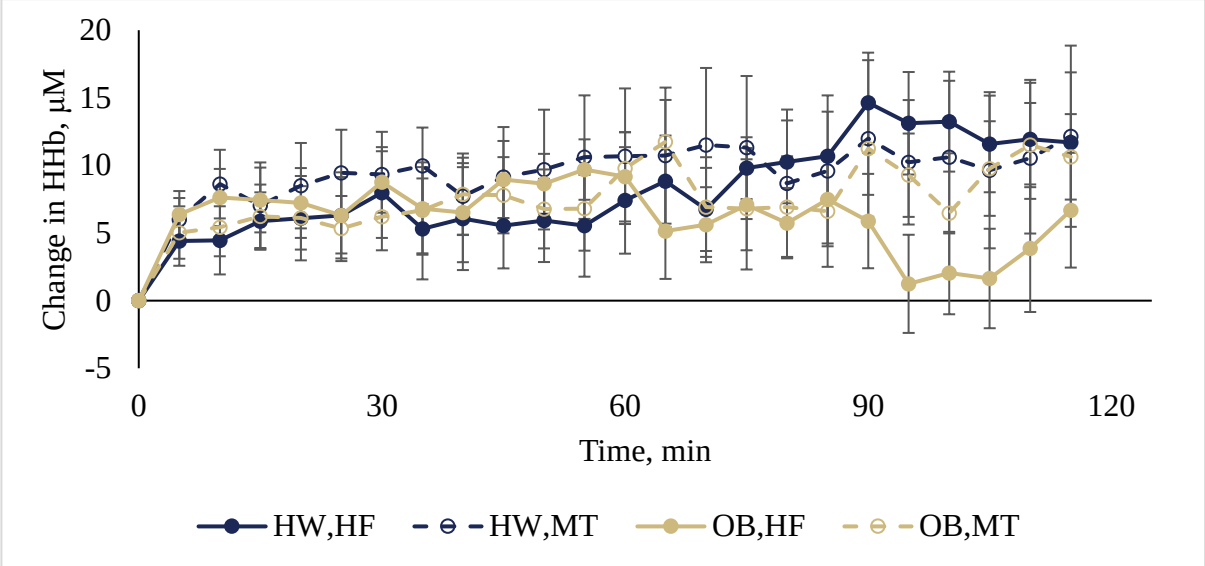

Figure 189: I. Change in HHb split into BMI group and flooring condition and II. Change in HHb split into BMI group and flooring condition displayed over time. Error bars are standard error of the mean.

I.

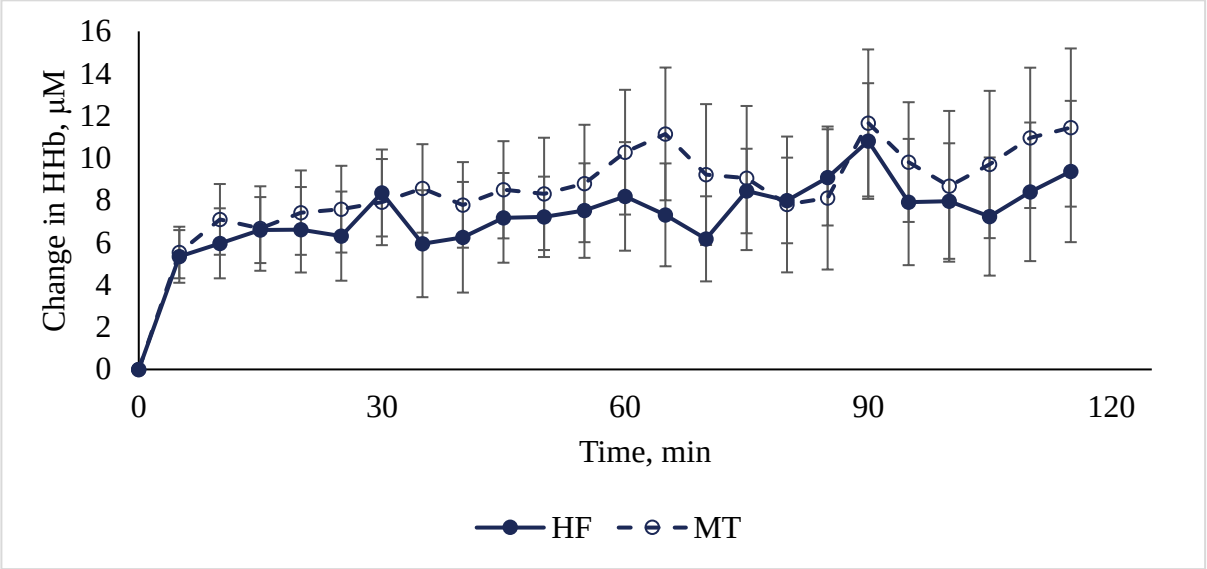

II.

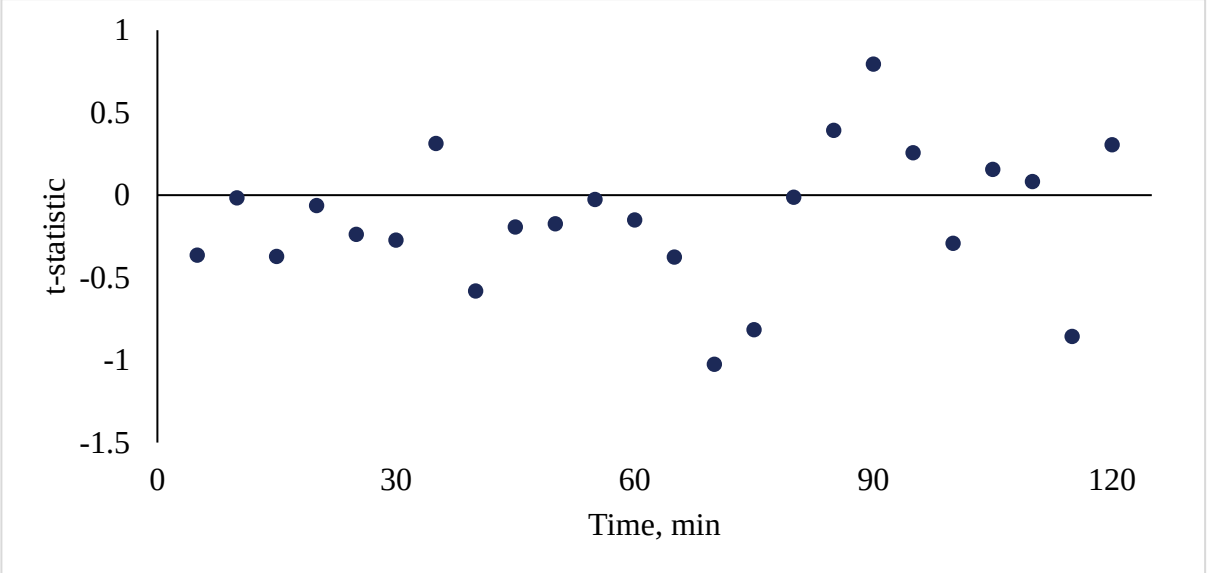

Figure 190: I. Change in HHb split into HF and MT flooring conditions and plotted over time. Error bars are standard error of the mean. II. Tukey HSD t statistic comparing mean change in HHb between flooring conditions at each five minute time interval.

I.

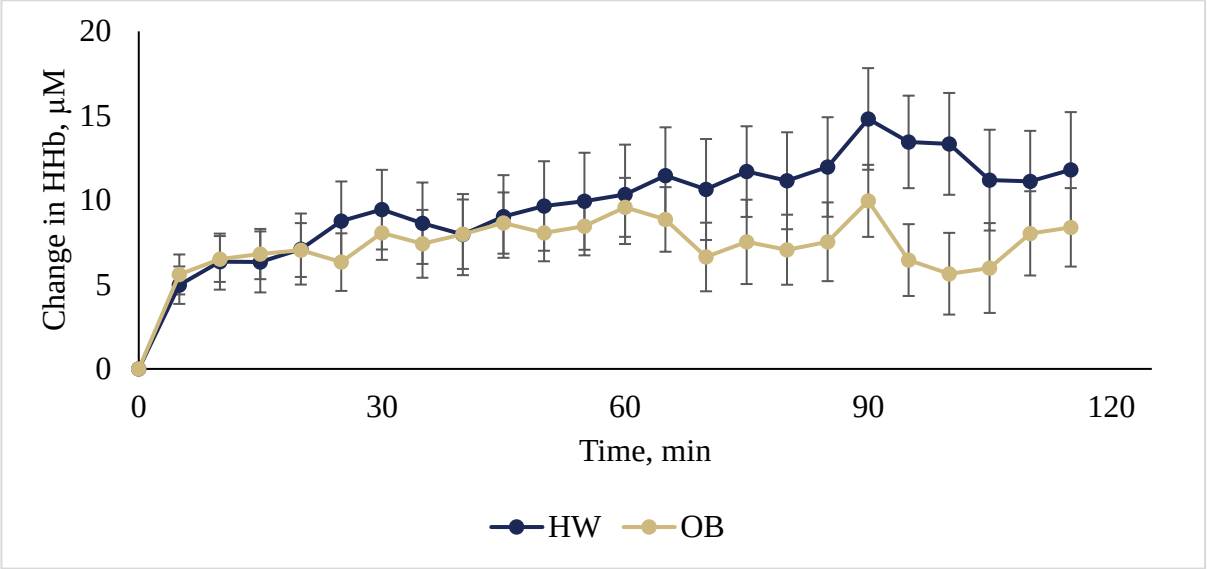

II.

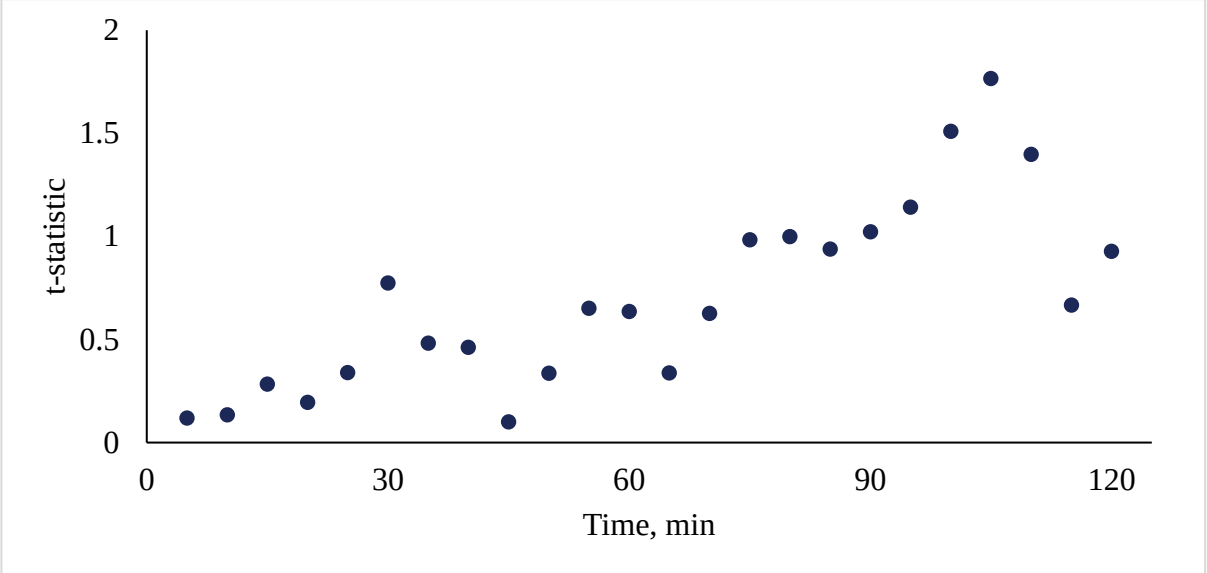

Figure 191: Change in HHb split into BMI groups and plotted over time. Error bars are standard error of the mean. II. Tukey HSD t statistic comparing mean change in HHb between BMI groups at each five minute time interval.

Appendix D.2.3 Total Hemoglobin

I.

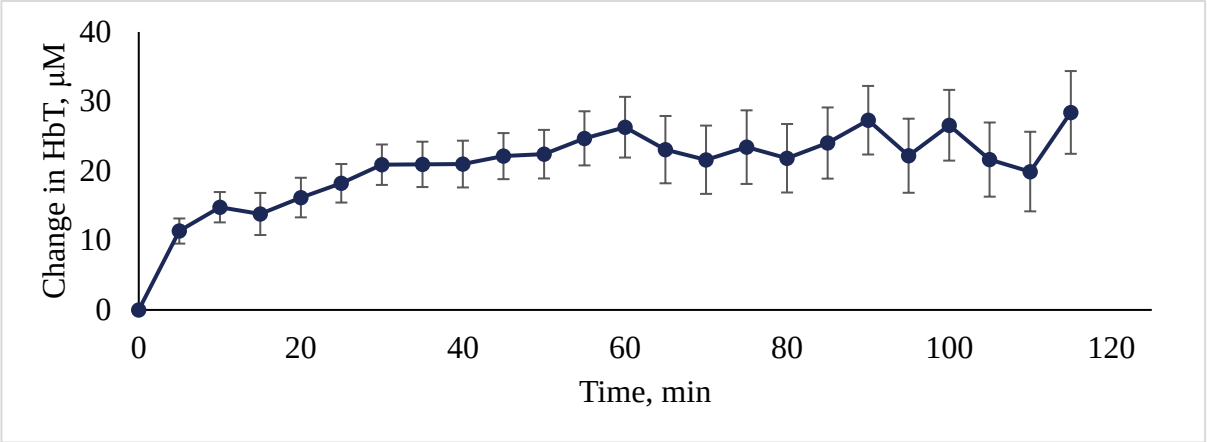

II.

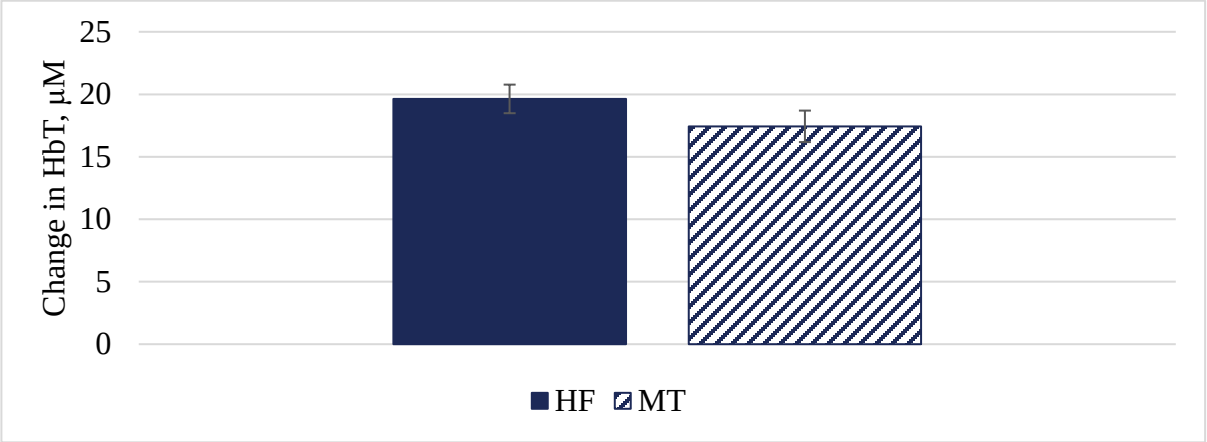

III.

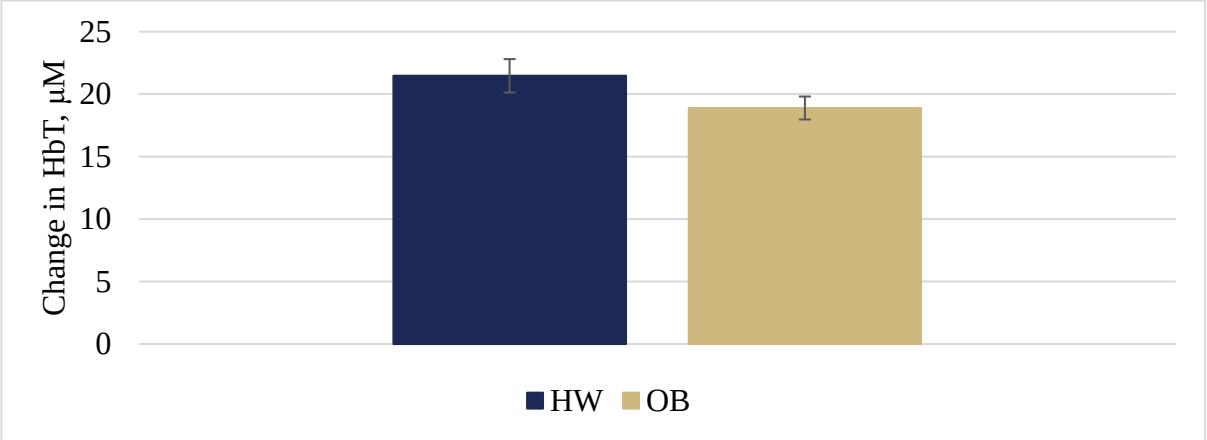

Figure 192: Change in HbT over time (I) and between flooring conditions (II) and BMI groups (III). Error bars are standard error of the mean.

I.

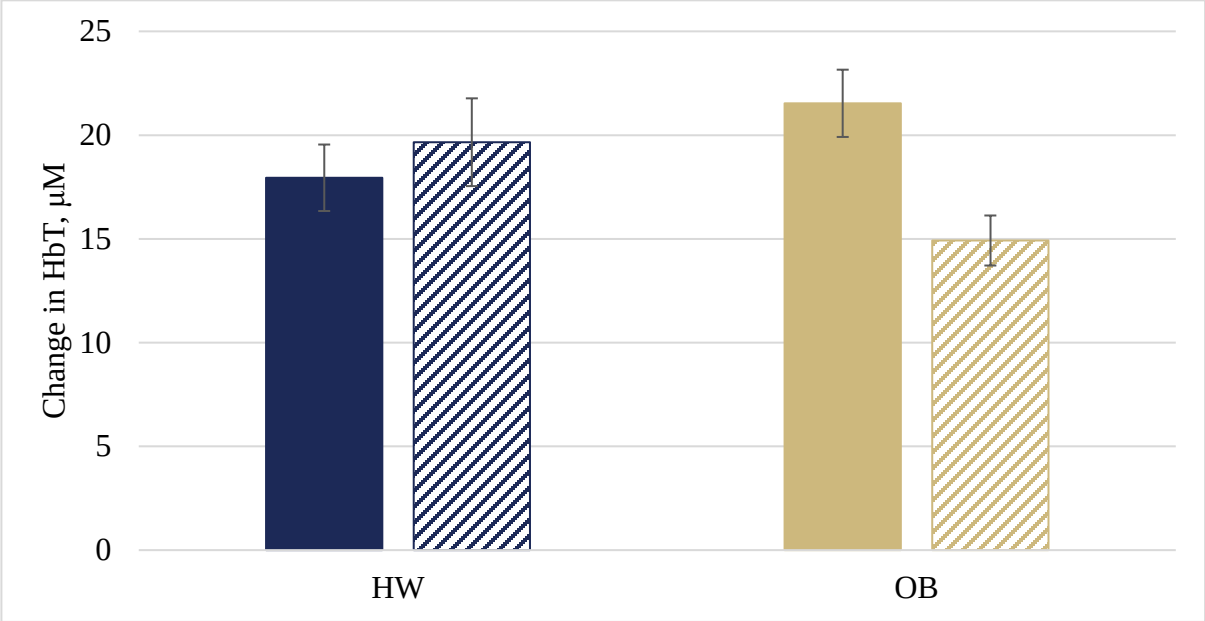

II.

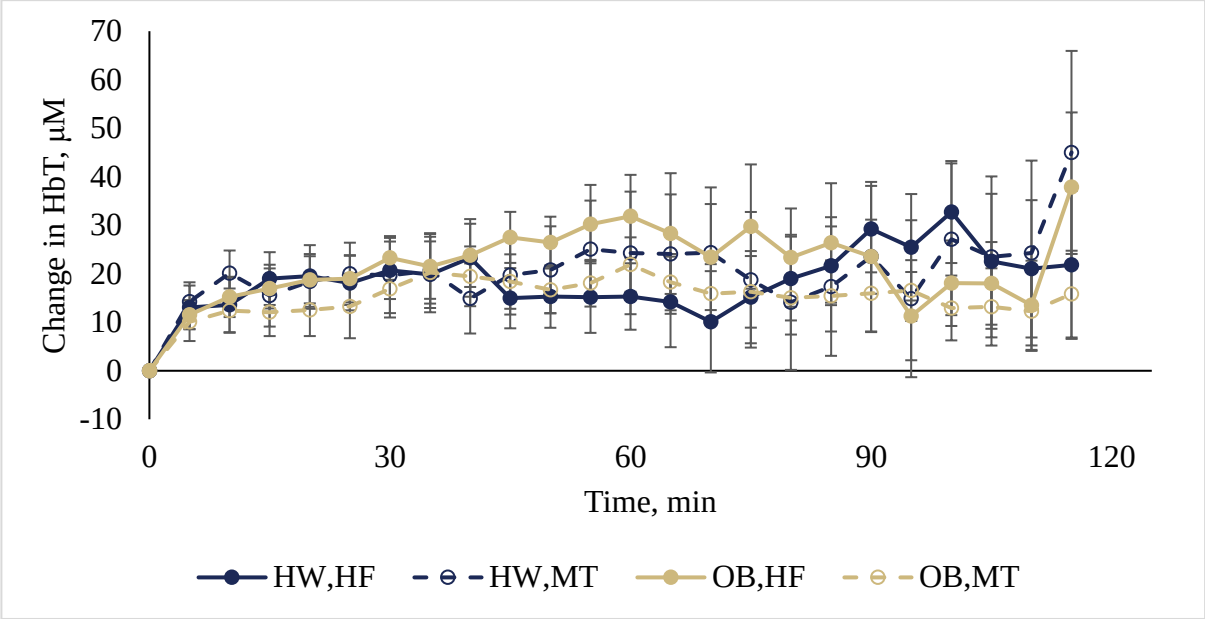

Figure 193: I. Change in HbT split into BMI group and flooring condition and II. Change in HbT split into BMI group and flooring condition displayed over time. Error bars are standard error of the mean.

I.

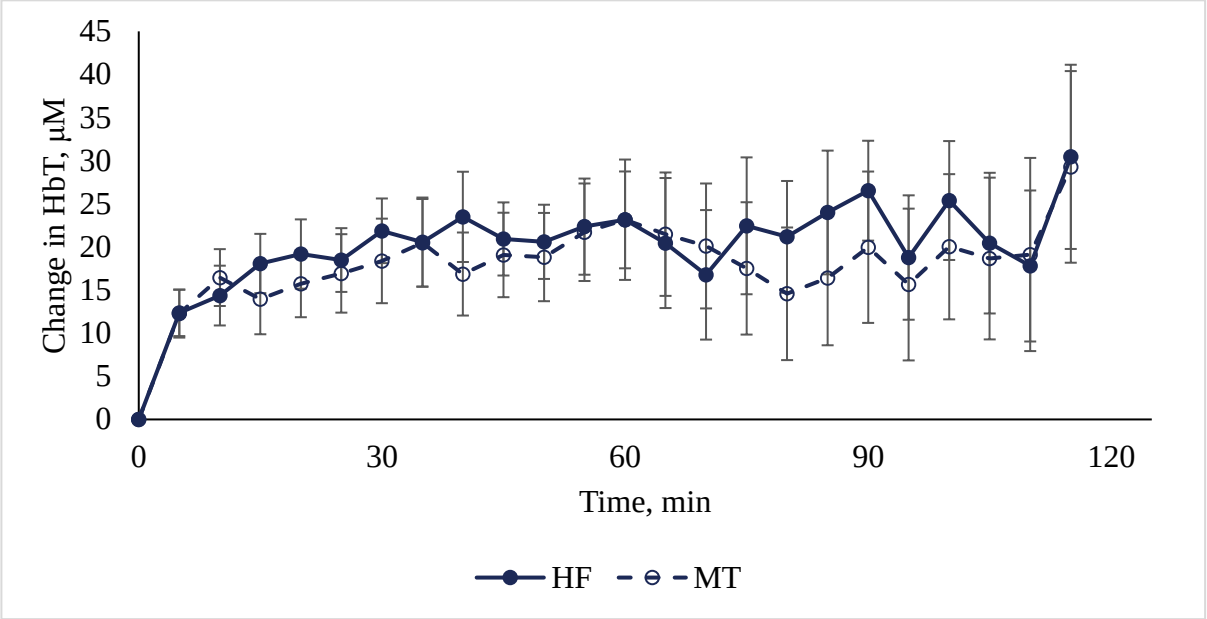

II.

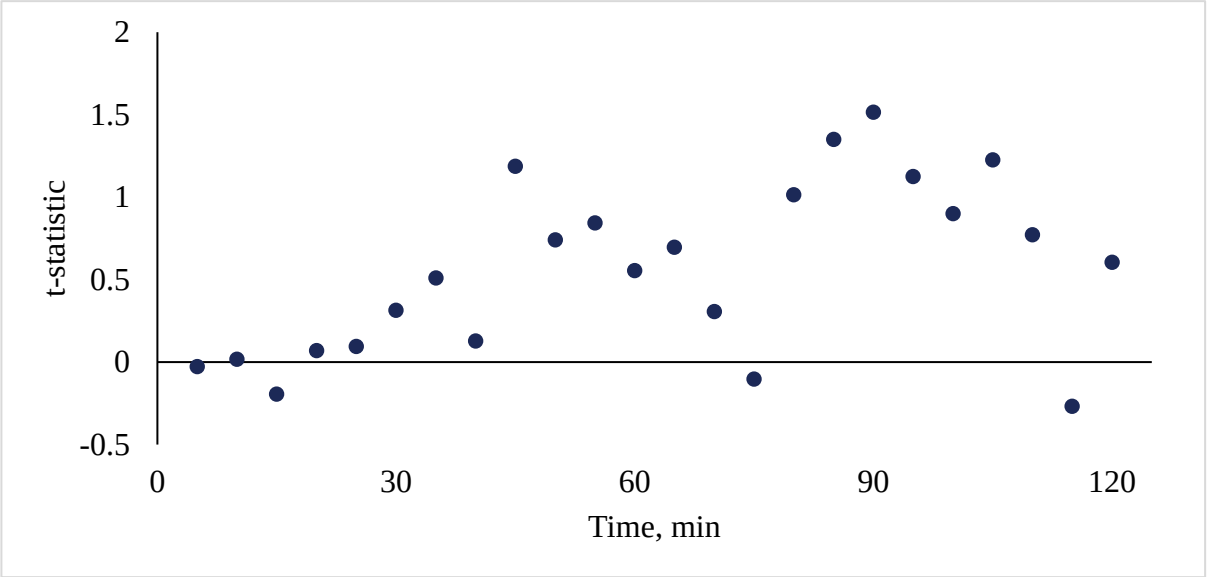

Figure 194: I. Change in HbT split into HF and MT flooring conditions and plotted over time. Error bars are standard error of the mean. II. Tukey HSD t statistic comparing mean change in HbT between flooring conditions at each five minute time interval.

I.

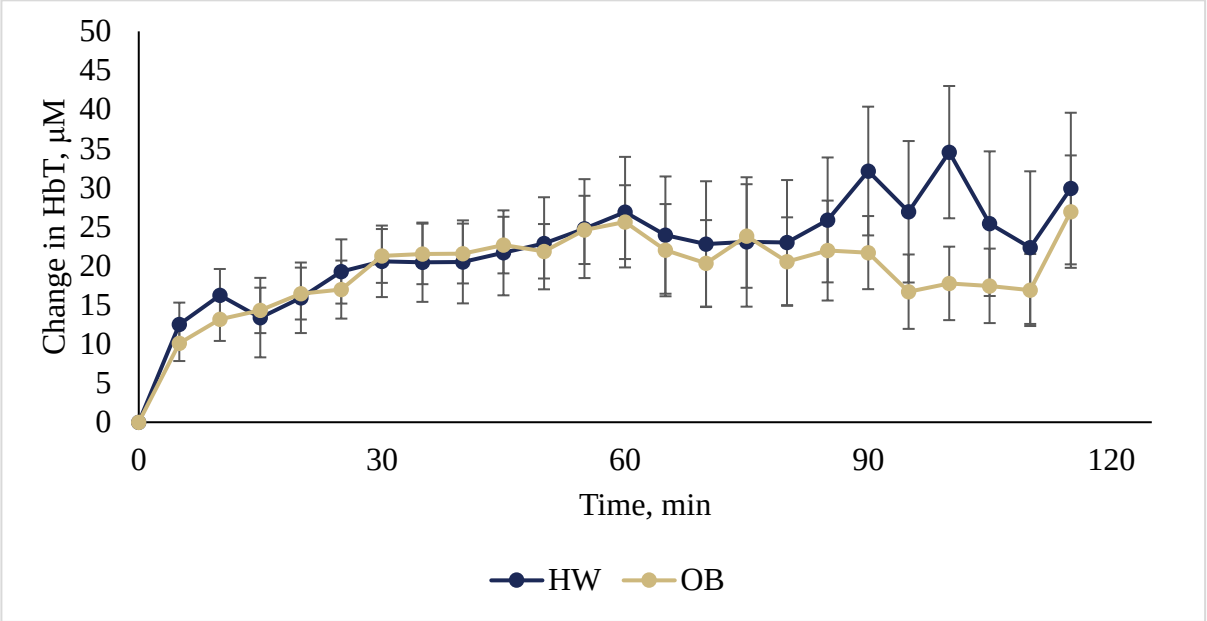

II..

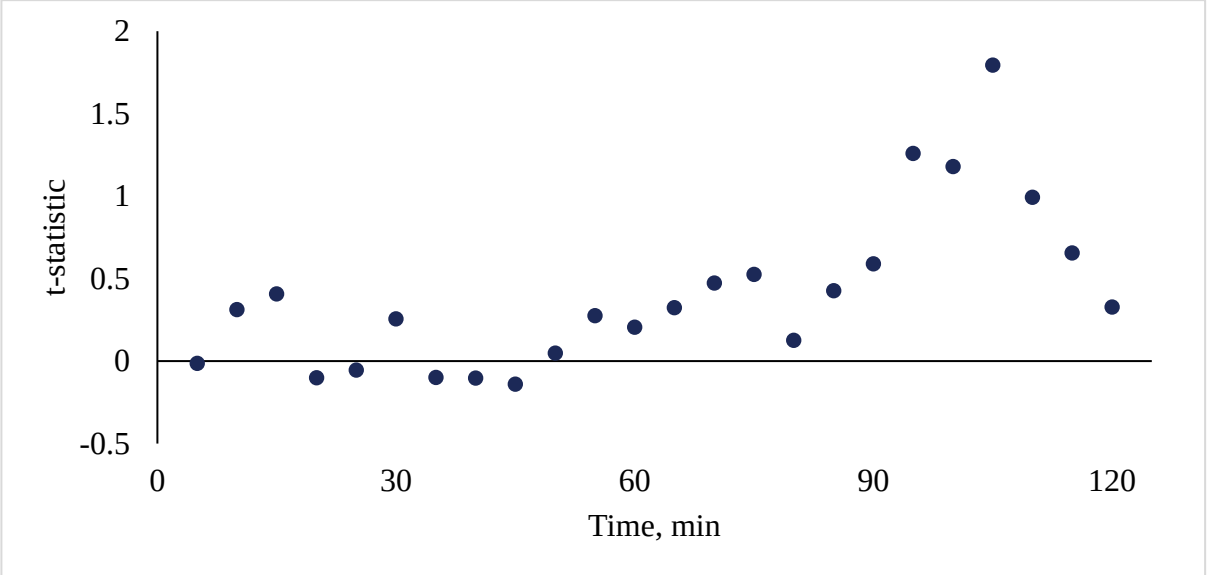

Figure 195: I. Change in HbT split into BMI groups and plotted over time. Error bars are standard error of the mean. II. Tukey HSD t statistic comparing mean change in HbT between BMI groups at each five minute time interval.

Appendix D.2.4 Pulsatile Flow

I.

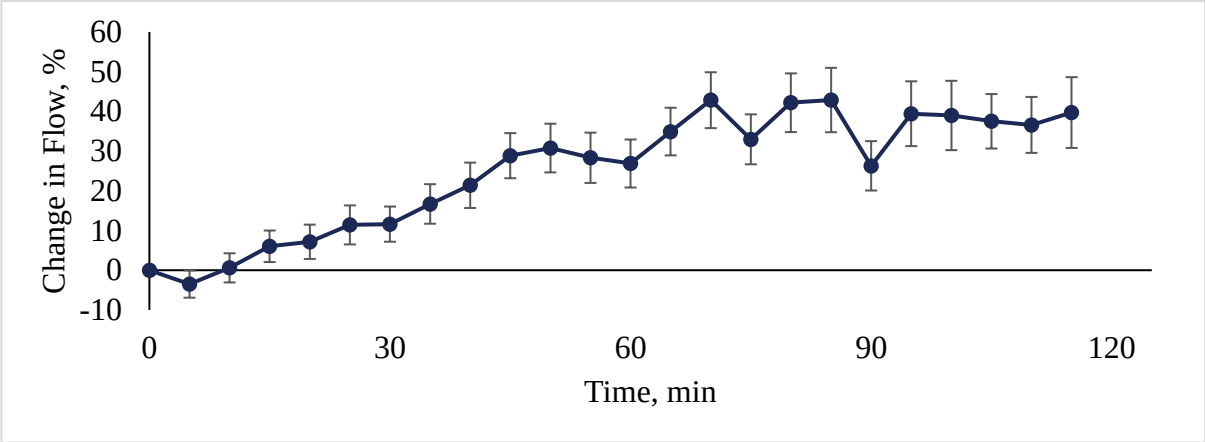

II.

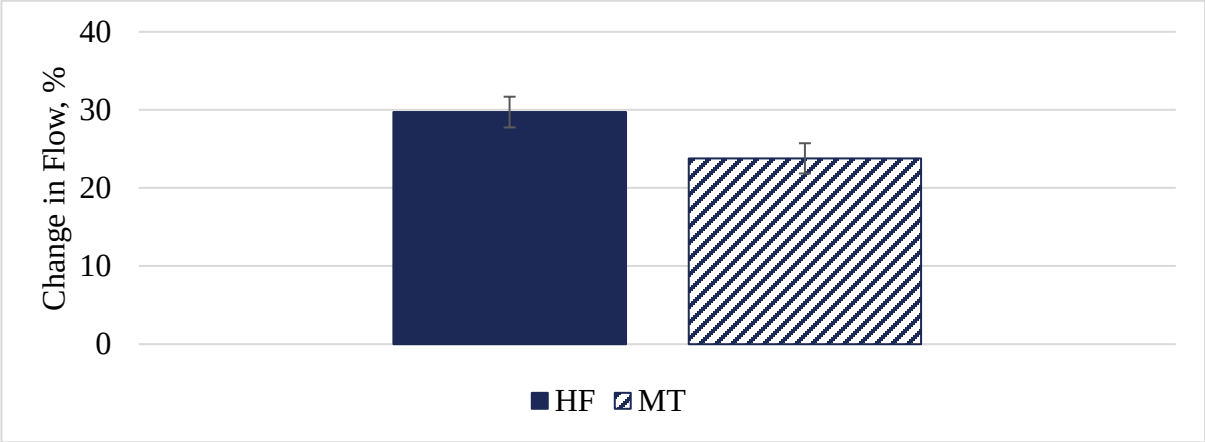

III.

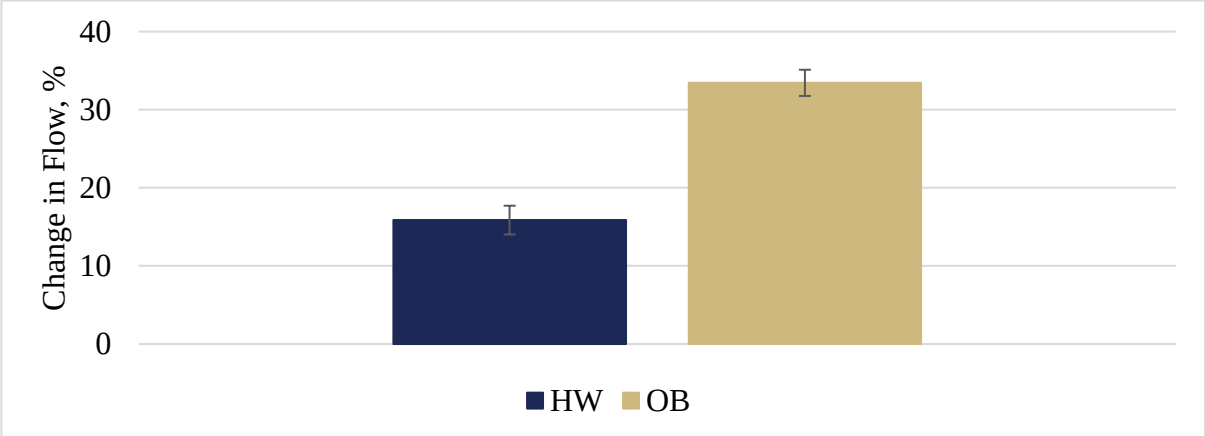

Figure 196: Change in Flow (%) over time (I) and between flooring conditions (II) and BMI groups (III). Error bars are standard error of the mean.

I.

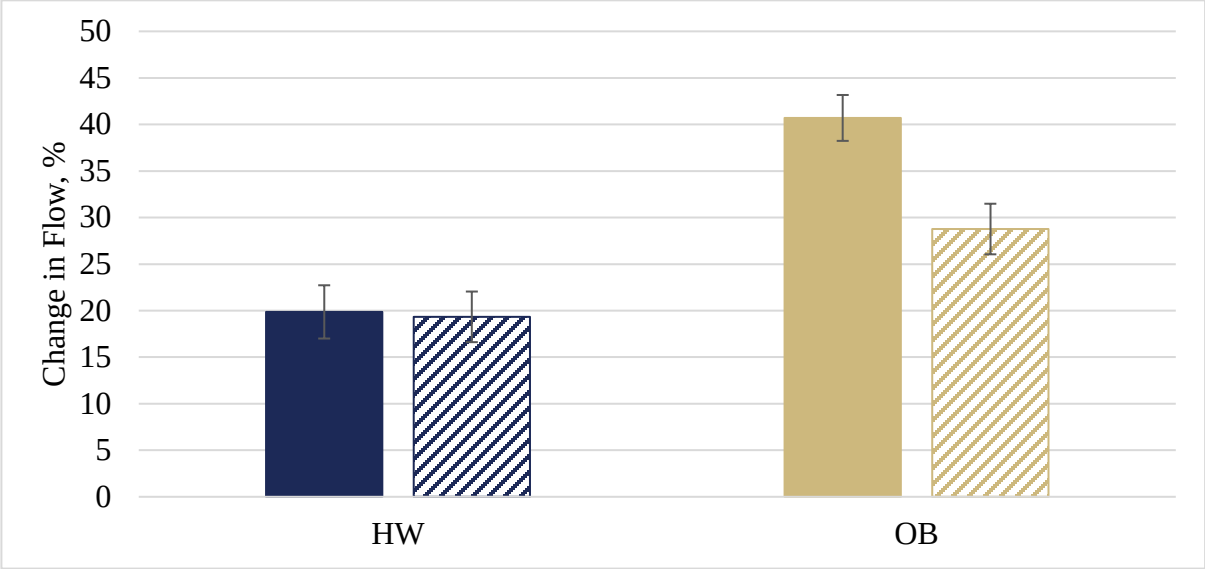

II.

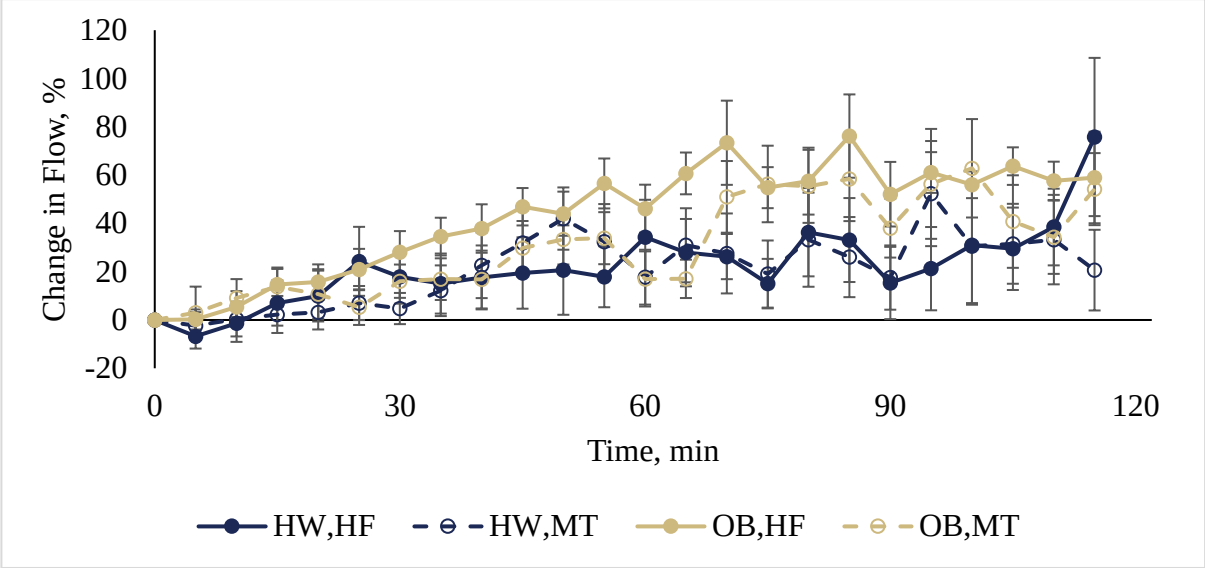

Figure 197: I. Change in Flow split into BMI group and flooring condition and II. Change in Flow split into BMI group and flooring condition displayed over time. Error bars are standard error of the mean.

I.

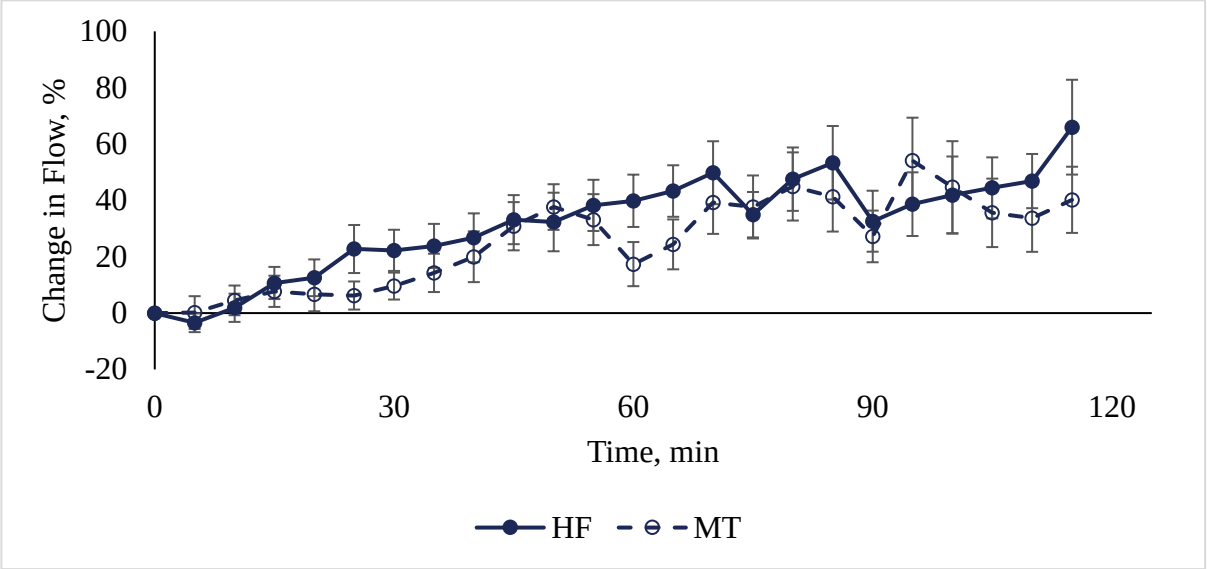

II.

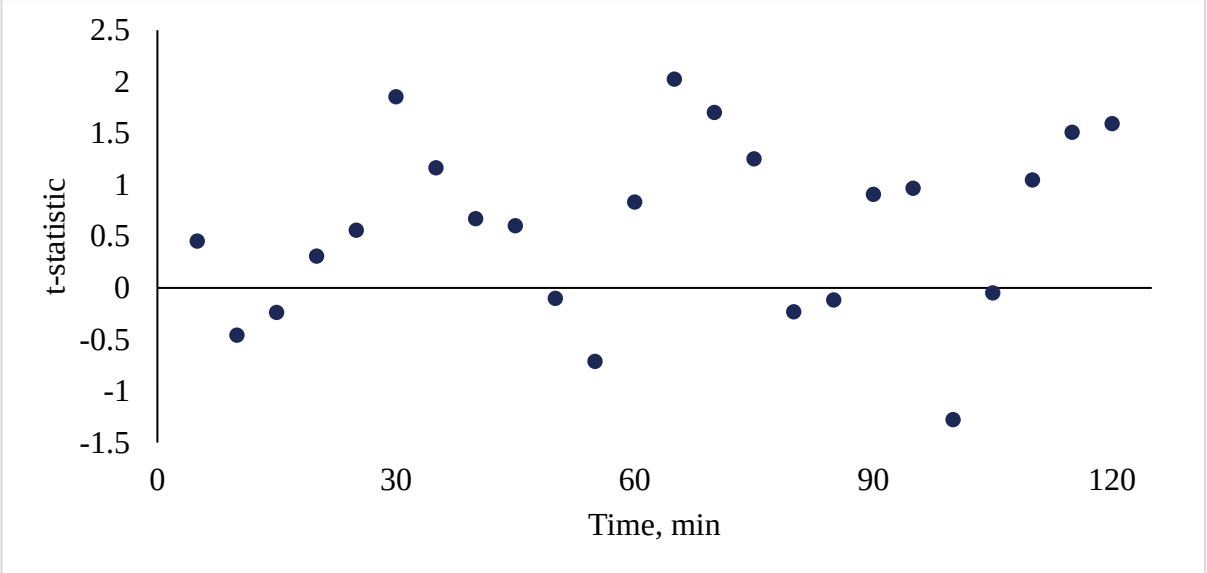

Figure 198: I. Change in Flow split into HF and MT flooring conditions and plotted over time. Error bars are standard error of the mean. II. Tukey HSD t statistic comparing mean change in Flow between flooring conditions at each five minute time interval.

I.

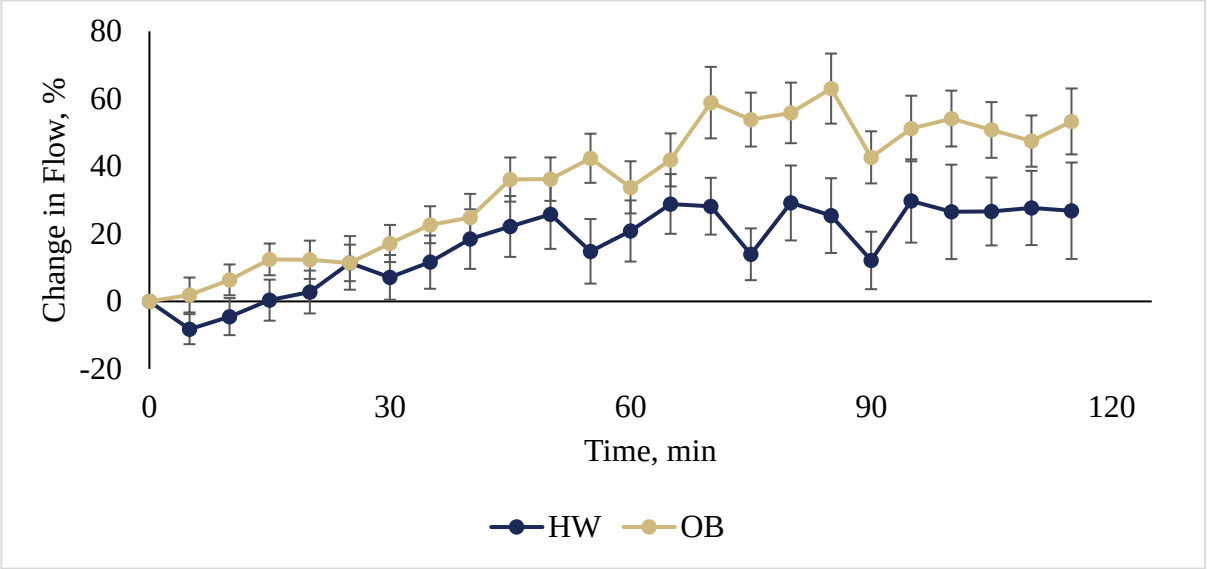

II.

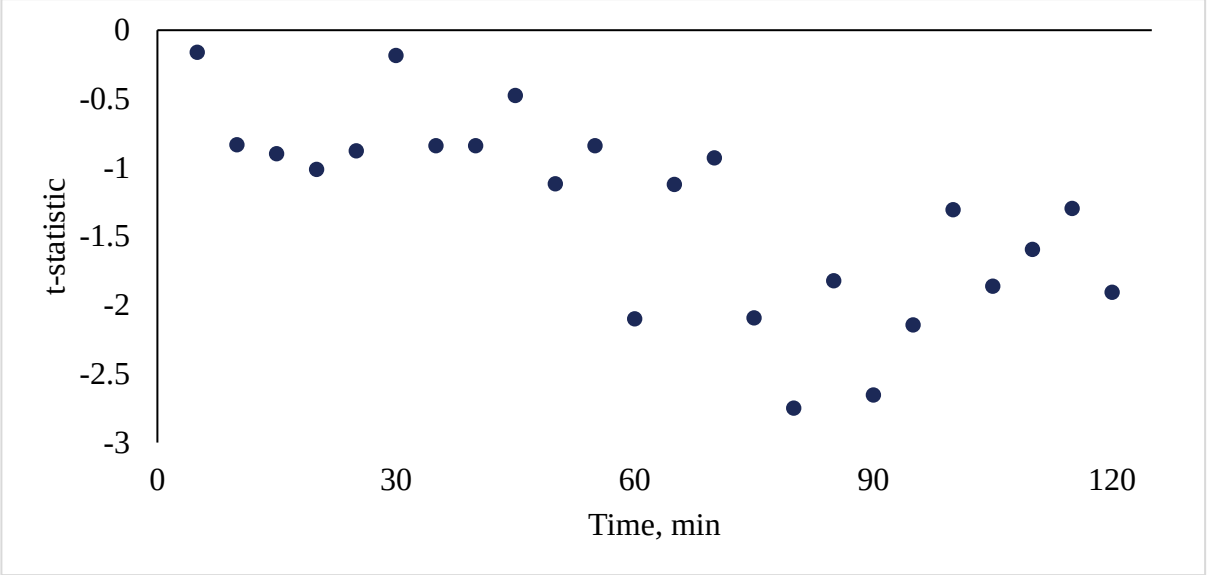

Figure 199: I. Change in Flow split into BMI groups and plotted over time. Error bars are standard error of the mean. II. Tukey HSD t statistic comparing mean change in Flow between BMI groups at each five minute time interval.

Appendix D.2.5 Tissue Oxygen Saturation

I.

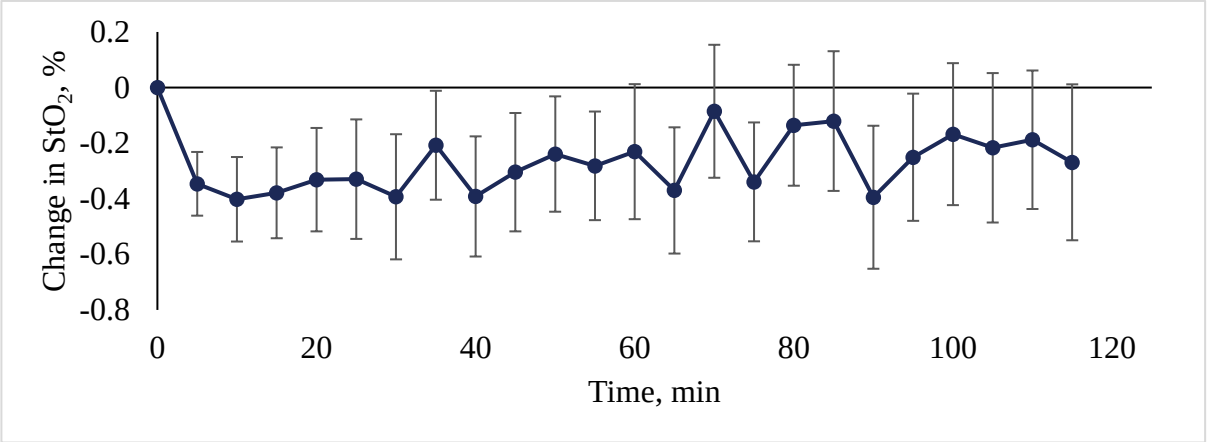

II.

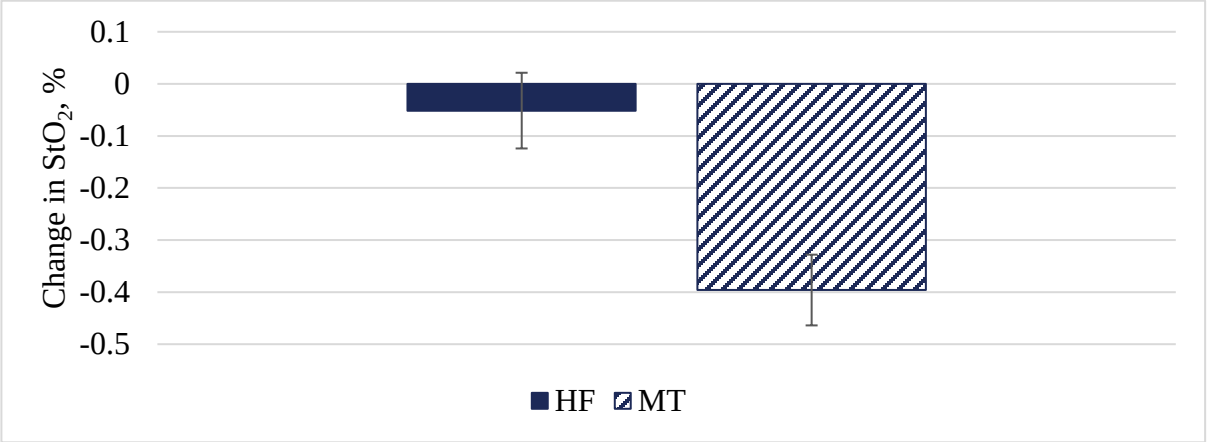

III.

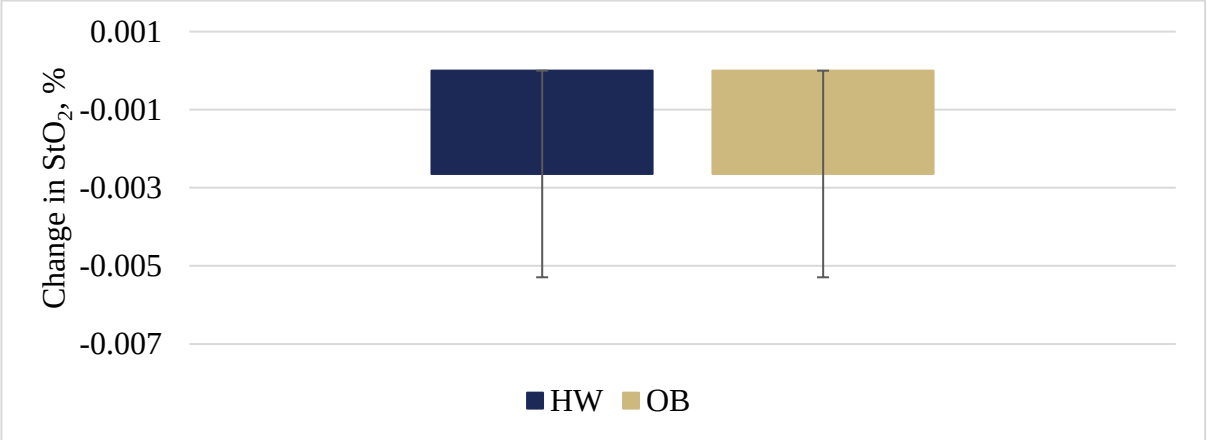

Figure 200: Change in StO_2 (%) over time (I) and between flooring conditions (II) and BMI groups (III). Error bars are standard error of the mean.

I.

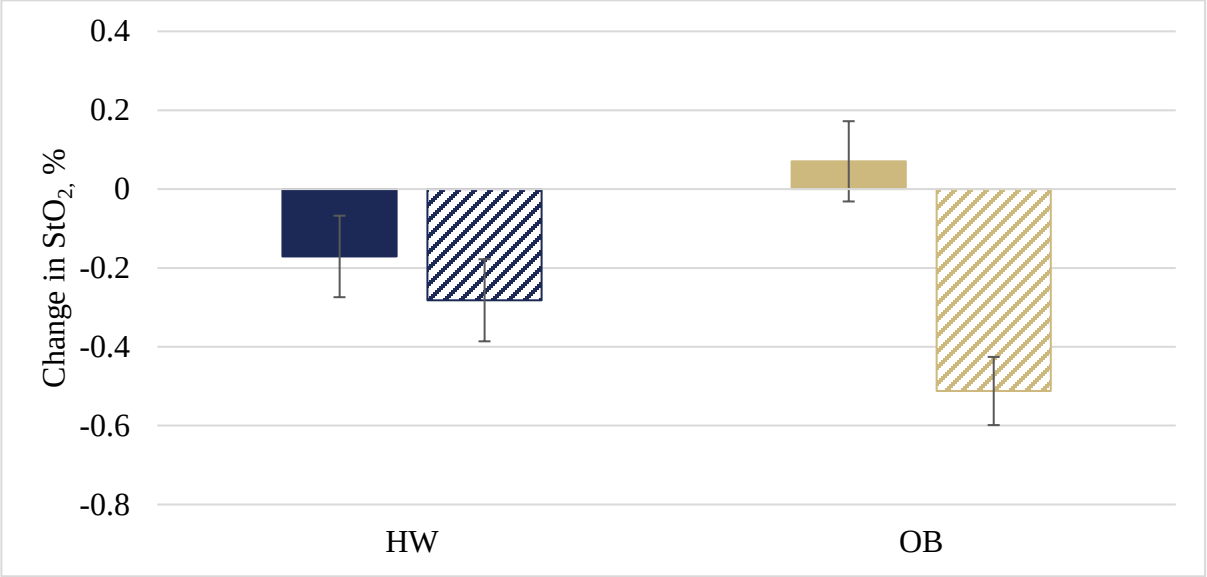

II.

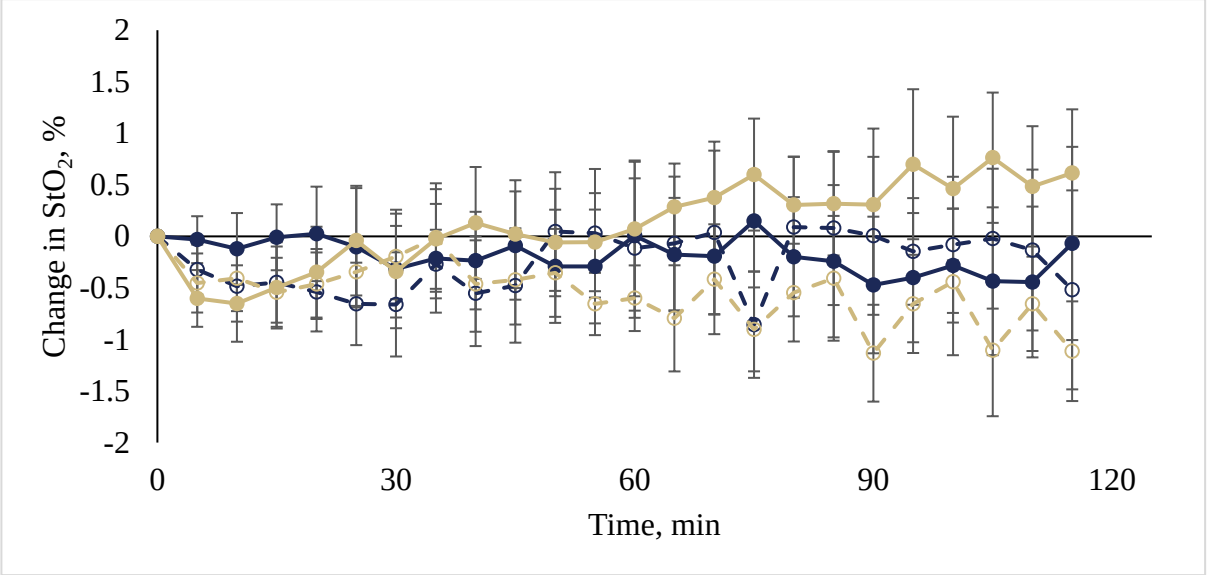

Figure 201: I. Change in StO_2 split into BMI group and flooring condition and II. Change in StO_2 split into BMI group and flooring condition displayed over time. Error bars are standard error of the mean.

I.

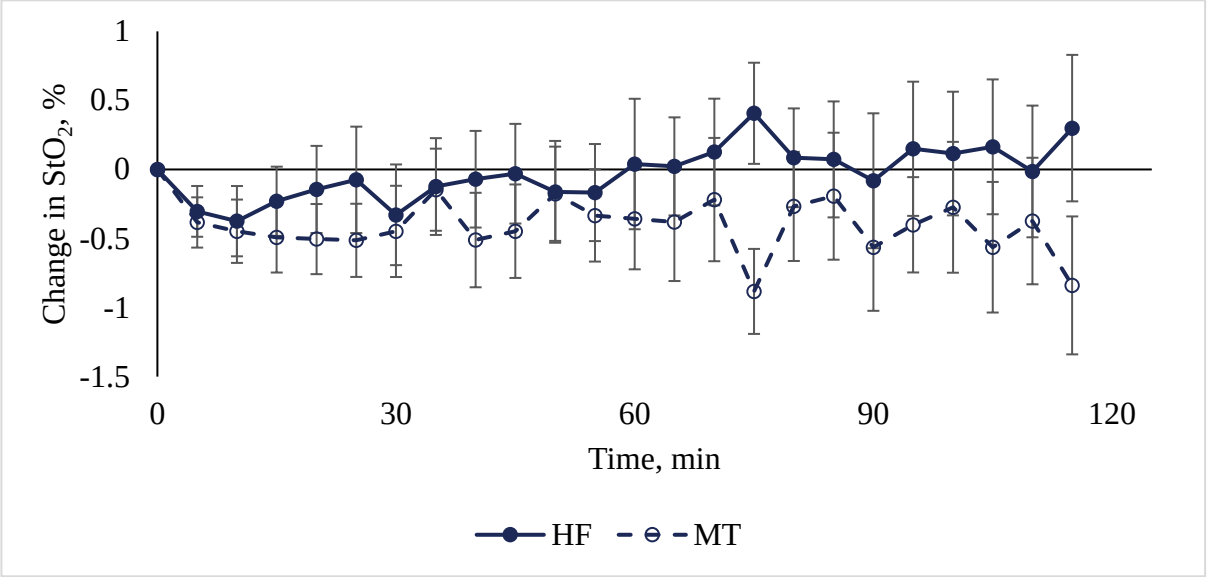

II.

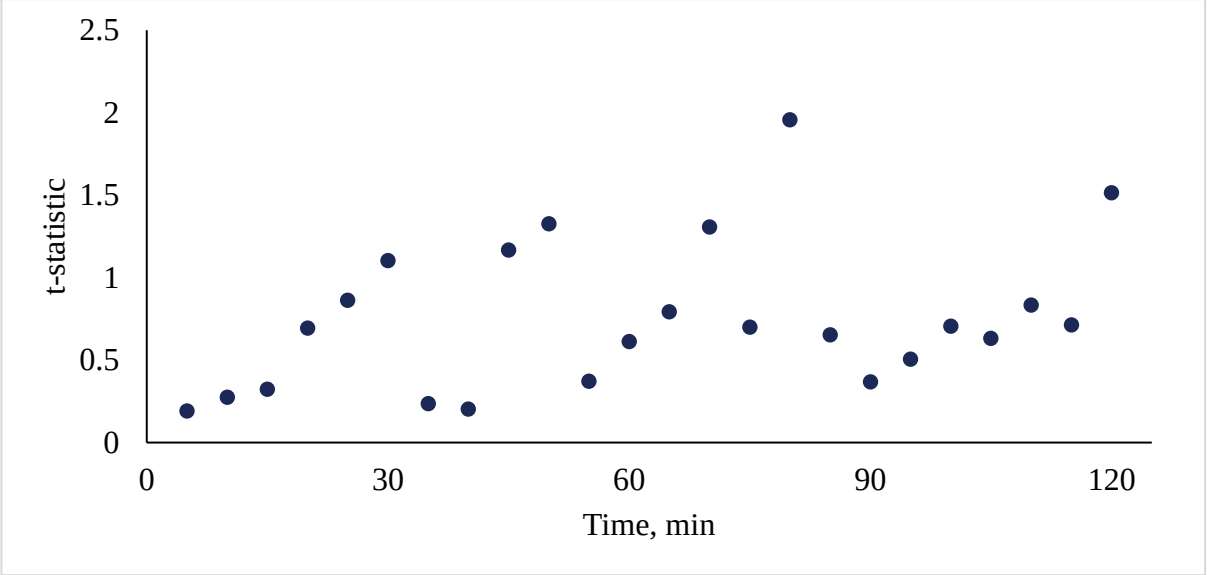

Figure 202: I. Change in StO_2 split into HF and MT flooring conditions and plotted over time. Error bars are standard error of the mean. II. Tukey HSD t statistic comparing mean change in StO_2 between flooring conditions at each five minute time interval.

I.

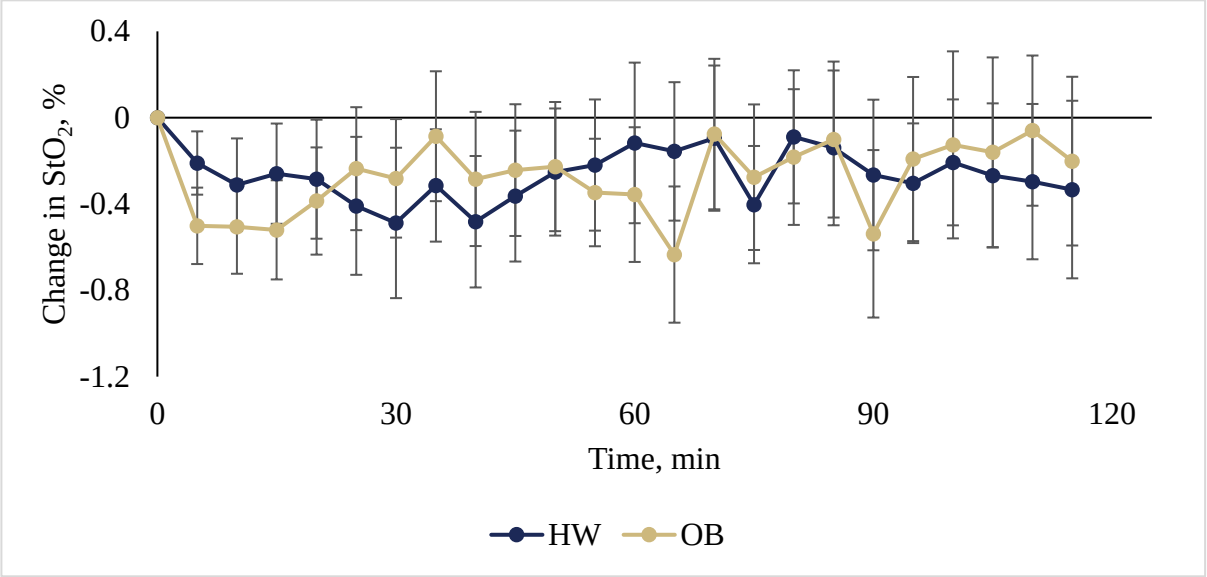

II.

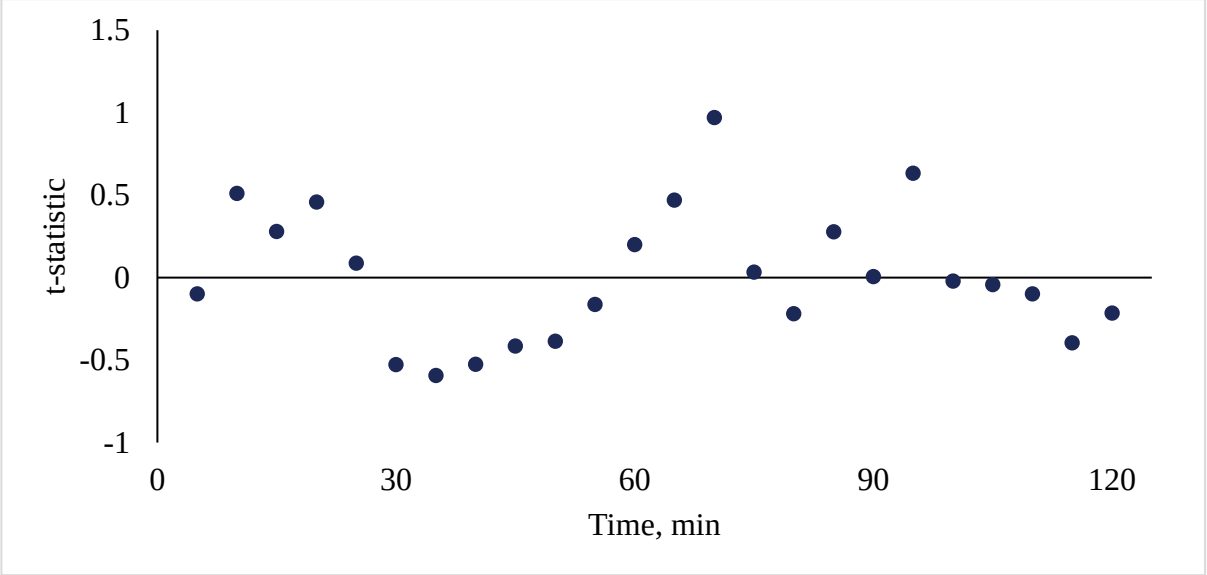

Figure 203: I. Change in StO_2 split into BMI groups and plotted over time. Error bars are standard error of the mean. II. Tukey HSD t statistic comparing mean change in StO_2 between BMI groups at each five minute time interval.

Appendix D.2.6 Pulsatile Oxygen Saturation

I.

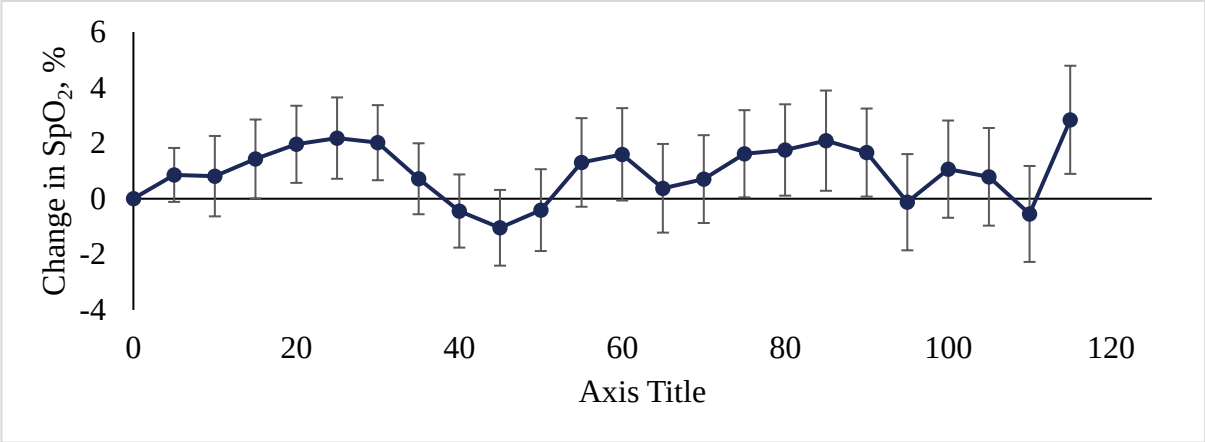

II.

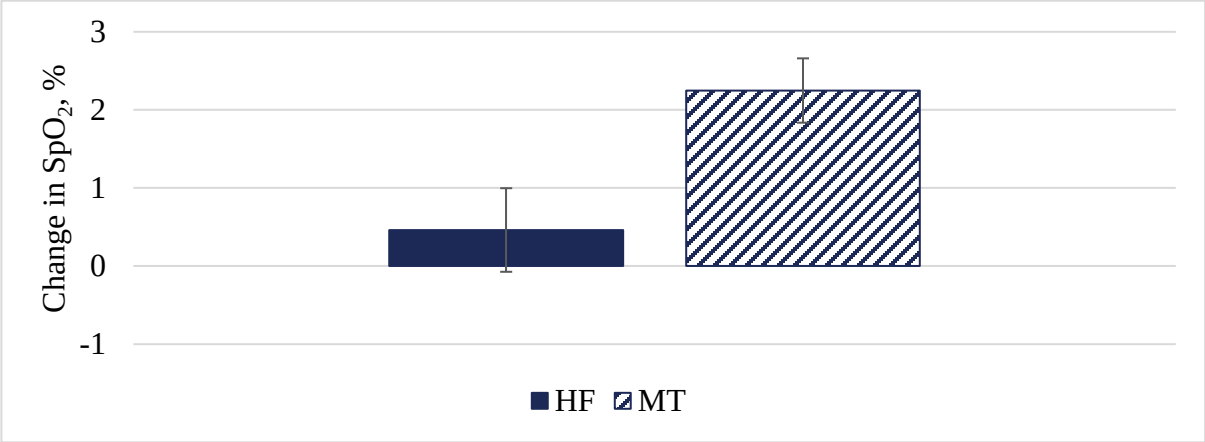

III.

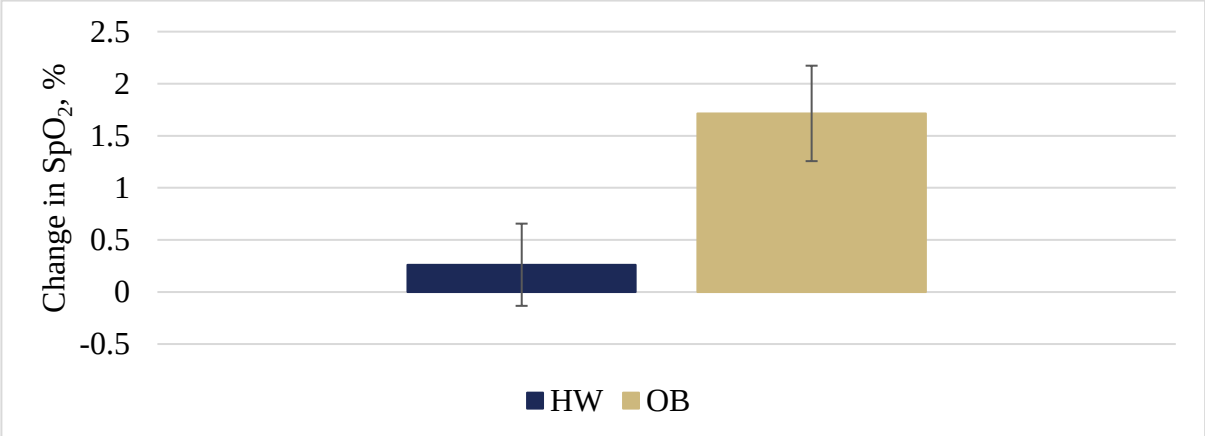

Figure 204: Change in StO_2 (%) over time (I) and between flooring conditions (II) and BMI groups (III). Error bars are standard error of the mean.

I.

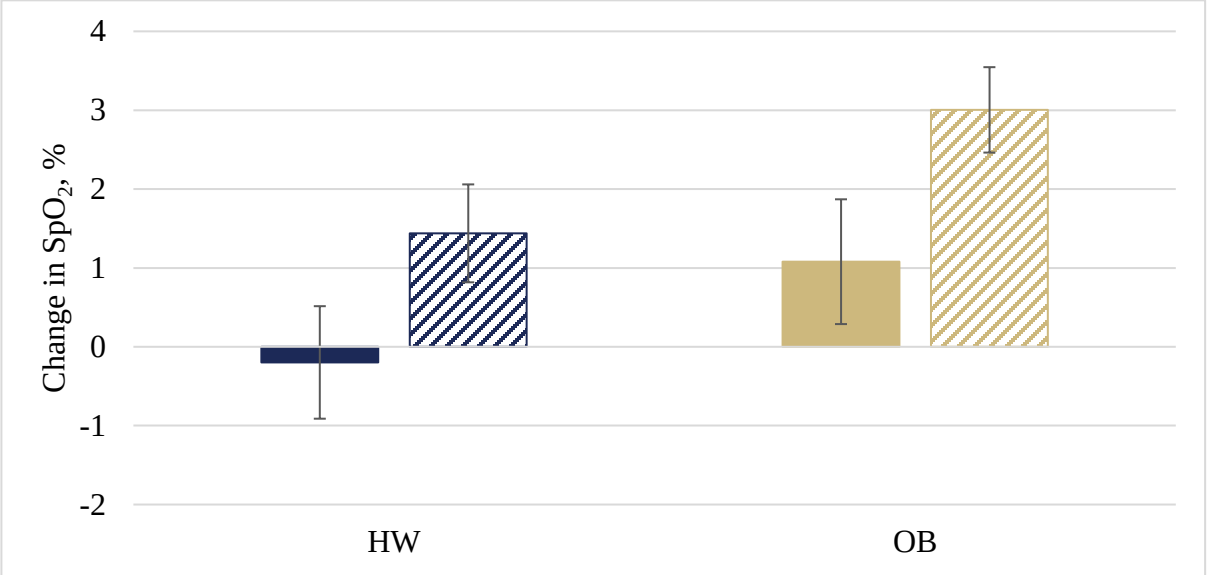

II.

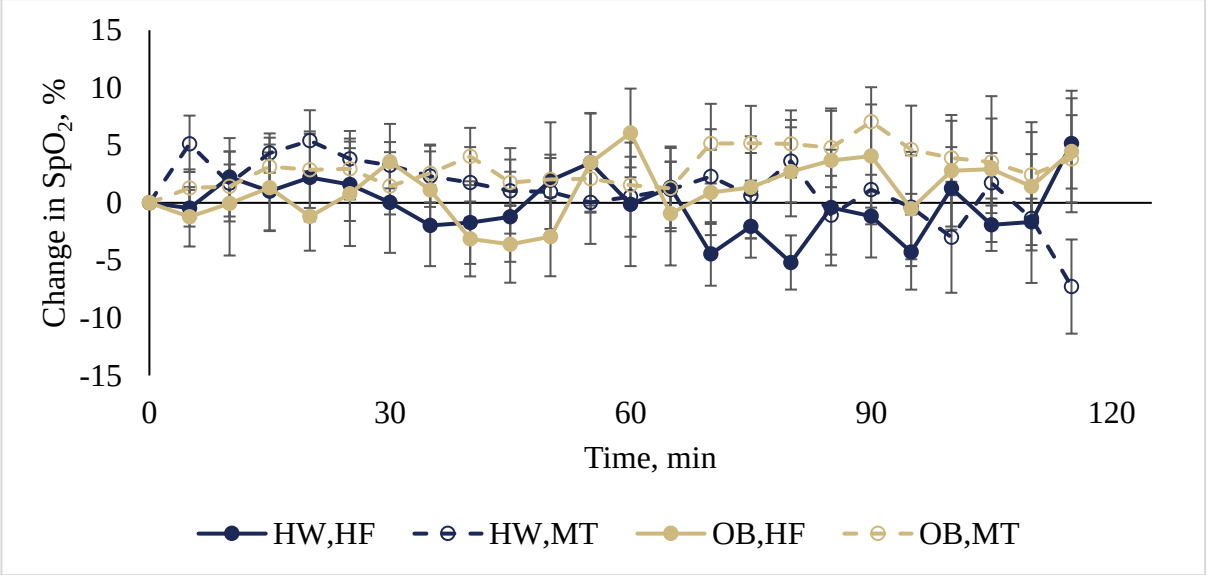

Figure 205: I. Change in SpO_2 split into BMI group and flooring condition and II. Change in SpO_2 split into BMI group and flooring condition displayed over time. Error bars are standard error of the mean.

I.

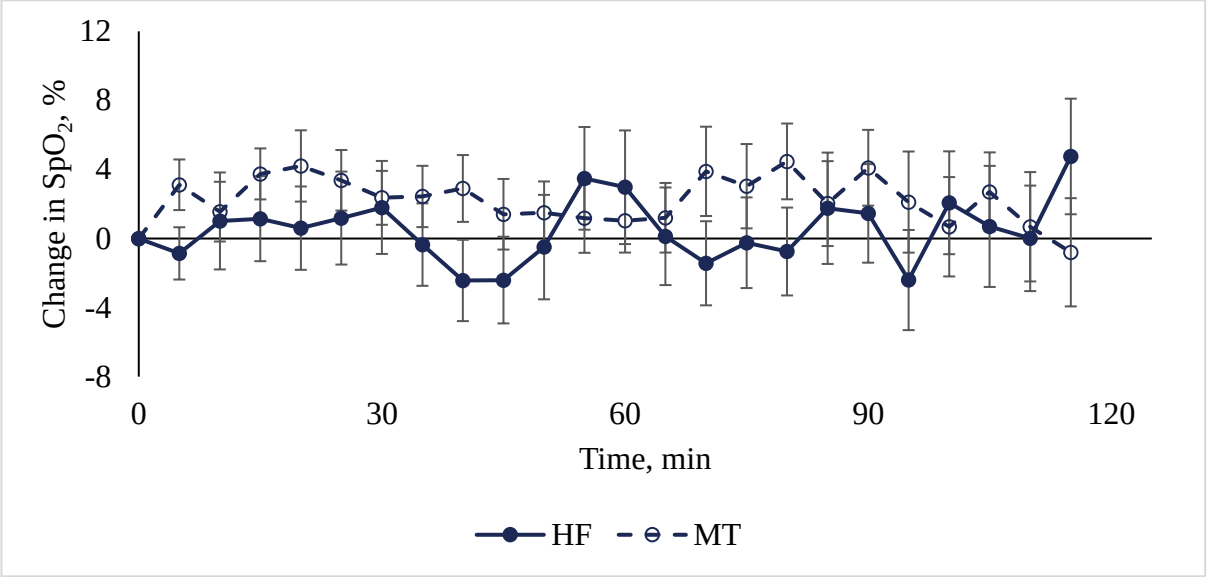

II.

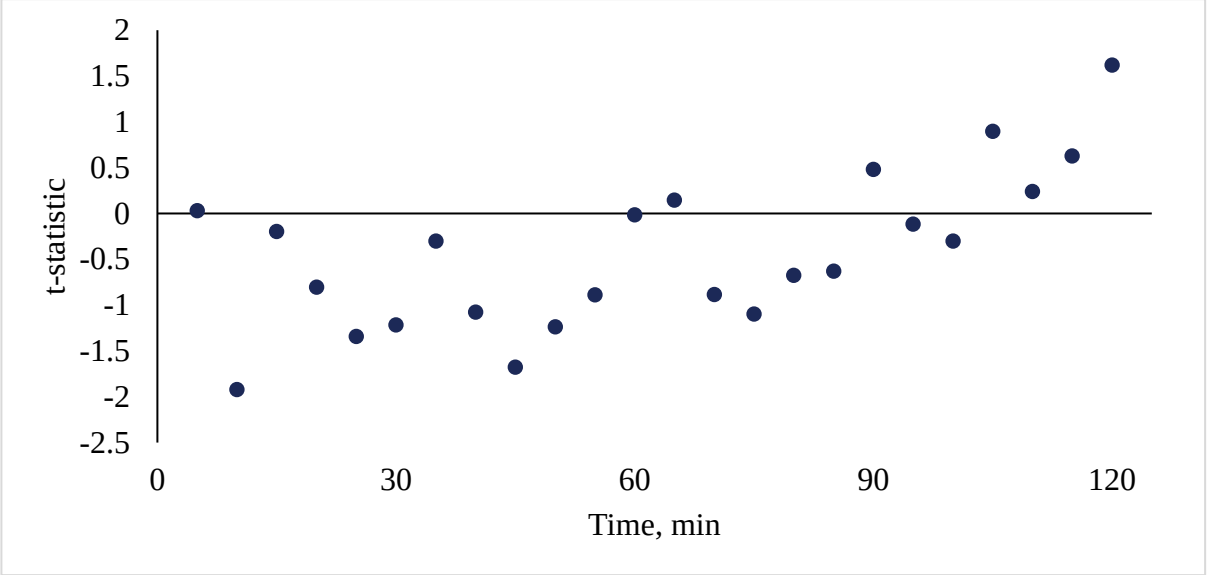

Figure 206: I. Change in SpO_2 split into HF and MT flooring conditions and plotted over time. Error bars are standard error of the mean. II. Tukey HSD t statistic comparing mean change in SpO_2 between flooring conditions at each five minute time interval.

I.

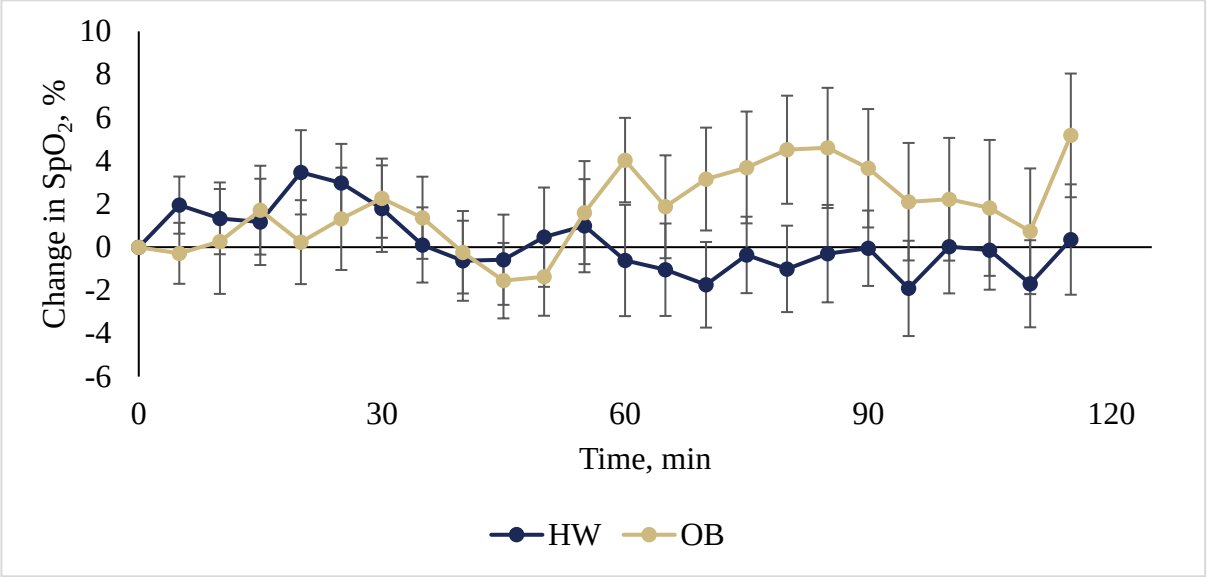

II.

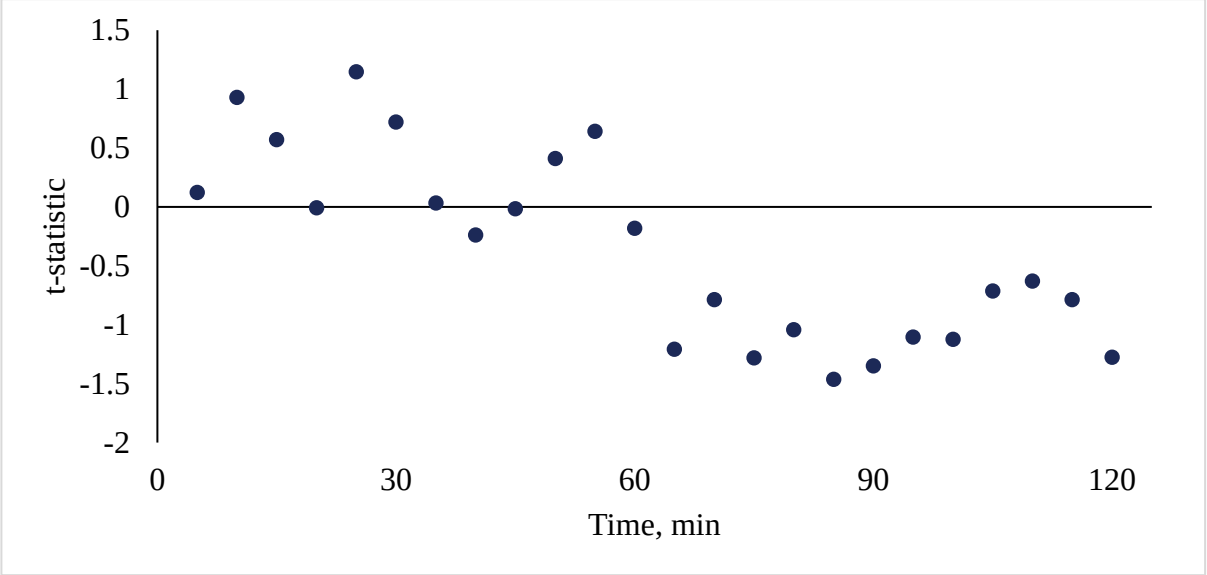

Figure 207: I. Change in SpO_2 split into BMI groups and plotted over time. Error bars are standard error of the mean. II. Tukey HSD t statistic comparing mean change in SpO_2 between BMI groups at each five minute time interval.

Bibliography

[1] R. Cham and M. S. Redfern, "Effect of Flooring on Standing Comfort and Fatigue," *Human Factors: The Journal of the Human Factors and Ergonomics Society,* vol. 43, no. 3, pp. 381-391, 2001.

[2] I. Halim, A. R. Omar, A. M. Saman, and I. Othman, "Assessment of muscle fatigue associated with prolonged standing in the workplace," *Safety and health at work,* vol. 3, no. 1, pp. 31-42, 2012.

[3] L. Hansen, J. Winkel, and K. Jørgensen, "Significance of mat and shoe softness during prolonged work in upright position: based on measurements of low back muscle EMG, foot volume changes, discomfort and ground force reactions," *Applied Ergonomics,* vol. 29, no. 3, pp. 217-224, 1998.

[4] P. M. King, "A comparison of the effects of floor mats and shoe in-soles on standing fatigue," *Applied Ergonomics,* vol. 33, no. 5, pp. 477-484, 2002.

[5] Y.-H. Lin, C.-Y. Chen, and M.-H. Cho, "Influence of shoe/floor conditions on lower leg circumference and subjective discomfort during prolonged standing," *Applied ergonomics,* vol. 43, no. 5, p. 965, 2012.

[6] P. Madeleine, M. Voigt, and L. Arendt-Nielsen, "Subjective, physiological and biomechanical responses to prolonged manual work performed standing on hard and soft surfaces," *European Journal of Applied Physiology and Occupational Physiology,* vol. 77, no. 1, pp. 1-9, 1997.

[7] A. R. Orlando and P. M. King, "Relationship of Demographic Variables on Perception of Fatigue and Discomfort Following Prolonged Standing Under Various Flooring Conditions," *Journal of Occupational Rehabilitation,* vol. 14, no. 1, pp. 63-76, 2004.

[8] J. M. Prado, M. C. M. Dinato, and M. Duarte, "Age-related difference on weight transfer during unconstrained standing," *Gait & posture,* vol. 33, no. 1, pp. 93-97, 2011.

[9] M. S. Redfern and D. B. Chaffin, "Influence of Flooring on Standing Fatigue," *Human Factors: The Journal of the Human Factors and Ergonomics Society,* vol. 37, no. 3, pp. 570-581, 1995.

[10] T. R. Waters and R. B. Dick, "Evidence of Health Risks Associated with Prolonged Standing at Work and Intervention Effectiveness," *Rehabilitation Nursing,* vol. 40, no. 3, pp. 148-165, 2015.

[11] N. Wiggermann and W. M. Keyserling, "Effects of Anti-Fatigue Mats on Perceived Discomfort and Weight-Shifting During Prolonged Standing," *Human Factors: The Journal of Human Factors and Ergonomics Society*, vol. 55, no. 4, pp. 764-775, 2013.

[12] B. o. L. Statistics. (2016, November 13). *Standing or walking versus sitting on the job in 2016* [Online]. Available: www.bls.gov.

[13] J. Engels, J. Van Der Gulden, T. F. Senden, C. Hertog, J. Kolk, and R. Binkhorst, "Physical work load and its assessment among the nursing staff in nursing homes," 1995.

[14] I. Halim, A. R. Omar, A. M. Saman, and I. Othman, "A review on health effects associated with prolonged standing in the industrial workplaces," *IJRRAS*, vol. 8, no. 1, pp. 14-21, 2011.

[15] U. S. D. o. Labor. (2017, November 26). *Minimum Length of Meal Period Required under State Law for Adult Employees in Private Sector* [Online]. Available: www.dol.gov.

[16] A. G. Ryan, "The prevalence of musculo-skeletal symptoms in supermarket workers," *Ergonomics*, vol. 32, no. 4, pp. 359-371, 1989.

[17] R. A. Werner, N. Gell, A. Hartigan, N. Wiggerman, and W. M. J. P. Keyserling, "Risk factors for Foot and Ankle Disorders Among Assembly Plant Workers," *American Journal of Industrial Medicine*, vol. 53, no. 12, pp. 1233-1239, 2010.

[18] M. Stolt, R. Suhonen, P. Virolainen, and H. Leino-Kilpi, "Lower extremity musculoskeletal disorders in nurses: A narrative literature review," *Scandinavian journal of public health*, vol. 44, no. 1, pp. 106-115, 2016.

[19] O. Hassan and H. Bayomy, "Occupational respiratory and musculoskeletal symptoms among Egyptian female hairdressers," *Journal of community health*, vol. 40, no. 4, pp. 670-679, 2015.

[20] H. A. Aweto, B. A. Tella, and O. Y. Johnson, "Prevalence of work-related musculoskeletal disorders among hairdressers," *International Journal of Occupational Medicine and Environmental Health*, vol. 28, no. 3, p. 545, 2015.

[21] R. Baker, P. Coenen, E. Howie, J. Lee, A. Williamson, and L. Straker, "A detailed description of the short-term musculoskeletal and cognitive effects of prolonged standing for office computer work," *Ergonomics*, vol. 61, no. 7, pp. 877-890, 2018.

[22] J. C. D'Souza, A. Franzblau, and R. A. Werner, "Review of epidemiologic studies on occupational factors and lower extremity musculoskeletal and vascular disorders and symptoms," (in eng), *Journal of Occupational Rehabilitation*, vol. 15, no. 2, pp. 129-65, Jun 2005.

[23] "Arthritis By The Numbers / Book of Trusted Facts & Figures," A. Foundation, Ed., ed, 2018.

[24] R. Plotnikoff *et al.*, "Osteoarthritis prevalence and modifiable factors: a population study," *BMC public health,* vol. 15, pp. 1195-1195, 2015.

[25] J. S. Schouten, F. A. van den Ouweland, and H. A. Valkenburg, "A 12 year follow up study in the general population on prognostic factors of cartilage loss in osteoarthritis of the knee," (in eng), *Ann Rheum Dis,* vol. 51, no. 8, pp. 932-937, 1992.

[26] H. Miranda, E. Viikari-Juntura, R. Martikainen, and H. Riihimäki, "A prospective study on knee pain and its risk factors," *Osteoarthritis and Cartilage,* vol. 10, no. 8, pp. 623-630, 2002/08/01/ 2002.

[27] P. Baker, I. Reading, C. Cooper, and D. Coggon, "Knee disorders in the general population and their relation to occupation," *Occupational and Environmental Medicine,* vol. 60, no. 10, p. 794, 2003.

[28] F. Tuchsen, N. Krause, H. Hannerz, H. Burr, and T. S. Kristensen, "Standing at work and varicose veins," (in eng), *Scandinavian journal of work, environment & health,* vol. 26, no. 5, pp. 414-20, Oct 2000.

[29] R. M. Krijnen, E. M. de Boer, and D. P. Bruynzeel, "Epidemiology of venous disorders in the general and occupational populations," (in eng), *Epidemiologic reviews,* vol. 19, no. 2, pp. 294-309, 1997.

[30] F. Tomei, T. P. Baccolo, E. Tomao, S. Palmi, and M. V. Rosati, "Chronic venous disorders and occupation," vol. 36, no. 6, pp. 653-665, 1999.

[31] R. Krijnen, E. De Boer, H. Ader, D. J. S. r. Bruynzeel, and technology, "Diurnal volume changes of the lower legs in healthy males with a profession that requires standing," vol. 4, no. 1, pp. 18-23, 1998.

[32] N. Krause, J. W. Lynch, G. A. Kaplan, R. D. Cohen, R. Salonen, and J. T. Salonen, "Standing at work and progression of carotid atherosclerosis," (in eng), *Scandinavian journal of work, environment & health,* vol. 26, no. 3, pp. 227-36, Jun 2000.

[33] (2018). *Occupational Injuries and Illnesses: Industry Data (2014 forward).*

[34] (2018). *Nonfatal cases involving days away from work: selected characteristics (2011 forward).*

[35] C. M. Torio and B. J. Moore. (2016, February 12). *National Inpatient Hospital Costs: The Most Expensive Conditions by Payer, 2013* [Online]. Available: https://www.hcup-us.ahrq.gov/reports/statbriefs/sb204-Most-Expensive-Hospital-Conditions.jsp.

[36] R. Carlton, R. Mallick, C. Campbell, A. Raju, T. O'Donnell, and M. Eaddy, "Evaluating the Expected Costs and Budget Impact of Interventional Therapies for the Treatment of Chronic Venous Disease," (in eng), *Am Health Drug Benefits,* vol. 8, no. 7, pp. 366-374, 2015.

[37] E. B. Kirkland *et al.*, "Trends in Healthcare Expenditures Among US Adults With Hypertension: National Estimates, 2003-2014," *Journal of the American Heart Association,* vol. 7, no. 11, p. e008731, 2018.

[38] S. Uzuner, M. L. Rodriguez, L. Li, and S. Kucuk, "Dual fluoroscopic evaluation of human tibiofemoral joint kinematics during a prolonged standing: A pilot study," *Engineering Science and Technology, an International Journal,* 2019.

[39] J. Brownie and B. J. Martin, "Muscle fatigue and discomfort associated with standing and walking: Comparison of work surfaces," in *Proceedings 19th Triennial Congress of the IEA*, 2015, vol. 9, p. 14.

[40] Y. L. Chen, B. Z. Wu, and D. H. Huang, "Effect of participant physiques on increases in shank circumference for the two prolonged standing conditions," *Human Factors and Ergonomics in Manufacturing & Service Industries,* vol. 27, no. 4, pp. 171-176, 2017.

[41] C. G. Drury, Y. L. Hsiao, C. Joseph, S. Joshi, J. Lapp, and P. R. Pennathur, "Posture and performance: sitting vs. standing for security screening," (in eng), *Ergonomics,* vol. 51, no. 3, pp. 290-307, Mar 2008.

[42] M.-G. Garcia, T. Läubli, and B. J. Martin, "Long-Term Muscle Fatigue After Standing Work," *Human Factors: The Journal of Human Factors and Ergonomics Society,* vol. 57, no. 7, pp. 1162-1173, 2015.

[43] J. Haney and P. University of, "Effect of flooring on lower extremity discomfort and fatigue during long-term standing/walking: evaluation of muscle oxygenation as an objective measure of fatigue using near infrared spectroscopy," Dissertation/Thesis, 2014.

[44] J. S. Rekant, S. A. Wiltman, A. J. Chambers, and H. Factors, "A Novel Method of Analysis for Prolonged-Standing Data: Accounting for Joint and Muscle Discomfort," *IISE Transactions on Occupational Ergonomics,* vol. 7, no. 2, pp. 142-152, 2019.

[45] L. ZHANG, C. G. DRURY, and S. M. WOOLLEY, "Constrained standing: evaluating the foot/floor interface," *Ergonomics,* vol. 34, no. 2, pp. 175-192, 1991.

[46] J. R. Jefferson, "The Effect of Cushioning Insoles on Back and Lower Extremity Pain in an Industrial Setting," *Workplace Health & Safety,* vol. 61, no. 10, pp. 451-457, 2013.

[47] J. T. Cacioppo, L. G. Tassinary, and G. Berntson, *Handbook of psychophysiology*. Cambridge University Press, 2007.

[48] S. Grant *et al.*, "A Comparison of the Reproducibility and the Sensitivity to Change of Visual Analogue Scales, Borg Scales, and Likert Scales in Normal Subjects During Submaximal Exercise," *Chest,* vol. 116, no. 5, pp. 1208-1217, 1999/11/01/ 1999.

[49] P. M. Podsakoff, S. B. MacKenzie, J.-Y. Lee, and N. P. Podsakoff, "Common Method Biases in Behavioral Research: A Critical Review of the Literature and Recommended Remedies," *Journal of Applied Psychology,* vol. 88, no. 5, pp. 879-903, 2003.

[50] D. A. Winter, *Biomechanics and motor control of human movement*, 3rd ed. (no. Book, Whole). Hoboken, New Jersey: John Wiley & Sons, 2005.

[51] D. A. Winter, *ABC (anatomy, biomechanics and control) of balance during standing and walking*. Waterloo Biomechanics, 1995.

[52] A. J. Sophia Fox, A. Bedi, and S. A. Rodeo, "The basic science of articular cartilage: structure, composition, and function," *Sports health,* vol. 1, no. 6, pp. 461-468, 2009.

[53] V. C. Mow and R. Huiskes, *Basic orthopaedic biomechanics & mechano-biology*. Lippincott Williams & Wilkins, 2005.

[54] D. W. Smith, *Articular Cartilage Dynamics* (no. Book, Whole). Singapore: Springer, 2018.

[55] A. Mak, W. Lai, and V. Mow, "Biphasic indentation of articular cartilage—I. Theoretical analysis," *Journal of biomechanics,* vol. 20, no. 7, pp. 703-714, 1987.

[56] V. C. Mow, S. Kuei, W. M. Lai, and C. G. Armstrong, "Biphasic creep and stress relaxation of articular cartilage in compression: theory and experiments," *Journal of biomechanical engineering,* vol. 102, no. 1, pp. 73-84, 1980.

[57] C. Armstrong, W. Lai, and V. Mow, "An analysis of the unconfined compression of articular cartilage," *Journal of biomechanical engineering,* vol. 106, no. 2, pp. 165-173, 1984.

[58] V. C. Mow, M. Gibbs, W. M. Lai, W. Zhu, and K. A. Athanasiou, "Biphasic indentation of articular cartilage—II. A numerical algorithm and an experimental study," *Journal of biomechanics,* vol. 22, no. 8-9, pp. 853-861, 1989.

[59] R. K. Korhonen *et al.*, "Comparison of the equilibrium response of articular cartilage in unconfined compression, confined compression and indentation," (in eng), *Journal of Biomechanics,* vol. 35, no. 7, pp. 903-9, Jul 2002.

[60] D. L. Burris and A. C. Moore, "Cartilage and joint lubrication: new insights into the role of hydrodynamics," *Biotribology,* vol. 12, pp. 8-14, 2017.

[61] A. C. Moore and D. L. Burris, "Tribological and material properties for cartilage of and throughout the bovine stifle: support for the altered joint kinematics hypothesis of osteoarthritis," *Osteoarthritis and cartilage,* vol. 23, no. 1, pp. 161-169, 2015.

[62] A. C. Moore and D. L. Burris, "Tribological rehydration of cartilage and its potential role in preserving joint health," *Osteoarthritis and cartilage,* vol. 25, no. 1, pp. 99-107, 2017.

[63] W. Anderst, R. Zauel, J. Bishop, E. Demps, and S. Tashman, "Validation of three-dimensional model-based tibio-femoral tracking during running," *Medical Engineering and Physics,* vol. 31, no. 1, pp. 10-16, 2009.

[64] C. A. Marsh, "The development and application of an arthrokinematic biomarker for the early detection of osteoarthritis," Dissertation/Thesis, ProQuest Dissertations Publishing, 2014.

[65] L. E. DeFrate, H. Sun, T. J. Gill, H. E. Rubash, and G. Li, "In vivo tibiofemoral contact analysis using 3D MRI-based knee models," *Journal of biomechanics,* vol. 37, no. 10, pp. 1499-1504, 2004.

[66] A. Hosseini *et al.*, "In-vivo time-dependent articular cartilage contact behavior of the tibiofemoral joint," *Osteoarthritis and Cartilage,* vol. 18, no. 7, pp. 909-916, 2010.

[67] G. Li *et al.*, "The cartilage thickness distribution in the tibiofemoral joint and its correlation with cartilage-to-cartilage contact," *Clinical biomechanics,* vol. 20, no. 7, pp. 736-744, 2005.

[68] C. S. Paranjape *et al.*, "A New Stress Test for Knee Joint Cartilage," *Scientific reports,* vol. 9, no. 1, p. 2283, 2019.

[69] C. Herberhold *et al.*, "In situ measurement of articular cartilage deformation in intact femoropatellar joints under static loading," *Journal of biomechanics,* vol. 32, no. 12, pp. 1287-1295, 1999.

[70] M. E. Mayerhoefer *et al.*, "The in vivo effects of unloading and compression on T1-Gd (dGEMRIC) relaxation times in healthy articular knee cartilage at 3.0 Tesla," *European radiology,* vol. 20, no. 2, pp. 443-449, 2010.

[71] J. V. Basmajian and C. J. De Luca, *Muscles alive, their functions revealed by electromyography*, 5th ed. (no. Book, Whole). Baltimore: Williams & Wilkins, 1985.

[72] D. A. Neumann, *Kinesiology of the musculoskeletal system: foundations for physical rehabilitation*, 1st ed. (no. Book, Whole). St. Louis: Mosby, Inc, 2002.

[73] A. J. Pappano, W. G. Wier, and M. N. Levy, *Cardiovascular physiology*, 10th ed. (no. Book, Whole). Philadelphia, PA: Elsevier/Mosby, 2013.

[74] M. Nordin, G. B. Andersson, and M. H. Pope, "Musculoskeletal disorders in the workplace," *Louis. Mosby,* 1997.

[75] R. E. Klabunde, *Cardiovascular physiology concepts*, 2nd ed. (no. Book, Whole). Baltimore, MD: Lippincott Williams & Wilkins/Wolters Kluwer, 2012.

[76] M. Ferrari, M. Muthalib, and V. Quaresima, "The use of near-infrared spectroscopy in understanding skeletal muscle physiology: recent developments," *Philosophical Transactions: Mathematical, Physical and Engineering Sciences,* vol. 369, no. 1955, pp. 4577-4590, 2011.

[77] A. Bakker, B. Smith, P. Ainslie, and K. Smith, "Near-infrared spectroscopy," in *Applied Aspects of Ultrasonography in Humans*: IntechOpen, 2012.

[78] S. Wray, M. Cope, D. T. Delpy, J. S. Wyatt, and E. O. Reynolds, "Characterization of the near infrared absorption spectra of cytochrome aa3 and haemoglobin for the non-invasive monitoring of cerebral oxygenation," (in eng), *Biochimica et biophysica acta,* vol. 933, no. 1, pp. 184-92, Mar 30 1988.

[79] N. L. Hughes, A. Nelson, M. W. Matz, and J. Lloyd, "AORN Ergonomic Tool 4: Solutions for prolonged standing in perioperative settings," *AORN journal,* vol. 93, no. 6, pp. 767-774, 2011.

[80] (2016, October 6). *Working in a Standing Position - Basic Information* [Online]. Available: https://www.ccohs.ca/oshanswers/ergonomics/standing/standing_basic.html.

[81] (2019, October 6). *Prolonged Standing* [Online]. Available: https://www.osha.gov/SLTC/youth/restaurant/drivethru_standing.html.

[82] N. L. Hughes, A. Nelson, M. W. Matz, and J. Lloyd, "AORN Ergonomic Tool 4: Solutions for Prolonged Standing in Perioperative Settings," *AORN Journal,* vol. 93, no. 6, pp. 767-774.

[83] C. M. Hales, M. D. Carroll, C. D. Fryar, and C. L. Ogden, "Prevalence of obesity among adults and youth: United States, 2015–2016," 2017.

[84] G. Eknoyan, "Adolphe Quetelet (1796–1874)—the average man and indices of obesity," *Nephrology Dialysis Transplantation,* vol. 23, no. 1, pp. 47-51, 2007.

[85] P. Buckle and J. Buckle, "Obesity, ergonomics and public health," *Perspectives in public health,* vol. 131, no. 4, pp. 170-176, 2011.

[86] T. Sturmer, K. P. Gunther, and H. Brenner, "Obesity, overweight and patterns of osteoarthritis: the Ulm Osteoarthritis Study," (in eng), *Journal of clinical epidemiology,* vol. 53, no. 3, pp. 307-13, Mar 1 2000.

[87] T. Østbye, J. M. Dement, and K. M. Krause, "Obesity and Workers' Compensation: Results From the Duke Health and Safety Surveillance System," *Archives of Internal Medicine,* vol. 167, no. 8, pp. 766-773, 2007.

[88] O. Hue *et al.*, "Body weight is a strong predictor of postural stability," *Gait & posture,* vol. 26, no. 1, pp. 32-38, 2007.

[89] F. Menegoni *et al.*, "Mechanisms underlying center of pressure displacements in obese subjects during quiet stance," *Journal of neuroengineering and rehabilitation,* vol. 8, no. 1, p. 20, 2011.

[90] D. Singh, W. Park, M. S. Levy, and E. S. Jung, "The effects of obesity and standing time on postural sway during prolonged quiet standing," *Ergonomics,* vol. 52, no. 8, pp. 977-986, 2009.

[91] E. F. Chehab, T. P. Andriacchi, and J. Favre, "Speed, age, sex, and body mass index provide a rigorous basis for comparing the kinematic and kinetic profiles of the lower extremity during walking," *Journal of Biomechanics,* vol. 58, pp. 11-20, 2017/06/14/ 2017.

[92] A. T. Collins *et al.*, "Obesity alters the in vivo mechanical response and biochemical properties of cartilage as measured by MRI," *Arthritis research & therapy,* vol. 20, no. 1, p. 232, 2018.

[93] A. Jawien, "The influence of environmental factors in chronic venous insufficiency," *Angiology,* vol. 54, no. 1, pp. S19-S31, 2003.

[94] K. Kohno *et al.*, "Standing posture at work and overweight exacerbate varicose veins: Shimane Co HRE Study," *The Journal of dermatology,* vol. 41, no. 11, pp. 964-968, 2014.

[95] C. f. D. Control. (2017, November 20). *Adult Obesity Facts* [Online]. Available: www.cdc.gov.

[96] G. Borg, *Borg's perceived exertion and pain scales*. Human kinetics, 1998.

[97] S. Tashman and W. Anderst, "In-vivo measurement of dynamic joint motion using high speed biplane radiography and CT: application to canine ACL deficiency," *Journal of biomechanical engineering,* vol. 125, no. 2, p. 238, 2003.

[98] B. M. You, P. Siy, W. Anderst, and S. Tashman, "In vivo measurement of 3-D skeletal kinematics from sequences of biplane radiographs: Application to knee kinematics," *IEEE Transactions on Medical Imaging,* vol. 20, no. 6, pp. 514-525, 2001.

[99] A. Iraqi, R. Cham, M. S. Redfern, and K. E. Beschorner, "Coefficient of friction testing parameters influence the prediction of human slips," *Applied Ergonomics,* vol. 70, pp. 118-126, 2018.

[100] S. M. S. F. Freitas, J. M. Prado, and M. Duarte, "The use of a safety harness does not affect body sway during quiet standing," *Clinical Biomechanics,* vol. 20, no. 3, pp. 336-339, 2005.

[101] W. J. Anderst and S. Tashman, "A method to estimate in vivo dynamic articular surface interaction," *Journal of Biomechanics,* vol. 36, no. 9, pp. 1291-1299, 2003/09/01/ 2003.

[102] E. S. Grood and W. J. Suntay, "A joint coordinate system for the clinical description of three-dimensional motions: application to the knee," *Journal of biomechanical engineering,* vol. 105, no. 2, pp. 136-144, 1983.

[103] J. Mauro and N. M. Briggs, "Assessment of variations in radiation exposure in the United States," 2005.

[104] B. L. Wise *et al.*, "Patterns of compartment involvement in tibiofemoral osteoarthritis in men and women and in whites and African Americans," (in eng), *Arthritis Care Res (Hoboken),* vol. 64, no. 6, pp. 847-852, 2012.

[105] T. J. Huppert, S. G. Diamond, M. A. Franceschini, and D. A. Boas, "HomER: a review of time-series analysis methods for near-infrared spectroscopy of the brain," (in eng), *Appl Opt,* vol. 48, no. 10, pp. D280-D298, 2009.

[106] M. Nitzan *et al.*, "Calibration-free pulse oximetry based on two wavelengths in the infrared - a preliminary study," (in eng), *Sensors (Basel),* vol. 14, no. 4, pp. 7420-7434, 2014.

[107] G. Themelis *et al.*, "Near-infrared spectroscopy measurement of the pulsatile component of cerebral blood flow and volume from arterial oscillations," (in eng), *Journal of biomedical optics,* vol. 12, no. 1, p. 014033, Jan-Feb 2007.

[108] D. Roman-Liu, "Age-related changes in the range and velocity of postural sway," (in eng), *Archives of gerontology and geriatrics,* vol. 77, pp. 68-80, Jul - Aug 2018.

[109] K. Aukland, "Why Don't Our Feet Swell in the Upright Position?," *Physiology,* vol. 9, no. 5, pp. 214-219, 1994.

[110] J.-A. Collins, A. Rudenski, J. Gibson, L. Howard, and R. O'Driscoll, "Relating oxygen partial pressure, saturation and content: the haemoglobin-oxygen dissociation curve," (in eng), *Breathe (Sheff),* vol. 11, no. 3, pp. 194-201, 2015.

[111] (2019). *Employed Persons by Detailed Occupation and Age*.